

Tectono-metamorphic and magmatic evolution of the Internal
Dinarides (Kopaonik area, southern Serbia)
and its significance for the geodynamic evolution
of the Balkan Peninsula

Inauguraldissertation

zur

Erlangung der Würde eines Doktors der Philosophie

vorgelegt der

Philosophisch-Naturwissenschaftlichen Fakultät der Universität Basel

von

Senecio Claudio Schefer

aus Teufen (AR), Schweiz

Basel, 2012

Genehmigt von der Philosophisch-Naturwissenschaftlichen Fakultät auf Antrag von

Prof. Dr. Stefan M. Schmid (Fakultätsverantwortlicher, Dissertationsleiter)

Geologisch-Paläontologisches Institut, Universität Basel

Prof. Dr. Bernhard Fügenschuh (Dissertationsleiter)

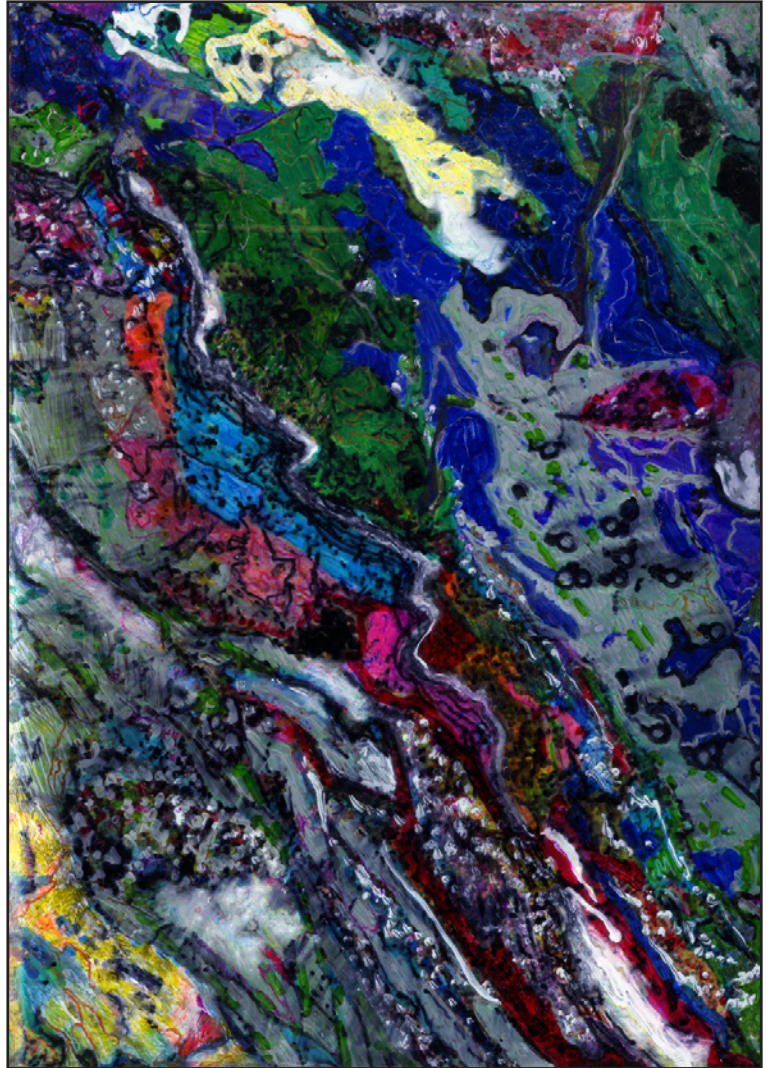
Institut für Geologie und Paläontologie, Universität Innsbruck

Basel, 27. April 2010

Prof. Dr. Eberhard Parlow

(Dekan der Philosophisch-Naturwissenschaftlichen Fakultät)

...to H el ene and our wonderful daughter Lou...



('Lou Stoja' by P. Stoffel 2008)

Abstract

This study is embedded in a Swiss Science Foundation (SNF) project entitled “Tisza and its role in the framework of the tectonic evolution of Alps, Dinarides and Carpathians“ (Project No. 20002-109278). The study presented here expands the area covered by this project towards southeast into Serbia where the contact between the Dacia Mega-Unit (which was fixed in respect to Tisza since mid-Cretaceous times) and the Dinarides can be studied. The study is devoted to the tectono-metamorphic and magmatic evolution of the Internal Dinarides and it furthermore addresses the geodynamic evolution of the Balkan Peninsula. The investigated area is located in the internal-most part of the Dinarides and covers the contact zone between the Dinaridic orogen that essentially formed in Latest Cretaceous to Paleogene times and the “Serbo–Macedonian Massif“, that is a part of the Carpatho–Balkan orogen (Dacia Mega-Unit) which is characterised by older (pre-Turonian) deformations. The widespread occurrences of ophiolitic rocks, separated by different fragments of continental basement rocks led to a ‘multi-ocean’ concept whereby the oceans were separated by elongate continental terranes or micro-plates. By investigating the stratigraphic and tectonic evolution of the various continent-derived units and by studying their relation with the intervening ophiolitic belts this ‘multi-terrane/multi-ocean’ problem is critically addressed and a one-ocean model is preferred. Thereby the continental terranes simply represent the passive margin of Adria, exposed in windows below the ophiolites, which were obducted in Late Jurassic times.

Strongly deformed and metamorphosed meta-sediments crop out in the Studenica valley and the Kopaonik area representing the easternmost occurrences of Triassic sediments within the Dinarides. Upper Paleozoic terrigenous sediments are overlain by Lower Triassic siliciclastics and limestones, followed by Anisian shallow-water carbonates. A pronounced facies change to hemipelagic and distal turbiditic, cherty meta-limestones (Kopaonik Formation) testifies to a late Anisian drowning of the former shallow-water carbonate shelf. Sedimentation of the Kopaonik Formation was contemporaneous with shallow-water carbonate production on nearby and more proximal carbonate platforms that were the source areas of diluted turbidity currents reaching the depositional area of this formation. The Kopaonik Formation was dated by conodont faunas as late Anisian to Norian and possibly extends into the Early Jurassic. It is therefore considered an equivalent of the grey Hallstatt facies of the Eastern Alps, the Western Carpathians and the Albanides–Hellenides. The coeval carbonate platforms were generally located in more proximal areas of the Adriatic margin, whereas the distal margin was dominated by hemipelagic/pelagic and distal turbiditic sedimentation, facing the evolving Neotethys Ocean to the east. A similar arrangement of Triassic facies belts can be recognised all along the evolving Meliata–Maliac–Vardar branch of Neotethys, which is in line with a ‘one-ocean-hypothesis’ for the Dinarides: all ophiolites presently located southwest of the Drina–Ivanjica and Kopaonik thrust sheets are derived from an area to the east, and the Drina–Ivanjica and Kopaonik units emerge in tectonic windows from below this ophiolite nappe. On the base of the Triassic facies distribution neither arguments for an independent Dinaridic Ocean nor evidence for isolated terranes or blocks was seen.

Two age groups for the Cenozoic granitoids in the Dinarides of southern Serbia were determined by high precision single grain U–Pb dating of thermally annealed and chemically abraded zircons: (i) Oligocene ages (Kopaonik, Drenje, Željin) ranging from 31.7 to 30.6 Ma and (ii) Miocene ages (Golija and Polumir) at 20.58–20.17 and 18.06–17.74 Ma, respectively. Apatite fission-track central ages and modelling combined with zircon central ages, together with local structural observations, constrain the subsequent exhumation history of the magmatic rocks. They indicate rapid cooling from above 300 to ca. 80 °C between 16 and 10 Ma for the Oligocene and the Miocene age group, caused by extensional exhumation of the plutons that are located in the footwall of

core-complexes. Miocene magmatism and core-complex formation thus not only affected the Pannonian basin but also a part of the mountainous areas of the internal Dinarides.

Four different deformation phases (D1–D4) are distinguished in the study area. D1 to D3 are related to compression and metamorphism that pre-date the intrusion of I-type Oligocene plutons in Early Oligocene times, whereas the fourth deformation phase (D4) is related to extensional tectonics and exhumation that are contemporaneous with the intrusion of Miocene S-type granitoids. The first event (D1) is probably linked to the obduction of the Western Vardar Ophiolitic Unit onto the distal Adriatic continental margin. It is associated with top-NW shear-senses observed in sigma-clasts in a ductilely deformed and slightly metamorphosed ophiolitic mélange as well as with a penetrative foliation and a stretching lineation coupled to greenschist facies metamorphism in the Late Paleozoic to Early Jurassic sediments. During the Late Cretaceous (110–85 Ma) these sediments witnessed a metamorphic event that occurred under lowermost greenschist-facies conditions, associated with the ductile deformation phase (D2) represented by a well developed foliation and isoclinal folds overprinting D1. A higher greenschist- to amphibolite-facies overprint is observed during the Late Eocene to Early Oligocene (40–30 Ma) due to nappe-stacking caused by out-of-sequence thrusting (D3). This event is associated with the E–W-oriented compression related to and following the closure of the Sava suture. During the Miocene the entire area of investigation underwent rapid exhumation, accompanied by intense N–S-oriented ductile stretching (D4). This extension is correlated with the Miocene extension in the Pannonian basin whose location is in the back-arc area of the W-directed subduction of the European lithosphere beneath the Carpathians.

For the geodynamical setting of the Balkan Peninsula, based on new Hf isotope analyses and the discussion of an extensive set of age data from the literature, it is proposed that Late Eocene to Oligocene magmatism, which affects the Adria-derived lower plate units of the internal Dinarides, was caused by delamination of the Adriatic mantle from the overlying crust, associated with post-collisional convergence that propagated outward into the external Dinarides. Miocene magmatism, on the other hand, is associated with core-complex formation along the southern margin of the Pannonian basin, probably associated with the W-directed subduction of the European lithosphere beneath the Carpathians and interfering with ongoing Dinaridic–Hellenic back-arc extension.

РЕЗИМЕ

Ова студија је део пројекта Швајцарске научне фондације под називом ‘Тиса и њена улога у тектонској еволуцији Алпа, Динарида и Карпата’ (бр. Пројекта 20002-109278). Студија обухвата веће истражно подручје од оног обухваћеним иницијалним пројектом, и шири се ка југоистоку Србије где се може посматрати контакт између Дачија-Мега јединице (која је била фиксирана за Тисију још од средње креде) и Динарида. Студија је посвећена тектоно-метаморфној и магматској еволуцији унутрашњих Динарида и као таква даје модел геодинамичке еволуције Балканског полуострва. Истражно подручје се налази у средишњем делу Динарида и покрива контактну зону између динаридског орогена, који је формиран током горње креде и палеогена, и Српско-Македонске масе, која припада карпато-балканском орогену (Дачија Мега- јединица) окарактерисаним пре- туронским деформацијама. Појављивање офиолита, који су раздојени различитим фрагментима стена континенталне базе, довела је до концепта ‘неколико океана’ према коме су ти океански простори били раздојени дугачким континенталним теранима или микро плочама. Испитивањем стратиграфске и тектонске еволуције различитих континенталних јединица, и проучавањем њихових односа са обдукованим офиолитским појасевима, дошло се до закључка да преовлађујући концепт, који подразумева неколико терана и неколико океана, није у складу са добијеним резултатима. Нови, једноставнији концепт је предложен и подразумева један океански простор док континентални терани, по овом моделу, једноставно представљају пасивну маргину Адрије, откривену у тектонским прозорима испод офиолита обдукованих у горњој јури.

Интензивно деформисани и метаморфисани мета-седименти се могу наћи у долини Студенице и области Копаоника и представљају најисточније појаве тријаских седимената у Динаридима. Горње палеозојски теригени седименти су покривени доњетријаским силицикластним стенама и кречњацима који се даље настављају у анизијске плитководне карбонате. Изражена промена фација од хемипелашких и дисталних турбидита ка рожначко-кречњачким творевинама (Копаоничка формација) сведочи о исушивању раније плитководне карбонатне платформе, током доњег анизијског ката.

Седименти Копаоничке формације настали су у исто време кад и плитководни карбонати исталожени на оближњим, проксималним карбонатним платформама које пак, представљају изворна подручја турбидитних токова. Старост Копаоничке формације, утврђене на основу конодоната, одговара анизијском до норијском кату и вероватно сеже у доњу јуру. Зато се сматра еквивалентом сиве Халштатске фације источних Алпа, западних Карпата и Албанида-Хеленида. Карбонатне платформе исте старости су генерално биле лоциране у оближњим областима маргине Адрије. Седименти дисталних маргина представљени су доминантно хемипелашким/пелашким и дисталним турбидитским јединицама. Сличан распоред тријаских фација се може наћи свуда дуж пружања Мелиата-Малиак-Вардар бранши Неотетиса, који је у складу са хипотезом о ‘једном океану’ за Динариде; све офиолитске појаве лоциране југозападно од дринско-ивањичких и копаоничких навлака потичу из области са истока, док се Дрина-Ивањица и Копаоник појављују као тектонски прозори базе офиолитских навлака. На основу дистрибуције тријаских фација не могу се наћи аргументи ни за независтан Динаридски океан као ни за теране и блокове који су радовајали независне океанске просторе на овом подручју.

Две старосне групе кенозојских гранита у Динаридима јужне Србије су издвојене на основу високо прецизне уран- олово методе одређивања старости на цирконима: (и) Олигосенски гранити (Копаоник, Дрење, Жељин) старости од 31.7 до 30.6 милиона година и (и) Миоценски гранити (Голија и Полумир) старости 20.58–20.17 одн. 18.06–17.74 милиона година. Апатит fission track старости и моделовање које

комбинује fission-track старости са структурним обсервацијама са терена, говоре у прилог субсекветној ексхумацији магматских стена. Ове старости указују на брзо хлађење од преко 3000 °C на 800 °C у размаку од 16 до 10 милиона година за стене олигоценске и миоценске старости. Хлађење је узроковано екстензивном ексхумацијом плутона који се налазе у подини core complex-а. Миоценски магматизам и формација core complex-а је стога утицала како на развиће Панонског басена, тако делом и на планинска подручја унутрашњих Динарида.

На терену су присутне 4 различите фазе деформације (Д1–Д4). Д1–Д3 фазе су повезане са компресијом и метаморфизмом који се јавља пре интрузије олигоценског плутонизма И-типа, док четврта фаза деформације (Д4) корелише са екстензивном тектоником и ексхумацијом које се дешавају истовремено кад и интрузија С-тип гранита током миоцена. Прва фаза (Д1) је вероватно повезана са обдукцијом офиолитске јединице западног Вардара на дисталну континенталну маргину Адрије. Повезана је са правцима смицања ка северозападу што се види и у сигма кластима дуктилно деформисаног и слабо метаморфисаног меланжа као и у пенетративној фолијацији и линеацији везаној за метаморфизам зелених шкриљаца седиментног протолита, током горњег палеозоика и доње јуре. О метаморфизму, који се десио под најнижим условима фације зелених шкриљаца током доње креде, (110–85 милиона година) сведоче и горе поменути седименти. Овај метаморфизам је асоциран са дуктилним деформацијама фазе (Д2) која је представљена добро развијеном фолијацијом и изоклиним наборима. Ретроградни метаморфизам фације зелених шкриљаца у амфиболите се догодио током средњег до горњег еоцена (45–35 милиона година) као последица западно вергентног набирања (Д3). Овај догађај је повезан са компресијом у правцу исток-запад узрокованој затварањем Сава зоне. Цело подручје је током миоцена претрпело брзу ексхумацију праћену интензивним дуктилном екстензијом правца север-југ (Д4). Горе поменута екстензија је повезана пак са миоценском екстензијом панонског басена који представља залучну област (баск-арс басин) западно вергентне субдукције европске литосфере под Карпате.

На основу нових анализа Хф изотопа, на зрима циркона, као и дискусије литературних података за старости Балканског полуострва, може се рећи да је геодинамичка еволуција текла на следећи начин:

Током горњег еоцена и олигоценца јавља се магматизам у доњим јединицама унутрашњих Динарида који су деривирани из Адрије, као одговор на деламинацију адријатског омотача. Деламинација се пак јавља као последица пост-колизионе конвергенције која се шири напоље ка спољашњим Динаридима. Миоценски магматизам је, с друге стране, асоциран са формацијом core complex-а дуж јужне маргине панонског басена и вероватно има везе са западном субдукцијом европске литосфере под Карпате ометајући текућу динаридско-хеленску залучна (баск-арс) екстензију.

(Translation by Milica Božović)

Contents

Abstract	i
РЕЗИМЕ	III
Organisation of the thesis	1
1. Introduction	5
1.1 Thesis motivation	5
1.2 Aim of the study and methodological approach	6
1.3 Geological setting	7
References	10
2. Triassic metasediments in the internal Dinarides (Kopaonik area, southern Serbia): stratigraphy, paleogeographic and tectonic significance	13
Abstract	13
2.1 Introduction	14
2.2 Geological setting and metamorphism	15
2.3 Location of sections	17
2.3.1 Studenica	17
2.3.2 Gradac	17
2.3.3 Kopaonik area	18
2.4. Stratigraphy	19
2.4.1 Quartz-phyllites	19
2.4.2 Werfen Formation	19
2.4.3 Shallow-water carbonates ('Wurstelkalk'; Gutenstein and Steinalm Formations equivalents)	20
2.4.4 Breccia horizon in the uppermost Steinalm Formation equivalent	21
2.4.5 Tuffites and metabasalts	23
2.4.6 Kopaonik Formation	23
2.4.7 Red hemipelagic limestones and radiolarites	30
2.4.8 Ophiolitic mélange	32
2.5 Regional correlation and reconstruction of the original sedimentary succession	32
2.6 Discussion	34
2.7 Conclusions	36
References	37

3. Cenozoic granitoids in the Dinarides of southern Serbia: age of intrusion, isotope geochemistry, exhumation history and significance for the geodynamic evolution of the Balkan Peninsula	43
Abstract	43
Introduction	44
Regional geology	44
U–Pb (ID-TIMS) dating and Hf isotope data	51
<i>Analytical techniques</i>	51
<i>Sample material and presentation of the results</i>	52
<i>Interpretation and discussion of U–Pb ages and Hf isotope data</i>	56
Zircon and apatite fission-track data	57
<i>Sampled material and presentation of data</i>	57
<i>Analytical techniques</i>	57
<i>Results</i>	57
<i>Thermal modelling of the apatite fission-track data</i>	57
<i>Interpretation and discussion of the fission-track ages and thermal modelling</i>	60
<i>Exhumation history of the granitoid intrusions of the Inner Dinarides</i>	61
Discussion of data within the regional geodynamic context	62
<i>Late Eocene to earliest Miocene (37–22 Ma) magmatic activity in the Balkan Peninsula</i>	62
<i>Miocene magmatic activity in the Dinarides</i>	66
Conclusions	68
Appendix A, Fission-track dating	69
References	71
4. Metamorphism and structural geology	79
4.1 Metamorphic conditions within the different tectonic units	79
<i>Studenica Metamorphic Series</i>	79
<i>Kopaonik Metamorphic Series</i>	81
<i>Western Vardar Ophiolitic Unit</i>	81
<i>Upper Cretaceous sediments ('Senonian flysch') of the Sava zone</i>	87
<i>Eastern Vardar Ophiolitic Unit</i>	88
4.2 Structural geology	89
<i>Pre-Senonian episode (D1 and D2)</i>	89
<i>Post-Senonian pre-Oligocene episode (D3)</i>	92
<i>Post-Oligocene episode (D4)</i>	95
<i>Summary and interpretation of the different phases of deformation</i>	99

4.3 Geochronology	102
<i>Introduction</i>	102
<i>Potassium–Argon system</i>	102
<i>Uranium–Lead system</i>	103
4.3.1 $^{40}\text{Ar}/^{39}\text{Ar}$ mineral ages	104
<i>Introduction</i>	104
<i>Analytical techniques used for $^{40}\text{Ar}/^{39}\text{Ar}$ age dating</i>	105
<i>Results</i>	106
<i>Summary of the results and interpretation of the $^{40}\text{Ar}-^{39}\text{Ar}$ dating</i>	113
4.3.2 Fission-track analyses	115
<i>Introduction</i>	115
<i>Sampling strategy</i>	116
<i>Preparation of samples</i>	116
<i>Results</i>	117
<i>Thermal modelling of apatite track lengths</i>	119
<i>Interpretation and discussion of the fission-track ages and thermal modelling</i>	119
<i>Exhumation history</i>	120
4.4 Summary of metamorphism, structural geology and geochronology	122
<i>Jurassic obduction</i>	122
<i>Cretaceous metamorphic event</i>	122
<i>Paleogene metamorphic event (Late Eocene to Early Oligocene, Dinaric phase)</i>	122
<i>Miocene extension</i>	123
References	124
Appendix A: Raman spectroscopy of carbonaceous matter	128
Appendix B: List of important samples discussed in Chapter 4	129
Appendix C: Additional Stereoplots	130
5. Summary	131
5.1 Main results	131
5.2 Geodynamic evolution of the study area	133
References	140
Bibliography	143
Appendix I: Schmid et al. 2008	159
Appendix II: Ustaszewski et al. 2009	211
Acknowledgments	231
Curriculum Vitae	233

Organisation of the thesis

This thesis is organised as a ‚cumulative thesis‘ and consists of five chapters. Chapter 1 introduces the reader to the overall context. Chapter 2 is already published in *Geologica Carpathica* and Chapter 3 is currently in the reviewing process after submission to the *International Journal of Earth Science*. Chapter 4 presents all additional data not yet included in Chapters 2 and 3 and deals with metamorphism, structural geology, and age-dating. Chapter 5 summarises all findings and presents an integrative model for the geodynamic evolution of the study area. The merged chapters 4 and 5 are currently prepared for submission to a peer-reviewed journal. An outline of each of these chapters and the contributions of the individual co-authors to the journal manuscripts is provided below.

Appendix I and II consist of two publications (Schmid et al. 2008; Ustaszewski et al. 2009), to which S. Schefer contributed as a member of the group involved in the ‚Tisza-project‘.

1. Introduction

The first chapter presents the scope and aims of this thesis, provides the general geological background and gives an outline of the methodological approach.

2. Triassic metasediments in the internal Dinarides (Kopaonik area, southern Serbia): stratigraphy, paleogeographic and tectonic significance

Senecio Schefer, Daniel Egli, Sigrid Missoni, Daniel Bernoulli, Bernhard Fügenschuh, Hans-Jürgen Gawlick, Divna Jovanović, Leopold Krystyn, Richard Lein, Stefan M. Schmid, Milan N. Sudar

*(This chapter was published in 2010 in *Geologica Carpathica*, 61 (2), and will be cited as **Schefer et al. 2010a** in the current thesis)*

This chapter is devoted to the stratigraphic evolution in the Studenica area in southern Serbia and to the question as to how many oceans might have existed in the area. In the working area Upper Palaeozoic terrigenous sediments are overlain by Lower Triassic siliciclastics and limestones and by Anisian shallow-water carbonates. A pronounced facies change to hemipelagic and distal turbiditic, cherty metalimestones (Kopaonik Formation) testifies to a late Anisian drowning of the former shallow-water carbonate shelf. The Kopaonik Formation was dated by conodont faunas as late Anisian to Norian and possibly extends into the Early Jurassic. The sedimentological and stratigraphic evolution of the different areas reflects the transition from a proximal to a distal continental margin. A similar arrangement of Triassic facies belts can be recognised all along the evolving Meliata–Maliac–Vardar branch of Neotethys, which is in line with a ‘one-ocean-hypothesis’ for the Dinarides: all ophiolites presently located southwest of the Drina–Ivanjica and Kopaonik thrust sheets are derived from an area to the east, and the Drina–Ivanjica and Kopaonik units emerge in tectonic windows from below this ophiolite nappe. On the base of the Triassic facies distribution neither arguments for an independent Dinaridic Ocean nor evidence for isolated terranes or blocks could be found.

S. Schefer and D. Egli (carrying out his MSc-thesis in the framework of this project) are responsible for the field data and the lithostratigraphy. The manuscript was coordinated by the first author. S. Missoni, H.-J. Gawlick, L. Krystyn and R. Lein prepared and dated the conodonts. D. Jovanović and M. N. Sudar provided help during reconnaissance fieldwork and helped with logistics (maps, publications, translations). S. M. Schmid and B.

Fügenschuh (the thesis supervisors) as well as D. Bernoulli and H.-J. Gawlick helped through discussions and interpretation of the data and substantially contributed in finalising the manuscript. All the various contributions are highly appreciated.

3. Cenozoic granitoids in the Dinarides of southern Serbia: age of intrusion, isotope geochemistry, exhumation history and significance for the geodynamic evolution of the Balkan Peninsula

Senecio Schefer, Vladica Cvetković, Bernhard Fügenschuh, Alexandre Kounov, Maria Ovtcharova, Urs Schaltegger, Stefan M. Schmid, submitted to: International Journal of Earth Sciences

(This chapter was submitted to the International Journal of Earth Sciences in January 2010 and will be cited as Schefer et al. 2010b in the current thesis)

Chapter 3 presents the results of high precision dating and Hf isotope analyses of the southern Serbian Ko-paonik, Drenje, Željina, Golija and Polumir intrusions. These data are complemented by zircon and apatite fission-track data together with structural observations. Finally, the potential magmatic sources and the geodynamic setting of the Cenozoic intrusions in Serbia will be discussed within the frame of the entire Balkan Peninsula and adjacent areas, based on a recent compilation of tectonic units (Schmid et al. 2008). Sources for the magmatic activity in the Balkan Peninsula will be discussed by integrating the large amount of published age data on other granites and contemporaneous basaltic rocks. Also the formation of sedimentary basins, many of them associated with volcanics and/or volcanoclastics, as well as information from seismic tomography will be discussed in that context.

The first author carried out the fieldwork and collected and prepared all samples for U–Pb and fission-track investigations. U–Pb (ID-TIMS) dating on single zircons was carried out by S. Schefer at the University of Geneva under the supervision of M. Ovtcharova and U. Schaltegger, who also helped during the interpretation. A first version of the manuscript including all figures and tables was prepared by the first author. V. Cvetković provided additional unpublished age data together with a new figure on the geochemistry. He also assisted in the discussion of the regional geodynamic context and helped finalising the manuscript. B. Fügenschuh provided all fission-track data and supported the sampling campaign and helped with the interpretation. A. Kounov provided regional literature data for Bulgaria, Macedonia and Greece and assisted the first author on the evaluation and interpretation of the fission-track data. S.M. Schmid helped with the interpretation of the regional geodynamic evolution and greatly assisted in tidying up the final version of the manuscript. All co-authors are thanked for their valuable input.

4. Metamorphism and structural geology

This chapter integrates metamorphism, structural geology and age-dating (^{40}Ar – ^{39}Ar and fission-track analysis) to characterise the different tectono-metamorphic events in the study area. The geochronological results constrain the different phases of deformation and metamorphism with absolute ages. Together with field evidence for the relative chronology of deformation and metamorphism, an attempt is made to reconstruct the tectono-metamorphic evolution of the study area.

The first author did all the fieldwork, supported by the thesis supervisors, and provided all analysed samples. He performed the sample preparation for the Ar–Ar analyses and part of the preparation for the fission-track

analyses. B. Fügenschuh provided part of the fission-track sample preparation and all of the fission-track data. W. Frank is responsible for the ^{40}Ar – ^{39}Ar isotopic analyses and helped in interpreting the results. The first author wrote a first version of the chapter including all figures and tables. B. Fügenschuh and S.M. Schmid provided substantial help during the writing process and improved the quality of the resulting manuscript.

5. Summary

This chapter combines the various conclusions and discussions emerging from the individual chapters. In a second step, the combined results are used to reconstruct a possible scenario for the geodynamic evolution of the Dinarides, illustrated by interpretative cross-sections for seven time-slices starting with the stratigraphic evolution. Finally, the still remaining questions are briefly discussed and some future research perspectives are given.

Appendix I: Schmid et al. 2008, *Swiss Journal of Earth Sciences*, 101: 139–183

This paper provides a tectonic map that includes the entire Alpine–Carpathian–Dinaridic system of orogens including the Pannonian and Transylvanian basins, and addresses its complex temporal and spatial evolution. This map was constructed by compiling the available geological maps and the subsurface information for those parts of the system covered by very thick Mio–Pliocene (in case of the Pannonian basin) or mid-Cretaceous to Late Miocene deposits (in case of the Transylvanian basin). Starting with a brief overview of the first order tectonic elements, detailed descriptions of the individual tectonic units are given. In support of these descriptions, a series of crustal-scale profiles are presented. These provide a three-dimensional picture of this complex system of orogens, which formed by a long-lasting evolution that started in Late Jurassic times and is still going on today. The map leads to a better understanding of the mobile belts formed during Late Jurassic, Cretaceous and Cenozoic times that are characterized by extreme changes along strike, including changes in subduction polarity. In addition it serves as a base map for future palinspastic reconstructions that are required to arrive at realistic paleogeographic and paleotectonic reconstructions.

Conclusions drawn from these correlations have serious paleogeographic implications: Jurassic opening of the Alpine Tethys was largely contemporaneous with partial closure of the Neotethys oceanic lithosphere and the obduction of its Jurassic parts represented by the Eastern and Western Vardar Ophiolitic Units. Both, Triassic and Jurassic ophiolites formed part of one and the same branch of Neotethys, referred to as the Meliata–Maliac–Vardar Ocean. In the area of the Sava zone, the main branch of the Alpine Tethys was connected with the Neotethyan Meliata–Maliac–Vardar Ocean, representing the only oceanic realm that can be traced via the Dinarides and Hellenides eastward into Turkey. We propose that all ophiolitic remnants of Neotethys found in the area under consideration formed part of one and the same oceanic basin that started to open in Triassic times and continued to open during the Jurassic, though its closure commenced during the Middle Jurassic at the same time as the Alpine Tethys began to open. Erroneous interpretation of the complex geometries that resulted from out-of-sequence thrusting during the Cretaceous and Palaeogene deformations underlies a variety of multi-ocean concepts that were advanced in the literature. We propose that such models are incompatible with field evidence we have gathered and/or synthesized from the literature.

This contribution is due to a major effort of S.M. Schmid and the collaboration of numerous colleagues from the entire area covered by the map. S. Schefer, as a part of the ‘Tisza-team’, assisted in the compilation of the tectonic map and mainly contributed to the crustal-scale profile through the Dinarides (Profile 5 on Plate 3) that crosses the Koaponik area. He took also part in the discussions about the different oceanic realms during different geological times, and helped to establish schematic serial sections depicting the plate tectonic evolution of the Alps–Carpathians–Dinarides system in pre-Cenozoic times (Fig. 5). He was also involved in revising figures and text of the manuscript.

Appendix II: Ustaszewski et al. 2009, *Lithos* 108: 106–125

This paper presents new biostratigraphic, geochronological and geochemical evidence for Late Cretaceous intra-oceanic magmatism within the Sava Zone. Campanian to Early Maastrichtian intra-oceanic magmatism is reported in several inselbergs in the Sava Zone and implies that the Adriatic and Europe-derived smaller plates (such as the Tisza and the Dacia Mega-Unit) were still separated by a deep basin floored by oceanic lithosphere at this time. The Campanian to Early Maastrichtian oceanic crust can be considered as a northwestern-most extension of the Vardar Ocean, which at the same time was linked with the Alpine Tethys in the area of the Kozara Mountains (Bosnia and Hercegovina). Late Cretaceous to Early Paleogene bimodal volcanism in the Tisza Mega-Unit is attributed to the formation of a continental volcanic arc located in the upper plate during subduction. The end of subduction is marked by both the cessation of volcanic activity and the end of turbidite sedimentation in the Sava Zone in the Paleocene to Eocene.

These results constrain the earliest possible age for the closure of the Vardar Ocean to the latest Cretaceous. A remnant or a ‘marginal basin’ of the Vardar Ocean must therefore have stayed open until the Campanian and support the interpretation of the Sava zone as a suture that formed during the collision of the internal Dinarides with the European continent s.l. during the Paleogene.

This contribution is mainly the work of K. Ustaszewski who elaborated most of the tectonic and stratigraphic framework based on his field work involving geological mapping and an extensive sampling campaign.

S. Schefer provided U–Pb analyses and participated in discussions concerning the geodynamic evolution. He also assisted in finalizing the figures and interpretation and reviewed an earlier version of the manuscript.

1. Introduction

1.1 Thesis motivation

This PhD-thesis was initiated by Profs. Bernhard Fügenschuh and Stefan Schmid and launched in the context of the Swiss NF project ‘Tisza and its role in the framework of the tectonic evolution of Alps, Dinarides and Carpathians’ (Project No. 20002-109278). The project generally aimed at the analysis of the pre-Miocene tectonic and paleogeographic evolution of the Alps–Dinarides–Carpathian system and primarily focused on the enigmatic Tisza block and its surrounding units. The multidisciplinary methodological approach combined structural field-work with the analysis of subsurface data. Two working areas have been defined for detailed studies, one in the Apuseni Mountains and around the eastern edge of Tisza and a second one, of which this PhD-project forms a part, dealing with the southern contact of Tisza with the Dinarides. The contact zone, i.e. the ‘Sava belt’, is mostly hidden below Neogene sediments, but can be traced into the inselbergs of Vojvodina, Slavonia, northern Bosnia and the Zagreb area (e.g. Pamić 1998; Tari and Pamić 1998).

It was in 2005 that during an excursion across the entire Dinarides the inferred Oligocene plutons of the Kopaonik Mountains attracted our attention by showing syn-emplacement deformation and extension (Polumir). This, together with the observation of a multiple deformed greenschist-facies belt of Mesozoic and Paleozoic rocks allowed to define the Kopaonik Mountains as a target area to address different topics:

Located in the internal-most part of the Dinarides, the working area represents the transition from the Cenozoic Dinaridic orogen to the pre-Turonian ‘Serbo–Macedonian Massif’, a part of the Dacia Mega-Unit across the Sava belt consisting of Upper Cretaceous sediments (‘Senonian flysch’). Further north this Sava belt contains a larger variety of lithologies (Ustaszewski et al. 2009), and this same suture zone possibly extends further to the south into the working area separating the Dinarides also from the Dacia Mega-Unit (including the ‘Serbo–Macedonian Massif’ in SE Serbia).

While petrography and geochemistry of the magmatic rocks in the wider Kopaonik area are rather well known, the formation ages are poorly constrained. Well defined formation ages place valuable constraints on the deformation history and thus should allow for establishing a deformation sequence.

The widespread occurrences of ophiolitic rocks separated by different fragments of continental basement rocks led to a ‘multi-ocean’ concept separating elongated microplates. By investigating the stratigraphic and tectonic evolution of the various basement units in combination with their relation to the intervening ophiolitic units the multi-plate/multi-ocean problem can be addressed.

1.2 Aim of the study and methodological approach

The current study expands the ‘Tisza-Project’ towards the southeast into Serbia at the contact between Tisza-Dacia and the Dinarides. The aim of this study can be summed up in terms of the following main questions:

Tectono-metamorphic evolution of the nappes in the study area and kinematic characterisation of bounding faults

The geological maps at hand (1:100'000 map sheets of Former Yugoslavia) provide valuable information about the geology but lack a modern tectonic understanding. It is important to know the original nappe-stack of the working area in order to assign the different phases of deformation to distinct tectonic events. Hence extensive geological mapping in an area of ca. 50x70 km around the Kopaonik mountain area gave insight into stratigraphy, nappe-stacking, and later extension of the different units. Modern structural analysis provides a relative chronology based on clear overprinting criteria. Structural and kinematic analyses are of great importance for the construction of cross-sections showing the overall architecture of the study area and providing hints towards a tectonic reconstruction.

Age and paleogeographic provenance of the metasedimentary rocks underlying the ophiolites

Since most of the sediments are (at least weakly) metamorphosed – sometimes up to amphibolite facies – it is challenging to determine their stratigraphic age and facies. Only in areas of very weak metamorphic overprint (lower greenschist facies and less) their history could be unravelled by means of conodont stratigraphy.

Age and grade of metamorphism of the basement rocks

Establishing the pressure-temperature-time history of the various nappes allows for correlation with deformation events and – in combination – leads to a plate tectonic model. Petrological and Ar–Ar isotopic investigations were thus performed on metasedimentary rocks of known stratigraphic age to provide information on the age and grade of metamorphism.

Age and genesis of magmatic rocks

The widespread occurrence of igneous rocks and their impressive impact on the landscape is one of the first impressions when visiting the Kopaonik region. Due to available or missing deformational features they place important timing constraints on the tectonic evolution. Literature data on their formation ages are scarce and sometimes ambiguous. High-precision U–Pb isotopic dating on single zircon grains made it possible to date the time of zircon growth in six different intrusive bodies. Furthermore, fission-track analyses on apatite and zircon crystals were used to date the formation of two large volcanic occurrences. Hf isotope chemistry gave new insight into possible sources of magma generation.

Exhumation of the plutons and their relationship with the regional geodynamic evolution

Mode and timing of the exhumation of the dated plutons are addressed by a combined structural and fission-track analysis. Thermal modelling of the apatite fission-track data constrains the near-surface cooling and exhumation history of the working area and relates them to landscape forming processes.

Therefore, a multi-disciplinary and integrative approach involving different specialists and demanding a close cooperation with an international team of experts from the Universities of Basel, Belgrade, Geneva, Innsbruck, Leoben, Vienna and Zurich was used to answer the above mentioned questions. Finally all these questions merge into one: how did it come that this part of the earth looks the way it does, and are we able to unravel the history back to when it began? In our case, it will not be the big-bang, but the end of the Paleozoic...

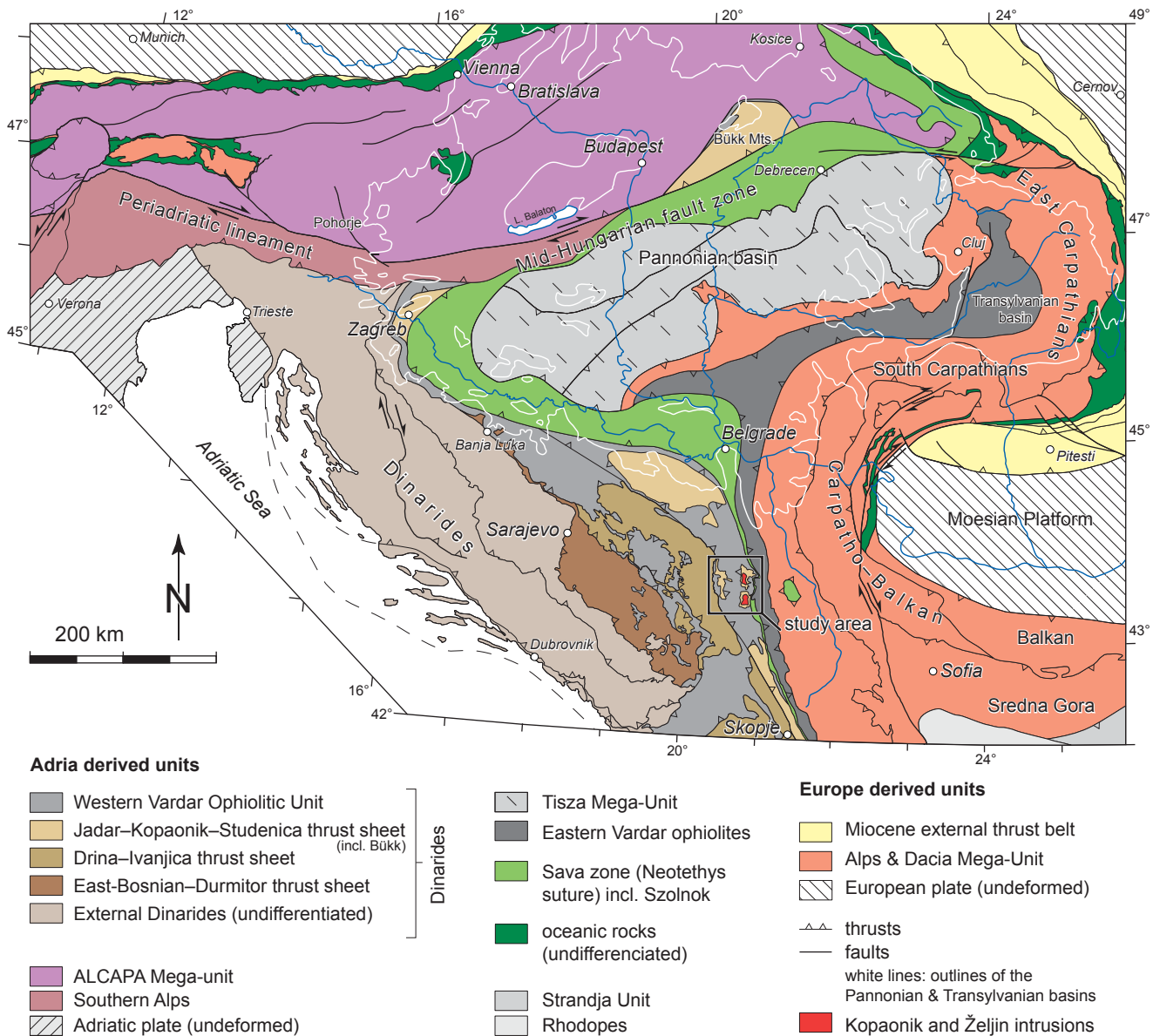


Fig. 1.1 – Tectonic map of the southern Dinarides, modified after Schmid et al. (2008)

1.3 Geological setting

The Dinarides represent a complex orogen consisting of thrust sheets that contain ophiolitic as well as Adria-derived continental material. These thrust sheets are located in a lower plate position with respect to an upper plate formed by the Tisza and Dacia Mega-Units with European affinities (Schmid et al. 2008, Ustaszewski et al. 2009). Ophiolites, derived from the Vardar branch of the Neotethys Ocean (Fig. 1.1, ‘Western Vardar Ophiolitic Unit’), were obducted already during the latest Jurassic onto the Adriatic margin and later involved in Late Cretaceous to

early Paleogene out-of-sequence thrusting. This led to the formation of a series of composite nappes that consist of continent-derived material in their lower part and ophiolitic material in the upper part.

The area around the Kopaonik massif in southern Serbia exposes the two innermost Dinaridic composite nappes, namely the Drina–Ivanjica and the Jadar–Kopaonik–Studenica composite thrust sheets. In the latest Cretaceous to Early Paleogene these innermost Dinaridic thrust sheets collided with the already existing (pre-Turonian) Carpatho–Balkan orogen that is part of the Dacia Mega-Unit and constitutes the upper plate of the complex collision zone (Schmid et al. 2008). A separating suture zone (Sava Zone) runs along the eastern rim of the innermost Dinarides located along the internal limit of the Jadar–Kopaonik–Studenica composite thrust sheet and separates the Dinarides from the Carpatho–Balkan orogen (Fig. 1.1).

The N–S-trending mountain range in the wider Kopaonik area exposes a part of the Jadar–Kopaonik–Studenica thrust sheet exposed in tectonic windows below the obducted ophiolites (Fig. 1.1). These windows are formed by the Kopaonik and the Studenica Metamorphic Series, which consist of metamorphosed Upper Paleozoic to Lower Jurassic sediments of the distal Adriatic margin (Schefer et al. 2010a). They are overlain by a (Middle?)–Upper Jurassic ophiolitic mélange found below the obducted Western Vardar Ophiolitic Unit. The two metamorphic series and the obducted ophiolites are unconformably overlain by post-Turonian sediments ('Upper Cretaceous sediments') that contain large olistoliths, including ophiolites and metamorphic rocks. This weakly metamorphosed N–S-trending 'Senonian' flysch belt, trending N–S along the eastern margin of the Kopaonik composite thrust sheet, is interpreted to represent the southern prolongation of the Sava Zone, i.e. the suture between the internal Dinarides and the Carpatho-Balkan orogen (Ustaszewski et al. 2009; Ustaszewski et al. submitted).

The Kopaonik Metamorphic Series east of the Ibar valley and the overlying Western Vardar Ophiolitic Unit were both intruded by the Kopaonik, Drenje and Željnj granitoids (Fig 1). Available structural data (Egli 2008; Schefer et al. 2008; Zelić et al. 2010; Schefer et al. 2010a) indicate that the intrusion of these plutons post-dates three phases of compressive deformation associated with thrusting in the internal Dinarides and suturing with the adjacent Carpatho-Balkan orogen, but pre-dates a latest extensional deformation event (D4) associated with movements along discrete faults that, however, were not observed in the plutons but are probably related to their final exhumation. The main Kopaonik pluton produced a contact metamorphic aureole consisting of hornfels and skarns that formed at 100 ± 50 MPa and ca. 550 °C according to Knežević et al. (1995).

Because of the metamorphic overprint, all metasedimentary sequences in the Kopaonik region and those developed west of the Ibar valley were often mapped as Paleozoic (Urošević et al. 1970a, b, 1973a, b; Brković et al. 1976, 1977; Mojsilović et al. 1978, 1980), although a Triassic-age of the carbonates in the Studenica area was postulated much earlier (Simić 1956). Indeed, conodonts of Carnian age were discovered in the metamorphic rocks of the Kopaonik area (Mičić et al. 1972).

The Studenica Metamorphic Series that crop out in a window west of the Ibar valley are intruded by the Polumir granite (Fig. 1.2). This granite shows high-temperature ductile deformation along its intrusive margin. The Golija granodiorite, located further west of the main thrust that separates the Jadar–Kopaonik–Studenica and Drina–Ivanjica composite thrust sheets, intruded Upper Paleozoic slates, siltstones and sandstones of the Drina–Ivanjica composite thrust sheet.

Suites of Oligocene to Miocene volcanic and volcanoclastic rocks are associated with these intrusions, representing their effusive equivalents. Most of the Oligocene volcanics intrude and/or overlie the ophiolites. They are confined to the Ibar Valley and are predominantly represented by extrusive to autoclastic dacitic/andesitic rocks. By contrast, the Miocene volcanics are quartz-latic in composition and are represented by effusive and

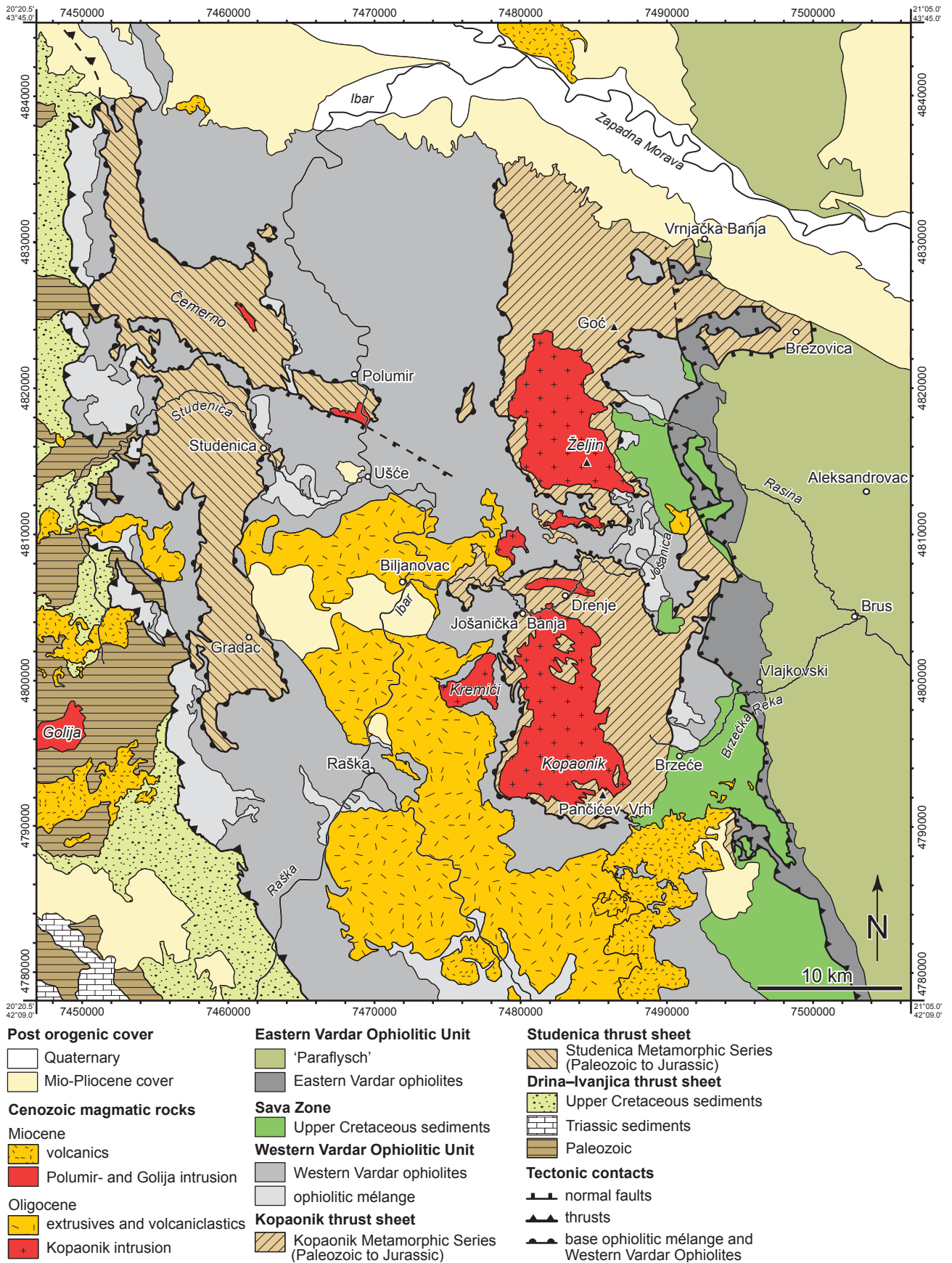


Fig. 1.2 – Tectonic map of the Kopaonik area, based on mapping by S. Schefer and compilation of the Basic Geological Map of Yugoslavia (1:100'000), Sheets Novi Pazar (Urošević et al. 1970a), Vrnjci (Urošević et al. 1970b), Sjenica (Mojsilović et al. 1978) and Ivanjica (Brković et al. 1976) as well as Simić (1956) for the Studenica area. Numbers at the border of the map are MGI Balkan 7 Cartesian coordinates.

pyroclastic rocks. The latter were related to Plinian to sub-Plinian events and ignimbrite formation. The Miocene volcanic rocks occur in the surroundings of the Golija pluton as well as southeastward from the Kopaonik intrusives (Fig. 1.2). These rocks are poorly studied in contrast to their counterparts in the north (Cvetković and Pécskay 1999; Cvetković 2002).

References

- Brković T, Malešević M, Urošević M, Trifunović S, Radanović Z, Dimitrijević M & Dimitrijević MN (1977): Geology of the Sheet Ivanjica (K34–17), Explanatory notes. *Savezni Geološki Zavod, Beograd*: 1–61.
- Cvetković V & Pécskay Z (1999): The Early Miocene eruptive complex of Borač (central Serbia): volcanic facies and evolution over time. *Carpatian Geology*.
- Cvetković V (2002): Nature and origin of pyroclastic deposits of the Miocene Eruptive Complex of Borač (Central Serbia). *Bull CXXXV de l' Acad. Serbe des Sci. et des Arts, Classe des Sci. math. et natur., Sci. natur.*, 342: 209–215.
- Egli D (2008): Das Kopaonik-Gebirge in Südserbien – Stratigraphie, Strukturen und Metamorphose. MSc Thesis, University of Basel, Basel.
- Klisić M, Mičić I, Pajić V, Simić D & Kandić M (1972): Contribution to the stratigraphy of the Trepča metamorphic series. *Zapiski Srpski geološki društva za 1968, 1969 i 1970 (Zbor 10. XII 1968)*: 105–107.
- Knežević V, Karamata S, Vasković N & Cvetković V (1995): Granodiorites of Kopaonik and contact metamorphic zone. In: *Geology and Metallogeny of the Kopaonik Mt.*, pp. 172–184, Belgrade.
- Mičić I, Urošević M, Kandić M, Klisić M & Simić D (1972): Findings of Triassic conodont fauna in the metamorphic complex of Kopaonik Mt. *Zapiski Srpski geološki društva za 1968, 1969 i 1970 (Zbor 10. XII 1968)*: 103–104.
- Mojsilović S, Baklajić D & Djoković I (1978): Basic Geological Map of the SFRY, 1:100'000, Sheet Sjenica (K32-29). *Savezni Geološki Zavod, Beograd (Geozavod – OOUR Geološki institut, Beograd, 1960-1973)*.
- Mojsilović S, Djoković I, Baklajić D & Rakić B (1980): Geology of the Sheet Sjenica (K32–29), Explanatory notes (in Serbo-Croatian, English and Russian summaries). *Savezni Geološki Zavod, Beograd*.
- Pamić J, Gusić I & Jelaska V (1998): Geodynamic evolution of the central Dinarides. *Tectonophysics*, 297: 251–268.
- Schefer S, Egli D, Frank W, Fügenschuh B, Ovtcharova M, Schaltegger U, Schoene B & Schmid SM (2008): Metamorphic and igneous evolution of the innermost Dinarides in Serbia. In: *6th Swiss Geoscience Meeting*, pp. 60–61, Lugano.
- Schefer S, Egli D, Missoni S, Bernoulli D, Fügenschuh B, Gawlick HJ, Jovanović D, Krystyn L, Lein R, Schmid SM & Sudar MN (2010a): Triassic metasediments in the Internal Dinarides (Kopaonik area, southern Serbia): stratigraphy, paleogeographic and tectonic significance. *Geologica Carpathica*, 61: ?
- Schmid SM, Bernoulli D, Fügenschuh B, Matenco L, Schefer S, Schuster R, Tischler M & Ustaszewski K (2008): The Alpine-Carpathian-Dinaridic orogenic system: correlation and evolution of tectonic units. *Swiss Journal of Geosciences*, 101: 139–183.
- Simić V (1956): Zur Geologie des Studenicegebietes (Südwestserbien). *Vesnik Bull. Serv. Geol. Geophys.*, 12: 5–66.

- Tari V & Pamić J (1998): Geodynamic evolution of the northern Dinarides and the southern part of the Pannonian basin. *Tectonophysics*, 297: 269–281.
- Urošević M, Pavlović Z, Klisić M, Brković T, Malešević M & Trifunović S (1970a): Geological map of Yugoslavia, Sheet Novi Pazar, 1:100'000, Savezni Geološki Zavod, Belgrade.
- Urošević M, Pavlović Z, Klisić M, Brković T, Malešević M & Trifunović S (1970b): Geological map of Yugoslavia, Sheet Vrnjci, 1:100'000, Savezni Geološki Zavod, Belgrade.
- Urošević M, Pavlović Z, Klisić M, Brković T, Malešević M & Trifunović S (1973a): Explanation to Geological map of Yugoslavia, Sheet Novi Pazar, Savezni Geološki Zavod, Belgrade.
- Urošević M, Pavlović Z, Klisić M, Malešević M, Stefanović M, Marković O & Trifunović S (1973b): Explanation to Geological map of Yugoslavia, Sheet Vrnjci, Savezni Geološki Zavod, Belgrade.
- Ustaszewski K, Schmid SM, Lugović B, Schuster R, Schaltegger U, Bernoulli D, Hottinger L, Kounov A, Fügenschuh B & Schefer S (2009): Late Cretaceous intra-oceanic magmatism in the internal Dinarides (northern Bosnia and Herzegovina): Implications for the collision of the Adriatic and European plates. *Lithos*, 108: 106–125.
- Ustaszewski K, Kounov A, Schmid SM, Schaltegger U, Frank W, Krenn E & Fügenschuh B (subm): Evolution of the Adria–Europe plate boundary in the northern Dinarides – from continent-continent collision to back-arc extension. *Tectonics*.
- Vukov M (1995): Petrologic characteristics of granitoid rocks of Željin and Polumir. In: *Geology and Metallogeny of the Kopaonik Mountain*, pp. 518, Belgrade.
- Zelić M, Levi N, Malasoma A, Marroni M, Pandolfi L & Trivić B (2010): Alpine tectono-metamorphic history of the continental units from Vardar zone: the Kopaonik Metamorphic Complex (Dinaric-Hellenic belt, Serbia). *Geological Journal*, 45: 59–77.

2. Triassic metasediments in the internal Dinarides (Kopaonik area, southern Serbia): stratigraphy, paleogeographic and tectonic significance

Senecio Schefer, Daniel Egli, Sigrid Missoni, Daniel Bernoulli, Bernhard Fügenschuh, Hans-Jürgen Gawlick, Divna Jovanović, Leopold Krystyn, Richard Lein, Stefan M. Schmid, Milan N. Sudar

Published in *Geologica Carpathica*, 61 (2), April 2010

Abstract

Strongly deformed and metamorphosed sediments in the Studenica valley and Kopaonik area in southern Serbia expose the easternmost occurrences of Triassic sediments in the Dinarides. In these areas, Upper Paleozoic terrigenous sediments are overlain by Lower Triassic siliciclastics and limestones and by Anisian shallow-water carbonates. A pronounced facies change to hemipelagic and distal turbiditic, cherty metalimestones (Kopaonik Formation) testifies to a late Anisian drowning of the former shallow-water carbonate shelf. Sedimentation of the Kopaonik Formation was contemporaneous with shallow-water carbonate production on nearby carbonate platforms that were the source areas of diluted turbidity currents reaching the depositional area of this formation. The Kopaonik Formation was dated by conodont faunas as late Anisian to Norian and possibly extends into the Early Jurassic. It is therefore considered an equivalent of the grey Hallstatt facies of the Eastern Alps, the Western Carpathians, and the Albanides–Hellenides. The coeval carbonate platforms were generally situated in more proximal areas of the Adriatic margin, whereas the distal margin was dominated by hemipelagic/pelagic and distal turbiditic sedimentation, facing the evolving Neotethys Ocean to the east. A similar arrangement of Triassic facies belts can be recognized all along the evolving Meliata–Maliac–Vardar branch of Neotethys, which is in line with a ‘one-ocean-hypothesis’ for the Dinarides: all ophiolites presently located southwest of the Drina–Ivanjica and Kopaonik thrust sheets are derived from an area to the east, and the Drina–Ivanjica and Kopaonik units emerge in tectonic windows from below this ophiolite nappe. On the base of the Triassic facies distribution we see neither argument for an independent Dinaridic Ocean nor evidence for isolated terranes or blocks.

Keywords: Stratigraphy, Triassic, Dinarides, Kopaonik, Serbia, conodonts

2.1 Introduction

Whereas the stratigraphy of the external zones of the Dinarides is relatively well known, the sedimentary and paleotectonic evolution of the internal zones is less understood. In part, this is due to Alpine metamorphic overprint, in part to the structural complexities of the area. In particular, there exists an ongoing controversy about the original paleogeography and as to how many basins underlain by oceanic lithosphere existed in Mesozoic times between the Adriatic microcontinent, of which the external Dinarides are part, and Europe including smaller continental fragments (Tisza, Dacia) detached from it. The case of a one-ocean model has been argued for by authors at different occasions (e.g. Bernoulli & Laubscher 1972; Gawlick et al. 2008; Schmid et al. 2008) and shall not be discussed in detail here. In brief, the one-ocean model according to Schmid et al. (2008) proposes that (a) all the Jurassic-age ophiolites of the Dinarides, including their supra-subduction magmatic rocks, originate from one and the same ocean and (b) this ocean also included Triassic-age oceanic crust bordering the Mesozoic Adriatic margin, from which only fragments referred to as Meliata in Slovakia and Maliac in Greece are preserved. Consequently, we shall call this oceanic branch of the Neotethys the Meliata–Maliac–Vardar Ocean. In contrast to our one-ocean model, Robertson & Karamata (1994), Dimitrijević (1997, 2001) and Karamata (2006) envisage at least two different oceanic basins floored by Jurassic oceanic crust originally separated from each other by intervening ‘terranes’ of continental crust, the Drina–Ivanjica, Jadar and Kopaonik ‘terranes’ (see Robertson et al. 2009 for discussion). In our interpretation, however, these ‘terranes’ are tectonic windows of the distal Adriatic margin below an ophiolite nappe referred to as Western Vardar Ophiolitic Unit, obducted in Late Jurassic time (Schlagintweit et al. 2008; Schmid et al. 2008) and including all ophiolites of the Dinarides west of the Sava Zone (Fig. 2.1; Western Vardar Ophiolites). In addition, our one-ocean model is in contrast with earlier models that attributed the remnants of Triassic-age oceanic crust found within Jurassic mélanges in Slovakia (Meliata; Channell & Kozur 1997), within Jurassic mélanges tectonically underlying obducted Jurassic ophiolites in the Dinarides (Vishnevskaya et al. 2009) or as tectonic imbricates below obducted Jurassic ophiolites in Greece (Maliac; Ferrière 1982) to other separate oceanic basins (e.g. Stampfli & Borel 2004). The basement complexes of the Drina–Ivanjica and the Jadar–Kopaonik thrust sheets including their formerly emplaced allochthonous ophiolitic cover have been involved in further out-of-sequence and frontal thrusting onto the more external East-Bosnian–Durmitor thrust sheet during the Late Cretaceous (Rampnoux 1970, 1974; Schmid et al. 2008).

The reconstruction of the Triassic–Jurassic paleogeography of the Dinarides, i.e. the reconstruction of the facies belts of the Triassic shallow-water carbonate platforms and their transition to the hemipelagic and pelagic (‘Hallstatt’) facies belt, play an important role for the various tectonic concepts and paleogeographic reconstructions. In a one-ocean model, we would expect a single continental-margin wedge of marine sediments with a general proximal-to-distal transition from shallow- to deep-water, facing the Triassic to Jurassic Meliata–Maliac–Vardar Ocean (or Neotethys) to the east. In contrast, according to various more-than-one ocean models, we would expect isolated fragments of shallow- or deep-water deposits with differing facies evolutions. In this contribution, we attempt to characterize the Mesozoic sedimentary evolution of an internal part of the Drina–Ivanjica thrust sheet (‘Studenica slice’ of Dimitrijević 1997) and of the Jadar–Kopaonik thrust sheet near Ušće in western Serbia (Fig. 2.2), which expose the easternmost occurrences of Triassic sediments in the Dinarides in windows below the ophiolites (Grubić et al. 1995; their Fig. 1).

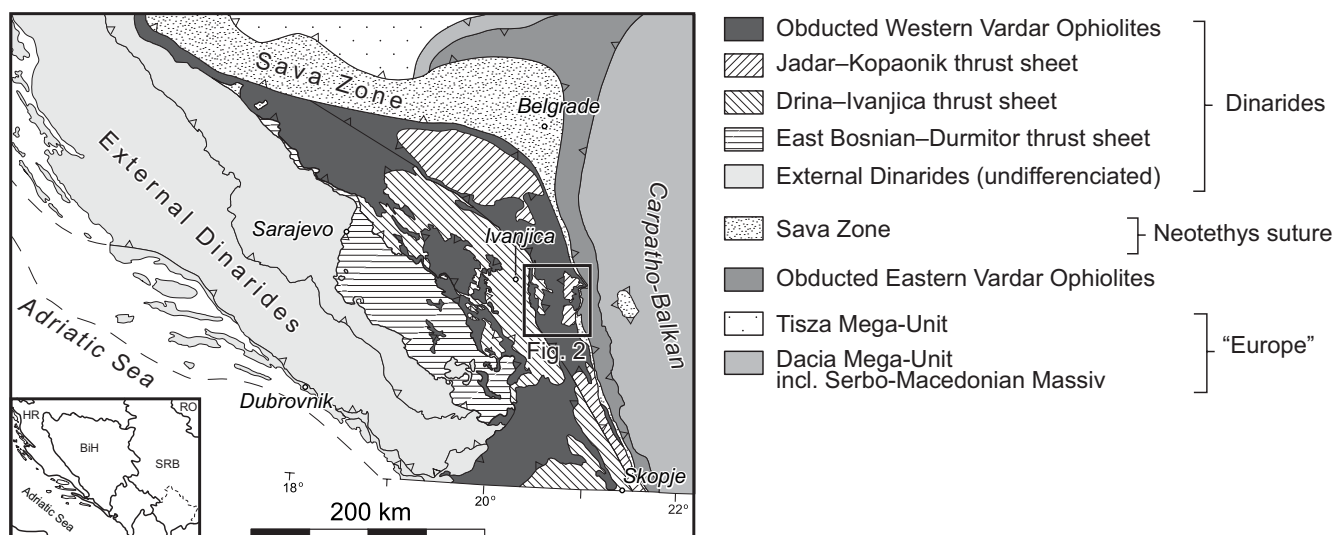
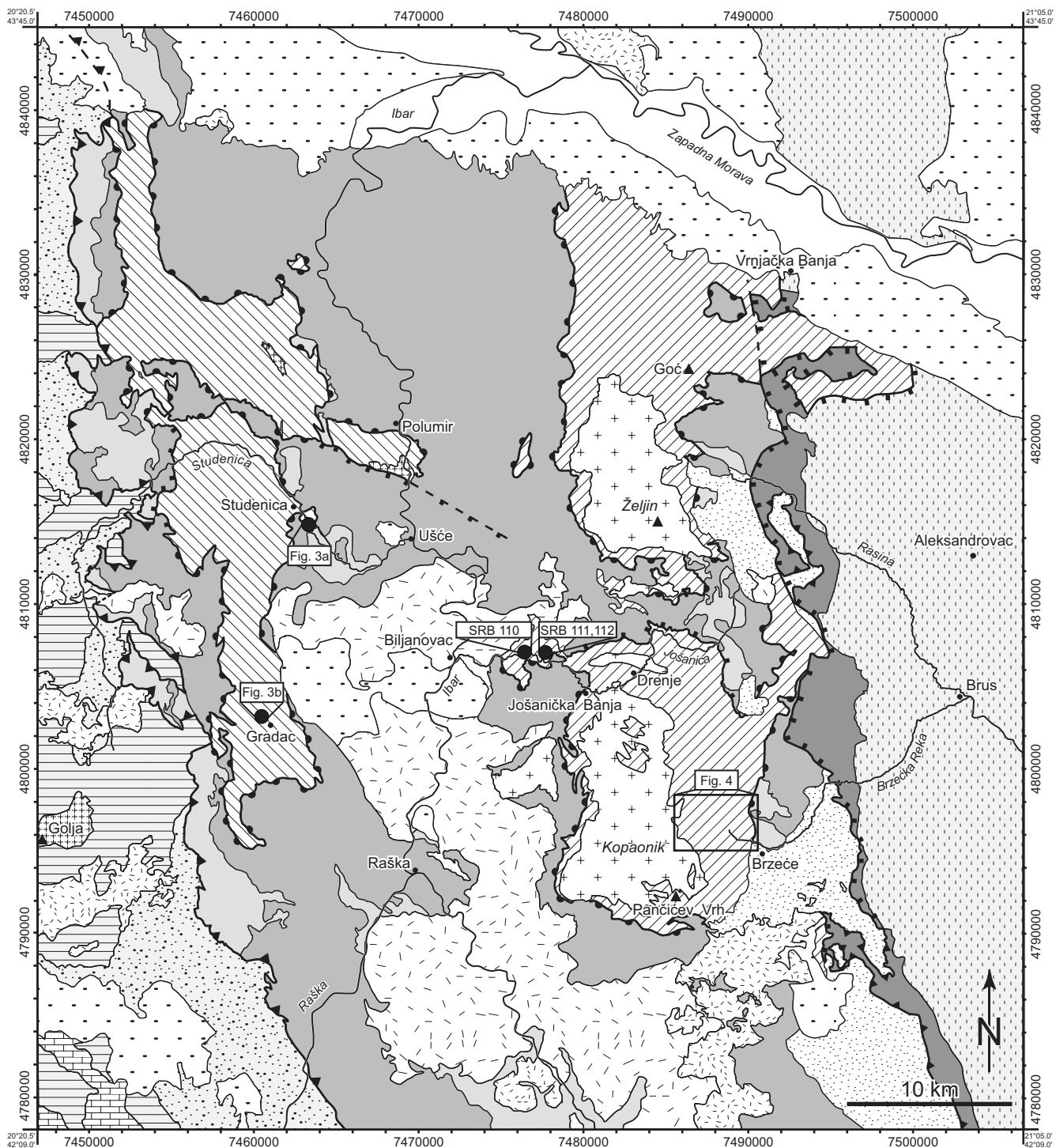


Fig. 2.1 – Tectonic map of the southern Dinarides, modified after Schmid et al. (2008)

2.2 Geological setting and metamorphism

The study area includes a metamorphic part of the internal Drina–Ivanjica thrust sheet (‘Studenica slice’) and the low-grade metamorphic Kopaonik thrust sheet. Both carry their previously emplaced allochthonous ophiolite covers (Fig. 2.2) (Schmid et al. 2008). These two units have been considered to be part of the Vardar Zone as originally defined by Kossmat (1924) including also the successions underlying the ophiolites (e.g. Rampoux 1974; Charvet 1978; Dimitrijević 1997, 2001). However, the co-occurrence of oceanic and continental basement rocks precludes such a simple definition and is unfortunate because the term ‘Vardar’ is usually associated with ophiolites. In our interpretation, both Studenica slice and Jadar–Kopaonik thrust sheet are part of the distal Adriatic margin, covered by the obducted Late Jurassic ophiolite nappe. The Studenica Metamorphic Series and the Kopaonik Metamorphic Series (Egli 2008; Schefer et al. 2008) of the internal Drina–Ivanjica and the Jadar–Kopaonik thrust sheet, respectively (Fig. 2.2), include a Paleozoic metasedimentary basement, overlain by metamorphic Triassic to Middle/?Upper Jurassic sediments. The Studenica Metamorphic Series and the Kopaonik Metamorphic Series have been thrust, together with their ophiolitic covers, as a composite nappe during the Late Cretaceous onto the Drina–Ivanjica thrust sheet to the west (Fig. 2.2).

The Mesozoic metasediments of the Kopaonik and Studenica Metamorphic Series show a polyphase penetrative tectonic overprint (Egli 2008), associated with polyphase Cretaceous and Paleogene greenschist-facies metamorphism that locally reaches lower-amphibolite grade conditions (Schefer et al. 2008). This greenschist-facies metamorphism is also reflected by the thermal alteration of conodonts, which change their colour from yellow to light brown, then to dark brown and black, later to grey and finally to white. This conodont colour change is expressed in terms of the Conodont Colour Alteration Index (CAI-values 1–8) that can be related to certain temperature intervals ranging from less than 80 °C to more than 600 °C (Epstein et al. 1977; Harris 1979; Rejebian et al. 1987). In addition, structural modifications of conodonts also provide information on contact-metamorphic/hydrothermal events (Epstein et al. 1977; Rejebian et al. 1987; Königshof 1992; Burnett et al. 1994). In part of our samples, conodonts with CAI 5.5–6.0 occur together with scarce specimens that exhibit CAI values of up to CAI 7.0. Such conodonts show a whitish patina and corrosion on their surface, in contrast to conodonts of CAI 5.5–6.0. We interpret the higher CAI-values related to a contact metamorphic event overprinting the already deformed and metamorphosed rocks. This later event can be correlated with the Oligocene intrusion of the Kopaonik



Post orogenic cover

- Quaternary
- Mio-Pliocene cover

Cenozoic magmatic rocks

Miocene

- volcanics
- Polumir- and Golja intrusion

Oligocene

- extrusives and volcanoclastics
- Kopaonik intrusion

Eastern Vardar Ophiolitic Unit

- "Paraflysch"
- Eastern Vardar Ophiolites

Sava Zone

- Upper Cretaceous sediments

Western Vardar Ophiolitic Unit

- Western Vardar Ophiolites
- ophiolitic mélange

Jadar–Kopaonik thrust sheet

- Kopaonik Metamorphic Series (Paleozoic to Jurassic)

Drina–Ivanjica thrust sheet

- Upper Cretaceous sediments
- Triassic sediments
- Paleozoic
- Studenica Metamorphic Series (Paleozoic to Jurassic)

Tectonic contacts

- normal faults
- thrusts
- base ophiolitic mélange and Western Vardar Ophiolites

Fig. 2.1 – Tectonic map of the Kopaonik area, based on mapping by S. Schefer and D. Egli and on the Basic Geological Map of the SFRY (1:100 000), Sheets Novi Pazar (Urošević et al. 1970a, 1973a), Vrnjci (Urošević et al. 1970b, 1973b), Sjenica (Mojsilović et al. 1978, 1980) and Ivanjica (Brković et al. 1976, 1977) as well as Simić (1956) for the Studenica area. Coordinates are in MGI Balkan 7.



granodiorite (Schefer et al. 2008) that thermally altered the surrounding host rocks (Knežević et al. 1995).

According to Knežević et al. (1995), the contact-metamorphic rocks (skarn and hornfelses) around the Kopaonik granodiorite record P-T-conditions of 565 °C and 100 ± 50 MPa, which is in line with CAI values of up to 7.0 (Epstein et al. 1977; Harris 1979) assuming a short time interval of heating to more than 550 °C (Nöth 1991; Burnett et al. 1994) associated with hot-fluid circulation derived from the Kopaonik intrusion. These mixed CAI values of CAI 5.5 and CAI 6.5–7.0 in one sample can only be explained by the contact-metamorphic overprint by the Kopaonik intrusion while the lower CAI values of 5.5–6.0 record the earlier regional metamorphic event contemporaneous with the main deformation (Egli 2008).

Because of the metamorphic overprint, all metamorphic sequences in the Kopaonik region and those developed west of the Ibar valley were often mapped as Paleozoic (Urošević et al. 1970a, b, 1973a, b; Brković et al. 1976, 1977; Mojsilović et al. 1978, 1980), although a Triassic-age of the carbonates in the Studenica area was postulated much earlier (Simić 1956). Indeed, conodonts of Carnian age were discovered in the metamorphic rocks of the Kopaonik area ('Central Kopaonik Series' in the north: Mičić et al. 1972; 'Metamorphic Trepča Series' in the south: Klisić et al. 1972). Sudar (1986) confirmed this Carnian age, and in addition, found Norian conodonts; he also established a biostratigraphic subdivision of the cherty limestones into conodont zones. The metamorphosed and ductilely deformed conodonts (CAI values 5-7) from Kopaonik Mt. were first described and illustrated by Sudar & Kovács (2006).

2.3 Location of sections

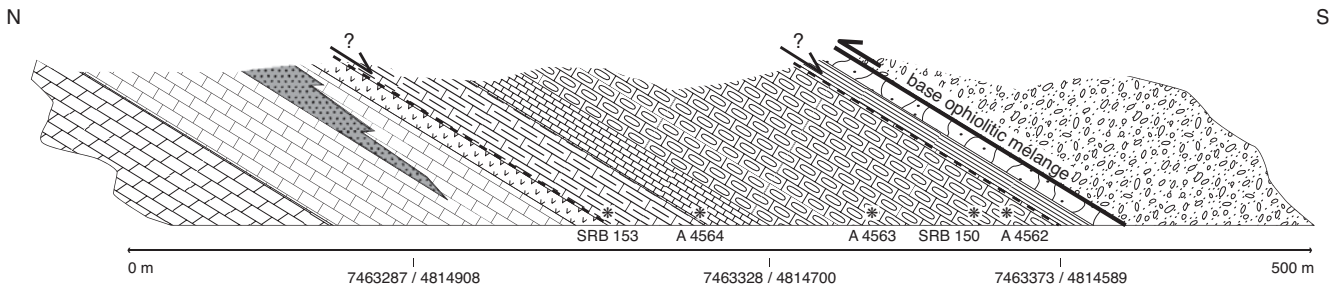
2.3.1 Studenica

This section (Fig. 2.3a) is located downstream from the Studenica monastery (Fig. 2.2) near a bridge over the Studenica River. After the Studenica quarry it follows the road for about 500 m downstream from the bridge. The northwestern base of the section is located at coordinates 7463300/4815000 (this and all following localities are given in the MGI Balkan 7 Cartesian coordinates also used for the 1:100'000 geological maps of former Yugoslavia). The highly deformed rocks were recrystallized under greenschist-facies conditions, and show a strong and occasionally mylonitic foliation and NNW–SSE- oriented stretching lineation. This resulted in a considerably reduced thickness of the sequence. The section starts with massive Anisian dolostones and ends in the ophiolitic mélange underlying the ophiolite nappe (Fig. 2.3a).

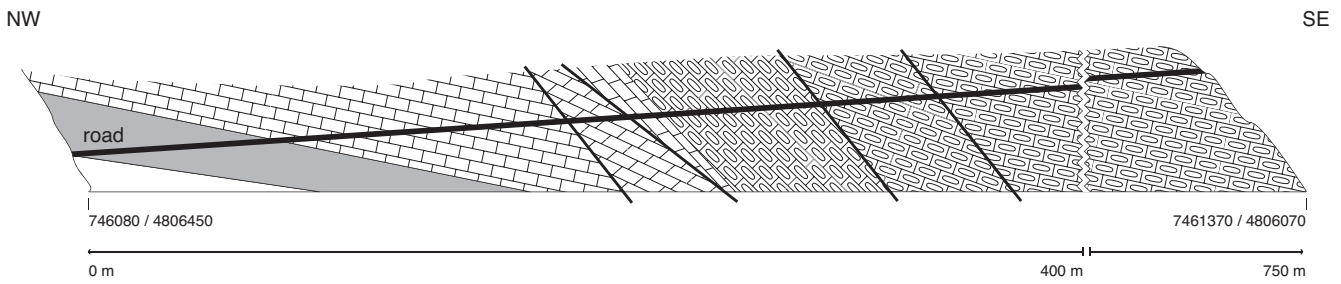
2.3.2 Gradac

The two sections near the village of Gradac are located further south in the Studenica unit, west of the Ibar River (Fig. 2.2). Both profiles, particularly section Gradac 2, show intense deformation under greenschist-grade metamorphic conditions. Section Gradac 1 starts some 3 km west of Gradac village and stretches along the road to Ivanjica between coordinates 7460710/4803253 and 7461274/4802826. This section includes the succession from the upper part of the Lower Triassic Werfen Formation (probably Campil Beds) to Anisian shallow-water

a Studenica road section



b Gradac 2 road section



Legend:

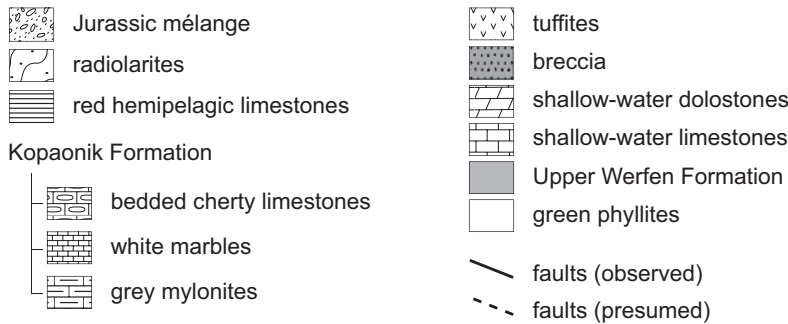


Fig. 2.3

a – Road section in the Studenica valley, starting from the quarry downstream of the Studenica monastery. Locations of the conodont samples are indicated. **b** – Stratigraphic section Gradac 2, starting north of the hamlet Jokovići on the road to Dolovi.

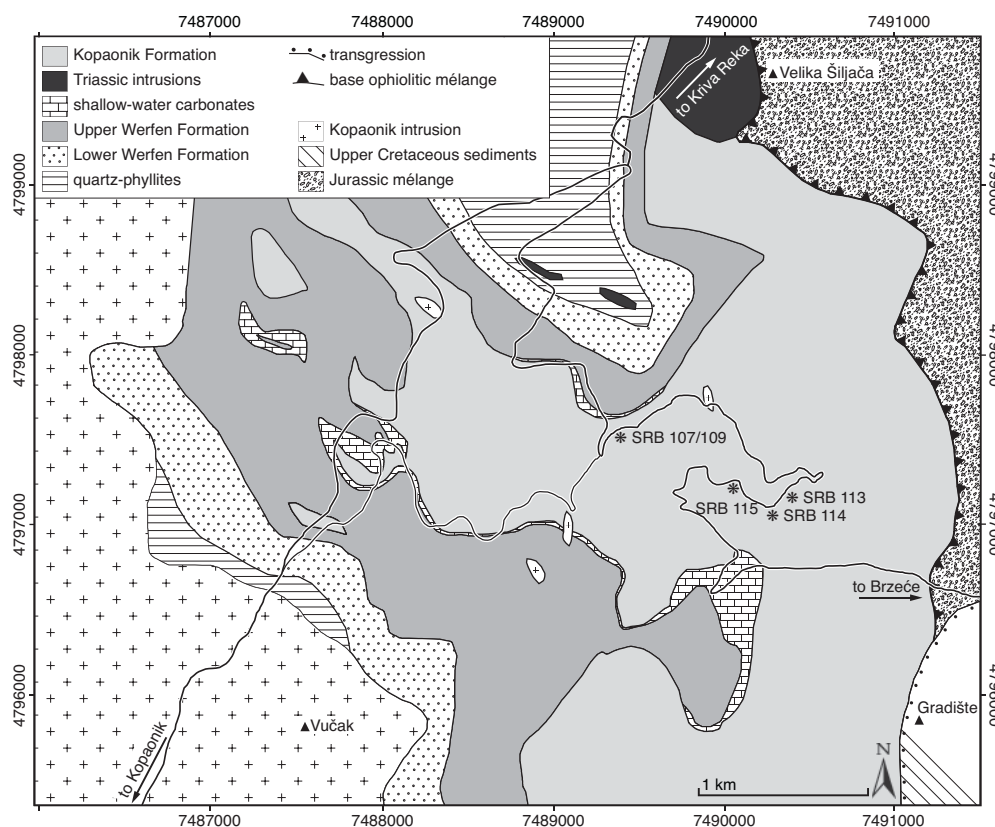
carbonates. Section Gradac 2 is located north of the hamlet Jokovići and along the road to Dolovi, between coordinates 7460889/4806460 and 7461163/4806257. It also starts with the Werfen Formation (probably Campil Beds) but exposes the succession up to the siliceous metalimestones of the Kopaonik Formation (Fig 3b); however, part of the succession is cut out by faults. In this section, the rocks are strongly deformed, showing a distinct stretching lineation and top-to-the-north shear-senses, whereas Gradac 1 is only slightly deformed, showing minor stretching in a NW–SE direction and open folding.

2.3.3 Kopaonik area

This area located east of the Ibar River and on the southeastern slope of the Kopaonik Mountain (NE of Pančičev Vrh) was mapped at the scale 1:10'000 by Egli (2008) (Fig. 2.4). The oldest rocks are quartz-phyllites of probably Paleozoic age, overlain by the Werfen Formation followed up-section by shallow-water carbonate sediments ('Gutenstein' and 'Steinalm' equivalents). A vast amount of the outcropping rocks, however, consists of well-bedded cherty metalimestones of the newly defined Kopaonik Formation (see below). This stratigraphic

succession underwent strong polyphase folding under greenschist-facies conditions (Egli 2008; Zelić et al. 2010). Near-isoclinal D2-folds dominate the map pattern. In the vicinity of the Kopaonik granodioritic intrusion (30.7–30.9 Ma; Schefer et al. 2008) we also find contact metamorphic rocks (skarns and hornfelses). Field evidence shows that intrusion and contact metamorphism postdate regional metamorphism and main deformation.

Fig. 2.4 – Geological map of the eastern Kopaonik area between Brzeće and the Kopaonik ski resort (mapped at scale 1:10'000 by D. Egli, coordinates are in MGI Balkan 7). Locations of the conodont samples are indicated



2.4. Stratigraphy

2.4.1 Quartz-phyllites

In the Kopaonik area, this formation is only preserved in some small outcrops bordering the Kopaonik granodiorite (Fig. 2.4). Layers of pelitic composition are interbedded with quartzitic layers. On weathered surfaces, the finely laminated rocks are of grey to reddish colour, but grey to greenish on fresh surfaces. While a narrow-spaced bedding-parallel foliation develops in the phyllitic layers, the quartzitic layers are often boudinaged. These rocks are probably of Paleozoic age but, alternatively, they may represent the lowermost part of the Lower Triassic Werfen Formation.

2.4.2 Werfen Formation

In the Kopaonik area, massive metasandstones, typical for the lower part of the Werfen Formation, are visible in small outcrops located close to the intrusion (Egli 2008). The sandstones are brownish to reddish on weathered surfaces and dark brown to black on fresh surfaces. Detrital grains (usually <1 mm) and cement are entirely made up of quartz. In coarse-grained layers, cross-bedding (Fig. 2.5a) or a faint parallel lamination, as well as a bedding-parallel foliation can be observed. In thin-section, small biotite flakes defining the foliation are present

besides quartz. In the vicinity of the intrusion, the rocks are overprinted by contact metamorphism, which leads to the formation of white mica, garnet and brown amphiboles with grains between 0.1 and 1 mm (Egli 2008).

The upper part of the Werfen Formation shows similarities with the basal part of the Gradac 1 and 2 successions and may stratigraphically overlie the siliciclastic sediments of the lower Werfen Formation in the Kopaonik area. There it consists of interbedded shales, sandstones and limestones with bed thicknesses of up to one metre. Sandy layers consist of quartz and limestone clasts of varying grain size, embedded in calcite cement. In section Gradac 1, shell fragments, mostly bivalves and gastropods, are preserved in the limestone layers. The pelitic layers are non-calcareous, show a strong foliation and reach thicknesses between one millimetre and several centimetres; stratification is arrhythmic.

In section Gradac 2 the Werfen Formation is more calcareous and less sandy. In the lower part there is a rhythmic stratification on a small scale: centimetre-thick layers of limestone are intercalated with pelitic material that becomes more abundant up-section, leading to a purely pelitic sequence. These pelitic layers are pale green with a silvery shine due to the relatively higher degree of metamorphism compared to section Gradac 1. Also the deformation, characterized by a pervasive bedding-parallel foliation and by isoclinal folding, is more intense than in section Gradac 2.

In the Kopaonik area, the Werfen Formation is again characterized by a rhythmic bedding pattern of non-calcareous shales, partly calcite-cemented sandstones and marlstones. Dynamically grown well-oriented biotite flakes, grown during regional metamorphism, define a bedding-parallel foliation visible in thin-section. In the immediate vicinity to the intrusion where contact metamorphism is accentuated, the abundance of calcareous beds diminishes (Egli 2008).

2.4.3 Shallow-water carbonates ('Wurstelkalk'; Gutenstein and Steinalm Formations equivalents)

The transition from the Werfen Formation into massive dark metalimestones is particularly well visible in section Gradac 1. Several metres of bioturbated, well-bedded grey to brownish weathering limestones are reminiscent of the basal Gutenstein Formation ('Wurstelkalk') of the Eastern Alps (Tollmann 1976) or the Szinpetri Limestone Formation in the Silica nappes (Aggtelek unit, Hungary) of the Inner Western Carpathians (Hips 2006). Up-section, these sediments give way to massive, dark grey to nearly black, slightly metamorphic limestones with quartz veins (middle to upper Gutenstein Formation equivalent).

In section Gradac 2 (Fig. 2.3b), these rocks are strongly deformed, and bioturbation is no longer visible in the lower part of the succession. The marbles show a distinct spaced cleavage of centimetre to decimetre size, and a N–S-oriented stretching lineation. Fissures filled with quartz and calcite are oriented perpendicular to the foliation. Calcite marble, probably belonging to the Gutenstein Formation, is followed by massive dolomitic marble of light grey colour with chaotic fissures without foliation. The latter is interpreted as shallow-water carbonate of the Steinalm Formation.

Dolostones reminiscent of the Steinalm Formation define the lowermost part of the Studenica section. The dolostones are massive, however, and no cleavage is visible. These dolostones are followed by a several tens of metres thick sequence of calcite marble. These marbles are strongly deformed and mylonitized (Fig. 2.5b), showing an alternation of differently coloured domains. An intense stretching lineation is NW–SE oriented. Minor amounts of dolomite are also found in the calcite marbles, dolomitic layers being less deformed and boudinaged, which leads to the development of sigma-clasts exhibiting top-to-the-north shear senses (Egli 2008).

In the Kopaonik area the marbles derived from shallow-water limestones reach a thickness of a few decametres;

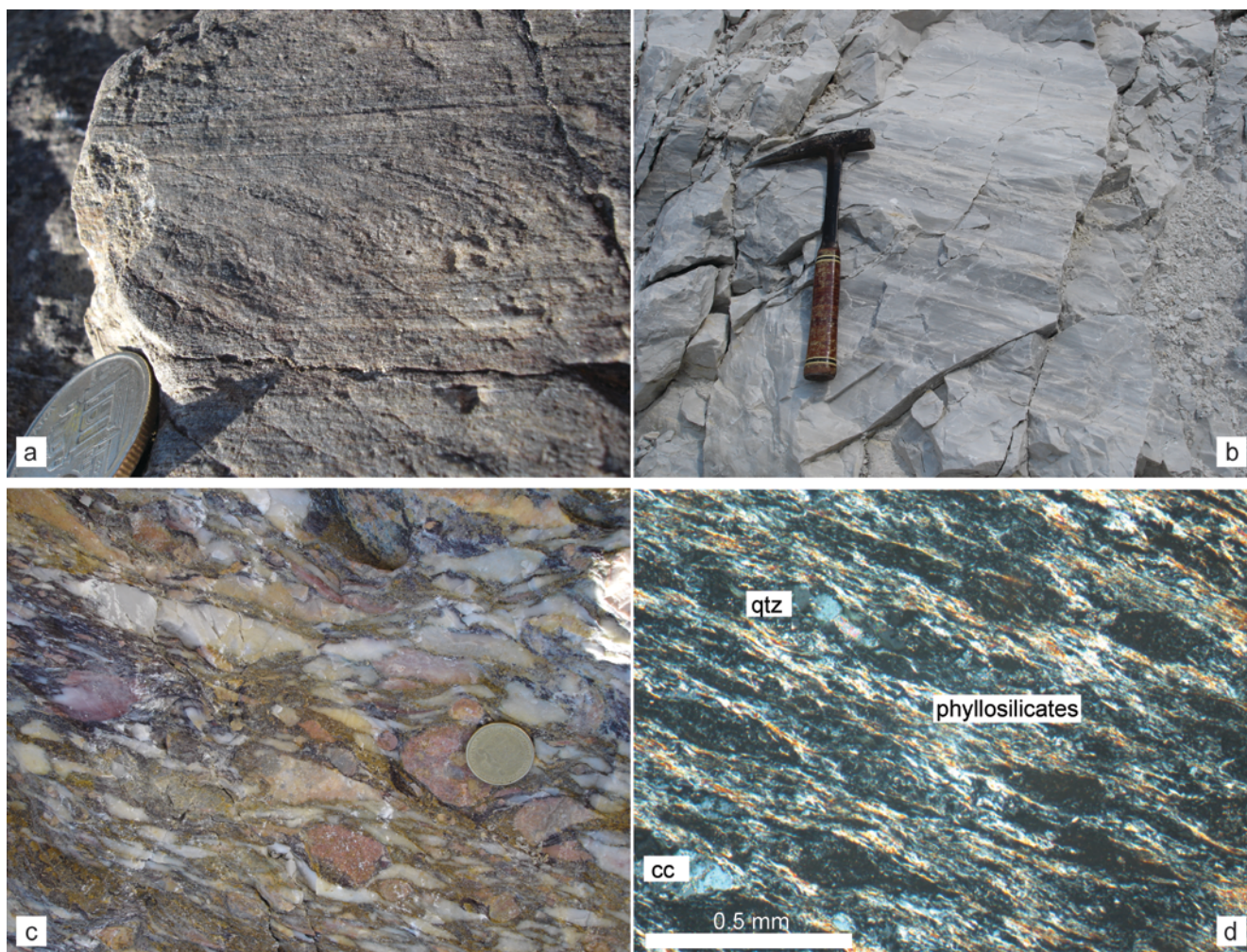


Fig. 2.5 – Early and Middle Triassic lithofacies. **a** – Cross-bedded sandstone, Lower Werfen Formation, Kopaonik area (7486570/4795890). **b** – Calcite-mylonite attributed to the Steinalm Formation (Anisian), Studenica quarry. **c** – Polymictic breccia overlying the Steinalm Formation, Studenica quarry. **d** – Tuffite, presumably Anisian/Ladinian boundary, Studenica quarry, thin-section crossed polarizers.

often they are only present as small layers or they may even be completely missing. The grain size of the marbles increases with the vicinity to the Kopaonik intrusion. The usually dark-coloured sediments pass into white coarse-grained marbles.

2.4.4 Breccia horizon in the uppermost Steinalm Formation equivalent

Only in the Studenica section, intercalated within the uppermost Steinalm Formation equivalent, limited to the quarry and wedging out towards the street (Fig. 2.3a), a layer of breccias of about 4 m thickness can be observed. The polymictic breccia is poorly sorted and consists of clasts one millimetre to several centimetres across (Fig. 2.5c). Rounded to sub-angular limestone clasts dominate, dolomite-marble clasts are rare. The matrix consists of red and greenish tuffites with a strong cleavage. Such tuffites also may occur as clasts in this breccia. The matrix becomes calcitic towards the top of the breccia, and is finally marly in the uppermost part. Isolated quartz grains and dynamically grown micas are also found in the matrix. Relics of probable foraminifera and pellets suggest a shallow-water origin of some of the components. The competence contrast between the different components causes heterogeneous deformation, which results in an undulating appearance and stretching lineations visible on the foliation planes. Strain analysis (Egli 2008) after Ramsay & Huber (1983) suggests thinning to 25% of the

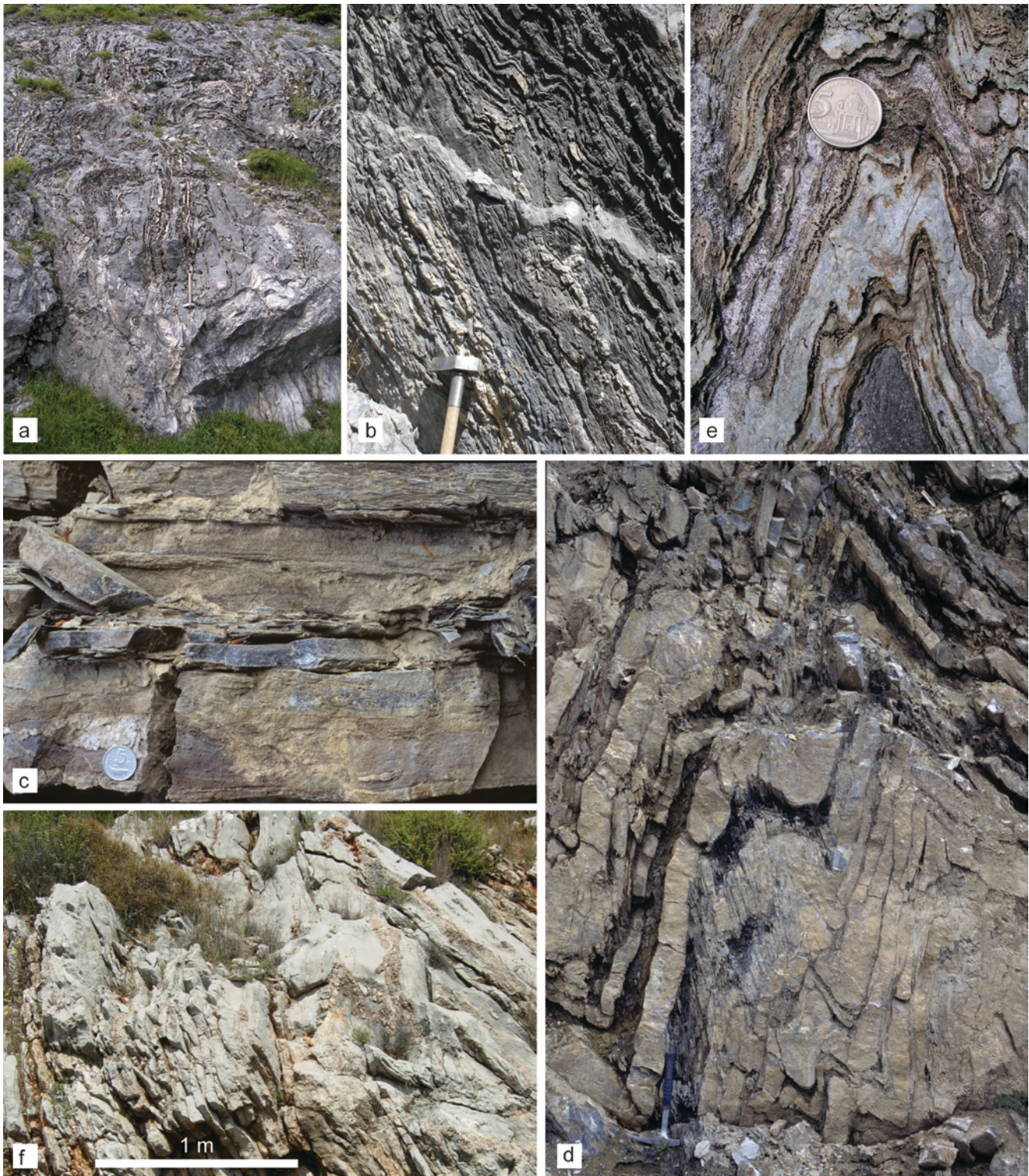


Fig. 2.6 – Lithofacies of Kopaonik Formation, Middle to Late Triassic, along road from Brzeće to Kopaonik. **a, b** – Intensely deformed and slightly contact-metamorphic grey, hemipelagic limestones with bands of diagenetic replacement chert (now quartzite). **c** – Graded fine-grained calcarenite, with diagenetic replacement chert, only weakly deformed. **d** – Chevron-type folds in a limestone-marl succession with well defined axial-plane schistosity in the marly layers. **e** – Cherty limestones transformed into calc-silicate rock due to contact metamorphism. **f** – Pelagic limestone with marly interbeds and bands of early diagenetic replacement chert, Adhami Limestone, Late Triassic–Sinemurian, Askiplion unit, road Palaio Epidhavros-Koliaki, Argolis, Greece; for details see Baumgartner (1985).

original thickness for the breccia horizon. This value is considered representative for the entire Studenica section, except for the dolomitic part at the base.

2.4.5 *Tuffites and metabasalts*

Intensely foliated tuffites, overlying the Steinalm Formation equivalent and with an intercalated breccia horizon at their top, can be observed only in the Studenica section. Their thickness is about 5 m. These tuffites of red and green colour are similar to those in the matrix of the underlying breccias (Fig. 2.5d). These rocks consist mainly of mica with some up to millimetre-sized clasts of quartz, dolomite, calcite and feldspar. According to Sudar (1986) these volcanoclastic sediments in the inner Dinarides were deposited near the Anisian-Ladinian boundary and up to the end of the Early Ladinian.

2.4.6 *Kopaonik Formation*

In the Studenica section and in the Kopaonik area, the shallow-water carbonates of the Middle Triassic and the associated tuffites are overlain by thin-bedded metalimestones with bands and nodules of chert (Figs. 2.6a, b). We refer to this formation as the Kopaonik Formation based on the following definition:

Derivatio nominis: after Kopaonik Mountain area (SW-Serbia). Compare ‘Central Kopaonik Series’ of Sudar (1986) and Sudar & Kovács (2006).

History: see chapter on geological setting and metamorphism.

Definition: bedded, hemipelagic grey metalimestones, in certain stratigraphic intervals including fine-grained calcarenites consisting of shallow-water components; chert nodules and/or marly and clayey intercalations are frequent (Fig. 2.7). The area of deposition appears to be far from shallow-water ramps or platforms.

Type area: Kopaonik thrust sheet and Studenica slice. A complete type section cannot be defined because deformation and metamorphism are too intense in the Kopaonik area. The formation overlies the shallow-water carbonates of the equivalents of the Steinalm Formation and is overlain by red hemipelagic limestones of probable Jurassic age.

Other localities: Smrekovnica limestones, ‘Metamorphic Trepča Series’, southern Kopaonik Mountain area, Kosovo (Sudar 1986; Sudar & Kovács 2006).

Age: Latest Anisian to (Late) Norian, defined by conodonts (this paper, Sudar 1986 and Sudar & Kovács 2006).

Facies: Grey hemipelagic basinal metalimestones with fine-grained redeposited calcarenites (deposited by low-density turbidity currents).

Differences to other and similar formations: The Kopaonik Formation is in parts similar to the Gučevo Limestone Formation (Sudar 1986; Filipović et al. 2003) or to the Grivska Formation (Dimitrijević 1997). However, the hemipelagic metalimestones of the latter include significantly more shallow-water debris from nearby carbonate platforms. By contrast, the hemipelagic condensed red or grey metalimestones of the Kopaonik Formation and the classical Hallstatt Limestones are devoid of coarser re-deposited shallow-water turbidites.

Fig. 2.7 – Microfacies of the ?Late Ladinian to (Early) Carnian fine-grained hemipelagic grey limestones in the Kopaonik region (Brzeće) and of the Early Norian grey micritic and partly cherty limestones of Studenica section. **A** – Laminated micritic limestone, strongly recrystallized. All fossil remnants are destroyed by recrystallization due to metamorphic overprint. The preserved laminae indicate probably a low energy turbiditic character of sedimentation and less bioturbation.

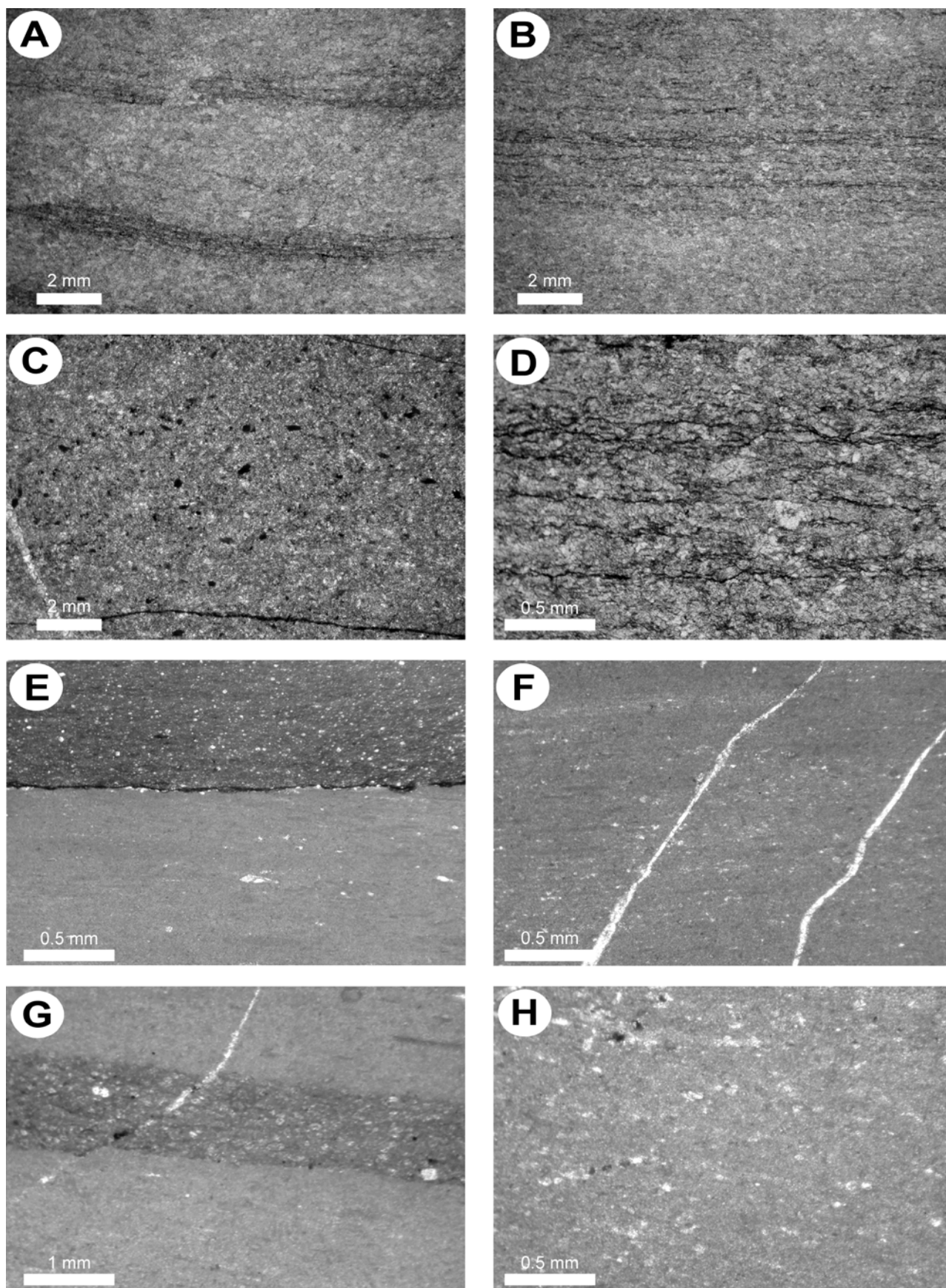


(**Fig. 2.7 continued:**) Sample SRB 113. **B** – Relatively homogenous micritic limestone with less content of clay and pyrite, recrystallized. Sample SRB 115. **C** – Relatively homogenous micritic limestone with pyrite. Some ghosts of organisms resemble filaments and radiolarians and probably peloids. Sample SRB 116. **D** – Partly some ghost of organisms are visible, probably representing remnants of crinoids and radiolarians. Sample SRB 115. **E** – The contact between the light and dark grey biomicrite is relatively sharp. The dark grey biomicrite is much richer in organisms, partly the shape of radiolarians is relatively well preserved. The dark grey biomicrite represents a more condensed facies in comparison with light grey micrite indicating highstand shedding. Sample SRB 150. **F** – Ghosts of radiolarians and filament-remnants occur mostly in the very fine-grained turbidites. Sample SRB 153. **G** – Overview showing the alternation of relatively organism-free light grey micrite and organisms enriched more condensed dark grey biomicrite. Sample SRB 153. **H** – Fig. E enlarged. Most organism/components are completely recrystallized and occur only as ghosts.



Table 2.1: Triassic conodont faunas of the Kopaonik and Studenica areas, southern Serbia.

Sample (coord.)	Conodont fauna	Age	CAI-values
Županj 1 (sample-nr. on Fig. 2.2)			
SRB 110 (7476443/4807045)	<i>Norigondolella</i> sp.,	Early–Middle Norian	5.5–6.0
	<i>Epigondolella</i> sp. (<i>abneptis</i> -group)		
Županj 2 (sample-nrs. on Fig. 2.2)			
SRB 111 (7477694/4806995)	<i>Neogondolella</i> cf. <i>excelsa</i> ,	Late Anisian	5.5–6.0
	<i>Neogondolella</i> cf. <i>eotrammeri</i> ,		
	<i>Neogondolella</i> cf. <i>cornuta</i>		
SRB 112 (7477694/4806995)	<i>Neogondolella</i> cf. <i>inclinata</i> (or <i>M. polygnathiformis</i>)	Ladinian–(Carnian)	5.5–6.0
Brzeće (Fig. 2.4)			
SRB 113 (7489302/4796146)	<i>Metapolygnathus</i> cf. <i>polygnathiformis</i>	Carnian	(5.0–)5.5 and 6.5–7.0
SRB 114 (7489269/4796084)	<i>Neogondolella</i> sp.	?Ladinian–Carnian	5.5
SRB 115 (7489107/4796221)	<i>Metapolygnathus polygnathiformis</i>	Carnian	5.5–6.0
Studenica (7463291/4814897, Fig. 2.3)			
A 4562	<i>Epigondolella quadrata</i>	Lacian (high 1 to 2)	5.5–6.0
A 4563	<i>Norigondolella</i> sp.,	Norian	5.5–6.0
	<i>Epigondolella</i> sp.		
A 4564	<i>Epigondolella</i> sp. indet,	Norian	5.5–6.0
SRB 150	<i>Neohindeodella triassica</i>	Lacian 2	5.5–6.0
	<i>Norigondolella navicula</i> ,		
	<i>Norigondolella</i> cf. <i>hallstattensis</i> ,		
SRB 153	<i>Epigondolella</i> cf. <i>triangularis</i>	Lacian 2	5.5–6.0
	<i>Norigondolella navicula</i> ,		
	<i>Norigondolella</i> cf. <i>hallstattensis</i> ,		
	<i>Epigondolella</i> sp. indet		

Remarks: The succession resembles that of the grey Hallstatt facies occurring within the Reifling and Pötschen Formations of the Eastern Alps (e.g. Lein 1987) as well as the Felsötárkány Limestone Formation of the Bükk Mountains, NE Hungary (Kozur 1991; Less et al. 2005). In addition, similar facies have been described from different locations in the internal Dinarides without specific formational names (Rampnoux 1974; Charvet 1978). A similar succession with hemipelagic Middle/Late Triassic metalimestones was described in Korabi/Pelagonia units of eastern Albania (Meco & Aliaj 2000; Gawlick et al. 2008).

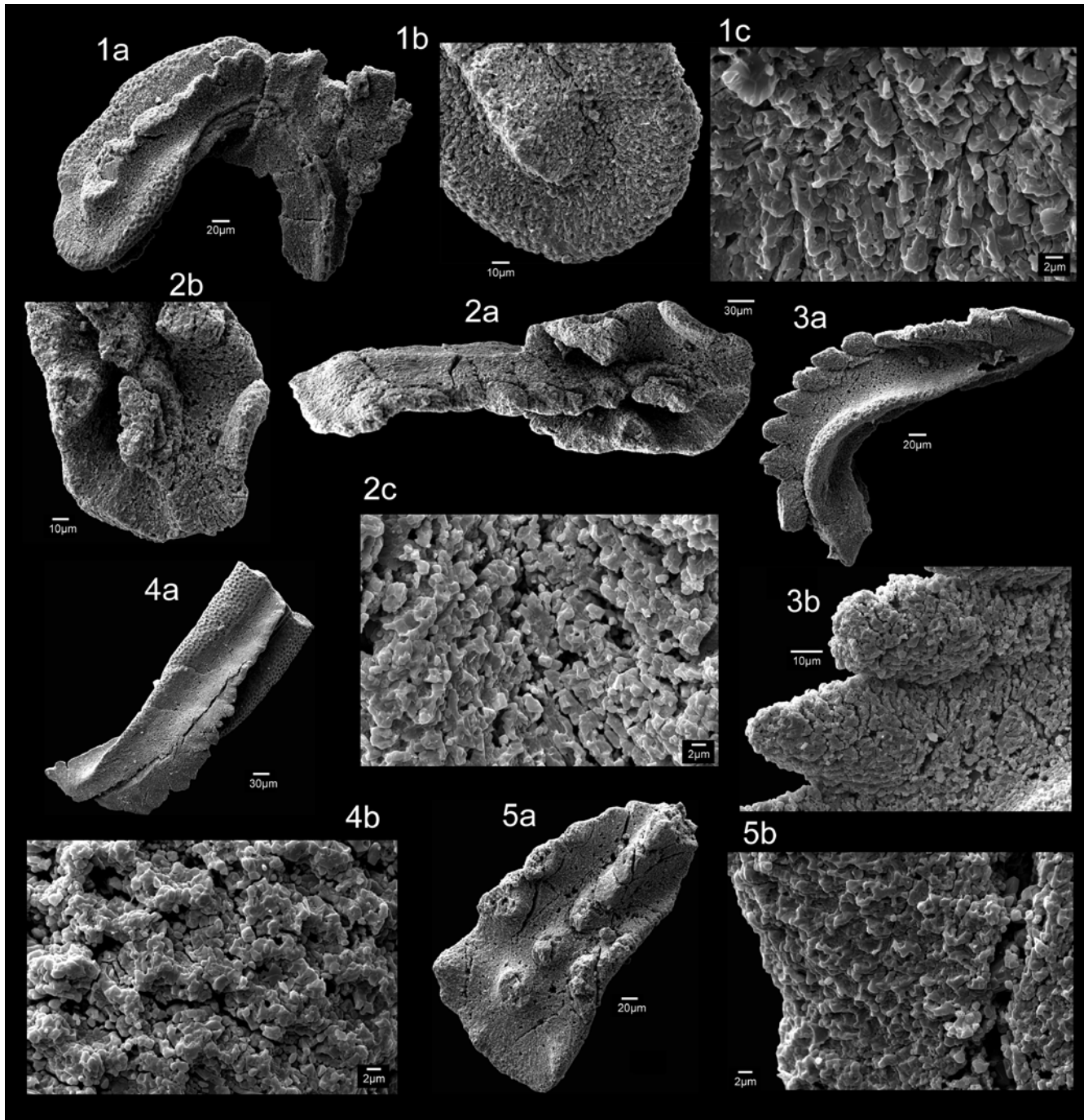
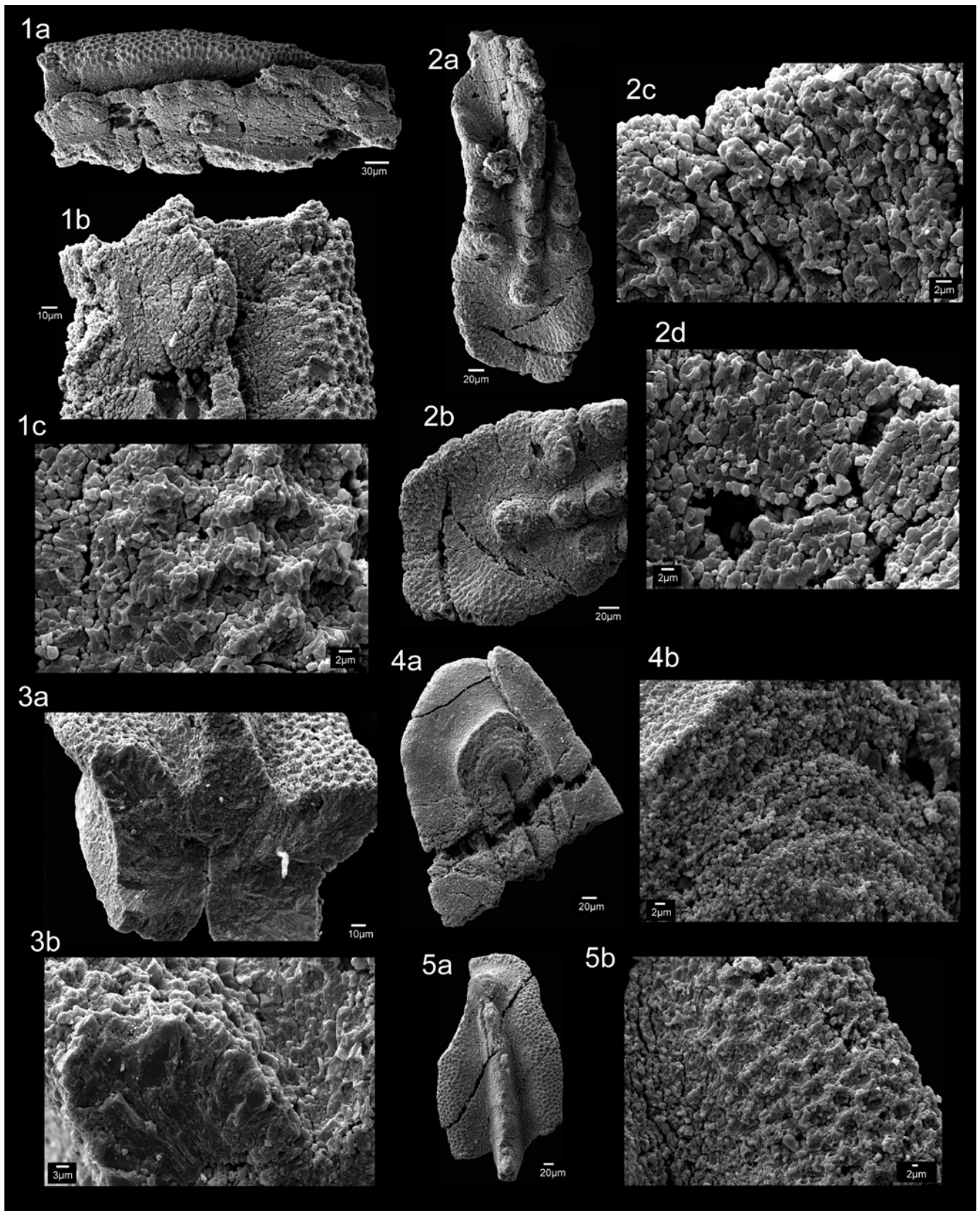


Fig. 2.8 – Metamorphosed and deformed conodonts with Conodont Colour Alteration (CAI) values 5.5–6.0 from the Studenica section (Sample SRB 150). These conodonts occur in grey cherty metalimestones and are of Early Norian (Lacian) age. **1a** – Ductilely deformed *Norigondolella navicula*. In this view the original ornamentation on the platform surface looks undeformed. **1b** – Platform end of *Norigondolella navicula*, enlarged, showing complete recrystallization of the original ornamentation by apatite crystal growth. **1c** – Enlarged detail of **1b** showing the growth of the apatite crystals. Corrosion is missing. **2a** – Slightly deformed *Epigondolella triangularis*. **2b** – Enlarged platform end showing the complete and relatively homogenous recrystallization of the conodont. **2c** – Enlarged detail showing the growth of apatite crystals. **3a** – Ductilely deformed *Norigondolella navicula*. **3b** – Recrystallized fabric, enlarged from **3a**. **4a** – Deformed and recrystallized part of ?*Norigondolella navicula*. The original ornamentation on the platform surface is preserved and looks undeformed. **4b** – Enlarged view on the ornamentation showing complete recrystallization of the ornamentation. **5a** – Undeformed but totally recrystallized *Epigondolella triangularis*. **5b** – Recrystallized fabric, enlarged from **5a**.

Fig. 2.9 – Metamorphosed and partly ductilely deformed conodonts with Conodont Colour Alteration (CAI) values 5.5–6.0 from the Studenica section (sample SRB 153). These conodonts are from Early Norian (Lacian) grey cherty metalimestones. **1a** – Slightly deformed and recrystallized *Norigondolella* sp. From this view, the original ornamentation on the platform



(*Fig. 2.9 continued*) surface looks undeformed. **1b** – Platform end, enlarged, showing complete recrystallization. **1c** – Enlarged view on the ornamentation showing the complete recrystallization of the ornamentation. **2a** – Undeformed but totally recrystallized *Epigondolella* sp. **2b** – Enlarged view of platform showing strong recrystallization. **2c, 2d** – Details of recrystallization, enlarged from **2b**. **3a** – Broken *Norigondolella* sp. showing recrystallization in the inner part of the conodont. **3b** – Enlarged detail from **3a**. **4a** – Basal view of *Norigondolella navicula*. **4b** – Enlarged detail from **4a**. **5a** – Broken *Norigondolella* cf. *hallstattensis*. The original ornamentation on the platform surface is preserved and looks undeformed. **5b** – Enlarged view of the ornamentation showing complete recrystallization of the ornamentation.

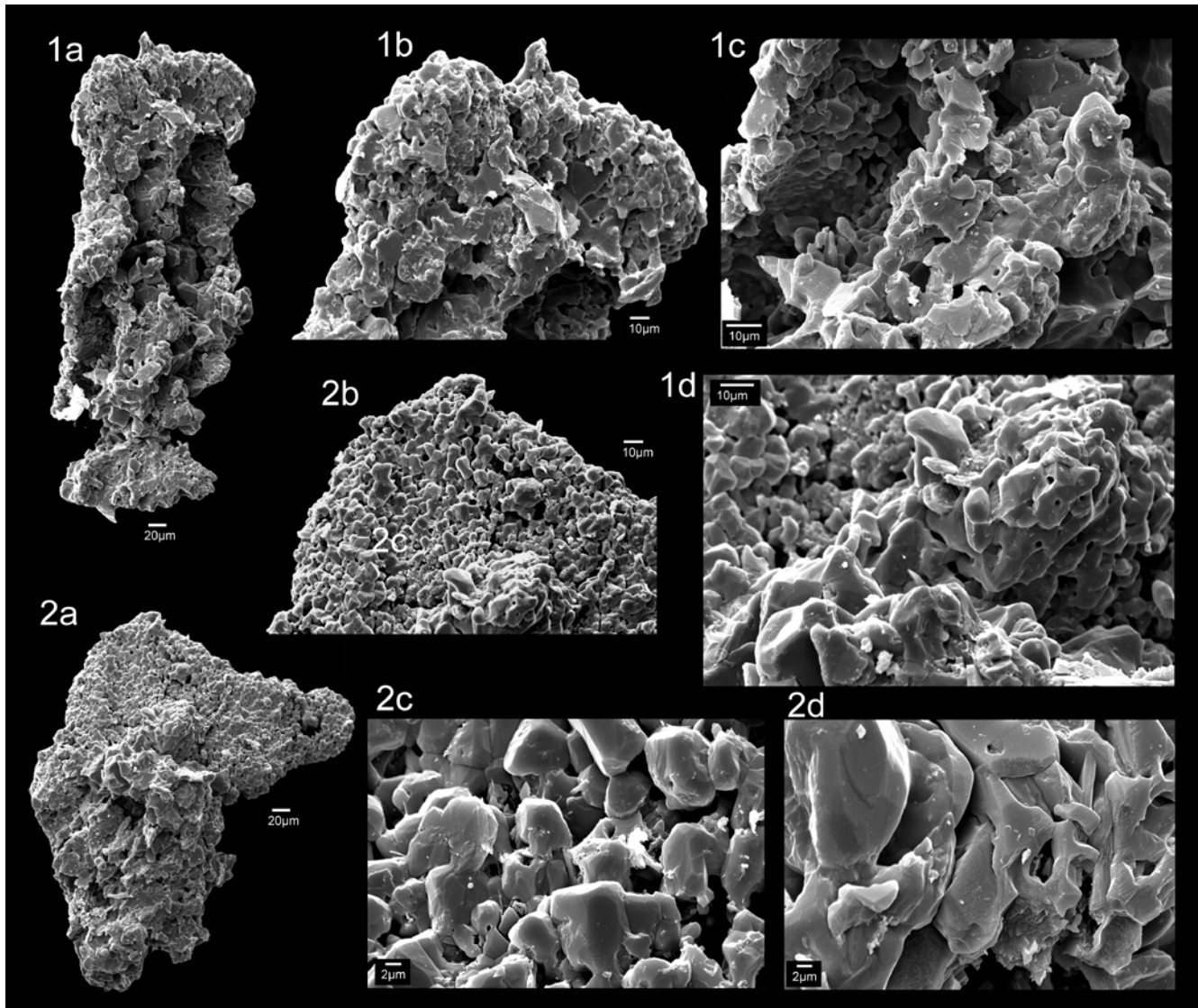


Fig. 2.10 – Metamorphosed and ductilely deformed conodonts (*Metapolygnathus polygnathiformis*) with Conodont Colour Alteration (CAI) values in average CAI 5.5–6.0 from Kopaonik, Brzeće section (sample SRB 115). These conodonts come from probably Late Carnian grey metalimestones. **1a** – Strongly recrystallized and corroded specimen. CAI 5.5–6.0. **1b** – Platform end enlarged showing strong recrystallization and growth of the apatite crystals. **1c** – Enlarged detail with strong recrystallization and partial corrosion of the surface. **1d** – Detail of the surface with relatively large apatite crystals. **2a** – Strongly recrystallized and slightly deformed specimen. CAI 6.0. **2b** – Platform end enlarged showing strong recrystallization and growth of the apatite crystals. The original surface is completely destroyed by recrystallization. **2c** – Enlarged detail showing strong recrystallization and growth of individual apatite crystals. **2d** – Enlarged detail showing strong recrystallization of apatite and enlargement of the crystallites.

In the Studenica section, the Steinalm Limestones are separated from the Kopaonik Formation by sparse outcrops of grey-weathering calcite mylonites (‘grey mylonites’) with a strong cleavage and with a few intercalated pelitic layers (Fig. 2.6c). In thin-section, the calcite grains are elongated and form sigma-clasts indicating top-to-the-northwest shear-sense. The white marbles overlying the mylonites are reminiscent of the Steinalm marbles found lower down in the Studenica section. However, the mylonites (sample SRB 153, Fig. 2.3a), the white marbles (sample A 4564), and the overlying well-bedded metalimestones with chert nodules (samples A 4563, SRB 150, A 4562, Table 2.1) include Norian conodonts (Figs. 2.8 and 2.9, Table 2.1). The conodont faunas cover only a very short time interval of the Early Norian, ranging from the higher part of the Lacion 1 or basal Lacion 2 (*Epigondolella quadrata*) to the Lacion 2 (*Epigondolella triangularis* and *Norigondolella hallstattensis*).

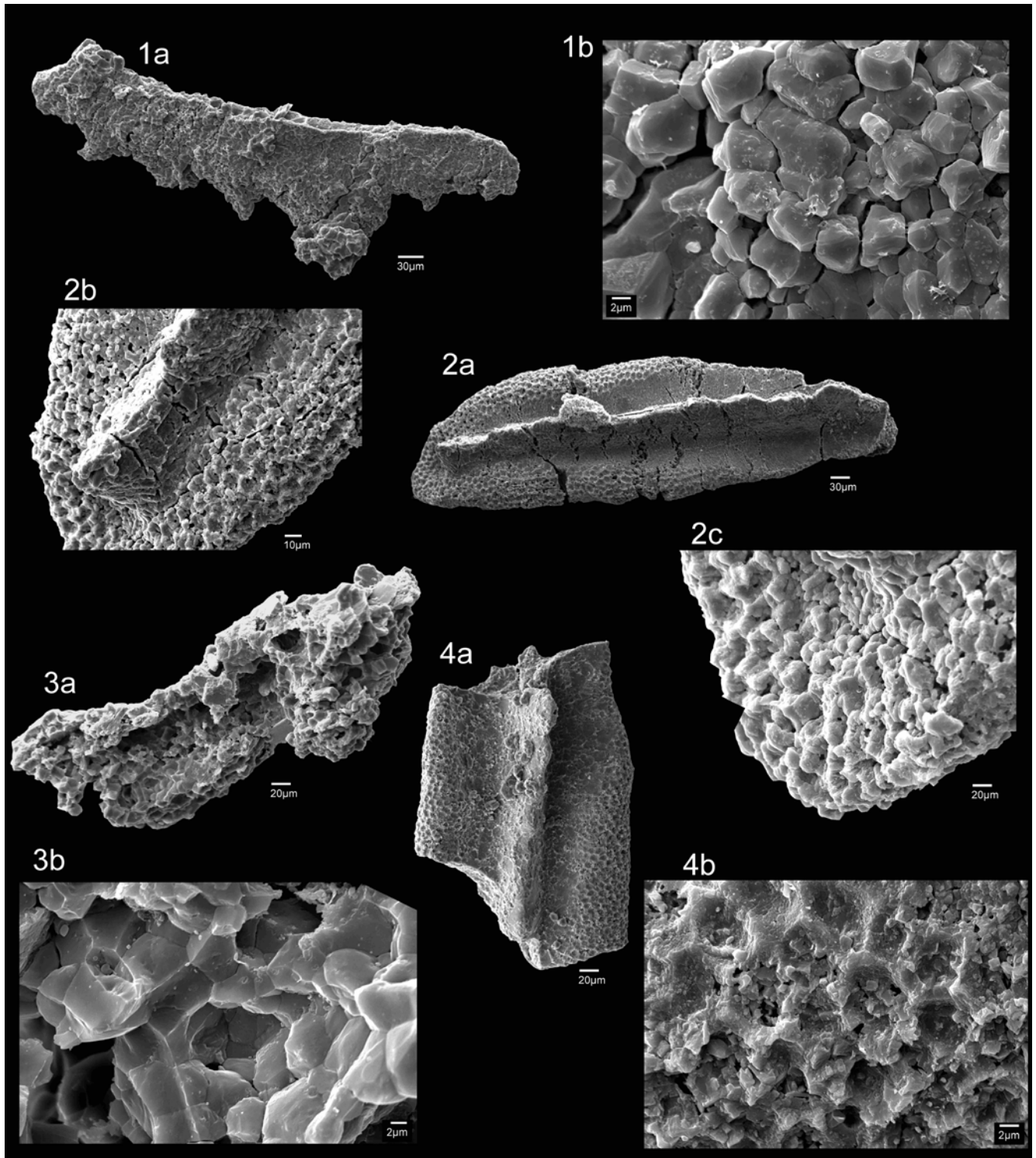


Fig. 2.11 – Metamorphosed and only slightly ductilely deformed conodonts from the Late Anisian resp. Late Ladinian to ?Early Carnian of locality Županje 2 with Conodont Colour Alteration (CAI) values of CAI 5.5–6.0. Samples SRB 111 and SRB 112. **1a** – *Neogondolella* cf. *cornuta*. CAI 5.5–6.0. **1b** – Enlarged part from **1a** showing the strong recrystallization and growth of the apatite crystals. The typical surface is completely destroyed by recrystallization. **2a** – *Neogondolella* cf. *eotrammeri*. CAI 5.5–6.0. **2b** – Enlarged platform end of the specimen figured in **2a** showing the complete recrystallization of the ornamentation. **2c** – Growth of apatite crystals, enlarged part from **2b**. **3a** – *Gondolella* cf. *excelsa*, extremely recrystallized. **3b** – Same specimen, enlarged part showing the strong recrystallization and growth of the apatite crystals. **4a** – Broken piece from the platform element of *Neogondolella* cf. *inclinata*. **4b** – Enlarged part from **4a** showing strong recrystallization and growth of apatite crystals in the area of platform ornamentation.

Because some important details of the conodont morphology were destroyed by intense deformation and low-grade metamorphism (CAI-values between CAI 5.5 and 6.0), the determination of the conodonts species cannot be more precise.

The conodont data from the grey calcite-mylonites, i.e., the Early Norian age pose a problem: obviously Ladinian and Carnian strata are missing in the Studenica section. As a primary stratigraphic gap by non-deposition and/or erosion appears unlikely to be the case, we suggest a tectonic contact along the calcite-mylonites.

In the Gradac 2 section, the Kopaonik Formation consists of thin-bedded marbles with interbedded marls. Weathering and fresh surfaces of the marbles are dark; the intercalated pelitic layers are yellowish. After a few metres of rhythmic alternations the metalimestones and marls give way to metalimestones with chert layers.

In the type area (Fig. 2.4), the Kopaonik Formation builds large cliffs and the most conspicuous outcrops. The formation is well stratified; calcareous beds alternate with chert-rich metalimestones or marly intercalations. The thickness of the beds varies between centimetres and decimetres (Fig. 2.6d). Where marly layers are absent, the chert layers and nodules are diagnostic for this formation. Weathered surfaces are greyish to brownish, depending on the amount of clay. In the vicinity of the intrusion, the Kopaonik Formation is transformed into massive skarns and hornfelses due to contact metamorphism (Fig. 2.6e). Metamorphosed chert layers and calcsilicates in marbles define the layering. In thin-section diopside, clinopyroxene, hornblende, garnet, and biotite are found. Calcite is consumed by reaction with quartz.

Our new conodont faunas from the Kopaonik Formation in the type area and near village of Brzeće, indicate a probable Early Carnian age based on the occurrence of *Metapolygnathus polygnathiformis* (samples SRB 113, SRB 114, SRB 115; Fig. 2.4, Table 2.1); however, a Late Ladinian to Late Carnian age cannot be excluded (Sudar 1986; Sudar & Kovács 2006) because the surface of *Metapolygnathus polygnathiformis* is destroyed by extreme polyphase deformation and (low-grade) metamorphism (CAI-values of CAI 5.5–6.0, reaching locally CAI 6.5–7.0, Fig. 2.10).

Two successions of metalimestones within the Kopaonik Formation are developed in the wider area of Kovači village, i.e. in Županj hamlet (north of the road from Jošanička Banja towards Biljanovac). In the locality Županj 1 an Early to Middle Norian conodont fauna, including *Norigondolella* sp. and *Epigondolella* sp. could be isolated from dark-grey micritic limestone beds (sample SRB 110 in Fig. 2.2, Table 2.1). These micritic metalimestones overlie a thick series of dark-grey, bedded metalimestones with fine-grained siliciclastic intercalations. In the locality Županj 2 (samples SRB 111, 112 in Fig. 2.2) a stratigraphically reduced series of dark-grey cherty and deformed metalimestones is dated as Late Anisian by the occurrence of *Neogondolella* cf. *excelsa* and *Neogondolella* cf. *cornuta*, and, higher up, as Late Ladinian/?Early Carnian by the occurrence of *Neogondolella* cf. *inclinata*. Due to the strong deformation of the conodonts a determination as *Metapolygnathus polygnathiformis* also seems possible (Fig. 2.11, Table 2.1). This locality is of special interest because it provides evidence of Middle Triassic (Late Anisian to Ladinian?) hemipelagic grey metalimestones in the Kopaonik region for the first time. Near to our samples from Županj 2, Sudar (1986) found several Carnian conodonts.

2.4.7 Red hemipelagic limestones and radiolarites

Only in the Studenica section such younger sediments are exposed. Here, the Kopaonik Formation is overlain by red to violet hemipelagic limestones with a thickness of only 1–2 metres showing a strong penetrative foliation. Limestone laminae, only up to one millimetre thickness, are separated by thin films of clay and occasional white marble layers. In thin-section accessory quartz grains and relics of radiolarians are visible. These red hemipelagic limestones probably represent an equivalent of the Middle Jurassic condensed Klaus Limestone of the

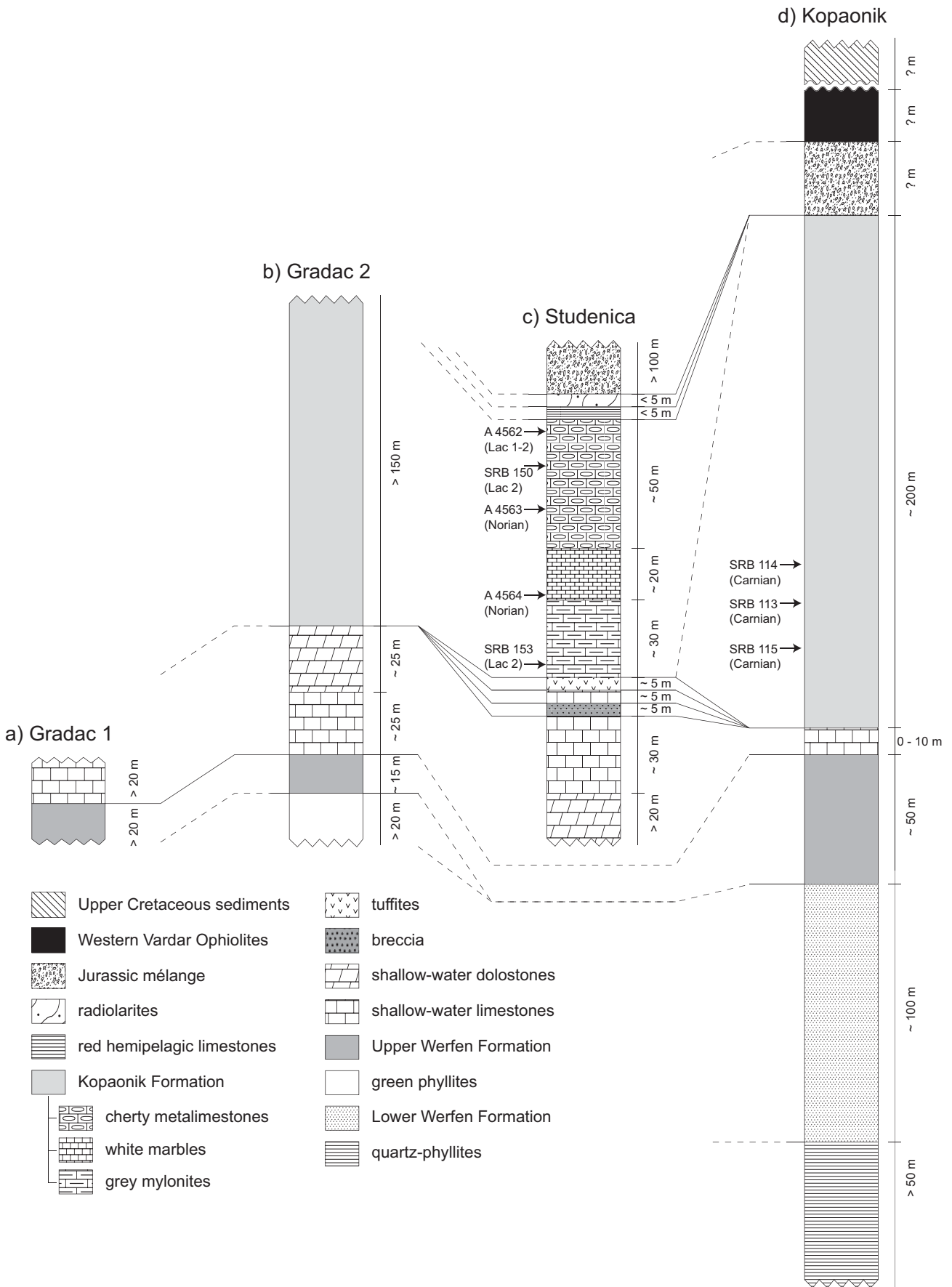


Fig. 2.12 – Stratigraphic successions of sections Gradac 1 (a), Gradac 2 (b) and Studenica (c) and of the Kopaonik region (d). The relative thicknesses of the formations are shown without correction for tectonic thinning. The original thicknesses are shown in Fig. 2.13.

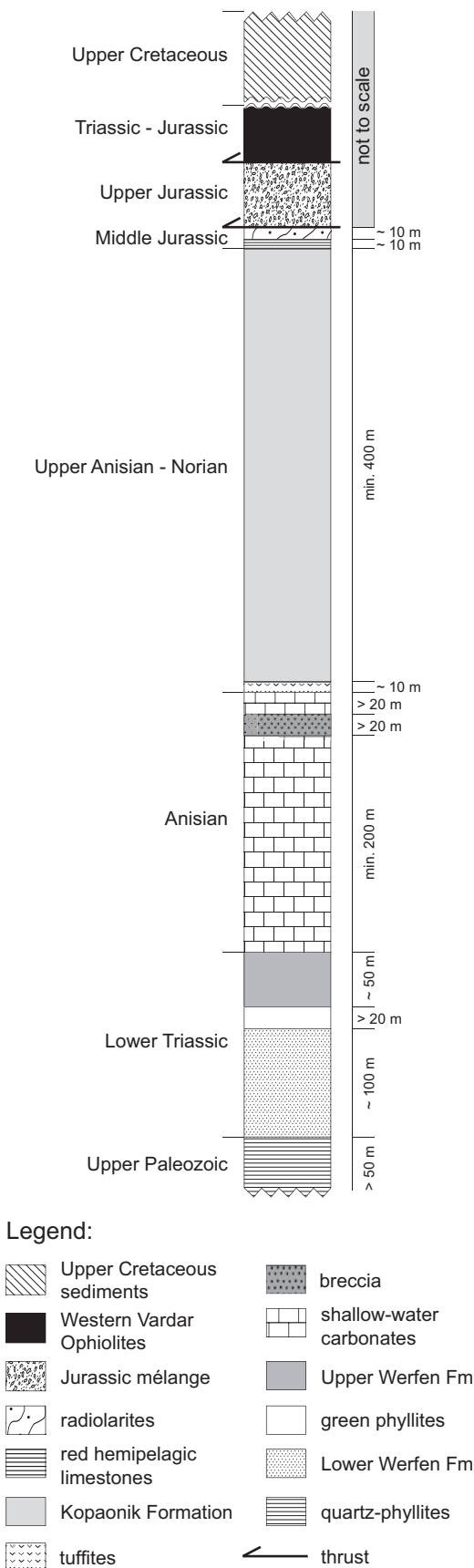


Fig. 2.13 – Synthetic sedimentary succession combining the stratigraphic columns of Fig. 2.12 a–d. The thicknesses are corrected for tectonic thinning according to the method of Ramsay & Huber (1983).

Eastern Alps and Western Carpathians (Krystyn 1971, Tollmann 1976, Gawlick et al. 2009), or of Toarcian–Middle Jurassic Rosso Ammonitico of the internal Hellenides (e.g. Baumgartner 1985). Similar condensed red Bositra limestones of Middle Jurassic age below siliceous sedimentary rocks were recently described also in SW Serbia (Radoičić et al. 2009) They are followed up-section by some metres of metamorphosed massive radiolarites of supposed late Middle to Late Jurassic age.

2.4.8 Ophiolitic mélangé

An ophiolite-bearing mélangé of considerable thickness tectonically overlies the Triassic–Jurassic succession in the Studenica section. In the Kopaonik area, the mélangé is thrust on top of the Kopaonik Formation while the sections Gradac 1 and Gradac 2 do not expose the contact to the mélangé. The mélangé contains, embedded in a brown to reddish mud matrix, blocks predominantly of serpentinite; basalts, turbiditic sandstones and carbonate rocks are also found as blocks. In the Studenica section the mélangé is often foliated due to a strong younger tectono-metamorphic overprint.

2.5 Regional correlation and reconstruction of the original sedimentary succession

Based on lithofacies and age dating we can correlate both the intensely folded strata of the Kopaonik area with the not visibly folded yet strongly foliated and metamorphosed strata from the sections Studenica and Gradac 1 and 2 (Fig. 2.12). It appears that all our sections are stratigraphically incomplete due to intense deformation leading to the thinning of strata. Hence each of the sections only reveals a part of what might be considered an originally complete stratigraphic succession for the study area.

According to our stratigraphic interpretation of the Studenica section, Ladinian as well as Carnian sediments are clearly missing in this section because the Anisian–Ladinian boundary tuffites are directly overlain by marbles yielding Norian (Lacian 1–2) conodonts that we attribute to the Kopaonik Formation. This omission of strata could have been caused by normal faulting; however, we were unable to detect normal faults in this section. On the other hand, strong penetrative deformation has reduced marbles and limestones in the Studenica section to 25% of their original

thickness as shown by a representative strain analysis of the breccia horizon (Egli 2008).

During mapping of the Kopaonik area, all Anisian shallow-water carbonates identified in the other profiles were included into one single formation ('shallow-water carbonates' in) because the succession is in most places too thin (or even lacking) to allow a subdivision into Gutenstein and/or Steinalm Formation. In this area, these formations are either stratigraphically reduced or tectonically thinned, or both.

In the Kopaonik area and in the section Gradac 2 the Kopaonik Formation mostly consists of typical fine-grained calcilutites with interbedded marls, cherty layers and nodules and calcarenites with some shallow-water material derived from a carbonate platform.

The overall sedimentary evolution of the Kopaonik Formation in the type-area can be summarized as follows: After shallow-water carbonate sedimentation prevailing during most of the Anisian, hemipelagic sedimentation started with a relatively thin succession of Upper Anisian to Ladinian grey cherty limestones that pass into a thick series of Lower Carnian limestones with some marls and few chert, followed by Upper Carnian to Lower Norian micritic limestones with an increase of cherts in the Middle Norian.

In the Studenica section the Kopaonik Formation is overlain by Jurassic hemipelagic limestones and radiolarites. These Jurassic sedimentary rocks occur a few metres above the Norian (Lacian 1–2) conodont-bearing horizon and testify to continuing subsidence of the distal continental margin before obduction of the ophiolites. In addition to continuing subsidence, shallowing of the calcite compensation depth (CCD) in the Middle–Late Jurassic, brought about by changes in plankton productivity, export of carbonate mud from adjacent platforms and in other paleoceanographic variables (e.g. Bernoulli & Jenkyns 2009), might have led to deposition of radiolarites near or below the CCD. The age of the distal continental-margin radiolarites is generally dated as Middle Jurassic in the internal Dinaride–Hellenide realm (e.g., Baumgartner 1985; Obradović & Goričan 1988; Djerić et al. 2007a, b), whereas the onset of radiolarite sedimentation in the more proximal parts of the continental margin occurred somewhat later (e.g., Charvet 1978; Obradović & Goričan 1988). Furthermore Middle Jurassic formation ages of ophiolitic mélanges in the Dinarides–Albanides (e.g., Goričan et al. 1999, 2005; Halamić et al. 1999; Babić et al. 2002; Chiari et al. 2002; Gawlick et al. 2008, 2009) suggest that early Late Jurassic obduction of the ophiolites was presumably preceded by the emplacement of olistostromes that were tectonically overprinted forming the mélanges below the ophiolites. In the closer Kopaonik region, however, sediments younger than the Kopaonik Formation were not found below the ophiolitic mélange, probably because obduction-related thrusts cut across older formations in this area.

Combining the four stratigraphic sections correlated in Fig. 2.12 with the other outcrops and the conodont data allows us to draw a reconstructed synthetic stratigraphic succession from the Upper Paleozoic up to the Upper Cretaceous showing the overall facies evolution (Fig. 2.13). Overlying an Upper Paleozoic basement, the some 100 m thick sedimentary succession starts with siliciclastic sediments, comparable to the Werfen Formation. A Late Permian onset of sedimentation cannot be excluded. Carbonate production started with the uppermost Werfen Formation, may be during the late Early Triassic, similar to the Southern or Eastern Alps. The Middle Triassic sequence starts with shallow-water carbonates (Gutenstein and Steinalm Formation equivalents), followed by Upper Anisian hemipelagic sediments in the wake of the drowning of the Steinalm ramp/platform. Hemipelagic carbonate sedimentation is proven for nearly the entire Middle and Late Triassic. The only preserved Jurassic sediments in the area consist of pelagic red metalimestones and radiolarites of probably Middle–?Late Jurassic age. These are followed by a ?Middle–Upper Jurassic ophiolitic mélange and the overriding West Vardar Ophiolites. From this reconstructed stratigraphic succession, where original thicknesses are estimated based on a representative strain determination (Egli 2008), it becomes clear that the original thickness of the Kopaonik Formation is at

least 400 metres. In the Kopaonik area, this is also apparent from the large outcrop areas appearing in the geological map (Fig. 2.4).

2.6 Discussion

Before discussing the paleogeographic setting of our study area in a wider context within the Alps–Carpathians–Dinarides system we compare the stratigraphy and facies of the study area with that of other parts of the Dinarides. The Mesozoic stratigraphy is rather well established in the more external units, i.e. in the main parts of the Drina–Ivanjica thrust sheet southwest of our study area (= ‘Zone de Golija’ of Aubouin et al. 1970) and in the East Bosnian–Durmitor thrust sheet (= ‘Zone Serbe’ of Aubouin et al. 1970), based on the work of Cadet (1970, 1978), Charvet (1970, 1978), Rampnoux (1970, 1974), Sudar (1986), Dimitrijević & Dimitrijević (1991), Dimitrijević (1997) and Sudar et al. (2008). In these areas a first platform-drowning event, which follows shallow-water carbonate sedimentation of the Gutenstein and Steinalm Formations is also recorded during the latest Anisian by the onset of condensed red pelagic limestones (Bulog Limestone of Rosso Ammonitico-type), first described by Hauer (1888, 1892). This facies is usually followed by volcanic tuffs that often occur around the Anisian/Ladinian boundary (Sudar 1986).

In our study area, the transition from shallow-water to hemipelagic sedimentation coincides with the occurrence of a breccia below the main tuffite horizon in the Studenica section. A similar breccia horizon (‘Podbukovi Conglomerate Member’) is observed in the uppermost Anisian dolomitic limestones of the Jablanica Formation (an equivalent of Steinalm limestone) of the Jadar–Kopaonik thrust sheet (i.e. in the ‘Jadar Block Terrane’ of Filipović et al. 2003). In the same area this breccia horizon is overlain by volcanics (metaandesites and accompanying pyroclastics of the Tronoša Formation).

According to our conodont data from Županj localities, the drowning in the Kopaonik area occurred during the latest Anisian (Fig. 2.13). Occasional calcarenites with shallow-water components in the ?Lower Carnian succession suggest redeposition of carbonate material derived from carbonate platforms, together with shedding of fine carbonate silt and lutum from the platforms during sea-level highstands (Schlager et al. 1994). This may explain the relatively high sedimentation rates during this time interval. A hemipelagic/deep-benthic setting, equivalent to the grey Hallstatt facies of the Eastern Alps–Western Carpathians (Lein 1987) is in line with the faunal content (radiolarians, conodonts, pelagic bivalves).

The most important facies difference with respect to the more external parts of the Drina–Ivanjica thrust sheet (including strata within so-called ‘olistoplacka’, which Dimitrijević (1997) interpreted as gravitationally emplaced olistoliths and that we consider as an integral part of the Drina–Ivanjica thrust sheet) and part of the East-Bosnian–Durmitor thrust sheet is, that the strata found up-section from the Bulog Limestone and the tuffites are typically shallow-water carbonate sequences, i.e. equivalents of the Late Ladinian to Carnian Wetterstein and the Norian to Rhaetian Dachstein formations (Dimitrijević & Dimitrijević 1991; Sudar et al. 2008). In some localities within these two more external thrust sheets, however, a base-of-slope to basinal hemipelagic facies of poorly known age (Middle to Late Triassic and/or Early to Middle Jurassic?) develops, that resembles the Kopaonik Formation (Fig. 2.13). It also consists of detrital carbonate and siliceous sediments and was referred to as Grivska Formation by Dimitrijević (1997). In the more external East-Bosnian–Durmitor thrust sheet Rampnoux (1970, 1974) described a similar basinal facies, his ‘calcaires lités pélagiques à silex’, for example from the ‘sillon de Zlatar’, which should be bordered, according to this author, by Wetterstein- and Dachstein-type platforms. The Grivska Formation and the age-equivalent Wetterstein and Dachstein platforms are overlain by Jurassic hemipelagic limestone

and radiolarites (Djerić et al. 2007a, b; Vishnevskaya et al. 2009) similar to those above the Kopaonik Formation in the Studenica section, followed by the ophiolitic mélangé. Carnian to Norian cherty limestones with conodonts (Gučevo Limestone) were also described from other parts of the Jadar–Kopaonik thrust sheet ('Jadar Zone' of Sudar 1986, 'Jadar Block Terrane' of Filipović et al. 2003).

In spite of some lithological similarities between the Grivska and the Kopaonik Formation we like to emphasize that the limestone succession of the Grivska Formation includes significantly more shallow-water debris from the nearby Ladinian to Rhaetian carbonate platforms. In addition, the Grivska Formation appears to be restricted to the more external paleogeographic domain (the Drina–Ivanjica and the East-Bosnian–Durmitor thrust sheets). Moreover, Bulog-type limestones and equivalents of the Wetterstein and Dachstein Formations were not found in our area. All this suggests that the grey hemipelagic sequences of the Kopaonik Formation, though yielding fine-grained shallow-water debris, represent a more distal facies of the Adriatic margin.

A paleogeographic position of the facies of the Kopaonik Formation at the distal Adriatic margin adjacent to the Neotethys (i.e. the Meliata–Maliac–Vardar Ocean) becomes even more convincing when we compare our area with the Eastern Alps and the Albanides–Hellenides. In the Northern Calcareous Alps of Austria (Lein 1987) and the Korabi–Pelagonia zone in Albania (Meco & Aliaj 2000; Gawlick et al. 2008), similar deposits are interpreted to have been deposited in a distal continental margin position (Haas et al. 1995; Gawlick et al. 1999, 2008) after rifting began during the Late Pelsonian leading to the opening of the Neotethys (Vardar–Meliata branch of Velliedits 2006). The Kopaonik Formation resembles also the so-called 'grey Hallstatt facies' or Zlambach facies zone (Pötschen Limestone) of the Eastern Alps (e.g. Lein 1987; Gawlick 2000). It further resembles the Felsőtárkány Limestone Formation in the Bükk Mountains (Kozur 1991; Less et al. 2005), as well as coeval deep-water limestones in the Korabi–Pelagonia zone of Albania (Gawlick et al. 2008). A paleogeographic derivation of the Kopaonik Formation close to the Meliata–Maliac–Vardar branch of the Neotethys is also suggested by the similarity with the Adhami Limestone that occurs in the distal part of the internal Pelagonian continental margin in the Argolis area of Greece and separates the shallow-water platforms (Pantokrator Limestone) of the more proximal margin from the oceanic realm (Baumgartner 1985).

Almost all the occurrences of Middle to Upper Triassic chert-rich deep-water limestones occur on the distal parts of the continental margin facing the Meliata–Maliac–Vardar Ocean. Towards the more proximal areas of the margin, the sites of hemipelagic deposition were linked to coeval carbonate platforms (Wetterstein, Dachstein platforms). Also the depositional area of the Kopaonik Formation must have been connected to one or more Middle to Upper Triassic rimmed carbonate platforms, like those preserved in the more external parts of the Dinarides, whereby the grain size and amount of the redeposited material decreases distally as can be observed from the Durmitor area across the Drina–Ivanjica zone to the Kopaonik area. Still, other carbonate platforms may have been present along the ocean–continent boundary, the deeper areas forming embayments like the modern Tongue of the Ocean. However, there seems to exist a general trend from the external to the internal Dinarides from shallow-water to pelagic near-oceanic environments. Applying Occam's razor (Thorburn 1918), we opt for a simple continental margin model. In fact, the paleogeographic location of the Jadar–Kopaonik thrust sheet is analogous to that of the Hallstatt facies of the Eastern Alps and to that of the depositional areas of similar facies in Albania or Greece adjacent to oceanic units attributed to the Meliata–Maliac–Vardar branch of the Neotethys and may represent the most distal parts of the Adriatic continental margin. Our data are conform with the one-ocean-hypothesis and an origin of all ophiolites, including the so-called Dinaridic ophiolites, from east of the

Drina–Ivanjica and Kopaonik units.

2.7 Conclusions

The metamorphic sedimentary succession of the Jadar–Kopaonik thrust sheet in the most internal Dinarides in southern Serbia includes a succession from the Upper Paleozoic terrigenous sediments to the Upper Jurassic ophiolitic mélangé and the Western Vardar ophiolites obducted in Late Jurassic time. Lower Triassic siliciclastics and limestones are overlain by Anisian shallow-water carbonates. A drowning event during the latest Anisian resulted in the deposition of a grey hemipelagic limestone succession characterized by fine-grained redeposited and often silicified calcarenites, shed by low-density turbidites from a carbonate platform. New conodont faunas date this hemipelagic sequence as Late Anisian to Norian, possibly extending into the Early Jurassic, which makes it to an equivalent of the grey Hallstatt facies of the Eastern Alps. The younger sediments overlying the Kopaonik Formation are red hemipelagic limestones and radiolarites of probably Middle–Late Jurassic age; they suggest that deep-pelagic conditions preceded the obduction of the Western Vardar Ophiolitic Unit.

Sedimentation of the hemipelagic Kopaonik Formation was contemporaneous with shallow-water carbonate production in nearby carbonate platforms that were part of the same passive continental margin. Most of these platforms were located on the more proximal parts of the Adriatic margin, whereas the distal margin was dominated by pelagic and distal turbiditic sedimentation, facing the evolving ocean to the east. Our data are in line with a continental margin model in which the facies belts are arranged in a logical order from the proximal margin to the Neotethys Ocean. In our interpretation the Drina–Ivanjica and Kopaonik thrust sheets expose the most distal portions of the Adriatic margin, emerging in tectonic windows below one and the same ophiolite nappe referred to as Western Vardar Ophiolitic Unit (including the so-called Dinaridic ophiolites) derived from the east and overthrusting the Durmitor zone.

We see no evidence for one or several independent Triassic oceans between the Adria, the Drina–Ivanjica and/or the Kopaonik areas. The sedimentological and stratigraphic evolution of the different areas reflects the transition from a proximal to a distal continental margin.

Acknowledgments

We thank S. Kovács and S. Kövér (Budapest) who participated in the field campaign for their valuable discussions and support, and J. Charvet and J. Michalik for thoughtful reviews. This project was financed by the Swiss National Fonds, Project No. 200020-109278 to S. M. Schmid, B. Fügenschuh and S. Schefer. The research of M. Sudar and D. Jovanović was supported by the Ministry of Science and Technological Development of the

Republic of Serbia, Project No. 146009.

References

- Aubouin J., Blanchet R., Cadet J.-P., Celet P., Charvet J., Chorowicz J., Cousin M. & Rampnoux J.-P. 1970: Essai sur la géologie des Dinarides. *Bull. Soc. Géol. France sér. 7*, 12, 1060–1095.
- Babić L., Hochuli P.A. & Zupanić J. 2002: The Jurassic ophiolitic mélange in the NE Dinarides: Dating, internal structure and geotectonic implications. *Eclogae Geol. Helv.* 95, 263–275
- Baumgartner P.O. 1985: Jurassic sedimentary evolution and nappe emplacement in the Argolis Peninsula (Peloponnesus; Greece). *Mém. Soc. Helv. Sci. Nat.* 99, 1–111.
- Bernoulli D. & Laubscher H. 1972: The palinspastic problem of the Hellenides. *Eclogae Geol. Helv.* 65, 107–118.
- Bernoulli D. & Jenkyns H.G. 2009: Ancient oceans and continental margins of the Alpine-Mediterranean Tethys: deciphering clues from Mesozoic pelagic sediments and ophiolites. *Sedimentology* 56, 149–190.
- Brković T., Malešević M., Urošević M., Trifunović S. & Radovanović Z. 1976: Basic Geological Map of the SFRY, 1:100'000, Sheet Ivanjica (K34–17), *Sav. geol. zavod, Beograd (Zav. geol. geofiz. istraž., Beograd, 1968)*.
- Brković T., Malešević M., Urošević M., Trifunović S., Radovanović Z., Dimitrijević M. & Dimitrijević M.N. 1977: Geology of the Sheet Ivanjica (K34–17), Explanatory notes, *Sav. geol. zavod, Beograd, (Zav. geol. geofiz. istraž., Beograd, 1968)*, 61 pp. (in Serbian, English and Russian summaries).
- Burnett R. D., Higgins A. C. & Austin R. L. 1994: Carboniferous-Devonian CAI in England, Wales and Scotland. The pattern and its interpretation: a synoptic review. *Cour. Forsch.-Inst. Senckenberg* 168, 267–280.
- Cadet J.-P. 1970: Esquisse géologique de la Bosnie-Herzégovine méridionale et du Monténégro occidental. *Bull. Soc. Géol. France sér. 7*, 12, 973–985.
- Cadet J.-P. 1978: Essai sur l'évolution alpine d'une paléomarge continentale: Les confins de la Bosnie-Herzégovine et du Monténégro (Yougoslavie). *Mém. Soc. Géol. France* 133, 1–84.
- Channell J.E.T. & Kozur H.W. 1997: How many oceans? Meliata, Vardar, and Pindos oceans in Mesozoic Alpine paleogeography. *Geology* 25, 183–186.
- Charvet J. 1970: Aperçu géologique des Dinarides aux environs du méridien de Sarajevo. *Bull. Soc. Géol. France sér. 7*, 12, 986–1002.
- Charvet J. 1978: Essai sur un orogène alpin. Géologie des Dinarides au niveau de la transversale de Sarajevo (Yougoslavie). *Soc. Géol. Nord Publ.* 2, 1–554.
- Chiari M., Marcucci M. & Prela M. 2002: New species of Jurassic radiolarians in the sedimentary cover of ophiolites in the Mirdita area, Albania. *Micropaleontology* 48 (Supplement 1), 61–87.
- Dimitrijević M. D. 1997: Geology of Yugoslavia. *Geol. Inst. Gemini, Spec. Publ.*, Barex, Belgrade, 187 pp.
- Dimitrijević M. D. 2001: Dinarides and the Vardar Zone: a short review of the geology. In: Downes H. & Vaselli O. (Eds.): Tertiary magmatism in the Dinarides. *Acta Vulcanol.* 13(1–2), 1–8.
- Dimitrijević M. N. & Dimitrijević M. D. 1991: Triassic carbonate platform of the Drina-Ivanjica element (Dinarides). *Acta Geol. Hung.* 34(1/2), 15–44.
- Djerić N., Vishnevskaya V. S. & Schmid S. M. 2007a: New data on radiolarians from the Dinarides (Bosnia and Serbia). *8th Alpine Workshop Davos, 10–12. October 2007, Abstract Volume*, 17–18.

- Djerić N., Gerzina N. & Schmid S.M. 2007b: Age of the Jurassic radiolarian chert formation from the Zlatar mountain (SW Serbia). *Ofioliti* 32, 101–108.
- Egli D. 2008: Das Kopaonik-Gebirge in Südserbien – Stratigraphie, Strukturen und Metamorphose. *Master thesis at Geologisch-Paläontologisches Institut*, Basel University, 1–97.
- Epstein A.G., Epstein J.B. & Harris L.D. 1977: Conodont Colour Alteration - An index to organic metamorphism. *U.S.Geol. Survey Prof. Paper* 995, Washington D.C., 1–27.
- Ferrière J. 1982: Paléogéographie et tectonique superposés dans les Hellenides internes: les massifs de l'Othrys et du Pélion (Grèce septentrionale). *Soc.Géol. Nord* 8, 1–970.
- Filipović I., Jovanović D., Sudar M., Pelikán P., Kovács S., Less G. & Hips K. 2003: Comparison of the Variscan – Early Alpine evolution of the Jadar Block (NW Serbia) and “Bükkium” (NE Hungary) terranes; some paleogeographic implications. *Slovak Geol. Mag.* 9, 23–40.
- Gawlick H.-J. 2000: Paläogeographie der Ober-Trias Karbonatplattform in den nördlichen Kalkalpen. *Mitt. Ges. Geol. Bergbaustud. Österreich.* 44, 45–95.
- Gawlick H.-J., Frisch W., Vecsei A., Steiger T. & Böhm F. 1999: The change from rifting to thrusting in the Northern Calcareous Alps as recorded in Jurassic sediments. *Geol. Rundsch.* 87, 644–657.
- Gawlick H.-J., Frisch W., Hoxha L., Dumitrica P., Krystyn L., Lein R., Missoni S. & Schlagintweit F. 2008: Mirdita Zone ophiolites and associated sediments in Albania reveal Neotethys Ocean origin. *Intl. J. Earth Sci.* 97, 865–881.
- Gawlick H.-J., Sudar M., Suzuki H., Djerić N., Missoni S., Lein R. & Jovanović D. 2009: Upper Triassic and Middle Jurassic radiolarians from the ophiolitic mélange of the Dinaridic Ophiolite Belt, SW Serbia. *N. Jb Geol. Paläont. – Abh.* 253, 293–311.
- Gawlick H.-J., Missoni S., Schlagintweit F., Suzuki H., Frisch W., Krystyn L., Blau J. & Lein R. 2009: Jurassic Tectonostratigraphy of the Austroalpine domain. *J. Alpine Geol.* 50, 1–152, Wien.
- Goričan Š., Slovenec D. & Kolar-Jurkovšek T. 1999: A Middle Jurassic Radiolarite-Clastic Succession from the Medvednica Mt. (NW Croatia). *Geol. Croat.* 52, 29–57.
- Goričan Š., Halamić J., Grgasović T. & Kolar-Jurkovšek T. 2005: Stratigraphic evolution of Triassic arc-backarc system in northwestern Croatia. *Bull. Soc. géol. France* 176, 1, 3–22.
- Grubić A., Djoković I. & Marović M. 1995: Tectonic outline of the Kopaonik area. In: Symposium “Geology and Metallogeny of the Kopaonik Mt.” (June 19–22, 1995), Kopaonik–Belgrade, 46–53 (in Serbian, English abstract).
- Haas J., Kovács S., Krystyn L. & Lein R. 1995: Significance of Late Permian-Triassic facies zones in terrane reconstructions in the Alpine-North Pannonian domain. *Tectonophysics* 242, 19–40.
- Halamić J., Goričan Š., Slovenec D. & Kolar-Jurkovšek T. 1999: A Middle Jurassic radiolarite-clastic succession from the Medvednica Mt. (NW Croatia). *Geol. Croat.* 52, 29–57.
- Harris A.G. 1979: Conodont Color Alteration, an organomineral metamorphic index, and its application to Appalachian Basin geology. *SEPM Spec. Publ.* 26, 3–16.
- Hauer F. von 1888: Die Cephalopoden des bosnischen Muschelkalkes von Han Bulog bei Sarajevo. *Denkschr. Akad. Wiss. Wien, Math.-Natw. Kl.* 54, 1–50.
- Hauer F. von 1892: Beiträge zur Kenntnis der Cephalopoden aus der Trias von Bosnien. I. Neue Funde aus dem Muschelkalk von Han Bulog bei Sarajevo. *Denkschr. Akad. Wiss. Wien, Math.-Natw. Kl.* 59, 232–296.

- Hips K. 2006: Facies pattern of western Tethyan Middle Triassic black carbonates: The example of Gutenstein Formation in Silica Nappe, Carpathians, Hungary, and its correlation to formations of adjoining areas. *Sediment. Geol.* 194, 99–114.
- Karamata S. 2006: The geological development of the Balkan Peninsula related to the approach, collision and compression of Gondwanan and Eurasian units. In: Robertson A.H.F., Mountrakis D. (Eds). Tectonic Development of the Eastern Mediterranean Region. *Geol. Soc. (London) Spec. Publ.* 260, 155–178.
- Klasić M., Mičić I., Pajić V., Simić D. & Kandić M. 1972: Contribution to the stratigraphy of the Trepča metamorphic series. *Zapiski Srp. geol. druš. za 1968, 1969 i 1970* (Zbor 10. XII 1968), 105–107 (in Serbo-Croatian, Cyrillic).
- Königshof P. 1992: Der Farbänderungsindex von Conodonten (CAI) in paläozoischen Gesteinen (Mitteldevon bis Unterkarbon) des Rheinischen Schiefergebirges. Eine Ergänzung zur Vitrinitreflexion. *Cour. Forsch.-Inst. Senckenberg* 146, 1–118.
- Kossmat F. 1924: Geologie der zentralen Balkanhalbinsel, mit einer Übersicht des dinarischen Gebirgsbaus. In: Wilder J. (Ed.): Die Kriegsschauplätze 1914–1918 geologisch dargestellt. *Verlag Gebrüder Bornträger*, Berlin, 198pp.
- Knežević V., Karamata S., Vasković N. & Cvetković V. 1995: Granodiorites of Kopaonik and contact metamorphic zone. In: Symposium “Geology and Metallogeny of the Kopaonik Mt.” (June 19–22, 1995), Kopaonik–Beograd, 172–184 (in Serbian, English abstract).
- Kozur H. W. 1991: The evolution of the Meliata-Hallstatt ocean and its significance for the early evolution of the Eastern Alps and Western Carpathians. *Palaeogeography, Palaeoclimatology, Palaeoecology* 87, 109–135.
- Krystyn L. 1971: Stratigraphie, Fauna und Fazies der Klaus-Schichten (Aalenium-Oxford) in den östlichen Nordalpen. *Verh. Geol. B.-A.*, 1971/3: 486–509, Wien.
- Lein R. 1987: Evolution of the Northern Calcareous Alps during Triassic times. In: Flügel, H.W. & Faupl, P. (Eds.): Geodynamics of the Eastern Alps), *Deuticke*, Wien, 85–102
- Less G., Kovács S., Pelikán P., Pentelényi P. & Sásdi L. 2005: In: Pelikán P. (Ed.) Geology of the Bükk Mountains, Regional map series of Hungary, Explanatory Book of the Geological map of the Bükk Mountains (1:50'000), Magyar Állami Földtani Intézet, Budapest (in Hungarian, English summary), 284 pp.
- Meco S. & Aliaj S. 2000: Geology of Albania. *Beiträge zur regionalen Geologie der Erde*, 28, *Schweizerbart*, Stuttgart, 1–246.
- Mičić I., Urošević D., Kandić M., Klasić M. & Simić D. 1972: Findings of Triassic conodont fauna in the metamorphic complex of Kopaonik Mt. *Zapiski Srp. geol. druš. za 1968, 1969 i 1970* (Zbor 10. XII 1968), 103–104 (in Serbian, Cyrillic).
- Mojsilović S., Baklajić D. & Djoković I. 1978: Basic Geological Map of the SFRY, 1:100'000, Sheet Sjenica (K32-29), *Sav. geol. zavod, Beograd (Geozavod – OOUR Geološki institut, Beograd, 1960-1973)*.
- Mojsilović S., Djoković I., Baklajić D. & Rakić B. 1980: Geology of the Sheet Sjenica (K32–29), Explanatory notes, *Sav. geol. zavod, Beograd, (Zav. geol. geofiz. istraž., Beograd, 1973)*, 46 pp. (in Serbo-Croatian, English and Russian summaries).
- Nöth S. 1991: Die Conodontendiagenese als Inkohlungsparameter und ein Vergleich unterschiedlich sensitiver Diageneseindikatoren am Beispiel von Triassedimenten Nord- und Mitteldeutschlands. *Bochumer Geol. Geotechn. Arb.* 37, 1–169.

- Obradović J. & Goričan Š. 1988: Siliceous Deposits in Yugoslavia: Occurrences, Types and Ages. In: Hein J.R. & Obradović J. (Eds.): *Siliceous Deposits of the Tethys and Pacific Regions*, New York (Springer-Verlag), 51–64.
- Radoičić R., Jovanović D. & Sudar, M.N. (2009): Stratigraphy of the Krs Gradac section (SW Serbia). *Ann. Géol. Péninsule Balkanique* 70, 23–41, Belgrade.
- Rampoux J.-P. 1970: Regard sur les Dinarides internes yougoslaves (Serbie-Monténégro oriental): stratigraphie, évolution paléogéographique, magmatisme. *Bull. Soc. Géol. France sér. 7*, 12, 948–966.
- Rampoux J.-P. 1974: Contribution à l'étude géologique des Dinarides: Un secteur de la Serbie méridionale et du Monténégro oriental (Yougoslavie). *Mém. Soc. Géol. France, n. sér.* 119, 1–99.
- Ramsay J. G. & Huber M. I. 1983: The Techniques of Modern Structural Geology Volume 1: Strain Analysis, *Academic Press*, London, 1–307.
- Rejebian V.A., Harris A.G. & Huebner J.S. 1987: Conodont colour and textural alteration: an index to regional metamorphism and hydrothermal alteration. *Geol. Soc. Am. Bull.* 99, 471–479.
- Robertson A.H.F. & Karamata S. 1994: The role of subduction-accretion processes in the tectonic evolution of the Mesozoic Tethys in Serbia. *Tectonophysics* 234, 73–94.
- Robertson A., Karamata S. & Šarić K. 2009: Overview of ophiolites and related units in the Late Paleozoic–Early Cenozoic magmatic and tectonic development of Tethys in the northern part of the Balkan region. *Lithos* 108, 1–36.
- Schefer S., Egli D., Frank W., Fügenschuh B., Ovtcharova M., Schaltegger U., Schoene B. & Schmid S.M. 2008: Metamorphic and igneous evolution of the innermost Dinarides in Serbia. *Abstract Volume 6th Swiss Geoscience Meeting Lugano*, 60–61.
- Schlager W., Reijmer J.J.G. & Droxler A. 1994: Highstand shedding of carbonate platforms. *J. Sediment. Res.* B64, 270–281.
- Schlagintweit F., Gawlick H.-J., Missoni S., Hoxha L., Lein R. & Frisch W. 2008: The eroded Late Jurassic Kurbanesh carbonate platform in the Mirdita Ophiolite Zone of Albania and its bearing on the Jurassic orogeny of the Neotethys realm. *Swiss J. Geosci.* 101, 125–138.
- Schmid S. M., Bernoulli D., Fügenschuh B., Matenco L., Schefer S., Schuster R., Tischler M. & Ustaszewski K. 2008: The Alpine-Carpathian-Dinaridic orogenic system: correlation and evolution of tectonic units. *Swiss J. Geosci.* 101, 139–183.
- Simić V. 1956: Zur Geologie des Studenica-gebietes (Südwestserbien). *Vesnik Bull. Serv. Geol. Geophys.* 12, 5–66 (in Serbo-Croatian, with German summary).
- Stampfli G.M. & Borel G. 2004: The TRANSMED transects in space and time: constraints on the paleotectonic evolution of the Mediterranean domain. In: Cavazza W., Roure F.M., Spakman W., Stampfli G.M. & Ziegler P.A. (Eds): *The TRANSMED Atlas: The Mediterranean Region from Crust to Mantle*. Springer, Berlin and Heidelberg, 53–80.
- Sudar M. 1986: Triassic microfossils and biostratigraphy of the Inner Dinarides between Gučevo and Ljubišnja Mts., Yugoslavia. *Ann. Géol. Péninsule Balkanique* 50, 151–394 (in Serbo-Croatian, English summary).
- Sudar M. & Kovács S. 2006: Metamorphosed and ductilely deformed conodonts from Triassic limestones situated beneath ophiolite complexes: Kopaonik Mountain (Serbia) and Bükk Mountains (NE Hungary) – a preliminary comparison. *Geol. Carpathica* 57(3), 157–176.

- Sudar M., Gawlick H.-J., Lein R., Missoni S., Jovanović D. & Krystyn L. 2008: Drowning and block tilting of Middle Anisian carbonate platform in the Middle Jurassic Zlatibor mélangé of the Dinaridic Ophiolite Belt (SW Serbia). *J. Alpine Geol.* 49, 106–107.
- Thorburn W. M. 1918: The Myth of Occam's Razor. *Mind* 27(107), 345–353.
- Tollmann A. 1976: Analyse des klassischen nordalpinen Mesozoikums. *Deuticke*, Wien, 1–580.
- Urošević M., Pavlović Z., Klisić M., Brković T., Malešević M. & Trifunović S. 1970a: Basic Geological Map of the SFRY, 1:100'000, Sheet Novi Pazar (K34–3), *Sav. geol. zavod, Beograd (Zav. geol. geofiz. istraž., Beograd, 1966)*.
- Urošević M., Pavlović Z., Klisić M., Brković T., Malešević M. & Trifunović S. 1970b: Basic Geological Map of the SFRY, 1:100'000, Sheet Vrnjci (K34–18), *Sav. geol. zavod, Beograd (Zav. geol. geofiz. ispit., Beograd, 1966)*.
- Urošević M., Pavlović Z., Klisić M., Karamata S., Malešević M. Stefanović K., Marković O. & Trifunović S. 1973a: Geology of Novi Pazar Sheet (K34–3), Explanatory notes, *Sav. geol. zavod, Beograd, (Zav. geol. geofiz. istraž., Beograd, 1966)*, 77 pp. (in Serbo-Croatian, English and Russian summaries).
- Urošević M., Pavlović Z., Klisić M., Malešević M., Stefanović M., Marković O. & Trifunović S. 1973b: Geology of Vrnjci Sheet (K34–18), Explanatory notes, *Sav. geol. zavod, Beograd, (Zav. geol. geofiz. ispit., Beograd, 1966)*, 69 pp. (in Serbo-Croatian, English and Russian summaries).
- Velledits F. 2006: Evolution of the Bükk Mountains (NE Hungary) during the Middle – Late Triassic asymmetric rifting of the Vardar-Meliata branch of the Neotethys. *Intl. J. Earth Sci.* 95, 395–412.
- Vishnevskaya V.S., Djerić N. & Zakariadze G.S. 2009: New data on Mesozoic Radiolaria of Serbia and Bosnia, and implications for the age and evolution of oceanic volcanic rocks in the Central and Northern Balkans. *Lithos* 108, 72–105,
- Zelić M., Levi N., Malasoma A., Marroni M., Pandolfi L. & Trivić B. 2010: Alpine tectono-metamorphic history of the continental units from Vardar zone: the Kopaonik Metamorphic Complex (Dinaric-Hellenic belt, Serbia). *Geol. J.* 45, 59–77, DOI: 10.1002/gj.1169.

3. Cenozoic granitoids in the Dinarides of southern Serbia: age of intrusion, isotope geochemistry, exhumation history and significance for the geodynamic evolution of the Balkan Peninsula

Senecio Schefer, Vladica Cvetković, Bernhard Fügenschuh, Alexandre Kounov, Maria Ovtcharova, Urs Schaltegger, Stefan M. Schmid

Accepted in International Journal of Earth Sciences, 29th of August 2010, online first

Abstract

Two age groups were determined for the Cenozoic granitoids in the Dinarides of southern Serbia by high precision single grain U–Pb dating of thermally annealed and chemically abraded zircons: (i) Oligocene ages (Kopaonik, Drenje, Željin) ranging from 31.7 to 30.6 Ma (ii) Miocene ages (Golija and Polumir) at 20.58–20.17 and 18.06–17.74 Ma, respectively. Apatite fission-track central ages, modelling combined with zircon central ages, and additionally, local structural observations constrain the subsequent exhumation history of the magmatic rocks. They indicate rapid cooling from above 300° to ca. 80°C between 16 and 10 Ma for both age groups, induced by extensional exhumation of the plutons located in the footwall of core-complexes. Hence, Miocene magmatism and core-complex formation not only affected the Pannonian basin but also a part of the mountainous areas of the internal Dinarides.

Based on an extensive set of existing age data combined with our own analyses we propose a geodynamical model for the Balkan Peninsula: The Late Eocene to Oligocene magmatism, which affects the Adria-derived lower plate units of the internal Dinarides, was caused by delamination of the Adriatic mantle from the overlying crust, associated with post-collisional convergence that propagated outward into the external Dinarides. Miocene magmatism, on the other hand, is associated with core-complex formation along the southern margin of the Pannonian basin, probably associated with the W-directed subduction of the European lithosphere beneath the Carpathians and interfering with ongoing Dinaridic–Hellenic back-arc extension.

Keywords: Periadriatic intrusions, Granitoids, Dinarides, U–Pb dating, Hf isotopes, Fission-track analysis

Introduction

Paleogene magmatic rocks within the Alpine–Carpathian–Pannonian–Dinaridic region occur in linear zones that surround the Adriatic plate (Periadriatic intrusions s.l.). At closer inspection three such linear zones can be distinguished (Fig. 3.1 and Kovács et al. 2007): (1) a belt that follows the Periadriatic line delimiting the Southern Alps from the rest of the Alps (Periadriatic intrusions s.str.; e.g. Rosenberg 2004), (2) an alignment along the Mid-Hungarian fault zone located within the Pannonian basin (e.g. Benedek 2002), and (3) a belt that follows the innermost Dinarides and extends across Bulgaria and northern Greece all the way to NW Turkey (e.g. Pamić et al. 2002a; Burchfiel et al. 2008). The distribution of the Neogene magmatic rocks within the Alpine-Carpathian-Pannonian-Dinaridic region, on the other hand, is by far more dispersed, many but by no means all of them being related to subduction in the Carpathians and the contemporaneous opening of the Pannonian basin (e.g. Seghedi et al. 2004). Only rarely is the Neogene magmatic activity spatially associated with Paleogene precursors, such as in the Pohorje region of Slovenia (Trajanova et al. 2008). The Neogene granites of Mt. Bukulja and Mt. Cer in northern Serbia have been studied by Karamata et al. (1992), Cvetković et al. (2007a) and Koroneos et al. (2010), and their petrogenesis has been attributed to the Pannonian extension. However, the Cenozoic granitoids in southern Serbia that are subject of this study remained very poorly studied in terms of their age and geodynamic significance.

This paper presents the results of high precision dating and Hf isotope analyses of the southern Serbian Kopaonik, Drenje, Željin, Golija, and Polumir intrusions (Fig. 3.2). These data are complemented by zircon and apatite fission-track data together and structural observations.

Additionally, the potential magmatic sources and the geodynamic setting of the Cenozoic intrusions in Serbia will be discussed within the frame of the entire Balkan Peninsula and adjacent areas, based on a recent compilation of tectonic units (Schmid et al. 2008). In particular, we shall discuss the much debated question as to whether the Paleogene Periadriatic intrusions of the Alps (Periadriatic intrusions s.str.) can be followed into the Mid-Hungarian fault zone and/or into the internal Dinarides and whether these intrusions represent the back-arc magmatism with respect to only one or two different subduction zones (Kovács et al. 2007), or alternatively, whether they are related to post-orogenic collapse of an overthickened crust in the internal Dinarides (Koroneos et al. 2010), mantle delamination and/or to extension in the Pannonian basin (e.g. Cvetković et al. 2007a). Sources for the magmatic activity in the Balkan Peninsula will be discussed by integrating the large amount of published age data on other granites and contemporaneous basaltic rocks (Cvetković et al. 2004a, b; Prelević et al. 2005). Also the formation of sedimentary basins, many of them associated with volcanics and/or volcanoclastics (e.g. Burchfiel et al. 2008), as well as information from seismic tomography (Piromallo and Morelli 2003), will be discussed in that context.

Regional geology

The Dinarides represent a complex orogen consisting of thrust sheets that contain ophiolitic as well as Adriatic-derived continental material. These thrust sheets are located in a lower plate position with respect to an upper plate formed by the Tisza and Dacia Mega-Units with European affinities (Schmid et al. 2008, Ustaszewski et al. 2009). Ophiolites, derived from the Vardar branch of the Neotethys Ocean (Fig. 3.1, ‘Western Vardar Ophiolitic Unit’), were obducted already during the latest Jurassic onto the Adriatic margin and later involved in Late Cretaceous to early Paleogene out-of-sequence thrusting. This led to the formation of a series of composite nappes that consist of continent-derived material in their lower part and ophiolitic material in the upper part.

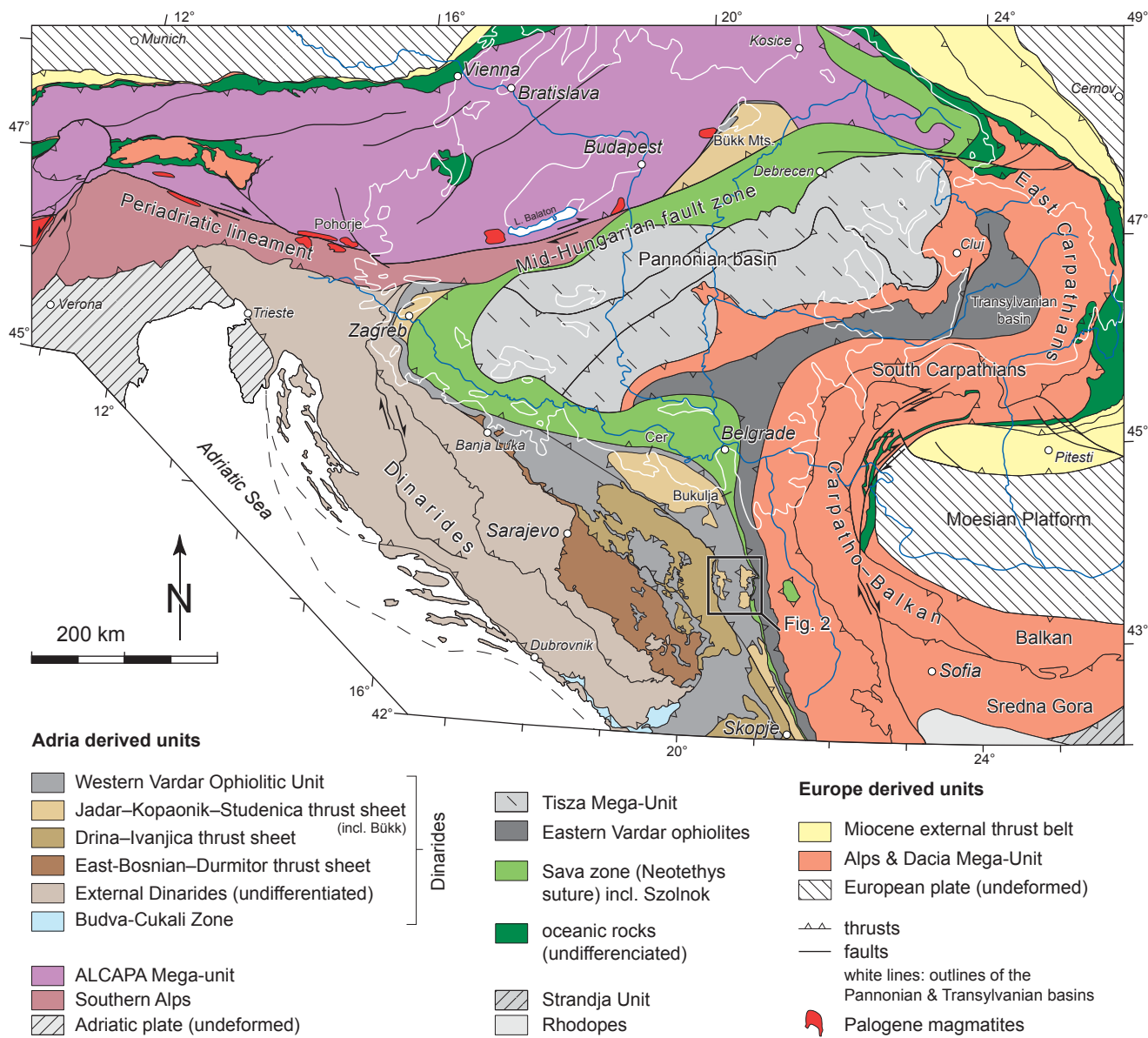


Fig. 3.1 – Tectonic map of the Alps, Carpathians and Dinarides, modified after Schmid et al. (2008). Note that only the Paleogene magmatites aligned along the Periadriatic lineament and the Mid-Hungarian fault zone are shown in this figure (Kovács et al. 2007). For Paleogene magmatites in the Balkan Peninsula see Fig. 3.10.

The area around the Kopaonik massif in southern Serbia exposes the two innermost Dinaridic composite nappes, namely the Drina–Ivanjica and the Jadar–Kopaonik–Studenica composite thrust sheets (Figs. 1 and 2; Schmid et al. 2008; Schefer et al. 2010). In the latest Cretaceous to Early Paleogene these innermost Dinaridic thrust sheets collided with the already existing (pre-Turonian) Carpatho–Balkan orogen that is part of the Dacia Mega-Unit and constitutes the upper plate of a complex collision zone (Schmid et al. 2008). A separating suture zone (Sava Zone) runs along the eastern rim of the innermost Dinarides, that is along the internal limit of the Jadar–Kopaonik–Studenica composite thrust sheet, and separates the Dinarides from the Carpatho–Balkan orogen (Fig. 3.1).

The N–S-trending mountain range in the wider Kopaonik area exposes a part of the Jadar–Kopaonik–Studenica thrust sheet as well as an exhumed deeper part of the deeper Drina–Ivanjica thrust sheet, both exposed in tectonic windows below the obducted ophiolites (Figs. 3.1 and 3.2). These windows are formed by the Kopaonik and the

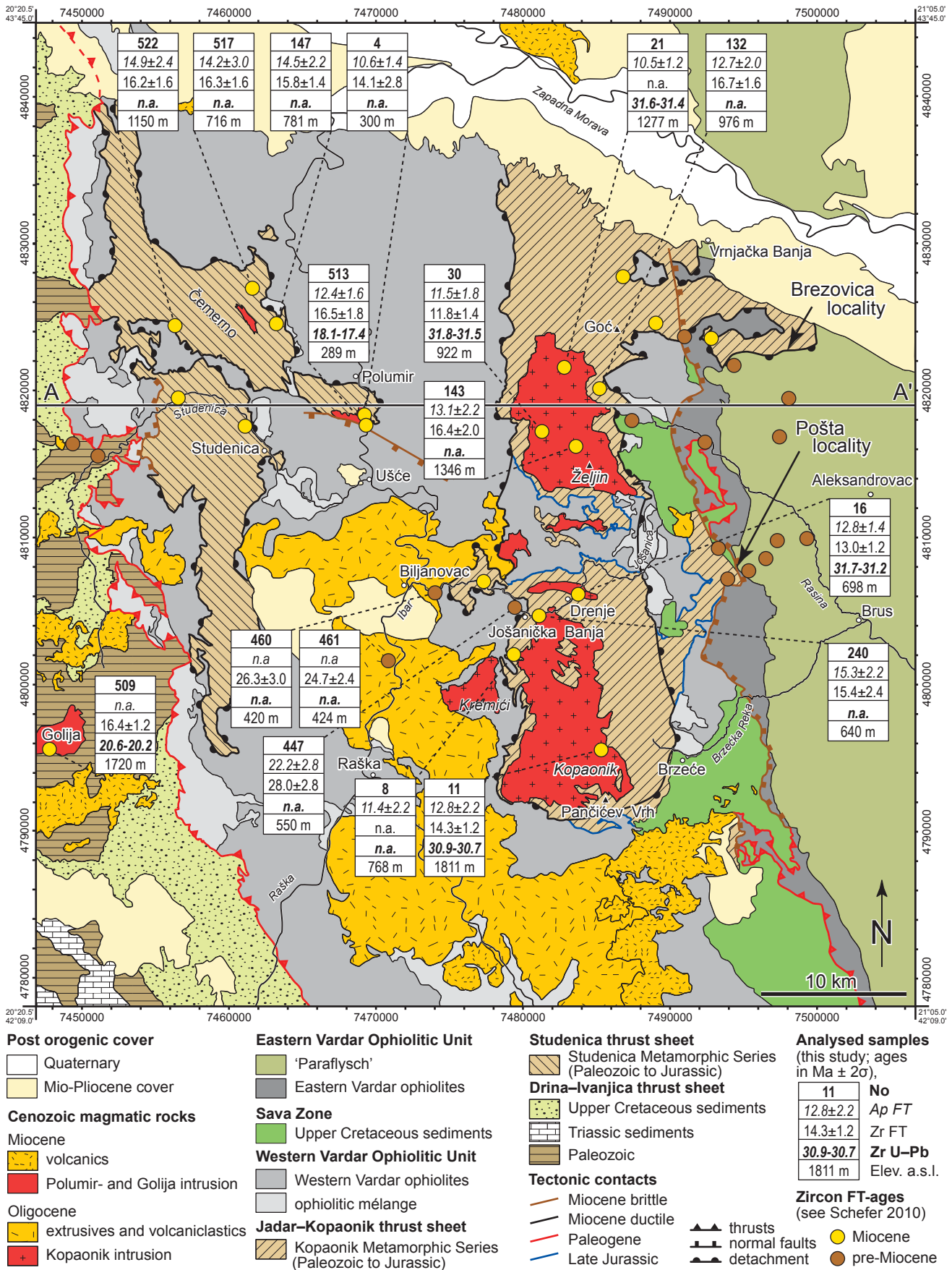


Fig. 3.2 – Tectonic map of the Kopaonik area with U–Pb and fission-track ages of the analysed samples (Tables 2 and 4), based on mapping by Schefer (2010) and on the Basic Geological Map of Yugoslavia (1:100'000),

Studenica Metamorphic Series, which consist of metamorphosed Upper Paleozoic to Lower Jurassic sediments of the distal Adriatic margin (Schefer et al. 2010). They are overlain by a (Middle?)–Upper Jurassic ophiolitic mélangé located below the obducted Western Vardar Ophiolitic Unit (Fig. 3.2). The two metamorphic series and the obducted ophiolites are unconformably overlain by post-Turonian sediments (Fig. 3.2; ‘Upper Cretaceous sediments’) that contain large olistoliths, including ophiolites and metamorphic rocks. This weakly metamorphosed N–S-trending ‘Senonian’ flysch belt, trending N–S along the eastern margin of the Kopaonik composite thrust sheet, is interpreted to represent the southern prolongation of the Sava zone, i.e. the suture between the internal Dinarides and the Carpatho-Balkan orogen (Ustaszewski et al. 2009; Ustaszewski et al. in press).

The Kopaonik Metamorphic Series east of the Ibar valley and the overlying Western Vardar Ophiolitic Unit were both intruded by the Kopaonik, Drenje and Željina granitoids (Fig. 3.2). Available structural data (Egli 2008; Schefer et al. 2008; Schefer 2010; Zelić et al. 2010) indicate that the intrusion of these plutons post-dates three phases of compressive deformation associated with thrusting in the internal Dinarides and suturing with the adjacent Carpatho-Balkan orogen, but pre-dates a latest D4 extensional deformation event associated with movements along normal faults that, although not observed within the plutons, will be shown to have led to their final exhumation.

While extension postdates the intrusion of the Kopaonik, Drenje and Željina intrusions it is at least partly contemporaneous with the emplacement of the younger Polumir granite. Extension is manifested by the following structures: (i) N–S stretching by ductile extensional deformation is mainly observed in the Studenica valley and around the Polumir intrusion in the Ibar valley (labelled ‘Miocene ductile’ in Fig. 3.2), (ii) ductile collapse folds characterized by sub-horizontal axial planes are found in the vicinity of the Kopaonik intrusion (Egli 2008) and (iii) brittle E–W and N–S trending normal faults (labelled ‘Miocene brittle’ in Fig. 3.2). Whereas ductile extension is exclusively associated with N–S stretching, brittle extension occurs along two contemporaneously active sets that lead to extension in both E–W and N–S direction. Furthermore, N-S striking brittle faults are seen to cut ductile E–W-striking faults, indicating that E–W-directed extension is younger. Post-Oligocene deformation is thus divided into two phases, an earlier ductile phase (D4a) and a later brittle phase (D4b).

A pronounced N–S-oriented stretching lineation and frequently observed boudins are the dominant macroscopic expression of the ductile D4a phase. Near Polumir locality in the Ibar valley (Fig. 3.2) the two-mica granite shows asymmetrically boudinaged dykes in the host rocks and S–C-fabrics both indicating top-N shearing (Fig. 3.3a,d). The dykes are progressively deformed under decreasing temperatures as indicated by kinematically consistent ductile to brittle faulting (Fig. 3.3c,d).

N–S-oriented extension is substantial within the entire study area. In the Studenica area this extension exhumes amphibolite-facies rocks in the form of a core-complex (Fig. 3.4). At the Brezovica locality (Fig. 3.2) large-scale shear bands found in meta-limestones of the Kopaonik Metamorphic Series exhume upper-most greenschist-facies rocks and bring them in contact with Cretaceous sediments referred to as ‘Paraflysch’ (cover of the Eastern Vardar ophiolitic Unit), thereby omitting the Eastern Vardar ophiolites, the Upper Cretaceous sediments of the Sava zone as well as the entire Western Vardar Ophiolitic Unit (see area around Brezovica locality in Fig. 3.2).

Brittle normal faults (D4b) are observed to affect all tectonic units throughout the entire study area at different scales. In many places brittle normal faults are seen to crosscut ductile detachments formed during D4a.

(Fig. 3.2 continued:) Sheets Novi Pazar (Urošević et al. 1970a), Vrnjci (Urošević et al. 1970b), Sjenica (Mojsilović et al. 1978) and Ivanjica (Brković et al. 1976) as well as Simić (1956) for the Studenica area. Numbers at the border of the map are MGI Balkan 7 Cartesian coordinates. ‘Miocene’ and ‘pre-Miocene’ zircon ages are unpublished data from Schefer (2010).

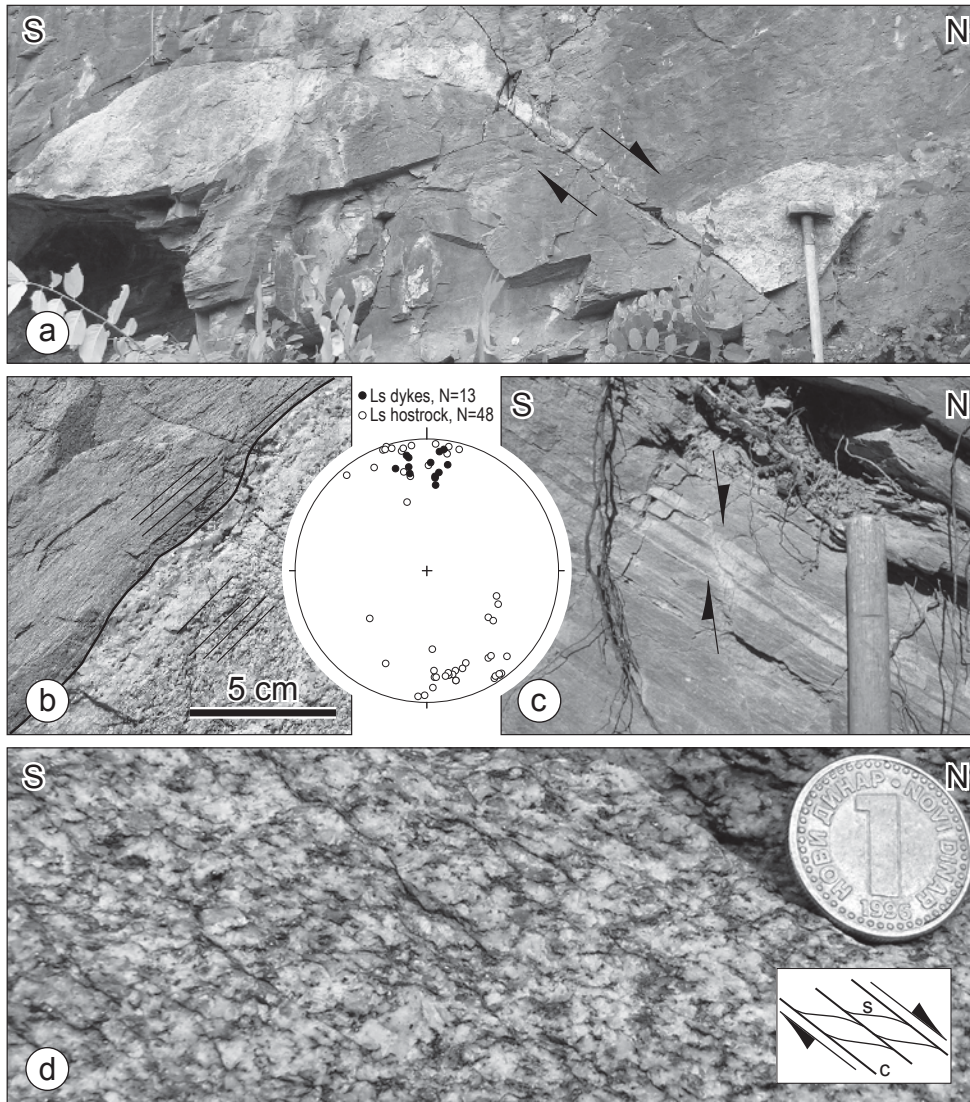


Fig. 3.3 – Structural features from the Polumir intrusion. **a** – Asymmetric boudinage indicating top-to-the-north extension (location 513 on Fig. 3.2). The stereoplot (lower hemisphere) compares stretching lineations from the dykes and the hostrocks (Studenica Metamorphic Series) showing N–S movement syn- to post intrusion of the Miocene Polumir granite. Ls=stretching lineation. **b** – The dykes intrude at a later stage of the foliation, but become foliated in the same way as the host-rock as observed along the margin of the dyke. **c** – Leucocratic layers in the mylonitized host-rocks offset by discrete normal faults, indicating that deformation continued into the brittle field with a similar orientation of the main stress-axis. **d** – C-S structures in the main body of the Polumir granite indicate top-to-the-north extensional deformation. Penetrative associations of foliation and ductile shear-bands usually develop during a retrogressive history from high to medium temperature. This scenario suits well with a syntectonic emplacement of the intrusion (Gapais 1989).

Small-scale normal faults, mainly expressed in serpentinised ophiolitic rocks, scatter in all directions. The major large-scale brittle normal faults, however, are N–S-striking. They border the core-complexes of the Studenica valley and the mountain chain of Kopaonik and Željina (Fig. 3.4). In between the two domes of Kopaonik and Željina mountains, E–W-striking brittle normal faults formed during D4b are also found (Fig. 3.2). The W-dipping D4b brittle normal fault at the western border of the Studenica dome is made up of several smaller faults that crosscut the former D4a detachment delimiting this core-complex to the west. Ductilely deformed amphibolite-facies rocks

are found in the footwall of this brittle normal fault whereas lower greenschist-facies rocks of the Studenica thrust sheet and formerly obducted ophiolitic rocks from the Western Vardar Ophiolitic Unit are exposed in its hanging wall (Figs. 2 and 4). The offset in metamorphic grade across this brittle fault is thus substantial, but most of this offset probably has to be attributed the D4a ductile precursor that was associated with N-S-directed extension and core-complex formation during D4a (faults marked ‘Miocene ductile’ in Fig. 3.2).

An E-dipping brittle normal fault is found at a locality referred to as ‘Pošta locality’ in Figs. 2 and 4. This brittle fault zone shows a sharp contact to the hanging-wall composed of fault gouges that include cataclastic fragments of ophiolitic rocks at its top, overprinting an older and more gently dipping foliation that might be associated with earlier N–S-oriented extension produced during D4a. Towards the base of the fault zone, the style of deformation changes from brittle to ductile, and an LS-tectonite exhibits top-E oriented shear-bands.

The main Kopaonik pluton produced a contact metamorphic aureole consisting of hornfels and skarns that formed at 1–2 kbar and ca. 550 °C according to Knežević et al. (1995). The Studenica Metamorphic Series that crop out in a window west of the Ibar valley are intruded by the Polumir granite (Fig. 3.2). The Polumir granite shows high-temperature ductile deformation along its intrusive margin. The Golija granodiorite, located further west of the main thrust that separates the Jadar–Kopaonik–Studenica and Drina–Ivanjica composite thrust sheets, intruded Upper Paleozoic slates, siltstones and sandstones of the Drina–Ivanjica composite thrust sheet (Fig. 3.2).

Suites of Oligocene to Miocene volcanic and volcanoclastic rocks are associated with these intrusions, representing their effusive equivalents. Most of the Oligocene volcanics intrude and/or overlie the ophiolites. They are confined to the Ibar Valley (Fig. 3.2) and are predominantly represented by extrusive to autoclastic dacitic/andesitic rocks. By contrast, the Miocene volcanics are quartzlatitic in composition and are represented by effusive and pyroclastic rocks. The latter were related to Plinian to sub-Plinian events and ignimbrite formation. The Miocene volcanic rocks occur in the surroundings of the Golija pluton as well as southeastward from the Kopaonik intrusives (Fig. 3.2). These rocks are poorly studied in

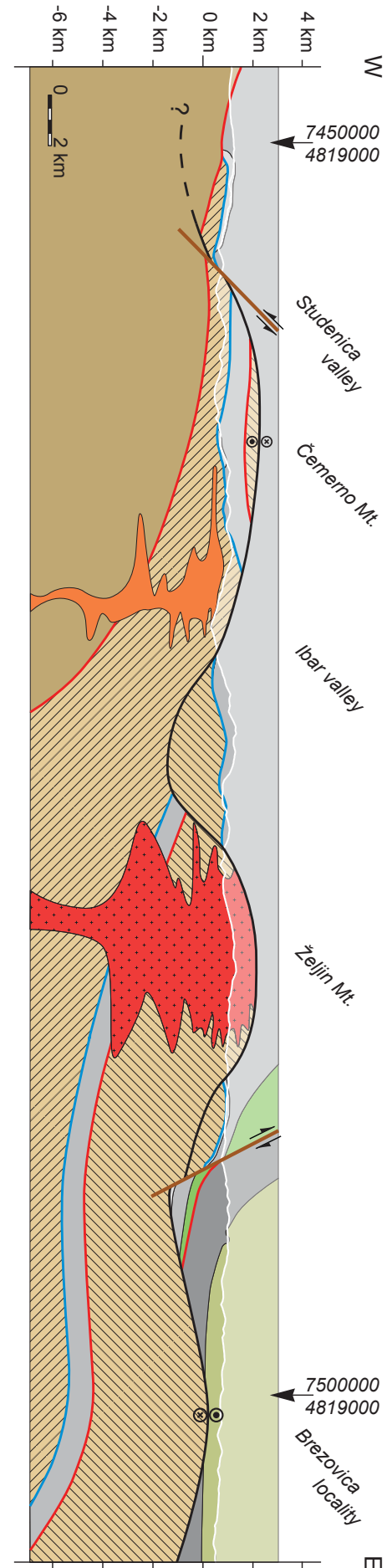


Fig. 3.4 – E–W-oriented cross-section across the entire study area; trace of profile is shown on Fig. 3.2. Ages of main activity along the major tectonic contacts are colour-coded as in Fig. 3.2.

contrast to their counterparts in the north (Cvetković and Pécskay 1999; Cvetković 2002).

Whereas the petrography of these intrusions and related volcanics is rather well known (e.g. Knežević et al. 1995; Vukov 1995), the geochronology is not yet well documented and high-precision U–Pb analyses are altogether missing. In a number of reviews (e.g. Karamata et al. 1992; Knežević et al. 1995; Prelević et al. 2001) the intrusive rocks of southern Serbia were separated into two different groups based on mineral and whole rock K–Ar ages: An Oligocene group including Kopaonik and its satellite Kremići and a Miocene group comprising the Željina, Golija, Drenje and Polumir intrusions (Fig. 3.2). While according to the existing literature the Oligocene group is regarded to represent I-type granites (Karamata et al. 1992; Knežević et al. 1995), the presumed Miocene group supposedly consists of both I-type (Željina, Golija and Drenje; Karamata et al. 1992) and S-type granitoids (Polumir; Vukov 1995; Vukov and Milovanović 2002). However, similarities in style of intrusion, as well as the close neighbourhood of the Kopaonik, Drenje and Željina intrusions suggest that they might be closely related and cogenetic. Cvetković et al. (2002), based on geochemical data, even proposed a co-magmatic evolution of the Kopaonik and Drenje intrusives, although this suggestion was in conflict with differences in their K–Ar radiometric ages as reported by Delaloye et al. (1989). Hence, at least part of the K–Ar age data seem suspicious and thus need closer inspection.

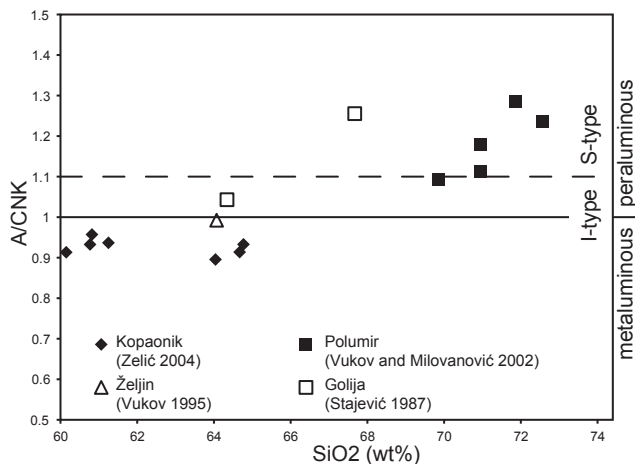


Fig. 3.5 – Diagram showing the $Al_2O_3/(NaO+K_2O+CaO)$ vs. SiO_2 relationships. Reference value for distinguishing peraluminous from metaluminous rocks after Shand (1947), reference value for distinguishing I- and S-types after Chappel and White (1974).

Drenje intrusion crops out as a separate, E–W elongated body, which is essentially similar to the equigranular granodiorite of the northern part of the Kopaonik pluton. In general, these granitoids are composed of quartz, plagioclase (An_{35-55}), potash feldspar ($Or > 86$), biotite and magnesiohornblende, with titanite, epidote, allanite, apatite, zircon and magnetite as accessory minerals. Decimetre-sized mafic enclaves are observed in all the varieties albeit with some differences. In the southern area they are larger and highly irregular in shape and sometimes contain felsic minerals apparently derived from the host granodiorite. These enclaves are typically biotite-rich and display a high-K composition. In the northern area they are smaller, usually rounded and rich in amphiboles.

Most Kopaonik and Drenje rocks have silica contents ranging from 57 to 67 wt% SiO_2 . They are medium-K calc-alkaline, metaluminous ($Al_2O_3 - [K_2O + Na_2O] < 1$), I-type granitoid rocks (Fig. 3.5), with LILE- and LREE-enriched trace element patterns. Because of slightly elevated K_2O concentrations (≥ 2.5 –3 wt%), the Kopaonik quartzmonzonites occurring in the south exhibit a high-K calc-alkaline character and are richer in incompatible elements compared to the Kopaonik and Drenje granodiorites.

Kopaonik and Drenje intrusives, although this suggestion was in conflict with differences in their K–Ar radiometric ages as reported by Delaloye et al. (1989). Hence, at least part of the K–Ar age data seem suspicious and thus need closer inspection.

Petrography and chemical composition of the granitoids

Kopaonik and Drenje intrusive(s)

The Kopaonik intrusive displays a zonal distribution of granitoid varieties that show gradual transitions between each other (Zelić 2009; Cvetković et al. 2002). The southern part is represented by porphyritic granodiorite to quartzmonzonite characterized by the presence of large cm-sized potash feldspars. Towards the north the intrusive rocks are more equigranular in texture and granodioritic to quartzdioritic in composition. The

Željina intrusive

The Željina intrusive ranges in composition from predominant quartzdiorite, tonalite and granodiorite to subordinate granite (Vukov 1989). These rocks show mineral compositions that are very similar to those of Kopaonik and Drenje, and they also show mutual compositional transitions characterized by increasing quartz and potash feldspar modal contents ranging from quartzdiorite to granite. Mafic enclaves are rare and more variable in composition compared to those from the Drenje intrusive.

The Željina quartzdiorite-granite suite is represented by typical medium-K calc-alkaline (SiO_2 mostly above 65 wt%, $\text{K}_2\text{O} \leq 2$ wt%), metaluminous, I-type rocks (Fig. 3.5; Vukov 1995). They have almost identical geochemical characteristics to those of the Kopaonik and Drenje intrusives.

Golija intrusive

These granitoid rocks are represented by relatively small irregularly shaped bodies or small dyke-like shallow intrusions cutting Paleozoic rocks of the Drina–Ivanjica thrust sheet. The granitoid body formed a contact-metamorphic aureole, to which small skarn-related deposits with iron, Pb-Zn and wolfram mineralization are related (Mojsilović et al. 1980). The rocks are granodiorites to quartzmonzonites and have inequigranular hypidiomorphic textures. They contain quartz, potash feldspar, plagioclase (andesine), biotite and amphibole, with tourmaline, allanite, sphene, apatite and zircon as accessory minerals.

According to scarce literature data, these rocks are high-K calc-alkaline ($\text{SiO}_2 > 65$ wt%, $\text{K}_2\text{O} \geq 3$ wt%), metaluminous ($\text{Al}_2\text{O}_3 - [\text{K}_2\text{O} + \text{Na}_2\text{O}] < 1$) and possess I-type characteristics (Fig. 3.5). Therefore, they are geochemically similar but slightly more potassium rich in comparison to the Kopaonik, Drenje and Željina granitoids (Mojsilović et al. 1980).

Polumir granite

This is a typical leucocratic two-mica granite composed of quartz, potash feldspar (Or_{82-93}), acid plagioclase ($\text{An} < 30$), biotite ($\text{Al}_2\text{O}_3 > 18$ wt%) and muscovite. Apatite, magnetite, monazite, allanite and zircon are the main accessory minerals. Plastic deformation along the intrusive margins, absent in case of all the other intrusions, resulted in a foliation formed by biotite and white mica.

In comparison to the other granitoid rocks, the Polumir granite is a more silica rich (SiO_2 mostly above 70 wt%) peraluminous ($\text{Al}_2\text{O}_3 - [\text{K}_2\text{O} + \text{Na}_2\text{O}] > 1$) S-type granitoid rock (Fig. 3.3). In addition, this granite has an overall lower content of incompatible elements, except for rubidium ($\text{Rb} \sim 200$ ppm; Vukov and Milovanović 2002).

U–Pb (ID-TIMS) dating and Hf isotope data

Analytical techniques

The analytical techniques of U–Pb dating closely follow those outlined in Schaltegger et al. (2008). Prior

Sample	Lithology	Locality	Coordinates	
11*	qz-monzonite	Kopaonik	7485417	4795565
16*	granodiorite	Drenje	7483641	4806274
21*	granodiorite	Željina	7482818	4821570
30	qz-diorite	Željina	7481290	4817210
509*	granodiorite	Golija	7445900	4795450
513	two-mica granite	Polumir	7469329	4817635

Table 3.1 – Locality and lithology of the samples selected for U–Pb age determination. Samples marked with an asterisk have been analysed additionally for Hf isotopic compositions (see Table 3.3). Coordinates are in the MGI Balkan 7 Cartesian system. For location of the samples see Fig. 3.2.

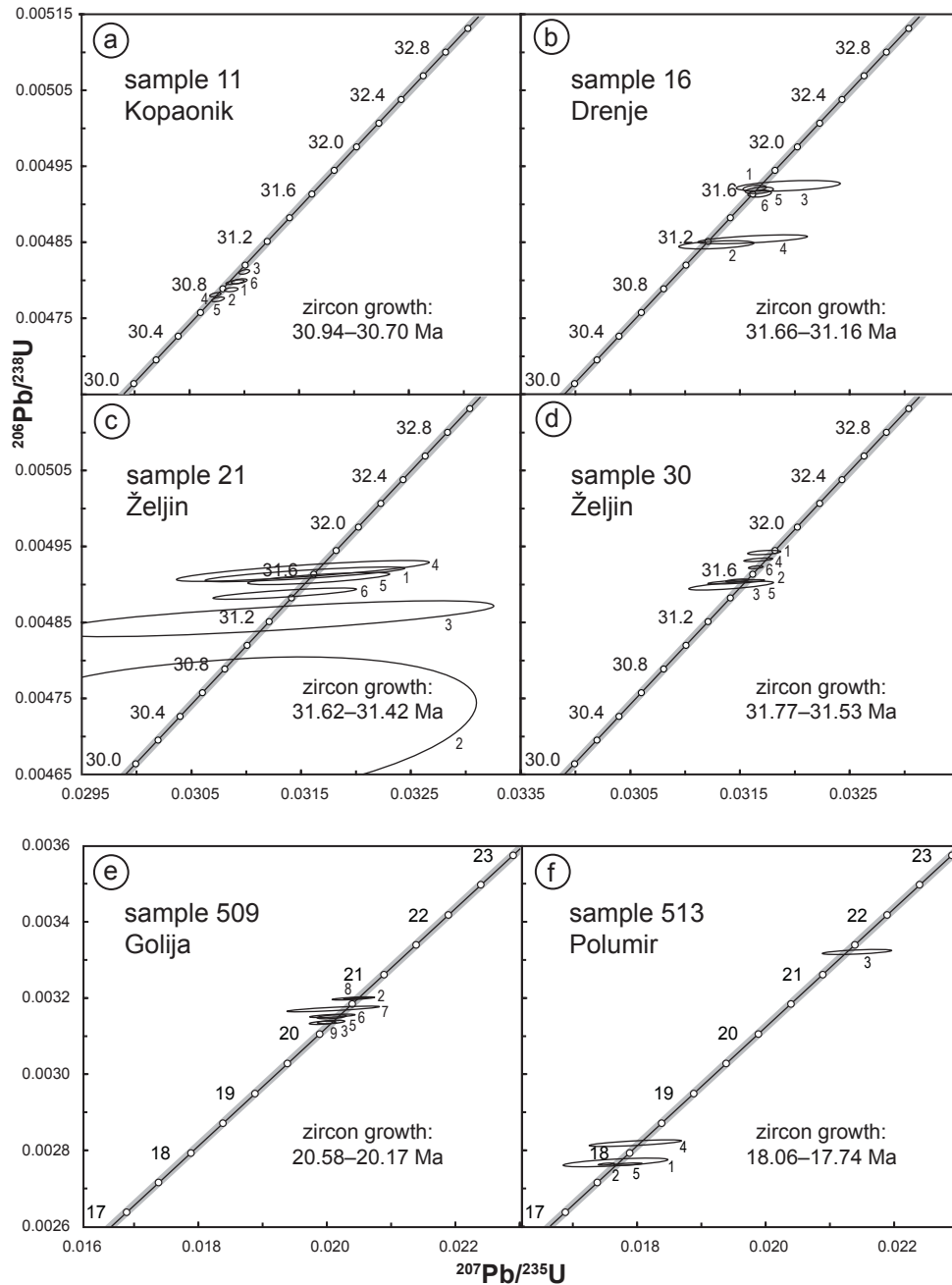


Fig. 3.6 – Concordia diagrams containing the results of zircon U–Pb dating of six samples. **a** – Kopaonik qz-monzonite. **b** – Drenje granodiorite. **c** – Granodiorite from the northern part of Željina. **d** – Granodiorite of the southern part of Željina. **e** – Granodiorite from the Golija mountain. **f** – Granite from Polumir near Ušće. Ellipses show the analytical uncertainties of the individual analyses. The gray bands straddling the concordia quantify the ^{238}U and ^{235}U decay constant uncertainties. For location of the samples see Fig. 3.2.

to analysis the zircons were treated by annealing-leaching (chemical abrasion). This minimizes the effects of post-crystallization lead loss (Mattinson 2005). Calculation of $^{206}\text{Pb}/^{238}\text{U}$ ages was done with the Isoplot/Ex v.3 program (Ludwig 2005). The techniques of the Hf isotope analysis are those described in Schaltegger and Brack (2007). Mean ages and mean Hf isotopic values are given with uncertainties at the 95% confidence level.

Sample material and presentation of the results

U–Pb age determinations were carried out on a total of 6 samples taken from five different intrusive bodies. Lithology, sample number and location are provided in Table 1 and Fig. 3.2. For each sample six to seven zircons were carefully selected and treated according to the criteria outlined in Schaltegger et al. (2008). This resulted in a total of 37 single grain analyses (Table 2). The results of the U–Pb age determinations based on these analyses

Sample	Zircon	Weight	Concentrations			Th/U	Atomic ratios								Apparent ages (Ma)		
			U	Pb Rad.	Pb Nonrad.		206/ 204	207/ 206	Error 2 σ	207/ 235	Error 2 σ	206/ 238	Error 2 σ	Error corr.	206/ 238	207/ 235	207/ 206
(Nr. on Fig. 2)	(a)	(mg)	(ppm)	(ppm)	(pg)	(b)	(c)	(d, e)	(%)	(d)	(%)	(d, e)	(%)		(e)		(e)
11	11-1	0.0081	961	4.84	1.03	0.14	2283.26	0.046744	0.20	0.030915	0.22	0.004797	0.05	0.42	30.85	30.92	43.42
	11-2	0.0053	1286	6.32	0.59	0.12	3477.16	0.046788	0.14	0.030880	0.15	0.004787	0.05	0.44	30.78	30.88	45.85
	11-3	0.0131	896	4.54	0.72	0.14	4945.70	0.046736	0.10	0.030999	0.12	0.004810	0.05	0.51	30.94	31.00	43.04
	11-4	0.0078	1138	5.61	0.59	0.12	4487.02	0.046631	0.11	0.030735	0.13	0.004780	0.05	0.47	30.74	30.74	37.81
	11-5	0.0026	2322	11.18	0.35	0.10	5177.13	0.046735	0.13	0.030764	0.14	0.004774	0.05	0.46	30.70	30.77	43.35
	11-6	0.0075	941	4.79	0.75	0.15	2854.68	0.046792	0.17	0.030955	0.19	0.004798	0.05	0.44	30.86	30.95	45.77
16	16-1	0.0138	274	1.43	1.34	0.43	911.62	0.046636	0.25	0.031637	0.26	0.004920	0.06	0.34	31.64	31.63	28.77
	16-2	0.0038	232	1.39	1.21	0.36	244.40	0.046832	0.85	0.031289	0.89	0.004846	0.09	0.51	31.16	31.28	39.02
	16-3	0.0093	153	0.83	1.32	0.43	365.24	0.047062	1.15	0.031944	1.20	0.004923	0.12	0.44	31.66	31.93	54.26
	16-4	0.0048	170	1.42	2.93	0.50	104.86	0.047254	1.22	0.031618	1.28	0.004853	0.10	0.66	31.21	31.61	64.42
	16-5	0.0023	1399	7.58	1.78	0.43	588.88	0.046718	0.31	0.031676	0.33	0.004918	0.07	0.33	31.62	31.66	33.94
	16-6	0.0020	1147	6.23	0.91	0.53	811.43	0.046769	0.26	0.031680	0.28	0.004913	0.08	0.39	31.59	31.67	39.02
21	21-1	0.0039	189	0.99	1.04	0.15	236.13	0.046574	2.22	0.031545	2.36	0.004912	0.17	0.83	31.59	31.54	34.41
	21-2	0.0048	166	0.80	2.52	0.11	110.60	0.046709	7.13	0.030232	7.77	0.004694	1.92	0.44	30.19	30.24	42.04
	21-3	0.0039	164	2.12	6.98	0.15	46.69	0.046646	5.08	0.031219	5.36	0.004854	0.39	0.74	31.22	31.21	38.23
	21-4	0.0037	213	1.10	1.64	0.14	165.33	0.046510	2.80	0.031528	2.99	0.004917	0.23	0.84	31.62	31.52	31.21
	21-5	0.0023	420	2.77	2.42	0.13	142.01	0.046804	1.59	0.031662	1.68	0.004906	0.13	0.71	31.55	31.65	46.31
	21-6	0.0027	282	2.27	2.72	0.14	105.42	0.046529	1.60	0.031349	1.70	0.004887	0.12	0.79	31.42	31.34	32.28
30	30-1	0.0160	224	1.14	0.85	0.12	1325.11	0.046567	0.37	0.031720	0.39	0.004940	0.05	0.55	31.77	31.71	34.25
	30-2	0.0085	471	2.27	0.68	0.07	1818.95	0.046548	0.26	0.031430	0.28	0.004897	0.03	0.52	31.54	31.47	33.72
	30-3	0.0062	154	0.81	0.62	0.08	489.10	0.046576	0.94	0.031668	1.00	0.004931	0.08	0.75	31.49	31.42	34.55
	30-4	0.0034	750	3.60	0.56	0.15	1404.92	0.046550	0.31	0.031476	0.34	0.004904	0.04	0.62	31.71	31.66	33.87
	30-5	0.0027	621	3.02	0.76	0.08	697.68	0.046550	0.62	0.031466	0.67	0.004903	0.05	0.78	31.53	31.46	33.79
	30-6	0.0086	677	3.28	0.61	0.08	2966.81	0.046628	0.16	0.031642	0.17	0.004922	0.03	0.47	31.65	31.63	37.81
509	509-2	0.0060	758	2.67	1.73	0.09	540.23	0.046285	1.25	0.020407	1.33	0.004940	0.11	0.71	20.58	20.51	24.10
	509-3	0.0050	915	3.31	1.83	0.12	506.05	0.046278	1.05	0.020000	1.12	0.004897	0.12	0.61	20.17	20.11	23.50
	509-5	0.0047	1280	4.38	1.30	0.12	928.47	0.046253	0.55	0.019986	0.59	0.004931	0.09	0.43	20.17	20.09	22.20
	509-6	0.0065	817	2.88	1.63	0.12	655.86	0.046226	0.88	0.020076	0.94	0.004904	0.15	0.49	20.27	20.18	20.76
	509-7	0.0051	318	2.81	10.12	0.11	50.83	0.045982	2.75	0.020096	2.90	0.004903	0.18	0.84	20.40	20.20	8.05
	509-8	0.0049	449	1.45	0.73	0.11	614.30	0.046394	0.71	0.020450	0.75	0.004922	0.06	0.79	20.58	20.56	29.57
509-9	0.0045	396	1.34	1.12	0.15	331.28	0.046208	1.36	0.020082	1.43	0.004940	0.11	0.72	20.29	20.19	19.54	
513	513-1	0.0048	513	1.60	1.61	0.04	287.17	0.044133	7.89	0.016837	8.14	0.002767	0.40	0.65	17.81	16.95	35.02
	513-2	0.0053	880	2.49	0.91	0.26	912.46	0.045697	0.39	0.017372	0.42	0.002756	0.09	0.40	17.74	17.49	5.06
	513-3	0.0060	434	1.66	1.97	0.03	291.71	0.046774	1.92	0.021418	2.04	0.003321	0.19	0.68	21.37	21.52	49.44
	513-4	0.0065	333	1.78	6.21	0.03	80.66	0.046198	2.36	0.017954	2.48	0.002806	0.15	0.81	18.06	18.07	11.11
	513-5	0.0027	986	2.85	0.95	0.13	509.19	0.046292	0.58	0.017639	0.61	0.002764	0.07	0.49	17.79	17.75	44.21
	513-6	0.0030	662	8.06	1.68	0.08	863.28	0.049603	0.50	0.078419	0.54	0.011466	0.06	0.62	73.49	76.66	179.56

Table 3.2 – Results of U–Pb age determination by single zircon ID-TIMS. For location of the samples see Fig. 3.2. Abbreviations: (a) all zircons annealed-leached (Mattinson 2005), all single grains – (b) calculated on the basis of radiogenic $^{208}\text{Pb}/^{206}\text{Pb}$ ratios – (c) corrected for fractionation and spike – (d) corrected for fractionation, spike, blank and common lead (Stacey and Kramers 1975) – (e) corrected for initial Th disequilibrium, using an estimated Th/U ratio of 4 for the melt.

Sample	Analysis	$^{176}\text{Hf}/^{177}\text{Hf}$ (normalised)	$^{176}\text{Hf}/^{177}\text{Hf}$ (T)	ϵHf (0)	ϵHf (T)	$\pm 2\sigma$	T2 (DM) (Ga)
11	11-1	0.283	0.283	0.71	1.43	0.5	0.94
	11-3	0.283	0.283	0.92	1.64	0.5	0.93
	11-4	0.283	0.283	0.74	1.46	0.5	0.94
	11-6	0.283	0.283	0.43	1.14	0.5	0.96
16	16-1	0.283	0.283	3.12	3.83	0.5	0.80
	16-2	0.283	0.283	3.01	3.73	0.5	0.81
	16-3	0.283	0.283	2.90	3.62	0.5	0.81
	16-4	0.283	0.283	2.90	3.62	0.5	0.81
21	21-1	0.283	0.283	3.01	3.73	0.5	0.81
	21-2	0.283	0.283	3.57	4.29	0.5	0.77
	21-3	0.283	0.283	1.20	1.92	0.5	0.91
	21-4	0.283	0.283	3.18	3.90	0.5	0.79
509	509-7	0.283	0.283	-1.13	-0.68	0.5	1.06
	509-8	0.283	0.283	-1.91	-1.46	0.5	1.10
	509-9	0.283	0.283	-3.15	-2.70	0.5	1.17

Table 3.3 – Hf isotopic compositions of selected dated zircons. Errors of the measured $^{176}\text{Hf}/^{177}\text{Hf}$ ratios are given as external 2σ reproducibility of standard measurements (i.e. ± 0.5). ϵHf values and T(DM) model ages were calculated with ($^{176}\text{Hf}/^{177}\text{Hf}$) CHUR(0) = 0.282772 and use present-day depleted mantle values of $^{176}\text{Hf}/^{177}\text{Hf} = 0.283252$, $^{176}\text{Lu}/^{177}\text{Hf} = 0.04145$ and a crustal $^{176}\text{Lu}/^{177}\text{Hf} = 0.017$ (Blichert-Toft and Albarède 1997). Mean Hf isotopic values are given at the 95% confidence level. For location of the samples see Fig. 3.2.

are shown in concordia diagrams in Fig. 3.6. Because of the often very small analytical uncertainties obtained for individual $^{206}\text{Pb}/^{238}\text{U}$ zircon dates (0.1–0.3 Ma) the results do generally not overlap within their 2σ errors and are represented as range of data rather than weighted mean $^{206}\text{Pb}/^{238}\text{U}$ values (Fig. 3.2).

Hf isotope analyses were carried out on 15 zircons (Table 3) separated from four samples taken at four localities (Table 1) in order to obtain petrogenetic information concerning the magma sources of the studied plutons.

Kopaonik intrusive (sample 11, Fig. 3.6a)

This sample is an isotropic inequigranular quartzmonzonite taken from the southeastern margin of the main Kopaonik intrusive body (Fig. 3.2). Six zircon analyses reveal $^{206}\text{Pb}/^{238}\text{U}$ dates between 30.94 and 30.70 Ma (Fig. 3.6a). The individual 2σ errors are ± 0.01 Ma due to high Pb*/Pbc (radiogenic/nonradiogenic lead) ratios (38–73) with uranium concentrations between 900 and 2300 ppm. Except for analyses 11-1 and 11-6 none of the data overlap. Because there is no indication for inheritance of old lead, we interpret the single zircon data to reflect zircon growth over some 240 ka, i.e. from 30.94 to 30.70 Ma, or as mixing from two growths episodes approximated by a maximum age of 30.70 and a minimum age of 30.94 Ma, respectively. The ϵHf values measured for zircons 11-1, 11-3, 11-4 and 11-6 are relatively uniform and fall between 1.1 and 1.6 (Table 3).

Drenje intrusive (sample 16, Fig. 3.6b)

The sample is a medium-grained, equigranular granodiorite exhibiting a synmagmatic foliation defined by hornblende (Fig. 3.2). Compared to sample 11 the individual 2σ errors of the $^{206}\text{Pb}/^{238}\text{U}$ dates are slightly higher (± 0.01 – 0.03 Ma) because of low Pb*/Pbc ratios. Based on the zircon ages for 16-1, 16-3 and 16-5 we were able to calculate a mean $^{206}\text{Pb}/^{238}\text{U}$ date of 31.64 ± 0.02 Ma (MSWD = 0.59). From the concordia plot one may infer two stages of zircon growth, one from 31.7 to 31.6 Ma and a second one at around 31.2 Ma (Fig. 3.6b). Zircon 16-2 could indicate that the last growth occurred at 31.16 Ma. However, we prefer to interpret the entire time span given by the single grain analyses as indicating the duration of zircon growth between 31.66 and 31.16 Ma, or, alternatively, mixing of zircon from two growth episodes. The 500 ka time span seems too long for the interpretation as protracted growth, a mixing hypothesis may therefore explain the data scatter better. The ϵHf values measured for zircons 16-1, 16-2, 16-3 and 16-4 (Table 3) show consistent values between 3.6 and 3.8, not indicating any old inherited zircon material.

Željina intrusive (sample 21, Fig. 3.6c)

The sample is a medium-grained, equigranular granodiorite. All six measured zircons yield concordant ages. Zircons 21-2 and 21-3 show large analytical uncertainties as well as potentially inaccurate $^{206}\text{Pb}/^{238}\text{U}$ dates due to low Pb^*/Pb_c ratios (0.5–1.5). We therefore do not include them for the interpretation of the age of the intrusion. The oldest three zircons (21-1, 21-4 and 21-5) overlap within their 2σ errors and give a mean $^{206}\text{Pb}/^{238}\text{U}$ date of 31.46 ± 0.03 Ma (MSWD = 0.26). Again, we prefer to interpret these data as indicating zircon growth over a time span of about 200 ka, i.e. from 31.62 (grain 4) to 31.42 Ma (grain 6), or mixing from two growth periods. The ϵHf values obtained for zircons 21-1, 21-2 and 21-4 fall between 3.7 and 4.3. Zircon 21-3, however, reveals a ϵHf value of 1.9, suggesting that traces of an older, crust-derived Hf component may be present.

Željina intrusive (sample 30, Fig. 3.6d)

This is a quartzdiorite showing a weak magmatic foliation defined by hornblende, taken from the eastern part of the Željina intrusion (Fig. 3.2). The individual 2σ errors on the $^{206}\text{Pb}/^{238}\text{U}$ data are ± 0.01 Ma due to high Pb^*/Pb_c ratios (20–40), except for 30-3 and 30-5 with Pb^*/Pb_c ratios of around 10 (Table 2) resulting in individual 2σ errors of the $^{206}\text{Pb}/^{238}\text{U}$ age of ± 0.03 Ma. We interpret these data to indicate zircon growth over some 250 ka, from 31.77 to 31.53 Ma, or mixing from two growth periods. The data possibly indicate that the younger zircons that exhibit smaller Pb^*/Pb_c ratios incorporated less uranium due to fractionation in the magma source.

Golija intrusive (sample 509, Fig. 3.6e)

Seven zircons were analysed from this granodiorite. One analysis (509-7) yields an elevated value for common lead (10.12 pg) and is thus excluded from the interpretation. The remaining analyses show individual 2σ errors of the $^{206}\text{Pb}/^{238}\text{U}$ data of 0.01–0.02 Ma. The $^{206}\text{Pb}/^{238}\text{U}$ single grain dates fall between 20.58 and 20.17 Ma. At first sight this time span of 400 ka seems rather long for being interpreted as a time interval of zircon growth, therefore mixing of zircon material from two episodes of growth seems to be more likely. The ϵHf values are significantly lower in comparison to the samples of the substantially older Kopaonik suite (Kopaonik, Drenje and Željina intrusion) and range between -0.7 and -2.7.

Polumir granite (sample 513, Fig. 3.6f)

This two-mica granite is different from the other intrusions by the fact that it is the only one showing a high-temperature C-S structures associated with a stretching lineation (Fig. 3.3). This solid-state fabric together with asymmetric boudinaged dykes observed in the host rocks (Fig. 3.3a) indicate top-to-the-north shearing along an extensional detachment that exhumed the Studenica Metamorphic Series and which was either active during the last stages of the intrusion and/or before the onset of substantial cooling of the Polumir granite (Fig. 3.3c). Two analyses, 513-3 and 513-6 (note that 513-6 is out of scale and not shown in Fig. 3.6f) are interpreted as inherited grains with $^{206}\text{Pb}/^{238}\text{U}$ ages of 21.3 and 73.5 Ma, respectively. The remaining four zircons that we regard to have grown during the intrusion yield closely grouped $^{206}\text{Pb}/^{238}\text{U}$ dates between 18.06 and 17.74 Ma. Three of them (513-1, 513-2, and 513-5) could be used to calculate a $^{206}\text{Pb}/^{238}\text{U}$ mean-age of 17.760 ± 0.048 Ma (MSWD = 0.37), 513-4 being statistically older with an age of 18.06 Ma. Again we interpret the data on these four zircons to indicate mineral growth during a magmatic event that occurred between 18.06 and 17.74 Ma, or, alternatively, being composed by mixing of an older and a younger age component in the zircon.

Interpretation and discussion of U–Pb ages and Hf isotope data

All the dated samples provide evidence for protracted or poly-episodic zircon growth over time spans of a few 10⁵ years, which can be resolved thanks to increased analytical precision in the ²⁰⁶Pb/²³⁸U dates. Since zircon may already start to grow during magma assembly at deeper crustal levels and continue during ascent and emplacement into the middle to upper crust (Miller et al. 2007), it is reasonable to assume that the youngest zircon date approximates the age of emplacement (Schaltegger et al. 2009). However, we cannot completely rule out the effect of lead loss, despite the pre-treatment by chemical abrasion.

Comparison of the ages amongst the six different intrusions (Fig. 3.6) clearly reveals two age groups: (i) The group of Oligocene plutons intruded within a narrow time span between 31.77 and 30.70 Ma. The Kopaonik pluton is the youngest (sample 11, 30.94 Ma to 30.70 Ma), and the remaining three (Drenje and the two analyses from Željina) cluster around 31.5 Ma. (ii) The group of Miocene intrusions consists of the Golija granodiorite and the Polumir granite, which intruded at 20.58–20.17 and 18.06–17.74 Ma, respectively. While the existence of two age groups has been postulated by previous studies (Karamata et al. 1992; Knežević et al. 1995), our study shows that the I-type Željina and Drenje intrusions are of the same Oligocene age as, and possibly cogenetic with the I-type Kopaonik intrusion, as suggested by Cvetković et al. (2002) on petrogenetic grounds. This contradicts the supposed Miocene age of the Željina and Drenje intrusions inferred by the previous studies based on K–Ar dating (Karamata et al. 1992).

Two out of the three Oligocene intrusions, samples 16 and 21 from Drenje and Željina, respectively, record uniform εHf values ranging from 3.6 to 4.3 whereas sample 11 of the Kopaonik quartzmonzonite shows distinctively lower values ranging from 1.1 to 1.6. The εHf values obtained for the Miocene Golija granitoid, on the other hand, are significantly lower in comparison with those obtained for the Oligocene intrusions, displaying εHf values ranging from -0.7 to -2.7.

The positive εHf values of all the three samples taken from Oligocene intrusives, along with their metaluminous I-type geochemistry, suggest a moderate crustal influence in the origin and evolution of these granitoids, especially given the fact that these granitoids intrude an old (Paleozoic) crust. In this context, the primary melts of the Oligocene intrusives could have formed via partial melting of mantle-derived lower crustal protoliths. Regarding the significantly lower εHf values shown by the Miocene Golija granitoid there are in principle at least two possible explanations: (1) This granitoid might have originated via melting of upper crustal material; but this possibility is unlikely given its distinctive I-type character. (2) The origin of the Golija intrusive could have involved an evolution that started with primary melts similar to those postulated for the Oligocene plutons. Such primary melts could have been modified either by assimilation of upper crustal material or, alternatively, by mixing with high-K calc-alkaline to ultrapotassic basic magmas. Although these two hypotheses cannot be unequivocally tested without more data including geochemical modelling, the second possibility, namely that the lower εHf values of the Golija granitoid (and possibly for the Kopaonik quartzmonzonite as well) did result from mixing between an acid and a high-K basic magma is supported by the following arguments: i) the Golija granitoid is a metaluminous, I-type, high-K calc-alkaline rock, ii) it contains mafic enclaves which are believed to represent petrographic evidence of magma mixing processes (Didier and Barbarin 1991; Poli et al. 1996), iii) generally, the Serbian ultrapotassic rocks have very unradiogenic Hf isotopes (εHf << 0; Prelević et al. submitted), similar to ~500 Ma old continental crust (Rudnick and Gao 2003), and iv) the role of magma mixing during Tertiary magmatism in Serbia has already been advocated by Prelević et al. (2001, 2004) and Cvetković et al. (2007b).

Accordingly, the only intrusive that is certainly related to significant melting of upper crustal material is the Polumir S-type granite for which, unfortunately, there are no data on Hf isotopes.

Zircon and apatite fission-track data

Sampled material and presentation of data

The sampling strategy aimed at obtaining an evenly distributed dataset involving most of the intrusive bodies, including some volcanic rocks, taken at different altitudes. Fourteen samples from the different intrusive bodies together with two samples from the volcanic bodies within the Ibar valley yielded fourteen apatite and fifteen zircon ages, twelve of them from both zircon and apatite. The analytical results are given in Table 4, the location of the samples in Fig. 3.2. The locations of additional yet unpublished data from (meta-) sedimentary rocks, taken from Schefer (2010), are shown in Fig. 3.2 and labelled ‘Miocene’ and ‘pre-Miocene’ zircon ages, respectively, in order to support the mapping of the outlines of the Miocene core-complexes.

Analytical techniques

After conventional mineral separation (crushing, sieving, magnetic and heavy liquid separation) samples were mounted in epoxy resin (apatite) and PFA Teflon (zircon). Revelation of fossil tracks was achieved by etching the polished zircon mounts in a NaOH-KOH eutectic melt at 210 °C. Apatite mounts were etched in 5 N HNO₃ at 20 °C for 20 s. Induced tracks in external detector muscovite were etched in 40 % HF for 45 minutes at 20 °C. Irradiation of samples was carried out at FRMII Garching (Technische Universität München, Germany). Neutron flux was monitored using CN5 (apatite) and CN1 (zircon) dosimeter glasses. Densities of spontaneous and induced tracks as well as lengths measurements for apatite (confined horizontal tracks and long axes of etch pits) were counted on a Zeiss Axioplan microscope equipped with an Autoscan® System at the University of Innsbruck. All samples have been analysed using the external detector method as described by Gleadow (1981). The fission-track central ages ($\pm 2\sigma$ error) (Galbraith and Laslett 1993) were calculated following the IUGS recommended approach of Hurford and Green (1983) with a zeta factor of 159 ± 3.6 (zircon, CN 1 glass) and 357 ± 5.2 (apatite, CN 5 glass) (analyst: B. Fügenschuh). Data processing was carried out using the TRACKKEY program (Dunkl 2002).

Results

All zircon central ages from the footwall of the D4b ductile normal faults range between 16.7 and 11.8 Ma (Table 4). However, three samples that stem from the hanging wall of the D4b ductile normal faults (447, 460 and 461) yielded ages between 28 and 25 Ma. Sample 447 comes from a very small satellite body of the Kopaonik intrusion intruding the ophiolites near Jošanička Banja but separated from the main intrusive bodies shown in Fig. 3.2 by a D4b ductile normal fault. Samples 460 and 461 are dacitic–andesitic rocks in the Ibar valley that are part of the volcanics formed at shallow depth and never buried to greater depth (Fig. 3.2).

The apatite central ages obtained from the Kopaonik, Drenje, Željina and Polumir intrusions in the footwall of the D4b ductile normal faults are only slightly younger compared to the zircon ages and range between 15.3 and 10.5 Ma. They all pass the Chi-square test. Mean track lengths range between 14.4 and 15.1 μm (Table 4). The apatite age of sample 447 from the hanging wall of the D4b ductile normal faults is of course older (22 Ma); samples 460 and 461 did not reveal enough apatite grains to obtain a fission-track age.

Thermal modelling of the apatite fission-track data

Thermal modelling of apatite fission-track data obtained on intrusive rocks was carried out for the Oligocene Kopaonik, Drenje and Željina intrusions (Fig. 3.7a, b and c), for the Miocene Polumir granite (Fig. 3.7d and e), for

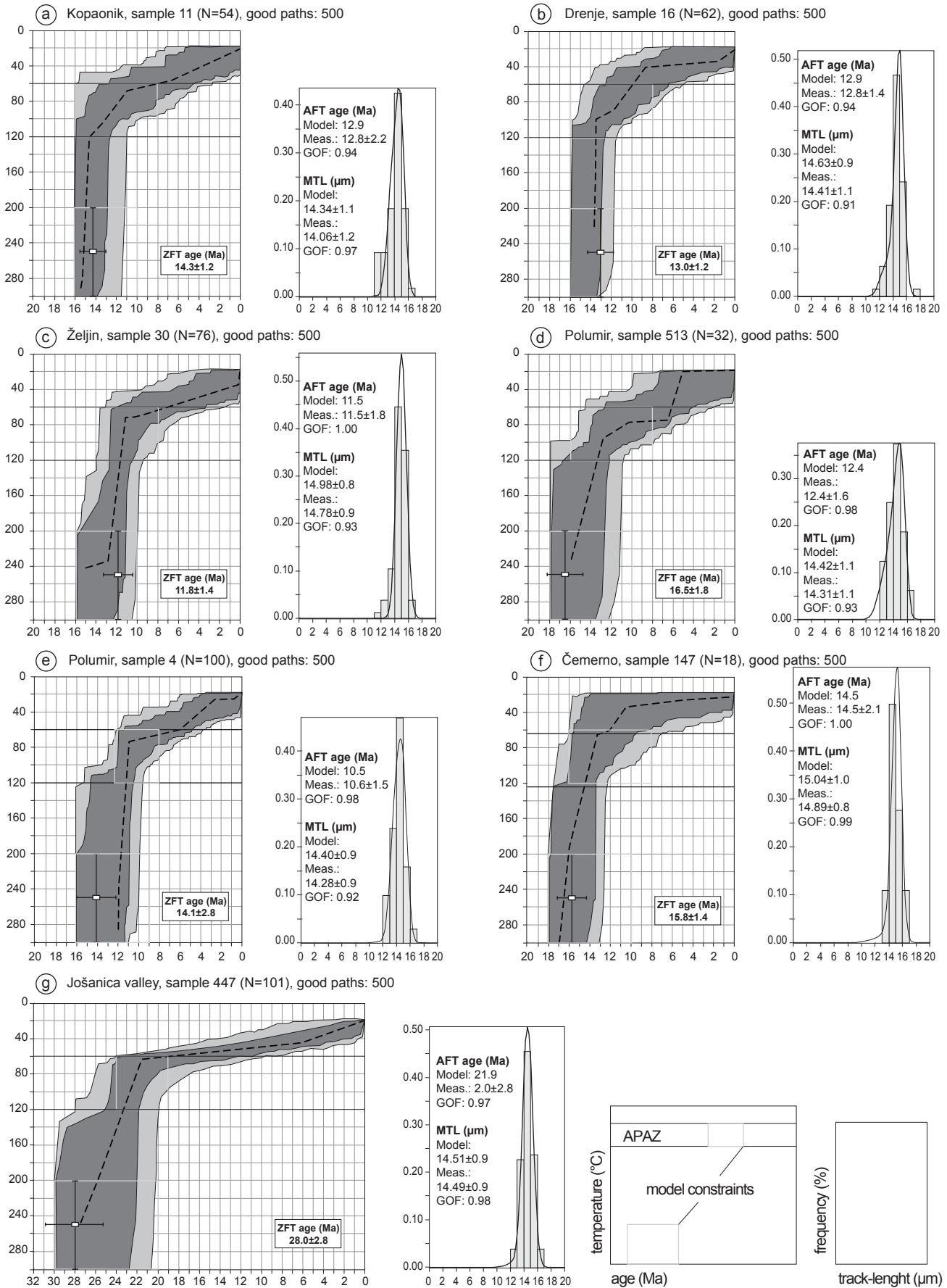


Table 3.4 – Sample details and results of zircon and apatite fission-track dating. All ages are central ages (Galbraith 1993). $P(\chi^2)$ is the probability of obtaining χ^2 values for ν degrees of freedom where $\nu = \text{number of crystals} - 1$. ρ_d , ρ_s and ρ_i represent the standard, sample spontaneous and sample induced track densities, respectively. N : Number of measurements; D_{par} : mean track pit length; MTL : mean track length; SD : standard deviation; All numbers in brackets are numbers of measurements. Locations are given in MGI Balkan 7 Cartesian coordinates (compare Fig. 3.2).

Sample no.	Min.	Location	Alt. (m)	Lithology	Intrusion	#	ρ_d x10 ⁶ cm ⁻²	ρ_s x10 ⁶ cm ⁻²	ρ_i x10 ⁶ cm ⁻²	N_s	N_i	$P(\chi^2)$ (%)	U conc. (ppm)	Central (Ma)	Error (2 σ)	MTL(meas) ± stat.error	SD (μm) (N)	D_{par} (μm)	
8	AP	7479347	768	granodiorite	Kopaonik	10	1.069	3206	3.186	125	53.442	2097	79	55±19	11.4	2.2	14.17±0.22	1.04(23)	2.32
	ZR	4802076												n.a.					
11	AP	7485417	1811	granodiorite	Kopaonik	20	1.062	3206	2.830	147	41.741	2168	100	46±13	12.8	2.2	13.26±0.18	1.34(54)	1.75
	ZR	4795565				20	0.474	3103	51.071	1449	134.393	3813	49	920±184	14.3	1.2			
240	AP	7481047	640	granitic dyke	Kopaonik	19	1.474	3100	4.161	232	71.628	3994	100	57±26	15.3	2.2	14.54±0.14	0.76(28)	2.63
	ZR	4804677				12	0.474	3504	9.885	288	24.091	704	68	163±31	15.4	2.4			
447	AP	7479698	550	granite	Kopaonik	20	1.441	3336	6.953	305	81.177	3561	100	70±42	22.0	2.8	13.66±0.91	1.11(101)	1.93
	ZR	4805525				22	0.474	3504	68.688	2582	90.902	3417	9	595±167	28.0	2.8			
16	AP	7483641	698	granodiorite	Drenje	20	1.064	3206	2.697	464	39.928	6869	82	44±14	12.8	1.4	13.60±0.19	1.49(62)	1.92
	ZR	4806274				20	0.473	3103	12.231	1016	35.417	2942	84	249±65	13.0	1.2			
21	AP	7482818	1277	granodiorite	Željina	20	1.056	3200	2.871	393	51.385	7033	74	56±11	10.5	1.2	14.41±0.20	1.09(29)	2.61
	ZR	7482818												n.a.					
30	AP	7481290	922	granodiorite	Željina	15	1.065	3206	2.273	21	37.448	3460	48	42±8	11.5	1.8	14.13±0.14	1.23(76)	3.10
	ZR	4817210				16	0.469	3103	10.632	608	31.984	1829	6	90±45	11.8	1.4			
132	AP	7485234	940	granodiorite	Željina	20	1.521	3663	1.373	165	29.332	3524	100	48±19	12.7	2.0	n.a.		1.42
	ZR	4819940				19	0.497	3204	19.882	847	46.970	2001	85	312±109	16.7	1.6			
143	AP	7483601	1346	granodiorite	Željina	20	1.512	3663	2.798	156	57.780	3222	100	44±8	13.1	2.2	n.a.		1.40
	ZR	4816215				20	0.499	3204	18.825	766	44.015	1791	7	285±125	16.4	2.0			
509	AP	7446900	1720	granite	Golja									n.a.					
	ZR	4795450				20	0.440	3063	77.902	2118	166.250	4520	100	1201±168	16.4	1.2			
513	AP	7469329	289	granite	Polumir	20	1.450	3100	3.815	265	79.607	5529	99	65±10	12.4	1.6	13.66±0.26	1.49(32)	1.96
	ZR	4817635				14	0.440	3063	37.002	660	78.152	1394	98	567±306	16.5	1.8			



Fig. 3.7 – Modelled thermal history and comparison between observed and predicted apatite fission-track parameters for samples from the main body of three different Oligocene intrusions (5a, b and c), the Miocene-age Polumir intrusion (5d) and from a small Oligocene magmatic body in the Jošanica valley (5e). Horizontal black lines within individual models at 60–120 °C bracket the partial annealing zone (PAZ) for apatite within the temperature limits assigned by Laslett et al. (1987). The segments of the thermal histories at temperatures lower than 60 °C only indicate a possible continuation of the thermal history because the annealing model is not sufficiently sensitive below 60 °C. The modelled t - T -paths are extended into the zircon partial annealing zone (Brandon et al. 1998) where the white squares represent the measured zircon fission-track central ages of the modelled samples including their 2σ errors. Modelling of apatite ages and track length distribution data were performed with the program HeFTy (Ketcham et al. 2000). Fission-track age, track-length distribution and etch pit diameters (D_{par}) as well as user-defined time-temperature boxes are used as input parameters. An inverse Monte Carlo algorithm with a multikinetic annealing model (Ketcham et al. 2007) was used to generate the time-temperature paths.

a (presumed) Miocene dyke in Čemerno mountain (Fig. 3.7f), and for a (presumed) Oligocene sample taken from a small intrusion in Jošanica valley located near the Kopaonik main intrusion (Figs. 3.2, 3.7g). All modelled samples yielded a significant number of measured confined horizontal tracks. The grey envelopes show ‘acceptable’, the dark ones ‘good’ fits between modelled and measured data (Ketcham et al. 2007). The models are mathematically well defined since the goodness of fit (GOF) is always between 0.9 and 1 (c.f. Appendix A).

All but the sample 447 from Jošanica valley (Fig. 3.7g) that was taken from the hanging wall of a D4b ductile normal fault show a similar cooling history, independent from the age of intrusion. Rapid cooling occurs from above the partial annealing zone for zircon, i.e. from around 300 °C, to some 80 °C between 16 and 10 Ma, followed by rather slow cooling to surface temperatures for the last 10 Ma. Sample 447 (Fig. 3.7g), however, shows a different cooling history. Rapid cooling starts between 30 and 21 Ma, i.e. shortly after the (presumed) age of intrusion at around 31 Ma, and hence, significantly earlier compared to the other samples shown in Fig. 3.7. This implies that sample 447 must have intruded at a very shallow level close to the surface, in order to cool rapidly through both the ZPAZ and the APAZ immediately after intrusion. After 22 Ma this sample cooled slowly from ca. 70 °C to surface temperatures, as indicated by the modelling. Note that the enhanced cooling rate between 16 and 10 Ma, monitored for the other samples by the modelling, is totally absent in sample 447. This will further be discussed below.

Interpretation and discussion of the fission-track ages and thermal modelling

The most obvious characteristics of the fission-track data obtained from the Oligocene Kopaonik, Drenje and Željina and the Miocene Polumir intrusions is that paired zircon and apatite ages display a small age difference within a given sample. This, together with the fact that these samples all pass the Chi-square test strongly indicates that these ages are cooling ages. The samples indicate fast cooling from temperatures above the zircon partial annealing zone (ZPAZ) to temperatures below the apatite PAZ during the time span between 16 and 10 Ma. This is confirmed by the modelling results (Fig. 3.7, Appendix A), as well as by the unimodal distribution and mean track lengths of >14 µm of the confined horizontal tracks in apatite (Table 4). The exact age of the time interval of enhanced cooling, as indicated by the apatite zircon pairs, however, slightly differs. The time interval of enhanced cooling reveals a regional trend indicating that the timing of extensional unroofing becomes slightly younger when going from S to N. Note that this interval of fast cooling observed in all the Oligocene intrusions, as indicated by fission-track age pairs and thermal modelling alike, significantly postdates the age of the intrusions at around 31 Ma that is documented by the U–Pb zircon data (Table 2). With respect to an assumed intrusion depth of 6–8 km the retardation of cooling through the zircon annealing window after the intrusion implies a slightly elevated ambient geothermal gradient, probably related to the emplacement, cooling and radioactive heat supply of the intrusion.

The Early Miocene Polumir intrusion yielded zircon fission-track ages of 16.5–14.1 Ma and apatite fission-track ages of 12.4–10.6 Ma (Table 4). As mentioned earlier, structural evidence (Fig. 3.3) suggests that the 18.06 to 17.74 Ma old Polumir intrusion started to be deformed by extensional unroofing during the last stages of its emplacement or shortly thereafter. Since this unroofing is seen to have continued all the way into the brittle field the apatite fission-track age of 12 Ma confines most of this extensional unroofing to have occurred during the 17–10 Ma time span. Hence, the timing of this Early to Middle Miocene period of rapid cooling, immediately following tectonically controlled exhumation in an extensional scenario near the Polumir granitoid, is comparable with the exhumation-related cooling history of the Kopaonik and Željina samples.

For the Golija intrusion, a similar and rather fast post-emplacement cooling can be inferred from the combined

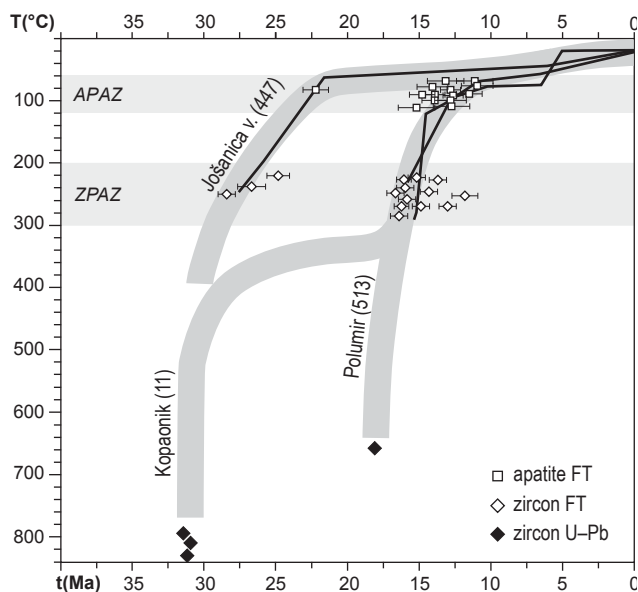


Fig. 3.8 – Thermal histories of three of the analysed granitoids of southern Serbia, as inferred from the radiometric U–Pb dating and the fission-track modelling presented in Fig. 3.6; the complete set of fission-track central ages obtained in the area is shown for comparison (c.f. Fig. 3.2 and Tables 3.2 and 3.4). The time-temperature paths (solid lines) correspond to the best-fit paths inferred from fission-track modelling (see Fig. 3.6) for samples 11 (Kopaonik), 513 (Polumir) and 447 (Jošanica valley); the thick gray lines represent an estimate of the complete *t*-*T* evolution that also take into account the age and estimated temperature of crystallization of the zircons. The U–Pb closure temperature corresponding to the zircon crystallization in sample 11 (Kopaonik *qz*-monzonite) was assumed to be around 820 °C (Lee et al. 1997). The S-type granite sample 513 (Polumir) must have intruded at lower temperatures. ZPAZ and APAZ are the partial annealing zones of zircon and apatite, respectively.

U–Pb (20.58–20.17 Ma) and fission-track zircon ages (16.4 ± 1.2 Ma). Due to the lack of apatite fission-track data, the post-16 Ma evolution is not constrained.

Exhumation history of the granitoid intrusions of the Inner Dinarides

A cooling path was constructed for three particular intrusive bodies for which the results of fission-track modelling could be combined with the results of U–Pb dating (Fig. 3.8) obtained from the same samples.

The *t*-*T*-path for the Oligocene Kopaonik intrusion (sample 11 in Fig. 3.8) is most likely characterized by a first period of rapid cooling due to heat conduction to the neighbouring rocks. Judging from the grade of regional metamorphism in the surrounding rocks (lowermost greenschist facies conditions), depth of intrusion must have been within the upper crust. The ambient temperature of the country rocks is estimated to have been slightly above 300 °C, i.e. above the upper limit of the PAZ for zircon, corresponding to at least some 10 km depth, and hence somewhat deeper than suggested by the pressures of 0.5–1.5 kbar inferred from the related contact metamorphic aureole (Knežević et al. 1995). Because the onset of the second period of rapid cooling through the zircon and apatite partial annealing zones indicated by the modelling considerably post-dates intrusion and its related first period of cooling by heat conduction, the Kopaonik intrusion must have remained at the ambient temperatures of the country rocks slightly above 300 °C for more than 10 Ma. However, until the onset of the second period of fast cooling between 16 and 10 Ma, these initial parts of the time-temperature history are rather loosely constrained by our data. The second period of rapid cooling is well constrained, however. In combination with the structural (Figs. 3 and 4) and metamorphic data (Schefer et al. 2008, Schefer 2010) this second period of rapid cooling can safely be interpreted as related to extensional unroofing in the footwall of normal faults that cut across the intrusion and surrounding metamorphic rocks (Figs. 2 and 4). Final cooling to near-surface temperatures occurred again at lower rates of around 10 °C/Ma from 10 Ma onwards.

The *t*-*T*-path of the Miocene Polumir granitoid revealed by fission-track data and modelling below 300°C (sample 513 in Fig. 3.8) is nearly identical with that of the Kopaonik intrusion. When combining the fission track ages with the intrusion age obtained by the zircon U–Pb dating (Fig. 3.8), however, it becomes evident that this Miocene-age intrusion underwent one single period of rapid cooling. This confirms the view that Miocene-age exhumation by normal faulting overlapped with and immediately followed the Polumir intrusion, as is independently evidenced by the field data (see Fig. 3.3; Schefer et al. 2008, Schefer 2010). Fission-track central ages for

zircon range from 16.7 to 11.8 Ma, those for apatite from 15.3 to 10.5 Ma for all specimens analysed (Fig. 3.7), but for one specimen discussed below (sample 447). This indicates that fast cooling related to Miocene-age extensional unroofing affected all the intrusions analysed but that from which sample 447 was taken.

Sample 447 that exhibits a different cooling history was taken from a small magmatic body in the Jošanica valley that intrudes the Western Vardar ophiolites (Fig. 3.2), and hence, a shallower structural level. At first sight, given its close vicinity to the main Kopaonik intrusive body and the same macroscopic appearance, it seems that this outcrop might be a coherent part of the Kopaonik intrusion. Structurally, however, this small body is located in the hanging-wall of the D4a ductile normal fault mapped in Fig. 3.2. This is supported by the fact that the zircon fission-track central age for this outcrop is 28 Ma, indicating cooling through the zircon PAZ shortly after the very probable Oligocene age of this intrusion. The fact that the sample fails the Chi-square test could indicate that the t-T-path of this sample is more likely due to cooling of the intrusion rather than recording tectonically induced rapid cooling during extensional unroofing. Hence, we propose that sample 447 stems from a much shallower part of the wider Kopaonik intrusive suite, which had already cooled to temperatures below the APAZ prior to Miocene extensional unroofing. This is independently supported by the fact that sample 447 is in close vicinity to the Oligocene-age extrusives (samples 460 and 461, Table 4) and volcanoclastics (32–29 Ma; Karamata et al. 1994) that crop out in the Ibar valley (Fig. 3.2).

Taken together the three cooling curves shown in Fig. 3.8 indicate that, after cooling of the Oligocene intrusions by heat conduction and before exhumation by Mid-Miocene extensional unroofing, the ambient temperatures differed by some 300°C. This indicates that Mid-Miocene extension was very substantial in the area investigated; it led to tectonic omission in the order of 10 km across the associated Miocene-age D4 normal faults.

Discussion of data within the regional geodynamic context

Late Eocene to earliest Miocene (37–22 Ma) magmatic activity in the Balkan Peninsula

The group of Oligocene intrusions within the investigated area (Kopaonik, Drenje Željin) is part of a NW-SE striking alignment of granitoids that follows the inner Dinarides (Sava-Vardar Belt or Zone of Pamić et al. 2002a and Kovács et al. 2007, respectively) from northern Bosnia (Motajica intrusion, Ustaszewski et al. in press) all the way to southern Serbia (Fig. 3.9). Further to the SE, however, this same belt crosses the Sava suture and strikes into the Dacia Mega-Unit, the Rhodopes and the Strandja Unit, which together form the upper plate with respect to the Dinarides (Schmid et al. 2008). Geographically, this belt runs across southern Bulgaria and northern Greece all the way into westernmost Turkey (Fig. 3.9 and references given in Table 5). The granitoids intruded between Late Eocene (37 Ma) and earliest Miocene (22 Ma) times. One has to be aware, however, that the age dates reported in Table 5 were obtained by different techniques and at different levels of accuracy.

As shown in Fig. 3.9, age and location of the granitoids coincide with that of a series of basaltic rocks (high-K calc-alkaline basalts, shoshonites and high-potassium volcanics; Cvetković et al. 2004a, Marchev et al. 2004; Prelević et al. 2005; ‘basalts’ in Fig. 3.9), volcanics and volcanoclastic basins, and additionally, non-volcanic sedimentary basins (e.g. Burchfiel et al. 2000, 2008; Dumurdzanov et al. 2005). Some of the basins are clearly associated with normal faulting and they date the onset of Aegean extension during Middle to Late Eocene times (e.g. Burchfiel et al. 2000, 2003; Kounov et al. 2004; Brun and Soukoutis 2007). The petrogenetic analyses of contemporaneous ultra-potassic volcanics (Prelević et al. 2005) in Serbia and in southern Bulgaria (Marchev et al. 2004) indicate that these volcanics were derived by melting a metasomatised mantle possessing a crustal signature. As

already discussed above, it is reasonable to assume that this same mantle source may also have contributed to the genesis of the I-type granitoid intrusions such as the Kopaonik quartzmonzonite. This ultrapotassic magmatism is generally contemporaneous with the formation of acidic volcanic and plutonic rocks. Its contribution, however, is minor in the case of the Oligocene granitoids and volcanics because these rocks are calc-alkaline, but without very high potassium contents.

For comparison, Fig. 3.9 also depicts the outlines of the occurrences of the older Tertiary basalts from the eastern Serbian ESPEMAR province (Paleocene to Mid-Eocene alkaline mafic volcanics). Most of these older Tertiary basalts are 60–50 Ma old according to the analyses that are mostly based on K–Ar dating of phlogopite and whole rock dating (Cvetković et al. 2004a). Note that this eastern Serbian ESPEMAR province is systematically located in a more internal position with respect to the Dinarides–Hellenides (Fig. 3.9). The ESPEMAR province was interpreted to have formed during the final stages of subduction of the Vardar branch of Neotethys and initial collision with ‘Europe’ (Cvetković et al. 2004a, b). The occurrences in eastern Serbia spatially coincide with another and still older magmatic province, referred to as Banatite Belt or Apuseni–Banat–Timok–Sredna Gora Belt. This is a 92–78 Ma old belt of calc–alkaline magmatism related to the subduction of a remnant of the Vardar branch of the Neotethys Ocean beneath the European continental margin during the Late Cretaceous (e.g. von Quadt et al. 2005). Note that, in contrast to the Late Eocene to earliest Miocene belt located within the Dinaridic lower plate, both these older magmatic belts are in a more internal position, i.e. they are confined to the upper (‘European’) plate with respect to the Sava suture.

The observation that the Late Eocene to earliest Miocene alignment of granitoids and associated features crosses the Sava suture implies that the last remnants of the Vardar branch of the Neotethys Ocean (Schmid et al. 2008) must have closed by Mid-Eocene times or earlier, in accordance with what is known from the literature (e.g. Pamić et al. 2002b; Ustaszewski et al. 2009, in press). Hence, it is clear that the Late Eocene to earliest Miocene magmatism is post-collisional with respect to the closure of the Vardar ocean. Since this magmatism is contemporaneous with the onset of extension in the Balkan area various scenarios may be proposed. All of them fit with the petrological evidence including the positive ϵ_{Hf} values:

(1) Post-collisional collapse of an overthickened orogen (e.g. Cvetković et al. 2004a), (2) Back-arc magmatism in relation to a more externally located subduction zone, with or without slab-break-off of the Adriatic plate (e.g. Pamić et al. 2002a; Kovács et al. 2007), and/or, (3) Slab delamination (Bird 1979) caused by roll-back (Funicello et al. 2006) of the former lower plate after collision, associated with foreland migration of thrusting within the external Dinarides. We exclude scenario (1) in view of the fact that compression in the Dinarides did not come to a halt after collision across the Sava Zone. Instead there appears to be a shift of the site of compression to the more external parts of the Dinarides (and Hellenides) during the Late Eocene (Figs. 9a and b). The external Dinarides formed in Late Eocene to Neogene times (e.g. Skourlis and Doutsos 2003; Mikes et al. 2008; Korbar 2009), whereby much of the shortening (at least some 300 km in the area of Dubrovnik; see profile 5 of plate 3 in Schmid et al. 2008) took place by shortening within the Budva–Pindos pelagic realm of the Dinarides and Hellenides, respectively. Foreland migration of the site of compression is also well established for the Hellenides (e.g. van Hinsbergen et al. 2005).

However, in contrast to Kovács et al. (2007) we do not regard the Budva–Pindos zone as a site of subduction associated with an ophiolitic suture zone, since there is no evidence for the existence of a NW-ward continuation of either an oceanic nor a non-oceanic Pindos zone into the Dinarides. Moreover, it is even uncertain if a ‘Pindos Ocean’ existed in the Pindos paleogeographic domain of Northwestern Greece (Schmid et al. 2008, Korbar 2009). Therefore we also regard scenario (2), namely the installation of a second and more externally located oceanic

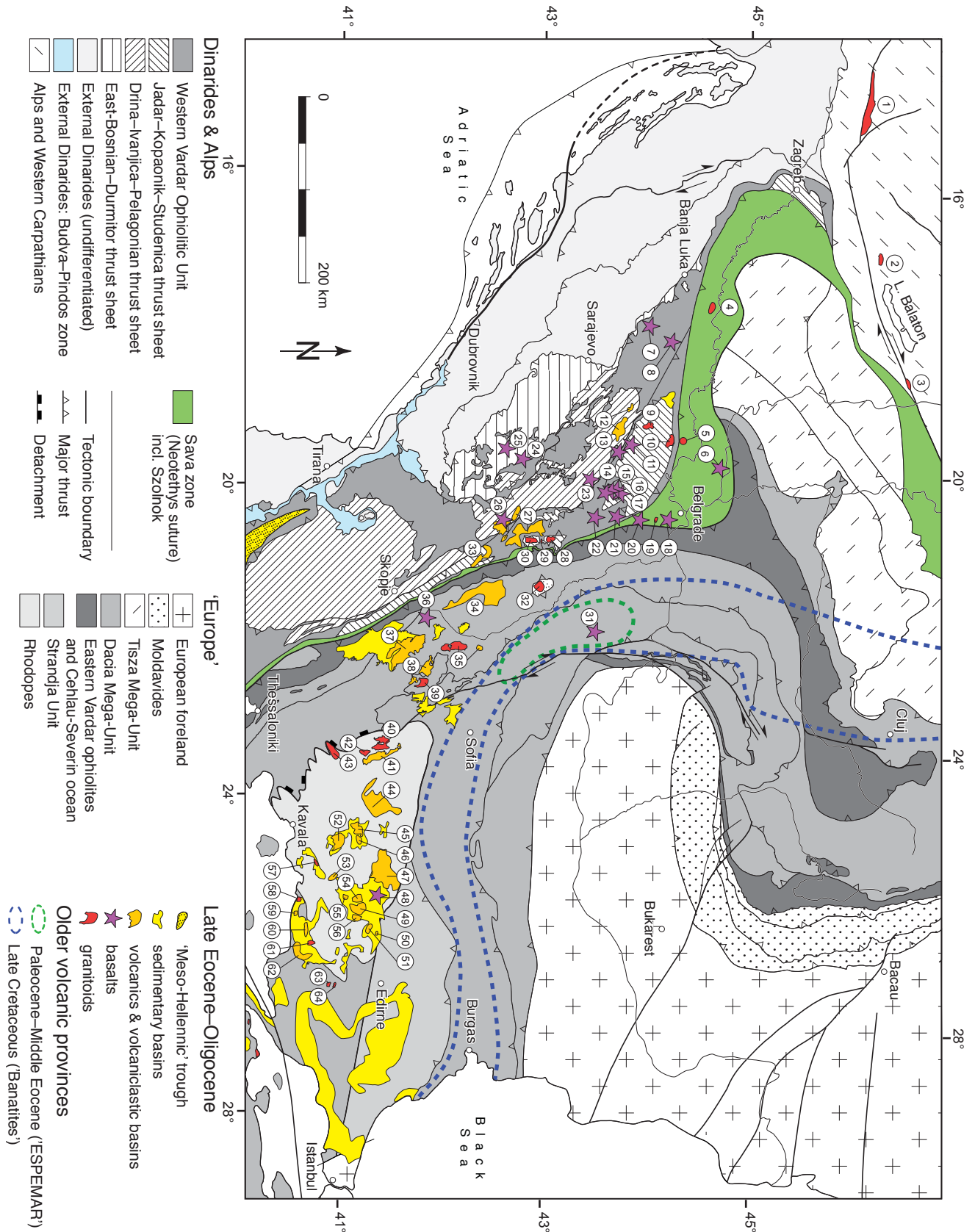


Fig. 3.9 – Distribution of Paleogene magmatism on the Balkan Peninsula. A compilation of literature data. For references to the numbers see Table 3.5. Geology modified after Schmid et al. (2008) and Marchev et al. (2005) for the Rhodopes.

subduction zone, unlikely. Rather, we prefer scenario 3, namely slab delamination and rollback of the Adriatic plate, whereby the Budva–Pindos zone merely represents an intra-continental site of compression (marked green in Fig. 3.9) that absorbs plate convergence. Note that this scenario is also in accordance with the evidence provided by Prelević et al. (2005) regarding the contemporaneous ultra-potassic volcanics being derived from a metasomatised mantle with a crustal signature.

We propose that after final closure of the Neotethys in the Eocene (Fig. 3.10a) the lithospheric mantle of the NE-ward subducted Adriatic plate started to delaminate (Bird 1979) and retreat. The thereby induced mantle flow (Funiciello et al. 2006; Piromallo et al. 2006) gave rise to mantle dominated magmas with various amounts of crustal contamination. Although lacking delamination, a similar scenario has been described with respect to the opening of the Tyrrhenian basins (Faccena et al. 2007), where the rapidly retreating Calabrian slab is continuously disrupted. In the case of the Dinarides the delamination model shown in Fig. 3.10b allows for (1) generation of chemically variable magmas, (2) magma emplacement in the lower (Adriatic) plate and (3) one single and continuously evolving subduction zone associated with one and the same (Adriatic) mantle slab.

Teleseismic tomography (Bijwaard and Spakman 2000; Piromallo and Morelli 2003) indeed monitored a through-going high velocity body in the southern Dinarides and northern Hellenides, i.e. from about Dubrovnik southwards. However, these authors documented a ca. 300 km long gap towards the north (cf. Ustaszewski et al. 2008). This suggests that in the Northern Dinarides the Adriatic slab did break off, while the central and southern Dinarides, as well as the Hellenides, are presently still characterized by roll back and mantle delamination.

Concerning the connection of the Dinaridic Late Eocene to earliest Miocene magmatic belt with the contemporaneous Periadriatic intrusions s.str. of the Alps and the magmatic belt paralleling the Mid-Hungarian fault zone (localities 1, 2 and 3 in Fig. 3.9), we emphasize that the subduction polarity in the Alps, including that within the Western Carpathians north of the Mid-Hungarian fault zone, merely representing the eastern prolongation of the Alps before Miocene lateral extrusion (Ratschbacher et al. 1991), is opposite to that of the Dinarides during the time span considered (Ustaszewski et al. 2008). Hence, in spite of the temporal coincidence there cannot be

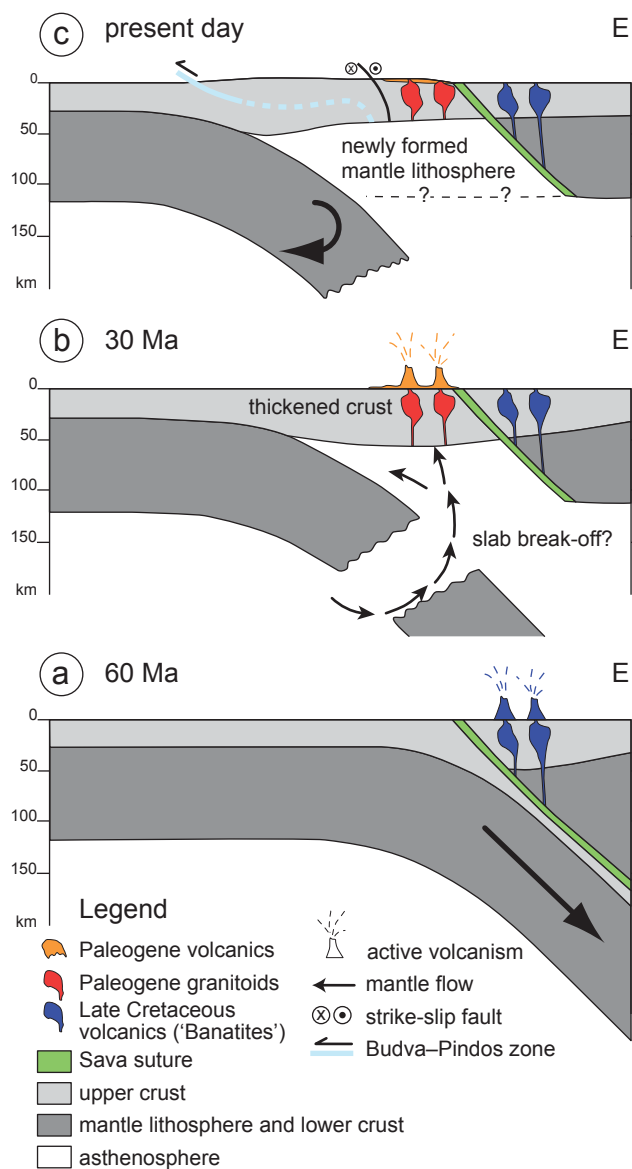


Fig. 3.10 – East–West profile sketches illustrating the migration of magmatism from the upper plate (Tisza-Dacia and Rhodopes) into the lower plate (present-day Dinarides) due to delamination of the lower plate (Adriatic) lithospheric mantle, possibly associated with slab break-off. Present-day geometry is that provided by the mantle tomography (Piromallo and Morelli 2003) and a by a crustal transect (Schmid et al. 2008).

a direct link between the Alpine–Mid-Hungarian magmatic belt and the Dinaridic–Hellenidic magmatic belt of which our area of investigation is a part. What is common to both, i.e. typical for the entire Periadriatic belt s.l., is the short distance between the site of subduction and the location of the magmatic arc, as well as the post-collisional scenarios. These two features, amongst others, led to the slab break-off model first proposed by von Blanckenburg and Davies (1995) for the Periadriatic intrusions of the Alps.

Miocene magmatic activity in the Dinarides

The Miocene Polumir intrusion (18 Ma) is part of a larger group of S-type granitoids in the Dinarides that includes a part of the Cer intrusive (albeit within an older I-type quartz monzonite; an age around 16 Ma (K–Ar) is reported for the S-type two-mica granite; Koroneos et al. 2010) and the two-mica Bukulja intrusion (20–17 Ma are reported for the two-mica granites; Cvetković et al. 2007b). It is uncertain, however, if the somewhat older I-type Golija intrusion with high-K affinity also belongs to this same suite. Regarding the Polumir intrusions, Vukov and Milovanović (2002) provided geochemical evidence to demonstrate partial melting of continental crust they interpreted to have formed in an extensional environment. This interpretation is supported by our own structural investigations (Fig. 3.3) and the fission-track data discussed above, which indicate the onset of extension during the last stages of granite emplacement or shortly thereafter (Fig. 3.8). Regarding the Cer and Bukulja intrusions (c.f. Fig. 3.9), Koroneos et al. (2010) and Cvetković et al. (2007b) proposed emplacement during the early stages of extension related to the formation of the Pannonian basin, the Bukulja intrusion being located in the footwall of a major core complex exhumed in early Miocene times (Marović et al. 2007). Hence, the location of these S-type granites at the southern margin of the Pannonian basin, their Early Miocene age and their association with core complex formation all argue for them being located in the backarc area of the W-directed subduction of the European lithosphere beneath the Carpathians, widely invoked to explain extension and magmatism in the main part of the Pannonian basin (Csontos 1995; Seghedi et al. 2004). However, the locations of the Miocene S-type granitoids of the Inner Dinarides also come to lie into within the Late Eocene to earliest Miocene (>22 Ma) belt of predominantly I-type granitoids. This, together with the fact that the Cer two-mica granite intrudes an older I-type quartz monzonite suggests that these S-type intrusions located at or close to the southern rim of the Pannonian basin may partly also have to do with them being located in the backarc area of the NE-directed subduction of the Adria plate. Hence it is not clear yet as to what extent this Miocene magmatic activity in the inner Dinarides might also interfere with ongoing extension in the Dinaridic–Hellenic back-arc during the Miocene.

Table 3.5 – References to the compilation shown in Fig. 3.8.

Nr	Locality	Rock Type	Age (Ma) Error ¹	Method	Min. ¹	Literature
Granitoids (red bodies)						
1	Karawanken	tonalite	30–28	K–Ar		Pamić and Palinkaš 2000
2	Zala	tonalite	35–27	K–Ar		Benedek 2002
3	Velence	andesite	37–29	K–Ar		Benedek 2002
4	Motajca	granitoid	26.7 ±0.1	U–Pb	Zr	Ustaszewski et al. subm.
5	Bogatić (well)	tonalite	44–36	K–Ar	Fsp	Pécskay unpubl.
5	Bogatić (well)	tonalite	30.5 ±1.2	K–Ar	Bio	Pécskay unpubl.
9	Boranje	granitoid	34–29	K–Ar	Bio	Karamata et al. 1992
10	Cer	granitoid	30–22	K–Ar	Fsp	Karamata et al. 1994
19	Kosmaj	granitoid	30–29	K–Ar	Bio, wr	Karamata et al. 1994
28	Željnj	granitoid	31.8–31.4	U–Pb	Zr	This study
29	Drenje	granitoid	31.7–31.2	U–Pb	Zr	This study
30	Kopaonik	granitoid	30.9–30.7	U–Pb	Zr	This study
32	Jastrebac	granitoid	37.3 ±5	Rb–Sr	Bio	Červenjak 1963
35	Surdulica	granodiorite	29–33	K–Ar	Bio, wr	Čebić 1990
39	Osogovo	granitoid	31.0 ±2	U–Pb	Zr	Graf 2001
40	Central Pirin	granitoid	34.3 ±2	U–Pb	Zr	Zagorchev et al. 1987
42	Teshovo	granitoid	32.0 ±0.2	U–Pb	Zr	Jahn–Awe et al. 2010
43	Leptokaria	granite	32.0 ±?	Rb–Sr		Delmoro et al. 1988
43	Vrondou	granodiorite	33–23	K–Ar	Hbl	Marakis 1969
57	Xanthi	granodiorite	34–30	U–Pb	Zr	Liaty 1986
58	Maronia	granite	29.0 ±?	Rb–Sr		Del Moro et al. 1988
58	Skaloti	granite	33.0 ±?	K–Ar		Marakis 1969
61	Kirki	granite	32.0 ±?	Rb–Sr		Del Moro et al. 1988
61	Lefkogia Granitis	granodiorite	28.0 ±?	K–Ar		Marakis 1969
63	Halasmata	granite	32.0 ±?	Rb–Sr		Del Moro et al. 1988
64	Tris Vrisses	granite	35.0 ±?	Rb–Sr		Del Moro et al. 1988
Volcanics and volcanoclastic basins (orange bodies)						
12	Srebrenica	andesite	31.7 ±?	K–Ar	Bio	Pamić 1997
27	Rogozna–Ibar	volcaniclastics	32–29	K–Ar		Karamata et al. 1994
33	Kosovska Mitrovica	volcaniclastics	33–28	K–Ar		Karamata et al. 1994
34	Lece	volcaniclastics	32–28	K–Ar		Pamić and Balen 2001
37	Ovchepole	volcanics	32–29	K–Ar		Dumurdzanov et al. 2005
38	Prekolnitsa	volcanics	34–33	U–Pb	Zr	Kounov et al 2004
38	Ruen	Volcanics	32–29	K–Ar		Harkovska and Pécskay 1997
41	Mesta	volcaniclastics	33.4 ±1.6	K–Ar		Pécskay et al. 2000
44	Bratsigovo–Dospat	volcaniclastics	34.0 ±3	K–Ar		Marchev et al. 2005
45	Perelik	volcaniclastics	32.9 ±1.2	K–Ar		Pécskay et al. 1991
46	Levochevo	volcaniclastics	33.4 ±1.4	K–Ar		Harkovska et al. 1998
47	Borovitsa	volcaniclastics	33–32	Ar/Ar		Singer and Marchev 2000
49	Sveti Iliya	volcaniclastics	35–31	K–Ar		Lilov et al. 1987
50	Lozen	volcaniclastics	37–35	K–Ar		Lilov et al. 1987
51	Madjarovo	volcaniclastics	33–31	K–Ar		Lilov et al. 1987
52	Kotili–Vitinia	volcaniclastics	30.8 ±0.1	U–Pb		Ovtcharova et al. Unpubl.
53	Kaloticho–Zlatograd	volcaniclastics	35–23	K–Ar		Eleftheriadis and Lippolt 1984
54	Dambalak	volcaniclastics	31–29	K–Ar		Georgiev et al. 2003
55	Zvezdel	volcaniclastics	31.9 ±0.5	Ar/Ar		Singer and Marchev 2000
56	Iran Tepe	volcaniclastics	37–35	K–Ar		Lilov et al. 1987
59	Petrota	volcaniclastics	30–27	K–Ar		Pécskay et al. 2003
60	Kirki–Esimi	volcaniclastics	33–22	K–Ar		Pécskay et al. 2003
62	Loutros–Fere–Dadia	volcaniclastics	33–20	K–Ar		Pécskay et al. 2003

Table 3.5 – (continued)

Nr	Locality	Rock Type	Age (Ma) Error ¹	Method	Min. ¹	Literature
Basalts (lila stars)						
6	Fruška Gora	trachyandesite	34.0 ±?	Rb–Sr	Fsp, Bio	Knežević et al. 1991
7	Veliki Majdan	Lamproite	33.5 ±1.3	K–Ar	Phl	Cvetković et al. 2004a
8	Maglaj	trachydacite	30.1 ±1.5	K–Ar	Bio	Pamić et al. 2000
11	Zabrdica	Ol-lamproite	25.6 ±1.0	K–Ar	wr	Cvetković et al. 2004a
13	Mionica	Lamproite	29.1 ±1.1	K–Ar	wr	Cvetković et al. 2004a
14	Šilopaj	Basalt	25.7 ±1.2	K–Ar	wr	Cvetković et al. 2004a
15	Mutanj	Basalt	24.2 ±1.0	K–Ar	wr	Cvetković et al. 2004a
16	Boljkovac	Phl-trachybasalt	29.7 ±1.1	K–Ar	wr	Cvetković et al. 2004a
17	Ozrem	Lamproite	35.0 ±1.6	K–Ar	wr	Cvetković et al. 2004a
17	Ozrem	Andesite	24.9 ±1.0	K–Ar	Bt	Cvetković et al. 2004a
18	Avala	Kersantite	30.9 ±1.2	K–Ar	Phl	Cvetković et al. 2004a
20	Bukulja	Minette	26.0 ±1.0	K–Ar	Phl	Cvetković et al. 2004a
21	Rudnik	Ol-Phl-lamproite	30.2 ±1.1	K–Ar	Phl	Cvetković et al. 2004a
21	Rudnik	Minette	31.9 ±1.2	K–Ar	Phl	Cvetković et al. 2004a
22	Borač	Phl-trachybasalt	22.7 ±0.9	K–Ar	Phl	Cvetković et al. 2004a
22	Borač	Minette	22.8 ±0.9	K–Ar	Phl	Cvetković et al. 2004a
22	Borač	Andesite	23.9 ±1.0	K–Ar	Hbl80%	Cvetković et al. 2004a
23	Družetići	Analcimite	23.9 ±2.1	K–Ar	wr	Cvetković et al. 2004a
24	Nova Varoš	Analcimite	21.5 ±1.1	K–Ar	wr	Cvetković et al. 2004a
25	Trijebine	Analcimite	23.0 ±1.3	K–Ar	wr	Cvetković et al. 2004a
26	Novi Pazar	Basaltic andesite	29.8 ±1.2	K–Ar	wr	Cvetković et al. 2004a
31	Bogovina	Lamproite	30.0 ±1.3	K–Ar	Phl	Cvetković et al. 2004a
35	Klinovac	Phl-trachybasalt	32.7 ±1.3	K–Ar	wr	Cvetković et al. 2004a
48	Kardjali	High-Ba-trachybasalt	33–29	K–Ar		Marchev et al. 2004

¹ if specified in original publication

Conclusions

1) U–Pb (ID-TIMS) dating on single zircons from different intrusions in southern Serbia revealed two age groups, an Oligocene (31.77–30.70 Ma) and a Miocene (20.58–17.74 Ma) one. The Oligocene group (Kopaonik, Drenje and Željina intrusive bodies) consists of I-type granitoids with positive ϵ_{Hf} values of the zircons, indicating a moderate crustal influence in their origin, and it is proposed that this group formed via partial melting of mantle-derived lower crustal protoliths. The Miocene group consists of the S-type Polumir granite and the Golija intrusion that shows negative ϵ_{Hf} values (-0.7 to -2.7), generally indicating a higher crustal influence during magma generation.

2) The zircon and apatite fission-track analyses show that the emplacement of all but one of the Oligocene intrusive bodies analysed occurred slightly above some 300 °C, i.e. within the upper crust. They cooled to the ambient temperatures and remained at this depth without further deformation for some 10 Ma before the onset of rapid cooling due to unroofing by substantial extension between 16 and 10 Ma. The onset of exhumation in an extensional scenario led to core-complex formation and was contemporaneous with the intrusion of the S-type Miocene-age Polumir granite. Final cooling to near-surface conditions occurred at lower rates of around 10 °C/Ma from 11 Ma onwards for both age groups.

3) It is proposed that Late Eocene to Oligocene magmatism, which affects the Adria-derived lower plate units of the Dinarides may be caused by delamination of the Adriatic mantle from the overlying crust after the closing of the Neotethys Ocean and Adria–Europe collision, associated with intra-plate convergence within the external Dinarides, i.e. within the lower plate, that started during the Late Eocene.

4) Miocene magmatism and core-complex formation at the southern rim of the Pannonian basin, believed to be mainly associated with back-arc extension, also affects a part of the mountainous areas of the internal Dinarides.

5) A connection of the Dinaridic Late Eocene to earliest Miocene magmatic belt with other contemporaneous Periadriatic intrusions in the Alps and along the Mid-Hungarian fault zone, as often proposed in the literature, is unlikely because the subduction polarity in the Alps and in the Western Carpathians north of the Mid-Hungarian fault zone is opposite to that of the Dinarides during the Paleogene. Hence, in spite of the temporal coincidence there cannot be a direct link between the Alpine–Mid-Hungarian magmatic belt and the Dinaridic–Hellenidic magmatic belt in Late Eocene to Oligocene times.

Acknowledgments

We thank B. Schoene for his help with sample preparation and mass spectrometry. K. Ustaszewski gave valuable input to the regional geological discussion. Yet unpublished radiometric ages were made available by the courtesy of D. Prelević. This manuscript greatly benefited from the comments and suggestions by D. Bernoulli. Very thorough and constructive revisions by C. B. Burchfiel and A. von Quadt are highly appreciated. S. Schefer thanks the Freiwillige Akademische Gesellschaft Basel for supporting him and his family during the final stage of his PhD thesis. This project was financed by the Swiss National Science Foundation, Project No. 200020-109278 granted to S. M. Schmid, B. Fügenschuh and S. Schefer.

Appendix A, Fission-track dating

Remarks regarding the interpretation of fission-track data

When interpreting fission-track results we took into account that the central ages obtained by dating the minerals are not necessarily a geological meaningful age because the tracks produced by the decay of ^{238}U are not stable at all temperature conditions. There is a temperature range, the partial annealing zone (PAZ), at which the tracks in the mineral lattice become annealed. As a result of the annealing process these tracks shorten and eventually disappear completely. The effective closure of the system lies within this PAZ and is dependent on the overall cooling rates and the kinetic properties of the minerals. The specific PAZ for apatite lies between 120–60 °C (Green and Duddy 1989; Corrigan 1993). The PAZ for zircon is not equally well defined and a wide range of temperature bounds has been published. Yamada et al. (1995) suggest temperature ranges of ca. 390–170 °C, whereas Tagami and Dumitru (1996) and Tagami et al. (1998) report ca. 310–230 °C. Recently, in his overview on the zircon fission-track dating method, Tagami (2005) reported temperature ranges for the zircon closure temperature of ca. 300–200 °C. Accordingly we use a value of 250 ± 50 °C for the closure temperature and a zircon PAZ of 300–200 °C.

Apatite fission-track thermal modelling

Fission-tracks in apatite form continuously through time with an approximately uniform initial mean length of

~16.3 μm (Gleadow et al. 1986). Upon heating, tracks gradually anneal and shorten to a length that is a function of the time and maximum temperature to which the apatites were exposed. For example, tracks are completely annealed at a temperature of 110–120 °C for a period of 105–106 years (Gleadow and Duddy 1981). These annealing characteristics allow the generation of time-temperature paths by inverse modelling (e.g. Gallagher 1995; Ketcham et al. 2003). As the resolution of the AFT thermo-chronometer is limited to the temperature range of 120–60 °C (Laslett et al. 1987), the paths of the t-T envelope defined for the zones outside of this range are not necessarily representative for the real thermal evolution of a sample.

Modelling of the apatite age and track length distribution data was carried out with the program HeFTy (Ketcham et al. 2003). Fission-track age, track-length distribution and etch pits diameters (Dpar) as well as user-defined time-temperature (t-T) boxes are used as input parameters. An inverse Monte Carlo algorithm with a multikinetic annealing model (Ketcham et al., 2007) was used to generate the time-temperature paths. The algorithm generates a large number of time-temperature paths, which are tested with respect to the input data. The t-T paths are forced to pass through the time-temperature boxes (constraints). The fitting of the measured input data and modelled output data are statistically evaluated and characterized by the value of ‘goodness of fit’ (GOF). A ‘good’ result corresponds to values >0.5 whereas a value of 0.05 or higher is considered to reflect an ‘acceptable’ fit between modelled and measured data.

It is important to remember that the ‘best’ thermal history obtained during this process is not necessarily the only possible one. Other thermal histories may match the observed data similarly well, and it is therefore imperative to consider as many other geological constraints as possible to determine the most likely path.

References

- Benedek K (2002) Paleogene igneous activity along the easternmost segment of the Periadriatic-Balaton lineament. *Acta Geol Hungarica* 45:359–371
- Bijwaard H, Spakman W (2000) Non-linear global P-wave tomography by iterated linearized inversion. *Geophys J Int* 141:71–82
- Bird P (1979) Continental Delamination and the Colorado Plateau. *J Geophys Res* 84:7561–7571
- Brandon MT, Roden-Tice MK, Garver JI (1998) Late Cenozoic exhumation of the Cascadia accretionary wedge in the Olympic Mountains, northwest Washington State. *Geol Soc Am Bull* 110:985–1009.
- Brković T, Malešević M, Urošević M, Trifunović S, Radanović Z, Dimitrijević M, Dimitrijević MN (1976) Geological map and explanatory text of the sheet Ivanjica. Savezni Geološki Zavod, Beograd
- Brun JP, Soukoutis D (2007) Kinematics of the Southern Rhodope Core Complex (North Greece). *Int J Earth Sci* 96:1079–1099
- Burchfiel BC, Nakov R, Tzankov T, Royden, L (2000) Cenozoic extension in Bulgaria and northern Greece: the northern part of the Aegean extensional regime. In: Bozkurt, E., Winchester, E and Piper, J.D.A. (eds.) – *Tectonics and Magmatism in Turkey and the Surrounding Area*. Geological Society (London) Special Publications, 173:325–352
- Burchfiel BC, Nakov R, Tzankov T (2003) Evidence from the Mesta half-graben, SW Bulgaria, for the Late Eocene beginning of Aegean extension in the Central Balkan Peninsula. *Tectonophysics* 375:61–76
- Burchfiel BC, Nakov R, Dumurdzanov N, Papanikolaou D, Tzankov T, Kotzev V, Todosov A, Nurce B (2008) Evolution and dynamics of the Cenozoic tectonics of the South Balkan extensional system. *Geosphere*. doi: 10.1130/GES00169.1.
- Čebić V (1990) Konačni izveštaj o geološko-petrološkom i geohemijskom izučavanju tercijarnog magmatskog kompleksa surduličke oblasti. Fond Geoinstituta, Beograd. (The final report on geological-petrological and geochemical investigations of the Tertiary magmatic complex of Surdulica area. Fund of Geoinstitute, Belgrade, in Serbo-Croatian)
- Červenjak Z, Ferrara G, Tongiorgi E (1963) Age determination of some Yugoslav granites and granodiorites by the rubidium-strontium method. *Nature* 197:893–893
- Chappell BJ and White AJR (1974) Two contrasting granite types. *Pacific Geol* 8:173–174
- Cherniak DJ, Watson EB (2001) Pb diffusion in zircon. *Chem Geol* 172:5–24
- Corrigan JD (1983) Apatite fission-track analysis of Oligocene strata in South Texas, USA; testing annealing models. *Chem Geol* 104:227–249
- Csontos L (1995) Tertiary tectonic evolution of the Intra-Carpathian area: a review. *Acta Vulcan* 7:1–13
- Cvetković V, Pécskay Z (1999) The Early Miocene eruptive complex of Borač (central Serbia): volcanic facies and evolution over time. Extended abstract. *Carpathian Geology 2000*, October 11–14, 1999, Smolenice. *Geol Carpathica* 50:91–93
- Cvetković V, Prelević D, Pécskay Z (2000) Lamprophyric rocks of the Miocene Borač eruptive complex (Central Serbia, Yugoslavia). *Acta Geol Hungarica* 43:25–41
- Cvetković V (2002) Nature and origin of pyroclastic deposits of the Miocene Eruptive Complex of Borač (Central Serbia). *Bull CXXV Acad Serbe Sci Arts, Classe Sci Math et Sci Natur* 342:209–215

- Cvetković V, Poli G, Resimić-Šarić K, Prelević D, Lazarov M (2002) Tertiary post-collision granitoid of Mt. Kopaonik (Serbia) – Petrogenetic constraints based on new geochemical data. In: Michalík J, Šimon L, Vozár J (eds) Proceedings of XVII. Congress of Carpathian-Balkan Geological Association Bratislava, September 1st–4th 2002. *Geol Carpathica* 53
- Cvetković V, Prelević D, Downes H, Jovanović M, Vaselli O, Pécskay Z (2004a) Origin and geodynamic significance of Tertiary postcollisional basaltic magmatism in Serbia (central Balkan Peninsula). *Lithos* 73:161–186
- Cvetković V, Downes H, Prelević D, Jovanovic M, Lazarov M (2004b) Characteristics of the lithospheric mantle beneath East Serbia inferred from ultramafic xenoliths in Palaeogene basanites. *Contrib Mineral Petrol* 148:335–357.
- Cvetković V, Downes H, Prelević D, Lazarov M, Resimić-Sarić K (2007a) Geodynamic significance of ultramafic xenoliths from Eastern Serbia: Relics of sub-arc oceanic mantle? *J Geodyn* 43:504–527
- Cvetković V, Poli G, Christofides G, Koroneos A, Pécskay Z, Resimić-Sarić K, Eric V (2007b) The Miocene granitoid rocks of Mt. Bukulja (central Serbia): evidence for pannonian extension-related granitoid magmatism in the northern Dinarides. *Europ J Mineral* 19:513–532
- Del Moro A, Innocenti F, Kyriakopoulos C, Manetti P, Papadopoulos P (1988) Tertiary granitoids from Thrace (northern Greece) – Sr isotopic and petrochemical data. *N J Mineral Abh* 159:113–135
- Delaloye M, Lovrić A, Karamata S (1989) Age of Tertiary granitic rocks of Dinarides and Vardar zone. 14th CBGA Congress Extended Abstracts, Sofia 1:1186–1189
- Didier J, Barbarin B (1991) The different types of enclaves in granites – Nomenclature. In: Didier J, Barbarin B (eds) *Enclaves and granite petrology, Developments in Petrology no. 13*, Amsterdam, pp 19–23
- Dumurdzanov N, Serafimovski T, Burchfiel BC (2005) Cenozoic tectonics of Macedonia and its relation to the South Balkan extensional regime. *Geosphere* 1:1–22
- Dunkl I (2002) TRACKKEY: a Windows program for calculation and graphical presentation of fission track data. *Comput Geosci* 18:3–12
- Egli D (2008) Das Kopaonik-Gebirge in Südserbien – Stratigraphie, Strukturen und Metamorphose. MSc Thesis, University of Basel, Basel.
- Faccenna C, Funicello F, Civetta L, D’Antonio M, Moroni M, Piromallo C (2007) Slab disruption, mantle circulation, and the opening of the Tyrrhenian basins. In: Beccaluva L, Bianchini G, Wilson M (eds) *Geol Soc Am Spec Paper* 418, pp 153–169
- Funicello F, Moroni M, Piromallo C, Faccenna C, Cenedese A, Bui HA (2006) Mapping mantle flow during retreating subduction: Laboratory models analyzed by feature tracking. *J Geophys Res* 111:B03402, doi:10.1029/2005JB003792
- Galbraith RF, Laslett GM (1993) Statistical models for mixed fission-track ages. *Nucl Tracks Radiation Meas* 21:459–470
- Gallagher K, Brown R & Johnson C (1998) Fission-track analysis and its applications to geological problems. *Ann Rev Earth Plan Sci* 26: 519–572
- Gapais D (1989) Shear structures within deformed granites: Mechanical and thermal indicators. *Geology* 17:1144–1147
- Georgiev V, Milovanov P, Monchev P (2003) K–Ar dating of the magmatic activity in the Momchilgrad volcano-tectonic depression. *CR Acad Bulgare Sci* 56:49–54

- Gleadow AJW (1981) Fission-track dating methods – what are the real alternatives. *Nucl Tracks Radiation Meas* 5:3–14
- Gleadow AJW & Duddy IR (1981) A natural long-term annealing experiment for apatite. *Nucl Tracks* 5:169–174
- Gleadow AJW, Duddy IR, Green PF & Lovering JF (1986) Confined fission track lengths in apatite: A diagnostic tool for thermal history analysis. *Contr Min Pet* 94:405–415
- Graf J (2001) Alpine Tectonics in Western Bulgaria: Cretaceous Compression of the Kraishte Region and Cenozoic Exhumation of the Crystalline Osogovo-Lisets Complex (PhD Thesis): ETH Zurich
- Green PF, Duddy IR (1989) Some comments on paleotemperature estimation from apatite fission track analysis. *J Petr Geol* 12:111–114
- Harkovska A, Pécskay Z (1997) The Tertiary magmatism in Ruen magmato-tectonic zone (W. Bulgaria) – A comparison of new K-Ar ages and geological data. In: Boev B, Serafimovski T (eds) *Magmatism, Metamorphism and Metallogeny of the Vardar Zone and Serbo-Macedonian Massif*. Faculty Mining Geology, Stip–Dojran, Rep. Macedonia, pp 137–142
- Harkovska A, Marchev P, Machev P, Pécskay Z (1998) Paleogene magmatism in the Central Rhodope area, Bulgaria — a review and new data. *Acta Vulcan* 10:199–216
- Hurford AJ, Green PF (1983) The zeta-age calibration of fission-track dating. *Isotope Geoscience* 1:285–317
- Jahn-Awe S, Froitzheim N, Nagel TJ, Frei D, Georgiev N, Pleuger J (2010) Structural and geochronological evidence for Paleogene thrusting in the Western Rhodopes (SW Bulgaria), *subm. Tectonics* 29:TC3008, doi:10.1029/2009TC002558
- Karamata S, Delaloye M, Lovrić A, Knežević V (1992) Two genetic groups of Tertiary granitic rocks of Central and Western Serbia. *Ann Géol Péninsule Balkan* 56:263–283
- Karamata S, Pécskay Z, Knežević V, Memović E (1994) Origin and age of Rogozna (central Serbia) volcanics in the light of new isotopic data. *Bull Acad Serb Sci* 35:41–46
- Ketcham RA, Donelick RA, Donelick M (2003) AFTSolve: A program for multi-kinetic modeling of apatite fission-track data. *Am Mineral* 88:929–929
- Ketcham RA, Carter A, Donelick RA, Barbarand J, Hurford AJ (2007) Improved measurement of fission-track annealing in apatite using c-axis projection. *Am Mineral* 92:789–798
- Knežević V, Szeki-Fux F, Steiger R, Pécskay Z, Boronihin VA, Karamata S (1991) Petrology of Fruška-Gora latites – volcanic precursors at the southern margin of the Pannonian basin. In: *Geodynamic Evolution of the Pannonian Basin*, *Serb Acad Sci Arts* 62:243–259
- Knežević V, Karamata S, Vasković N, Cvetković V (1995) Granodiorites of Kopaonik and contact metamorphic zone. In: *Geology and Metallogeny of the Kopaonik Mt., Belgrade*, pp 172–184
- Korbar T (2009) Orogenic evolution of the External Dinarides in the NE Adriatic region: a model constrained by tectonostratigraphy of Upper Cretaceous to Paleogene carbonates. *Earth Sci Rev* 96:296–312
- Koroneos A, Poli G, Cvetković V, Christofides G, Krstić D, Pécskay Z (2010) Petrogenetic and tectonic inferences from the study of the Mt Cer pluton (West Serbia). *Geol Mag* doi:10.1017/S0016756810000476
- Kounov A, Seward D, Bernoulli D, Burg JP, Ivanov Z (2004) Thermotectonic evolution of an extensional dome: the Cenozoic Osogovo-Lisets core complex (Kraishte zone, western Bulgaria). *Int J Earth Sci* 93:1008–1024

- Kovács I, Csontos L, Szabó C, Bali E, Falus G, Benedek K, Zajacz Z (2007) Paleogene–early Miocene igneous rocks and geodynamics of the Alpine–Carpathian–Pannonian–Dinaric region: An integrated approach. In: Beccaluva L, Bianchini G, Wilson M (eds) *Cenozoic Volcanism in the Mediterranean Area*, Geol Soc Am Spec Paper 418:93–112
- Laslett GM, Green PF, Duddy IR & Gleadow AJW (1987) Thermal annealing of fission tracks in apatite: 2. A quantitative analysis. *Chem Geol* 65:1–13
- Lee JKW, Williams IS, Ellis DJ (1997) Pb, U and Th diffusion in natural zircon. *Nature* 390:159–162
- Liati A (1986) Regional metamorphism and overprinting contact metamorphism of the Rhodope Zone, near Xanthi (N. Greece). Ph.D. Thesis, Technische Universität Braunschweig
- Lilov P, Yanev Y, Marchev P (1987) K–Ar dating of the Eastern Rhodopes Paleogene magmatism. *Geol Balcanica* 17:49–58
- Ludwig K (2005) Isoplot – A plotting and regression program for radiogenic isotope data. USGS Open File report, Boulder
- Marakis G (1969) Geochronologic studies of some granites from Macedonia. *Ann Géol Pays HELL* 21:121–252
- Marchev P, Raicheva R, Downes H, Vaselli O, Chiaradia M, Moritz R (2004) Compositional diversity of Eocene–Oligocene basaltic magmatism in the Eastern Rhodopes, SE Bulgaria: implications for genesis and tectonic setting. *Tectonophysics* 393:301–328
- Marchev P, Kaiser-Rohrmeier M, Heinrich C, Ovtcharova M, von Quadt A, Raicheva R (2005) Hydrothermal ore deposits related to post-orogenic extensional magmatism and core complex formation: The Rhodope Massif of Bulgaria and Greece. *Ore Geol Rev* 27:53–89
- Marović M, Djoković I, Toljić M, Spahić D, Milivojević J (2007) Extensional Unroofing of the Veliki Jastrebac Dome (Serbia). *Ann Géol Péninsule Balkan* 68:21–27
- Mattinson JM (2005) Zircon U–Pb chemical abrasion (“CA-TIMS”) method: Combined annealing and multi-step partial dissolution analysis for improved precision and accuracy of zircon ages. *Chem Geol* 220:47–66
- Mikes T, Baldi-Beke M, Kazmer M, Dunkl I, von Eynatten H (2008) Calcareous nannofossil age constraints on Miocene flysch sedimentation in the Outer Dinarides (Slovenia, Croatia, Bosnia-Herzegovina and Montenegro). *Geol Soc (London) Spec Pub* 298:335–363
- Miller JS, Matzel JEP, Miller CF, Burgess SD, Miller RB (2007) Zircon growth and recycling during the assembly of large, composite arc plutons. *J Volcan Geotherm Res* 167:282–299
- Mojsilović S, Baklajić D, Djoković I (1978) Basic Geological Map of the SFRY, 1:100'000, Sheet Sjenica (K32-29), Savezni Geološki Zavod, Beograd (1960–1973)
- Mojsilović S, Djoković I, Baklajić D, Rakić B (1980) Geology of the Sheet Sjenica (K32–29), Explanatory notes, Savezni Geološki Zavod, Beograd (1973, in Serbo-Croatian, English and Russian summaries).
- Pamić J (1997) Volcanic rocks of the Sava–Drava interfluvium and Baranja. *Nafta Monograph*, Zagreb
- Pamić J, Palinkas L (2000) Petrology and geochemistry of Paleogene tonalites from the easternmost parts of the Periadriatic Zone. *Mineral Petrol* 70:121–141
- Pamić J, Pécskay Z, Balen D (2000) Lower oligocene K–Ar ages of high-K calc-alkaline and shoshonite rocks from the North Dinarides in Bosnia. *Mineral Petrol* 70:313–320
- Pamić J, Balen D (2001) Tertiary magmatism of the Dinarides and the adjoining South Pannonian Basin, an overview. *Acta Vulcan* 13:9–24
- Pamić J, Balen D, Herak M (2002a) Origin and geodynamic evolution of Late Paleogene magmatic associations along the Periadriatic–Sava–Vardar magmatic belt. *Geodin Acta* 15:209–231

- Pamić J, Tomljenović B, Balen D (2002b) Geodynamic and petrogenetic evolution of Alpine ophiolites from the central and NW Dinarides: an overview. *Lithos* 65:113–142
- Pécskay Z, Balogh K, Harkovska A (1991) K–Ar dating of the Perelik volcanic massif (Central Rhodopes, Bulgaria). *Acta Geol Hungarica* 34:101–110
- Pécskay Z, Harkovska A, Hadjiev A (2000) K–Ar dating of Mesta volcanics (SW Bulgaria). *Geol Balcanica* 30:3–11
- Pécskay Z, Eleftheriadis G, Koroneos A, Soldatos T, Christofides G (2003) K–Ar dating, geochemistry and evolution of the Tertiary volcanic rocks (Thrace, northeastern Greece). In: Eliopoulos DG (ed) *Mineral Exploration and Sustainable Development*, Millpress, Rotterdam, pp 1229–1232
- Piomallo C, Morelli A (2003) P wave tomography of the mantle under the Alpine–Mediterranean area. *J Geophys Res* 108:ESE1.1–ESE1.23
- Piomallo C, Becker TW, Funiciello F, Faccenna C (2006) Three-dimensional instantaneous mantle flow induced by subduction. *Geophys Res Lett* 33:L08304, doi:10.1029/2005GL025390
- Poli G, Tommasini S, Halliday AN (1996) Trace elements and isotopic exchange during acid-basic magma interaction processes. *Trans R Soc Edinburgh: Earth Sci* 87:225–232.
- Prelević D, Cvetković V, Foley SF (2001) Composite igneous intrusions from Serbia; two case studies of interaction between lamprophyric and granitoid magmas. Tertiary magmatism in the Dinarides. *Acta Vulcan* 13:145–157
- Prelević D, Foley SF, Cvetković V, Romer RL (2004) Origin of minette by mixing of lamproite and felsic magmas in Veliki Majdan, Serbia. *J Petrol* 45:759–792
- Prelević D, Foley SF, Romer RL, Cvetković V, Downes H (2005) Tertiary ultrapotassic volcanism in Serbia: Constraints on petrogenesis and mantle source characteristics. *J Petrol* 46:1443–1487
- Prelević D, Foley SF, Stracke A, Romer RL, Conticelli S (subm.) Hf isotopes in Mediterranean lamproites: mixing of melts from asthenosphere and crustally contaminated lithosphere. *Chem Geol*, submitted
- Ratschbacher L, Frisch W, Linzer H-G, Merle O (1991) Lateral extrusion in the Eastern Alps, 2, structural analysis. *Tectonics* 10:257–271.
- Rosenberg CL (2004) Shear zones and magma ascent: A model based on a review of the Tertiary magmatism in the Alps. *Tectonics* 23:TC3002, doi:10.1029/2003TC001526
- Rudnick RL, Gao S (2003) Composition of the Continental Crust. In: Heinrich DH, Karl KT (eds.) *Treatise on Geochemistry*. Pergamon, Oxford, pp 1–64.
- Schaltegger U, Brack P (2007) Crustal-scale magmatic systems during intracontinental strike–slip tectonics: U, Pb and Hf isotopic constraints from Permian magmatic rocks of the Southern Alps. *Int J Earth Sci* 96:1131–1151.
- Schaltegger U, Guex J, Bartolini A, Schoene B, Ovtcharova M (2008) Precise U–Pb age constraints for end-Triassic mass extinction, its correlation to volcanism and Hettangian post-extinction recovery. *Earth Planet Sci Lett* 267:266–275.
- Schaltegger U, Brack P, Ovtcharova M, Peytcheva I, Schoene B, Stracke A, Marocchi M, Bargossi GM (2009) 700,000 years of magma accretion, crystallization and initial cooling in a composite pluton recorded by zircon and titanite (Adamello batholith, northern Italy). *Earth Planet Sci Lett* 286:208–218

- Schefer, S (2010) Tectono-metamorphic and magmatic evolution of the Internal Dinarides (Kopaonik area, southern Serbia) and its significance for the geodynamic evolution of the Balkan Peninsula. PhD Thesis, University of Basel, Switzerland.
- Schefer S, Egli D, Frank W, Fügenschuh B, Ovtcharova M, Schaltegger U, Schoene B, Schmid SM (2008) Metamorphic and igneous evolution of the innermost Dinarides in Serbia. In: 6th Swiss Geoscience Meeting, Lugano. Abstract Volume, pp 60–61
- Schefer S, Egli D, Missoni S, Bernoulli D, Fügenschuh B, Gawlick HJ, Jovanović D, Krystyn L, Lein R, Schmid SM, Sudar MN (2010) Triassic metasediments in the Internal Dinarides (Kopaonik area, southern Serbia): stratigraphy, paleogeographic and tectonic significance. *Geol Carpathica* 61:89–109
- Schmid SM, Bernoulli D, Fügenschuh B, Matenco L, Schefer S, Schuster R, Tischler M, Ustaszewski K (2008) The Alpine–Carpathian–Dinaridic orogenic system: correlation and evolution of tectonic units. *Swiss J Geosci* 101:139–183
- Seghedi I, Downes H, Szakacs A, Mason PRD, Thirlwall MF, Rosu E, Pécskay Z, Marton E, Panaiotu C (2004) Neogene–Quaternary magmatism and geodynamics in the Carpathian–Pannonian region: A synthesis. *Lithos* 72:117–146
- Shand SJ (1947) Eruptive Rocks. Their genesis, composition, classification, and their relation to ore deposits (3rd ed.). J. Wiley & Sons, New York, N.Y.
- Simić V (1956) Zur Geologie des Studenicegebietes (Südwestserbien). *Vesnik Bull Serv Geol Geophys* 12:5–66
- Singer B, Marchev P (2000) Temporal evolution of arc magmatism and hydrothermal activity including epithermal gold veins, Borovitsa caldera, southern Bulgaria. *Econ Geol* 95:1155–1164
- Skourlis K, Doutsos T (2003) The Pindos Fold-and-thrust belt (Greece): inversion kinematics of a passive continental margin. *Int J Earth Sci* 92:891–903
- Stacey JS, Kramers JD (1975) Approximation of terrestrial lead isotope evolution by a 2-stage model. *Earth Planet Sci Lett* 26:207–221
- Stajević B (1987) Magmatizam Golije i njegov metalogenetski značaj. *Zbornik radova Rudarsko-geološkog fakulteta* 26:7–17
- Tagami T, Dimitru TA (1996) Provenance and history of the Franciscan accretionary complex: Constraints from zircon fission-track thermochronology. *J Geophys Res* 101:11353–11364
- Tagami T, Galbreith RF, Yamada R, Laslett GM (1998) Revised annealing kinetics of fission tracks in zircon and geological implications. In: Van den Haute P, de Corte F (eds) *Advances in Fission-Track Geochronology*. Kluwer Academic Publishers, Dordrecht, pp 99–114
- Tagami T (2005) Zircon fission-track thermochronology and applications to fault studies. *Rev Mineral Geochem* 58:95–122
- Trajanova M, Pécskay Z, Itaya T (2008) K–Ar geochronology and petrography of the Miocene Pohorje Mountains batholith (Slovenia). *Geol Carpathica* 59:247–260
- Urošević M, Pavlović Z, Klisić M, Brković T, Malešević M, Trifunović S (1970a) Basic Geological Map of the SFRY, 1:100'000, Sheet Novi Pazar (K34–3), Savezni Geološki Zavod, Beograd (1966).
- Urošević M, Pavlović Z, Klisić M, Brković T, Malešević M, Trifunović S (1970b) Basic Geological Map of the SFRY, 1:100'000, Sheet Vrnjci (K34–18), Savezni Geološki Zavod, Beograd (1966).
- Ustaszewski K, Schmid SM, Fügenschuh B, Tischler M, Kissling E, Spakman W (2008) A map-view restoration of the Alpine–Carpathian–Dinaridic system for the Early Miocene. *Swiss J Geosci* 101:S273–S294

- Ustaszewski K, Schmid SM, Lugović B, Schuster R, Schaltegger U, Bernoulli D, Hottinger L, Kounov A, Fügenschuh B, Schefer S (2009) Late Cretaceous intra-oceanic magmatism in the internal Dinarides (northern Bosnia and Herzegovina): Implications for the collision of the Adriatic and European plates. *Lithos* 108:106–125
- Ustaszewski K, Kounov A, Schmid SM, Schaltegger U, Frank W, Krenn E, Fügenschuh B (in press) Evolution of the Adria–Europe plate boundary in the northern Dinarides – from continent-continent collision to back-arc extension. *Tectonics*
- van Hinsbergen DJJ, Hafkenscheid E, Spakman W, Meulenkamp JE, Wortel R (2005) Nappe stacking resulting from continental lithosphere below subduction of oceanic and Greece. *Geology* 33:325–328
- von Blanckenburg F, Davies JH (1995) Slab breakoff: A model for syncollisional magmatism and tectonics in the Alps. *Tectonics* 14: 120–131
- von Quadt A, Moritz R, Peytcheva I, Heinrich CA (2005) 3: Geochronology and geodynamics of Late Cretaceous magmatism and Cu-Au mineralization in the Panagyurishte region of the Apuseni–Banat–Timok–Srednogorie belt, Bulgaria. *Ore Geol Rev* 27:95–126
- Vukov M (1989) Petrology and geochemistry of Željina granitoid (in Serbian). PhD Thesis, Faculty of Mining and Geology, University of Belgrade
- Vukov M (1995) Petrologic characteristics of granitoid rocks of Željina and Polumir. In: *Geology and Metallogeny of the Kopaonik Mountain*, Belgrade, pp 518–216
- Vukov M, Milovanović D (2002) The Polumir Granite – Additional data on its origin. *Ann Géol Péninsule Balkan* 64:167–185
- Yamada R, Tagami T, Nishimura S, Ito H (1995) Annealing kinetics of fission tracks in zircon: an experimental study. *Chem Geol* 122:249–258
- Zagorchev I, Moorbath S, Lilov P (1987) Radiogeochronological data on the Alpine igneous activity in the western part of the Rhodope Massif. *Geol Balcanica* 17: 59–71
- Zelić M (2004) Tectonic history of the Vardar zone: constraints from the Kopaonik area (Serbia). PhD Thesis, Università di Pisa, Italy.
- Zelić M, Levi N, Malasoma A, Marroni M, Pandolfi L, Trivić B (2010) Alpine tectono-metamorphic history of the continental units from Vardar zone: the Kopaonik Metamorphic Complex (Dinaric–Hellenic belt, Serbia). *Geol J* 45: 59–77, doi: 10.1002/gj.1169

4. Metamorphism and structural geology

4.1 Metamorphic conditions within the different tectonic units

The study area includes two metamorphic complexes separated from each other by outcrops of the Western Vardar Ophiolitic Unit (Fig.4.1): the Studenica Metamorphic Series of the more external and structurally lower amphibolite-facies metamorphic Studenica thrust sheet and the Kopaonik Metamorphic Series of the more internal and structurally higher lower greenschist facies metamorphic Kopaonik thrust sheet. Both thrust sheets formed parts of the distal Adriatic margin and carried remnants of the previously (Late Jurassic) emplaced Western Vardar Ophiolitic Unit before they were thrust onto each other. The Studenica Metamorphic Series and the Kopaonik Metamorphic Series (Egli 2008; Schefer et al. 2010a) consist of a pre-Mesozoic metasedimentary basement that is stratigraphically overlain by metamorphosed Triassic to Middle (?Upper) Jurassic sediments (Fig. 4.1). Both have been thrust, together with their overlying ophiolitic sheets that were previously obducted, as composite nappes or thrust sheets, i.e. the Studenica and Kopaonik thrust sheets, during Late Cretaceous–Early Paleogene times onto the Drina–Ivanjica thrust sheet to the west (Schefer et al. 2010a).

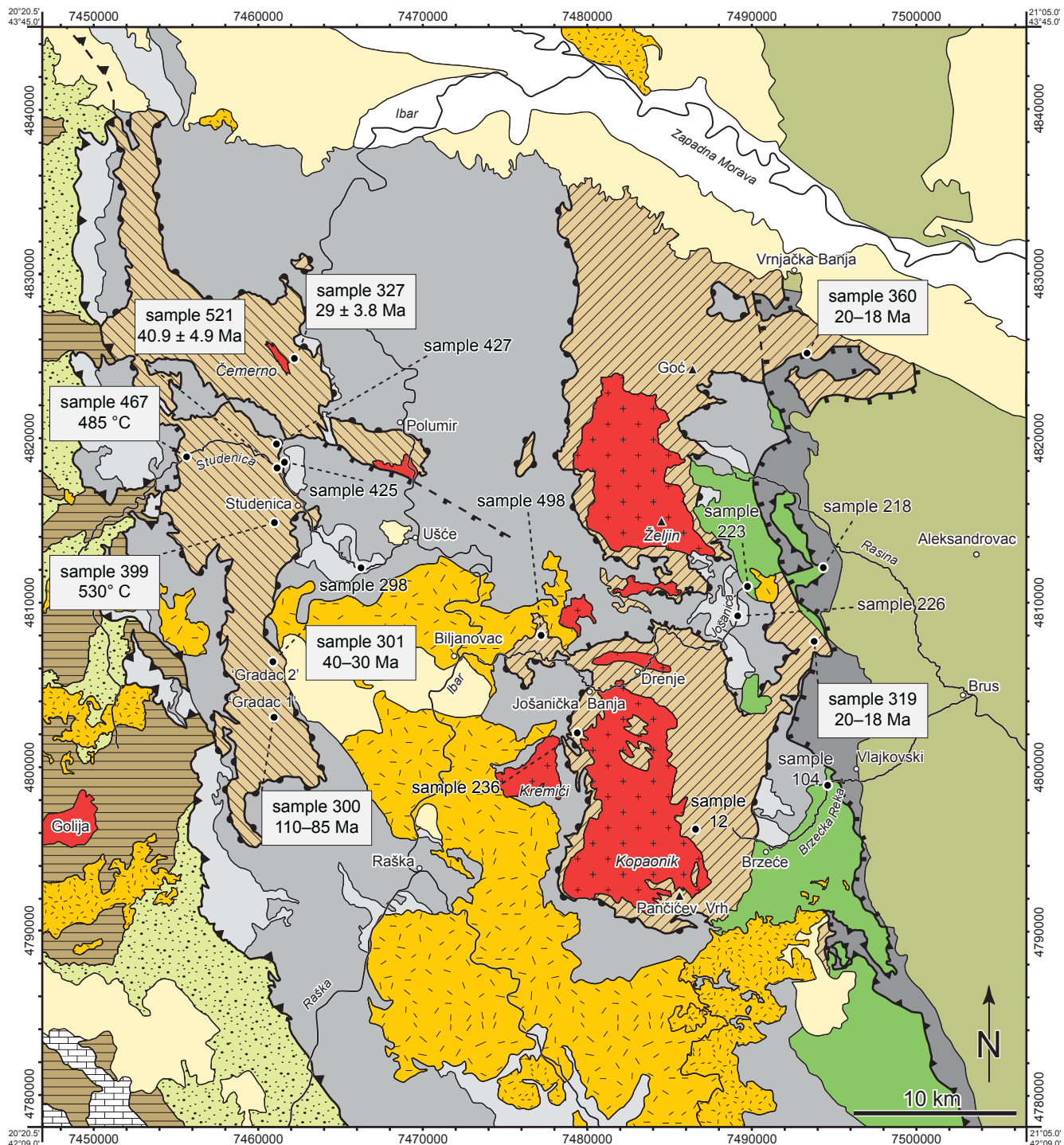
The Mesozoic metasediments of the Kopaonik and Studenica Metamorphic Series show a polyphase penetrative tectonic overprint (see chapter 4.2; Egli 2008; Zelić 2004; Zelić et al. 2010), associated with polyphase, latest Jurassic, Cretaceous, and Paleogene, greenschist-facies metamorphism that locally reaches lower-amphibolite grade conditions (see chapter 4.3; Schefer et al. 2008, 2010a). This greenschist-facies metamorphism also causes thermal alteration of conodonts (Sudar & Kovács 2006; Schefer et al. 2010a).

The Kopaonik and Studenica Metamorphic Series and the Western Vardar Ophiolitic Unit are unconformably overlain by post-Turonian sediments ('Senonian flysch' of Dimitrijević 1997; Fig. 4.1, 'Upper Cretaceous sediments') that contain large olistoliths, including ophiolites and metamorphic rocks. Thrust on top of this 'Senonian flysch' is the Eastern Vardar Ophiolitic Unit.

This chapter discusses the metamorphic conditions of the different units in the study area, starting with the tectonically lowermost unit (Studenica thrust sheet), going tectonically upwards (Fig. 4.1).

Studenica Metamorphic Series

The Studenica Metamorphic Series are located in the area of the Studenica valley and crop out in a window below the Western Ophiolitic Unit (Fig. 4.1). The lithologies range from lowermost greenschist-facies metamorphic limestones in the south (profile Gradac1, Schefer et al. 2010a) to amphibolite-facies biotite-garnet-schists and amphibolites in the main valley of the Studenica River (Fig. 4.2). Except for the southern area (near profile Gradac 1) the metamorphic conditions within the Studenica Metamorphic Series are usually higher than in their equivalent found further east (Kopaonik Metamorphic Series). The mineral assemblage garnet, biotite, white mica, quartz, and minor feldspar as well as quartz-textures showing grain-boundary migration recrystallization, indicate amphibolite facies metamorphic conditions. The garnets are rotated and broken during ongoing deformation related to exhumation. During this (retrograde) path, part of the biotite is replaced by chlorite. Sigma-clasts and shear-bands reveal a sense of shear indicating top-to-the-north movement. Raman spectroscopy of carbonaceous material was carried out by M. Wiederkehr on two samples for exploratory reasons (Appendix A). Both samples contain a large amount of carbonaceous material (Fig. 4.2e). The peak-temperatures derived from Raman spectroscopy for samples 399 and 467 (Fig. 4.2e–g) are 531 ± 14 and 485 ± 15 °C, respectively (Fig. 4.3). These results fit the metamorphic conditions inferred from the petrographic observations in other samples (Fig. 4.2) that



Post orogenic cover

- Quaternary
- Mio-Pliocene cover

Cenozoic magmatic rocks

- Miocene**
- volcanics
- Polumir- and Golija intrusion
- Oligocene**
- extrusives and volcanoclastics
- Kopaonik intrusion

Eastern Vardar Ophiolitic Unit

- 'Paraflysch'
- Eastern Vardar ophiolites

Sava Zone

- Upper Cretaceous sediments

Western Vardar Ophiolitic Unit

- Western Vardar ophiolites
- ophiolitic mélange

Kopaonik thrust sheet

- Kopaonik Metamorphic Series (Paleozoic to Jurassic)

Studenica thrust sheet

- Studenica Metamorphic Series (Paleozoic to Jurassic)

Drina-Ivanjica thrust sheet

- Upper Cretaceous sediments
- Triassic sediments
- Paleozoic

Tectonic contacts

- normal faults
- ▲ thrusts
- ▲ base ophiolitic mélange and Western Vardar Ophiolites

indicate lower amphibolite-facies conditions.

Kopaonik Metamorphic Series

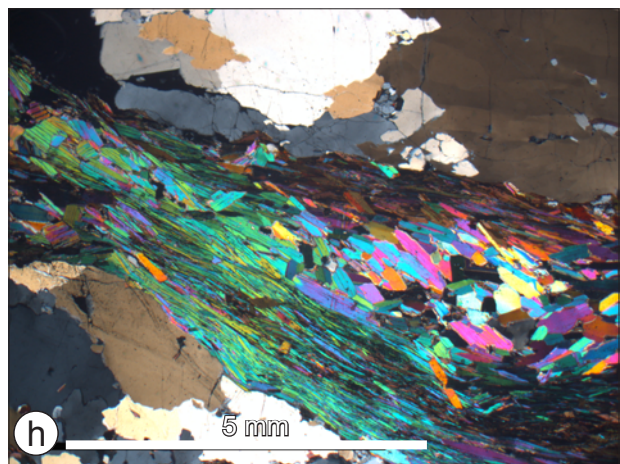
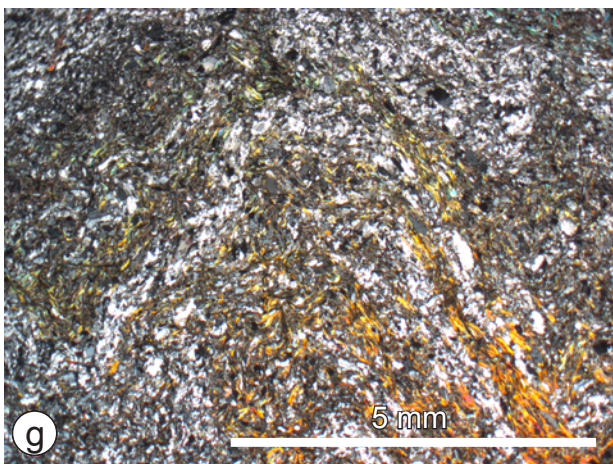
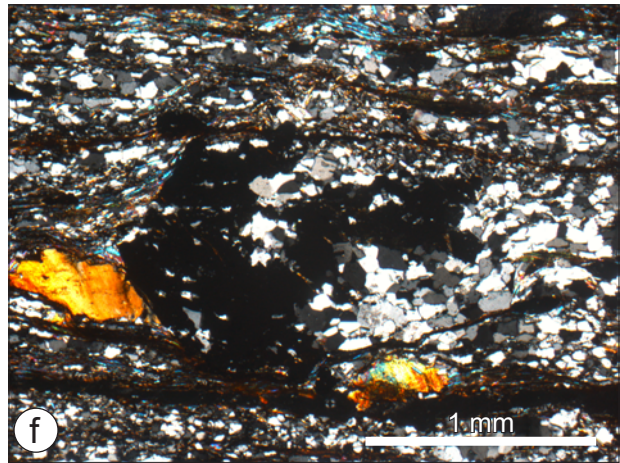
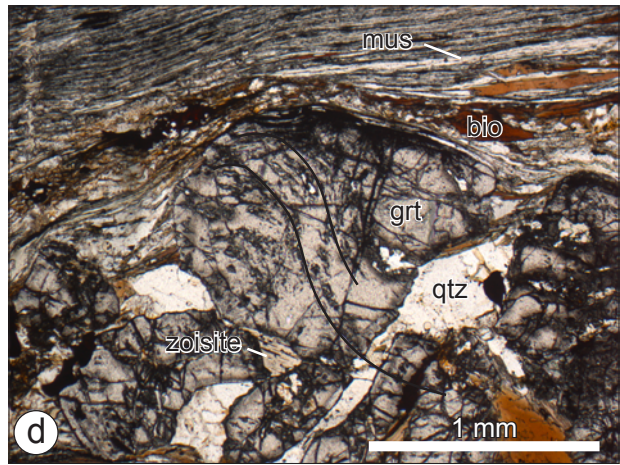
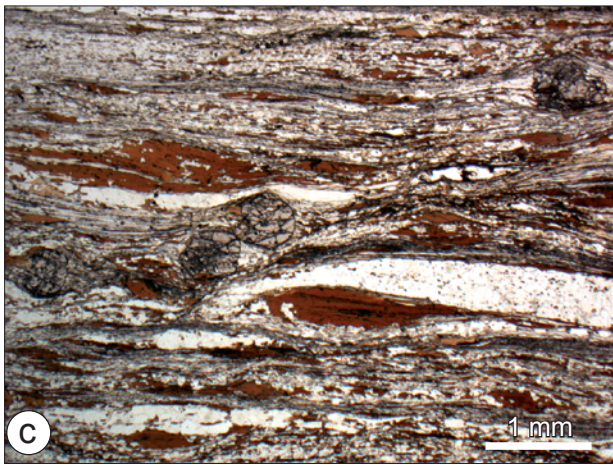
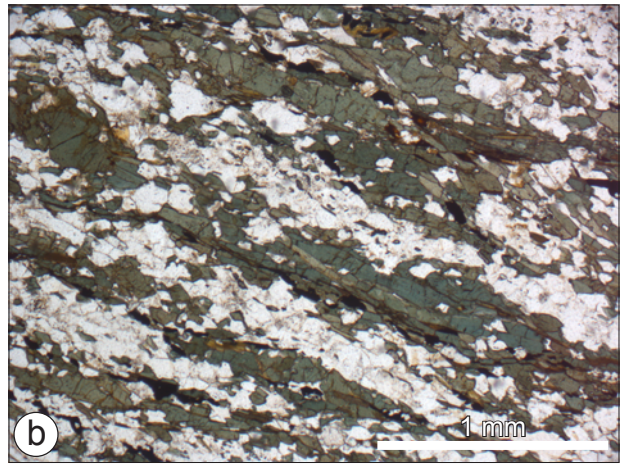
The Kopaonik Metamorphic Series are found east of the Ibar River and in the area of the Kopaonik and Željina mountain chains. The oldest rocks are quartz-phyllites of probably Paleozoic age, overlain by the Werfen Formation, followed up-section by shallow-water carbonate sediments ('Gutenstein' and 'Steinalm' equivalents). A vast amount of the Mesozoic cover, however, consists of well-bedded cherty meta-limestones of the newly defined Kopaonik Formation (Schefer et al. 2010a). Chlorite-epidote-actinolite schists originating from Triassic intrusions are also found in this series (Fig. 4.4a), showing a strong retrograde greenschist-facies metamorphic overprint. The Kopaonik Formation stems from diluted turbidity currents sourced by nearby carbonate platforms. This stratigraphic succession underwent strong polyphase deformation under greenschist-facies conditions (Egli 2008; Zelić et al. 2010). Contact metamorphic rocks (skarns and hornfelses) are found in the vicinity of the Oligocene Kopaonik granodioritic intrusion (Schefer et al. 2010b). They contain layers of calcsilicate and tremolite (Fig. 4.4b,c) that grew after deformation and newly grown garnet as a result of contact-metamorphism (Fig. 4.4d).

Field evidence shows that intrusion and contact metamorphism postdate regional metamorphism and main deformation (chapter 4.2). The highest grade of regional metamorphism in this unit is monitored in biotite-chlorite schists and calc-silicate rocks (Fig. 4.4e,f) showing a N-S-oriented stretching lineation and found between Biljanovac and Jošanička Banja (Fig. 4.1). Temperature estimates based on the coexistence of biotite, chlorite and feldspar range from 350 to 450 °C. Other work on metamorphism in this unit is sparse, but Sudar and Kovács (2006) calculated peak metamorphic conditions based on the conodont alteration index (CAI) to be at least 400 °C, but less than 500 °C at ca. 300 MPa pressure (upper-most greenschist-facies conditions). Zelić et al. (2010) report P-T-conditions of 200–500 MPa and > 420 °C for the mica-schists and phyllites and 200–600 MPa and 420–470 °C for the Triassic metabasites from the Kopaonik Metamorphic Series.

Western Vardar Ophiolitic Unit

The base of the Western Vardar Ophiolitic Unit is marked by an ophiolite-bearing *mélange* of considerable thickness, which tectonically overlies the Kopaonik and Studenica Metamorphic Series. The *mélange* contains, embedded in a brown to reddish muddy matrix, predominantly blocks of serpentinite, but blocks and components of basalts, turbiditic sandstones and carbonate rocks are also frequently found. In the Kopaonik area, the *mélange* is thrust on top of the Kopaonik Formation while in the Studenica area the original contact to the *mélange* is rarely exposed. Outcrops between Ušće and Studenica (sample 425 on Fig. 4.1) expose *mélange* with a well developed foliation and a considerable tectono-metamorphic overprint. The *mélange* shows a silty matrix and contains blocks of sandstone and ophiolitic detritus, also olistostromes with radiolarites and sandstones are observed. Lithified greywacke containing large amounts of feldspar and mica in a silty basaltic matrix is also found. The large components are mostly angular, in contrast to smaller ones, indicating rather short distances between source and sink

Fig. 4.1 – Geological map of the Kopaonik area based on mapping by S. Schefer and compilation of the Geological Map of Yugoslavia (1:100'000), sheets Novi Pazar (Urošević et al. 1970a), Vrnjci (Urošević et al. 1970b), Sjenica (Mojsilović et al. 1978), and Ivanjica (Brković et al. 1976) as well as Simić (1956) for the Studenica area. Numbers at the border of the map are MGI Balkan 7 Cartesian coordinates. The map also indicates the locations of the samples for ⁴⁰Ar–³⁹Ar analyses and the samples used for measuring peak metamorphic temperatures by Raman spectroscopy (boxes), as well as other important samples discussed in the text (no boxes).



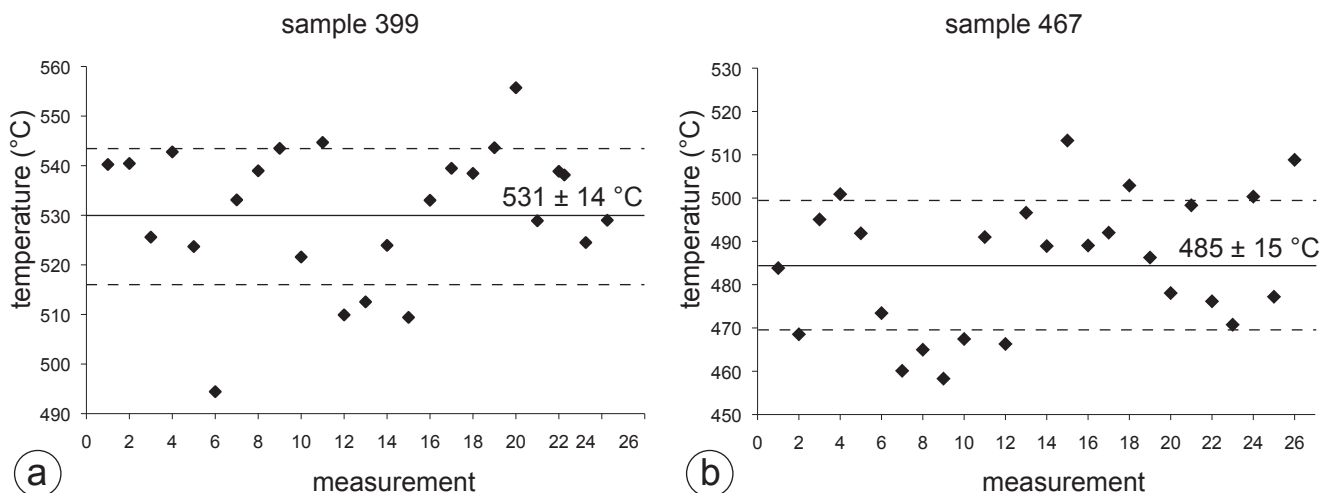


Fig. 4.3 – Peak metamorphic temperatures (points) obtained on two samples from Studenica valley by Raman spectroscopy. Solid lines represent the mean temperature, dashed lines the standard deviation. Location of the samples is indicated on Fig. 4.1.

regions, as expected for a tectonic mélange. All components were already lithified and later ductilely deformed, the smaller ones forming sigma-clasts indicating top-NW directed transport (Fig. 4.5a; chapter 4.2).

In large parts of the Western Vardar Ophiolitic Unit elsewhere a high-grade metamorphic sole typically underlies the obducted ultramafic massifs. Metamorphic conditions span a large range of temperatures from 300 to 850 °C together with a reported P-range of 4–10 kbar (Carosi et al. 1996; Karamata et al. 2000b; Operta et al. 2003). Mafic rocks (amphibolites) predominate, though intercalated metasediments, probably derived from the sedimentary cover of the lower plate during intra-oceanic subduction, occur as well (Karamata et al. 2000b; Bortolotti et al. 2005). In the study area, however, the metamorphic sole could only be observed in the form of a reworked component in the ophiolite-bearing mélange (Fig. 4.5b).

The Western Vardar Ophiolitic Unit is dominated by depleted mantle rocks (harzburgites). It contains abundant extrusive rocks with a supra-subduction geochemical signature (i.e. Karamata et al. 1980; Spray et al. 1984; Lugović et al. 1991). Metamorphic conditions of the strongly serpentinised mantle rocks are generally difficult to determine. Only at one locality in the Studenica valley (sample 425 on Fig. 4.1), coexisting olivine, talc and antigorite show an amphibolite-facies overprint together with a greenschist-facies retrogression evidenced by calcite-rims around olivine (Fig. 4.5c) and magnetite being replaced by Fe-Hydroxide (probably goethite). Talk was determined by means of infrared spectroscopy (Fig. 4.5e). When comparing the sample with two standards

Fig. 4.2 – Characterisation of selected lithologies of the Studenica Metamorphic Series. *a* – Triassic breccia (Schefer et al. 2010a) from the quarry near Studenica, ca. 1 km downstream from the Studenica Monastery (Fig. 4.1). The components are strongly deformed, reducing the original thickness to 20% (Egli 2008). *b* – Thin-section of a hornblende schist (sample 521, Fig. 4.1). The minerals were ductilely deformed under at least lower amphibolite-facies conditions, evidenced by dynamically recrystallised hornblende. *c, d* – Syn-tectonically growing garnets formed during peak metamorphic conditions (sample 427, Fig. 4.1). A schistosity is developed in the inclusions inside the garnets that is rotated during ongoing deformation. Pressure shadows contain quartz, biotite and white mica. This deformation outlasts the stability field of garnet, implying exhumation related deformation during D4a. During this (retrograde) path, part of the biotite is replaced by chlorite and the garnets are first rotated and then broken into pieces. Sigma-clasts and shear-bands reveal a sinistral sense of shear that indicates top-to-the-north movement during extension. *e, f* – Biotite-schist with a large amount of carbonaceous matter used for Raman spectroscopy. Garnet porphyroblasts with pre-existing schistosity, quartz and mica indicate uppermost greenschist-facies conditions, which is in line with the results of Raman spectroscopy (sample 399, Fig. 4.1). *g* – White mica, quartz and minor chlorite in a greenschist-facies rock from the Studenica Metamorphic Series used for Raman spectroscopy (sample 467, Fig. 4.1). *h* – Two mica-schist from the Studenica Metamorphic Series at Čemerno mountain (sample 327, Fig. 4.1) with syn-kinematically grown biotite.

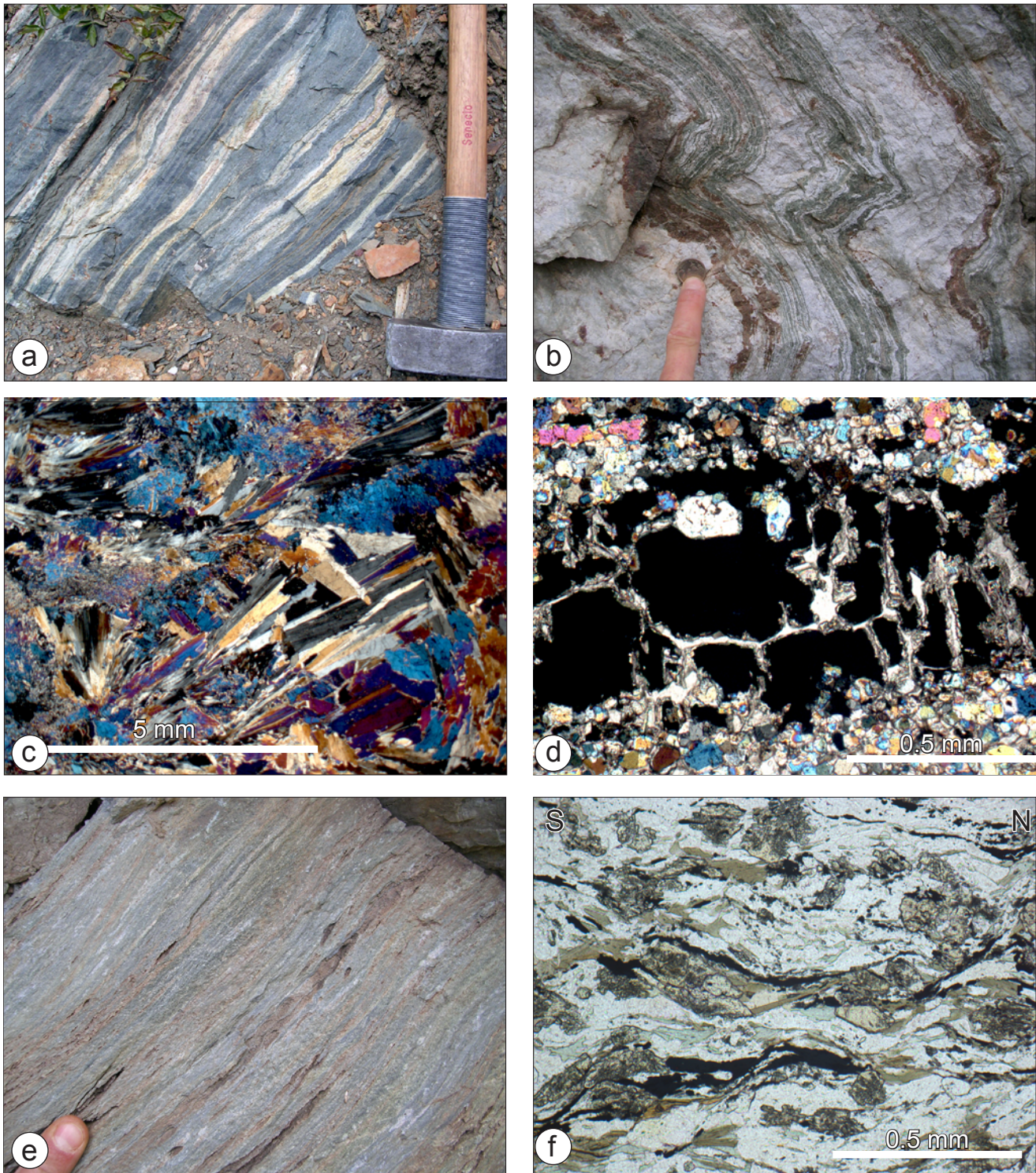


Fig. 4.4 – Characterisation of selected lithologies from the Kopaonik Metamorphic Series. *a* – Chlorite-epidote-actinolite-schist representing metamorphosed Triassic intrusions into the Mesozoic sediments now forming part of the Kopaonik Metamorphic Series (sample 236, Fig. 4.1). *b* – Layers of calcsilicate and tremolite in hornfels at the rim of the Kopaonik intrusion found within the Kopaonik Metamorphic Series (sample 12, Fig. 4.1). *c* – Thin-section of a hornfels (sample 12) with large tremolite crystals that grew after deformation. *d* – Garnet growing as a result of contact-metamorphism in sample 12. *e* – Calcsilicate rock within the Kopaonik Metamorphic Series with layers of calcite (brownish) and a N–S oriented (probably D4a) stretching lineation (sample 498, Fig. 4.1). *f* – Thin-section of sample 498 (*e*) with biotite, chlorite, epidote, feldspar quartz and calcite showing greenschist-facies metamorphic conditions (350–450 °C) with an associated sinistral deformation (top-S) conditions, which is in line with the results of Raman spectroscopy (sample 399, Fig. 4.1). *g* – White mica, quartz and minor chlorite in a greenschist-facies rock from the Studenica Metamorphic Series used for Raman spectroscopy (sample 467, Fig. 4.1). *h* – Two mica-schist from the Studenica Metamorphic Series at Čemerno mountain (sample 327, Fig. 4.1) with syn-kinematically grown biotite.

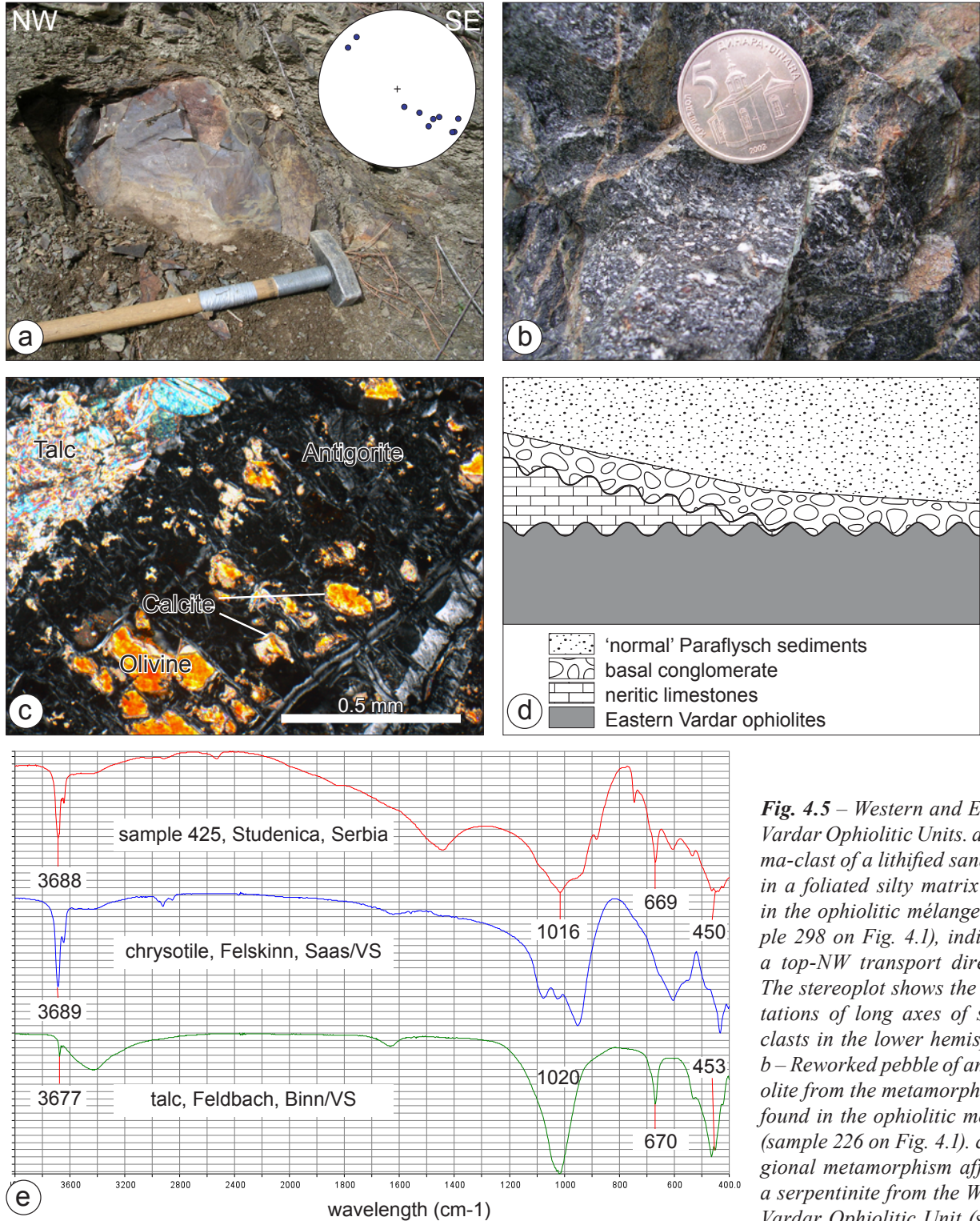
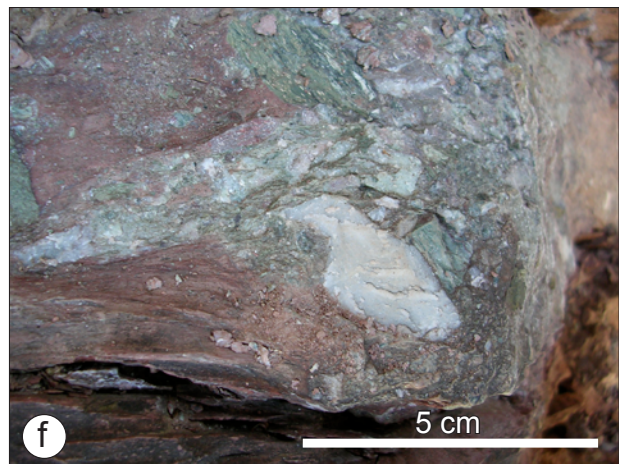
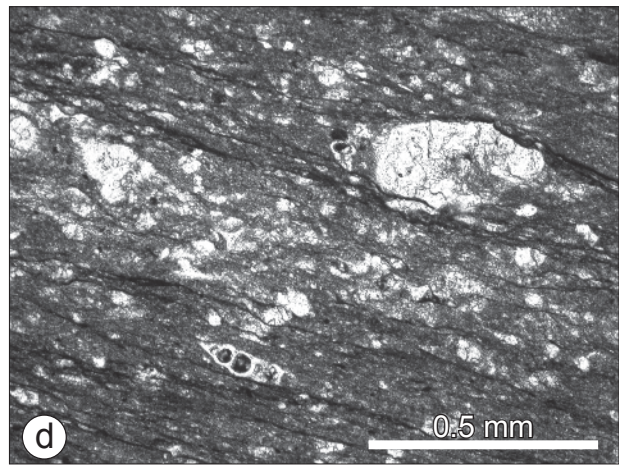
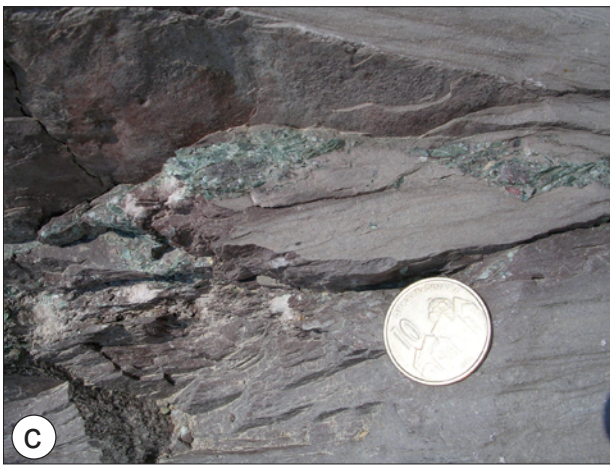
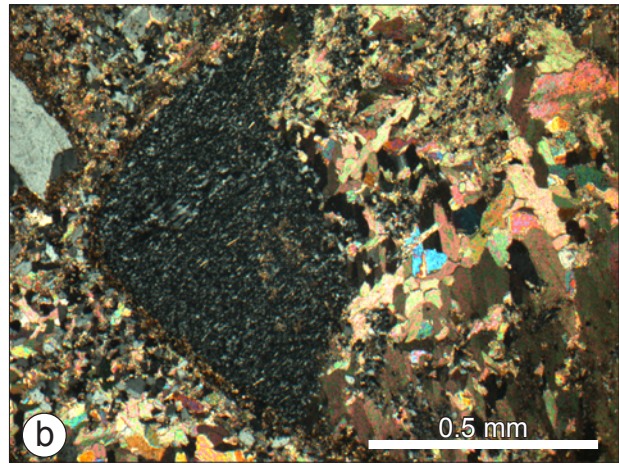


Fig. 4.5 – Western and Eastern Vardar Ophiolitic Units. *a* – Sigma-clast of a lithified sandstone in a foliated silty matrix found in the ophiolitic mélangé (sample 298 on Fig. 4.1), indicating a top-NW transport direction. The stereonet shows the orientations of long axes of sigma-clasts in the lower hemisphere. *b* – Reworked pebble of amphibolite from the metamorphic sole found in the ophiolitic mélangé (sample 226 on Fig. 4.1). *c* – Regional metamorphism affecting a serpentinite from the Western Vardar Ophiolitic Unit (sample

425, Fig. 4.1). The paragenesis olivine, talc and antigorite indicates amphibolite-facies conditions, the calcite-rims around olivine suggest a greenschist-facies retrograde overprint. *d* – Sketch of a double unconformity found at the Vljakovsci locality (between Brus and Brzeće, Fig. 4.1) between the Eastern Vardar ophiolites and the sediments of the Paraflysch. Neritic limestones (Albian–Cenomanian; Rampoux 1974) transgress unconformably onto the ophiolites. Transgressing these neritic limestones are the basal conglomerates of the ‘Paraflysch’. This indicates a long and ongoing phase of erosion during Beriasian–Albian times, followed by the sedimentation of neritic limestones until the Cenomanian. Uplift and erosion during a rather short interval at the end of the Cenomanian until the Turonian is then followed by the basal conglomerate of the ‘Paraflysch’. *e* – Infrared spectra of sample 425 (red line) from the Western Vardar Ophiolitic Unit and the standards for chrysotile (blue line, Felskinn, Saas/VS) and talc (green line, Feldbach, Binn/VS). The characteristic peaks for talc are all reproduced (3688, 670 and 450 cm⁻¹), but some superposition with chrysotile is also obvious (1016 cm⁻¹). This proves the existence of talc and thus the amphibolite-facies paragenesis of sample 425 (c).



(talk from Feldbach, Binn/VŠ and chrysotile from Felskinn, Saas/VŠ), the characteristic peaks of talk were all reproduced (3688, 670 and 450 cm⁻¹). Some superposition with chrysotile is also visible (1016 cm⁻¹). This implies that this part of the Western Vardar Ophiolitic Unit was subjected to a considerable post-obduction (Cretaceous?) regional metamorphic overprint.

Upper Cretaceous sediments ('Senonian flysch') of the Sava zone

The Kopaonik and Studenica Metamorphic Series and the Western Vardar Ophiolitic Unit are unconformably overlain by post-Turonian sediments (Fig. 4.1, 'Upper Cretaceous sediments') that contain large olistoliths, including ophiolites and metamorphic rocks. The base is formed by a calcitic sedimentary breccia (basal breccia of the 'Senonian flysch', sample 223 on Fig. 4.1) containing ophiolitic detritus as well as previously metamorphosed components (Fig. 4.6a). The thin-section shows strongly deformed and recrystallised detrital conglomerates. Quartz and lithic fragments make up most of the rock surrounded by a fine-grained mixture of quartz and calcite (Fig. 4.6b). Zelić (2004) even reports amphibolite-facies pebbles from the same breccia. Red pelagic limestones ('Scaglia rossa') are typical for this unit (Fig. 4.6c). A key outcrop is found between Brzeće and Brus close to the contact to the overlying Eastern Vardar Ophiolitic Unit (sample 104 on Fig. 4.1). Olistoliths ranging in size from some 100 m to dm are incorporated into the 'Senonian flysch'. They comprise calc-arenites, a conglomerate from a carbonate platform with a high proportion of biogenetic particles, i.e. orbitolinae (Barremian–Cenomanian), echinoderms, molluscs and radiolarians. Other olistoliths are grainstones containing rudist fragments and orbitolinae, indicating an age not older than late Early Cretaceous. These metamorphosed grainstones contain megacryst quartz crystals, which grew during metamorphism or diagenesis. Sometimes also orbitolina are overgrown by megacryst quartz. Magmatic components with boreholes are also observed. In some olistoliths globotruncanids could be separated in the matrix yielding a Campanian–Maastrichtian age. The globotruncanids are strongly recrystallised, sometimes even replaced by quartz (Fig. 4.6d), and a clear foliation parallel to bedding can be observed at outcrop and microscopic scale.

In terms of deformation two phases could be distinguished (Fig. 4.6e; chapter 4.2). Asymmetric boudinage in layers containing ophiolitic detritus is observed (Fig. 4.6c) and some quartz clasts in the pelagic matrix show ductile deformation after sedimentation (Fig. 4.6f,g). Sigma clasts indicate top-W-oriented shear senses and are later overprinted by brittle E-dipping normal faults (Fig. 4.6h).

The fact that metamorphic components are reworked by these Upper Cretaceous sediments and that they progressively overlie not only the obducted Western Vardar Ophiolitic Unit, but also the metasediments of the Kopaonik Metamorphic Series, implies that they transgress an already eroded and polyphase metamorphosed distal part of a continental margin (i.e. the Adriatic margin; Schefer et al. 2010a). This greenschist-facies metamorphic 'Senonian flysch' belt trending N–S along the eastern margin of the Kopaonik composite thrust sheet is interpreted



Fig. 4.6 – Lithologies and deformation features in Upper Cretaceous sediments ('Senonian flysch'). a – Limestone breccia that contains ophiolitic detritus and metamorphic components from the Kopaonik Metamorphic Series (basal breccia of the 'Senonian flysch', sample 223 on Fig. 4.1). b – Strongly deformed and recrystallised conglomerate. Quartzite and lithic fragments make up most of the rock, the fine-grained matrix consists of quartz and calcite. Note that the fragments show a pre-existing cleavage from an earlier deformation event. c – Red pelagic limestone ('Scaglia rossa') with ophiolitic detritus, both show ductile deformation (sample 104 on Fig. 4.1). d – Strongly recrystallised globotruncanids. The thin-section shows pressure-solution cleavage probably through tectonic overburden, possibly parallel to bedding. e – Hinge of an earlier isoclinal fold in the 'Senonian flysch', indicating that it underwent more than one deformation phase. f – Quartzite clasts within the matrix of pelagic limestones from the 'Senonian flysch' are ductilely deformed and indicate that deformation occurred at least under lowermost greenschist-facies conditions (sample 104). g,h – Sigma-clasts indicate top-W-oriented shear senses (g) and are later overprinted by brittle E-dipping normal faults (h). Locality 'Grčak' on Fig. 4.7.

to represent the southern prolongation of the Sava zone, i.e. the suture zone between the internal Dinarides and the Carpatho-Balkan orogen (Schmid et al. 2008; Ustaszewski et al. 2009; Ustaszewski et al. submitted). Parts of this ‘Senonian flysch’ are interpreted as ‘wildflysch’ that formed during the Upper Cretaceous to Early Paleogene closing of the last remnants of the Vardar branch of Neotethys Ocean (Schmid et al. 2008).

Eastern Vardar Ophiolitic Unit

The Eastern Vardar Ophiolitic Unit represents a piece of MORB-type oceanic lithosphere that is overstepped by Late Jurassic reef Limestones (Karamata 2006), followed by supposedly Cretaceous-age terrigenous sediments (‘Paraflysch’; Urošević et al. 1970a,b; Brković et al. 1976; Mojsilović et al. 1978). The main difference between the Western Vardar- and the Eastern Vardar Ophiolitic Unit lies in the missing underlying mélange formation and metamorphic sole of the latter. A discussion of the different ophiolitic units can be found in Schmid et al. (2008). It is difficult to determine the metamorphic conditions, since the ultramafics mostly underwent strong serpentinisation and hence lost their peak metamorphic information. The overlying Cretaceous sediments of the ‘Paraflysch’, however, do show a weak metamorphic overprint, also evidenced by partial resetting of the apatite fission-track ages (c.f. chapter 4.3), but sedimentary structures are still observable. At Vljakovsci (between Brus and Brzeće, Fig. 4.1) a double unconformity is seen between the Eastern Vardar ophiolites and the sediments of the ‘Paraflysch’ (Fig. 4.5d). The ophiolites show an erosion surface, on which neritic limestones (Albian–Cenomanian; Rampnoux 1974) transgress unconformably, followed by a second erosion phase visible on top of the neritic limestones. Transgressing these neritic limestones are the basal conglomerates of the ‘Paraflysch’, a badly sorted conglomerate with quartz, feldspars, and lithic fragments of a metamorphic continental basement as well as ophiolitic detritus. No matrix is visible, the grains show large grain-boundaries with pressure solution at its rims. In summary, there must have been a long and ongoing phase of erosion during Berriasian–Albian times, followed by the sedimentation of neritic limestones until the Cenomanian. Uplift and erosion during a rather short interval at the end of the Cenomanian until the Turonian is then followed by the basal conglomerate of the ‘Paraflysch’, which started to be sedimented contemporaneously with the basal breccia of the ‘Senonian flysch’ of the Sava zone.

4.2 Structural geology

This chapter presents the field structural data obtained during some seven months of fieldwork. The study area is affected by distinct ductile deformation phases related to nappe-stacking which were later overprinted by a set of ductile and brittle normal faults related to exhumation. A relative chronological order can be established by means of overprinting criteria. The deformation phases can be grouped into three different episodes:

(i) Pre-Senonian deformation, sealed by a sedimentary unconformity at the base of the ‘Senonian flysch’, is witnessed mainly within the Kopaonik Metamorphic Series (Fig. 4.7) and best established in the vicinity of the Kopaonik intrusion. This episode is purely ductile and takes place in a compressive setting. It resulted in the formation of a pervasive foliation and large scale folds affecting the Paleozoic–Mesozoic metasediments.

(ii) Post-Senonian pre-Oligocene deformation, predating the intrusion of the Kopaonik granitoids but affecting the Late Cretaceous cover, is observed in the Kopaonik and Studenica Metamorphic Series as well as within Upper Cretaceous sediments (‘Senonian flysch’ and ‘Paraflysch’ on Fig. 4.7). This phase takes mainly place in the ductile field of deformation and is manifested by chevron-type folding in a compressive regime.

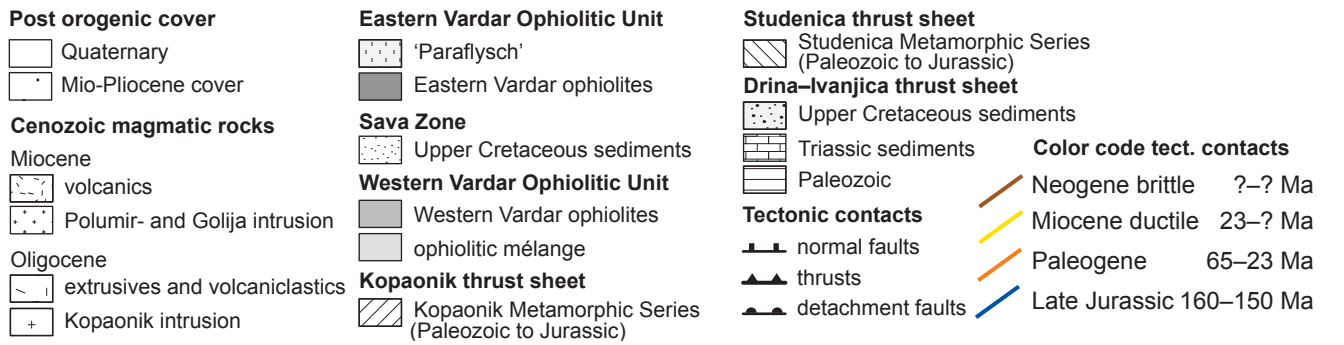
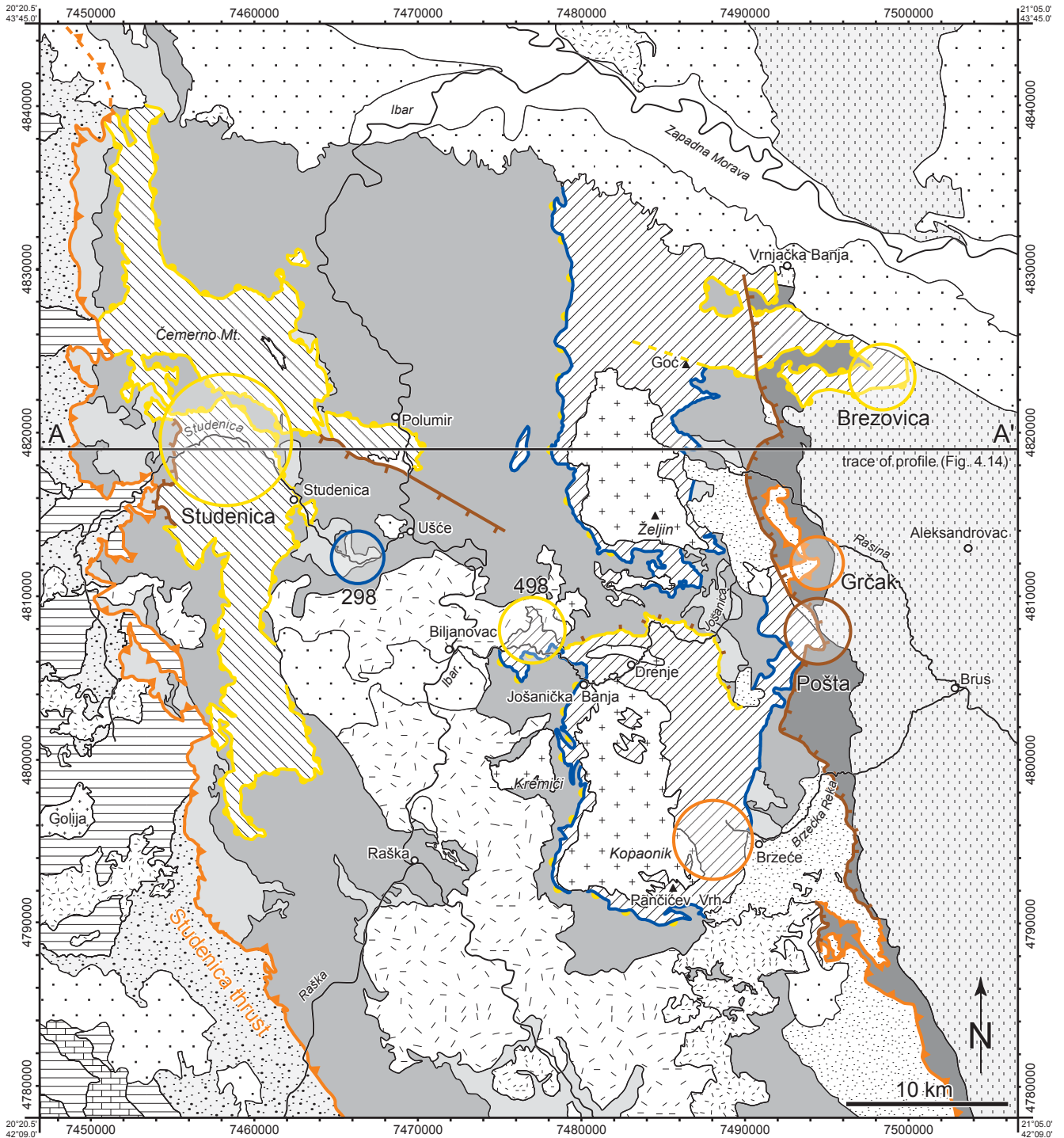
(iii) Post-Oligocene deformation affects all tectonic units within the study area. It is related to extension and exhumation and ranges from ductile extensional deformation (core-complex formation) to brittle normal faulting. It led to the exhumation of the metamorphic series and large intrusive bodies and was particularly intense in the case of the amphibolite-facies metasediments found in the Studenica valley.

Pre-Senonian episode (D1 and D2)

Pre-Senonian deformation can best be studied in the vicinity of the Kopaonik intrusion (i.e. its southeastern flank located between Brzeće and the Kopaonik ski resort) because of numerous good outcrops along and in the vicinity of the main road that provide ample relative age-constraints, aided by marked topography, outcrops exposing a variety of different lithologies and tectonic units, and intense overprint by contact metamorphism. The Kopaonik area thus serves as the basis for setting up a scheme to be correlated with the outcrops in the Studenica valley that were heavily overprinted by post-Oligocene deformation.

A first phase of deformation (D1) in the Kopaonik area can only be observed in the form of relictic and dismembered hinges of isoclinal F1 folds within the Kopaonik Metamorphic Series (Fig. 4.8a,b). It produced a first penetrative foliation containing a first stretching lineation, both being refolded by the later D2 deformation phase characterized by NE-dipping axial planes (Fig. 4.8c). The D2 structures are the prominent features seen in map view and at the outcrop. These first two phases of deformation (D1 and D2) affected all stratigraphic units of the Kopaonik Metamorphic Series. In contrast, the overlying Western Vardar Ophiolitic Unit does not distinctively show these two deformation phases. This may be due to the contrasting rheology of the different lithologies; at least locally the contact at the base of the ophiolitic units is overprinted by later extensional faulting. The Upper Cretaceous sediments (‘Senonian flysch’), however, are not affected by these two deformation phases. A transgressive contact between the latter and the Kopaonik Metamorphic Series is observed, whereby the entire Western Vardar Ophiolitic Unit is missing due to erosion. The basal conglomerate of the Upper Cretaceous sediments includes reworked and previously metamorphosed components of the Kopaonik Metamorphic Series (Fig. 4.6).

Within the metasediments of the Studenica Metamorphic Series of the Studenica valley the presence of the different pre-Senonian deformation phases is not evident, probably since the D1 and D2 deformations were totally erased by intense shearing during later exhumation. The overlying ophiolitic mélange in the hanging-wall of the



Studenica core-complex, on the other hand, is affected by deformation interpreted to belong to D1. In one particular outcrop (between Ušće and Studenica, sample 298 on Fig. 4.1) the *mélange* shows a silty matrix and contains blocks of sandstone and ophiolitic detritus. All components were previously lithified and ductilely deformed later on, the smaller ones forming sigma-clast that show a top-NW transport direction interpreted to be related to D1 deformation (Fig. 4.5a). Deformation that can be related to the second deformation phase (D2) is rarely observed in the form of refolded hinges of isoclinal folds in the lower amphibolite-facies rocks (Fig. 4.8d) or as newly grown white mica parallel to the axial planes of tight folds in lower-most greenschist-facies pelitic rocks in Gradac 1 (Fig. 4.1). These folds affect a compositional layering and not a cleavage, it is therefore locally representing the first deformation phase. Only the style of folding (small inter-limb angles and newly developed axial-plane cleavage) allows for a correlation with the regional D2. The occurrence of a similarly folded amphibolite-facies serpentinite rock (Fig. 4.5c) from the obducted Western Vardar Ophiolitic Unit found in the Studenica valley implies that D2 post-dates the Late Jurassic obduction as the Western Vardar Ophiolitic Unit that therefore seems to be part of a stack of composite nappes during D2.

Interpretation

Taking into account the age of the rocks affected by D1 and D2, these deformation phases must be younger than the Middle to Late Jurassic. The foliated and metamorphosed matrix of the ophiolitic *mélange* that includes sigma-clasts with top-NW shear-senses (sample 298 on Fig. 4.7) allows for correlating this first deformation phase (D1) to the NW-directed obduction of the Western Vardar Ophiolitic Unit onto the Kopaonik and Studenica Metamorphic Series during the Late Jurassic as observed elsewhere in the Dinarides. An intense shear zone must have developed at the base of this thrust/obduction plane comprising the ophiolitic *mélange* and the underlying sediments of the Adriatic margin. This shear zone is visible in the mylonitic metamorphic sole at different localities of the Dinarides (e.g. Zlatibor, Brezovica in Kosovo; Karamata et al. 2000b; Schmid et al. 2008) as well as in the Mirdita ophiolites of Albania (Carosi et al. 1996). Shear sense indicators (Simpson and Schmid 1983) consistently vary between top-W and top-NW. The shear senses measured in the ophiolitic *mélange* found in the study area also show top-NW movement (Fig. 4.5a), indicating that intra-oceanic obduction was NW-directed, hence oblique to nearly parallel in respect to the present-day strike of the Dinaridic chain (Schmid et al. 2008). The stretching lineations related to D1 in the Kopaonik area cannot be used to infer the transport direction, since they were refolded, and hence reoriented by at least two subsequent deformation phases (Fig. 4.9a). In the Studenica valley (Fig. 4.7) this first deformation phase is altogether missing and the ophiolitic *mélange* is only rarely found in this area, suggesting that the shear zone of the obduction must have been oblique to present-day topography and the outcropping rocks have not been affected by it.

The second deformation phase (D2) also affects the obducted Western Vardar Ophiolitic Unit (at least in the Studenica valley) and D2 is thus younger than Late Jurassic. Since the the Upper Cretaceous sediments of the ‘Senonian flysch’ are not affected by D2, it is attributed to a (pre-Senonian, >89 Ma) Cretaceous tectono-metamorphic event, that is also evidenced by new $^{40}\text{Ar}/^{39}\text{Ar}$ ages obtained from pelitic rocks in the Studenica valley (see Chapter 4.3.1). A Cretaceous metamorphic event in the Dinarides (lower greenschist grade and, in case of the Fruška Gora blue-schist metamorphism) was already proposed by different authors (Milovanović 1984; Belak et

Fig. 4.7 – Tectonic map of the Kopaonik area. The ages of main activity along major tectonic contacts are colour-coded. Important areas for the respective deformation phases are circled with the corresponding colour. The map is based on field-work by S. Schefer and a compilation of the Basic Geological Map of Yugoslavia (1:100'000); sheets Novi Pazar (Urošević et al. 1970a), Vrnjci (Urošević et al. 1970b), Sjenica (Mojsilović et al. 1978) and Ivanjica (Brković et al. 1976) as well as Simić (1956) for the Studenica area. Numbers at the border of the map are MGI Balkan 7 Cartesian coordinates.

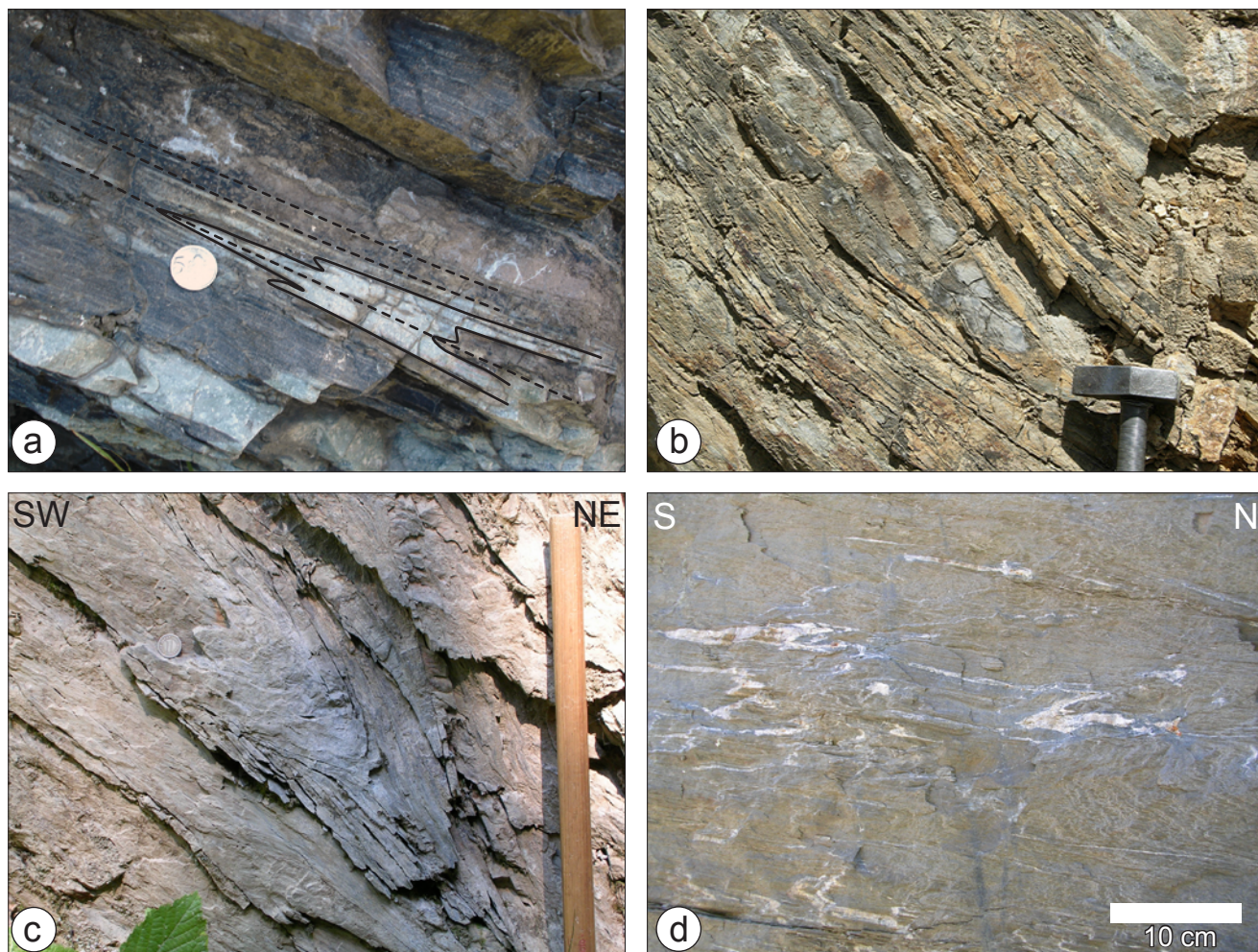


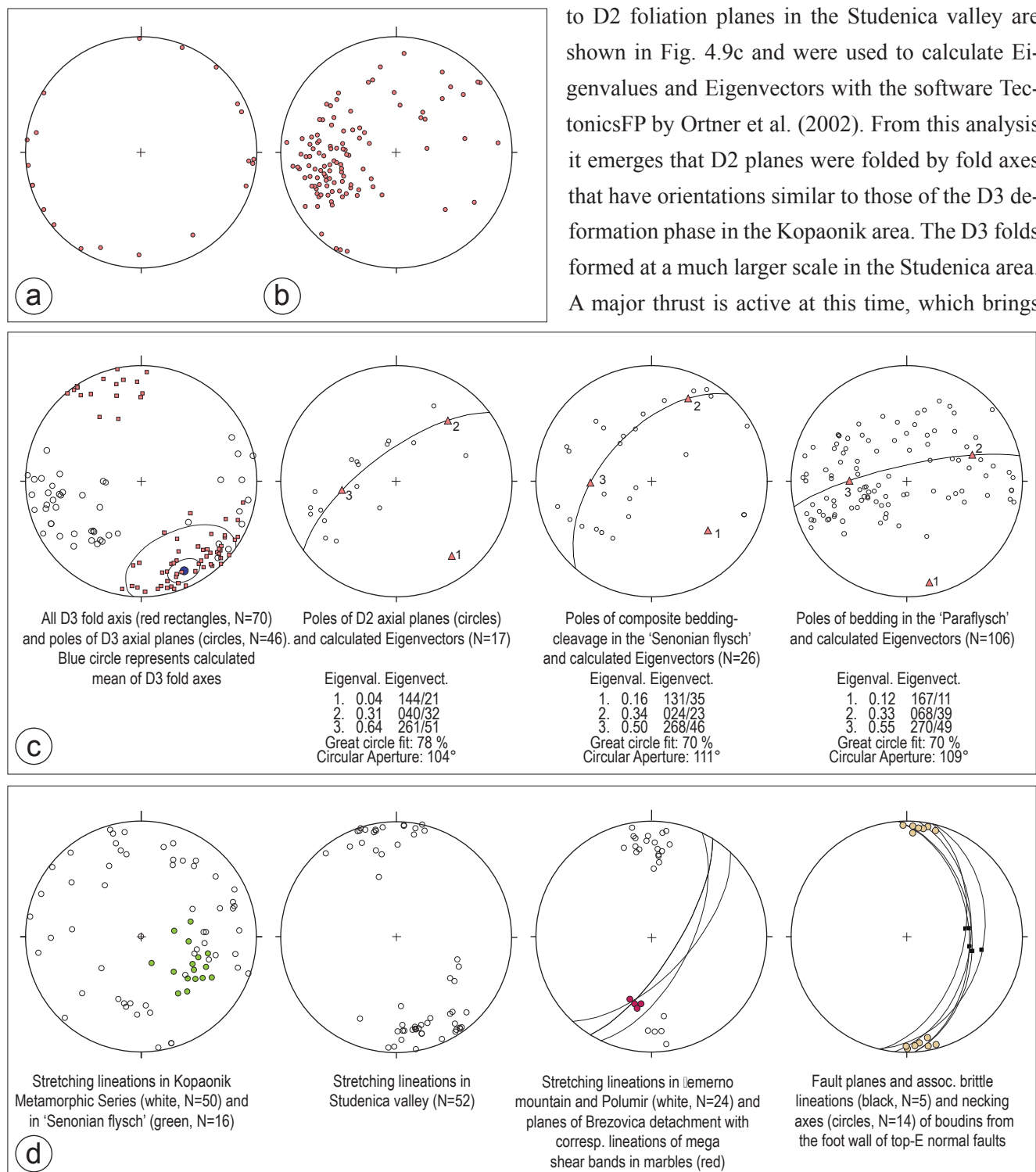
Fig. 4.8 – Deformation features of the pre-Senonian episode (D1–D2). *a* – Relict D1-folds in contact-metamorphic sediments of the Kopaonik Metamorphic Series. *b* – Hinge of D1 isoclinal fold (FA=348/06) in the Kopaonik Metamorphic Series: D1 produces new axial planar cleavage. *c* – Isoclinal D2-folds in Kopaonik Metamorphic Series with newly developed east-dipping axial plane cleavage. *d* – Relicts of D2-folds in actinolite-schist of the Studenica Metamorphic Series. Fold axes are rotated into parallelism with a later (D4a) N–S oriented stretching lineation (sample 312).

al. 1995; Milovanović et al. 1995; Pamić et al. 2004; Ilić et al. 2005), the regionally closest locality was described by Milovanović (1984) for the Drina–Ivanjica thrust sheet based on K/Ar ages in the 139–129 Ma range obtained for phyllites and greenschists. This is in line with a massive Early Cretaceous (Beriasian–Albian, 142–99 Ma, i.e. post Austrian phase) erosional event, witnessed in the entire Dinarides by unconformably transgressing Late Cretaceous sediments (Gosau-type conglomerates and ‘Senonian flysch’) onto the units of the distal Adriatic margin (Brković et al. 1976; Mojsilović et al. 1978; Tomljenović et al. 2008).

Post-Senonian pre-Oligocene episode (D3)

Folds formed during D3 are characterized by N–S striking sub-vertical axial planes and sub-horizontal NNW–SSE trending fold axes (Fig. 4.9c). This folding is interpreted to be associated with WSW-vergent thrusting (Paleogene thrusts in Fig. 4.7). East of the Kopaonik and Željina mountains D3 folds appear as chevron-type folds in the Cretaceous metasediments (‘Senonian flysch’ and ‘Paraflysch’). Chevron-type D3 folds are also found in the Paleozoic to Mesozoic metasediments of the Kopaonik Metamorphic Series exposed on the Kopaonik ridge (Fig. 4.10). Sigma-clasts found within low-grade metamorphic Late Cretaceous sediments (‘Senonian flysch’)

indicate top-W-oriented shearing (Fig. 4.6g) in the footwall of the thrust contact of the Eastern Vardar Ophiolitic Unit ('Grčak' on Fig. 4.7). The metasediments of the Studenica Metamorphic Series usually do not show such chevron-type folds, but were folded on a larger scale (larger wavelengths and amplitudes) during D3. The poles



to D2 foliation planes in the Studenica valley are shown in Fig. 4.9c and were used to calculate Eigenvalues and Eigenvectors with the software TectonicsFP by Ortner et al. (2002). From this analysis it emerges that D2 planes were folded by fold axes that have orientations similar to those of the D3 deformation phase in the Kopaonik area. The D3 folds formed at a much larger scale in the Studenica area. A major thrust is active at this time, which brings

Fig. 4.9 – Stereoplots (lower hemisphere) for different deformation phases and their respective overprints. Eigenvectors were calculated using the software TectonicsFP (Ortner et al. 2002). a – L1-lineations measured within the main foliation of D1, back-rotated by undoing the tilt of the foliation around the average fold axes produced during D3 (N=20). The lineation still scatter in all directions, which indicates that they were already reoriented by an earlier phase, namely by D2. b – Poles to the pervasive D2 foliations (N=109). The average orientation of the foliation plane (D2 axial cleavage) dips with 30–60° to the E–NE. c – Stereoplots that characterize D3, see legend below the stereoplots for more details. d – Structures related to D4 (D4a and D4b), see legend below the stereoplots for more details.

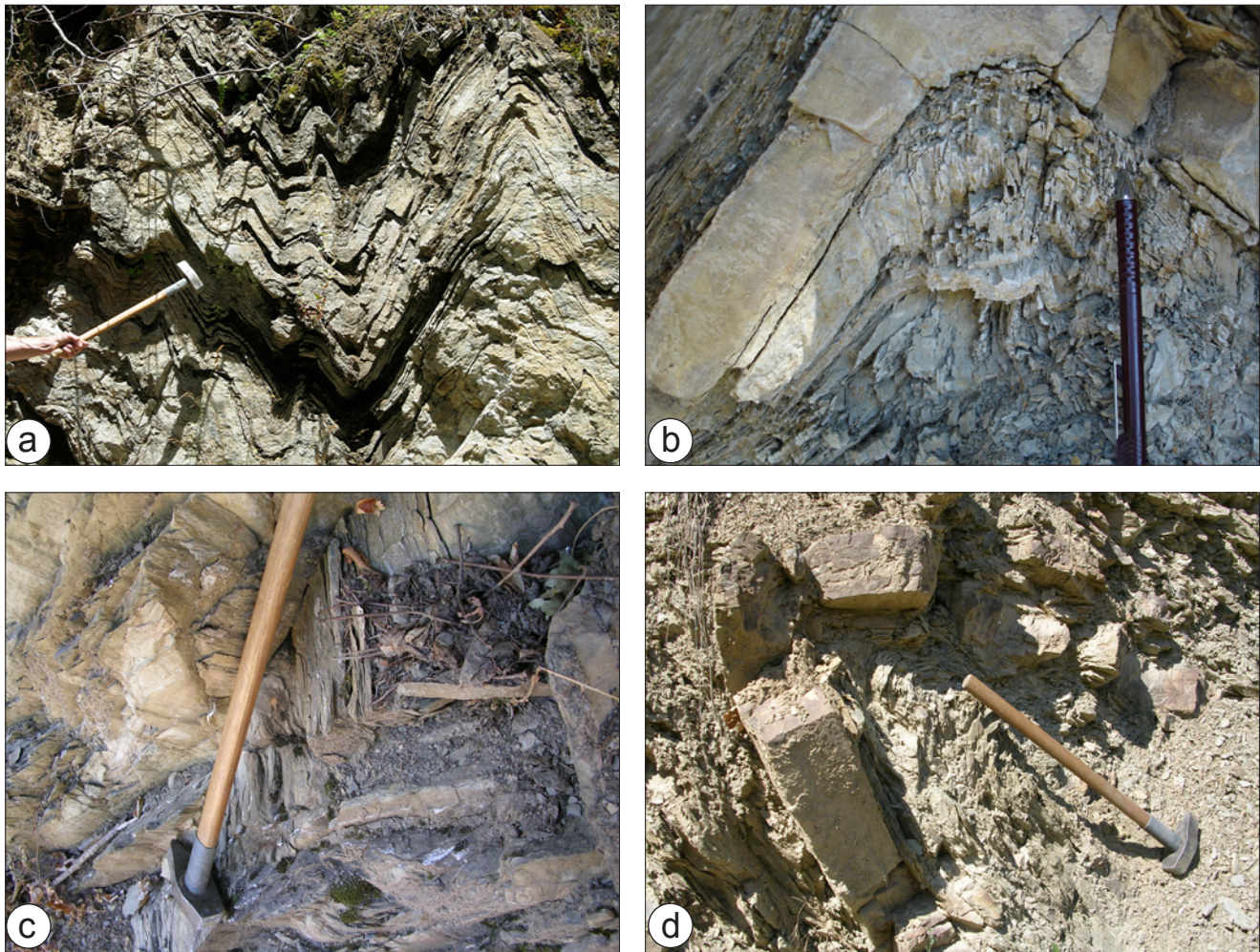


Fig. 4.10 – Details relating to the D3 phase of deformation expressed in different tectonic units. a – Chevron-type folds in the Kopaonik Fm (Schefer et al. 2010a) showing vertical N–S striking axial planes and sub-horizontal N–S trending fold axes. b – Hinge of a chevron-type fold with a developing axial plane cleavage in a marly layer of the Kopaonik Fm. c – D3 folds in Upper Cretaceous sediments ('Senonian flysch') with SE-dipping fold axes and E-dipping axial planes. d – Inclined E-dipping axial plane and sub-horizontal N–S trending fold axis of D3 in Cretaceous sediments ('Paraflysch').

the Studenica thrust sheet on top of the non-metamorphic Upper Cretaceous Sediments of the Drina–Ivanjica thrust sheet ('Studenica thrust' on Fig. 4.7). This thrust comprises also a dextral strike-slip component (Schmid et al. 2008).

The Oligocene intrusives were clearly not affected by D3 deformation. This is evident from the observation that the competence contrasts in D3 folds between pelitic material (future skarns and hornfelses) and calcitic layers at the margin of the Kopaonik intrusion were not yet inverted when the folds formed, indicating that the D3-structures pre-date the Oligocene intrusions (Schefer et al. 2010b). This is further supported by granitic veins related to the Oligocene granodiorite body which cut across D3 chevron folds in the Kopaonik Metamorphic Series (Fig. 4.11b). In summary, these observations bracket the time-interval for D3 between the Early Paleocene (post-dating the deposition of the 'Senonian flysch') and the Latest Eocene (pre-dating the Oligocene-age intrusion of the Kopaonik granodiorite).

Interpretation

The post Senonian pre-Oligocene deformation (D3) is related to WSW–ENE-oriented compression that is associated with out-of-sequence thrusting in the internal Dinarides during the final stages of collision that followed the subduction of the last remnants of Neotethys (Sava Zone) and the final suturing of the Dinarides with the adjacent Carpatho-Balkan orogen. This D3-related deformation is observed across the entire Dinarides and is generally characterized by NW–SE-trending thrusts and minor strike-slip faults. In the area of the Southern Alps this event is known as the ‘Dinaric phase’ and there it ranges from the Late Eocene to the Early Oligocene (Channell and Doglioni, 1994; Tari 2002; Schmid et al. 2008; Rainer et al. 2009; Ustaszewski et al. submitted), i.e. it appears to be slightly younger in the Southern Alps. In the study area the thrusts are N–S-trending and the direction of transport is top west (Fig. 4.6b). Since the overall strike of the southern Dinarides in our working area is N–S, compared to NW–SE-strike in the main part of the Dinarides, this departure to top-W seems obvious.

In the Kopaonik area east of the Ibar valley this post-Senonian pre-Oligocene deformation phase is mainly visible in the form of chevron-type folds, whereas west of the Ibar valley such folds are absent. A possible explanation might be that a major thrust, contemporaneous with the ‘Studenica thrust’ (Fig. 4.7) located at the base of the Kopaonik thrust sheet, brings the Kopaonik thrust sheet on top of the Studenica thrust sheet during the Eocene. Part of the shortening is accommodated in the hanging-wall by folding (chevron-type folds), the rest of the shortening is accommodated by the basal thrust. Unfortunately, this thrust is not visible on the surface, it may be hidden in the vast masses of the serpentinitised ophiolitic rocks of the Western Vardar Ophiolitic Unit in the Ibar valley (c.f. chapter 4.4).

Post-Oligocene episode (D4)

The episode of extension observed throughout the study area is associated with D4 deformation that can be subdivided into D4a and D4b. This extension postdates the Oligocene intrusion of the Kopaonik, Drenje and Željnj intrusions and is at least partly contemporaneous with the emplacement of the Polumir two-mica granite in the Miocene (Schefer et al. 2010b). Extension is manifested by a variety of structures: (i) N–S stretching by ductile extensional deformation is mainly observed in the Studenica valley, around the Polumir intrusion in the Ibar valley and at Brezovica (Fig. 4.7), (ii) ductile collapse folds characterized by sub-horizontal axial planes are found in the vicinity of the Kopaonik intrusion and (iii) brittle E–W and N–S trending normal faults such as mapped in Fig. 4.7. Whereas ductile extension is exclusively associated with N–S stretching, the brittle extension occurs along the two contemporaneously active sets that lead to extension in E–W and N–S direction. Furthermore, the N-S striking brittle faults are seen to cut the ductile E-W-striking faults, indicating that E-W-directed extension is younger. The post-Oligocene deformation episode is thus divided into two phases, an earlier ductile phase (D4a) and a later brittle phase (D4b).

Deformation phase D4a

This predominantly ductile deformation phase is best visible along E-W-striking normal faults found in the Studenica area west of the Ibar valley, but also in two areas in the Kopaonik area (near Brezovica and in the area east of Biljanovac; see Fig. 4.7). A pronounced N–S-oriented stretching lineation and frequently observed boudins are the dominant macroscopic expression of this phase (Figs. 4.2e and 4.9d, Fig. 4.12a,e). In thin-section shear-bands (or S-C’ structures; Choukroune et al. 1987) indicate a top-to-the-north sense of shear. Garnet porphyroclasts are rotated and broken during ongoing deformation along the exhumation path, as evidenced by syn-kinematic growth of biotite and white mica in the pressure shadows (Figs. 4.3c–f and 4.12c). Near Polumir

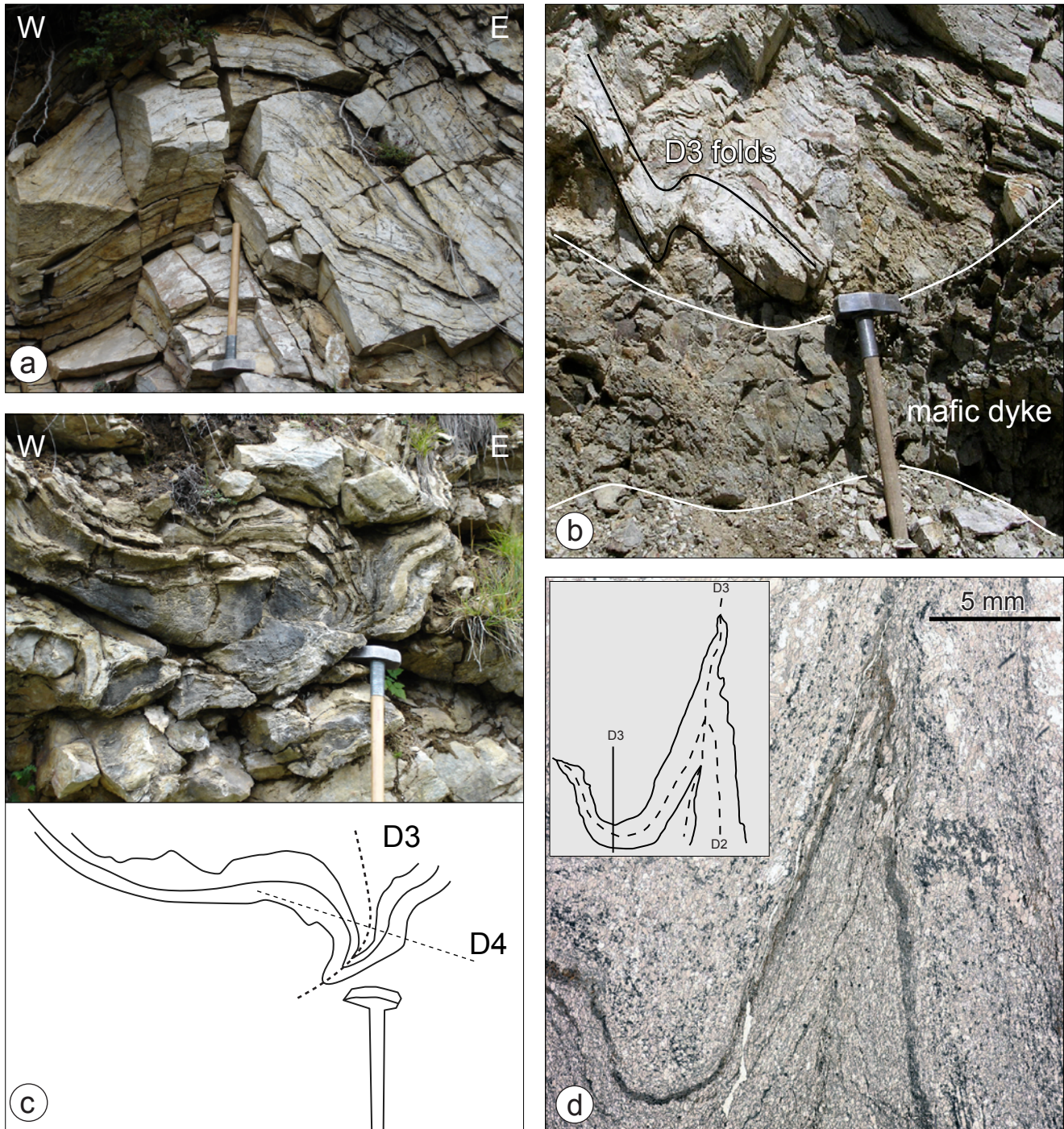


Fig. 4.11 – Field evidence illustrating overprinting criteria between different deformation phases. *a* – Isoclinal D2 fold in the Kopaonik Fm (Schefer et al. 2010a) of the Kopaonik Metamorphic Series refolded by D3 folds with a sub-vertical axial plane (sample 68). *b* – Dyke related to the Oligocene Kopaonik intrusion cross-cutting preexisting D3 chevron-type folds in the Kopaonik Fm of the Kopaonik Metamorphic Series. *c* – Overprinting of a D2–D3 interference pattern by a D4a collapse fold in the Kopaonik Fm in the vicinity of the Kopaonik intrusion. *d* – Thin-section from a cherty meta-limestone from the Kopaonik Fm showing the main foliation overprinted by D2 and D3 folds (see inset).

locality in the Ibar valley (Fig. 4.7) the Miocene two-mica granite (18 Ma; Schefer et al. 2010b) also shows such S-C-fabrics. Asymmetrically boudinaged dykes in the host rocks also indicate top-N shearing (Fig. 4.12e,f). The dykes are progressively deformed under decreasing temperatures as indicated by kinematically consistent ductile to brittle faulting. East of the Ibar valley (i.e. in Brezovica and at locality 498, Fig. 4.7), however, N-S extension is related to top-S shearing (Figs. 4.2f, 4.9d, and 4.12b,d). In the vicinity of the Kopaonik intrusion collapse folds

(Froitzheim 1992) with sub-horizontal axial planes also are attributed to D4a (e.g. Egli 2008; Zelić 2010). In some outcrops of the Oligocene intrusive bodies (i.e. in the gorge of Drenje and at the northwestern margin of the Željnj pluton, Fig. 4.7) a N-dipping foliation of hornblende minerals also indicates N–S-oriented extension.

The N–S-oriented extension is well visible in the entire study area. In the Studenica area this extension exhumes amphibolite-facies rocks in the form of a core-complex. In the Brezovica locality large scale shear bands found in meta-limestones of the Kopaonik Metamorphic Series exhume upper-most greenschist-facies rocks and bring them in contact to the Cretaceous sediments of the ‘Paraflysch’, thereby omitting the Eastern Vardar ophiolites, the Upper Cretaceous sediments of the Sava zone as well as the entire Western Vardar Ophiolitic Unit (Fig. 4.12g). Although it is not clear whether this nappe stack ever existed with its thickness seen elsewhere at this time, the S-dipping normal fault at Brezovica is of rather big importance for the understanding of the northeastern sector of the tectonic map (Fig. 4.7).

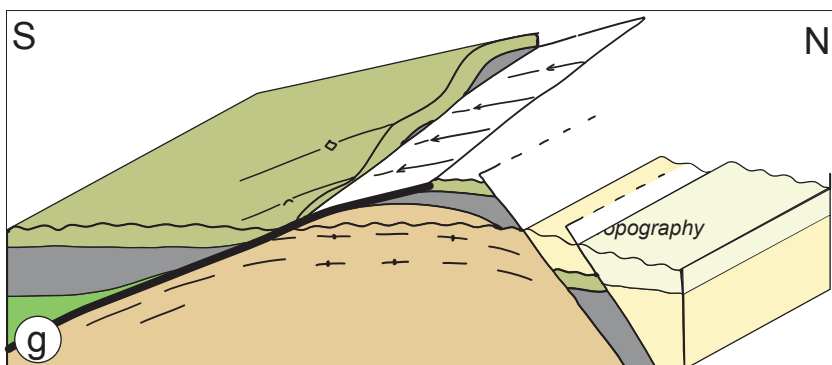
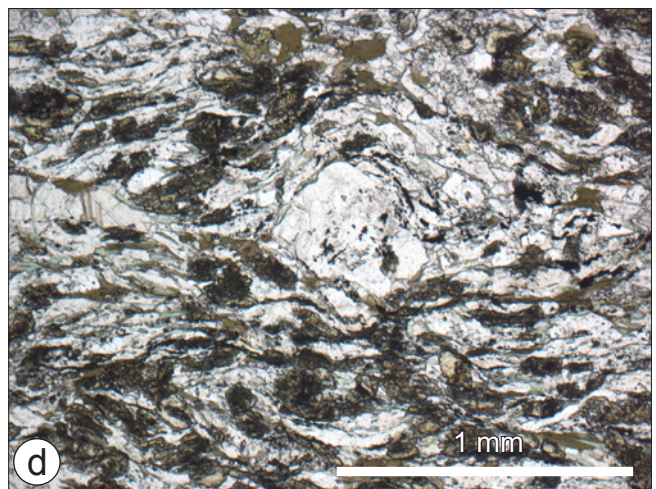
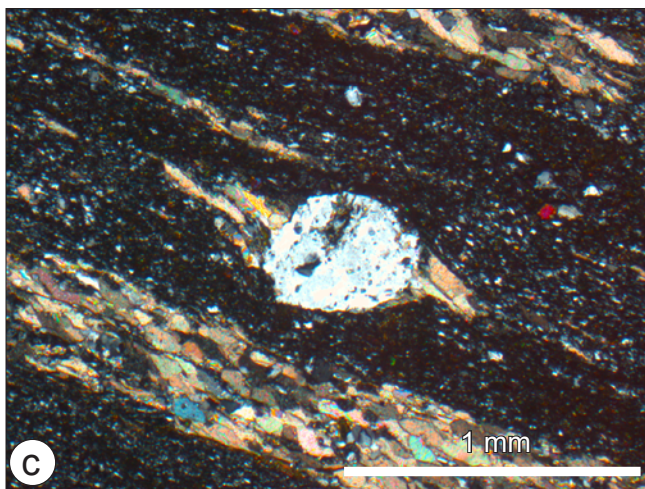
Deformation phase D4b

Brittle normal faults are observed to affect all tectonic units throughout the entire study area at different scales. This brittle deformation postdates the ductile phase D4a in many places where brittle normal faults are seen to cross-cut a ductile detachment. Small-scale normal faults, mainly expressed in serpentinised ophiolitic rocks, scatter in all directions. The major large-scale brittle normal faults, however, are N–S-striking. They border the core-complexes of the Studenica valley and the mountain chain of Kopaonik and Željnj (Fig. 4.7). In between the two domes of Kopaonik and Željnj mountains, E–W-striking brittle normal faults formed during D4b are also found (Fig. 4.7). The W-dipping normal fault at the western border of the Studenica dome (‘Studenica normal fault’; Fig. 4.13f) is made up of several smaller faults (Fig. 4.13a,b) that cross-cut the boundary of the core-complex. In its footwall ductilely deformed amphibolite-facies rocks are found whereas in the hanging wall lower greenschist-facies rocks of the Studenica thrust sheet and formerly obducted ophiolitic rocks from the Western Vardar Ophiolitic Unit are exposed (Figs. 4.13f, 4.14). The offset in metamorphic grade across this fault is substantial, and hence most of this offset probably has to be attributed to core-complex formation during D4a.

The E-dipping normal fault (Fig. 4.13c) at ‘Pošta’ locality (Fig. 4.7) is a fault zone that shows a sharp contact to the hanging-wall composed of fault gauges that include cataclastic fragments of ophiolitic rocks at its top, overprinting an older and more gently dipping foliation (Fig. 4.13d) that might be associated with earlier N–S-oriented extension produced during D4a. Towards the base of the fault zone, the style of deformation changes from brittle to ductile, and an LS-tectonite exhibits top-E oriented shear-bands (Figs. 4.13e and 4.9d). Judging from the substantial tectonic omission observed at the Pošta locality (the entire sediments of the ‘Senonian flysch’ are missing and only ca. 1 m of overlying Eastern Vardar ophiolitic rocks are preserved), this normal fault seems to contribute substantially to the exhumation of the Kopaonik–Željnj dome. However, the fission-track results (chapter 4.3) mainly show an offset of the zircon ages and only minor changes in the apatite ages across this normal fault. This indicates that tectonic omission was mainly produced during earlier and ductile N–S-oriented extension during D4a.

Interpretation

The older deformation phase (D4a) is interpreted as the more important one regarding the exhumation of metamorphic units in the study area. The fission-track data obtained on zircon and apatite discussed later (chapter 4.3; Schefer et al. 2010b) point towards fast cooling between 21 and 10 Ma (c.f. chapter 4.3). This fast cooling significantly postdates the age of the Oligocene intrusions (ca. 31 Ma; Schefer et al. 2010b). After cooling of the



- Quaternary
- Mio-Pliocene cover
- 'Paraflysch'
- Eastern Vardar ophiolites
- 'Senonian flysch'
- Kopaonik thrust sheet

Oligocene intrusions by heat conduction and before exhumation by Early to Mid-Miocene extensional unroofing, the ambient temperatures in the intrusions and the host rock differed by some 300 °C (Schefer et al. 2010b). This indicates that Mid-Miocene N–S-extension was very substantial in the area investigated; it led to tectonic omission of about 10 km across the normal faults associated with D4a. This N–S extension is correlated with Miocene extension in the Pannonian basin whose location in the back-arc area of the W-directed subduction of the European lithosphere beneath the Carpathians is widely invoked in order to explain extension and magmatism in the main part of the Pannonian basin (Csontos 1995; Seghedi et al. 2004). D4b, on the other hand, represents a younger stage of exhumation and its importance must be subordinate concerning omission of strata. During the Middle Miocene (16.5–11 Ma), the collision of Tisza with the European continent slowed the retreating subduction processes (Seghedi et al. 2004) and may thus have reduced the amount of extension in the back-arc area. Extension during D4b is mainly E–W-oriented, but N–S-oriented extension appears to occur contemporaneously. A scenario of NE–SW-oriented transtension similar to pull-apart basins is proposed and fits well with both directions observed in the field.

Summary and interpretation of the different phases of deformation

The deformation history of the study area is characterized by three phases of compressional deformation associated with metamorphism (D1–D3), followed by a phase of intense extension leading to exhumation (D4).

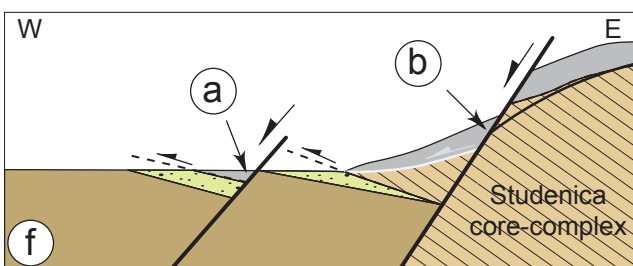
The first phase of penetrative deformation (D1) produces a penetrative foliation and stretching lineations, visible in sparse outcrops and always overprinted by the later stages in the Kopaonik Metamorphic Series. The foliated and metamorphosed matrix of the ophiolitic *mélange* including sigma-clasts with top-NW shear-senses suggests that this first deformation phase (D1) has to be correlated with the NW-directed obduction of the Western Vardar Ophiolitic Unit onto the Kopaonik and Studenica Metamorphic Series during the Late Jurassic.

The second phase of penetrative deformation (D2) is characterized by isoclinal folds that overprint D1 and that are associated with a well developed foliation S2 that completely transposes S1. D2 deformation affects the basement rocks of the Kopaonik and Studenica Metamorphic Series and probably also some ophiolites of the obducted Western Vardar Ophiolitic Unit, but not the Late Cretaceous sediments of the Sava zone. It is attributed to a (pre-Senonian, >89 Ma) Cretaceous metamorphic event that is also evidenced by new $^{40}\text{Ar}/^{39}\text{Ar}$ ages obtained from pelitic rocks in the Studenica valley (chapter 4.3).

The post-Senonian pre-Oligocene deformation phase (D3) is related to E–W-directed compression that produces chevron-type folds in the east and large-scale open folds in the west (Fig. 4.14). At the same time map-scale W-vergent thrusts accumulate a large amount of shortening that is interpreted to be associated with collision and out-of-sequence thrusting in the internal Dinarides during the final closure of oceanic realms found in the Sava zone and the suturing of the Dinarides with the adjacent Carpatho-Balkan orogen.

← Intense multi-directional post-Oligocene extension characterizes the last deformation phase (D4). This event is

Fig. 4.12 – Structures related to the ductile post-Oligocene D4a deformation. *a* – Asymmetric boudinage in chlorite-sericite-schists of the Studenica Metamorphic Series in the Studenica valley indicating dextral (top-N) shearing. *b* – Large scale sinistral (top-S) shear bands in meta-limestones of the Kopaonik Metamorphic Series (Brezovica locality, Fig. 4.7). *c* – Rotated feldspar sigma-clast with relict foliation in a matrix of quartz and calcite indicating sinistral sense of shear (top-N) from the Studenica Metamorphic Series (sample 301, Fig. 4.1); biotite grows in the pressure shadow. *d* – Sinistral (top-S) sense of shear in a calcsilicate rock (sample 498, Fig. 4.1) from the Kopaonik Metamorphic Series. *e* – Asymmetric top-N boudinage of a syn-extensional Miocene-age dyke (Polumir, c.f. Schefer et al. 2010b, their Fig. 5). *f* – S–C structures within the main body of the Polumir granite indicating dextral (top-N) extensional deformation. Such S–C fabrics in granitoids usually develop by ongoing deformation during rapid cooling from high to medium temperatures. *g* – Sketch of the high-temperature detachment at Brezovica locality (Fig. 4.7).



- Western Vardar ophiolites
- Upper Cretaceous sediments
- Studenica thrust sheet
- Drina-Ivanjica thrust sheet

correlated with Miocene extension in the Pannonian basin. Initial N–S-oriented extension and core-complex formation during D4a represents the more important phase of exhumation and is contemporaneous with the intrusion of the S-type Miocene-age Polumir granite. D4b, on the other hand, is the latest stage of exhumation, but its importance is subordinate.

Fig. 4.13 – Structures related to the brittle post-Oligocene D4b deformation. *a* – Brittle normal fault at the western margin of the Studenica core-complex (Fig. 4.7) with obducted Western Vardar Ophiolites in the hanging wall juxtaposed with the Studenica Metamorphic Series. *b* – Large scale normal faults cross-cut the detachment fault (D4a) that exhumed the amphibolite-facies rocks of the Studenica core-complex. *c* – Overview of the brittle normal fault (top-E) at the locality ‘Pošta’ (Fig. 4.7). *d* – Fault gauge at the ‘Pošta locality cross-cutting an earlier foliation. *e* – Shear-bands (top-E) from the footwall of the brittle Pošta normal fault’. *f* – Schematic drawing showing the location of the W-dipping D4b normal faults cross-cutting the boundary of the Studenica core-complex (D4a).

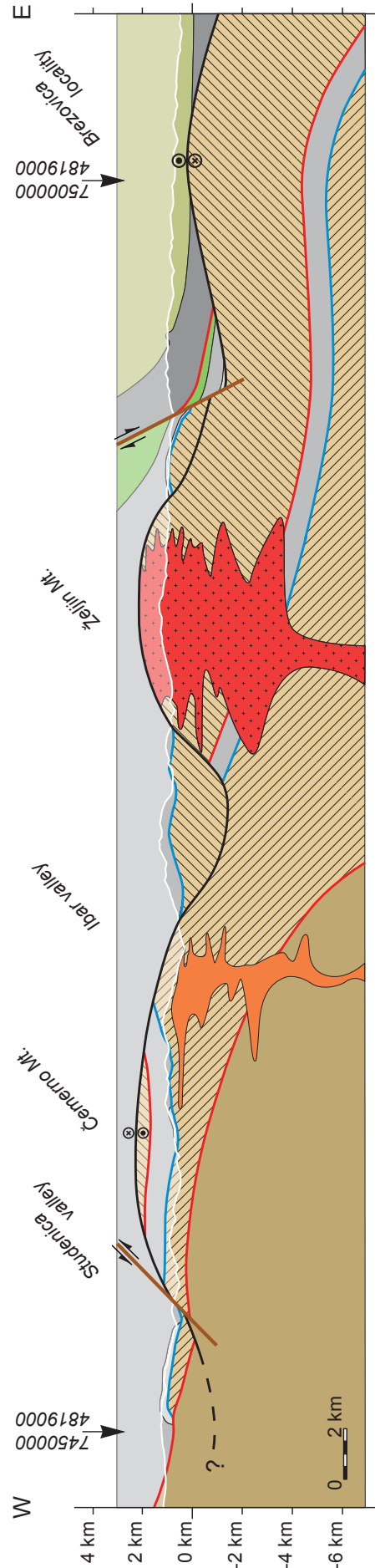


Fig. 4.14 – E–W-oriented cross-section across the entire study area, trace of profile is shown on Fig. 4.7. Ages of main activity along the major tectonic contacts are colour-coded as in Fig. 4.7.

4.3 Geochronology

Introduction

A large number of isotopic systems are currently applied in earth sciences in order to address different questions. A simple analogue, namely an hourglass, illustrates the general principle of radiometric dating: For each grain of sand that disappears from the upper reservoir (parent isotope), a grain is added to the lower reservoir (daughter isotope). If we stop the hourglass at some time (the time of the analysis in the laboratory), we can determine how long the hourglass had been running from the ratio of the sand in the two reservoirs. In order to know this time, several conditions must be known:

- (i) The number of grains dropping from one reservoir into the other per time must be known. This ratio is called the decay constant λ and is independently calculated for each isotopic system by physical experiments.
- (ii) The lower reservoir should ideally be empty at the starting time, i.e. our dated sample behaves like an open system.
- (iii) After start of the hourglass no sand may be added from or lost to the outside, i.e. the glass is fully closed. This condition is known as ‘closed system condition’, and there is no possibility to calculate a meaningful age, if this condition is violated. Applied to geochronology this implies that the system containing parent and daughter isotopes must keep the total number of isotopes constant.

If one wants to choose the appropriate system for dating a particular kind of rock or mineral, it is important to consider some facts:

- (i) Since the amount of daughter isotope is a function of time *and* amount of parent isotope, one has to choose an isotopic system in which the parent isotope is available in a measurable quantity.
- (ii) The decay constants and thus the half-lives of the different isotopic systems are different, ranging from several years (e.g. ^{210}Pb) to many billion years (e.g. ^{187}Re). This makes geochronological studies possible over the entire range of possible ages (Geyh and Schleicher 1990). The methods used in geology, however, are more often based on the long-lived radionuclides with half-lives between 700 Ma (^{235}U) and >40 Ga (^{187}Re).

It follows that the method of choice is the one with a high amount of parent isotopes built into the minerals or rocks to be dated and a half-life that is short enough to produce as much of the daughter isotope as possible and long enough to still leave some amount of parent isotopes left to be measured. This thesis used two suitable isotopic systems: the K–Ar and the U–Pb systems.

Potassium–Argon system

The decay of ^{40}K continuously produces ^{40}Ar , which itself is a radiogenic noble gas. Such gases are usually not incorporated in mineral lattices. However, in spite of its gaseous character, due to the large atomic radius of argon (1.9 Å), they are retained and accumulated within most crystals at relatively low temperatures. The abundance of potassium bearing minerals in the crust is probably the biggest advantage for using this system. K–Ar dating can be divided into two slightly different dating methods, the ^{40}K – ^{40}Ar and the ^{39}Ar – ^{40}Ar method, the latter being a modification of the former based on incremental heating of the sample, and it may be applied to igneous or metamorphic rocks containing potassium but only minor calcium (e.g. mica, feldspar, amphibole; Geyh and Schleicher

1990). The measurements are interpreted by analysing the degassing spectra (see below) and the accuracy of $^{39}\text{Ar}/^{40}\text{Ar}$ plateau ages is often better than that of conventional K/Ar ages (i.e. $\leq 1\%$). The advantages with respect to the conventional K/Ar method are as follows:

(i) Potassium and argon are measured simultaneously on the same sample aliquots, thus eliminating errors due to inhomogeneity.

(ii) Stepwise heating permits the distribution of argon isotopes in the sample to be checked, so that possible argon loss or extraneous argon can be recognised. Differences in the $^{40}\text{Ar}/^{39}\text{Ar}$ ratios for the individual degassing steps indicate disturbance of the K–Ar system, which would mean that the conditions for the calculation of a conventional K/Ar age are not present.

(iii) The calculation of plateau ages provides a more accurate age that is not influenced by argon loss at the rim of the mineral grain.

The interpretation, however, is different from case to case and may yield an age of crystallization, cooling, sedimentation or diagenesis.

Uranium–Lead system

Uranium has three different isotopes and all of them are unstable: ^{238}U (99.275% abundance), ^{235}U (0.720%) and ^{234}U (0.005%). Only ^{238}U and ^{235}U are initial nuclides of that decay series with ^{206}Pb and ^{207}Pb as their respective stable end-members, and ^{234}U is an intermediate member of the ^{238}U decay series. The uranium–lead system is a complex decay system involving 20 different steps from ^{238}U to ^{206}Pb and 17 steps from ^{235}U to ^{207}Pb , including α and β decays as well as isomeric transitions. The different transition products are all unstable with half-life times between several seconds and 4.47 Ga (^{238}U – ^{234}Th). Lead has four natural isotopes, ^{208}Pb , ^{207}Pb , ^{206}Pb and ^{204}Pb , whereas only ^{204}Pb is entirely non-radiogenic. The U–Pb system gives two independent age dates ($^{207}\text{Pb}/^{235}\text{U}$ and $^{206}\text{Pb}/^{238}\text{U}$) as well as a dependent one ($^{207}\text{Pb}/^{206}\text{Pb}$). The three ages are concordant and yield the age of the mineral, if the following three conditions are met:

- (i) The three decay constants are known with sufficient precision
- (ii) The initial lead isotope ratios are known, or alternatively, they can be neglected
- (iii) The minerals were kept in a closed system since their formation

Nowadays condition (i) is mostly fulfilled since physical experiments constrained the decay constants of the considered isotopes to a precise number within known errors that are small enough to give reasonable results for geological interpretations. It is harder to fulfil conditions (ii) and (iii). At time zero there is usually a small portion of so-called „common lead“ present, for which the isotopic composition must be known in order to correct for it. Stacey and Kramers (1975) made a promising approach and this correction is also used in this study. The closed system condition opens up a wide field of discussion about closing temperatures of different minerals.

4.3.1 $^{40}\text{Ar}/^{39}\text{Ar}$ mineral ages

Introduction

$^{40}\text{Ar}/^{39}\text{Ar}$ ages obtained from fine-fractions of pelitic rocks may reveal information concerning one or several thermal events during the geological history of the analysed samples. The fractions 2–6 and 6–12 μm were obtained by grinding the pelitic rocks as little as possible, de-carbonating them and separating the different fractions by the use of Attenberg cylinders. During this process the grains may get destroyed and thus may alter their grain-size. It is therefore important to gather as much information as possible from the thin-section to avoid misinterpreting the resulting age dates (detrital grains or older cores). Loss of ^{39}Ar by recoil was quoted to severely restrict the applicability of the $^{40}\text{Ar}/^{39}\text{Ar}$ dating technique for clay-size fractions (e.g. Turner and Cadogan 1974; Faure 1986; McDougall and Harrison 1999). On the other hand, Dong et al. (1995; 1997a,b) demonstrated how vacuum encapsulation prior to irradiation mitigated this effect, yielding geologically meaningful ages even on $<2 \mu\text{m}$ fractions. Frank and Schlager (2006) successfully demonstrated the applicability of this technique on small grain size fractions. Hence this technique was considered a viable approach for dating fine fractions from sub-greenschist-facies and greenschist-facies pelites. Nevertheless, the fact that recoil was not dominant in the release spectra shown must be discussed individually. The contribution of low-K phase impurities to the released ^{39}Ar was evaluated by inspecting the K/Ca ratio. One must keep in mind that not only single mineral phases, but aggregates of mica with some amount of quartz and, depending on the lithology, subordinate amounts of feldspar and chlorite are dated by this technique. This may lead to rather discordant age-spectra and the interpretation will become more difficult.

Grain-sizes of mica in fine-grained pelitic rocks usually cluster around 20–40 μm . Neither bigger nor smaller grains contribute significantly to the volume of the pelite. The grain-sizes of 2–6 and 6–12 μm are therefore mostly produced during preparation of the sample. This implies that (younger) parts from the rim are enriched in the small fraction, resulting in a systematic age difference between the fraction 2–6 μm (younger and from the rims) and the fraction 6–12 μm (older).

Plateau-ages are usually calculated for two or more steps that show similar ages and sum up to at least 50% of all argon released. A more pragmatic approach was chosen and this (arbitrary) definition was disregarded by calculating plateau-ages even when steps showing similar ages sum up to only ca. 40% of all argon released.

Total gas-ages are calculated by integrating over all the plateaus. If the spectrum shows strongly discordant ages, such calculation is geologically irrelevant. For plateau-like spectra with only erratic steps it is nevertheless better to indicate total gas-ages instead of giving too much weight to one or several relatively small plateau-ages.

If one observes steps with continuously increasing ages in an interval of about 10–25 Ma this usually indicates a period of crystal growth in fine-grained, low-temperature metamorphic phyllitic rocks. Whether older parts of the core contribute to this age can hardly be distinguished from the spectrum alone; one needs to look closely at the thin-section and integrate the knowledge of the regional geology. Detrital grains coexisting with newly grown mica can usually be distinguished even longer in the spectrum than in thin-section.

Analytical techniques used for $^{40}\text{Ar}/^{39}\text{Ar}$ age dating

Mineral concentrates were enclosed in high purity quartz vials and irradiated for 4–6 h at the 9MW ASTRA reactor at the Austrian Research centre Seibersdorf. After a cooling period of at least 3 weeks, the samples were filled in small annealed (low-blank) cylindrical tantalum capsules. Two Ar-extraction lines were used during this study, a manually operated and a fully automatic extraction and purification line. Both were built in-house at the Institute of Geology of Vienna University. They are made mainly of glass and fitted with a radio frequency (RF)-induction furnace made of quartz glass. The hot portion of the extraction furnace is doubly walled and continuously pumped to avoid diffusion of argon from ambient air during the high temperature steps. Argon was released at progressively higher temperatures, typically ranging between 600 and 1300 °C, on average in 30 °C intervals.

During the analysis only one tantalum capsule was in the heating position. Due to the geometry of the cylindrical capsules, which always have a horizontal position within the RF-induction coil, a uniform temperature distribution in the sample is guaranteed. Temperatures were monitored by a calibrated pyrometer, with the energy output of the RF generator being governed by the pyrometer reading. The stability at the pre-set diffusion temperature is within 1 °C. The temperature rise was rather quick and practically no overheating took place. The heating time for the low temperature steps was typically 10 min and was continuously lowered to 3 min for the high temperature steps.

Between the heating procedures the RF was switched off and no gas was released. After measuring >400 samples of different ages, mineral composition and age-patterns it can be stated that samples with uniform distribution of radiogenic Ar yield perfect plateau-type patterns. Small disturbances in the samples are easily detected, because diffusion is restricted to the pre-set temperature time span. Samples with a strong thermal overprint or old cores are characterized by pronounced age variations derived from the individual domains. Even such complex release patterns are surprisingly reproducible with the method used. Experiments during which the sample was held at a temperature of ≤ 500 °C between the diffusion steps essentially showed the same results as experiments in which the sample was not heated between the steps.

Cleaning of the gas was done by a combination of cold traps, Ti-sponge and SAE-getters. A collection of the argon with a cold trap before sample inlet was not performed. Two-thirds of the gas were introduced into a VG-5400 gas mass spectrometer. The rest of the gas was pumped away from the extraction line. Isotopic ratios were determined for a measuring period of 10 min, with the local ratios having been extrapolated back to the time of sample inlet to determine the original isotopic composition. Ages were calculated after corrections for mass discrimination and radioactive decay, especially of ^{37}Ar , using the formulas given by McDougall and Harrison (1988). The specific production ratios of the interfering Ar isotopes at the ASTRA reactor of Seibersdorf are: $^{36}\text{Ar}/^{37}\text{Ar}$ (Ca)=0.0003, $^{39}\text{Ar}/^{37}\text{Ar}$ (Ca)=0.00065, $^{40}\text{Ar}/^{39}\text{Ar}$ (K)=0.025. The K/Ca ratio is determined from the $^{39}\text{Ar}/^{37}\text{Ar}$ ratio (calculated for the end of irradiation) using a conversion factor of 0.247. This factor was determined from a plagioclase with uniform and well known composition. A plateau age is considered to be defined if the ages recorded by three or more contiguous gas fractions with similar apparent K/Ca ratios each representing >4 % of the total ^{39}Ar evolved, and together constituting >55 % of the total quantity of ^{39}Ar evolved, are mutually similar within a ± 1 % uncertainty.

The ^{40}Ar line blank at 1000 °C is $2\text{--}5 \times 10^{-10}$ cm³ STP and the $^{40}\text{Ar}/^{36}\text{Ar}$ ratio of the line blank is close to air composition. Determination of the background, blank corrections and careful checking of the peak positions were routinely performed. J-values were determined with internal laboratory standards, calibrated by international standards including muscovite Bern 4M (Burghele 1987), amphibole Mm1Hb (Samson and Alexander 1987) and Fish Canyon sanidine (Renne et al. 1994). The errors of the calculated ages for the individual steps are given as

1σ , and the error of the plateau ages or total gas ages includes an additional error of $\pm 0.4\%$ on the J-value. The age data obtained are reproducible with the same analytical equipment within this error. Inter-laboratory reproducibility can be expected within 1–1.5%. The gas from the monitors was measured in two fractions and the value was accepted when both results differed by $<0.4\%$.

The analytical techniques adapted and slightly modified after Frimmel and Frank (1998).

Results

The 16 analyses from 8 different localities (compare Fig. 4.1) can be separated into four age groups: Permian (sample 285), Cretaceous (sample 300), Paleogene (samples 301, 302 and 521) and Miocene (samples 319, 327 and 360). They will be discussed from older to younger ages. The analytical results are as shown in Table 1.

Permian ages

Only sample 285 of the matrix of the Senonian flysch near Podujevo (Kosovo) showed Permian ages. The sample consists of low-grade metamorphic sandstones with some large (>1 mm) detrital micas and small (ca. 0.02 mm) newly grown grains. The volume of the detrital grains is ca. 30 times larger than that of the newly grown grains. A well-defined schistosity is visible. Hence it is to be expected that the detrital grains might lose radiogenic argon that is incorporated into the newly formed small-sized grains.

The two analyses performed, 4569 (2–6 μm) and 4575 (6–12 μm), reveal apparent ages of 256–276 Ma and a plateau age of 207.9 ± 6 Ma, respectively (Fig. 4.15 a,b). The spectrum of analysis 4569 (2–6 μm , Fig. 2a) shows a decrease in age during the first two steps followed by an age-spectrum that continuously rises from 256 to 276 Ma. This increase is interpreted as a typical growth age. This growth age probably represents the age of the detrital grains that were reduced in grain-size during preparation. The spectrum of analysis 4575 (6–12 μm , Fig. 4.15 b) is difficult to interpret: after an increase in age within the first two steps (245–278 Ma) it gradually decreases down to 204 Ma. Since this implies that the cores of the grains are younger than their rims. Hence analysis 4575 is discarded.

Cretaceous ages

Three different samples (300/1, 300/2, 300/3) obtained at locality 300 (Fig. 4.1) all yielded Cretaceous ages. The analysed samples are sandy pelites as part of the Campil Beds of the Werfen Formation (Schefer et al. 2010a), containing only very few detrital grains. Thin-section analysis indicates lowermost greenschist-facies metamorphic conditions (Fig. 4.16a,b). Four analyses (4567, 4589, 4573, 4581; see Figs. 4.15c–f) were performed on these three samples. All three samples, including both size fractions analysed for sample 300/3, generally show similar and slightly increasing age-steps from rim to core and reveal apparent ages within the 85–110 Ma age interval (Fig. 4.15c–f). Only analysis 4567 shows younging during the first three steps (Fig. 4.15c), interpreted as being artificial and probably related to Ar-excess. No plateau ages were calculated, but all diagrams in Fig. 4.15c–f show spectra that are typical for formation ages. There is no evidence for inherited older ages from the cores or from detrital grains, except for sample 300/2 that shows older ages for the last steps in comparison with the other three analyses.

This group of data is interpreted to indicate a period of progressive and prograde metamorphism that led to crystal growth. Assuming that the oldest plateaus in analysis 4589 are due to an inherited signature, this event took place within the 110–85 Ma time period (Albian to Coniacian). It is difficult to assess whether this indicates slow heating or imprecise dating of a more short-lived event.

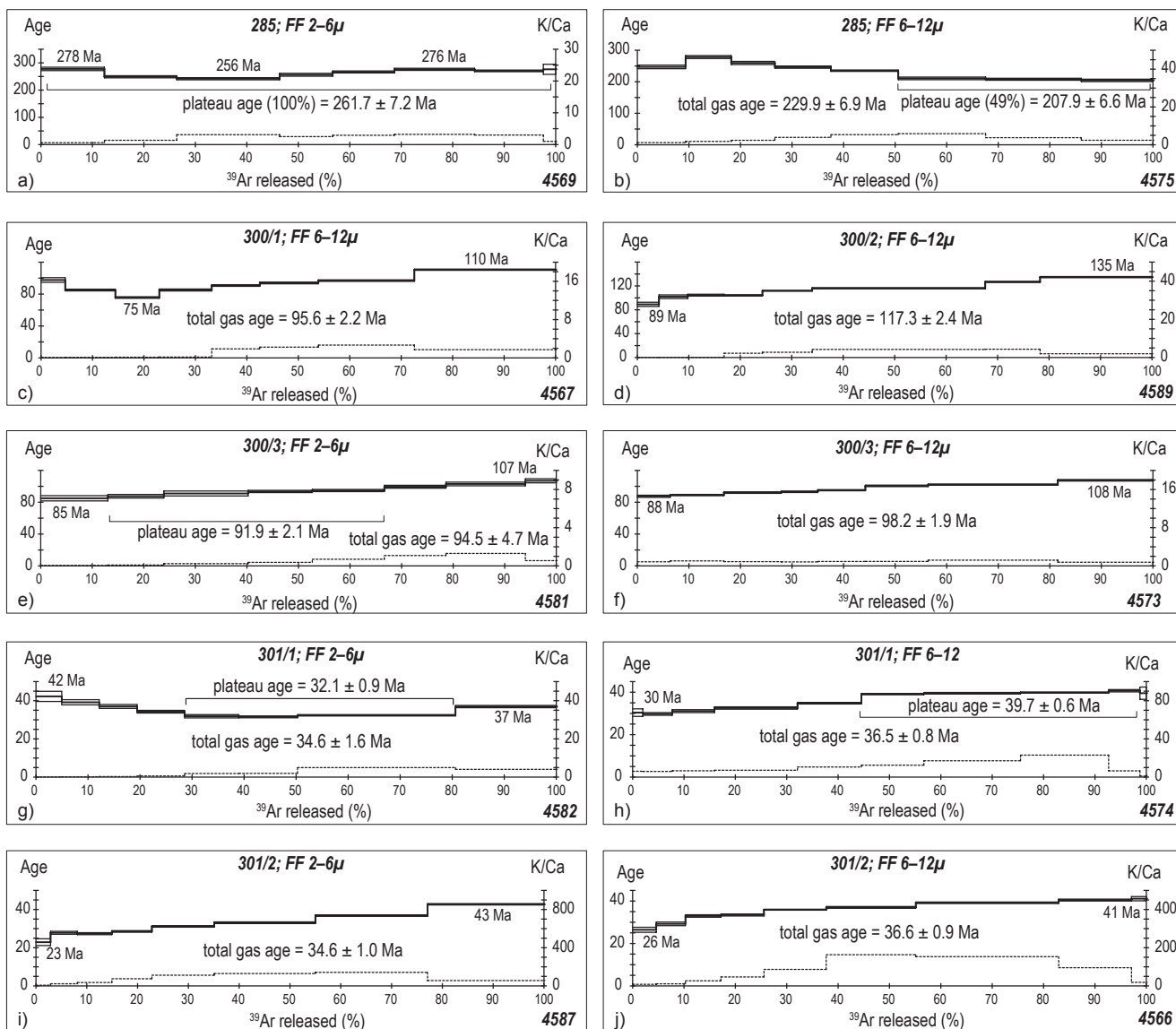


Fig. 4.15 – ^{40}Ar – ^{39}Ar incremental release spectra obtained for fine fraction (2–6 and/or 6–12 μm) of samples 285, 300 and 301 whose location is indicated in Fig. 4.1. The analytical results are shown in Table 1.

Paleogene ages

Paleogene ages were obtained at two localities, namely within the Campil Beds from Gradac 2 (sample 301, Fig. 4.1) and from an amphibolite in the Studenica valley (sample 521, Fig. 4.1).

Two specimens from locality Gradac 2 revealed a total of four analyses. These two samples are fine-grained pelitic schists. The micas are well equilibrated with no detrital grains visible. However, in outcrop as well as in thin-section (Figs. 4.12c; 4.16c,d), the degree of metamorphism appears distinctively higher in comparison to sample 300 (Fig. 4.16a,b) that yielded a Cretaceous age of metamorphism.

On specimen 301/1 two analyses (4574 and 4582; see Figs. 4.15g and 4.15h) were carried out. They reveal plateau ages of 32.1 ± 0.9 (2–6 μm fraction, Fig. 4.15g) and 39.7 ± 0.6 Ma (6–12 μm fraction, Fig. 4.15h), respectively. The analysis 4582 on the finer fraction (2–6 μm) shows artificial younging during the first four steps attributed to a recoil-effect, partly also because these negative steps were not observed in the coarser fraction of analysis 4574 (6–12 μm , Fig. 4.15h). The two analyses carried out on specimen 301/2 (4587 and 4566, Figs. 4.15i,

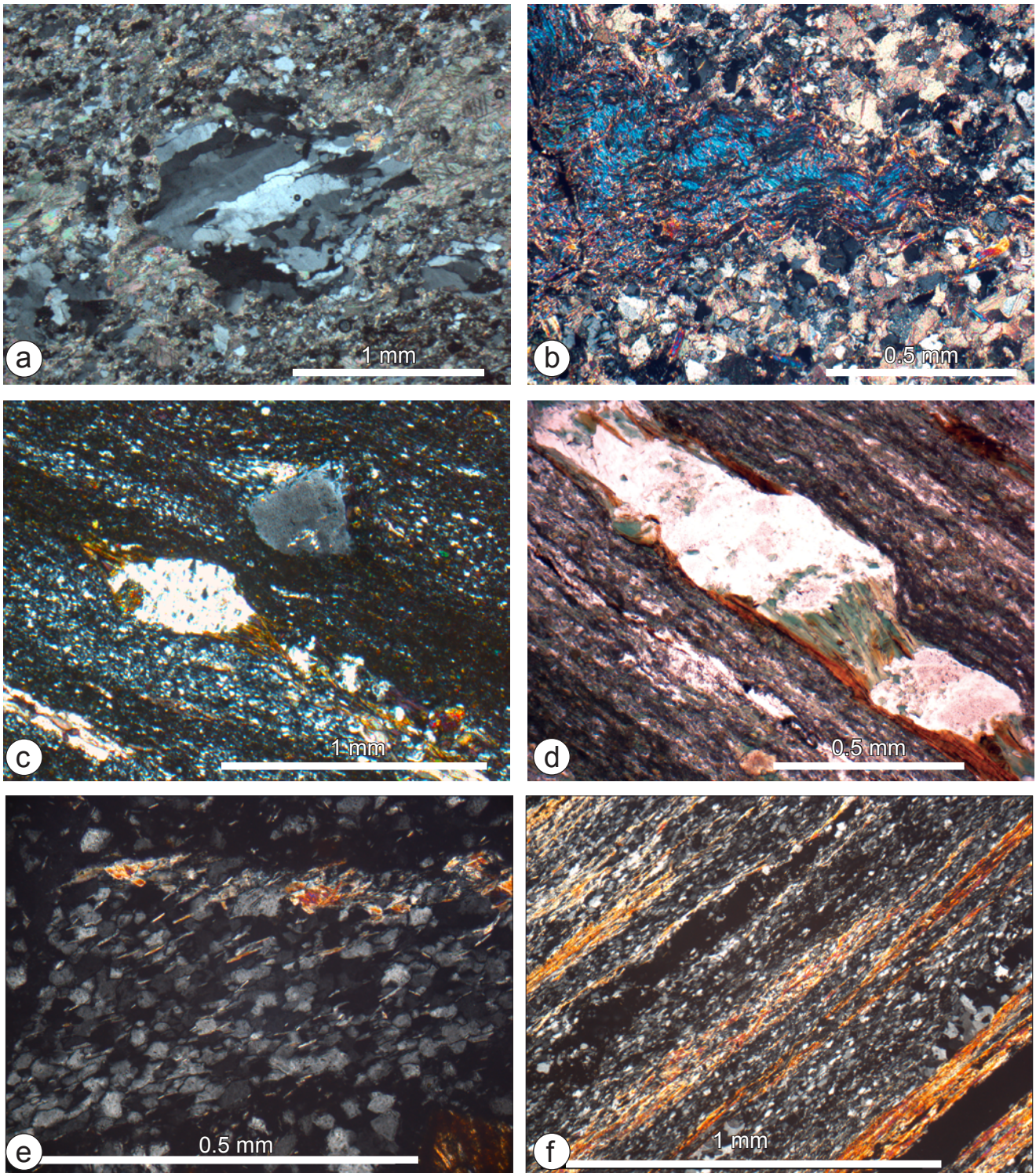


Fig. 4.16 – Thin-sections of selected samples used for ^{40}Ar – ^{39}Ar isotopic analyses. *a* – Quartz-clast in a sandy pelite of the Upper Werfen Formation (sample 300, Gradac 1 on Fig. 4.1). The quartz microstructures show deformation bands and beginning sub-grain-rotation recrystallization (SGR). The sub-grain boundaries are parallel to the *c*-axis, indicating basal-a glide, usually the first slip system activated above some 270 °C. *b* – Growth of white mica and chlorite at temperatures of an estimated 300–350 °C in sample 300. *c* – Quartz, chlorite, white mica, biotite and minor calcite are observed in sample 301 (Campil Beds of the Werfen Formation, Gradac 2 on Fig. 4.1). Quartz is completely recrystallised. The presence of biotite infers that metamorphic conditions are distinctively higher than those encountered in sample 300 (Fig. 4.16a), reaching upper greenschist-facies conditions. *d* – Chlorite replaces biotite in a pressure shadow in the fringes of larger quartz clasts (sample 301). This implies that deformation started at higher temperatures at which biotite was still stable (> 420 °C, reaction of biotite and white mica to chlorite and K-feldspar; Bucher and Frey 2002) and continued along a retrograde path. The quartz grains show relatively straight grain-boundaries and no internal bending, indicating static annealing after dynamic recrystallization. Furthermore, shear-sense indicators such as sigma-clasts and shear-bands give sinistral

and 4.15j) do not reveal plateau ages but show the typical spectra expected for mineral growth (slightly positive steps), the steps ranging from 30 to 40 Ma. The youngest apparent ages of 23 and 26 Ma, respectively, presumably reflect latest growth at the rim of grains and might be geologically relevant. Note, however, that the volume of the analysed material from the rim is very small. Analysis 4587 (2–6 μm , Fig. 4.15i) shows rather large steps in the apparent ages, which suggests that older (Cretaceous or older) relic cores might contribute to this effect.

All four analyses show a high ratio of $^{36}\text{Ar}/\text{blank}$ (Table 1), making the results analytically reliable. In view of the fine-grained lithology, disregarding the oldest steps and taking into account possible recoil effects these ages are interpreted as indicating an interval of mineral growth between 40 and 30 Ma.

Sample 521 (4570, Fig. 4.17a) is a mineral concentrate of hornblende from an amphibolite from the Studenica valley, located even further to the north compared to Gradac 2 (Fig. 4.1). Hornblende sigma-type porphyroclasts and shear bands indicate that these amphibolites were ductilely deformed after the growth of hornblende (Fig. 4.2b). They carry a N–S oriented stretching-lineation. In the Studenica valley metamorphic conditions reached ca. 500 °C, i.e. lower amphibolite-facies conditions (Fig. 4.2). This is also evidenced by the graphite thermometry on two samples (Fig. 4.3) revealing peak-temperatures of 513 and 485 °C, respectively, and additionally, by the quartz microstructures in quartzitic veins showing sub-grain rotation recrystallization, a deformation regime active at temperatures above some 450 °C (Stipp et al. 2002).

The spectrum shows negative steps at the beginning. Hornblende concentrates often show an effect of Ar-excess, usually due to small biotite inclusions in the rim (Frimmel and Frank 1998). The first two steps were therefore discarded and an apparent mean age of 40.9 ± 4.9 Ma was calculated from the remaining steps. Technically the analytical conditions during analysis 4570 were only sub-optimal, resulting in very low intensities and therefore large analytical errors. Nevertheless, this date clearly represents a metamorphic overprint, which took place at around 40 Ma.

In summary, all the five analyses of this age group (4574, 4582, 458, 4566, 4570, Fig. 4.15g–j and 4.17a) indicate a Late Eocene to Early Oligocene metamorphic overprint in an area that was formerly affected by lower greenschist facies metamorphism during the Cretaceous.

Miocene ages

All the three samples yielding Miocene ages (samples 319, 327 and 360) originate from the Kopaonik Metamorphic Series and were collected in an area northeast of Željina mountain (Fig. 4.1). Two of them (319, 360) represent fine-fractions (2–6 and 6–12 μm) obtained from fine-grained sericite-schists; sample 327 is a mineral separate of biotite from a strongly deformed biotite-schist collected at the Čemerno mountain west of the Ibar valley near Polumir (Fig. 4.1). Its protolith probably is a Paleozoic sediment from the Studenica Metamorphic Series.

The thin-section of sample 327 (Fig. 4.2g) shows a microstructure that formed under peak temperature conditions. There are no signs of retrogression and/or deformation during cooling and exhumation. Analysis 4571 (Fig. 4.17b) obtained on this specimen shows low intensity due to technical difficulties, which results in larger analytical errors. The age-spectrum only shows slightly decreasing steps for most of the spectrum. The weighted

(Fig. 4.16 continued) shear senses resulting in top-N shearing. *e* – Newly grown white mica within foliation plane in a greenschist-facies sericite-schist from the Kopaonik Metamorphic Series (sample 319). *f* – Strongly foliated sericite-schist from the Kopaonik Metamorphic Series mainly consisting of dynamically recrystallised quartz and mica (sample 360).

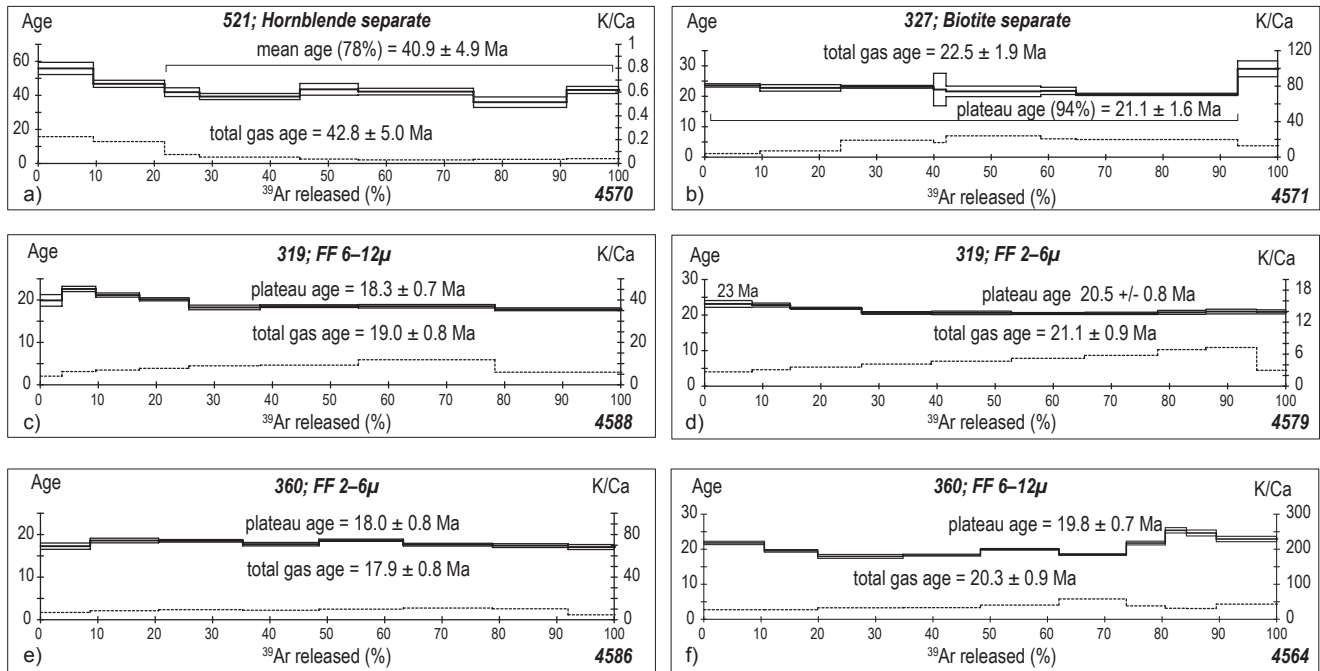


Fig. 4.17 – $^{40}\text{Ar}/^{39}\text{Ar}$ incremental release spectra obtained for fine fraction (2–6 and/or 6–12 μm) of samples 521, 327, 319 and 360 whose location is indicated in Fig. 4.1. The analytical results are shown in Table 1.

Table 4.1 – ^{40}Ar – ^{39}Ar analytical data for incremental heating experiments. Location of samples indicated on Fig. 4.1.

Correcting factors:

$$\text{Daly}/\text{HF} = 9.64 \pm 5.0\%$$

$$^{40}\text{Ar}/^{36}\text{Ar}_{\text{air}} = 299 \pm 1\%$$

$$\text{K}/\text{Ca}\text{-conv.} = 0.247$$

$$^{36}\text{Ca}/^{37}\text{Ca} = 0.00027$$

$$^{39}\text{Ca}/^{37}\text{Ca} = 0.0003$$

$$^{40}\text{K}/^{39}\text{K} = 0.0254$$

Measurement		Nr: 4569	Weight: 12.9 mg		J =	0.014 ± 0.4%			
Step	T(°C)	^{39}Ar (%)	$^{40}\text{Ar}^*$ (mV)	rad (%)	$^{39}\text{Ar}/^{37}\text{Ar}$	^{36}Ca (%)	$^{40}\text{Ar}^*/^{39}\text{Ar}$	age (Ma)	
1 *	590	12.3%	8.07	91.8%	2.395	0.03	12.05 ± 2.4%	277.8 ± 6.2	
2 *	620	14.1%	8.18	91.1%	5.467	0.01	10.71 ± 1.7%	248.9 ± 3.9	
3 *	645	20.0%	11.27	93.7%	12.614	0.01	10.38 ± 1.8%	241.7 ± 4.0	
4 *	670	10.3%	6.19	93.1%	10.181	0.01	11.05 ± 2.2%	256.3 ± 5.3	
5 *	710	12.0%	7.51	89.1%	11.824	0.00	11.53 ± 1.5%	266.7 ± 3.6	
6 *	760	15.6%	10.15	94.0%	13.004	0.01	11.98 ± 1.5%	276.2 ± 3.9	
7 *	860	13.3%	8.49	95.2%	12.153	0.01	11.71 ± 1.2%	270.6 ± 3.0	
8 *	1250	2.4%	1.56	80.7%	4.086	0.01	11.98 ± 7.2%	276.3 ± 18.5	
							100%	total gas age:	261.7 ± 7.2
								plateau age:	261.7 ± 7.2

Measurement		Nr: 4575	Weight: 23.0 mg		J =	0.014 ± 0.4%			
Step	T(°C)	^{39}Ar (%)	$^{40}\text{Ar}^*$ (mV)	rad (%)	$^{39}\text{Ar}/^{37}\text{Ar}$	^{36}Ca (%)	$^{40}\text{Ar}^*/^{39}\text{Ar}$	age (Ma)	
1	590	9.4%	19.78	83.1%	4.657	0.01	10.63 ± 2.5%	247.1 ± 5.7	
2	520	8.8%	21.27	90.5%	7.244	0.01	12.09 ± 1.8%	278.4 ± 4.6	
3	645	8.5%	18.89	86.4%	9.640	0.00	11.21 ± 2.1%	259.7 ± 5.0	
4	670	10.9%	22.89	89.7%	15.882	0.00	10.80 ± 1.6%	246.4 ± 3.6	
5 *	710	13.1%	26.21	91.6%	21.752	0.00	10.08 ± 1.0%	235.1 ± 2.2	
6 *	760	16.9%	30.24	91.6%	23.848	0.00	8.98 ± 2.1%	210.7 ± 4.2	
7 *	860	18.6%	32.66	88.7%	15.257	0.00	8.95 ± 1.6%	208.0 ± 3.2	
8 *	1250	13.9%	24.02	78.0%	9.728	0.00	8.69 ± 2.0%	204.4 ± 3.8	
							49%	total gas age:	229.9 ± 6.9
								mean age:	207.9 ± 6.6

Measurement		Nr: 4567	Weight: 18.6 mg		J =	0.014 ± 0.4%			
Step	T(°C)	^{39}Ar (%)	$^{40}\text{Ar}^*$ (mV)	rad (%)	$^{39}\text{Ar}/^{37}\text{Ar}$	^{36}Ca (%)	$^{40}\text{Ar}^*/^{39}\text{Ar}$	age (Ma)	
1	590	4.7%	4.55	88.1%	0.360	0.30	4.03 ± 3.1%	97.7 ± 2.9	
2	620	9.7%	8.21	88.9%	0.462	0.30	3.49 ± 1.3%	85.1 ± 1.1	
3	645	8.5%	6.36	91.4%	0.568	0.35	3.10 ± 1.3%	75.7 ± 1.0	
4	670	10.2%	8.60	90.9%	0.713	0.26	3.50 ± 1.5%	85.1 ± 1.2	
5	710	9.3%	8.41	91.2%	7.646	0.03	3.73 ± 1.1%	90.7 ± 1.0	
6	760	11.4%	10.63	92.3%	9.102	0.03	3.87 ± 1.2%	93.9 ± 1.1	
7	860	18.7%	17.99	92.2%	10.820	0.02	3.99 ± 1.0%	96.9 ± 0.9	
8	1250	27.4%	30.29	90.1%	6.963	0.02	4.57 ± 0.7%	110.5 ± 0.7	
								total gas age:	95.6 ± 2.2

Measurement		Nr: 4589	Weight: 30.8 mg		J =	0.014 ± 0.4%			
Step	T(°C)	^{39}Ar (%)	$^{40}\text{Ar}^*$ (mV)	rad (%)	$^{39}\text{Ar}/^{37}\text{Ar}$	^{36}Ca (%)	$^{40}\text{Ar}^*/^{39}\text{Ar}$	age (Ma)	
1	590	4.2%	16.68	69.8%	0.271	0.16	3.67 ± 4.0%	89.1 ± 3.5	
2	620	5.6%	25.47	83.0%	0.306	0.24	4.21 ± 3.1%	101.9 ± 3.1	
3	645	7.1%	32.94	91.4%	0.413	0.34	4.32 ± 1.5%	104.6 ± 1.5	
4	670	7.4%	34.67	93.9%	9.052	0.03	4.30 ± 1.0%	104.2 ± 1.0	
5	720	9.7%	48.49	94.3%	11.162	0.03	4.63 ± 0.5%	111.9 ± 0.5	
6	760	33.6%	175.17	95.8%	17.167	0.02	4.83 ± 0.7%	116.1 ± 0.8	
7	860	10.7%	60.82	91.4%	17.620	0.01	5.27 ± 0.7%	126.8 ± 0.9	
8	1250	21.7%	132.18	93.1%	7.990	0.03	5.62 ± 0.7%	134.8 ± 0.9	
								total gas age:	117.3 ± 2.4

Table 4.1 – (continued)

		300/3; FF 2–6μ						
Measurement	Nr: 4581	Weight:	7.8 mg	J =		0.014 ± 0.4%		
Step	T(°C)	³⁹ Ar (%)	⁴⁰ Ar* (mV)	rad (%)	³⁹ Ar/ ³⁷ Ar	³⁶ Ca (%)	⁴⁰ Ar*/ ³⁹ Ar	age (Ma)
1	590	13.0%	10.01	74.2%	0.199	0.25	3.50 ± 4.0%	85.0 ± 3.3
2	620	10.9%	8.60	71.7%	0.370	0.14	3.60 ± 2.6%	87.5 ± 2.3
3	645	16.3%	13.49	66.2%	0.955	0.04	3.75 ± 3.5%	91.0 ± 3.1
4	670	12.4%	10.57	81.3%	1.496	0.06	3.86 ± 1.6%	93.5 ± 1.4
5	710	14.0%	12.02	86.4%	2.818	0.05	3.91 ± 1.5%	94.7 ± 1.4
6	760	12.0%	10.82	85.9%	4.392	0.03	4.11 ± 1.9%	99.5 ± 1.8
7	860	15.4%	14.43	83.1%	5.283	0.02	4.26 ± 2.3%	102.9 ± 2.3
8	1250	6.0%	5.84	69.2%	2.239	0.02	4.43 ± 2.5%	106.9 ± 2.6
							total gas age:	94.5 ± 4.7
		300/3; FF 6–12μ						
Measurement	Nr: 4573	Weight:	18.6 mg	J =		0.014 ± 0.4%		
Step	T(°C)	³⁹ Ar (%)	⁴⁰ Ar* (mV)	rad (%)	³⁹ Ar/ ³⁷ Ar	³⁶ Ca (%)	⁴⁰ Ar*/ ³⁹ Ar	age (Ma)
1	590	6.4%	14.65	86.3%	3.470	0.04	3.60 ± 1.6%	87.5 ± 1.3
2	620	10.4%	24.45	94.1%	4.214	0.09	3.66 ± 0.9%	89.0 ± 0.8
3	645	11.1%	27.02	97.0%	3.594	0.20	3.79 ± 1.1%	92.1 ± 0.9
4	670	7.1%	17.45	93.0%	3.368	0.08	3.84 ± 1.0%	93.1 ± 0.9
5	710	9.2%	23.13	94.6%	3.740	0.10	3.92 ± 0.7%	95.1 ± 0.7
6	760	12.2%	32.36	93.1%	3.783	0.07	4.15 ± 0.9%	100.6 ± 0.9
7	860	25.2%	67.93	92.4%	4.866	0.05	4.22 ± 0.7%	102.1 ± 0.7
8	1250	18.4%	52.53	85.6%	3.101	0.03	4.45 ± 0.9%	107.5 ± 0.9
							total gas age:	98.2 ± 1.9
		301/1; FF 2–6μ						
Measurement	Nr: 4582	Weight:	18.0 mg	J =		0.014 ± 0.4%		
Step	T(°C)	³⁹ Ar (%)	⁴⁰ Ar* (mV)	rad (%)	³⁹ Ar/ ³⁷ Ar	³⁶ Ca (%)	⁴⁰ Ar*/ ³⁹ Ar	age (Ma)
1	590	5.0%	6.37	42.3%	0.333	0.09	1.72 ± 6.3%	42.3 ± 2.7
2	620	7.2%	8.59	64.6%	0.662	0.13	1.59 ± 3.5%	39.2 ± 1.4
3	645	7.3%	8.19	74.8%	1.066	0.14	1.50 ± 2.8%	37.0 ± 1.0
4	670	9.1%	9.49	79.1%	2.405	0.09	1.39 ± 2.1%	34.2 ± 0.7
5	710	10.4%	10.08	88.2%	7.621	0.07	1.29 ± 2.7%	31.8 ± 0.9
6	760	11.3%	10.80	80.0%	7.860	0.03	1.28 ± 1.6%	31.5 ± 0.5
7	860	30.4%	29.84	89.1%	20.194	0.03	1.31 ± 1.1%	32.4 ± 0.4
8	1250	19.4%	21.75	77.4%	16.461	0.01	1.50 ± 1.6%	36.9 ± 0.6
							total gas age:	34.6 ± 1.6
							plateau age:	32.1 ± 0.9
							52%	
		301/1; FF 6–12μ						
Measurement	Nr: 4574	Weight:	26.9 mg	J =		0.014 ± 0.4%		
Step	T(°C)	³⁹ Ar (%)	⁴⁰ Ar* (mV)	rad (%)	³⁹ Ar/ ³⁷ Ar	³⁶ Ca (%)	⁴⁰ Ar*/ ³⁹ Ar	age (Ma)
1	600	2.0%	3.32	84.7%	24.677	0.02	1.23 ± 5.9%	30.4 ± 1.8
2	640	5.7%	9.32	79.8%	23.885	0.01	1.20 ± 2.1%	29.8 ± 0.6
3	700	8.2%	14.02	84.8%	26.781	0.01	1.26 ± 2.2%	31.1 ± 0.7
4	740	16.2%	28.85	90.4%	29.153	0.02	1.32 ± 1.7%	32.5 ± 0.5
5	770	12.5%	23.81	93.7%	42.803	0.03	1.41 ± 1.1%	34.8 ± 0.4
6	800	12.2%	26.16	97.4%	50.410	0.09	1.59 ± 0.8%	39.1 ± 0.3
7	840	18.8%	40.88	96.4%	69.218	0.03	1.60 ± 0.9%	39.5 ± 0.4
8	900	17.1%	37.54	97.3%	93.196	0.04	1.62 ± 0.6%	39.8 ± 0.3
9	980	6.1%	13.63	90.0%	26.493	0.02	1.65 ± 1.4%	40.7 ± 0.6
10	1250	1.2%	2.70	56.1%	4.245	0.02	1.61 ± 7.4%	39.5 ± 2.9
							total gas age:	36.5 ± 0.8
							plateau age:	39.7 ± 0.6
							54%	
		301/2; FF 2–6μ						
Measurement	Nr: 4587	Weight:	? mg	J =		0.014 ± 0.4%		
Step	T(°C)	³⁹ Ar (%)	⁴⁰ Ar* (mV)	rad (%)	³⁹ Ar/ ³⁷ Ar	³⁶ Ca (%)	⁴⁰ Ar*/ ³⁹ Ar	age (Ma)
1	590	2.9%	7.71	60.3%	29.927	0.00	0.93 ± 7.8%	22.9 ± 1.8
2	620	5.3%	17.23	83.4%	91.344	0.00	1.13 ± 2.8%	27.8 ± 0.8
3	645	6.8%	21.81	80.5%	144.488	0.00	1.11 ± 1.9%	27.3 ± 0.5
4	670	7.9%	26.38	83.5%	303.746	0.00	1.16 ± 1.4%	28.5 ± 0.4
5	710	12.3%	44.90	90.1%	454.164	0.00	1.26 ± 1.3%	31.2 ± 0.4
6	760	19.9%	77.47	91.4%	524.594	0.00	1.34 ± 1.3%	33.1 ± 0.4
7	860	22.1%	95.66	89.3%	574.471	0.00	1.49 ± 1.0%	36.8 ± 0.4
8	1250	22.9%	115.49	77.1%	227.443	0.00	1.74 ± 0.8%	42.7 ± 0.3
							total gas age:	34.6 ± 1.0
		301/2; FF 6–12μ						
Measurement	Nr: 4566	Weight:	20.5 mg	J =		0.014 ± 0.4%		
Step	T(°C)	³⁹ Ar (%)	⁴⁰ Ar* (mV)	rad (%)	³⁹ Ar/ ³⁷ Ar	³⁶ Ca (%)	⁴⁰ Ar*/ ³⁹ Ar	age (Ma)
1	590	4.6%	5.48	58.5%	33.719	0.00	1.07 ± 4.5%	26.4 ± 1.2
2	620	5.7%	7.49	75.7%	44.486	0.01	1.18 ± 2.9%	29.2 ± 0.9
3	645	6.9%	10.29	89.4%	108.403	0.01	1.33 ± 1.8%	32.9 ± 0.6
4	670	8.4%	12.64	92.4%	190.174	0.00	1.35 ± 1.4%	33.4 ± 0.5
5	710	12.1%	19.66	95.9%	350.205	0.00	1.46 ± 0.6%	35.9 ± 0.2
6	760	17.4%	29.17	93.1%	661.891	0.00	1.50 ± 1.1%	37.0 ± 0.4
7	830	27.8%	49.33	90.2%	620.806	0.00	1.59 ± 0.9%	39.2 ± 0.3
8	960	14.2%	25.94	90.5%	386.026	0.00	1.64 ± 1.1%	40.5 ± 0.4
9	1250	2.9%	5.37	80.1%	75.692	0.00	1.67 ± 2.5%	41.1 ± 1.0
							total gas age:	36.6 ± 0.9
		521; Hornblend						
Measurement	Nr: 4570	Weight:	27.2 mg	J =		0.014 ± 0.4%		
Step	T(°C)	³⁹ Ar (%)	⁴⁰ Ar* (mV)	rad (%)	³⁹ Ar/ ³⁷ Ar	³⁶ Ca (%)	⁴⁰ Ar*/ ³⁹ Ar	age (Ma)
1	850	9.5%	3.61	64.1%	0.912	0.07	2.28 ± 6.5%	55.8 ± 3.6
2	950	12.3%	3.90	62.5%	0.744	0.09	1.90 ± 4.5%	46.8 ± 2.1
3	1015	6.0%	1.71	59.5%	0.304	0.19	1.70 ± 6.2%	41.9 ± 2.6
4	1090	17.3%	4.60	80.9%	0.216	0.51	1.60 ± 4.6%	39.3 ± 1.8
5	1140	10.1%	2.98	69.2%	0.149	0.41	1.77 ± 8.0%	43.6 ± 3.4
6	1200	19.9%	5.68	87.6%	0.121	0.75	1.71 ± 4.7%	42.2 ± 1.9
7	1280	16.0%	3.90	69.6%	0.140	0.48	1.46 ± 8.7%	36.0 ± 3.1
8	1340	8.9%	2.61	61.4%	0.164	0.31	1.75 ± 4.9%	43.2 ± 2.1
							total gas age:	42.8 ± 5.0
							mean age:	40.6 ± 5.0
							78%	

apparent plateau age from these geologically relevant (younger) steps yields 21.1 ± 1.6 Ma and is interpreted as dating cooling of biotite below temperatures of around 320 °C ('closure-temperature' of biotite; Von Blanckenburg et al. 1989; Hames and Bowring 1994) and after the Paleogene event that must also have overprinted this specimen before it was subject to extensional denudation. Apparent ages increase abruptly for the last step, possibly reflecting an older isotopic equilibrium preserved in the cores of biotite.

Sample 360 is a sericite-schist from the Kopaonik Metamorphic Series at Goč mountain, south of Vrnjačka Banja (Fig. 4.1). It was collected directly underneath the tectonically overlying ophiolites. The rocks are strongly ductilely deformed (Fig. 4.16f), probably during D4a normal faulting, since the Upper Cretaceous sediments, usually found on top of the Kopaonik Metamorphic Series, are missing. The grade of metamorphism is similar to that of sample 319 (greenschist-facies, Fig. 4.16f).

Sample 360 is a sericite-schist from the Kopaonik Metamorphic Series on Goč mountain, south of Vrnjačka Banja (Fig. 4.1). It was collected directly underneath the tectonically overlying ophiolites. The rocks are strongly ductilely deformed (Fig. 4.16f), probably during D4a normal faulting, since the Upper Cretaceous sediments, usually found on top of the Kopaonik Metamorphic Series, are missing. The grade of metamorphism is similar to that found in sample 319 (greenschist-facies, Fig. 4.16f).

Table 4.1 – (continued)

327; Biotite										
Measurement	Nr: 4571	Weight:	10.9 mg	J =	0.014 ± 0.4%					
Step	T(°C)	³⁹ Ar (%)	⁴⁰ Ar* (mV)	rad (%)	³⁹ Ar/ ³⁷ Ar	³⁶ Ca (%)	⁴⁰ Ar*/ ³⁹ Ar	age (Ma)		
1	610	9.6%	4.07	77.7%	16.364	0.02	0.95 ± 2.3%	23.6 ± 0.5		
4	710	14.1%	5.75	80.6%	28.628	0.01	0.92 ± 4.7%	22.8 ± 1.1		
5	760	16.2%	6.72	84.0%	77.082	0.01	0.93 ± 2.0%	23.1 ± 0.5		
6	810	2.2%	0.87	55.0%	66.337	0.00	0.90 ± 24.2%	22.2 ± 5.3		
7 *	860	16.5%	6.41	72.8%	97.154	0.00	0.87 ± 8.0%	21.6 ± 1.7		
8 *	940	6.1%	2.40	43.2%	83.531	0.00	0.88 ± 5.5%	21.8 ± 1.2		
9 *	1020	28.2%	10.42	78.8%	80.249	0.01	0.83 ± 1.8%	22.5 ± 1.9		
10	1250	7.0%	3.64	29.8%	51.921	0.00	1.17 ± 9.1%	29.0 ± 2.6		
							total gas age:	22.5 ± 1.9		
							51%	mean age:	21.1 ± 1.6	
319; FF 2–6μ										
Measurement	Nr: 4588	Weight:	23.2 mg	J =	0.014 ± 0.4%					
Step	T(°C)	³⁹ Ar (%)	⁴⁰ Ar* (mV)	rad (%)	³⁹ Ar/ ³⁷ Ar	³⁶ Ca (%)	⁴⁰ Ar*/ ³⁹ Ar	age (Ma)		
1	690	3.8%	4.77	54.4%	16.556	0.01	0.80 ± 6.9%	19.9 ± 1.4		
2	620	5.8%	8.39	80.4%	25.328	0.02	0.91 ± 2.8%	22.6 ± 0.6		
3	645	7.5%	10.18	82.3%	28.164	0.02	0.85 ± 2.3%	21.2 ± 0.5		
4	670	8.5%	10.95	82.8%	31.447	0.02	0.81 ± 1.9%	20.2 ± 0.4		
5 *	720	12.3%	14.32	78.4%	36.276	0.01	0.74 ± 3.0%	18.2 ± 0.5		
6 *	760	16.9%	20.03	84.5%	37.603	0.02	0.75 ± 1.7%	18.6 ± 0.3		
7 *	860	23.5%	27.81	83.6%	47.888	0.01	0.75 ± 2.2%	18.5 ± 0.4		
8 *	1250	21.7%	24.64	73.7%	24.120	0.01	0.72 ± 1.9%	17.8 ± 0.3		
							total gas age:	19.0 ± 0.8		
							74%	plateau age:	18.3 ± 0.7	
319; FF 6–12μ										
Measurement	Nr: 4579	Weight:	23.9 mg	J =	0.014 ± 0.4%					
Step	T(°C)	³⁹ Ar (%)	⁴⁰ Ar* (mV)	rad (%)	³⁹ Ar/ ³⁷ Ar	³⁶ Ca (%)	⁴⁰ Ar*/ ³⁹ Ar	age (Ma)		
1	590	8.2%	6.41	58.5%	10.865	0.01	0.94 ± 4.2%	23.1 ± 1.0		
2	615	6.6%	5.08	77.0%	12.490	0.03	0.92 ± 2.5%	22.8 ± 0.6		
3	655	12.3%	9.10	80.7%	14.473	0.03	0.89 ± 1.3%	21.9 ± 0.3		
4 *	685	12.0%	8.36	83.5%	16.776	0.03	0.83 ± 1.8%	20.6 ± 0.4		
5 *	720	13.8%	9.64	81.8%	18.945	0.03	0.83 ± 2.4%	20.6 ± 0.5		
6 *	750	12.6%	8.69	89.9%	21.129	0.05	0.83 ± 1.3%	20.4 ± 0.3		
7 *	795	12.6%	8.74	86.4%	23.375	0.03	0.83 ± 1.6%	20.5 ± 0.3		
8 *	840	8.3%	5.84	87.1%	27.755	0.03	0.84 ± 2.7%	20.8 ± 0.6		
9 *	920	8.7%	6.22	83.3%	29.363	0.02	0.85 ± 3.2%	21.0 ± 0.7		
10 *	1250	5.0%	3.54	78.1%	12.044	0.03	0.84 ± 2.8%	20.9 ± 0.6		
							total gas age:	21.1 ± 0.9		
							73%	plateau age:	20.6 ± 0.8	
360; FF 2–6μ										
Measurement	Nr: 4586	Weight:	26.6 mg	J =	0.014 ± 0.4%					
Step	T(°C)	³⁹ Ar (%)	⁴⁰ Ar* (mV)	rad (%)	³⁹ Ar/ ³⁷ Ar	³⁶ Ca (%)	⁴⁰ Ar*/ ³⁹ Ar	age (Ma)		
1	590	8.7%	11.06	61.2%	27.717	0.01	0.70 ± 4.3%	17.3 ± 0.7		
2 *	620	11.9%	16.36	73.1%	34.279	0.01	0.75 ± 2.9%	18.6 ± 0.5		
3 *	645	14.7%	20.07	80.5%	38.267	0.01	0.75 ± 1.6%	18.5 ± 0.3		
4 *	670	13.3%	17.39	76.4%	36.162	0.01	0.72 ± 2.3%	17.7 ± 0.4		
5 *	710	14.7%	20.24	84.6%	40.169	0.02	0.75 ± 1.4%	18.7 ± 0.3		
6 *	760	15.5%	20.22	82.6%	44.454	0.01	0.71 ± 1.8%	17.6 ± 0.3		
7 *	860	13.2%	16.92	78.9%	41.638	0.01	0.70 ± 2.6%	17.4 ± 0.4		
8 *	1250	8.0%	10.13	60.1%	18.757	0.01	0.69 ± 3.4%	17.1 ± 0.6		
							total gas age:	17.9 ± 0.8		
							91%	plateau age:	18.0 ± 0.8	
360; FF 6–12μ										
Measurement	Nr: 4564	Weight:	26.7 mg	J =	0.014 ± 0.4%					
Step	T(°C)	³⁹ Ar (%)	⁴⁰ Ar* (mV)	rad (%)	³⁹ Ar/ ³⁷ Ar	³⁶ Ca (%)	⁴⁰ Ar*/ ³⁹ Ar	age (Ma)		
1	590	10.6%	11.19	83.6%	110.575	0.00	0.88 ± 2.2%	21.8 ± 0.5		
2	615	9.3%	8.84	78.9%	110.694	0.00	0.79 ± 2.0%	19.5 ± 0.4		
3	655	14.9%	12.98	76.9%	132.904	0.00	0.72 ± 3.1%	18.0 ± 0.6		
4 *	685	13.5%	12.02	80.0%	134.642	0.00	0.74 ± 1.6%	18.3 ± 0.3		
5 *	720	13.7%	13.30	89.4%	164.171	0.01	0.81 ± 1.2%	20.0 ± 0.2		
6 *	755	11.8%	10.54	86.8%	235.272	0.00	0.75 ± 1.3%	18.5 ± 0.2		
7 *	795	6.8%	7.18	72.7%	155.019	0.00	0.88 ± 2.5%	21.8 ± 0.5		
8 *	840	3.7%	4.56	67.1%	127.199	0.00	1.03 ± 3.0%	25.4 ± 0.8		
9	920	5.2%	6.24	70.2%	124.520	0.00	1.00 ± 3.5%	24.6 ± 0.8		
10	1250	10.5%	11.73	54.9%	175.152	0.00	0.93 ± 3.4%	22.9 ± 0.8		
							total gas age:	20.3 ± 0.9		
							49%	plateau age:	19.8 ± 0.7	

Both analyses of sample 360 (4586 and 4564, Fig. 4.17e,f) show erratic steps, analysis 4586 (Fig. 4.17e) being analytically more reliable. 4564 shows possible Ar-excess content at the rims and rather large age differences between steps, possibly due to chlorite (or other mineral inclusions). The plateau ages calculated give apparent ages of 18.0 ± 0.8 Ma (4586, Fig. 8a) and 20.3 ± 0.9 Ma (4564, Fig. 4.17f) and are similar to those of sample 360. These dates are also interpreted as indicating the age of deformation and recrystallization during the initial stages of the exhumation.

Strong similarities amongst the different analyses are found when comparing the data from the three samples that yielded Miocene ages (Fig. 4.17b–f). All spectra are fairly balanced, not taking into account the turbulence of Ar-excess on most of the rims and some polyminerall problems (mainly on 4564, Fig. 4.17f). Slightly decreasing age-steps are also observed in all analysed spectra. This indicates that the minerals grew or recrystallised last in a dynamic tectonic and thermally not equilibrated environment, which favoured incorporation of excess argon. All geologically relevant steps lie within the 21–17 Ma time-span. This period of time is regarded as that of rapid exhumation, the isotopic signature being preserved within the footwall of normal faults and within strongly deformed fault rocks.

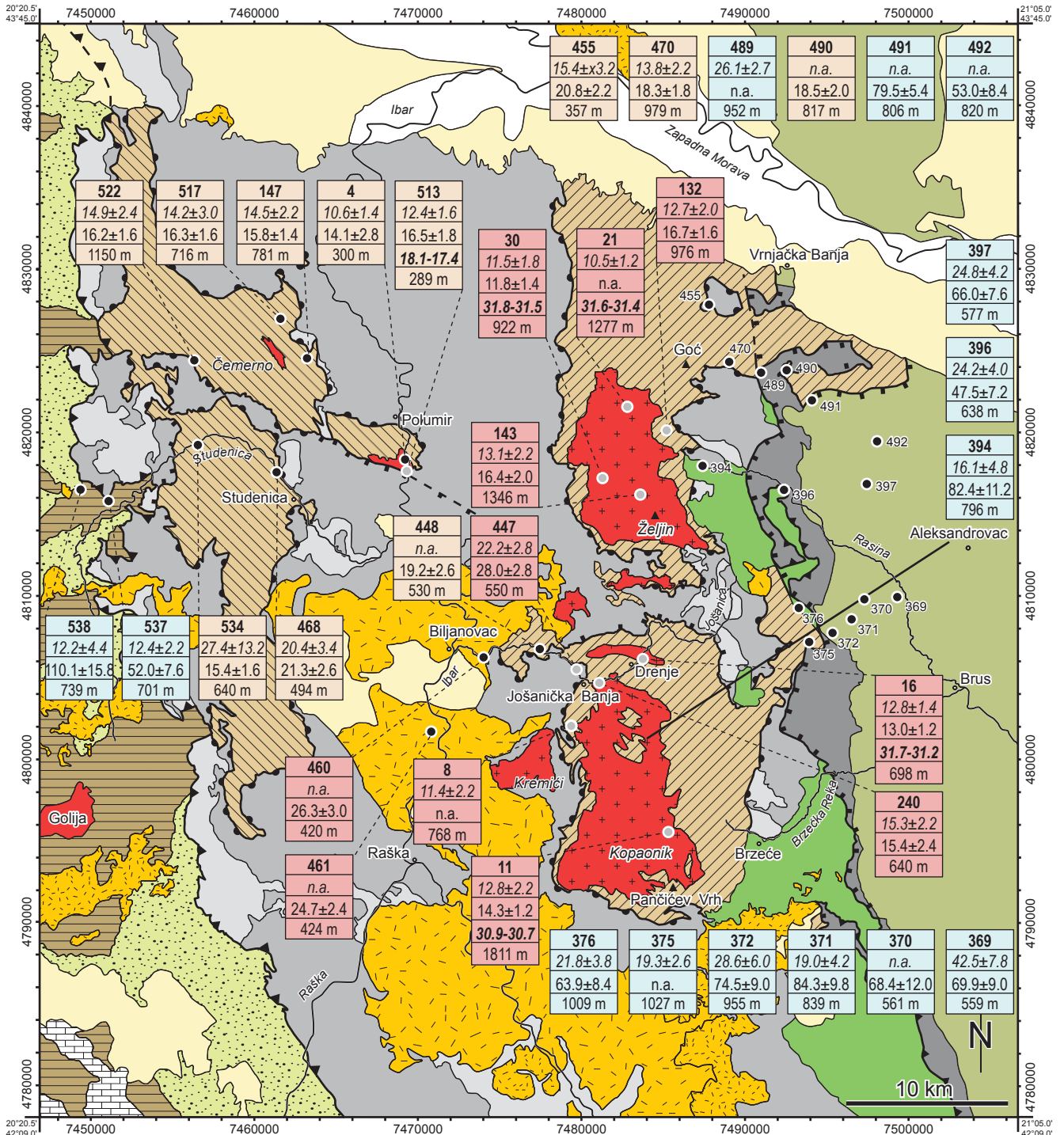
Summary of the results and interpretation of the ^{40}Ar – ^{39}Ar dating

Sample 285 from the matrix of the Upper Cretaceous sediments (‘Senonian flysch’) near Podujevo (Kosovo), representing the continuation of the Sava zone (Schmid et al. 2008), shows a Permian age-range from 276–256 Ma. This age range probably represents the metamorphic age of the detrital mica in these sediments which implies that the temperatures prevailing at this locality from the Sava zone were insufficient to overprint the ages. The Sava zone might therefore lose its importance as an accretionary wedge further to the south.

The sediments of the Studenica Metamorphic Series of Late Paleozoic to Early Jurassic age (Simić 1956; Schefer et al. 2010a) witnessed a first metamorphic event during the Late Cretaceous (110–85 Ma, Fig. 4.15c–f). This event took place under lowermost greenschist-facies conditions and is only manifested in the analyses from locality 300 (Fig. 4.1). This age-range partly overlaps with that obtained for Cretaceous low-grade metamorphism in the pre-Karst unit of the Dinarides (121–92 Ma; Pamić et al. 2004). The more internal parts of the Drina-Ivanjica thrust sheet locally also exhibit radiometrically dated Cretaceous-age low-grade metamorphism (Milovanović 1984), followed by erosion and an angular unconformity at the base of the ‘Senonian’ (Turonian and younger, i.e. <93.5 Ma) flysch that locally transgresses down onto the basement (Schmid et al. 2008, their profile 6 of Plate 3). Also the Late Cretaceous (<100 Ma according to Mikes et al. 2008) Ugar Formation found in the Pre-Karst Unit transgresses above an angular unconformity on an older flysch (Schmid et al. 2008) and contains zircon grains, which are indicative for rapid ‘mid’ to Late Cretaceous exhumation of the Adriatic basement (Mikes et al. 2008). In summary, this Cretaceous age group confirms the existence of a ‘mid’ to Late Cretaceous metamorphic event in the most internal parts of the Dinarides.

Samples 301 and 521 further north (Fig. 4.1) witnessed higher greenschist- to amphibolite-facies overprint (Fig. 4.2) during the Late Eocene to Early Oligocene. Since the same formation suffered an earlier Cretaceous metamorphism nearby (at locality Gradac 1, see above), it is likely that the Campil Beds of the larger Gradac area suffered two metamorphic events, whereby the Paleogene-age event must have been stronger at locality Gradac 2, completely wiping out the Cretaceous signature which must also have formerly overprinted this nearby locality. This reflects an increase in Paleogene metamorphic temperatures from south (Gradac 1) to north (Gradac 2) for the currently exposed levels. The strong deformation and the associated metamorphic overprint of the samples from Gradac 2 and the Studenica valley (301 and 521) led to recrystallization of the minerals, erasing the Cretaceous history formerly stored in these sample.

The Cretaceous and the Late Eocene to Early Oligocene events are only observed west of the Ibar valley and in the Studenica valley. During the Miocene the entire area of investigation (Fig. 4.1) underwent rapid exhumation accompanied by a high amount of N–S-oriented ductile deformation (deformation phase D4a; Fig. 4.12) evidenced by samples 319, 327 and 360 that all show reset $^{40}\text{Ar}/^{39}\text{Ar}$ ages of 21–17 Ma. This exhumation can also be observed independently by syn-extensional boudinage of the granitic dykes at the Polumir locality (Fig. 4.12e,f), which has been dated by U–Pb (ID-TIMS on single grain zircons) to be of Miocene age (18.1– 17.7 Ma, Schefer et al. 2010b).



<p>Post orogenic cover</p> <ul style="list-style-type: none"> Quaternary Mio-Pliocene cover <p>Cenozoic magmatic rocks</p> <p>Miocene</p> <ul style="list-style-type: none"> volcanics Polumir- and Golija intrusion <p>Oligocene</p> <ul style="list-style-type: none"> extrusives and volcaniclastics + Kopaonik intrusion 	<p>Eastern Vardar Ophiolitic Unit</p> <ul style="list-style-type: none"> 'Paraflysch' Eastern Vardar ophiolites <p>Sava Zone</p> <ul style="list-style-type: none"> Upper Cretaceous sediments <p>Western Vardar Ophiolitic Unit</p> <ul style="list-style-type: none"> Western Vardar ophiolites ophiolitic mélange <p>Kopaonik thrust sheet</p> <ul style="list-style-type: none"> Kopaonik Metamorphic Series (Paleozoic to Jurassic) 	<p>Studenica thrust sheet</p> <ul style="list-style-type: none"> Studenica Metamorphic Series (Paleozoic to Jurassic) <p>Drina-Ivanjica thrust sheet</p> <ul style="list-style-type: none"> Upper Cretaceous sediments Triassic sediments Paleozoic <p>Tectonic contacts</p> <ul style="list-style-type: none"> normal faults ▲ thrusts ▲ base ophiolitic mélange and Western Vardar Ophiolites 	<p>Analysed samples (ages in Ma ± 2σ)</p> <table border="1" style="width: 100%; border-collapse: collapse;"> <tr> <td style="text-align: center;">447</td> <td>Sample</td> </tr> <tr> <td style="text-align: center;">16.5±2.2</td> <td>Ap FT</td> </tr> <tr> <td style="text-align: center;">23.8±5.9</td> <td>Zr FT</td> </tr> <tr> <td style="text-align: center;">30.3-30.1</td> <td>Zr U-Pb</td> </tr> <tr> <td style="text-align: center;">1034m</td> <td>Elev. a.s.l.</td> </tr> </table> <p>● age data published in Schefer et al. (2010b)</p>	447	Sample	16.5±2.2	Ap FT	23.8±5.9	Zr FT	30.3-30.1	Zr U-Pb	1034m	Elev. a.s.l.
447	Sample												
16.5±2.2	Ap FT												
23.8±5.9	Zr FT												
30.3-30.1	Zr U-Pb												
1034m	Elev. a.s.l.												

4.3.2 Fission-track analyses

Introduction

The fission-track dating method is based on the spontaneous decay of ^{238}U . The currently preferred model for the formation of fission tracks is the ion spike explosion model (Fleischer et al 1975), whereby two highly charged heavy particles are produced. The highly charged particles recoil as a result of Coulomb repulsion and interact with other atoms in the lattice initially by electron stripping or ionisation. This leads to further deformation of the lattice as the ionised lattice atoms repel each other. As the fission particles capture electrons, they slow down and begin to interact by atomic collisions, further reducing the energy of the particles until they come to rest, leaving a damage trail or fission track. These cannot be observed optically unless chemically etched. A thorough overview of the fission-track technique and its geological applications is found in Gallagher et al. (1998).

Since uranium is included in several minerals as a trace element (e.g. apatite, zircon, monazite, etc.), this method is applicable to a variety of geological problems, including provenance studies, thermal history analysis in sedimentary basins, the evolution of orogenic or mountain belts, and applications in non-orogenic settings (Gallagher et al. 1998). This study concentrates on age-dating and thermal history analysis. When interpreting fission-track results one has to take into account that the central ages obtained by dating the minerals are not necessarily a geological meaningful age because the produced tracks are not stable at all temperature conditions. There is a temperature range referred to as partial annealing zone (PAZ) within which the tracks in the mineral lattice become annealed. As a result of the annealing process these tracks shorten and eventually completely disappear. The effective closure of the system lies within this PAZ and is dependent on the overall cooling rates and the kinetic properties of the minerals. The specific PAZ for apatite is between 120–60 °C (Green and Duddy 1989; Corrigan 1993). The PAZ for zircon is not so well defined and a wide range of temperature bounds have been published. Yamada et al. (1995) suggest temperature ranges of ca. 390–170 °C, whereas Tagami and Dumitru (1996) and Tagami et al. (1998) report ca. 310–230 °C. Recently, in an overview on the zircon fission-track dating method, Tagami (2005) reported temperature ranges for the zircon closure temperature of ca. 300–200 °C. Accordingly a value of 250 ± 50 °C for the closure temperature and a zircon PAZ of 300–200 °C was used in this study.

Apatite fission-track thermal modelling

Fission-tracks in apatites continuously form through time, with an approximately uniform initial mean length of ~ 16.3 μm (Gleadow et al. 1986). Upon heating, tracks gradually anneal and shorten to a length that is a function of the time and temperature within the partial annealing zone. For example, tracks are completely annealed at a temperature of 110–120 °C for a period of 105–106 years (Gleadow and Duddy 1981). These annealing characteristics allow the generation of time-temperature paths by inverse modelling (e.g. Gallagher 1995; Ketcham et al. 2003). As the resolution of the AFT thermo-chronometer is limited to the temperature range of 120–60 °C (Laslett et al. 1987), the paths of the t-T envelope defined for the zones outside this range are not necessarily representative for the real thermal evolution of a sample.

Fig. 4.18 – Fission-track central ages for zircon and apatite obtained from samples whose location is indicated on the tectonic map of the Kopaonik area. The age boxes are colour-coded in terms of three groups as follows: **red** – ages obtained for Oligocene intrusive and extrusive rocks; **yellow** – Miocene zircon central ages, **blue** – pre-Miocene zircon central ages. The map is based on fieldwork by S. Schefer and a compilation of the Basic Geological Map of Yugoslavia (1:100'000), Sheets Novi Pazar (Urošević et al. 1970a), Vrnjci (Urošević et al. 1970b), Sjenica (Mojsilović et al. 1978) and Ivanjica (Brković et al. 1976) as well as Simić (1956) for the Studenica area. Numbers at the border of the map are MGI Balkan 7 Cartesian coordinates.

Sampling strategy

The sampling strategy aimed at providing an overview of the cooling histories within the different units in the study area. 36 samples from the different stratigraphic units yielded 29 apatite and 32 zircon ages, with 25 age pairs. Ten of these samples (most of the Oligocene intrusive rocks) were previously published in Schefer et al. (2010) together with U–Pb age data, focussing on the cooling and exhumation of the plutons. These dates are included into this chapter in order to better understand the exhumation of the entire study area. All analytical results are given in Table 2 (data from Schefer et al. 2010b are marked with an asterisk), the locations of the samples are given in Fig. 4.18.

Preparation of samples

After conventional mineral separation (crushing, sieving, magnetic and heavy liquid separation) samples were mounted in epoxy resin (apatite) and PFA Teflon (zircon). Revelation of fossil tracks was achieved by etching the polished zircon mounts in a NaOH-KOH eutectic melt at 210 °C. Apatite mounts were etched in 5 N HNO₃ at 20 °C for 20 s. Induced tracks in external detector muscovite were etched in 40 % HF for 45 minutes at 20 °C. Irradiation of samples was carried out at FRMII Garching (Technische Universität München, Germany). Neutron flux was monitored using CN5 (apatite) and CN1 (zircon) dosimeter glasses. Densities of spontaneous and induced tracks as well as lengths measurements for apatite (confined horizontal tracks and long axes of etch pits) were counted on a Zeiss Axioplan microscope equipped with an Autoscan® System at the University of Innsbruck. All samples have been analysed using the external detector method as described by Gleadow (1981). The fission-track

Table 4.2 – Sample details and results of zircon and apatite fission-track dating. All ages are central ages (Galbraith 1993). $P(\chi^2)$ is the probability of obtaining χ^2 values for ν degrees of freedom where $\nu = \text{number of crystals} - 1$. pd , ps and pi represent the standard, sample spontaneous and sample induced track densities, respectively. N : Number of measurements; $Dpar$: mean track pit length; MTL : mean track length; SD : standard deviation; all numbers in brackets are numbers of measurements. Locations are given in MGI Balkan 7 Cartesian coordinates (compare Fig. 4.18).

Sample number	Min.	Location	Alt. (m)	Lithology	Stratigraphic Division	Num. gr.	pd x106 cm-2	Nd	ps x106 cm-2	Ns	pi x106 cm-2	Ni	$P(\chi^2)$ (%)	U conc. ppm(±)	Central (Ma)	Error (2σ)
Oligocene intrusive and extrusive rocks																
* 8	AP	7479347 4802076	768	granodiorite	Kopaonik	10	1.069	3206	3.186	125	53.442	2097	79.33	55 (19)	11.4	2.2
* 11	AP ZR	7485417 4795565	1811	granodiorite	Kopaonik	20 20	1.062 0.474	3206 3103	2.830 51.071	147 1449	41.741 134.393	2168 3813	99.88 49.41	46 (13) 920 (184)	12.8 14.3	2.2 1.2
* 240	AP ZR	7481047 4804677	640	granitic dyke	Kopaonik	20 12	1.474 0.474	3100 3504	4.474 9.885	263 288	73.220 24.091	4304 704	98.01 67.63	57 (26) 163 (31)	15.3 15.4	2.2 2.4
* 447	AP ZR	7479698 4805525	550	granite	Kopaonik	20 22	1.441 0.474	3336 3504	6.953 68.688	305 2582	81.177 90.902	3561 3417	100.00 9.06	70 (42) 595 (167)	22.0 28.0	2.8 2.8
* 16	AP ZR	7483641 4806274	698	granodiorite	Drenje	20 20	1.064 0.473	3206 3103	2.697 12.231	464 1016	38.794 35.417	6674 2942	64.05 83.85	42 (13) 249 (65)	12.8 13.0	1.4 1.2
* 21	AP	7482818 7482818	1277	granodiorite	Željin	20	1.056	3200	2.871	393	51.385	7033	73.63	56 (11)	10.5	1.2
* 30	AP ZR	7481290 4817210	922	granodiorite	Željin	15 16	1.065 0.469	3206 3103	2.273 10.632	21 608	37.448 31.984	3460 1829	47.80 6.43	42 (8) 90 (45)	11.5 11.8	1.8 1.4
* 132	AP ZR	7485234 4819940	976	granodiorite	Željin	20 19	1.521 0.497	3663 3204	1.373 19.882	165 847	29.332 46.970	3524 2001	100.00 85.27	48 (19) 312 (109)	12.7 16.7	2.0 1.6
* 143	AP ZR	7483601 4816215	1346	granodiorite	Željin	20 20	1.512 0.499	3663 3204	2.798 18.825	156 766	57.780 44.015	3222 1791	100.00 7.48	44 (8) 285 (125)	13.1 16.4	2.2 2.0
* 513	AP ZR	7469329 4817635	289	granite	Polumir	20 14	1.450 0.440	3100 3063	3.815 37.002	265 660	79.607 78.152	5529 1394	99.12 97.73	65 (10) 567 (306)	12.4 16.5	1.6 1.8
4	AP ZR	7465213 4818926	370	granitic dyke	Polumir	20 6	1.441 0.440	3336 3063	4.462 0.955	244 158	108.537 2.368	5935 392	99.93 99.29	88 (5) 18 (8)	10.6 14.1	1.4 2.8
460	AP ZR	7473995 4806265	420	dacite andesite	Volcanics	17	0.474	3504	12.860	702	18.410	1005	98.44	262 (100)	26.3	3.0
461	AP ZR	7470788 4801728	424	dacite andesite	Volcanics	20	0.474	3504	26.076	949	39.760	1447	79.95	276 (83)	24.7	2.4

Table 4.2 – (continued)

Sample number	Min.	Location	Alt. (m)	Lithology	Stratigraphic Division	Num. gr.	pd x106 cm-2	Nd	ps x106 cm-2	Ns	pi x106 cm-2	Ni	P(x2) (%)	U conc. ppm(±)	Central age (Ma)	(2σ)
Miocene zircon central ages																
375	AP	7493913	1027	qz-phyllite	Kopaonik Met. Series	20	1.457	3205	1.325	60	17.792	806	99.86	15 (4)	19.3	2.6
	ZR	4807265														
448	AP	7477865	530	qz-phyllite	Kopaonik Met. Series	11	0.474	3504	30.546	632	59.739	1236	10.20	439 (198)	19.2	2.6
	ZR	4806689														
455	AP	7487366	357	qz-phyllite	Kopaonik Met. Series	20	1.521	3663	2.151	109	37.838	1917	100.00	29 (16)	15.4	3.2
	ZR	4827891				20	0.501	3204	26.154	755	50.014	1482	99.33	326 (114)	20.8	2.2
470	AP	7488959	979	qz-phyllite	Kopaonik Met. Series	20	1.243	3189	2.963	169	47.719	2722	99.07	44 (28)	13.8	2.2
	ZR	4824345				20	0.498	3204	33.090	803	71.620	1738	45.73	481 (164)	18.3	1.8
489	AP	7490498	952	qz-phyllite	Kopaonik Met. Series	20	1.454	3205	1.044	91	11.399	994	91.90	16 (12)	23.7	2.7
	ZR	4824076														
490	AP	7492507	817	qz-phyllite	Kopaonik Met. Series	20	0.497	3204	32.279	790	68.889	1686	67.25	432 (143)	18.5	2.0
	ZR	4824099														
468	AP	7461394	494	qz-phyllite	Studenica Met. Series	19	1.460	3100	2.763	158	35.278	2017	89.78	27 (28)	20.4	3.4
	ZR	4817574				12	0.474	3504	28.259	649	50.118	1151	23.17	347 (135)	21.3	2.6
534	AP	7456553	640	qz-phyllite	Studenica Met. Series	9	1.456	3100	0.702	19	6.653	180	99.19	5 (2)	27.4	13.2
	ZR	4819234				19	0.474	3504	19.873	738	48.686	1808	88.86	350 (193)	15.4	1.6
147	AP	7463250	781	Paragneis	Čemerno dyke	20	1.472	3100	3.560	219	64.591	3973	97.30	50 (10)	14.5	2.2
	ZR	4824540				14	0.474	3504	34.594	1808	82.294	4301	3.57	934 (364)	15.8	1.4
517	AP	7461599	716	two-mica granite	Čemerno dyke	5	1.472	3100	7.067	105	130.646	1941	87.53	102 (18)	14.2	3.0
	ZR	4826953				19	0.474	3504	29.692	2275	67.398	5164	0.44	854 (359)	16.3	1.6
522	AP	7456137	1150	aplite	Čemerno dyke	11	1.441	3336	1.758	170	30.377	2938	99.70	82 (42)	14.9	2.4
	ZR	4824427				19	0.474	3504	27.543	1049	63.829	2431	17.13	466 (289)	16.2	1.6
pre-Miocene zircon central ages																
376	AP	7493116	1009	sandstone	Senonian Flysch	20	1.443	3205	0.552	154	6.515	1818	86.06	32 (19)	21.8	3.8
	ZR	4809248				18	0.496	3204	102.807	1714	63.040	1051	0.13	430 (142)	63.9	8.4
394	AP	7487361	796	sandstone	Senonian Flysch	12	1.521	3663	1.328	64	21.722	1047	61.16	55 (73)	16.1	4.8
	ZR	4817971				15	0.497	3204	112.559	864	53.674	412	35.65	375 (128)	82.4	11.2
396	AP	7492770	638	sandstone	Senonian Flysch	20	1.521	3663	5.065	168	56.708	1881	100.00	43 (25)	24.2	4.0
	ZR	4816529				20	0.500	3204	74.526	892	61.910	741	0.69	408 (131)	47.5	7.2
491	AP	7493829	806	qz-phyllite	Kopaonik Met. Series	15	0.499	3204	89.342	943	44.244	467	28.35	323 (162)	79.5	5.4
	ZR	4822078														
369	AP	7499247	559	sandstone	Paraflysch	20	1.454	3205	4.422	141	27.287	80	91.01	25 (24)	41.9	7.8
	ZR	4809994				20	0.499	3204	112.807	1500	63.022	838	1.81	413 (132)	69.9	9.0
370	AP	7497239	561	sandstone	Paraflysch	12	0.497	3204	4.888	792	2.752	446	1.89	131 (162)	68.4	12.0
	ZR	4809874														
371	AP	7496435	839	sandstone	Paraflysch	18	1.451	3205	1.717	87	23.432	1187	96.18	18 (12)	19.0	4.2
	ZR	4808653				20	0.497	3204	60.104	1220	27.983	568	87.95	182 (58)	84.3	9.8
372	AP	7494802	955	sandstone	Paraflysch	16	1.446	3205	3.372	112	30.529	1014	33.45	26 (12)	28.6	6.0
	ZR	4807780				20	0.499	3204	39.541	1062	20.925	562	49.26	248 (92)	74.5	9.0
397	AP	7497448	577	sandstone	Paraflysch	17	1.521	3663	5.198	166	56.775	1813	96.47	46 (29)	24.8	4.2
	ZR	4816894				20	0.498	3204	117.056	1177	69.816	702	62.59	455 (146)	66.0	7.6
492	AP	7497927	820	sandstone	Paraflysch	12	0.502	3204	52.332	432	39.249	324	57.38	266 (85)	53.0	8.4
	ZR	4819456														
537	AP	7451114	701	sericite-schist	Drina Ivanjica Paleozoic	20	1.441	3205	1.339	139	27.665	2872	88.86	41 (20)	12.4	2.2
	ZR	4815814				13	0.500	3204	52.107	565	39.565	429	38.38	277 (130)	52.0	7.6
538	AP	7449391	739	sandstone	Upper Cretaceous sed.	6	1.452	3100	1.929	34	40.785	719	43.98	32 (32)	12.2	4.4
	ZR	4816513				10	0.474	3504	81.529	911	27.653	309	72.35	208 (71)	110.1	15.8

* Previously published in Schefer et al. (2010b)

central ages ($\pm 2\sigma$ error) (Galbraith and Laslett 1993) were calculated following the IUGS recommended approach of Hurford and Green (1983) with a zeta factor of 159 ± 3.6 (zircon, CN 1 glass) and 357 ± 5.2 (apatite, CN 5 glass) (analyst: B. Fügenschuh). Data processing was carried out using the TRACKKEY program (Dunkl 2002). For thermal modelling the HeFTy® modelling program, version 1.6.7 (Ketcham 2005) and the annealing model of Ketcham et al. (2007) were used. Measured long axis of etch pits on the polished surface (= Dpar values; Donelick 1993) were included in the modelling as indicators for the chemical composition of the single grains.

Results

The samples were divided into the following three different groups: (i) Group of 11 samples from the Oligocene intrusive and extrusive rocks east of the Ibar river, (ii) Group of 11 samples with Miocene zircon central ages and (iii) Group of 14 samples yielding pre-Miocene zircon central ages.

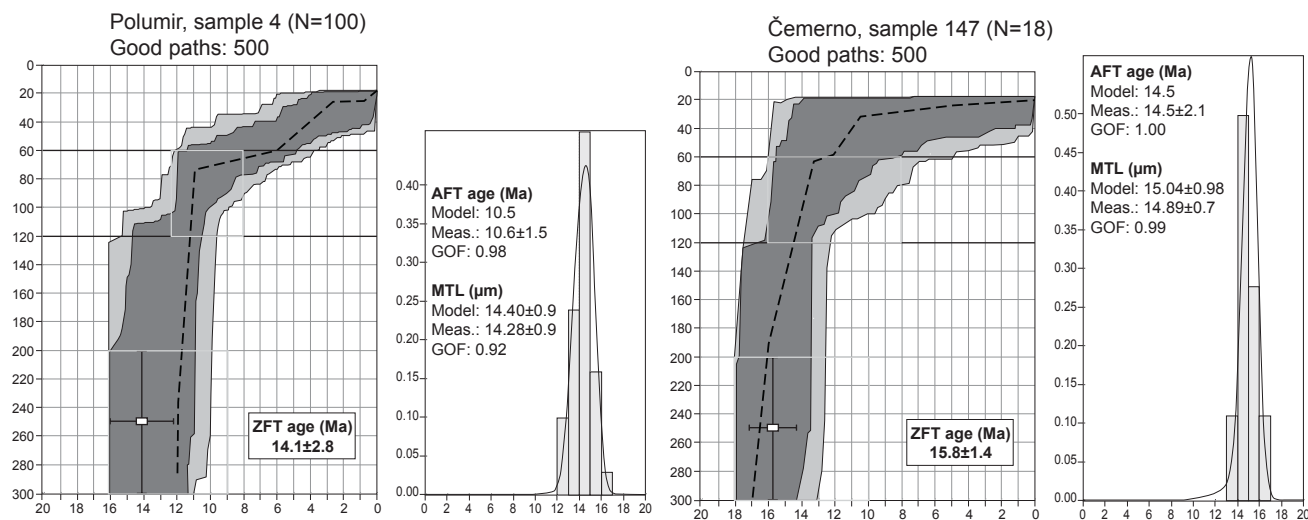


Fig. 4.19 – Modelled thermal history and comparison between observed and predicted apatite fission-track parameters for two samples from dykes within the Studenica Metamorphic Series. Horizontal black lines within individual models at 60–120 °C bracket the partial annealing zone (PAZ) for apatite within the temperature limits assigned by Laslett et al. (1987). The segments of the thermal histories at temperatures lower than 60 °C only indicate a possible continuation of the thermal history because the annealing model is not sufficiently sensitive below 60 °C. The modelled *t*-*T*-paths are extended into the zircon partial annealing zone (Brandon et al. 1998) where the white squares represent the measured zircon fission-track central ages of the modelled samples including their 2σ errors. Modelling of apatite ages and track length distribution data was performed with the program HeFTy (Ketcham et al. 2003). Fission-track age, track-length distribution and etch pit diameters (*D*_{par}) as well as user-defined time-temperature boxes are used as input parameters. An inverse Monte Carlo algorithm with a multi-kinetic annealing model (Ketcham et al. 2007) was used to generate the time-temperature paths.

(i) Oligocene intrusive and extrusive rocks

The zircon central ages reveal two different age groups, one ranging between 16.7 and 11.8 Ma (samples 11, 16, 30, 132, 143 and 240, Table 2) and another one that is significantly older, i.e. between 28.0 and 24.7 Ma (samples 447, 460 and 461, Table 2). The oldest sample (447: 28.0 Ma) comes from a very small satellite body of the Kopaonik pluton intruding the ophiolites near Jošanička Banja. It is located in the hanging wall of the normal faults that surrounds the large intrusive bodies shown in Fig. 4.18. Samples 460 and 461 are dacitic andesites from the Ibar valley; they are also part of the hanging wall in relation to the Cenozoic intrusive rocks.

The apatite central ages obtained from the Kopaonik, Drenje and Željina intrusions range between 15.3 and 10.5 Ma and all pass the Chi-square test. Mean track lengths range between 14.4 and 15.1 μm (Schefer et al. 2010b). Again sample 447 yielded an older age compared to the rest, i.e. 22 Ma. Apatite age data for samples 460 and 461 are lacking due to the poor number and quality of the grains.

(ii) Miocene zircon central ages

Zircon central ages of the 11 samples from the footwall of the N–S extensional fault zone (D4a) range from 21.3 to 14.1 Ma and all but two samples (147 and 517) pass the Chi-square test.

The central ages of all but one (sample 534) of the 10 apatite central ages fall between 20.4 and 10.6 Ma. Sample 534 reveals an apatite central age of 27.4 Ma with a 2σ error of 13.2 Ma due to its very low uranium content (5 ± 2 ppm). With respect to its 2σ error this sample therefore also falls into the above mentioned time span. Confined horizontal tracks could only be measured for three samples (samples 4, 147 and 517), all from intrusive rocks within the Studenica Metamorphic Series. For samples from the metasediments only statistically meaningless numbers of tracks could be measured.

(iii) Pre-Miocene zircon central ages

Within this group 10 out of the 12 samples measured revealed zircon central ages ranging between 110.1 and 47.5 Ma. Nine samples revealed apatite central ages, all but one sample (369) fall in the range 28.6 to 12.2 Ma. This time-span seems rather long compared to the usually short ones found in the other groups. Sample 369 is clearly older than all the others (42.5 ± 7.8 Ma). Unfortunately no track-length measurements could be carried out due to the very poor quality of the grains and the low number of tracks.

Thermal modelling of apatite track lengths

(i) Thermal modelling of the Oligocene intrusive rocks is discussed in Fig. 6 of Schefer et al. (2010b) and will only briefly be summarised here. All, with the exception of sample 447, show a similar cooling history that does not depend on the intrusion age. Rapid cooling occurs from the upper limit of the zircon partial annealing zone (ZPAZ), i.e. from around 300 °C, to some 80 °C between 16 and 10 Ma, followed by rather slow cooling to surface temperatures for the last 10 Ma. Sample 447, however, suggests rapid cooling between 30 and 21 Ma, i.e. shortly after the (presumed) age of this intrusion at around 31 Ma, and hence, significantly earlier compared to the other samples from this group. This implies that sample 447 must have intruded at a very shallow level close to the surface, in order to cool rapidly through both the ZPAZ and the APAZ immediately after its emplacement. After 22 Ma this sample cooled slowly from ca. 70 °C to surface temperatures, as indicated by the modelling, and the enhanced cooling rate between 16 and 10 Ma, monitored for the other samples by the modelling, is totally absent in sample 447.

Unfortunately there are only two samples with enough confined horizontal tracks in apatite to be measured (samples 4 and 147). These samples both come from granitic dykes intruding the basement rocks of the Studenica Metamorphic Series (Fig. 4.18) and belong to the group of Miocene zircon central ages. Most of the other samples stem from Cretaceous sediments, and the quality of the apatites was not good enough to reveal a sufficient number of confined horizontal tracks for enabling modelling (some 3–4 confined horizontal tracks per sample).

The results of the thermal modelling are presented in Fig. 4.19. They show the same pattern as the models obtained for the Oligocene intrusive rocks, i.e. rapid cooling from above the partial annealing zone for zircon, i.e. from around 300 °C to some 70 °C, between 16 and 10 Ma, followed by rather slow cooling to surface temperatures for the last 10 Ma.

Interpretation and discussion of the fission-track ages and thermal modelling*(i) Oligocene intrusive and extrusive rocks*

The most obvious characteristics of the fission-track data obtained from the Oligocene Kopaonik, Drenje and Željina intrusions is that paired zircon and apatite ages display a small age difference within a given sample. This, together with the fact that all these samples pass the Chi-square test and can thus best be interpreted as cooling ages, points to fast cooling from temperatures above the zircon partial annealing zone (PAZ) to temperatures below the apatite PAZ during the time span between 16 and 10 Ma as also shown by the modelled Tt-paths (Schefer et al. 2010b). Samples 460 and 461 represent volcanic rocks belonging to the same magmatic event as the Oligocene intrusions, extruding at a later stage. From their zircon central ages, and the fact that they pass the Chi-square test, it can be inferred that the ages of 26.3 and 24.7 Ma, respectively, represent the time of cooling after crystallization. For volcanic rocks, as is the case here, this time-lag should be sufficiently small to interpret these ages as formation ages. The few existing age data also point to an Oligocene age of these extrusive and volcanoclastic rocks in the Ibar valley (32–29 Ma; Karamata et al. 1994). Sample 447, on the other hand, shows

a different cooling history (c.f. Schefer et al. 2010b): Rapid cooling starts at 30 to 21 Ma, shortly after intrusion, and it lacks the enhanced cooling between 16 and 10 Ma observed in the other intrusive rocks. This small body is located in the hanging-wall of a normal fault (Fig. 4.18). The fact that the sample fails the Chi-square test could indicate that the t-T-path of this sample is more likely related to cooling of the intrusion rather than recording tectonically induced rapid cooling due to extensional unroofing. Hence we propose that sample 447 stems from a much shallower part of the wider Kopaonik intrusive suite, which had already cooled to temperatures below the APAZ prior to Miocene extensional unroofing. This is independently supported by the fact that sample 447 is in close vicinity to the Oligocene-age dacitic andesites (460 and 461).

(ii) Miocene zircon central ages

This group generally shows a small age difference between zircon and apatite central ages which indicates fast cooling from temperatures above the ZPAZ to temperatures below the APAZ during a time span between 21 and 10 Ma. This time span for cooling is somewhat longer than that for the Oligocene intrusions but nevertheless comparable. All samples of this group are part of the Kopaonik and Studenica Metamorphic Series (Fig. 4.18; Schefer et al. 2010b) and are hence from the footwall of the core-complexes (chapter 4.2). Thermal modelling again reveals rapid cooling between 16 and 10 Ma, identical to what was found for the Oligocene magmatic rocks. This leads to the conclusion that all rocks located in the core-complex below the D4a detachments experienced the same cooling history, irrespective of stratigraphic or magmatic age.

(iii) Pre-Miocene zircon central ages

This age group reveals pre-Miocene zircon ages within the time span 110–47 Ma. This large time span indicates that the samples of this group did not undergo complete resetting of zircon ages and thus did not experience a significant thermal overprint. Since all dated zircons from this group are detrital grains within Cretaceous sediments it is obvious that these samples are only partially annealed.

The apatite data can be divided into two groups. The first one shows fully annealed apatite with central ages ranging between 19 to 16 Ma. A second one comprises partially annealed apatites, whereby the single-grain age range falls between 75 and 8 Ma (Fig. 4.20), still passing the chi-square test. With one exception (sample 371) these two groups of ages nicely reflect the position of the groups of samples in the foot-wall and hanging-wall, respectively, of late D4b normal faults (such as the ‘Pošta’ normal fault on Fig. 4.7) that separate the Eastern Vardar Ophiolitic Unit from the underlying Sava zone (Fig. 4.14). Only sample 371, is located on the hanging-wall and nevertheless shows fully annealed apatites (19.6 ± 4.2 Ma) as is usually the case for the footwall. A possible reason for this erratic behaviour are large land slides shown on the geological map in this area (Urošević et al. 1970b), which might have disturbed the original context.

Exhumation history

The exhumation of the units in the study area is largely dictated by tectonic unroofing via N–S-stretching during the D4a deformation phase characterized by ductile detachment faults that formed during the Miocene (Figs. 4.7, 4.12g, and 4.14). All the samples from the footwall of such detachment faults yield the same small difference between zircon and apatite central ages (Fig. 4.18; Table 4.2), indicating fast cooling from temperatures above the zircon PAZ to temperatures below the apatite PAZ between 21 and 10 Ma. Thermal modelling of apatite fission track data from the Oligocene intrusions (Schefer et al. 2010b) indicates rather slow cooling to surface temperatures for the last 10 Ma. This is in line with the fact that zircon central ages on the sections crossing the

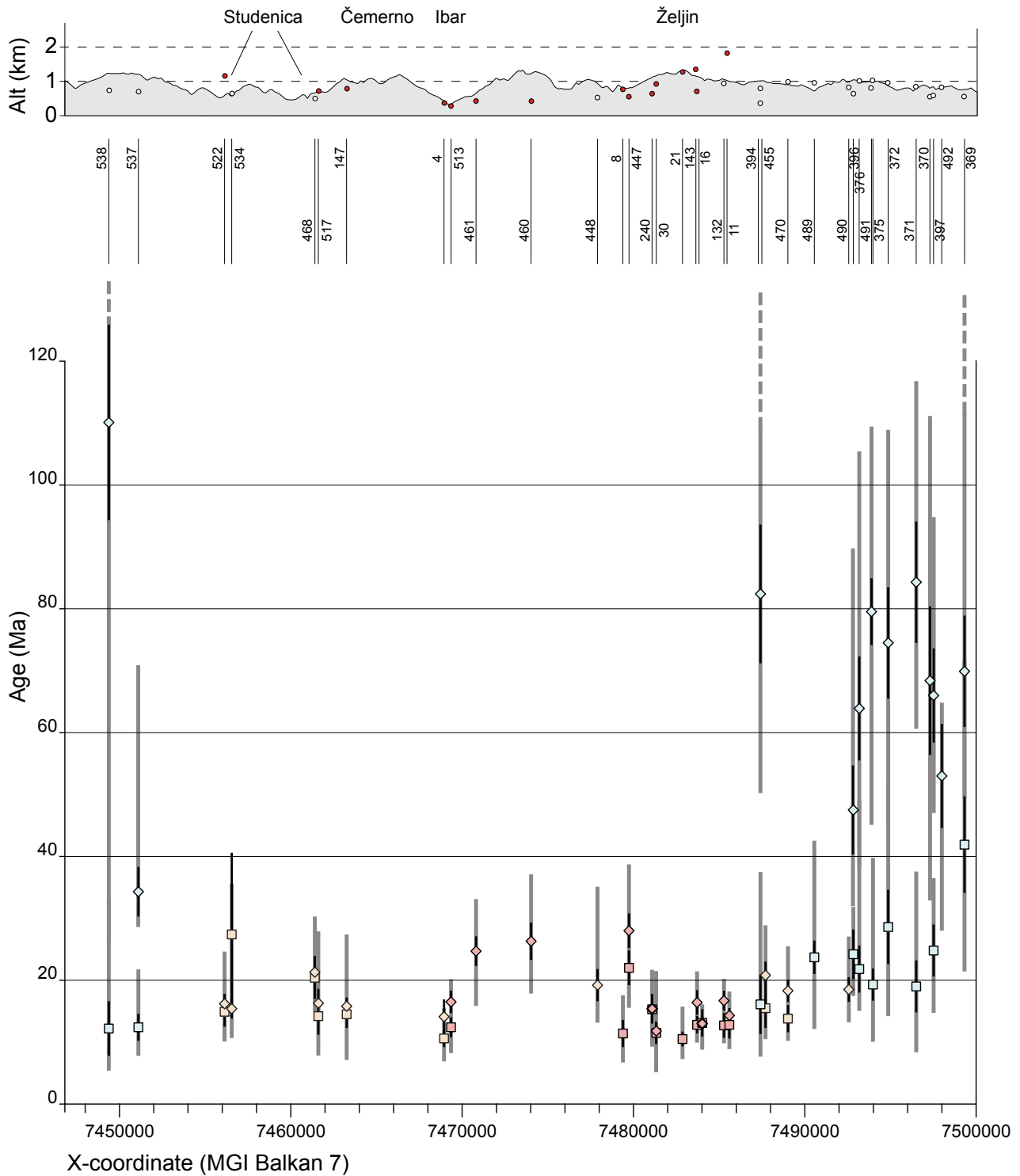


Fig. 4.20 – E–W profile (vertical exaggeration 2x; for location, see profile trace A–A’ of Fig. 4.7) across the study area showing the fission-track data. **Top:** sample location and altitude (Alt). All samples are projected in a N–S and horizontally into the profile trace. Red circles represent samples obtained on intrusive rocks, white circles those obtained for sediments. **Bottom:** apatite (squares) and zircon (diamonds) central ages with respective 2σ errors (bold line) and range between oldest and youngest single grain age (thin line). Colour code corresponds to that of Fig. 4.18.

brittle normal faults at the eastern border of the Kopaonik and Željina mountains (e.g. locality Pošta on Fig. 4.7, deformation phase D4b) are not reset, while apatite fission-track ages are only moderately affected.

4.4 Summary of metamorphism, structural geology and geochronology

This chapter integrates data on metamorphism, structural geology and age-dating and characterizes the various tectono-metamorphic events recorded in the study area. The results of geochronology constrain the different phases of deformation and metamorphism with absolute ages. Therefore, an attempt is made to reconstruct the tectono-metamorphic evolution of the study area, together with field-evidence regarding the relative chronology of deformation and metamorphism. An E–W-oriented cross-section over the entire study area (Fig. 4.14, see trace given in Fig. 4.7) demonstrates how the available data may fit into a tectonic model.

Jurassic obduction

This first event implies the obduction of the Western Vardar Ophiolitic Unit onto the Adriatic continental margin, i.e. onto its most distal parts preserved in the Kopaonik and Studenica thrust sheets and the Drina–Ivanjica thrust sheet (blue line in Figs. 4.7 and 4.14). Obduction is associated with top-NW shear-senses observed in sigma-clasts in a ductilely deformed and slightly metamorphosed ophiolitic mélange (see Fig. 4.5a). On the eastern flank of the Kopaonik mountain a penetrative foliation S1 and a stretching lineation L1 developed during this time (D1), probably associated with lower green-schist facies metamorphism; but evidence regarding kinematics and metamorphic conditions is sparse. An intense shear zone is inferred to have developed at the base of the Western Vardar Ophiolitic Unit, comprising the ophiolitic mélange and also the top-part of the underlying sediments of the Kopaonik Metamorphic Series. In the dome of the Studenica core-complex (Fig. 4.14) effects of this D1 event are not visible. Since the rocks in this area exhibit Paleogene amphibolite-facies metamorphic ages, they were exhumed from a deeper crustal level, where the obduction event did not leave any imprint.

Cretaceous metamorphic event

The Late Paleozoic to Early Jurassic sediments of the Kopaonik and Studenica Metamorphic Series (Simić 1956; Schefer et al. 2010a) witnessed a metamorphic event of lowermost greenschist-facies conditions during the Late Cretaceous (110–85 Ma). This metamorphism is interpreted to have been associated with the ductile D2 deformation phase, associated with isoclinal folding overprinting D1 and the development of a well developed second foliation S2. The Cretaceous age, however, can only be inferred from the Ar–Ar dating at locality ‘Gradac 1’ located at the southern margin of the Studenica core-complex (sample 300; Fig. 4.1). This radiometric age confirms the existence of a „mid“ to Late Cretaceous metamorphic event in the most internal parts of the Dinarides (Milovanović 1984; Belak et al. 1995; Milovanović et al. 1995; Pamić et al. 2004; Ilić et al. 2005).

Paleogene metamorphic event (Late Eocene to Early Oligocene, Dinaric phase)

The rocks from the Studenica metamorphic dome witnessed higher greenschist- to lower amphibolite-facies metamorphic overprint (Fig. 4.2) during Middle to Late Eocene (45–35 Ma). Temperatures increased from south (Gradac 1) to north (Gradac 2) during the Paleogene, as indicated by the Cretaceous age only preserved at Gradac 1 (Fig. 4.1). East of the Ibar valley, none of the metasediments of the Kopaonik Metamorphic Series witnessed such an amphibolite-facies overprint, and Paleogene metamorphic ages could not be obtained. This is probably due to its position in the hanging wall of the presumed Kopaonik thrust that induced the amphibolite-facies metamorphism in the Studenica Metamorphic Series. Since the E–W-oriented compression during the closure of the Sava suture (Schmid et al. 2008) is also associated with out-of-sequence thrusting (D3), a major thrust similar to the ‘Studenica thrust’ (Fig. 4.7) at the base of the Kopaonik Metamorphic Series might have created the tectonic

overburden that caused the Paleogene high-grade metamorphism in the Studenica dome (orange line on Fig. 4.14).

Miocene extension

During the Miocene the entire area of investigation underwent rapid exhumation, assisted by intense N–S-oriented extension (deformation phase D4a). Exhumation is evidenced by three $^{40}\text{Ar}/^{39}\text{Ar}$ ages within 21–17 Ma obtained on micas that grew or recrystallised last in a dynamic tectonic and thermally not equilibrated setting, as well as by zircon and apatite fission-track ages from the Oligocene intrusions (Schefer et al. 2010b) and from the Kopaonik and Studenica Metamorphic Series (Fig. 4.7). The latter indicate fast cooling from temperatures higher than 300 °C (upper limit of the ZPAZ) to temperatures lower than 60 °C (lower limit of the APAZ) between 21 and 10 Ma. Moreover, this N–S-oriented extension and core-complex formation during D4a (yellow lines on Fig. 4.14) is contemporaneous with the syn-extensional intrusion of the S-type Miocene-age Polumir granite (18 Ma; Schefer et al. 2010b).

This extension is correlated with the Miocene extension in the Pannonian basin, whose location in the back-arc area of the W-directed subduction of the European lithosphere beneath the Carpathians is generally invoked to explain extension and magmatism in the main part of the Pannonian basin (Csontos 1995; Seghedi et al. 2004). D4b, on the other hand, represents the latest stage of exhumation whose importance is subordinate, as is shown by the non-reset fission-track central ages on apatite in the footwall of the brittle normal faults. During the Middle Miocene (16.5–11 Ma), the collision of Tisza with the European continent slowed the retreating subduction processes (Seghedi et al. 2004) and may thus have reduced the amount of extension in the back-arc area.

Acknowledgments

The structural data obtained at the margin of the Oligocene Kopaonik intrusion greatly benefited from the work done in corporation with Daniel Egli, who spent two summers of fieldwork on the south-eastern flank of the Kopaonik Mt. working for his Master Thesis at the University of Basel (Egli 2008). Wolfgang Frank provided the results of and participated in important discussions on the $^{40}\text{Ar}/^{39}\text{Ar}$ age dates. Stefan Graeser provided IR- and Michael Wiederkehr Raman spectroscopy on some samples. All fission-track ages were counted by Bernhard Fügenschuh. Daniel Bernoulli was of great help regarding the determination of fossils in the sediments.

References

- Belak M, Pamić J, Kolar-Jurkovšek T, Pécskay Y & Karan D (1995): Alpinski regionalno metamorni kompleks Medvednice (sjeverozapadna Hrvatska). In: *1st Croatian Geological Congress Proceedings* (ed Vlahović Iea), pp. 67–70.
- Bortolotti V, Marroni M, Pandolfi L & Principi G (2005): Mesozoic to Tertiary tectonic history of the Mirdita ophiolites, northern Albania. *Island Arc*, 14: 471–493.
- Brković T, Malešević M, Urošević M, Trifunović S & Radanović Z (1976): Basic Geological Map of the SFRY, 1:100'000, Sheet Ivanjica (K34–17). *Savezni Geološki Zavod, Beograd*.
- Bucher K & Frey M (2002): *Petrogenesis of Metamorphic Rocks*. Springer, New York.
- Burghelle A (1987): Propagation of error and choice of standard in the ^{40}Ar – ^{39}Ar technique. *Chemical Geology*, 66: 17–19.
- Carosi R, Cortesogno L, Gaggero L & Marroni M (1996): Geological and petrological features of the metamorphic sole from the Mirdita ophiolites, northern Albania. *Ophioliti*, 21: 21–40.
- Channell JET & Doglioni C (1994): Early Triassic paleomagnetic data from the Dolomites (Italy). *Tectonics*, 13: 157–166.
- Choukroune P, Gapais D & Merle O (1987): Shear criteria and structural symmetry. *Journal of Structural Geology*, 9: 525–530.
- Csontos L (1995): Tertiary tectonic evolution of the Intra-Carpathian area: a review. *Acta Vulcanologica*, 7: 1–13.
- Dimitrijević MD (1997): Geology of Yugoslavia. In: *Geological Institute GEMINI Special Publication*, pp. 187, Belgrade.
- Donelick RA (1993): A method of fission track analysis utilizing bulk chemical etching of apatite. *U.S. Patent 5,267,274*.
- Dong H, Hall CM & Halliday AN (1995): Mechanisms of argon retention in clays revealed by laser ^{40}Ar – ^{39}Ar dating. *Science*, 267: 355–359.
- Dong H, Hall CM, Halliday AN & Peacor DR (1997a): Laser ^{40}Ar – ^{39}Ar dating of microgram-size illite samples and implications for thin section dating. *Geochimica et Cosmochimica Acta*, 61: 3803–3808.
- Dong H, Hall CM, Halliday AN, Peacor DR, Merriman RJ & Roberts B (1997b): ^{40}Ar – ^{39}Ar illite dating of Late Caledonian (Acadian) metamorphism and cooling of K-bentonites and slates from the Welsh Basin, U.K. *Earth and Planetary Science Letters*, 150: 337–351.
- Dunkl I (2002): TRACKKEY: A Windows program for calculation and graphical presentation of fission track data. *Computers & Geosciences*, 18: 3–12.
- Egli D (2008): Das Kopaonik-Gebirge in Südserbien – Stratigraphie, Strukturen und Metamorphose. MSc Thesis, University of Basel, Basel.
- Ehlers TA (2005): Crustal thermal processes and the interpretation of thermochronometer data. In: *Low-Temperature Thermochronology: Techniques, Interpretations, and Applications*, pp. 315–350, Mineralogical Society of America, vol 58, Chantilly.
- Faure G (1986): *Principles of Isotope Geology*. John Wiley & Sons, New York.
- Fleischer RL, Price PB & Walker RM (1975): *Nuclear Tracks in Solids*. University of California Press, Berkeley.
- Frank W & Schlager W (2006): Jurassic strike slip versus subduction in the Eastern Alps. *International Journal of Earth Sciences*, 95: 431–450.
- Frimmel HE & Frank W (1998): Neoproterozoic tectono-thermal evolution of the Gariiep Belt and its basement, Namibia and South Africa. *Precambrian Research*, 90: 1–28.
- Froitzheim N (1992): Formation of recumbent folds during synorogenic crustal extension (Austroalpine nappes, Switzerland). *Geology*, 20: 923–926.
- Galbreith RF & Laslett GM (1993): Statistical models for mixed fission-track ages. *Nuclear Tracks and Radiation Measurements*, 21: 459–470.

- Gallagher K, Brown R & Johnson C (1998): Fission-track analysis and its applications to geological problems. *Annual Reviews of Earth and Planetary Sciences*, 26: 519–572.
- Geyh MA & Schleicher H (1990): Absolute Age Determination, Physical and Chemical Dating Methods and Their Application. Springer, Berlin.
- Gleadow AJW (1981): Fission-track dating methods – what are the real alternatives. *Nuclear Tracks and Radiation Measurements*, 5: 3–14.
- Gleadow AJW & Duddy IR (1981): A natural long-term annealing experiment for apatite. *Nuclear Tracks*, 5: 169–174.
- Gleadow AJW, Duddy IR, Green PF & Lovering JF (1986): Confined fission track lengths in apatite: A diagnostic tool for thermal history analysis. *Contributions to Mineralogy and Petrology*, 94: 405–415.
- Hames WE & Bowring SA (1994): An empirical evaluation of the argon diffusion geometry in muscovite. *Earth and Planetary Science Letters*, 124: 161–167.
- Hurford AJ & Green PF (1983): The zeta-age calibration of fission-track dating. *Isotope Geoscience*, 1: 285–317.
- Ilić A, Neubauer F & Handler R (2005): Late Paleozoic-Mesozoic tectonics of the Dinarides revisited: Implications from $^{40}\text{Ar}/^{39}\text{Ar}$ dating of detrital white micas. *Geology*, 33: 233–236.
- Karamata S, Korikovskiy S & Kurdyukov E (2000): Prograde contact metamorphism of mafic and sedimentary rocks in the contact aureole beneath the Bresovica harzburgite Massif. In: *International Symposium Geology and Metallogeny of the Dinarides and the Vardar zone* (eds Karamata S & Janković S), pp. 171–177, Academy of Sciences & Arts Republic of Srpska, vol 1, Banja Luka, Sarajevo.
- Karamata S (2006): The geological development of the Balkan Peninsula related to the approach, collision and compression of Gondwanan and Eurasian units. In: *Tectonic Development of the Eastern Mediterranean Region* (eds Robertson AHF & Mountrakis D), pp. 155–178, Geol. Soc. London Spec. Publ., vol 260.
- Ketchum RA (2005): Forward and Inverse Modeling of Low-Temperature Thermochronometry Data. *Reviews in Mineralogy & Geochemistry*, 58: 275–314.
- Ketchum RA, Carter A, Donelick RA, Barbarand J & Hurford AJ (2007): Improved measurement of fission-track annealing in apatite using c-axis projection. *American Mineralogist*, 92: 789–798.
- Laslett GM, Green PF, Duddy IR & Gleadow AJW (1987): Thermal annealing of fission tracks in apatite: 2. A quantitative analysis. *Chemical Geology*, 65: 1–13.
- McDougall I & Harrison TM (1999): Geochronology and Thermochronology by the $^{40}\text{Ar}/^{39}\text{Ar}$ method. Oxford University Press, New York.
- Mikes T, Christ D, Petri R, Dunkl I, Frei D, Baldi-Beke M, Reitner J, Wemmer K, Hrvatović H & Von Eynatten H (2008): Provenance of the Bosnian Flysch. *Swiss Journal of Geosciences*, 101: S31–S54.
- Milovanović D (1984): Petrology of low metamorphosed rocks of the central part of the Drina-Ivanjica Palaeozoic. *Bulletin du Musée de l'Histoire Naturelle Beograd*, A39: 1–139.
- Milovanović D, Marchig V & Stevan K (1995): Petrology of the crossite schist from Fruska Gora Mts (Yugoslavia), relic of a subducted slab of the Tethyan oceanic crust. *Journal of Geodynamics*, 20: 289–304.
- Mojsilović S, Baklajić D & Djoković I (1978): Basic Geological Map of the SFRY, 1:100'000, Sheet Sjenica (K32-29). *Savezni Geološki Zavod, Beograd (Geozavod – OOUR Geološki institut, Beograd, 1960-1973)*.
- Mojsilović S, Djoković I, Baklajić D & Rakić B (1980): Geology of the Sheet Sjenica (K32–29), Explanatory notes (in Serbo-Croatian, English and Russian summaries). *Savezni Geološki Zavod, Beograd*.
- Operta M, Pamić J, Balen D & Tropper P (2003): Corundum-bearing amphibolites from the metamorphic basement of the Krivaja-Konjuh ultramafic massif (Dinaride Ophiolite Zone, Bosnia). *Mineralogy and Petrology*, 77: 287–295.
- Ortner H, Reiter F & Acs P (2002): Easy handling of tectonic data: the programs TectonicVB for Mac and TectonicsFP for Windows(TM). *Computers & Geosciences*, 28: 1193–1200.
- Pamić J, Balogh K, Hrvatović H, Balen D, Jurković I & Palinkas L (2004): K–Ar and Ar–Ar dating of the Palaeozoic metamorphic complex from the Mid-Bosnian Schist Mts., central Dinarides, Bosnia and Hercegovina. *Mineralogy and Petrology*, 82: 65–79.

- Rainer T, Sachsenhofer RF, Rantitsch G, Herlec U & Vrabec M (2009): Organic maturity trends across the Variscan discordance in the Alpine-Dinaric Transition Zone (Slovenia, Austria, Italy): Variscan versus Alpidic thermal overprint. *Austrian Journal of Earth Sciences*, 102: 120–133.
- Rampnoux JP (1974): Contribution à l'étude géologique des Dinarides: Un secteur de la Serbie méridionale et du Monténégro oriental (Yougoslavie). *Mémoires de la Société Géologique de France (Nouvelle Serie)*, 119: 1–99.
- Renne PR, Deino AL, Walter RC, Turrin BD, Swisher CC, Becker TA, Curtis GH, Sharp WD & Jaouni A-R (1994): Intercalibration of astronomical and radioisotopic time. *Geology*, 22: 783–786.
- Samson SD & Alexander EC (1987): Calibration of the interlaboratory ^{40}Ar – ^{39}Ar dating standard MMhb-1. *Chemical Geology*, 66: 27–34.
- Schefer S, Egli D, Missoni S, Bernoulli D, Fügenschuh B, Gawlick HJ, Jovanović D, Krystyn L, Lein R, Schmid SM & Sudar MN (2010a): Triassic metasediments in the Internal Dinarides (Kopaonik area, southern Serbia): stratigraphy, paleogeographic and tectonic significance. *Geologica Carpathica*, 61: ?
- Schefer S, Cvetković V, Fügenschuh B, Kounov A, Ovtcharova M, Schaltegger U & Schmid SM (2010b): Cenozoic granitoids in the Dinarides of southern Serbia: age of intrusion, isotope geochemistry, exhumation history and significance for the geodynamic evolution of the Balkan Peninsula. *International Journal of Earth Sciences*, in Review.
- Schmid SM, Bernoulli D, Fügenschuh B, Matenco L, Schefer S, Schuster R, Tischler M & Ustaszewski K (2008): The Alpine-Carpathian-Dinaridic orogenic system: correlation and evolution of tectonic units. *Swiss Journal of Geosciences*, 101: 139–183.
- Seghedi I, Downes H, Szakacs A, Mason PRD, Thirlwall MF, Rosu E, Pécskay Z, Marton E & Panaiotu C (2004): Neogene–Quaternary magmatism and geodynamics in the Carpathian–Pannonian region: A synthesis. *Lithos*, 72: 117–146.
- Simić V (1956): Zur Geologie des Studenicegebietes (Südwestserbien). *Vesnik Bull. Serv. Geol. Geophys.*, 12: 5–66.
- Simpson C & Schmid SM (1983): An evaluation of criteria to deduce the sense of movement in sheared rocks. *Bulletin Geological Society America*, 94: 1281–1288.
- Stipp M, Stünitz H, Heilbronner R & Schmid SM (2002): The eastern Tonale fault zone: a 'natural laboratory' for crystal plastic deformation of quartz over a temperature range from 250 to 700 °C. *Journal of Structural Geology*, 24: 1861–1884.
- Sudar M & Kovács S (2006): Metamorphosed and ductilely deformed conodonts from Triassic limestones situated beneath ophiolite complexes: Kopaonik Mountain (Serbia) and Bukk Mountains (NE Hungary) - a preliminary comparison. *Geologica Carpathica*, 57: 157–176.
- Tari V (2002): Evolution of the northern and western Dinarides: a tectonostratigraphic approach. *EGU Stephan Mueller Special Publications*, 1: 223–236.
- Tomljenović B, Csontos L, Marton E & Marton P (2008): Tectonic evolution of the northwestern Internal Dinarides as constrained by structures and rotation of Medvednica Mountains, North Croatia. In: *Tectonic Aspects of the Alpine-Dinaride-Carpathian system* (eds Siegesmund S, Fügenschuh B & Froitzheim N), pp. 145–167, Geological Society, London, Special Publications, vol 298.
- Turner G & Cadogan PH (1974): Possible effects of ^{39}Ar recoil in ^{40}Ar – ^{39}Ar dating. *Geochimica et Cosmochimica Acta*, 2, Supplement 5: 1601–1615.
- Urošević M, Pavlović Z, Klisić M, Brković T, Malešević M & Trifunović S (1970a): Geological map of Yugoslavia, Sheet Novi Pazar, 1:100'000, Savezni Geološki Zavod, Belgrade.
- Urošević M, Pavlović Z, Klisić M, Brković T, Malešević M & Trifunović S (1970b): Geological map of Yugoslavia, Sheet Vrnjci, 1:100'000, Savezni Geološki Zavod, Belgrade.

- Ustaszewski K, Schmid SM, Lugović B, Schuster R, Schaltegger U, Bernoulli D, Hottinger L, Kounov A, Fügenschuh B & Schefer S (2009): Late Cretaceous intra-oceanic magmatism in the internal Dinarides (northern Bosnia and Herzegovina): Implications for the collision of the Adriatic and European plates. *Lithos*, 108: 106–125.
- Ustaszewski K, Kounov A, Schmid SM, Schaltegger U, Frank W, Krenn E & Fügenschuh B (subm): Evolution of the Adria–Europe plate boundary in the northern Dinarides – from continent-continent collision to back-arc extension. *Tectonics*.
- von Blanckenburg F, Villa IM, Baur H, Morteani G & Steiger RH (1989): Time calibration of a PT-path from the Western Tauern Window, Eastern Alps: the problem of closure temperatures. *Contributions to Mineralogy and Petrology*, 101: 1–11.
- Wiederkehr M (2009): From subduction to collision: a combined metamorphic, structural and geochronological study of polymetamorphic metasediments at the NE edge of the Lepontine dome (Swiss Central Alps). PhD Thesis, University of Basel, Basel.
- Zelić M (2004): Tectonic history of the Vardar zone: constraints from the Kopaonik area (Serbia). PhD Thesis, Università di Pisa, Italy.
- Zelić M, Levi N, Malasoma A, Marroni M, Pandolfi L & Trivić B (2010): Alpine tectono-metamorphic history of the continental units from Vardar zone: the Kopaonik Metamorphic Complex (Dinaric-Hellenic belt, Serbia). *Geological Journal*, 45: 59–77.

Appendix A: Raman spectroscopy of carbonaceous matter

The two analyses presented here were kindly performed by M. Wiederkehr in the framework of his PhD-Thesis (Wiederkehr 2009). A brief overview on the method and its possibility is given here without further references because it is not in the aim of this thesis to provide a scientific background on this method. For additional information please refer to Wiederkehr (2009) and references therein.

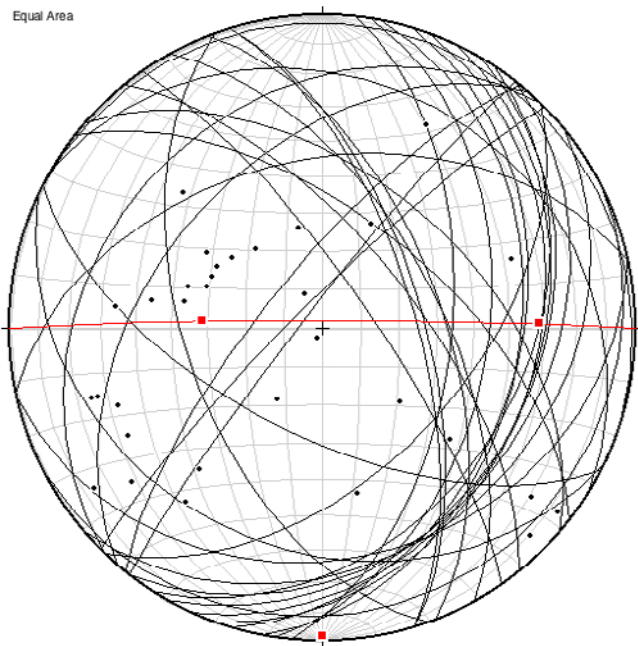
Method

The crystalline structure of carbonaceous material (CM) changes with increasing temperature from amorphous organic matter to fully ordered graphite. The analysis of the crystalline structure of CM can therefore be used as a geothermometer. Using Raman spectroscopy, the degree of ordering within the crystallographic structure can be visualised. The relationship between the degree of crystallinity, as is expressed by the shape of the Raman spectra, and the metamorphic conditions have been calibrated as a geothermometer over a wide temperature interval from 100 to 700 °C. It is important to note that this geothermometer always records peak-metamorphic conditions, since the degree of ordering in the crystallographic structure is strictly irreversible and will therefore not change on the retrograde path. Micro-Raman spectroscopy was performed at the Raman Laboratory of the Institute of Geosciences at Potsdam University by M. Wiederkehr.

Appendix B: List of important samples discussed in Chapter 4

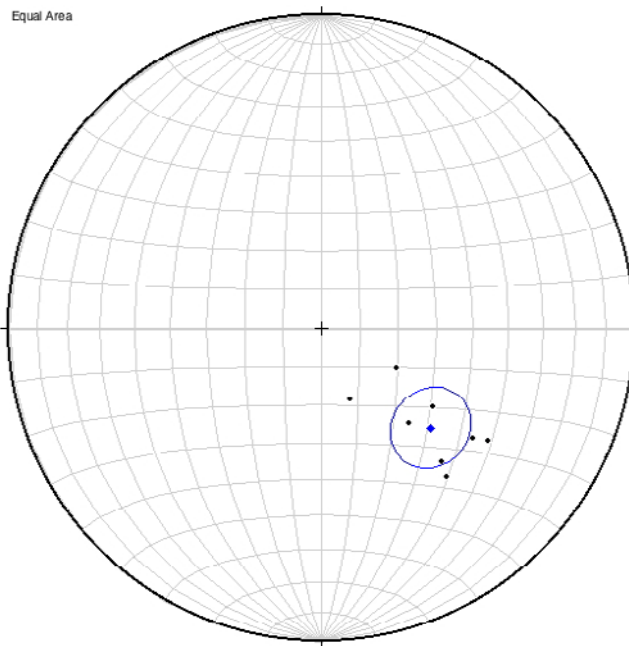
No.	Coord. (MGI Balkan 7)	Formation	Lithology	Remarks
4	7465213 4818926	Miocene intrusion	granitic dyke	Miocene extension (D4)
12	7486620 4796018	Kopaonik Metamorphic Series	calcsilicate	contact metamorphism
68	7487522 4795944	Kopaonik Metamorphic Series	cherty limestone	overprinting evidence (D1–D4)
104	7494684 4799141	Senonian flysch'	pelagic limestone	Scaglia rossa' with ophiolitic detritus
111	7489079 4795833	Kopaonik Metamorphic Series	cherty limestone	Kopaonik Fm, D1–D3
121	7492150 4811368	Senonian flysch'	neritic limestone	olistolith
190	7488889 4797616	Kopaonik Metamorphic Series	granitic dyke	D3 overprints D2
197	7494723 4799143	Senonian flysch'	pelagic limestone	Microfauna (globotruncanids etc.)
218	7494497 4812231	Senonian flysch'	pelitic schist	Grčak' (D3 and D4b)
223	7489439 4811263	Senonian flysch'	breccia	basal breccia incl. reworked metamorphic rocks
226	7488932 4808762	ophilitic mélange	amphibolite pebble	pebbles of metamorphic sole
236	7479494 4802718	Kopaonik Metamorphic Series	metabasite	Triassic intrusions
285	7506399 4758506	Senonian flysch' (Kosovo)	sandstone	Ar-Ar sample
300	7460928 4803072	Kopaonik Metamorphic Series	pelitic schist	Ar-Ar sample
301	7460858 4806453	Kopaonik Metamorphic Series	chlorite schist	Ar-Ar sample
305	7466825 4812432	ophilitic mélange	sandstone	Jurassic obduction (top-NW)
312	7458931 4819720	Studenica Metamorphic Series	actinolite schist	D2 in Studenica core-complex
319	7493436 4807296	Kopaonik Metamorphic Series	sericite schist	Ar-Ar sample
327	7462166 4824729	Studenica Metamorphic Series	pegmatite	Ar-Ar sample
351	7492727 4811675	Senonian flysch'	pelitic schist	Paleogene thrust (Sava suture) and D4b
360	7493270 4825216	Kopaonik Metamorphic Series	sericite schist	Ar-Ar sample
373	7494550 4807750	Kopaonik Metamorphic Series	kakirite	Pošta' locality (D4b)
374	7494238 4807278	Kopaonik Metamorphic Series	pelitic schist	footwall of D4b
386	7498615 4823510	Kopaonik Metamorphic Series	mylonitic marble	Brezovica quarry (D4a)
399	7460953 4814917	Studenica Metamorphic Series	garnet schist	Raman spectroscopy
423	7461227 4817842	Studenica Metamorphic Series	sericite schist	Miocene extension (D4)
425	7461333 4818628	Western Vardar ophiolites	serpentinite	amphibolite-facies serpentinite
427	7461249 4819612	Studenica Metamorphic Series	biotite schist	Paleogene peak metamorphism
433	7503224 4780334	Senonian flysch'	pelitic schist	deformation
445	7455258 4818650	Studenica Metamorphic Series	pelitic schist	locality of 'Studenica normal fault'
467	7455625 4818916	Studenica Metamorphic Series	phylite	Raman spectroscopy
498	7477036 4807997	Kopaonik Metamorphic Series	biotite schist	deformation phases D1–D4
513	7469329 4817635	Miocene intrusion	two-mica granite	Miocene extension (D4)
521	7461149 4818423	Studenica Metamorphic Series	amphibolite schist	Ar-Ar sample

Appendix C: Additional Stereoplots



Great Circle:
 N = 35 ; first plane = 1 ; last plane = 35
 Pattern = solid
 Scatter Plot:
 N = 35 ; Symbol = •
 Bingham Axes:
 N = 35 ; first line = 1 ; last line = 35
 Eigenvalue Eigenvector (T&P) Confidence Cones
 1. .6175 275.3° 58.4° Max = 16.5° Min = 12.5°
 2. .2108 88.8° 31.5°
 3. .1717 180.1° 2.0° Max = -1.0° Min = -1.0°

Axial planes of D2 in the Upper Cretaceous flysch, refolded by D3



Scatter Plot:
 N = 8 ; Symbol = •
 Mean Vector:
 N = 8 ; first line = 1 ; last line = 8
 Mean Vector T & P = 132.4° 50.9° Length = .9698/1
 conc. factor, k = 33.1; 99% cone = 13.8° 95% = 10.5°

Stretching lineation on shear bands associated with sinistral shearing within the Upper Cretaceous flysch

5. Summary

This chapter first combines the various conclusions and discussions from the individual chapters. In a second step, the combined results will be used to reconstruct a possible scenario for the geodynamic evolution of the Dinarides, illustrated by a series of interpretative large-scale cross-sections (Fig. 5.1). Finally, the still remaining questions are briefly discussed and some future research perspectives are given.

5.1 Main results

In the following the most important results and conclusions of the thesis are summarised with reference to the relevant chapters.

Stratigraphy and Paleogeography

Whereas the stratigraphy of the external zones of the Dinarides is relatively well known, the sedimentary and paleotectonic evolution of the internal zones is less understood. In part, this is due to Alpine metamorphic overprint, in part to the structural complexities of the area. In *Chapter 2*, we attempted to characterize the Mesozoic sedimentary evolution of part of the internal Jadar–Kopaonik–Studenica thrust sheet (Fig. 1.1), which expose the easternmost occurrences of Triassic sediments in the Dinarides in windows below the Jurassic ophiolite nappe (Fig. 1.2).

The metamorphic sedimentary succession of the internal Jadar–Kopaonik–Studenica thrust sheet includes a succession from Upper Paleozoic terrigenous sediments to the Upper Jurassic ophiolitic mélangé and the Western Vardar ophiolites obducted in Late Jurassic time (e.g. Schmid et al 2008). Lower Triassic siliciclastics and limestones are overlain by Anisian shallow-water carbonates. A drowning event during the latest Anisian resulted in the deposition of a grey hemipelagic limestone succession characterized by fine-grained, redeposited and often silicified, calcarenites shed by low-density turbidity currents from a carbonate platform. New conodont faunas date this hemipelagic sequence as Late Anisian to Norian, possibly extending into the Early Jurassic, which makes it an equivalent of the grey Hallstatt facies of the Eastern Alps. The younger sediments overlying the Kopaonik Formation are red hemipelagic limestones and radiolarites of probably Middle–Late Jurassic age; they suggest that deep pelagic conditions preceded the obduction of the Western Vardar Ophiolitic Unit.

Sedimentation of the hemipelagic Kopaonik Formation (*Chapter 2*) was contemporaneous with shallow-water carbonate production in nearby carbonate platforms that were part of the same passive continental margin. Most of these platforms were located on the more proximal parts of the Adriatic margin, whereas the distal margin was dominated by pelagic and distal turbiditic sedimentation, facing the evolving ocean to the east. Our data are in line with a continental margin model in which the facies belts are arranged in a logical order from the proximal margin to the Neotethys Ocean. In our interpretation the Drina–Ivanjica and Kopaonik–Studenica thrust sheets expose the most distal portions of the Adriatic margin, emerging in tectonic windows below one and the same ophiolite nappe referred to as Western Vardar Ophiolitic Unit (including the so-called Dinaridic ophiolites) derived from the east and overthrusting the Durmitor zone.

The sedimentary and stratigraphic evolution of the different areas reflects the transition from a proximal to a distal continental margin and we see no evidence for one or several independent Triassic oceans between the Adria, the Drina–Ivanjica and/or the Kopaonik areas.

Tectono-metamorphic evolution and kinematics of the bounding faults

A first phase of penetrative deformation (D1) produced a penetrative foliation and stretching lineations, visible in sparse outcrops and always overprinted by the later deformation in the Kopaonik Metamorphic Series. The foliated and metamorphosed matrix of the ophiolitic mélangé includes sigma-clasts with top-NW shear-senses suggesting that this first deformation phase (D1) has to be correlated with the NW-directed obduction of the Western Vardar Ophiolitic Unit onto the Kopaonik and Studenica Series during the Late Jurassic.

The sediments of the Studenica Metamorphic Series witnessed a metamorphic event during the Late Cretaceous (110–85 Ma). This event took place under lowermost greenschist-facies conditions and confirms the existence of a „mid“ to Late Cretaceous metamorphic event in the most internal parts of the Dinarides. This metamorphism is associated with the ductile D2 deformation phase, including isoclinal folding overprinting D1 and the development of a well developed second foliation S2.

According to our Ar–Ar-data (*Chapter 4.3*) the higher greenschist- to amphibolite-facies overprint (*Chapter 4.1*) occurs during Late Eocene to Early Oligocene and is associated with deformation phase D3, which is stratigraphically constrained by the deformed Upper Cretaceous sediments (‘Senonian flysch’) and the cross-cutting 31 Ma Kopaonik intrusion. It was related to E–W-directed compression that produced chevron-type folds in the east and large-scale open folds in the west (*Chapter 4.2*). At the same time, map-scale W-vergent thrusts accommodated a large amount of shortening that is contemporaneous with and interpreted to be associated with collision and out-of-sequence thrusting in the internal Dinarides during the final closure of the remnant oceanic realms in the Sava zone and the suturing of the Dinarides with the adjacent Carpatho-Balkan orogen.

During the Miocene the entire area underwent rapid exhumation accompanied by a high amount of N–S-oriented ductile deformation (D4). This exhumation left also its trace by syn-extensional boudinage of the Miocene granitic dykes at the Polumir locality (*Chapter 3*). This intense multi-directional post-Oligocene extension is correlated with Miocene extension in the Pannonian basin. Initial N–S-oriented extension and core-complex formation during D4a represents the more important phase of exhumation. D4b, on the other hand, is the latest stage of exhumation, but its importance is subordinate.

Age and genesis of magmatic rocks and their significance for the geodynamic evolution of the Balkan Peninsula

Paleogene magmatic rocks of the Alpine–Carpathian–Pannonian–Dinaridic region occur in linear zones that surround the Adriatic plate (Periadriatic intrusions s.l.). At closer inspection, three such linear zones can be distinguished (Fig. 3.8): (1) a belt that follows the Periadriatic line delimiting the Southern Alps from the rest of the Alps (Periadriatic intrusions s.str.; e.g. Rosenberg 2004), (2) an alignment along the Mid-Hungarian fault zone located within the Pannonian basin (e.g. Benedek 2002), and (3) a belt that follows the innermost Dinarides and extends across Bulgaria and northern Greece all the way to NW Turkey (e.g. Pamić et al. 2002a; Burchfiel et al. 2008). *Chapter 3* presents the results of high precision dating and Hf isotope analyses of the Kopaonik, Drenje, Željina, Golija and Polumir intrusions (Fig. 3.2). U–Pb (ID-TIMS) dating on single zircons from these intrusions revealed two age groups, an Oligocene (31.77–30.70 Ma) and a Miocene (20.58–17.74 Ma) one. The Oligocene group (Kopaonik, Drenje and Željina intrusive bodies) consists of I-type granitoids with positive ϵ_{Hf} values of the zircons indicating a moderate crustal influence in their origin and it is proposed that this group formed via partial melting of mantle-derived lower crustal protoliths. The Miocene group consists of the S-type Polumir granite and the Golija intrusion, which shows negative ϵ_{Hf} values (-0.7 to -2.7) generally indicating a higher crustal influence during magma generation.

It is proposed that Late Eocene to Oligocene magmatism, which affects the Adria-derived lower plate units of the Dinarides may be caused by delamination of the Adriatic mantle from the overlying crust after the closing of the Neotethys Ocean and the Adria–Europe collision, contemporaneous with intra-plate convergence within the external Dinarides, i.e. within the lower plate, that started during the Late Eocene (Fig. 3.9).

A connection of the Dinaridic Late Eocene to earliest Miocene magmatic belt with other contemporaneous Periadriatic intrusions in the Alps and those along the Mid-Hungarian fault zone, as proposed in the literature, is unlikely because the subduction polarity in the Alps and in the Western Carpathians north of the Mid-Hungarian fault zone is opposite to that of the Dinarides during the Paleogene. Hence, in spite of the temporal coincidence there was no direct link between the Alpine–Mid-Hungarian magmatic belt and the Dinaridic–Hellenidic magmatic belt in Late Eocene to Oligocene times.

Exhumation history

The zircon and apatite fission-track analyses (*Chapter 3*) show that the exhumation of the different tectonic units was largely taking place by tectonic unroofing via N–S-stretching during the D4a deformation phase. All the samples from the footwall of such detachment faults yield the same small difference between zircon and apatite central ages, indicating fast cooling from temperatures above the zircon PAZ to temperatures below the apatite PAZ between 21 and 10 Ma.

The emplacement of all but one of the Oligocene intrusive bodies analysed occurred slightly above some 300 °C, i.e. within the upper crust. They cooled to the ambient temperatures and remained at this depth without further deformation for some 10 Ma before the onset of rapid cooling due to unroofing by substantial extension between 16 and 10 Ma. Exhumation in an extensional setting during D4a led to core-complex formation and tectonic omission in the order of 10 km across the bounding normal faults. Final cooling to near-surface conditions occurred at lower rates of around 10 °C/Ma from 11 Ma onwards for both age groups. This is in line with the fact that zircon central ages from the metasediments on the sections crossing the brittle normal faults (D4b, e.g. locality Pošta on Fig. 4.7) are not reset, while apatite fission-track ages are only moderately affected.

5.2 Geodynamic evolution of the study area

Based on our findings and available literature data an attempt is made to reconstruct the geodynamic evolution of the internal Dinarides, starting in the Late Paleozoic. A series of interpretative cross-sections are drawn to assist the understanding (Fig. 5.1).

Upper Paleozoic to Middle–Late Jurassic: Sedimentation

Upper Paleozoic terrigenous sediments were followed by Lower Triassic siliciclastics and limestones overlain by Anisian shallow-water carbonates. A pronounced vertical facies change to hemipelagic and turbiditic, cherty limestones (Kopaonik Formation, *Chapter 2*) testifies to late Anisian drowning of the former shallow-water carbonate shelf. Sedimentation of the Kopaonik Formation was contemporaneous with shallow-water carbonate production on nearby carbonate platforms that were the source areas of diluted turbidity currents reaching the depositional area of this formation that possibly extends into the Early Jurassic (*Chapter 2*). The sedimentary and stratigraphic evolution of the study area reflects the transition from a proximal to a distal continental margin (Fig. 5.1a), where the younger sediments overlying the Kopaonik Formation (red hemipelagic limestones and radiolarites of probably Middle–Late Jurassic age) suggest that deep-pelagic conditions preceded the obduction of

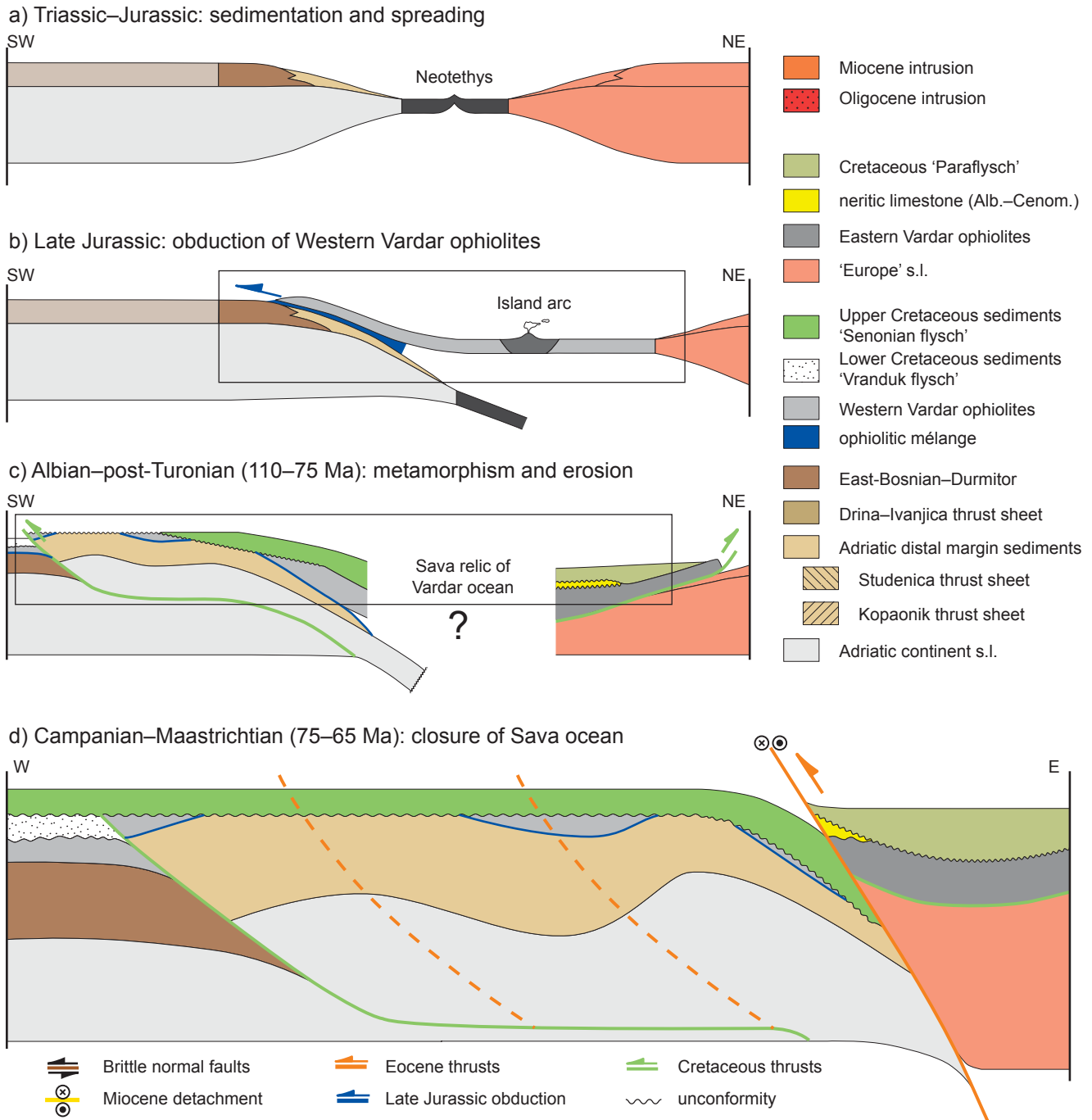


Fig. 5.1 – Interpretative large scale cross-sections through the Dinarides. The individual time-slices are indicated in the figure. The change in scale between individual steps is shown by black rectangles surrounding the area of the next picture relative to the precedent. The colours of the tectonic contacts are identical with those from Fig. 4.7 and dashed lines mark the position of future tectonic contacts.

the Western Vardar Ophiolitic Unit. Sedimentation took place on a distal part of the Adriatic continent, as argued for on the base of the Triassic facies distribution (Chapter 2).

Middle to Late Jurassic: Ophiolite obduction onto the Adriatic margin

Intra-oceanic subduction within Neotethys started at around 180 Ma (Toarcian; Schmid et al. 2008) as is evidenced by ages of formation of the metamorphic sole at the base of the obducted ophiolites (Aalian–Oxfordian, Lanphere et al. 1975; Okrusch et al. 1978; Dimo-Lahitte et al. 2001). Ongoing sedimentation on the distal

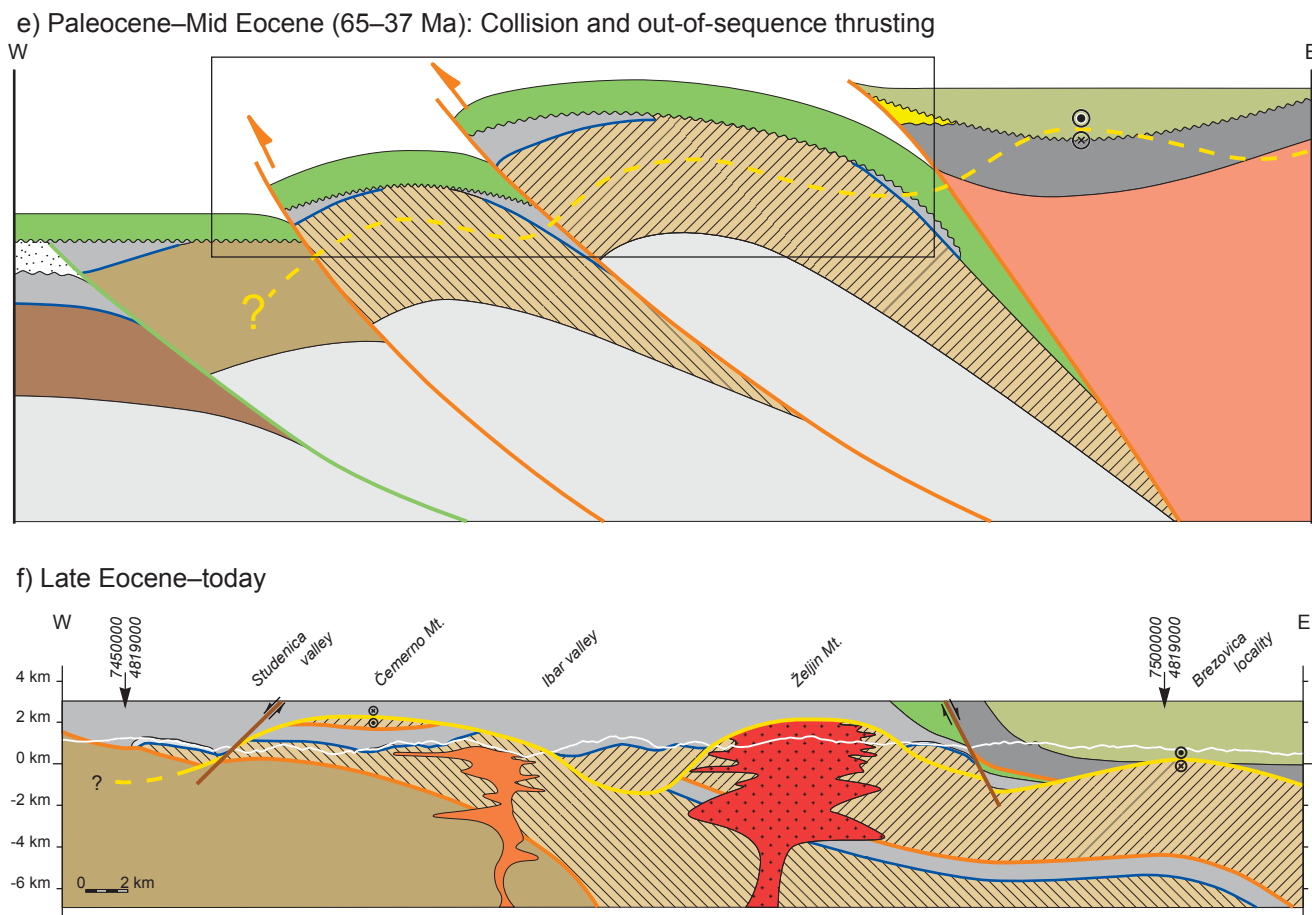


Fig. 5.1 – (continued)

continental margin during this time implies that obduction onto the Adriatic margin could not have started prior to Middle–Late Jurassic. The obduction is associated with top-NW thrusting as determined from shear-sense indicators such as sigma-clasts in the ductilely deformed and slightly metamorphosed ophiolitic mélangé. A wide shear zone must have developed at the base of the Western Vardar Ophiolitic Unit, involving also the ophiolitic mélangé and parts of the underlying sediments of the Adriatic margin, where a penetrative foliation and a stretching lineation, associated with greenschist-facies metamorphism, are developed (deformation phase D1; Chapter 4.2).

Near Zagreb, the matrix of the ophiolitic mélangé (Fig. 1.1) associated with the obducted Western Vardar ophiolites contains palynomorphs that yield ages ranging from the Hettangian to the Late Bajocian (Babić et al. 2002), giving a maximum age for the mélangé formation of Late Bajocian. The end of ophiolite obduction and mélangé formation are dated by strata, which overstep the previously emplaced Western Vardar Ophiolitic Unit (Schmid et al. 2008). After a period of erosion, during which parts of the obducted ophiolites were removed, sedimentation locally resumed with Tithonian to Berriasian fluvial conglomerates and sandstones (Blanchet et al. 1970; Pamić and Hrvatović 2000; Neubauer et al. 2003). These overstepping formations indicate that the final stages of obduction occurred during Late Jurassic times (Fig. 5.1b; Schmid et al. 2008).

Early to Late Cretaceous (142–65 Ma): Metamorphism in the internal Dinarides and erosion

Age data on Cretaceous metamorphism within the Dinarides are known from the following areas: Barremian age (123 ± 5 Ma) blueschist metamorphic rocks from the Fruška Gora inselberg (K–Ar on amphibole concentrate, Milovanović et al. 1995), Valanginian–Hauterivian (139–129 Ma) greenschist-facies metamorphism in the Drina–Ivanjica thrust sheet (K–Ar on phyllites and greenschists, Milovanović 1984), Aptian to Turonian (121–92 Ma) low-grade metamorphism in the Pre-Karst Unit (K–Ar and Ar–Ar on whole rock and mineral concentrates, Pamić et al. 2004), and Aptian to Albian (122–111 Ma) greenschist-facies metamorphism (K–Ar ages, whole rock and mica concentrates) in greenschists from the Medvednica mountains (Tomljenović et al. 2008). Hence, the available radiometric ages span the entire 139–92 Ma time interval (Barremian–Turonian), either suggesting a large error range or, alternatively, a rather continuous tectonic and metamorphic evolution during a large part of the Cretaceous (Schmid et al. 2008). The sediments of the Kopaonik and Studenica Metamorphic Series witnessed lowermost greenschist-facies metamorphism that was dated as early Late Cretaceous by the present study (Albian–Coniacian, i.e. 110–85 Ma, *Chapter 4.3*). This metamorphism is associated with a ductile deformation phase (locally D2) documented by isoclinal folds (*Chapter 4.2*).

Enhanced erosion after this Cretaceous age metamorphic event during the latest Early and earliest Late Cretaceous is testified by prominent angular unconformities below the basal strata of the Turonian to uppermost Cretaceous ('Senonian') over-stepping series (Fig. 5.1c). In the hangingwall of the Drina–Ivanjica thrust sheet, that was emplaced during the Cretaceous tectono-metamorphic event, erosion was particularly pronounced. This led to the transgression of the Upper Cretaceous onto Paleozoic strata (Fig. 4.1) and also led to a substantial exhumation of the low-grade metamorphic rocks in section Gradac 1 (*Chapters 2 and 4.3*). The Kopaonik thrust sheet (occupying a more internal position) was also metamorphosed before the Late Cretaceous transgression. This is evidenced by a basal breccia of Late Cretaceous age including metamorphic pebbles and ophiolitic detritus (Fig. 4.6).

Ongoing compression between Adria and Europe led to E-ward thrusting of the Eastern Vardar ophiolites onto Europe s.l. (Fig. 5.1d; Schmid et al. 2008), where Early Cretaceous erosion has been described by Rampoux (1974). Nevertheless, at the same time (Albian–Cenomanian) neritic limestones were deposited onto the Eastern Vardar ophiolites, following an Early Cretaceous unconformity at Vlajkovsci (Fig. 4.5; Rampoux 1974), and a basal conglomerate of the 'Paraflysch' (Upper Cretaceous sediments of Gosau-type), overlies a second unconformity (post-Cenomanian). This implies, that the 'Paraflysch' unit, mapped as Lower Cretaceous (Barremian–Aptian) sediments in our area (Urošević et al. 1970a,b) must be younger than Cenomanian, which is also supported by nanofossils (Turonian–Late Cretaceous, Rampoux 1974; post-Upper Coniacian, CC14, Zelić 2004).

In the Kozera Mountains (northern Bosnia and Hercegovina), a bimodal igneous succession (U–Pb ages on zircons from dolerites and rhyolites of 82–81 Ma) is intercalated with pelagic limestones yielding a Campanian globotruncanid association (Ustaszewski et al. 2009). The bimodal igneous succession is unconformably overlain by Maastrichtian to Paleocene siliciclastics that contain abundant ophiolitic detritus, suggesting reworking of the Campanian magmatics. An Eocene turbiditic sandstone succession unconformably covers both the Western Vardar Ophiolitic Unit and the Late Cretaceous bimodal igneous successions. These observations suggest that the Adriatic Plate and the Europe-derived Dacia Mega-Unit were still separated by a deep basin floored by oceanic lithosphere until the Campanian and that its closure did not occur before the Maastrichtian to earliest Paleogene (Ustaszewski et al. 2009). The Upper Cretaceous sediments of the 'Senonian flysch' are related to this closure.

Paleocene to Late Eocene (65–37 Ma): Collision and out-of-sequence thrusting

Continuing compression in an E-W direction resulted in the collision between Adria and the Serbo-Macedonian massif. In our area, it first activated the Kopaonik thrust separating the Kopaonik- from the Studenica thrust sheet (in Fig. 5.1 this step is not individually shown). This nappe-stacking led to amphibolite-facies metamorphism in the Studenica thrust sheet, dated by ^{40}Ar – ^{39}Ar ages on hornblende (Studenica valley: 40.9 ± 4.9 Ma) and sericite (section Gradac 2: 40–30 Ma; *Chapter 4.3*). In the Kopaonik thrust sheet, such an amphibolite-facies metamorphism is not observed due to its higher tectonic position. The Studenica thrust was activated next, now separating the Studenica from the Drina–Ivanjica thrust sheet. However, this tectonic contact represents a transpressive fault rather than a pure thrust fault. This Palogene phase is evidenced by folds with sub-vertical axial planes and sub-horizontal N–S trending fold axis (deformation phase D3; *Chapter 4.2*), as observed in the Kopaonik Metamorphic Series and the Upper Cretaceous sediments (‘Senonian flysch’) within the Kopaonik thrust sheet. In the ophiolitic units this deformation phase cannot be identified unequivocally.

Compression in the Dinarides did not come to a halt after the collision across the Sava Zone. Instead there appears to be a shift of the site of compression to the more external parts of the Dinarides during the Late Eocene (Fig. 3.8, *Chapter 3*). The external Dinarides formed in Late Eocene to Neogene times (e.g. Skourlis and Doutsos 2003; Mikes et al. 2008; Korbar 2009), whereby much of the shortening (at least some 300 km in the area of Dubrovnik; see profile 5 of plate 3 in Schmid et al. 2008) took place by shortening within the Budva–Pindos pelagic realm of the Dinarides and Hellenides, respectively. Foreland migration of the site of compression is also well established for the Hellenides (e.g. van Hinsbergen et al. 2005).

Late Eocene to earliest Miocene (37–22 Ma): Magmatic activity in the Balkan Peninsula

The Oligocene intrusions Kopaonik, Drenje, and Željina are part of a NW–SE striking alignment of granitoids, whose ages range from the Late Eocene (37 Ma) to the earliest Miocene (22 Ma). They follow the inner Dinarides all the way to southern Serbia (*Chapter 3*). Age and location of these granitoids coincide with that of a series of basaltic rocks (Cvetković et al. 2004; Marchev et al. 2004; Prelević et al. 2005), volcanics and volcanoclastic basins, and additionally, non-volcanic sedimentary basins (e.g. Burchfiel et al. 2000, 2008; Dumurdzanov et al. 2005). Some of the basins are clearly associated with normal faulting and contemporaneous with the onset of Aegean extension during Middle to Late Eocene times (e.g. Burchfiel et al. 2000, 2003; Kounov et al. 2004; Brun and Soukoutis 2007). The fact that this trace of magmatism crosses the Sava suture implies that the last remnants of the Vardar branch of the Neotethys Ocean must have been closed by Mid-Eocene times or earlier, in accordance with what is known from the literature (e.g. Pamić et al. 2002; Ustaszewski et al. 2009, submitted). Hence, it is clear that the Late Eocene to earliest Miocene magmatism is post-collisional with respect to the closure of the Vardar ocean. A model of slab-retreat and delamination (Bird 1979) and thereby induced mantle flow (Funicello et al. 2006; Piromallo et al. 2006) allows for magmatism in the lower (Adriatic) plate, associated with an intracontinental subduction zone that now led to thrusting in the external Dinarides during the Late Eocene Dinaric phase (Schefer et al. 2010b).

Neogene (23–3 Ma): Extensional tectonics in the Dinarides

During the Miocene our area underwent rapid exhumation accommodated by a high amount of N–S-oriented extension (deformation phase D4a; *Chapter 4.2*). The timing of this exhumation is evidenced by ^{40}Ar – ^{39}Ar ages of 21–17 Ma obtained on micas that are interpreted to have recrystallised during extension, as well as by zircon (ca. 21 Ma) and apatite (ca. 10 Ma) fission-track ages (*Chapter 4.3*, Fig. 4.7). This N–S-oriented extension and core-

complex formation is contemporaneous with the syn-extensional intrusion of the S-type Miocene-age Polumir granite (18 Ma; *Chapter 3*). On a larger scale this stage is correlated with the Miocene extension in the Pannonian basin (*Chapter 4.4*). The latest stage of exhumation is marked by the transition from a purely N–S-directed extensional regime to an E–W-oriented extensional setting. E–W-oriented extension was predominantly brittle (e.g. ‘Pošta normal fault’, Fig. 4.13). It accommodated the final exhumation of the metamorphic rocks and of the intrusive bodies, but its importance is relatively minor compared to D4a, as shown by the non-reset zircon- and the partially reset apatite fission-track central ages in the footwall of the brittle normal faults (*Chapter 4.3*). The soft collision of Tisza with the European continent during the Middle Miocene (16.5–11 Ma) slowed down the subduction retreat in the Carpathians (Seghedi et al. 2004) and may thus have reduced the amount of extension in the back-arc area of the Pannonian basin, of which our working area is a part. N–S-extension, on the other hand, appears to have persisted until the Pliocene, forming several NW–SE-striking basins, such as the Kraljevo basin. This also implies that there are two \pm contemporaneous extensional directions during this period.

5.3 Future research perspectives

The new data obtained during this thesis shed new light on the tectono-metamorphic evolution of the area and are important for the understanding of the geodynamic evolution of the internal Dinarides. While we answered some questions, it also gave rise to new ones that should be addressed by future studies. Some are outlined below.

Whereas the first evidence of Paleogene amphibolite-facies metamorphism in the internal Dinarides obtained during this thesis is spectacular, it still needs further petrological and geochronological investigation, mainly to obtain better constrained P-T-conditions. Moreover, the Cretaceous greenschist-facies event proposed in this thesis is still weakly constrained, and its geodynamic context is enigmatic. The only Cretaceous age obtained comes from the Studenica Metamorphic Series in section Gradac 1, but the Kopaonik Metamorphic Series must also have witnessed this event. A sampling strategy focusing on this Cretaceous event should concentrate on lithologies from the hanging wall of the Miocene detachment faults (outside of the core-complexes) within the Kopaonik Metamorphic Series.

Miocene detachment faults that mainly accommodated the exhumation of the Oligocene intrusions and the high-grade metamorphic rocks were observed and dated by fission-track analyses. Their exact position is seen in some outcrops, but due to the dense vegetation could not be traced with certainty on the map. Moreover, shear-senses in the eastern part of our area are opposite to those from the western part.

The contact between the Western Vardar and the Eastern Vardar Ophiolitic Units is usually made up by the Upper Cretaceous sediments of the 'Senonian flysch' that is believed to be a relic of the Sava zone (e.g. Schmid et al. 2008; Schefer et al. 2007, 2008; Ustaszewski et al. 2009, *subm.*). However, where these sediments are missing, the contact must lie within strongly serpentinised ophiolitic rocks and it becomes difficult to distinguish between the Western and Eastern Vardar Ophiolitic Units, i.e. between upper and lower plate during Cenozoic suturing between the Dinarides and the Dacia Mega-Unit. Very detailed mapping and structural analysis may possibly give better answers to this question.

The sediments of the 'Paraflysch' (Lower Cretaceous after Urošević et al. 1970a,b) show a sedimentation age not older than Turonian in our area (nannofossil dating by Rampnoux 1974; Zelić 2004). Partial resetting of apatite fission-track ages together with our structural observations suggest that the 'Paraflysch' unit also underwent low-temperature metamorphism to some degree. A revision of the sedimentary age, the depositional environment, and the tectono-metamorphic history of this unit is needed in order to understand its geological significance.

References

- Bird P (1979): Continental Delamination and the Colorado Plateau. *Journal of Geophysical Research*, 84: 7561–7571.
- Blanchet R, Durand Delga M, Moullade M & Sigal J (1970): Contribution à l'étude du Crétacé des Dinarides internes: la région de Maglaj, Bosnie (Yougoslavie). *Bulletin de la Société Géologique de France*, 12: 1003–1009.
- Brun JP & Soukoutis D (2007): Kinematics of the Southern Rhodope Core Complex (North Greece). *International Journal of Earth Sciences*, 96: 1079–1099.
- Burchfiel BC, Nakov R, Tzankov T & Royden L (2000): Cenozoic extension in Bulgaria and northern Greece: the northern part of the Aegean extensional regime. In: *Tectonics and Magmatism in Turkey and the Surrounding Area* (eds Bozkurt E, Winchester E & Piper JDA), pp. 325–352, Geological Society Special Publications, London.
- Burchfiel BC, Nakov R & Tzankov T (2003): Evidence from the Mesta half-graben, SW Bulgaria, for the Late Eocene beginning of Aegean extension in the Central Balkan Peninsula. *Tectonophysics*, 375: 61–76.
- Burchfiel BC, Nakov R, Dumurdzanov N, Papanikolaou D, Tzankov T, Kotzev V, Todosov A & Nurce B (2008): Evolution and dynamics of the Cenozoic tectonics of the South Balkan extensional system. *Geosphere*, 4: 919–938.
- Cvetković V, Prelević D, Downes H, Jovanović M, Vaselli O & Pecskey Z (2004): Origin and geodynamic significance of Tertiary postcollisional basaltic magmatism in Serbia (central Balkan Peninsula). *Lithos*, 73: 161–186.
- Dimo-Lahitte A, Monié P & Vergély P (2001): Metamorphic soles from the Albanian ophiolites: Petrology, $^{40}\text{Ar}/^{39}\text{Ar}$ geochronology, and geodynamic evolution. *Tectonics* 20: 78–96.
- Djerić N, Gerzina N & Schmid SM (2007a): Age of the Jurassic radiolarian chert formation from the Zlatar mountain (SW Serbia). *Ofioliti*, 32: 101–108.
- Djerić N, Vishnevskaya VS & Schmid SM (2007b): New data on radiolarians from the Dinarides (Bosnia and Serbia). Davos, 10.-12.October 2007, Abstract Volume p. 17-18. In: *8th Alpine Workshop*, pp. 17–18, Davos.
- Dumurdzanov N, Serafimovski T & Burchfiel BC (2005): Cenozoic tectonics of Macedonia and its relation to the South Balkan extensional regime. *Geosphere*, 1: 1–22.
- Funiciello F, Moroni M, Piromallo C, Faccenna C, Cenedese A & Bui HA (2006): Mapping mantle flow during retreating subduction: Laboratory models analyzed by feature tracking. *Journal of Geophysical Research-Solid Earth*, 111: B03402, doi:10.1029/2005JB003792.
- Korbar T (2009): Orogenic evolution of the External Dinarides in the NE Adriatic region: a model constrained by tectonostratigraphy of Upper Cretaceous to Paleogene carbonates. *Earth Science Reviews*, 96: 296–312.
- Kounov A, Seward D, Bernoulli D, Burg JP & Ivanov Z (2004): Thermotectonic evolution of an extensional dome: the Cenozoic Osogovo-Lisets core complex (Kraishte zone, western Bulgaria). *International Journal of Earth Sciences*, 93: 1008–1024.
- Lanphere M, Coleman RG, Karamata S & Pamić J (1975): Age of amphibolites associated with Alpine peridotites in the Dinaride ophiolite zone, Yugoslavia. *Earth and Planetary Science Letters* 26: 271–276.
- Marchev P, Raicheva R, Downes H, Vaselli O, Chiaradia M & Moritz R (2004): Compositional diversity of Eocene–Oligocene basaltic magmatism in the Eastern Rhodopes, SE Bulgaria: implications for genesis and tectonic setting. *Tectonophysics*, 393: 301–328.

- Milovanović D (1984): Petrology of low metamorphosed rocks of the central part of the Drina-Ivanjica Palaeozoic. *Bulletin du Musée de l'Histoire Naturelle Beograd*, A39: 1–139.
- Milovanović D, Marchig V & Stevan K (1995): Petrology of the crossite schist from Fruska Gora Mts (Yugoslavia), relic of a subducted slab of the Tethyan oceanic crust. *Journal of Geodynamics*, 20: 289–304.
- Neubauer F, Pamić J, Dunkl I, Handler R & Majer V (2003): Exotic granites in the Cretaceous Pogari Formation overstepping the Dinaric Ophiolite Zone mélange in Bosnia. *Annales Universitatis Scientiarum Budapestinensis, Sectio Geologica*, 35: 133–134.
- Okrusch M, Seidel E, Kreuzer H & Harre W (1978): Jurassic age of metamorphism at the base of the Brezovica peridotite (Yugoslavia). *Earth and Planetary Science Letters* 39: 291–297.
- Pamić J & Hrvatović H (2000): Dinaride Ophiolite Zone (DOZ). *Pancardi 2000 Fieldtrip Guidebook. Vijesti*, 37: 60–68.
- Pamić J, Balen D & Herak M (2002): Origin and geodynamic evolution of Late Paleogene magmatic associations along the Periadriatic–Sava–Vardar magmatic belt. *Geodinamica Acta*, 15: 209–231.
- Pamić J, Balogh K, Hrvatović H, Balen D, Jurković I & Palinkas L (2004): K–Ar and Ar–Ar dating of the Palaeozoic metamorphic complex from the Mid-Bosnian Schist Mts., central Dinarides, Bosnia and Hercegovina. *Mineralogy and Petrology*, 82: 65–79.
- Piomallo C, Becker TW, Funicello F & Faccenna C (2006): Three-dimensional instantaneous mantle flow induced by subduction. *Geophysical Research Letters*, 33: L08304.
- Prelević D, Foley SF, Romer RL, Cvetković V & Downes H (2005): Tertiary ultrapotassic volcanism in Serbia: Constraints on petrogenesis and mantle source characteristics. *Journal Of Petrology*, 46: 1443–1487.
- Rampnoux JP (1974): Contribution à l'étude géologique des Dinarides: Un secteur de la Serbie méridionale et du Monténégro oriental (Yougoslavie). *Mémoires de la Société Géologique de France (Nouvelle Serie)*, 119: 1–99.
- Schefer S, Fügenschuh B, Schmid SM, Egli D & Ustaszewski K (2007): Tectonic evolution of the suture zone between Dinarides and Carpatho–Balkan: field-evidence from the Kopaonik region, southern Serbia. In: *EGU General Assembly 2007, Geophysical Research Abstracts*, pp. 03891, Vienna.
- Schefer S, Egli D, Frank W, Fügenschuh B, Ovtcharova M, Schaltegger U, Schoene B & Schmid SM (2008): Metamorphic and igneous evolution of the innermost Dinarides in Serbia. In: *6th Swiss Geoscience Meeting*, pp. 60–61, Lugano.
- Schefer S, Egli D, Missoni S, Bernoulli D, Fügenschuh B, Gawlick HJ, Jovanović D, Krystyn L, Lein R, Schmid SM & Sudar MN (2010a): Triassic metasediments in the Internal Dinarides (Kopaonik area, southern Serbia): stratigraphy, paleogeographic and tectonic significance. *Geologica Carpathica*, 61: ?
- Schefer S, Cvetković V, Fügenschuh B, Kounov A, Ovtcharova M, Schaltegger U & Schmid SM (2010b): Cenozoic granitoids in the Dinarides of southern Serbia: age of intrusion, isotope geochemistry, exhumation history and significance for the geodynamic evolution of the Balkan Peninsula. *International Journal of Earth Sciences*, in Review.
- Schmid SM, Bernoulli D, Fügenschuh B, Matenco L, Schefer S, Schuster R, Tischler M & Ustaszewski K (2008): The Alpine-Carpathian-Dinaridic orogenic system: correlation and evolution of tectonic units. *Swiss Journal of Geosciences*, 101: 139–183.

- Seghedi I, Downes H, Szakacs A, Mason PRD, Thirlwall MF, Rosu E, Pécskay Z, Marton E & Panaiotu C (2004): Neogene–Quaternary magmatism and geodynamics in the Carpathian–Pannonian region: A synthesis. *Lithos*, 72: 117–146.
- Skourlis K & Doutsos T (2003): The Pindos Fold-and-thrust belt (Greece): inversion kinematics of a passive continental margin. *International Journal of Earth Sciences*, 92: 891–903.
- Ustaszewski K, Schmid SM, Lugović B, Schuster R, Schaltegger U, Bernoulli D, Hottinger L, Kounov A, Fügenschuh B & Schefer S (2009): Late Cretaceous intra-oceanic magmatism in the internal Dinarides (northern Bosnia and Herzegovina): Implications for the collision of the Adriatic and European plates. *Lithos*, 108: 106–125.
- Ustaszewski K, Kounov A, Schmid SM, Schaltegger U, Frank W, Krenn E & Fügenschuh B (subm): Evolution of the Adria–Europe plate boundary in the northern Dinarides – from continent-continent collision to back-arc extension. *Tectonics*.
- van Hinsbergen DJJ, Hafkenscheid E, Spakman W, Meulenkamp JE & Wortel R (2005): Nappe stacking resulting from continental lithosphere below subduction of oceanic and Greece. *Geology* 33: 325–328.

Bibliography

- Aubouin J, Blanchet R, Cadet J-P, Celet P, Charvet J, Chorowicz J, Cousin M & Rampnoux J-P (1970): Essai sur la géologie des Dinarides. *Bulletin de la Société Géologique de France*, 12: 1060–1095.
- Babić L, Hochuli PA & Zupanić J (2002): The Jurassic ophiolitic melange in the NE Dinarides: Dating, internal structure and geotectonic implications. *Eclogae Geologicae Helveticae*, 95: 263–275.
- Baumgartner PO (1985): Jurassic sedimentary evolution and nappe emplacement in the Argolis Peninsula (Peloponnesus; Greece). *Mémoires de la Société Helvétique des Sciences Naturelles*, 99: 1–111.
- Belak M, Pamić J, Kolar-Jurkovišek T, Pécskay Y & Karan D (1995): Alpinski regionalno metamorni kompleks Medvednice (sjeverozapadna Hrvatska). In: *1st Croatian Geological Congress Proceedings* (ed Vlahović Iea), pp. 67–70.
- Benedek K (2002): Paleogene igneous activity along the easternmost segment of the Periadriatic-Balaton lineament. *Acta Geologica Hungarica*, 45: 359–371.
- Bernoulli D & Laubscher H (1972): The palinspastic problem of the Hellenides. *Eclogae Geologicae Helveticae*, 65: 107–118.
- Bernoulli D & Jenkyns HC (2009): Ancient oceans and continental margins of the Alpine-Mediterranean Tethys: deciphering clues from Mesozoic pelagic sediments and ophiolites. *Sedimentology*, 56: 149–190.
- Bijwaard H & Spakman W (2000): Non-linear global P-wave tomography by iterated linearized inversion. *Geophysical Journal International*, 141: 71–82.
- Bird P (1979): Continental Delamination and the Colorado Plateau. *Journal of Geophysical Research*, 84: 7561–7571.
- Blanchet R, Durand Delga M, Moullade M & Sigal J (1970): Contribution à l'étude du Crétacé des Dinarides internes: la région de Maglaj, Bosnie (Yougoslavie). *Bulletin de la Société Géologique de France*, 12: 1003–1009.
- Bortolotti V, Marroni M, Pandolfi L & Principi G (2005): Mesozoic to Tertiary tectonic history of the Mirdita ophiolites, northern Albania. *Island Arc*, 14: 471–493.
- Brandon MT, Roden-Tice MK & Garver JI (1998): Late Cenozoic exhumation of the Cascadia accretionary wedge in the Olympic Mountains, northwest Washington State. *GSA Bulletin*, 110: 985–1009.
- Brković T, Malešević M, Urošević M, Trifunović S & Radanović Z (1976): Basic Geological Map of the SFRY, 1:100'000, Sheet Ivanjica (K34–17). *Savezni Geološki Zavod, Beograd*.
- Brković T, Malešević M, Urošević M, Trifunović S, Radanović Z, Dimitrijević M & Dimitrijević MN (1977): Geology of the Sheet Ivanjica (K34–17), Explanatory notes. *Savezni Geološki Zavod, Beograd*: 1–61.
- Brun JP & Soukoutis D (2007): Kinematics of the Southern Rhodope Core Complex (North Greece). *International Journal of Earth Sciences*, 96: 1079–1099.
- Bucher K & Frey M (2002): *Petrogenesis of Metamorphic Rocks*. Springer, New York.

- Burchfiel BC, Nakov R, Tzankov T & Royden L (2000): Cenozoic extension in Bulgaria and northern Greece: the northern part of the Aegean extensional regime. In: *Tectonics and Magmatism in Turkey and the Surrounding Area* (eds Bozkurt E, Winchester E & Piper JDA), pp. 325–352, Geological Society Special Publications, London.
- Burchfiel BC, Nakov R & Tzankov T (2003): Evidence from the Mesta half-graben, SW Bulgaria, for the Late Eocene beginning of Aegean extension in the Central Balkan Peninsula. *Tectonophysics*, 375: 61–76.
- Burchfiel BC, Nakov R, Dumurdzanov N, Papanikolaou D, Tzankov T, Kotzev V, Todosov A & Nurce B (2008): Evolution and dynamics of the Cenozoic tectonics of the South Balkan extensional system. *Geosphere*, 4: 919–938.
- Burghelle A (1987): Propagation of error and choice of standard in the ^{40}Ar – ^{39}Ar technique. *Chemical Geology*, 66: 17–19.
- Burnett RD, Higgins AC & Austin RL (1994): Carboniferous-Devonian CAI in England, Wales and Scotland. The pattern and its interpretation: a synoptic review. *Courier Forschungsinstitut Senckenberg*, 168: 267–280.
- Cadet J-P (1970): Esquisse géologique de la Bosnie-Herzégovine méridionale et du Monténégro occidental. *Bulletin de la Société Géologique de France*, 12: 973–985.
- Cadet J-P (1978): Essai sur l'évolution alpine d'une paléomarge continentale: Les confins de la Bosnie-Herzégovine et du Monténégro (Yougoslavie). *Mémoires de la Société Géologique de France*, 133: 1–84.
- Carosi R, Cortesogno L, Gaggero L & Marroni M (1996): Geological and petrological features of the metamorphic sole from the Mirdita ophiolites, northern Albania. *Ofoliti*, 21: 21–40.
- Ćebić V (1990): *Konačni izveštaj o geološko-petrološkom i geochemijskom izučavanju tercijarnog magmatskog kompleksa surduličke oblasti. (The final report on geological-petrological and geochemical investigations of the Tertiary magmatic complex of Surdulica area)*, Belgrade.
- Červenjak Z, Ferrara G & Tongiorgi E (1963): Age determination of some Yugoslav granites and granodiorites by the rubidium-strontium method. *Nature*, 197: 893–893.
- Channel JET & Kozur HW (1997): How many oceans? Meliata, Vardar, and Pindos oceans in Mesozoic Alpine paleogeography. *Geology*, 25: 183–186.
- Channell JET & Doglioni C (1994): Early Triassic paleomagnetic data from the Dolomites (Italy). *Tectonics*, 13: 157–166.
- Chappel BJ & White AJR (1974): Two contrasting granite types. *Pacific Geology*, 8: 173–174.
- Charvet J (1970): Aperçu géologique des Dinarides aux environs du méridien de Sarajevo. *Bulletin de la Société Géologique de France*, 12: 986–1002.
- Charvet J (1978): Etude géologique des Dinarides de la côte dalmate au Bassin pannonique: le profil Mostar-Sarajevo-Tuzla (Yougoslavie). *Thèse Sciences Naturelles Lille*, 1: 1–422.
- Chiari M, Marcucci M & Prella M (2002): New species of Jurassic radiolarians in the sedimentary cover of ophiolites in the Mirdita area, Albania. *Micropaleontology*, 48: 61–87.
- Choukroune P, Gapais D & Merle O (1987): Shear criteria and structural symmetry. *Journal of Structural Geology*, 9: 525–530.

- Corrigan JD (1983): Apatite fission-track analysis of Oligocene strata in South Texas, USA; testing annealing models. *Chemical Geology*, 104: 227–249.
- Csontos L (1995): Tertiary tectonic evolution of the Intra-Carpathian area: a review. *Acta Vulcanologica*, 7: 1–13.
- Cvetković V (2002): Nature and origin of pyroclastic deposits of the Miocene Eruptive Complex of Borač (Central Serbia). *Bulletin CXXXV de l' Académie Serbe des Sciences et des Arts, Classe des Science mathématiques et naturelles*, 342: 209–215.
- Cvetković V & Pecskey Z (1999): The Early Miocene eruptive complex of Borač (central Serbia): volcanic facies and evolution over time. *Carpatian Geology*.
- Cvetković V, Prelević D & Pecskey Z (2000): Lamprophyric rocks of the Miocene Borač eruptive complex (Central Serbia, Yugoslavia). *Acta Geologica Hungarica*, 43: 25–41.
- Cvetković V, Poli G, Resimić-Šarić K, Prelević D & Lazarov M (2002): Tertiary post-collision granitoid of Mt. Kopaonik (Serbia) – Petrogenetic constraints based on new geochemical data. *Geologica Carpathica*, 53.
- Cvetković V, Downes H, Prelević D, Jovanović M & Lazarov M (2004a): Characteristics of the lithospheric mantle beneath East Serbia inferred from ultramafic xenoliths in Palaeogene basanites. *Contributions to Mineralogy and Petrology*, 148: 335–357.
- Cvetković V, Prelević D, Downes H, Jovanović M, Vaselli O & Pecskey Z (2004b): Origin and geodynamic significance of Tertiary postcollisional basaltic magmatism in Serbia (central Balkan Peninsula). *Lithos*, 73: 161–186.
- Cvetković V, Downes H, Prelević D, Lazarov M & Resimić-Sarić K (2007a): Geodynamic significance of ultramafic xenoliths from Eastern Serbia: Relics of sub-arc oceanic mantle? *Journal Of Geodynamics*, 43: 504–527.
- Cvetković V, Poli G, Christofides G, Koroneos A, Pecskey Z, Resimić-Sarić K & Eric V (2007b): The Miocene granitoid rocks of Mt. Bukulja (central Serbia): evidence for pannonian extension-related granitoid magmatism in the northern Dinarides. *European Journal Of Mineralogy*, 19: 513–532.
- Del Moro A, Innocenti F, Kyriakopoulos C, Manetti P & Papadopoulos P (1988): Tertiary granitoids from Thrace (northern Greece) - Sr isotopic and petrochemical data. *Neues Jahrbuch für Mineralogie-Abhandlungen*, 159: 113–135.
- Delaloye M, Lovrić A & Karamata S (1989): Age of Tertiary granitic rocks of Dinarides and Vardar zone. *14th CBGA Congr. Extended Abstracts, Sofia*, 1: 1186–1189.
- Deleon G (1969): Pregled rezultata određivanja apsolutne geološke starost granitoidnih stena u Jugoslaviji. *Rad inst. geol. rud. istraž. ispit nukl. drug. min. sirov.*, 6: 165–182.
- Didier J & Barbarin B (1991): The different types of enclaves in granites – Nomenclature. In: *Enclaves and granite petrology* (eds Didier J & Barbarin B), pp. 19–23, Developments in Petrology, vol 13, Amsterdam.
- Dimitrijević MD (1997): Geology of Yugoslavia. In: *Geological Institute GEMINI Special Publication*, pp. 187, Belgrade.
- Dimitrijević MD (2001): Dinarides and the Vardar Zone; a short review of the geology.; Tertiary magmatism in the Dinarides. *Acta Vulcanologica*, 13: 1–8.

- Dimitrijević MN & Dimitrijević MD (1991): Triassic carbonate platform of the Drina-Ivanjica element (Dinarides). *Acta Geologica Hungarica*, 34: 15–44.
- Dimo-Lahitte A, Monié P & Vergély P (2001): Metamorphic soles from the Albanian ophiolites: Petrology, $^{40}\text{Ar}/^{39}\text{Ar}$ geochronology, and geodynamic evolution. *Tectonics*, 20: 78–96.
- Dinter DA, Macfarlane A, Hames W, Isachsen C, Bowring S & Royden L (1995): U–Pb and $^{40}\text{Ar}/^{39}\text{Ar}$ geochronology of the Symvolon granodiorite - implications for the thermal and structural evolution of the Rhodope Metamorphic Core Complex, northeastern Greece. *Tectonics*, 14: 886–908.
- Djerić N, Gerzina N & Schmid SM (2007a): Age of the Jurassic radiolarian chert formation from the Zlatar mountain (SW Serbia). *Ofioliti*, 32: 101–108.
- Djerić N, Vishnevskaya VS & Schmid SM (2007b): New data on radiolarians from the Dinarides (Bosnia and Serbia). Davos, 10.-12.October 2007, Abstract Volume p. 17-18. In: *8th Alpine Workshop*, pp. 17–18, Davos.
- Donelick RA (1993): A method of fission track analysis utilizing bulk chemical etching of apatite. . *U.S. Patent 5,267,274*.
- Dong H, Hall CM & Halliday AN (1995): Mechanisms of argon retention in clays revealed by laser ^{40}Ar – ^{39}Ar dating. *Science*, 267: 355–359.
- Dong H, Hall CM, Halliday AN & Peacor DR (1997a): Laser ^{40}Ar – ^{39}Ar dating of microgram-size illite samples and implications for thin section dating. *Geochimica et Cosmochimica Acta*, 61: 3803–3808.
- Dong H, Hall CM, Halliday AN, Peacor DR, Merriman RJ & Roberts B (1997b): ^{40}Ar – ^{39}Ar illite dating of Late Caledonian (Acadian) metamorphism and cooling of K-bentonites and slates from the Welsh Basin, U.K. *Earth and Planetary Science Letters*, 150: 337–351.
- Dumurdzanov N, Serafimovski T & Burchfiel BC (2005): Cenozoic tectonics of Macedonia and its relation to the South Balkan extensional regime. *Geosphere*, 1: 1–22.
- Dunkl I (2002): TRACKKEY: a Windows program for calculation and graphical presentation of fission track data. *Computers & Geosciences*, 18: 3–12.
- Egli D (2008): Das Kopaonik-Gebirge in Südserbien – Stratigraphie, Strukturen und Metamorphose. MSc Thesis, University of Basel, Basel.
- Ehlers TA (2005): Crustal thermal processes and the interpretation of thermochronometer data. In: *Low-Temperature Thermochronology: Techniques, Interpretations, and Applications*, pp. 315–350, Mineralogical Society of America, vol 58, Chantilly.
- Epstein AG, Epstein JB & Harris LD (1977): Conodont Colour Alteration - An Index to Organic Metamorphism. - Geol. Surv. Prof. Pap. 995: 1-27, Washington. *U.S. Geol. Surv. Prof. Pap.*, 995: 1–27.
- Faccenna C, Funicciello F, Civetta L, D'Antonio M, Moroni M & Piromallo C (2007): Slab disruption, mantle circulation, and the opening of the Tyrrhenian basins. In: *Geological Society of America Special Paper* (eds Beccaluva L, Bianchini G & Wilson M), pp. 153–169.
- Faure G (1986): *Principles of Isotope Geology*. John Wiley & Sons, New York.
- Ferrière J (1982): Paléogéographie et tectonique superposés dans les Hellenides internes: les massifs de l'Othrys et du Pélion (Grèce septentrionale). *Société Géologique du Nord*, 8: 1–970.

- Filipović I, Jovanović M, Sudar M, Pelikán P, Kovács M, Less G & Hips K (2003): Comparison of the Variscan – Early Alpine evolution of the Jadar Block (NW Serbia) and “Bükkium” (NE Hungary) terranes; some paleogeographic implications. *Slovak Geological Magazine*, 9: 23–40.
- Fleischer RL, Price PB & Walker RM (1975): *Nuclear Tracks in Solids*. University of California Press, Berkeley.
- Frank W & Schlager W (2006): Jurassic strike slip versus subduction in the Eastern Alps. *International Journal of Earth Sciences*, 95: 431–450.
- Frimmel HE & Frank W (1998): Neoproterozoic tectono-thermal evolution of the Gariep Belt and its basement, Namibia and South Africa. *Precambrian Research*, 90: 1–28.
- Froitzheim N (1992): Formation of recumbent folds during synorogenic crustal extension (Austroalpine nappes, Switzerland). *Geology*, 20: 923–926.
- Funciello F, Moroni M, Piromallo C, Faccenna C, Cenedese A & Bui HA (2006): Mapping mantle flow during retreating subduction: Laboratory models analyzed by feature tracking. *Journal of Geophysical Research-Solid Earth*, 111: B03402, doi:10.1029/2005JB003792.
- Galbreith RF & Laslett GM (1993): Statistical models for mixed fission-track ages. *Nuclear Tracks and Radiation Measurements*, 21: 459–470.
- Gallagher K, Brown R & Johnson C (1998): Fission-track analysis and its applications to geological problems. *Annual Reviews of Earth and Planetary Sciences*, 26: 519–572.
- Gapais D (1989): Shear structures within deformed granites: Mechanical and thermal indicators. *Geology*, 17: 1144–1147.
- Gawlick HJ (2000): Paläogeographie der Ober-Trias Karbonatplattform in den nördlichen Kalkalpen. *Mitteilungen der Gesellschaft der Geologie- & Bergbaustudenten Österreich*, 44: 45–95.
- Gawlick HJ, Frisch W, Vecsei A, Steiger T & Böhm F (1999): The change from rifting to thrusting in the Northern Calcareous Alps as recorded in Jurassic sediments. *Geologische Rundschau*, 87: 644–657.
- Gawlick HJ, Frisch W, Hoxha L, Dumitrica P, Krystyn L, Lein R, Missoni S & Schlagintweit F (2008): Mirdita Zone ophiolites and associated sediments in Albania reveal Neotethys Ocean origin. *International Journal of Earth Sciences*, 97: 865–881.
- Gawlick HJ, Sudar M, Suzuki H, Đerić N, Missoni S, Lein R & Jovanović D (2009a): Upper Triassic and Middle Jurassic radiolarians from the ophiolitic melange of the Dinaridic Ophiolite Belt, SW Serbia. *Neues Jahrbuch für Geologie und Palaontologie-Abhandlungen*, 253: 293–311.
- Gawlick HJ, Missoni S, Schlagintweit F, Suzuki H, Frisch W, Krystyn L, Blau J & Lein R (2009b): Jurassic Tectonostratigraphy of the Austroalpine domain. *Journal of Alpine Geology*, 50: 1–152.
- Georgiev V, Milovanov P & Monchev P (2003): K–Ar dating of the magmatic activity in the Momchilgrad volcano-tectonic depression. *Comptes Rendus de l'Academie Bulgare Scientifique*, 56: 49–54.
- Geyh MA & Schleicher H (1990): *Absolute Age Determination, Physical and Chemical Dating Methods and Their Application*. Springer, Berlin.

- Gleadow AJW (1981): Fission-track dating methods – what are the real alternatives. *Nuclear Tracks and Radiation Measurements*, 5: 3–14.
- Gleadow AJW & Duddy IR (1981): A natural long-term annealing experiment for apatite. *Nuclear Tracks*, 5: 169–174.
- Gleadow AJW, Duddy IR, Green PF & Lovering JF (1986): Confined fission track lengths in apatite: A diagnostic tool for thermal history analysis. *Contributions to Mineralogy and Petrology*, 94: 405–415.
- Goričan Š, Slovenec D & Kolar-Jurkovšek T (1999): A Middle Jurassic Radiolarite-Clastic Succession from the Medvednica Mt. (NW Croatia). *Geologia Croatia*, 52: 29–57.
- Goričan Š, Halamić J, Grgasović T & Kolar-Jurkovšek T (2005): Stratigraphic evolution of Triassic arc-backarc system northwestern Croatia. *Bulletin de la Société Géologique de France*, 176: 3–22.
- Graf J (2001): Alpine Tectonics in Western Bulgaria: Cretaceous Compression of the Kraishite Region and Cenozoic Exhumation of the Crystalline Osogovo–Lisets Complex. ETH, Zürich.
- Green PF & Duddy IR (1989): Some comments on paleotemperature estimation from apatite fission track analysis. *Journal of Petroleum Geology*, 12: 111–114.
- Grubić A, Djoković I & Marović M (1995): Tectonic outline of the Kopaonik area. In: *Geology and Metallogeny of the Kopaonik Mt.*, pp. 46–53, Belgrade.
- Haas J, Kovács S, Krystyn L & Lein R (1995): Significance of Late Permian-Triassic facies zones in terrane reconstructions in the Alpine-North Pannonian domain. *Tectonophysics*, 242: 19–40.
- Halamić J, Goričan Š, Slovenec D & Kolar-Jurkovšek T (1999): A Middle Jurassic radiolarite-clastic succession from the Medvednica Mt. (NW Croatia). *Geologia Croatia*, 52.
- Hames WE & Bowring SA (1994): An empirical evaluation of the argon diffusion geometry in muscovite. *Earth and Planetary Science Letters*, 124: 161–167.
- Harkovska A & Pécskay Z (1997): The Tertiary magmatism in Ruen magmato-tectonic zone (W. Bulgaria) – A comparison of new K-Ar ages and geological data. In: *Magmatism, Metamorphism and Metallogeny of the Vardar Zone and Serbo-Macedonian Massif* (eds Boev B & Serafimovski T), pp. 137–142, Faculty Mining Geology, Stip–Dojran, Rep. Macedonia.
- Harkovska A, Marchev P, Machev P & Pecskey Z (1998): Paleogene magmatism in the Central Rhodope area, Bulgaria — a review and new data. *Acta Vulcanologica*, 10: 199–216.
- Harris AG (1979): Conodont Color Alteration, an organomineral metamorphic index, and its application to Appalachian Basin geology. *SEPM Special Publications*, 26: 3–16.
- Hauer von F (1888): Die Cephalopoden des bosnischen Muschelkalkes von Han Bulog bei Sarajevo. *Denkschriften / Akademie der Wissenschaften in Wien, Mathematisch-Naturwissenschaftliche Klasse*, 54: 1–50.
- Hauer von F (1892): Beiträge zur Kenntnis der Cephalopoden aus der Trias von Bosnien. I. Neue Funde aus dem Muschelkalk von Han Bulog bei Sarajevo. *Denkschriften / Akademie der Wissenschaften in Wien, Mathematisch-Naturwissenschaftliche Klasse*, 59: 232–296.

- Hips K (2006): Facies pattern of western Tethyan Middle Triassic black carbonates: The example of Gutenstein Formation in Silica Nappe, Carpathians, Hungary, and its correlation to formations of adjoining areas. *Sedimentary Geology*, 194: 99–114.
- Hurford AJ & Green PF (1983): The zeta-age calibration of fission-track dating. *Isotope Geoscience*, 1: 285–317.
- Ilić A, Neubauer F & Handler R (2005): Late Paleozoic-Mesozoic tectonics of the Dinarides revisited: Implications from $^{40}\text{Ar}/^{39}\text{Ar}$ dating of detrital white micas. *Geology*, 33: 233–236.
- Jahn-Awe S, Froitzheim N, Nagel TJ, Frei D, Georgiev N & Pleuger J (2010): Structural and geochronological evidence for Paleogene thrusting in the Western Rhodopes (SW Bulgaria). *Tectonics*, doi:10.1029/2009TC002558.
- Karamata S (2006): The geological development of the Balkan Peninsula related to the approach, collision and compression of Gondwanan and Eurasian units. In: *Tectonic Development of the Eastern Mediterranean Region* (eds Robertson AHF & Mountrakis D), pp. 155–178, Geological Society (London) Special Publication, vol 260.
- Karamata S, Delaloye M, Lovrić A & Knežević V (1992): Two genetic groups of Tertiary granitic rocks of Central and Western Serbia. *Annales Géologiques de la Péninsule Balkanique*, 56: 263–283.
- Karamata S, Pecskay Z, Knežević V & Memović E (1994): Origin and age of Rogozna (central Serbia) volcanics in the light of new isotopic data. *Bull. Acad. Serb. Sci.*, 35: 41–46.
- Karamata S, Korikovskiy S & Kurdyukov E (2000): Prograde contact metamorphism of mafic and sedimentary rocks in the contact aureole beneath the Bresovica harzburgite Massif. In: *International Symposium Geology and Metallogeny of the Dinarides and the Vardar zone* (eds Karamata S & Janković S), pp. 171–177, Academy of Sciences & Arts Republic of Srpska, vol 1, Banja Luka, Sarajevo.
- Ketcham RA (2005): Forward and Inverse Modeling of Low-Temperature Thermochronometry Data. *Reviews in Mineralogy & Geochemistry*, 58: 275–314.
- Ketcham RA, Donelick RA & Donelick MB (2000): AFTSolve: A program for multi-kinetic modeling of apatite fission-track data. *Geological Materials Research*, 2: (electronic).
- Ketcham RA, Carter A, Donelick RA, Barbarand J & Hurford AJ (2007): Improved measurement of fission-track annealing in apatite using c-axis projection. *American Mineralogist*, 92: 789–798.
- Klisić M, Mičić I, Pajić V, Simić D & Kandić M (1972): Contribution to the stratigraphy of the Trepča metamorphic series. *Zapisnici Srpski geološki društva za 1968, 1969 i 1970 (Zbor 10. XII 1968)*: 105–107.
- Knežević V, Szeki-Fux F, Steiger R, Pecskay Z, Boronihin VA & Karamata S (1991): Petrology of Fruška-Gora latites - volcanic precursors at the southern margin of the Pannonian basin. *Geodynamic Evolution of the Pannonian Basin, Serbian Academy of Science and Arts, Academic Conference*, 62: 243–259.
- Knežević V, Karamata S, Vasković N & Cvetković V (1995): Granodiorites of Kopaonik and contact metamorphic zone. In: *Geology and Metallogeny of the Kopaonik Mt.*, pp. 172–184, Belgrade.
- Königshof P (1992): Der Farbänderungsindex von Conodonten (CAI) in paläozoischen Gesteinen (Mitteldevon bis Unterkarbon) des Rheinischen Schiefergebirges. Eine Ergänzung zur Vitritreflexion. *Courier Forschungsinstitut Senckenberg*, 146: 1–118.

- Korbar T (2009): Orogenic evolution of the External Dinarides in the NE Adriatic region: a model constrained by tectonostratigraphy of Upper Cretaceous to Paleogene carbonates. *Earth Science Reviews*, 96: 296–312.
- Koroneos A, Poli G, Cvetković V, Christofides G, Krstić D & Pécskay Z (in press): Contrasting plutonic bodies in the northern Dinarides – South Pannonian Basin: Petrogenetic and tectonic implications inferred from the study of Mt. Cer granitoids (West Serbia). *Geological Magazine*.
- Kossmat F (1924): Geologie der zentralen Balkanhalbinsel, mit einer Übersicht des dinarischen Gebirgsbaus. In: *Die Kriegsschauplätze 1914–1918 geologisch dargestellt*. (ed Wilder J), pp. 198, Verlag Gebrüder Bornträger, Berlin.
- Kounov A, Seward D, Bernoulli D, Burg JP & Ivanov Z (2004): Thermotectonic evolution of an extensional dome: the Cenozoic Osogovo-Lisets core complex (Kraishte zone, western Bulgaria). *International Journal of Earth Sciences*, 93: 1008–1024.
- Kovács I, Csontos L, Szabó C, Bali E, Falus G, Benedek K & Zajacz Z (2007): Paleogene–early Miocene igneous rocks and geodynamics of the Alpine-Carpathian-Pannonian-Dinaric region: An integrated approach. In: *Cenozoic Volcanism in the Mediterranean Area* (eds Beccaluva L, Bianchini G & Wilson M), pp. 93–112, Geological Society of America Special Paper, vol 418.
- Kozur HW (1991): The evolution of the Meliata-Hallstatt ocean and its significance for the early evolution of the Eastern Alps and Western Carpathians. *Palaeogeography, Palaeoclimatology, Palaeoecology*, 87: 109–135.
- Krystyn L (1971): Stratigraphie, Fauna und Fazies der Klaus-Schichten (Aalenium-Oxford) in den östlichen Nordalpen. *Verh. der Geologischen Bundesanstalt Wien*, 1971: 486–509.
- Lanphere M, Coleman RG, Karamata S & Pamić J (1975): Age of amphibolites associated with Alpine peridotites in the Dinaride ophiolite zone, Yugoslavia. *Earth and Planetary Science Letters*, 26: 271–276.
- Laslett GM, Green PF, Duddy IR & Gleadow AJW (1987): Thermal annealing of fission tracks in apatite: 2. A quantitative analysis. *Chemical Geology*, 65: 1–13.
- Lee JKW, Williams IS & Ellis DJ (1997): Pb, U and Th diffusion in natural zircon. *Nature*, 390: 159–162.
- Lein R (1987): Evolution of the Northern Calcareous Alps During Triassic Times. In: *Geodynamics of the Eastern Alps* (eds Flügel HW & Faupl P), pp. 85–102, Deuticke, Wien.
- Less G, Kovács M, Pelikán P, Pentelényi P & Sásdi L (2005): *Geology of the Bükk Mountains*, Budapest.
- Liati A (1986): Regional metamorphism and overprinting contact metamorphism of the Rhodope Zone, near Xanthi (N. Greece). Technische Universität, Braunschweig.
- Lilov P, Yanev Y & Marchev P (1987): K–Ar dating of the Eastern Rhodopes Paleogene magmatism. *Geologica Balcanica*, 17: 49–58.
- Ludwig K (2005): Isoplot - A plotting and regression program for radiogenic isotope data. In: *USGS Open File report 91–445* (ed edited), Boulder.
- Marakis G (1969): Geochronologic studies of some granites from Macedonia. *Annales Géologiques des Pays Helleniques*, 21: 121–252.

- Marchev P, Raicheva R, Downes H, Vaselli O, Chiaradia M & Moritz R (2004): Compositional diversity of Eocene–Oligocene basaltic magmatism in the Eastern Rhodopes, SE Bulgaria: implications for genesis and tectonic setting. *Tectonophysics*, 393: 301–328.
- Marchev P, Kaiser-Rohrmeier M, Heinrich C, Ovtcharova M, von Quadt A & Raicheva R (2005): 2: Hydrothermal ore deposits related to post-orogenic extensional magmatism and core complex formation: The Rhodope Massif of Bulgaria and Greece. *Ore Geology Reviews*, 27: 53–89.
- Marović M, Djoković I, Toljić M, Spahić D & Milivojević J (2007): Extensional Unroofing of the Veliki Jastrebac Dome (Serbia). *Annales Géologiques de la Péninsule Balkanique*, 68: 21–27.
- Mattinson JM (2005): Zircon U-Pb chemical abrasion („CA-TIMS“) method: Combined annealing and multi-step partial dissolution analysis for improved precision and accuracy of zircon ages. *Chemical Geology*, 220: 47–66.
- McDougall I & Harrison TM (1999): *Geochronology and Thermochronology by the $^{40}\text{Ar}/^{39}\text{Ar}$ method*. Oxford University Press, New York.
- Meco S & Aliaj S (2000): *Geology of Albania*. Schweizerbart, Stuttgart.
- Mićić I, Urošević M, Kandić M, Klisić M & Simić D (1972): Findings of Triassic conodont fauna in the metamorphic complex of Kopaonik Mt. *Zapiski Srpski geološki društva za 1968, 1969 i 1970 (Zbor 10. XII 1968)*: 103–104.
- Mikes T, Baldi-Beke M, Kazmer M, Dunkl I & von Eynatten H (2008a): Calcareous nannofossil age constraints on Miocene flysch sedimentation in the Outer Dinarides (Slovenia, Croatia, Bosnia-Herzegovina and Montenegro). *Geological Society, London, Special Publications*, 298: 335–363.
- Mikes T, Christ D, Petri R, Dunkl I, Frei D, Baldi-Beke M, Reitner J, Wemmer K, Hrvatović H & Von Eynatten H (2008b): Provenance of the Bosnian Flysch. *Swiss Journal of Geosciences*, 101: S31–S54.
- Miller JS, Matzel JEP, Miller CF, Burgess SD & Miller RB (2007): Zircon growth and recycling during the assembly of large, composite arc plutons. *Journal Of Volcanology And Geothermal Research*, 167: 282–299.
- Milovanović D (1984): Petrology of low metamorphosed rocks of the central part of the Drina-Ivanjica Palaeozoic. *Bulletin du Musée de l' Histoire Naturelle Beograd*, A39: 1–139.
- Milovanović D, Marchig V & Stevan K (1995): Petrology of the crossite schist from Fruska Gora Mts (Yugoslavia), relic of a subducted slab of the Tethyan oceanic crust. *Journal of Geodynamics*, 20: 289–304.
- Mojsilović S, Baklajić D & Djoković I (1978): Basic Geological Map of the SFRY, 1:100'000, Sheet Sjenica (K32-29). *Savezni Geološki Zavod, Beograd (Geozavod – OOUR Geološki institut, Beograd, 1960-1973)*.
- Mojsilović S, Djoković I, Baklajić D & Rakić B (1980): Geology of the Sheet Sjenica (K32–29), Explanatory notes (in Serbo-Croatian, English and Russian summaries). *Savezni Geološki Zavod, Beograd*.
- Neubauer F, Pamić J, Dunkl I, Handler R & Majer V (2003): Exotic granites in the Cretaceous Pogari Formation overstepping the Dinaric Ophiolite Zone mélange in Bosnia. *Annales Universitatis Scientiarium Budapestinensis, Sectio Geologica*, 35: 133–134.
- Nöth S (1991): Die Conodontendiagenese als Inkohlungsparameter und ein Vergleich unterschiedlich sensitiver Diageneseindikatoren am Beispiel von Triassedimenten Nord- und Mitteldeutschlands. *Boch. geol. und geotechn. Arb.*, 37: 1–169.

- Obradović J & Goričan Š (1988): Siliceous deposits in Yugoslavia: occurrences, types and ages. In: *Siliceous deposits of the Tethys and Pacific regions* (eds Hein JR & Obradović J), pp. 51–64, Springer, New York.
- Okrusch M, Seidel E, Kreuzer H & Harre W (1978): Jurassic age of metamorphism at the base of the Brezovica peridotite (Yugoslavia). *Earth and Planetary Science Letters*, 39: 291–297.
- Operta M, Pamić J, Balen D & Tropper P (2003): Corundum-bearing amphibolites from the metamorphic basement of the Krivaja-Konjuh ultramafic massif (Dinaride Ophiolite Zone, Bosnia). *Mineralogy and Petrology*, 77: 287–295.
- Ortner H, Reiter F & Acs P (2002): Easy handling of tectonic data: the programs TectonicVB for Mac and TectonicsFP for Windows(TM). *Computers & Geosciences*, 28: 1193–1200.
- Pamić J (1997): Volcanic rocks of the Sava–Drava interfluvium and Baranja. *Nafta Monograph, Zagreb*: 192pp.
- Pamić J & Palinkas L (2000): Petrology and geochemistry of Paleogene tonalites from the easternmost parts of the Periadriatic Zone. *Mineralogy and Petrology*, 70: 121–141.
- Pamić J & Hrvatović H (2000): Dinaride Ophiolite Zone (DOZ). *Pancardi 2000 Fieldtrip Guidebook. Vijesti*, 37: 60–68.
- Pamić J & Balen D (2001): Tertiary magmatism of the Dinarides and the adjoining South Pannonian Basin, an overview. *Acta Vulcanologica*, 13: 9–24.
- Pamić J, Gusić I & Jelaska V (1998): Geodynamic evolution of the central Dinarides. *Tectonophysics*, 297: 251–268.
- Pamić J, Pécskay Z & Balen D (2000): Lower oligocene K–Ar ages of high-K calc-alkaline and shoshonite rocks from the North Dinarides in Bosnia. *Mineralogy and Petrology*, 70: 313–320.
- Pamić J, Balen D & Herak M (2002a): Origin and geodynamic evolution of Late Paleogene magmatic associations along the Periadriatic–Sava–Vardar magmatic belt. *Geodinamica Acta*, 15: 209–231.
- Pamić J, Tomljenović B & Balen D (2002b): Geodynamic and petrogenetic evolution of Alpine ophiolites from the central and NW Dinarides: an overview. *Lithos*, 65: 113–142.
- Pamić J, Balogh K, Hrvatović H, Balen D, Jurković I & Palinkas L (2004): K–Ar and Ar–Ar dating of the Palaeozoic metamorphic complex from the Mid-Bosnian Schist Mts., central Dinarides, Bosnia and Hercegovina. *Mineralogy and Petrology*, 82: 65–79.
- Pécskay Z, Balogh K & Harkovska A (1991): K–Ar dating of the Perelik volcanic massif (Central Rhodopes, Bulgaria). *Acta Geologica Hungarica*, 34: 101–110.
- Pécskay Z, Harkovska A & Hadjiev A (2000): K–Ar dating of Mesta volcanics (SW Bulgaria). *Geologica Balcanica*, 30: 3–11.
- Pécskay Z, Eleftheriadis G, Koroneos A, Soldatos T & Christofides G (2003): K–Ar dating, geochemistry and evolution of the Tertiary volcanic rocks (Thrace, northeastern Greece). In: *Mineral Exploration and Sustainable Development* (ed Eliopoulos DG), pp. 1229–1232, Millpress, Rotterdam.
- Piomallo C & Morelli A (2003): P wave tomography of the mantle under the Alpine-Mediterranean area. *Journal of Geophysical Research-Solid Earth*, 108.

- Piromallo C, Becker TW, Funicello F & Faccenna C (2006): Three-dimensional instantaneous mantle flow induced by subduction. *Geophysical Research Letters*, 33: L08304.
- Poli G, Tommasini S & Halliday AN (1996): Trace elements and isotopic exchange during acid-basic magma interaction processes. 87: 225–232.
- Prelević D, Cvetković V & Foley SF (2001): Composite igneous intrusions from Serbia; two case studies of interaction between lamprophyric and granitoid magmas.; Tertiary magmatism in the Dinarides. *Acta Vulcanologica*, 13: 145–157.
- Prelević D, Foley SF, Cvetković V & Romer RL (2004): Origin of minette by mixing of lamproite and felsic magmas in Veliki Majdan, Serbia. *Journal Of Petrology*, 45: 759–792.
- Prelević D, Foley SF, Romer RL, Cvetković V & Downes H (2005): Tertiary ultrapotassic volcanism in Serbia: Constraints on petrogenesis and mantle source characteristics. *Journal Of Petrology*, 46: 1443–1487.
- Prelević D, Foley SF, Stracke A, Romer RL & Conticelli S (submitted): Hf isotopes in Mediterranean lamproites: mixing of melts from asthenosphere and crustally contaminated lithosphere. *Chemical Geology*, submitted.
- Radoičić R, Jovanović D & Sudar MN (2009): Stratigraphy of the Krs Gradac section (SW Serbia). *Annales Géologiques de la Péninsule Balkanique*, 70: 23–41.
- Rainer T, Sachsenhofer RF, Rantitsch G, Herlec U & Vrabec M (2009): Organic maturity trends across the Variscan discordance in the Alpine-Dinaric Transition Zone (Slovenia, Austria, Italy): Variscan versus Alpidic thermal overprint. *Austrian Journal of Earth Sciences*, 102: 120–133.
- Rampnoux JP (1970): Regards sur les Dinarides internes yougoslaves (Serbie-Monténégro oriental): stratigraphie, évolution paléogéographique, magmatisme. *Bulletin de la Société Géologique de France*, 12: 948–966.
- Rampnoux JP (1974): Contribution à l'étude géologique des Dinarides: Un secteur de la Serbie méridionale et du Monténégro oriental (Yougoslavie). *Mémoires de la Société Géologique de France (Nouvelle Serie)*, 119: 1–99.
- Ramsay JG & Huber MI (1983): *Modern Structural Geology Vol. 1: Strain Analysis*. Academic Press.
- Ratschbacher L, Frisch W & Winzer H-G (1991): Lateral extrusion in the Eastern Alps, 2, structural analysis. *Tectonics*, 10: 257–271.
- Rejebian VA, Harris AG & Huebner JS (1987): Conodont colour and textural alteration: an index to regional metamorphism and hydrothermal alteration. *Geological Society of America Bulletin*, 99.
- Renne PR, Deino AL, Walter RC, Turrin BD, Swisher CC, Becker TA, Curtis GH, Sharp WD & Jaouni A-R (1994): Intercalibration of astronomical and radioisotopic time. *Geology*, 22: 783–786.
- Robertson AHF & Karamata S (1994): The role of subduction-accretion processes in the tectonic evolution of the Mesozoic Tethys in Serbia. *Tectonophysics*, 234: 73–94.
- Robertson AHF, Karamata S & Sarić K (2009): Ophiolites and related geology of the Balkan region. *Lithos*, 108: vii–x.
- Rosenberg CL (2004): Shear zones and magma ascent: A model based on a review of the Tertiary magmatism in the Alps. *Tectonics*, 23.

- Rudnick RL & Gao S (2003): Composition of the Continental Crust. In: *Treatise on Geochemistry* (eds Heinrich DH & Karl KT), pp. 1–64, Pergamon, Oxford.
- Samson SD & Alexander EC (1987): Calibration of the interlaboratory ^{40}Ar – ^{39}Ar dating standard MMhb-1. *Chemical Geology*, 66: 27–34.
- Schaltegger U & Brack P (2007): Crustal-scale magmatic systems during intracontinental strike-slip tectonics: U, Pb and Hf isotopic constraints from Permian magmatic rocks of the Southern Alps. *International Journal of Earth Sciences*, 96: 1131–1151.
- Schaltegger U, Guex J, Bartolini A, Schoene B & Ovtcharova M (2008): Precise U–Pb age constraints for end-Triassic mass extinction, its correlation to volcanism and Hettangian post-extinction recovery. *Earth and Planetary Science Letters*, 267: 266–275.
- Schaltegger U, Brack P, Ovtcharova M, Peytcheva I, Schoene B, Stracke A, Marocchi M & Bargossi GM (2009): 700,000 years of magma accretion, crystallization and initial cooling in a composite pluton recorded by zircon and titanite (Adamello batholith, northern Italy). *Earth and Planetary Science Letters*, 286: 208–218.
- Schefer S, Fügenschuh B, Schmid SM, Egli D & Ustaszewski K (2007): Tectonic evolution of the suture zone between Dinarides and Carpatho–Balkan: field-evidence from the Kopaonik region, southern Serbia. In: *EGU General Assembly 2007, Geophysical Research Abstracts*, pp. 03891, Vienna.
- Schefer S, Egli D, Frank W, Fügenschuh B, Ovtcharova M, Schaltegger U, Schoene B & Schmid SM (2008): Metamorphic and igneous evolution of the innermost Dinarides in Serbia. In: *6th Swiss Geoscience Meeting*, pp. 60–61, Lugano.
- Schefer S, Egli D, Missoni S, Bernoulli D, Fügenschuh B, Gawlick HJ, Jovanović D, Krystyn L, Lein R, Schmid SM & Sudar MN (2010a): Triassic metasediments in the Internal Dinarides (Kopaonik area, southern Serbia): stratigraphy, paleogeographic and tectonic significance. *Geologica Carpathica*, 61: ?
- Schefer S, Cvetković V, Fügenschuh B, Kounov A, Ovtcharova M, Schaltegger U & Schmid SM (2010b): Cenozoic granitoids in the Dinarides of southern Serbia: age of intrusion, isotope geochemistry, exhumation history and significance for the geodynamic evolution of the Balkan Peninsula. *International Journal of Earth Sciences*, in Review.
- Schlager W, Reijmer JJG & Droxler A (1994): Highstand shedding of carbonate platforms. *Journal Sedimentary Research*, 64: 270–281.
- Schlagintweit F, Gawlick HJ, Missoni S, Hoxha L, Lein R & Frisch W (2008): The eroded Late Jurassic Kurbnesh carbonate platform in the Mirdita Ophiolite Zone of Albania and its bearing on the Jurassic orogeny of the Neotethys realm. *Swiss Journal of Geosciences*, 101: 125–138.
- Schmid SM, Bernoulli D, Fügenschuh B, Matenco L, Schefer S, Schuster R, Tischler M & Ustaszewski K (2008): The Alpine-Carpathian-Dinaridic orogenic system: correlation and evolution of tectonic units. *Swiss Journal of Geosciences*, 101: 139–183.
- Seghedi I, Downes H, Szakacs A, Mason PRD, Thirlwall MF, Rosu E, Pécskay Z, Marton E & Panaiotu C (2004): Neogene–Quaternary magmatism and geodynamics in the Carpathian–Pannonian region: A synthesis. *Lithos*, 72: 117–146.
- Shand SJ (1947): Eruptive Rocks. Their genesis, composition, classification, and their relation to ore deposits (3rd ed.). J. Wiley & Sons, New York, N.Y.

- Simić V (1956): Zur Geologie des Studenicegebietes (Südwestserbien). *Vesnik Bull. Serv. Geol. Geophys.*, 12: 5–66.
- Simpson C & Schmid SM (1983): An evaluation of criteria to deduce the sense of movement in sheared rocks. *Bulletin Geological Society America*, 94: 1281–1288.
- Singer B & Marchev P (2000): Temporal evolution of arc magmatism and hydrothermal activity including epithermal gold veins, Borovitsa caldera, southern Bulgaria. *Economic Geology*, 95: 1155–1164.
- Skourlis K & Doutsos T (2003): The Pindos Fold-and-thrust belt (Greece): inversion kinematics of a passive continental margin. *International Journal of Earth Sciences*, 92: 891–903.
- Stacey JS & Kramers JD (1975): Approximation of terrestrial lead isotope evolution by a 2-stage model. *Earth and Planetary Science Letters*, 26: 207–221.
- Stajević B (1987): Magmatizam Golije i njegov metalogenetski značaj. *Zbornik radova Rudarsko-geološkog fakulteta*, 26: 7–17.
- Stampfli GM & Borel G (2004): The TRANSMED transects in space and time: constraints on the paleotectonic evolution of the Mediterranean domain. In: *The TRANSMED Atlas: The Mediterranean Region from Crust to Mantle*. (eds Cavazza W, Roure FM, Spakman W, Stampfli GM & Ziegler PA), pp. 53–80, Springer, Berlin and Heidelberg.
- Stipp M, Stünitz H, Heilbronner R & Schmid SM (2002): The eastern Tonale fault zone: a ‘natural laboratory’ for crystal plastic deformation of quartz over a temperature range from 250 to 700 °C. *Journal of Structural Geology*, 24: 1861–1884.
- Sudar M (1986): Triassic microfossils and biostratigraphy of the Inner Dinarides between Gučevo and Ljubišnja Mts., Yugoslavia (in Serbian, English summary). *Annales Géologiques de la Péninsule Balkanique*, 50: 151–394.
- Sudar M & Kovács S (2006): Metamorphosed and ductilely deformed conodonts from Triassic limestones situated beneath ophiolite complexes: Kopaonik Mountain (Serbia) and Bukk Mountains (NE Hungary) - a preliminary comparison. *Geologica Carpathica*, 57: 157–176.
- Sudar M, Gawlick HJ, Missoni S, Jovanović M & Krystyn L (2008): Drowning and block tilting of Middle Anisian carbonate platform in the Middle Jurassic Zlatibor melange of the Dinaridic Ophiolite Belt (SW Serbia). *Journal of Alpine Geology*, 49: 106–107.
- Tagami T (2005): Zircon fission-track thermochronology and applications to fault studies. *Reviews in Mineralogy and Geochemistry*, 58: 95–122.
- Tagami T & Dimitru TA (1996): Provenance and history of the Franciscan accretionary complex: Constraints from zircon fission-track thermochronology. *Journal of Geophysical Research*, 101: 11353–11364.
- Tagami T, Galbreith RF, Yamada R & Laslett GM (1998): Revised annealing kinetics of fission tracks in zircon and geological implications. In: *Advances in Fission-Track Geochronology* (eds Van den Haute P & de Corte F), pp. 99–114, Kluwer Academic Publishers, Dordrecht.
- Tari V & Pamić J (1998): Geodynamic evolution of the northern Dinarides and the southern part of the Pannonian basin. *Tectonophysics*, 297: 269–281.

- Tari V (2002): Evolution of the northern and western Dinarides: a tectonostratigraphic approach. *EGU Stephan Mueller Special Publications*, 1: 223–236.
- Thorburn WM (1918): The Myth of Occam's Razor. *Mind*, 27: 345–353.
- Tollmann A (1976): *Analyse des klassischen nordalpinen Mesozoikums*. Deuticke, Wien.
- Tomljenović B, Csontos L, Marton E & Marton P (2008): Tectonic evolution of the northwestern Internal Dinarides as constrained by structures and rotation of Medvednica Mountains, North Croatia. In: *Tectonic Aspects of the Alpine-Dinaride-Carpathian system* (eds Siegesmund S, Fügenschuh B & Froitzheim N), pp. 145–167, Geological Society, London, Special Publications, vol 298.
- Trajanova M, Pecskey Z & Itaya T (2008): K–Ar geochronology and petrography of the Miocene Pohorje Mountains batholith (Slovenia). *Geologica Balcanica*, 59: 247–260.
- Turner G & Cadogan PH (1974): Possible effects of ^{39}Ar recoil in ^{40}Ar - ^{39}Ar dating. *Geochimica et Cosmochimica Acta*, 2, Supplement 5: 1601–1615.
- Urošević M, Pavlović Z, Klisić M, Brković T, Malešević M & Trifunović S (1970a): Geological map of Yugoslavia, Sheet Novi Pazar, 1:100'000, Savezni Geološki Zavod, Belgrade.
- Urošević M, Pavlović Z, Klisić M, Brković T, Malešević M & Trifunović S (1970b): Geological map of Yugoslavia, Sheet Vrnjci, 1:100'000, Savezni Geološki Zavod, Belgrade.
- Urošević M, Pavlović Z, Klisić M, Brković T, Malešević M & Trifunović S (1973a): Explanation to Geological map of Yugoslavia, Sheet Novi Pazar, Savezni Geološki Zavod, Belgrade.
- Urošević M, Pavlović Z, Klisić M, Malešević M, Stefanović M, Marković O & Trifunović S (1973b): Explanation to Geological map of Yugoslavia, Sheet Vrnjci, Savezni Geološki Zavod, Belgrade.
- Ustaszewski K, Schmid SM, Fügenschuh B, Tischler M, Kissling E & Spakman W (2008): A map-view restoration of the Alpine-Carpathian-Dinaridic system for the Early Miocene. *Swiss Journal of Geosciences*, 101: S273–S294.
- Ustaszewski K, Schmid SM, Lugović B, Schuster R, Schaltegger U, Bernoulli D, Hottinger L, Kounov A, Fügenschuh B & Schefer S (2009): Late Cretaceous intra-oceanic magmatism in the internal Dinarides (northern Bosnia and Herzegovina): Implications for the collision of the Adriatic and European plates. *Lithos*, 108: 106–125.
- Ustaszewski K, Kounov A, Schmid SM, Schaltegger U, Frank W, Krenn E & Fügenschuh B (subm): Evolution of the Adria–Europe plate boundary in the northern Dinarides – from continent-continent collision to back-arc extension. *Tectonics*.
- van Hinsbergen DJJ, Hafkenscheid E, Spakman W, Meulenkamp JE & Wortel R (2005): Nappe stacking resulting from continental lithosphere below subduction of oceanic and Greece. *Geology*, 33: 325–328.
- Velledits F (2006): Evolution of the Bükk Mountains (NE Hungary) during the Middle-Late Triassic asymmetric rifting of the Vardar-Meliata branch of the Neotethys Ocean. *International Journal of Earth Sciences*, 95: 395–412.
- Vishnevskaya VS, Djerić N & Zakariadze GS (2009): New data on Mesozoic Radiolaria of Serbia and Bosnia, and implications for the age and evolution of oceanic volcanic rocks in the Central and Northern Balkans. *Lithos*, 108: 72–105.

- von Blanckenburg F, Villa IM, Baur H, Morteani G & Steiger RH (1989): Time calibration of a PT-path from the Western Tauern Window, Eastern Alps: the problem of closure temperatures. *Contributions to Mineralogy and Petrology*, 101: 1–11.
- von Blanckenburg F & Davies JH (1995): Slab breakoff: A model for syncollisional magmatism and tectonics in the Alps. *Tectonics*, 14: 120–131.
- von Quadt A, Moritz R, Peytcheva I & Heinrich CA (2005): Geochronology and geodynamics of Late Cretaceous magmatism and Cu-Au mineralization in the Panagyurishte region of the Apuseni–Banat–Timok–Srednogorie belt, Bulgaria. *Ore Geology Reviews*, 27: 95–126.
- Vukov M (1989): Petrology and geochemistry of Zeljin granitoid (in Serbian), PhD-Thesis. University of Belgrade, Belgrade.
- Vukov M (1995): Petrologic characteristics of granitoid rocks of Željina and Polumir. In: *Geology and Metallogeny of the Kopaonik Mountain*, pp. 518, Belgrade.
- Vukov M & Milovanović D (2002): The Polumir Granite - Additional data on its origin. *Annales Géologiques de la Péninsule Balkanique*, 64: 167–185.
- Wiederkehr M (2009): From subduction to collision: a combined metamorphic, structural and geochronological study of polymetamorphic metasediments at the NE edge of the Lepontine dome (Swiss Central Alps). PhD Thesis, University of Basel, Basel.
- Yamada R, Tagami T, Nishimura S & Ito H (1995): Annealing kinetics of fission tracks in zircon: an experimental study. *Chemical Geology*, 122: 249–258.
- Zagorchev I, Moorbath S & Lilov P (1987): Radiogeochronological data on the Alpine igneous activity in the western part of the Rhodope Massif. *Geologica Balcanica*, 17: 59–71.
- Zelić M (2004): Tectonic history of the Vardar zone: constraints from the Kopaonik area (Serbia). PhD Thesis, Università di Pisa, Italy.
- Zelić M, Levi N, Malasoma A, Marroni M, Pandolfi L & Trivić B (2010): Alpine tectono-metamorphic history of the continental units from Vardar zone: the Kopaonik Metamorphic Complex (Dinaric-Hellenic belt, Serbia). *Geological Journal*, 45: 59–77.

Appendix I: Schmid et al. 2008

1661-8726/08/010139-45
DOI 10.1007/s00015-008-1247-3
Birkhäuser Verlag, Basel, 2008

Swiss J. Geosci. 101 (2008) 139–183

The Alpine-Carpathian-Dinaridic orogenic system: correlation and evolution of tectonic units

STEFAN M. SCHMID¹, DANIEL BERNOULLI¹, BERNHARD FÜGENSCHUH², LIVIU MATENCO³, SENECIO SCHEFER¹, RALF SCHUSTER⁴, MATTHIAS TISCHLER¹ & KAMIL USTASZEWSKI¹

Key words: tectonics, collisional Orogens, Ophiolites, alps, Carpathians, Dinarides

ABSTRACT

A correlation of tectonic units of the Alpine-Carpathian-Dinaridic system of orogens, including the substrate of the Pannonian and Transylvanian basins, is presented in the form of a map. Combined with a series of crustal-scale cross sections this correlation of tectonic units yields a clearer picture of the three-dimensional architecture of this system of orogens that owes its considerable complexity to multiple overprinting of earlier by younger deformations.

The synthesis advanced here indicates that none of the branches of the Alpine Tethys and Neotethys extended eastward into the Dobrogea Orogen. Instead, the main branch of the Alpine Tethys linked up with the Meliata-Maliac-Vardar branch of the Neotethys into the area of the present-day Inner Dinarides. More easterly and subsidiary branches of the Alpine Tethys separated Tisza completely, and Dacia partially, from the European continent. Remnants of the Triassic parts of Neotethys (Meliata-Maliac) are preserved only as ophiolitic mélanges present below obducted Jurassic Neotethyan (Vardar) ophiolites. The opening of the Alpine Tethys was largely contemporaneous with the Latest Jurassic to Early Cretaceous obduction of parts of the Jurassic Vardar ophiolites. Closure of the Meliata-Maliac Ocean in the Alps and West Carpathians led to Cretaceous-age orogeny associated with an eclogitic overprint of the adjacent continental margin. The Triassic Meliata-Maliac and Jurassic Western and Eastern Vardar ophiolites were derived from one single branch of Neotethys: the Meliata-Maliac-Vardar Ocean. Complex

geometries resulting from out-of-sequence thrusting during Cretaceous and Cenozoic orogenic phases underlay a variety of multi-ocean hypotheses, that were advanced in the literature and that we regard as incompatible with the field evidence.

The present-day configuration of tectonic units suggests that a former connection between ophiolitic units in West Carpathians and Dinarides was disrupted by substantial Miocene-age dislocations along the Mid-Hungarian Fault Zone, hiding a former lateral change in subduction polarity between West Carpathians and Dinarides. The SW-facing Dinaridic Orogen, mainly structured in Cretaceous and Palaeogene times, was juxtaposed with the Tisza and Dacia Mega-Units along a NW-dipping suture (Sava Zone) in latest Cretaceous to Palaeogene times. The Dacia Mega-Unit (East and South Carpathian Orogen, including the Carpatho-Balkan Orogen and the Bihar nappe system of the Apuseni Mountains), was essentially consolidated by E-facing nappe stacking during an Early Cretaceous orogeny, while the adjacent Tisza Mega-Unit formed by NW-directed thrusting (in present-day coordinates) in Late Cretaceous times. The polyphase and multi-directional Cretaceous to Neogene deformation history of the Dinarides was preceded by the obduction of Vardar ophiolites onto the Adriatic margin (Western Vardar Ophiolitic Unit) and parts of the European margin (Eastern Vardar Ophiolitic Unit) during Late Jurassic to Early Cretaceous times.

1. Introduction

Our analysis of the Alpine-Carpathian-Dinaridic system of orogens including the Pannonian and Transylvanian basins, and of its complex temporal and spatial evolution, is based on a tectonic map that includes the entire system and crosses many national boundaries. This map, presented in Plate 1, was constructed by compiling of available geological maps and subsurface information for those parts of the system covered by

very thick Mio-Pliocene (in case of the Pannonian basin) or mid-Cretaceous to Late Miocene deposits (in case of the Transylvanian basin).

The map leads to a better understanding of the mobile belts formed during Late Jurassic, Cretaceous and Cenozoic times that are characterized by extreme changes along strike, including changes in subduction polarity (Alpine-Carpathian polarity vs. Dinaridic polarity; e.g. Laubscher 1971; Schmid et al. 2004b; Kissling et al. 2006). In addition it serves as a base map for

¹Geologisch-Paläontologisches Institut, Basel University, Bernoullistr. 35, 4058 Basel, Switzerland. E-mail: Stefan.Schmid@unibas.ch

²Geology and Palaeontology, Innsbruck University, Innrain 52f, A-6020 Innsbruck, Austria.

³Netherlands Centre for Integrated Solid Earth Sciences, Vrije Universiteit, Faculty of Earth and Life Sciences, De Boelelaan 1085, 1081 HV Amsterdam, The Netherlands. E-mail: liviu.Matenco@falw.vu.nl

⁴Geologische Bundesanstalt, Neulinggasse 38, A-1030 Wien, Austria. E-mail: Ralf.Schuster@cc.geoloba.ac.at

future palinspastic reconstructions that are required to arrive at realistic paleogeographic and paleotectonic reconstructions. The first obvious step towards this goal consists in establishing the Early Miocene geometry of the various tectonic units of the system. A retro-deformation of the very substantial Miocene rotations and translations was first sketched by the pioneering work of Balla (1987). Subsequent attempts included kinematic inversion of pre-Miocene rotations and translations in order to establish the motion and deformation of the different tectono-stratigraphic units involved in the system during the earlier Palaeogene and/or Cretaceous orogenic phases (i.e. Royden & Baldi 1988; Csontos et al. 1992; Csontos 1995; Fodor et al. 1999; Csontos & Vörös 2004). Moreover, numerous contrasting reconstructions have been advanced for the opening and closure of the different oceanic domains that form part of Neo-Tethys, including its Alpine branch (e.g. Săndulescu 1980, 1988; Golonka 2004; Haas & Pero 2004; Stampfli & Borel 2004).

All attempts at retro-deformation for Palaeogene and/or Mesozoic times must consider the present-day complex three-dimensional configuration of the entire Alpine-Carpathian-Dinaridic system. Our maps and profiles attempt to provide correlations on the basis of which the paleogeographic and paleotectonic evolution can be deduced. The data presented here are derived from literature studies and extensive own fieldwork. Naturally the divisions shown on the map (Plate 1) build on existing compilations (e.g. Săndulescu 1975; Channell & Horvath 1976; Royden & Horvath 1988; Csontos & Vörös 2004; Kovács et al. 2004), but use only primary data and own observations for defining the individual units.

Starting with a brief overview of the first order tectonic elements, we proceed with detailed descriptions of the individual tectonic units. In support of these descriptions, a series of crustal-scale profiles will be presented. These provide a three-dimensional picture of this complex system of orogens, which formed by a long-lasting evolution, that started in Late Jurassic times and is still going on today (Weber et al. 2005).

2. Method of map compilation

The tectonic map of the Carpathian-Balkan Mountain Systems edited by Mahel (1973) served as base map for the entire area covered by our compilation (Plate 1), apart from the Alps, for which we used a simplified version of the tectonic map published by Schmid et al. (2004a). The tectonic map by Mahel (1973) was progressively updated by new data. The most important sources of information are referenced. Longitudes and latitudes are marked at the margins of Plate 1. A version of this map giving 1° longitude and latitude grid points can be obtained from the first author. Figure 1 gives geographic and geological names mentioned in the text.

The Pannonian and Transylvanian basin fills, covering large parts of the Alpine-Carpathian-Dinaridic tectonic units, must be removed to understand the correlations and relationships between the different units. The sedimentary fill of these basins is regarded as “post-tectonic” as it rests unconformably on

parts of the Alpine, Carpathian and Dinaridic orogens; however, these sediments were later deformed in many places by deformation associated with basin formation and inversion. In Plate 1, white lines give the outlines of the Pannonian and Transylvanian Basin, and of numerous “inselbergs” in which units of the basin floor are exposed. Buried tectonic boundaries were drawn by projecting their suspected or known position to the surface. However, in many places the location of tectonic boundaries below the basin fill remains rather uncertain.

In the Pannonian basin, the post-tectonic fill conceals many crucial contacts between Alpine, Dinaride and Carpathian tectonic units. The basin fill mostly consists of Miocene sediments up to 6 km thick (see overview given in Haas 2001). The sediments of the post-tectonic cover of the Pannonian basin typically start with either Late Cretaceous or Palaeogene strata.

Note that we assigned the Cretaceous to Eocene Szolnok Flysch (Haas 2001) to the “bedrock”-units rather than to the post-tectonic fill of the Pannonian basin, because the evolution of this flysch basin clearly differs from that of the rest of the Pannonian Basin (e.g. Baldi & Baldi-Becke 1985). In our compilation the Szolnok Flysch is correlated with similar units occurring in the “Pienides” of Northern Romania (Săndulescu et al. 1981a; Tischler 2005; Tischler et al. 2007) and in the “Penine” units known from the subsurface of the East Slovak Basin (Iňačovce-Krichevo Unit; i.e. Soták et al. 1999). The subsurface information for this basin largely stems from drill holes (e.g. Fülöp & Dank 1987) and from seismic data (e.g. Tari et al. 1999).

The Late Cretaceous to Miocene fill of the Transylvanian Basin (e.g. Huismans et al. 1997; de Broucker et al. 1998) covers many of the more internal units of the East Carpathians and Apuseni Mountains. Only recently, a wealth of information from the floor of this basin became available from hydrocarbon exploration (e.g. Kreszek & Bally 2006). Much of this as yet largely unpublished information, consisting of seismic reflection data partly calibrated by bore holes was used during compilation of Plate 1.

The crustal-scale cross-sections given in Plates 2 & 3 were constructed during the compilation the map (Plate 1). Profile construction led to additional insights that significantly improved parts of the map. Note however, that the deeper portions of the crustal-scale profiles in Plates 2 & 3 are not constrained by geophysical or borehole data.

3. Overview of the major groups of tectono-stratigraphic units

The tectono-stratigraphic units described in detail below define eight groups (Plate 1). Before going into greater details regarding map compilation and individual tectonic units, these groups are briefly introduced.

3.1. Undeformed foreland

The northern and eastern flexural foredeep of the Alps and Carpathians (“External Foredeep”) is variably floored by Va-

riscan, Caledonian or Precambrian basement that is overlain by little or undeformed Mesozoic to Cenozoic sediments. The East European and Scythian platforms were essentially consolidated during Precambrian times. More recently, the Scythian Platform was re-interpreted as the passive margin of the East European craton that was strongly involved in latest Precambrian to Early Paleozoic (pre-Variscan) tectonic events and that was reactivated during younger and less important events (Stephenson et al. 2004; Saintot et al. 2006). The SW boundary of the East European Platform (“Precambrian platform” in Plate 1) coincides with the NW–SE striking Teisseyre-Tornquist Zone that was repeatedly reactivated during Late Paleozoic, Mesozoic and early Cenozoic times (Ziegler 1990). The Pre-Mesozoic basement of areas located to the SW of the Tornquist-Teisseyre Zone consists of an array of essentially Gondwana-derived terranes that were accreted to the margin of the East European craton during the Caledonian and Variscan orogenies (Ziegler 1981, 1990; Pharaoh et al. 2006). The Moesian Platform, for example, underwent significant Variscan deformation and was accreted to the Scythian Platform during the Late Carboniferous (Seghedi 2001). In the process of this, the latter also became overprinted by Variscan deformation (e.g. Zonenshain et al. 1990).

The most external units of the allochthonous East Carpathian Miocene flysch belt partly override the Teisseyre-Tornquist Zone. Following an Early Triassic rifting event, the Moesian Block was probably separated from the Scythian Platform along the SE-most segment of the Teisseyre-Tornquist Zone, only to be re-accreted to it during the Jurassic Cimmerian North Dobrogean orogeny (e.g. Murgoci 1929; Seghedi 2001) that occupies a special position within the Alpine-Carpathian-Dinaridic system (Plate 1). Along the SE-most segment of the Teisseyre-Tornquist Line the Moesian Platform and the North Dobrogea Orogen were welded along the Peceneaga-Camena Fault Zone before the end of the Early Cretaceous (e.g. Murgoci 1915; Hippolyte 2002) when intense tectonic activity along it ceased. Both units are separated by the pre-Neogene Trotus fault from the Scythian Platform (Săndulescu & Visarion 1988).

With respect to the post-Early Cretaceous tectonic activity, the North Dobrogea Orogen, and the Moesian and Scythian platforms are considered as “undeformed foreland”. Only minor reactivation along faults shown by thick black lines in Plate 1 occurred in Miocene-Quaternary times (Tărăpoancă et al. 2003; Leever et al. 2006). The northern fault segment near Bacău (Plate 1), however, is not part of the pre-Neogene Trotus fault, but a Quaternary northern splay of the latter (see Matenco et al. 2007).

The term “Adriatic plate” often refers to the undeformed lithospheric plate or “subplate” (Channell & Horvath 1976) that includes the present day undeformed areas of Istria and the Apulian carbonate platform and is framed by the external thrust belts of Southern Alps, Dinarides and Apennines. This part of the Adriatic plate acted as a rigid indenter during its collisional interaction with the Alpine and Dinaridic orogens to the north and east (Fig. 2c), respectively (e.g. Channell et

al. 1979; Schmid & Kissling 2000; Pinter et al. 2005). However, note that the term “Adria” is also used for denoting the paleogeographical affiliation of structural entities that had originally formed part of a larger Adriatic (or “African/Adriatic”; Channell & Horvath 1976) promontory or micro-continent but later became involved in its fringing folded belts (Dercourt et al. 1986). In this contribution the term “Adria” and “Adriatic” will therefore be used for the broader paleogeographical realm that flanked the Alpine Tethys to the south (“Apulia” in the sense of Schmid et al. 2004a), rather than just for the present-day rigid Adriatic plate. Structural entities that later became incorporated into the Alpine-Carpathian-Dinaridic system will be referred to as “Adria-derived”.

3.2. Miocene external thrust belt:

This thrust belt is the only structural element that extends continuously along the margin of the Alpine-Carpathian orogenic system from the Western Alps through the Western and Eastern Carpathians into the South Carpathians where it ends (Plate 1). In the Carpathians this foreland fold-and-thrust-belt (i.e. Săndulescu et al. 1981a,b; Morley 1996; Matenco & Bertotti 2000; Krzywiec 2001; Oszczytko 2006) formed during the Neogene when the ALCAPA (Alps-Carpathians-Pannonia) and Tisza-Dacia Mega-Units moved to the northeast and east into an eastward concave embayment in the European foreland. Their soft collision with the European foreland (e.g. Balla 1987) was triggered by a combination of lateral extrusion (e.g. Ratschbacher et al. 1991a,b) and, more importantly, by the retreat (roll-back) of a subducting eastern European oceanic lithospheric slab (in the sense of Royden 1988, 1993). Calc-alkaline and alkaline magmatism within the Carpathian arc was closely related to subduction, slab-rollback, slab-detachment and extension in the overriding plate (Nemčok et al. 1998; Wortel & Spakman 2000; Seghedi et al. 2004). In the South Carpathians, where the Miocene fold-and-thrust-belt ends, the inner units of the South Carpathians were juxtaposed with the Moesian Platform during Palaeogene-Miocene time in response to a combination of strike-slip movements along curved fault systems (Plate 1) and by oblique thrusting (Ratschbacher et al. 1993; Răbăgia & Matenco 1999; Fügenschuh & Schmid 2005; Răbăgia et al. 2007).

3.3. Europe-derived units in the Alps and in the “Dacia” Mega-Unit

This rather heterogeneous group of tectonic units denotes allochthonous units, commonly interpreted to have been derived from the European continent. In the Alps these units comprise the Helvetic, Ultrahelvetic and Subpenninic nappes, as well as nappes derived from the continental Briançonnais fragment that broke off Europe (Fig. 2c) in the Early Cretaceous in conjunction with opening of a partly oceanic scar (Valais ocean, e.g. Schmid et al. 2004a). In the Carpathians analogous allochthonous units, but not considered as the direct lateral continuation

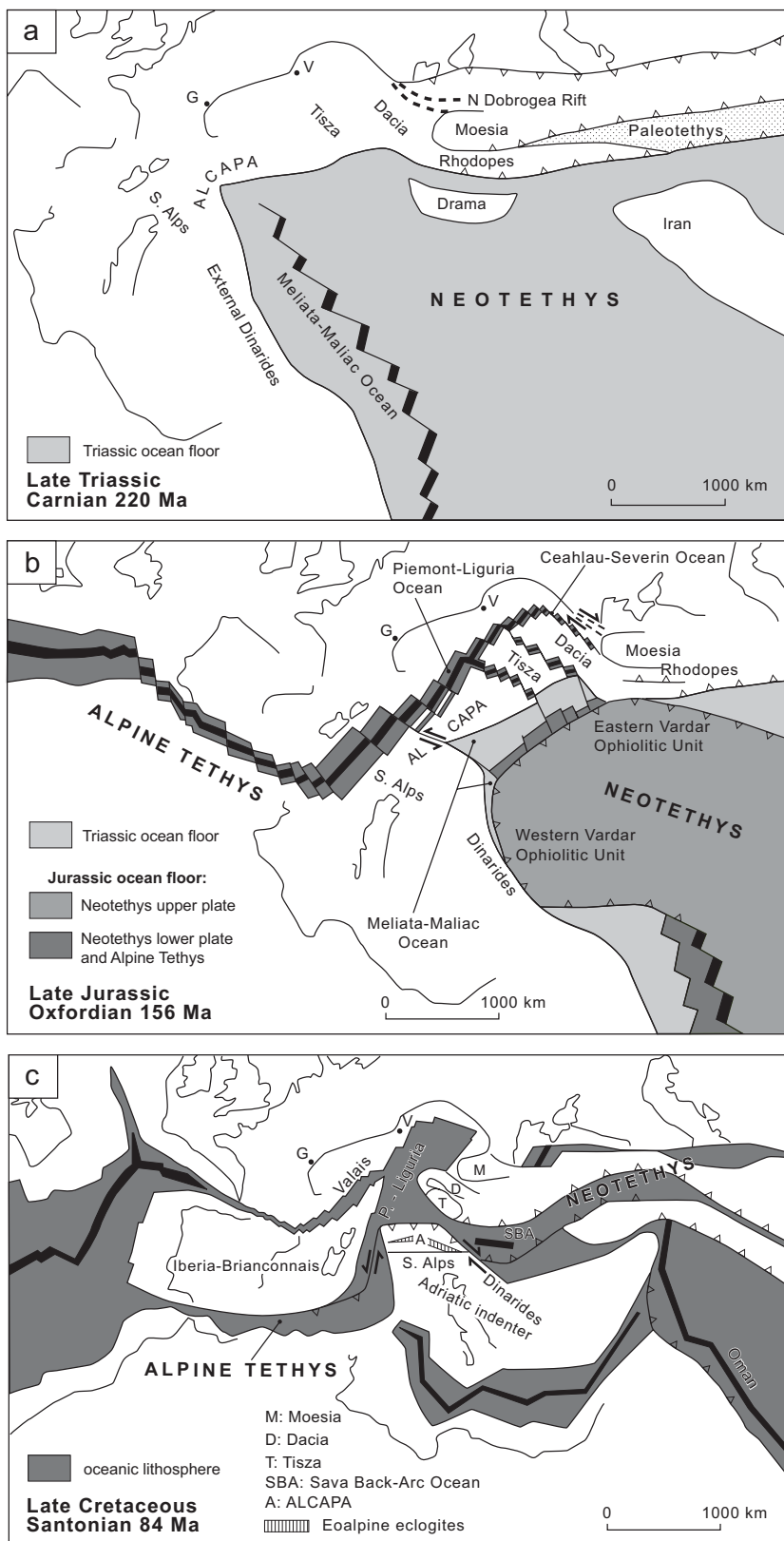


Fig. 2. Schematic palinspastic sketches visualizing concepts presented in the text and incorporating ideas mainly taken from Frisch (1979), Frank (1987), Dercourt et al. (1993), Stampfli (1993), Săndulescu (1994), Stampfli et al. (2001), Marroni et al. (2002) & Schmid et al. (2004a). Positions and projections of the outlines of the European and African continents are those given by Stampfli et al. (2001), except for the coastlines of the Adriatic Sea that we assume to remain firmly attached to the African continent until Cretaceous times. G: Geneva; V: Vienna.

a) Opening of the Neotethyan Meliata-Maliac Ocean in the Triassic (Carnian, 220 Ma).

b) Opening of the Piemont-Liguria Ocean (Alpine Tethys), leading to the separation of the Adria Plate (including the future Southern Alps and ALCAPA), as well as the Tisza and Dacia Mega-Units from the European continent in Oxfordian time (156 Ma). Simultaneously, the Triassic Meliata-Maliac Ocean is being subducted south-eastward below the upper plate Jurassic parts of Neotethys (future Western and Eastern Vardar Ophiolitic Units). The latter are about to become obducted onto the Adria margin, i.e. the future Dinarides, as well as onto the Dacia Mega-Unit.

c) In Santonian times (84 Ma) the two branches of the Alpine Tethys (Valais and Piemont-Liguria Oceans) connect via the Carpathian embayment with younger, i.e. Cretaceous-age branches of Neotethys such as the back-arc ocean that will form the future Sava Zone. Note the onset of northward movement of the Adriatic indenter, contemporaneous with the opening of the East Mediterranean Ocean and the northward drift of Africa.

of their Alpine counterparts, define what is commonly referred to as the Dacia (Fig. 2) Mega-Unit or terrane in the Hungarian literature (e.g. Csontos & Vörös 2004). Parts of this Mega-Unit consist of an assemblage of far-travelled nappes (Infrabucovinian-Getic-Kraishite-Sredna Gora and Serbo-Macedonian-Supragetic-Subbucovinian-Bucovinian-Biharia units; also referred to as Median Dacides by Săndulescu 1994) that were derived from blocks, which were detached from the European margin during Jurassic rifting (Fig. 2b). Whilst oceanic lithosphere of the Ceahlau-Severin Ocean separated parts of these units from Europe, it is unlikely that oceanic lithosphere had separated other units from the European margin. It appears that some nappes, such as the Danubian nappes of the South Carpathians (also referred to as Marginal Dacides; Săndulescu 1994; Krättnér 1996), and units such as the Central Balkan and Prebalkan units of Bulgaria (Georgiev et al. 2001) were directly scraped off the European margin (Moesian Platform; Fig. 1) in response to strong collisional coupling of the orogenic wedge and the foreland (Ziegler et al. 1995).

3.4. Inner Balkanides

While the External Balkanides (Prebalkan, Central Balkan and Sredna Gora units; e.g. Ivanov 1988) can be correlated with other units that form part of Dacia, the Inner Balkanides (“inner” with respect to the Moesian foreland of the Balkanides) form a distinct group of tectonic elements whose origin remains controversial. Two of these units, that are not the focus of our analysis, reach the southern margin of the map of Plate 1. These are: (i) the Strandja Unit (e.g. Georgiev et al. 2001; Okay et al. 2001) that was strongly deformed, metamorphosed and thrust northward during Late Jurassic to Early Cretaceous time and represents a fragment of an older (“Cimmerian”) orogen, located near the Paleotethys-Eurasia-Gondwana triple point, that was later incorporated into the N-vergent Balkan Orogen; (ii) The Rhodope core complex delimited to the north and west by Cenozoic normal and strike-slip faults (e.g. Sokoutis et al. 1993; Kiliyas et al. 1999; Brun & Sokoutis 2007). Its bounding Cenozoic faults post-date Early Jurassic to Cretaceous top-S (SW) nappe stacking and high- to ultrahigh-pressure metamorphism within the gneissic units of the Rhodope Mountains, and they obscure the original relationships of the Rhodope core complex with the neighbouring units (Burg et al. 1996; Turpaud 2006; Perraki et al. 2006; Mposkos & Krohe 2006). The structurally lower unit within the Rhodope core complex possibly represents a terrane (Drama terrane in Fig. 2a) that collided with the rest of the Rhodopian units in Jurassic times along the eclogite-bearing Nestos suture (Turpaud 2006; Bauer et al. 2007).

3.5. Units with mixed European and Adriatic affinities: Tisza

The crustal fragment, which presently constitutes the nappe sequence of the Tisza Mega-Unit, was separated from Europe during the Middle Jurassic (Fig. 2b), presumably in conjunction

with the opening of the eastern parts of the Alpine Tethys (or Piemont-Liguria Ocean; Haas & Pero 2004). With the opening of an ocean between Europe and Tisza, the latter moved into a paleogeographic position comparable to that of the Austroalpine or Southalpine realm. The facies of the post-rift sediments within Tisza, such as radiolarites and pelagic Maiolica-type limestones, exhibits Adriatic affinities; the faunal provinces are of the “Mediterranean” type (e.g. Vörös 1977, 1993; Lupu 1984; Haas & Pero 2004). Much of the tectonic units of Tisza (Mecsek, Bihor and Codru nappe systems) are only exposed in isolated and rather small inselbergs within the Pannonian plain (i.e. Mecsek nappe system in the Mecsek Mountains in Hungary; Haas 2001). A coherent nappe sequence is only present in the North Apuseni Mountains of Romania (Bihor and Codru nappe systems; Balintoni 1994). The tectonically highest and most internal nappe system of the North Apuseni Mountains is the Biharia nappe system (Balintoni 1994), traditionally considered as a constituent of Tisza (Csontos & Vörös 2004), i.e. the Internal Dacides (Săndulescu 1984; Balintoni 1994). However, we correlate this Biharia nappe system with the Bucovinian nappes (Plate 1) and hence attribute it to Dacia (i.e. the Median Dacides in the sense of Săndulescu 1984) for reasons discussed later.

3.6. Adria-derived far-travelled nappes of the internal Alps and the West Carpathians (ALCAPA Mega-Unit):

This group of tectonic elements is referred to as the Austroalpine nappes in the Alps (e.g. Schmid et al. 2004a) and as the Central and Inner West Carpathians in the Carpathians (e.g. Plašienka et al. 1997a,b). In the Alpine literature these elements are often referred to as being derived from Adria (or “Apulia” in the sense of Schmid et al. 2004a). In the Alps this implies that their initial paleogeographical position was to the south of the Piemont-Liguria Ocean, the main branch of the Alpine Tethys (Fig. 2b). Presently, these elements represent far-travelled thin crustal slices found in an upper plate position above the Upper Penninic (or Vahic in case of the West Carpathians) suture zone and the underlying Europe-derived elements of the Alps and West Carpathians.

Note, however, that the notion of Adria as a single paleogeographic entity becomes problematic in the easternmost Alps and the adjacent Carpathians and Dinarides owing to the occurrence of branches of a second group of oceanic realms that formed part of the so-called “Neotethys” (e.g. Haas 2001). Neotethys formed an eastward opening oceanic embayment in the Adria paleogeographical realm that had opened during Triassic times (Fig. 2a) and is referred to as Meliata Ocean in the Alps and Carpathians (i.e. Channell & Kozur 1997), but as Maliac Ocean in the Hellenides (e.g. Stampfli & Borel 2004). Hence the Austroalpine nappes and their extension into the West Carpathians include tectonic elements that were positioned north, west and south of the Meliata-Maliac Ocean (Fig. 2; Schmid et al. 2004a). Sea-floor spreading continued in Neotethys during the Jurassic, but the connections between the various oceanic

realms formed in Jurassic times with those of the Alpine Tethys are not yet properly understood; Figure 2 merely represents an attempt to satisfy the data compiled in this work.

3.7. *Adria-derived thrust sheets: Southern Alps and Dinarides*

The units that comprise parts of the Adria paleogeographic realm presently located south of the Periadriatic Line and its eastern continuation (Balaton Line), i.e. south of the ALCAPA Mega-Unit, constitute the Southern Alps and all the non-ophiolitic tectonic units of the Dinarides, including a fragment dislocated along the Mid-Hungarian Fault Zone (Bükk Mountains of Northern Hungary). During the Triassic these units were also located south (or rather southwest, Fig. 2a) of the Meliata Ocean, and thus they were derived from the northern passive margin of Adria that faced the Meliata-Maliac-Vardar branch of Neotethys. In our view the Drina-Ivanjica, Korab-Pelagonian, Bükk, Jadar and Kopaonik “terranes” or “blocks” (e.g. Dimitrijević 2001; Karamata 2006) all represent units that structurally underlie remnants of what we refer to as Vardar Ocean in this contribution, i.e. Neotethyan ophiolites of Jurassic age that were obducted onto the Adria margin during the Late Jurassic (Fig. 2b). Presently, the most external northern Dinaridic units are separated from the Southern Alps by the eastward continuation of a south verging dextrally transpressive thrust front, which formed at a late stage (Mio-Pliocene) in the tectonic history of the Alpine-Carpathian-Dinaridic system. From northeastern Italy and Slovenia we trace this transpressive thrust front into Hungary as far to the east as south of lake Balaton (Plate 1).

In summary, this group of units was derived from continental crustal domains located far to the south of the Alpine Tethys, and even south (or southwest in case of the Southern Alps) of the Neotethys (Fig. 2). Note that many of the detached units of this group overlie an autochthonous basement that is presently still associated with its lithospheric underpinnings (Schmid et al. 2004b); they thus represent deformed parts of the present-day Adriatic plate.

3.8. *Ophiolites and accretionary prisms*

This group of tectonic units is characterized by ophiolitic and/or flysch-type rock associations and is extremely heterogeneous. It comprises tectonic elements, some of which can be traced along strike over long distances; they often define important sutures and/or important mobile zones between and occasionally also within the above described groups of tectonic elements.

Here we will use the term “ophiolite” in a wider sense, that is we do not restrict the term to rock associations formed at mid-ocean ridges. We also include other types of magmatic and sedimentary rock associations that are indicative of the presence of former oceanic lithosphere. Hence we include, for example, supra-subduction ophiolites and/or subduction-related volcanic arc rocks that developed within pre-existing oceanic crust (see discussion on ophiolite models in Robertson 2002). Moreover, we use the term “ocean” as denoting paleo-

graphic domains we suspect to have been floored by oceanic rather than continental lithosphere.

It is important to realize, however, that in some cases the ophiolites were obducted as thrust sheets and hence do not mark the location of a deeper suture zone (e.g. Western Vardar Ophiolitic Unit of Plate 1). Others (e.g. the remnants of the Meliata-Maliac Ocean) are only found as blocks within mélange formations beneath coherent ophiolitic thrust sheets such as the Western Vardar Ophiolitic Unit that were obducted during the Late Jurassic (Fig. 2b). Some ophiolitic mélange and obducted ophiolites became subsequently involved in the development of composite thrust sheets or nappes, consisting of continental units and previously obducted ophiolites that formed by out-of-sequence thrusting during Cretaceous and Cenozoic orogenic cycles.

The interrelationships between individual elements of this group of tectonic units still remain uncertain in many cases. This is due to a poor understanding on how Miocene deformations and even more so Palaeogene and Cretaceous deformations and translations ought to be retro-deformed. In this sense, all existing paleogeographic reconstructions for the Alpine-Carpathian-Dinaridic area for Triassic, Jurassic or Cretaceous times, of course including those presented in Fig. 2, must be regarded as purely speculative.

These uncertainties necessitate the continued use of many regional or local names for these ophiolitic and/or accretionary wedge units (see discussion by Zacher & Lupu 1999). Nevertheless, we find it convenient to use the terms Alpine Tethys and Neotethys in order to denote two groups of oceans that began to open in Permian (?) to Mesozoic times in conjunction with the break-up of Pangaea (e.g. Stampfli & Borel 2004).

We use the term “Alpine Tethys” collectively for all oceanic realms in the Alpine-Carpathian domain, the opening of which was kinematically directly linked to sea-floor spreading in the Central Atlantic (Figs. 2b and 2c) that was initiated in late Early Jurassic times (Favre & Stampfli 1992). The term “Neotethys” is used for all oceanic realms located in an area southeast of the Alpine Tethys and the future Western Alps that opened during and after the Permian to Triassic closure of Paleotethys, which at the end of the Variscan orogeny had still separated Gondwana and Laurussia (e.g. Stampfli & Borel 2004). Opening of the oceanic Neotethys basins was neither temporally nor kinematically linked to the opening of the Alpine Tethys. In contrast to the Alpine Tethys, parts of Neotethys were consumed in the context of obduction during Late Jurassic times (Fig. 2b), with a kinematic link to the opening of the Central Atlantic (e.g. Dinaridic ophiolites; Laubscher 1971; Pamić et al. 2002a), while others opened later during the Cretaceous (Sava Back-Arc Ophiolites of Fig. 2c). Yet it is debatable whether during the Jurassic the oceanic realms of the Alpine Tethys and Neotethys were completely separated or linked somewhere in the Alpine-Carpathian-Dinaridic realm (as proposed in Fig. 2b). However, we will present arguments to propose that Cretaceous-age oceanic branches of Neotethys (such as the Sava Back-Arc Ocean,

Fig. 2c) were directly linked with the Alpine Tethys along the present-day Sava-Zone mapped in Plate 1.

We attribute the following oceanic basins to the Alpine Tethys: (i) The Valais, Rhenodanubian and Magura flysch units forming a northern branch (Schnabel 1992; Plašienka 2003; Schmid et al. 2004a), and (ii) the Piemont-Liguria-Vahicium-Pieniny Klippen Belt (Birkenmajer 1986; Plašienka 1995a) units defining a southern branch. Both branches were at least partly separated by the continental Briançonnais fragment of the Western Alps (Frisch 1979; Stampfli 1993) and possibly by smaller analogous units found as relics in the Pieniny Klippen Belt of the West Carpathians (Birkenmajer 1986; Trümpy 1988) that probably were not directly linked with the Briançonnais.

According to our interpretation the Magura Flysch and the Piemont-Liguria-elements of the Alpine Tethys can be traced SE-ward via the Iňačovce-Kriscevo Unit of Eastern Slovakia and the Ukraine (Soták et al. 1993, 1999) into the flysch units referred to as the Pienides of northern Romania (Săndulescu et al. 1981a). In map view, the latter form a tight E-verging arc (Plate 1) and were thrust onto the Tisza-Dacia Mega-units during Miocene times (Fig. 3; Tischler et al. 2007). We propose to connect the Pienides with the Szolnok Flysch in the subsurface of the Pannonian Basin. The ophiolitic Szolnok Flysch belt (“ophiolite-bearing Intrapannonian belt” of Channell et al. 1979) can be traced westward along the Mid-Hungarian Fault Zone towards Zagreb where it links up with the ophiolite-bearing Sava Zone (Plate 1). This zone consists of a belt of ophiolitic (relics of the Sava Back-Arc Ocean, Fig. 2c), magmatic and metamorphic rocks that extends SE-ward from Zagreb to Belgrade (“North-western Vardar Zone” of Pamić 1993; “Sava-Vardar Zone” of Pamić 2002). The Sava Zone defines the Late Cretaceous to Palaeogene suture between Tisza and the Dinarides. Between Zagreb and Belgrade this Sava Zone connects the SE branch of the Alpine Tethys with the Cretaceous-age branches of Neotethys further to the southeast (Fig. 2c). At present the Sava Zone, located between the Western and Eastern Vardar Ophiolitic Units (see Plate 1), represents the suture between the Dinarides and the Tisza-Dacia Mega-Units. The latter are derived from older branches of Neotethys.

The narrow, possibly only partly oceanic Ceahlau-Severin rift opened during Middle to Late Jurassic times (e.g. Ștefănescu 1995; Fig. 2b). Hence it is considered as the easternmost branch of the Alpine Tethys rather than a branch of Neotethys. Note, however, that in present-day map view (Plate 1) it does not directly connect with the easternmost branch of the Alpine Tethys of the Western Carpathians in Northern Romania and adjacent Ukraine, nor does it link up with the Transylvanian branch of the Eastern Vardar Ophiolitic Unit. Westward, units attributed to the narrow Ceahlau-Severin Ocean join the Magura Flysch Unit (Plate 1) that in Miocene times was thrust towards the SE (Fig. 3; Tischler et al. 2007) and that connects with the Mid-Hungarian Fault Zone (see above). Southward, the Ceahlau-Severin Ophiolitic Unit, which is well exposed in the South Carpathians, eventually appears to wedge out in western Bulgaria and eastern Serbia; no equivalents of this narrow

ocean have been ascertained in the Balkan Orogen. Figure 2b depicts two additional eastern branches of the Alpine Tethys, which are proposed to kinematically connect with the Triassic Neotethys Ocean and whose opening led to the separation of the Dacia and Tisza blocks from Europe. The relics of the branch between the Dacia and Tisza Mega-Units (Fig. 2b) will form the suture between the Dacia and Tisza Mega-Units in Early Cretaceous times, only preserved in the subsurface (see Plate 3, Profile 3). The branch between the Tisza and ALCAPA Mega-Units (Fig. 2b) forms part of the Mid-Hungarian Fault Zone (Fig. 1, Plate 1), i.e. the “ophiolite-bearing Intrapannonian belt” of Channell et al. (1979).

In the Alpine-Carpathian-Dinaridic system of orogens the westernmost branch of Neotethys (Fig. 2a) is known as the Meliata Ocean (Kozur 1991) that had opened earlier, i.e. in Triassic times (e.g. Velledits 2006). However, in our area, the ophiolitic remnants of the Meliata-Maliac Ocean do not form coherent thrust sheets, but are only preserved as blocks contained in Mid to Late Jurassic-age ophiolitic mélange formations. Such mélange formations occur in the Eastern Alps and West Carpathians (Kozur & Mostler 1991). Remnants of this same Meliata-Maliac Ocean are also found as blocks in Jurassic mélange formations that immediately underlie the obducted Western Vardar ophiolites in the Bükk Mountains (Monosbel nappe of Csontos 1999, 2000) and in the Dinarides (ophiolitic mélange formations; e.g. Babić et al. 2002). In the Dinarides these mélange formations are also referred to as “Diabas-Hornstein” (Kossmat 1924), “Diabase-Radiolarite” Formation (Ćirić & Karamata 1960) or “wildflysch with ophiolitic detritus” (Laubscher & Bernoulli 1977). Note that all obducted ophiolitic thrust sheets, which overlie these ophiolitic mélange formations, as seen in the Bükk Mountains (Darno-Szavarskö ophiolites; Csontos 2000) and Dinarides (Western Vardar Ophiolitic Unit; e.g. Pamić et al. 1998; Dimitrijević 2001; Karamata 2006), consist of Jurassic age ophiolites. We suggest that these Jurassic Western Vardar ophiolites, together with the Triassic Meliata-Maliac ophiolites, once formed part of one and the same Neotethyan oceanic branch before obduction began (Fig. 2b), i.e. before Mid-Jurassic times. During the latest Jurassic to Early Cretaceous the young (Early to Mid-Jurassic) Western Vardar Ophiolitic Unit was obducted onto the passive continental margin of Adria, the ophiolite mélange formation defining the tectonic contact zone.

The Eastern Vardar Ophiolitic Unit extends into the South Apuseni and Transylvanian ophiolite belt and represents another part of the Meliata-Maliac-Vardar Neotethys (Săndulescu 1984) that was probably obducted onto the European Margin (Dacia Mega-Unit, Fig. 2b). Its original location with respect to that of the Western Vardar ophiolites is still enigmatic. We emphasize that the Eastern Vardar ophiolitic belt does not extend along the Sava Zone towards Zagreb. Hence, the Eastern Vardar Ophiolitic Unit does not form part of the Dinarides. Instead, it is now the most internal, structurally highest tectonic element on top of the Dacia Mega-Unit. In turn this implies that the Eastern Vardar ophiolites cannot be linked with the

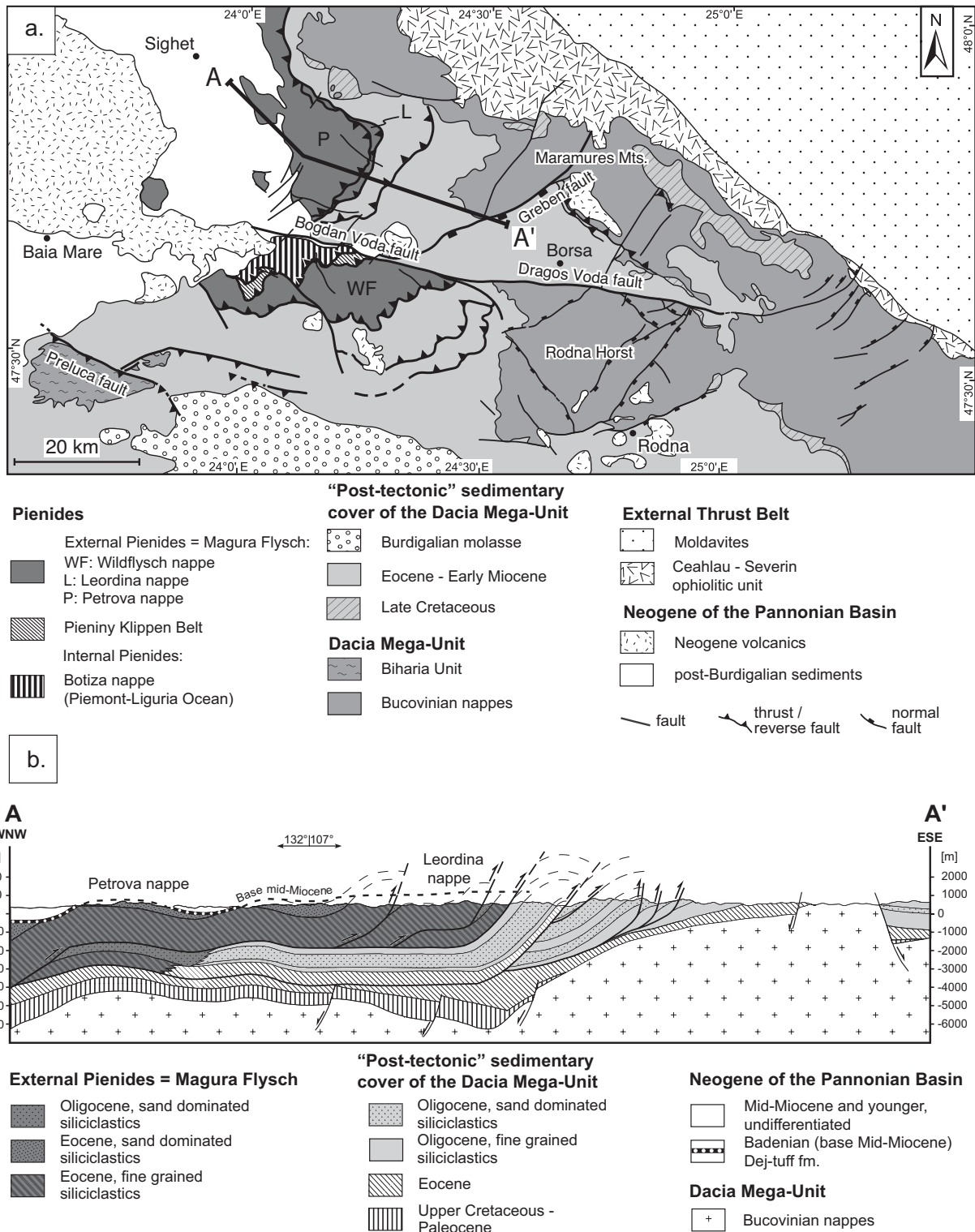


Fig. 3. Map (a) and cross-section (b) through the contact area between the ALCAPA and the Tisza-Dacia Mega-Units in Northern Romania (Maramures) after Tischler (2005) and Tischler et al. (2007). The Pienides of the Maramures area in Northern Romania form a tight arc in map view and were thrust onto the Tisza-Dacia Mega-units during Miocene times.

Alpine Tethys around the western margin of Tisza, nor do they extend E-ward into the North Dobrogea Orogen. In the south, i.e. between Beograd and Skopje, the Neotethyan Western and Eastern Vardar Ophiolitic Units parallel each other but are separated by a narrow band of the Sava Zone that, in our view, represents a suture zone between the Dinarides and the Tisza-Dacia Mega-Units which, in the Late Cretaceous, included their earlier obducted ophiolite sheets (Plate 1).

We conclude (1) that none of the branches of the Alpine Tethys and of Neotethys extends eastward into the North Dobrogea Orogen, although such connections have been proposed by many paleogeographic reconstructions (e.g. Stampfli & Borel 2004). The Triassic North Dobrogea rift (i.e. the Niculitel Zone; Savu et al. 1977; Seghedi 2001), which formed during a Permo-Triassic rifting event that affected also central Moesia, dies out rather rapidly northwestward (see review by Tari et al. 1997). We propose (2) that the ophiolitic remnants of Neotethys (the Triassic-age Meliata-Maliac ophiolites and the Jurassic-age Vardar ophiolites) occurring in the area of consideration formed part of one and the same Meliata-Maliac-Vardar oceanic basin. We will show later that there is no evidence for the existence of a “Pindos Ocean” and thereby accept the “one-ocean hypothesis” first formulated by Bernoulli & Laubscher (1972). We are convinced (3), that the different branches of Tethys found in the Alpine-Carpathian-Dinaridic system can only be followed eastward via the Dinarides and Hellenides into Turkey, but not into the Cimmerian system of the Black Sea to the north.

4. Detailed description of individual tectonic units of the Alps, Carpathians and Dinarides

This section provides the most important sources used for defining tectonic units and constructing the map (Plate 1). Moreover, a more detailed overview of all the tectonic units is presented and supported by a series of crustal-scale cross-sections (Plates 2 & 3). Names of tectonic units listed in the legend of Plate 1 are given in bold letters. The Alps will not be treated in detail (see Schmid et al. 2004a for a comprehensive review). We provide a relatively more comprehensive overview of the Dinarides since they are the least known part of the system.

4.1. The Miocene fold-and-thrust belt of the Alps and Carpathians

The Cretaceous and Cenozoic flysch units of the external Carpathian fold-and-thrust belt underwent most, though probably not all their total shortening during Miocene times. Deformation progressively migrated towards the foreland (Săndulescu et al. 1981a,b; Roca et al. 1995; Morley 1996; Zweigel et al. 1998; Matenco & Bertotti 2000).

The Neogene evolution of this flysch belt was mainly driven by the retreat of the Alpine Tethys subduction slab into the Carpathian embayment (Royden 1988). Prior to the Late Cretaceous onset of subduction, this embayment was occupied by Late Jurassic to Early Cretaceous oceanic lithosphere of the

Alpine Tethys that was attached to the European continent (Balla 1987; Fig. 2c). Subduction of this oceanic lithosphere started from the Late Aptian to Albian onwards. Its covering Late Jurassic – Early Cretaceous sediments were scraped off, forming the Ceahlau/Severin nappe that was emplaced about 75 Ma ago (“Laramide” emplacement of the Ceahlau-Severin Ophiolitic Unit; e.g. Săndulescu et al. 1981a,b). There are several popular models such as slab detachment (e.g. Wortel & Spakman 2000; Sperner et al. 2005; Weidle et al. 2005), slab delamination (e.g. Girbacea & Frisch 1998; Gvirtzman 2002; Knapp et al. 2005), or thermal re-equilibration of the lithosphere (e.g. Cloetingh et al. 2004) that have been proposed to explain the evolution of this subduction and its present-day expression as a near vertical high velocity mantle anisotropy beneath Vrancea (e.g. Martin et al. 2006). Whatever model is adopted, all of them invoke a Miocene retreat of the subducted oceanic slab as the principal driving force for the final emplacement of the continental ALCAPA and Tisza-Dacia Mega-Units that occupy the internal parts of the Carpathian loop.

The Carpathian thrust belt consists mainly of flysch units in its inner part and grades outward into progressively more shallow-water strata, the most frontal thrusts involving the inner parts of the Carpathian foredeep. The most internal thrusts were emplaced in Late Cretaceous time whereas the external thrusts are of Neogene age. The age of the youngest thrust deformation at the front of this fold-and-thrust belt decreases from the West Carpathians (ca. 18 Ma) towards the Polish and Ukrainian Carpathians where the latest movements are dated as Late Miocene (ca. 12 Ma; Krzywiec 2001). Further to the SE and S along the entire East Carpathians to the bending zone north of Bucharest the age of the youngest thrusts remains constant at around 11 Ma, though the amount of shortening accomplished across them increases significantly in the Romanian segment (Roure et al. 1993; Dicea 1995; Matenco & Bertotti 2000; Krzywiec 2001). This was partly accommodated in the internal parts of the Carpathians by coeval late-stage sinistral strike-slip motion along the contact between ALCAPA and Tisza-Dacia (e.g. Tischler et al. 2007). The external flysch belt in the East Carpathians is completely allochthonous and contains sediments formerly deposited on continental or oceanic crust of the Carpathian embayment. However, these sediments, which are incorporated in the Miocene-age nappe sequence, do not contain any detritus from an oceanic basement (e.g. Săndulescu 1988). Hence the hypothesis that parts of the Carpathian embayment were underlain by oceanic crust (e.g. Balla 1987) remains speculative.

The external Carpathian fold-and-thrust belt consists of three nappes or thrust systems, some of which can be traced all the way along strike. These nappe systems are best developed in the East Carpathians where they are referred to as the Moldavides (Săndulescu 1994).

The external-most tectonic unit consisting of Middle Eocene to Late Miocene sediments, the *thrust internal foredeep*, is called Subcarpathian nappe in the East Carpathians (Săndulescu 1981a,b; Dicea 1995). This unit, which is thrust over

the undeformed sediments of the Carpathians foreland, i.e. the external foredeep (Plate 3, Profile 3), can be traced north along strike into Ukraine where it wedges out between external foredeep and more internal thrust sheets (e.g. Kováč et al. 1999; Oszczytko 2006). In the foreland of the Romanian Carpathian bend zone and the South Carpathians this unit is partly buried beneath the latest Miocene-Pliocene (post-11 Ma), essentially undeformed sediments of the Dacic Basin (e.g. Jipa 2006) (Plate 2, Profile 4). The depocenter of these sediments is located near the town of Focsani ("Focsani Depression"; Tărăpoancă et al. 2003).

The Cenozoic Dacic basin forms the western branch of the larger and endemic Eastern Paratethys basin that was isolated from the Mediterranean and World Ocean since the beginning of the Oligocene in response to orogenic uplift of the Alpine-Carpathian-Tauride Caucasus domains (e.g. Rögl 1999). Parts of the Dacic basin, located between the Intramoesian and Trotus/Peceneaga-Camena Faults, were inverted during the Quaternary by folds and reverse faults involving the lower plate of the Eastern Carpathian thrust system; this led to the development of the synclinal configuration of the Focsani Depression (Plate 3, Profile 3; see also Leever et al. 2006).

In the South Carpathians foreland, the most internal and deformed part of the foredeep is referred to as Getic Depression. Although its latest Cretaceous to Late Miocene sediments are buried beneath the post-tectonic cover of the Dacic basin, subsurface data show that these were thrust over the Moesian foreland (Motaş & Tomescu 1983; Săndulescu 1988) (Plate 2, Profile 4). During the progressive N-, NE-, E- and ESE-ward transport of the Tisza-Dacia Mega-Units around Moesia, the Getic Depression was dominated by dextral strike-slip displacements. However, the total amount of Cenozoic shortening in the East Carpathians (<160 km; Ellouz et al. 1994) was largely accommodated within the South Carpathians (Fügenschuh & Schmid 2005; Răbăgia et al. 2007) rather than by shortening within the sediments of the Getic Depression. Palaeogene orogen-parallel extension within the South Carpathians (Schmid et al. 1998) was followed by Palaeogene to Early Miocene dextral movements and transtension along curved faults systems such as the Cerna-Jiu and Timok faults (Berza & Drăgănescu 1988; Ratschbacher et al. 1993; Krätner & Krstić 2002, 2006). For this reason it is suspected that the predominantly Miocene-age shortening in the East Carpathians may have already started in Palaeogene times and that Middle to Late Miocene transpression and thrusting of the internal foredeep over Moesia is only of secondary importance (Răbăgia & Matenco 1999).

The *Marginal Folds* and *Tarcau* thrust system makes up the middle of three major Neogene thrust systems of the East Carpathians and involves Early Cretaceous to Early Miocene flysch series. Towards the SW the amount of shortening across this thrust system decreases and is gradually transformed into limited transpressional deformations where it merges into the South Carpathians (Plate 1). To the west of the bending area this thrust system wedges out completely and is missing in the South Carpathians where transpression was absorbed in the

Subcarpathian nappe (Ştefănescu et al. 2000; Matenco et al. 2003). Northwards, these two units are traced into the *Skole* Unit of Poland (e.g. Oszczytko 2006) where this intermediate thrust system wedges out to the west.

Only the oldest and most internal thrust system of the Carpathian Miocene fold-and-thrust belt can be followed all along the East and West Carpathians into the Alps. In the East Carpathians it consists of, from external to internal, of the *Audia*, *Macla* and *Convolute Flysch* units that contain Late Cretaceous to Palaeogene strata (Săndulescu 1981a,b). These units gradually wedge out westward in the South Carpathians where they record SE-directed thrusting. Their internal geometry indicates associated strike-slip movements (Matenco & Bertotti 2000). Northwards, these units can be correlated with the external *Subsilesian*, intermediate *Silesian* and internal *Dukla* units of the Polish West Carpathians (Morley 1996; Kováč et al. 1999) that comprise Late Jurassic to Miocene sediments (Oszczytko 2006). Further west, in Slovakia, where the Dukla Unit is tectonically covered by the Magura Flysch Unit (Plate 2, Profile 2), the Silesian and Subsilesian Units can be traced westward into the Czech Republic (Zdanice Unit; Picha & Stranik 1999) and finally into the Waschbergzone of the easternmost Alps ("Molasse Zone" of Wessely 1987 in Profile 1 of Plate 2). Further westwards this unit wedges out. The Subalpine Molasse thrust slices of the Alps in western Austria and Switzerland were also mapped as part of this thrust system. Note, however, that in terms of basin evolution and tectonic position these Molasse sediments have little in common with their counterparts in the Eastern Alps and Carpathians.

4.2. Alps and West Carpathians (ALCAPA Mega-Unit)

4.2.1. What is ALCAPA?

The term ALCAPA (Alps-Carpathians-Pannonia) as defined by Csonotos & Vörös (2004) stands for a tectonic mega-unit that includes the Eastern Alps, the West Carpathians and the Transdanubian ranges north of Lake Balaton. The Miocene fill of the Pannonian Basin separates these three major areas of older rock exposures from one another. We mapped the exact boundaries of ALCAPA as follows on Plate 1:

The contact between the Rhenodanubian and Magura flysch units along with the Miocene flysch fold-and-thrust belt delimits the northern boundary of this Mega-Unit, which underwent a combination of lateral escape, thinning and subsidence during the Miocene evolution of the Pannonian Basin in Miocene times (Ratschbacher et al. 1991a,b; Horvath et al. 2006). The Periadriatic Line and its eastern extension, the Balaton Line (Fodor et al. 1998), that were active during this escape, define the southern boundary of ALCAPA all the way to Lake Balaton. The Balaton Line was delineated according to the compilation of subsurface data provided by Haas et al. (2000). Further east, we define the southern boundary of ALCAPA according to subsurface data provided by Csonotos & Nagymarosy (1998) and Fülöp & Dank (1987). However, and in contrast to the us-

age of the term ALCAPA by previous authors, we exclude the Bükk Mountains from this Mega-Unit. The principal reason is that the Bükk Mountains can nowadays be considered as a piece of the Dinarides (Kovács et al. 2000, 2004; Dimitrijević et al. 2003; Velledits 2006) rather than part of the Alpine-West Carpathian chain. The Bükk Mountains were displaced within the Mid-Hungarian Fault Zone (Tischler et al. 2007), a broader fault zone that is delimited to the south by the Mid-Hungarian Line (Csontos & Nagymarosy 1998), or “Zagreb-Zemplin Line” (Haas et al. 2000), and to the north by the eastern continuation of the Balaton Line. Consequently, we let the southern boundary of ALCAPA coincide with the southern part of the Darno Line and further eastwards with the Nekésény Fault (Haas 2001; see Fig. 1). These fault zones separate the Bükk Mountains from two inselbergs that we consider as part of the Inner West Carpathians (Uppony and Szendrő Mountains of NW Hungary; see Haas 2001, his Figs. 78 & 106). The eastern tip of ALCAPA extends into Northern Romania where it was identified from subsurface and field data (Săndulescu et al. 1978, 1993; Kováč et al. 1995; Tischler et al. 2007).

4.2.2. Europe-derived units within ALCAPA

In Plate 1, and regarding the Alps, we grouped the Helvetic and Ultrahelvetic cover nappes including the External Massifs (*Helvetic*) together with the *Subpenninic* nappes. The term “Subpenninic” denotes pre-Mesozoic basement units, on which the sediments now exposed in the Helvetic and Ultrahelvetic nappes were originally deposited, as well as more distal parts of the European upper crust, and its metamorphic cover, as exposed in the Tauern window (Schmid et al. 2004a; see Fig. 1). The most internal Europe-derived nappes are paleogeographically assigned to the *Briançonnais*, a crustal block that was detached from the European passive margin during the Early Cretaceous opening of the Valais branch of the Alpine Tethys (Fig. 2c; Frisch 1979; Stampfli 1993). The easternmost Briançonnais nappes are exposed in the Engadine window (Fig. 1).

However, according to our interpretation Subpenninic units extend in the subsurface much further to the east. For instance Subpenninic units, referred to as “Penninic” in the crustal-scale profile across the easternmost Alps by Tari (1996), are needed to fill the space between the base of ophiolitic nappes attributed to the Alpine Tethys (as exposed nearby in the Rechnitz window) and the Moho (Plate 2, Profile 1). However, we suspect the presence of such Subpenninic units in the subsurface also further to the east, namely in the West Carpathians (Plate 2, Profiles 1 & 2). Information on the deep structure of the West Carpathians is provided by a seismic transect presented by Tomek (1993) who assigned a large rock volume below the Alpine Tethys suture (Vahicum; Plašienka 1995a,b) to the Briançonnais. Yet, as the Briançonnais paleogeographic domain proper terminates west of the Tauern window (Schmid et al. 2004a), except for some small analogous crustal slivers found in the Pieniny Klippen Belt of the West Carpathians (Birkenmajer

1986; Trümpy 1988), we prefer to attribute this rock volume to the distal European margin, that is, to the Subpenninic units.

A direct comparison of the profiles across the Eastern Alps and West Carpathians (Plate 2, Profiles 1 & 2) highlights an important difference pertaining to the northern boundary of ALCAPA, which is only evident in cross sections. In the profile across the easternmost Alps (Plate 2, Profile 1) the basement of the undeformed European foreland is traced along a gently inclined thrust at the base of the Alpine accretionary wedge far to the south into the area of the Hungarian Plain (Tari 1996). By contrast, the profile through the West Carpathians (Plate 2, Profile 2) depicts a steeply dipping dextral strike-slip zone in the depth projection of the Pieniny Klippen Belt according to our interpretation. This crustal-scale sinistral strike-slip fault zone was active during the Miocene and formed the northern boundary of the ALCAPA Mega-Unit (Central and Inner West Carpathians) during its eastward escape (i.e. Nemčok 1993; Sperner et al. 2002). It thus post-dates nappe emplacement in the Inner West Carpathians. The northern parts of Profile 2 (Plate 2) suggest that the European foreland crust was imbricated (modified after Roca et al. 1995) during the transpressional emplacement of ALCAPA and the development of the Miocene West Carpathian fold-and-thrust belt. In this process the Outer West Carpathian Magura Flysch Unit was imbricated and accreted to ALCAPA whilst severe late-stage Miocene NNE-SSW-directed back-thrusts affected the more internal units in the High Tatra Mountains (Plate 2, Profile 2) (Sperner et al. 2002).

4.2.3. Remnants of the Alpine Tethys in ALCAPA

Most authors accept the existence of two branches of the Alpine Tethys, the *Piemont-Liguria* and *Valais* Oceans, respectively. However, this division can only be made where remnants of the intervening Briançonnais micro-continent are present. This is no longer possible east of the Engadine window. Hence, at first sight a paleogeographic separation of the Alpine Tethys into two separate branches (Froitzheim et al. 1996; Schmid et al. 2004a) becomes redundant in the Eastern Alps (see discussion in Kurz 2005 and Schmid et al. 2005) where these branches apparently merged into one single oceanic basin. Nevertheless, we make a distinction between the eastern equivalents of these two branches since an evaluation of the timing of accretion of these oceanic units (Late Cretaceous vs. Cenozoic) to the Austroalpine, respectively to the West Carpathian Tatric-Veporic-Gemic upper plate, is an important criterion for distinguishing between the equivalents of the two branches of the Alpine Tethys east of the Engadine window (for additional criteria see discussion in Schmid et al. 2005). Consequently, we correlate the Valais Ocean with the *Rhenodanubian Flysch* since accretion of both units to the Alpine nappe sequence occurred in Eocene times. The lateral equivalent even further east and in the West Carpathians is the *Magura Flysch* accreted to the Tatric-Veporic-Gemic orogenic wedge during Late Oligocene to Miocene times.

The **Pieniny Klippen Belt** (Birkenmajer 1986) was mapped separately (Plate 1) because it represents a rather peculiar, sub-vertical and narrow structural unit at the surface (Plate 2, Profile 2). It forms the boundary between Outer and Central West Carpathians for some 700 km from the St. Veit Klippen near Vienna to northern Romania. This belt typically consists of relatively erosion-resistant non-metamorphic blocks of Mesozoic strata of many different facies surrounded by less competent Late Cretaceous to Palaeogene marlstones and flysch. Only small parts of this belt, that were derived from the pelagic Kysuca-Pieniny Basin, hint to the former presence of a now completely subducted eastern continuation of the Piemont-Liguria Ocean, referred to in the West Carpathians as the **Vahic** Ocean (Plašienka 1995a, 2003). Southward subduction of the Vahic oceanic crust started in the Senonian (Plašienka 1995a,b). This ocean was located south of sedimentary rocks assigned to the Czorsztyn Ridge, the second major constituent of the Pieniny Klippen Belt that probably represents an eastern equivalent of the Briançonnais continental block (Birkenmajer 1986). It is important to emphasize that pebbles of Jurassic-age blueschists, thought to be derived from the Pieniny Klippen Belt (Dal Piaz et al. 1995), were not encountered in primary deposits, but were found as recycled components in the Gosau-type sediments of the Klappe Unit (“Periklippen Zone”; Ivan et al. 2006). This unit is not considered as forming part of the Pieniny Klippen Belt s.str., but as a displaced fragment of the Central West Carpathians (Plašienka 1995b). Hence these blueschist pebbles more likely originated from the Meliata-Maliac oceanic domain which crops out further to the south in the Central and Inner West Carpathians (see below) and which is not part of the Alpine Tethys.

In contrast to the Alps, in which ophiolitic nappes derived from the Piemont-Liguria Ocean are well exposed (Schmid et al. 2004a), remnants of the Vahicum that represents the eastern extension of the latter do not outcrop, except for very small tectonic windows some 10 km south of the Pieniny Klippen Belt (Belice Unit exposed in the Považský Inovec Mountains; see Plašienka 1995a,b for details). Based on seismic data (Tomek 1993), we suspect, however, that in the Central West Carpathians remnants of the Vahicum separate the Tatricum from suspected Subpenninic elements at depth (Plate 2, Profile 2). In Eastern Slovakia and Ukraine boreholes have reached, in the subsurface of the East Slovak basin, the **Iňačovce-Kriscevo** Unit that includes some serpentinite bodies (Soták et al. 1993, 1994, 2000) (Fig. 1). These rocks are along strike with the Vahicum and hence we regard them as equivalents of the Piemont-Liguria Ocean.

The easternmost occurrences of the Pieniny Klippen Belt (Kysuca-Pieniny-type sediments) form part of the so-called Pienides of the Maramures area in Northern Romania (Poiana Botizei locality; Săndulescu et al. 1979/1980; Bombitá & Savu 1986). In map view they form a tight arc (Plate 1, Fig. 3). These easternmost Pieniny Klippen Belt lithologies are a key-element for understanding the relationship between West and East Carpathians (Săndulescu et al. 1981a, 1993; Tischler et

al. 2007). This is because they separate, within the Pienides, the more internal Botiza nappe, a lateral equivalent of the Iňačovce-Kriscevo Unit of Eastern Slovakia and Ukraine that is attributed to the Piemont-Liguria Ocean, from the easternmost equivalents of the Magura Flysch (Wildflysch nappe of the External Pienides, see Fig. 3). The Pienides, including both these oceanic units and the Pieniny Klippen Belt in between them, were thrust SE-ward during the Early Burdigalian over the Dacia Mega-Unit, including its “post-tectonic” Late Cretaceous to Cenozoic cover. Later they were dissected by the Bogdan-Drăgos-Voda fault system (Tischler et al. 2007). As such, the Pienides define the easternmost tip of ALCAPA that is thrust over the Tisza-Dacia Mega-Units (Fig. 3; see Tischler 2005; Tischler et al. 2007; Márton et al. 2007). This thrusting was kinematically linked to movements along the Mid-Hungarian fault zone during the lateral extrusion of ALCAPA. The geometry of the tight Pienides arc in northern Romania led us to correlate the Botiza nappe, which we consider as the lateral equivalent of the Piemont-Liguria branch of the Alpine Tethys, with the Szolnok Flysch that occurs in the subsurface of the Pannonian Basin in eastern Hungary near Debrecen (Plate 1). Furthermore, we propose to connect this Szolnok flysch belt, which forms part of the Mid-Hungarian Fault Zone (or the ophiolitic “Intrapannonian Belt” in the sense of Channell et al. 1979) with the westernmost parts of the ophiolite-bearing Sava Zone of the Dinarides near Zagreb. According to our interpretation, Miocene dextral movements within the Mid-Hungarian Fault Zone (Zagreb-Zemplin line; Haas et al. 2000) disrupted the original connection between the Sava Zone of Croatia and northern Bosnia and the Pienides of northern Romania.

4.2.4. Adria-derived nappes in ALCAPA and remnants of the Triassic Meliata-Maliac Ocean

The compilation of Adria-derived units, known as the Austroalpine nappes in the Alps, follows the scheme proposed by Schmid et al. (2004a), except for minor modifications in the easternmost Alps that are discussed below. Correlation of these Alpine units across the Vienna Basin and the Little Hungarian Plain with the equivalent ones in the West Carpathians is based on compilations of subsurface (seismic and/or borehole) data provided by Fülöp & Dank (1967), Fülöp et al. (1987), Tari (1994, 1996), Plašienka et al. (1997a), Tari et al. (1999), Haas et al. (2000), and Haas (2001).

The **Lower Austroalpine** nappes representing the structurally lowermost units of the Austroalpine nappe sequence were derived from the northern passive margin of Adria that faced the Piemont-Liguria Ocean. At the eastern margin of the Alps, the subdivision proposed by Schmid et al. (2004a) was slightly modified: the Semmering nappe, without the overlying nappes that are built up by the so-called Grobgneiss Unit and the Strallegg Complex (Schuster et al. 2001, 2004), was included into the Lower Austroalpine nappe pile. This permits a correlation of the Lower Austroalpine units with an equivalent nappe sequence of the West Carpathians known as the **Tatricum** (i.e.

Plašienka et al. 1997a). Very probably the rocks in the Leitha Mountains of the easternmost Alps SE of Vienna extend eastward into the Hainburg Hills and the Malé Karpaty Mts. of the West Carpathians near Bratislava (Plašienka et al. 1991). Structurally, the Tatricum represents the lowermost Adria-derived nappe that consists of Variscan basement and its sedimentary cover and that was derived from a position adjacent to the Vahic (= Piemont-Liguria) Ocean (Dumont et al. 1996; Plašienka et al., 1997a). As revealed by deep seismic transects, the Tatricum forms a tabular, upwards slightly convex and more than 10 km thick thrust sheet (Plate 2, Profile 2) that extends into the lower crust below the Veporic units (Tomek 1993; Bielik et al. 2004).

Subdivision of the Upper Austroalpine nappe system and its West Carpathian equivalents into *northern margin of Meliata*, *Eoalpine high-pressure belt* and *southern margin of Meliata units*, as proposed in our compilation (Plate 1), follows essentially the new subdivision of the Upper Austroalpine units of the Alps as proposed by Schuster et al. (2004) and Schmid et al. (2004a). Note, however, that this concept, as briefly outlined below, applies strictly only to the West Carpathians and the eastern parts of the Eastern Alps since the oceanic Meliata-Maliac embayment did not extend into the Austroalpine domain of the more western areas. This applies also to the related Eoalpine high-pressure belt, the westernmost parts of which are present in the southern Ötztal basement (Schmid et al. 2004a).

This new subdivision is supported by the following data and/or concepts:

(1) The sedimentary nappes of the Northern Calcareous Alps were derived from the northern passive margin of the Triassic *Meliata Ocean* that formed a branch of the Neotethys. The most distal parts of this margin are characterized by the classical Hallstatt facies (e.g. Mandl 2000; Gawlick & Frisch 2003). We do not share the view of Neubauer et al. (2000) who proposed that within the domain of the present-day Northern Calcareous Alps a Meliata “suture” separates two conjugate passive margins. Instead, we interpret the stratigraphic evidence for Late Jurassic compressional tectonics in the Northern Calcareous Alps (Gawlick & Frisch 2003; Gawlick & Schlagintweit 2006) to be related to the development of an accretionary wedge at the front of an obducted Jurassic-age ophiolite body (Vardar Ocean). This obduction event followed an earlier pulse of intra-oceanic subduction (see chapter Dinarides) during which the Triassic parts of the Neotethyan oceanic lithosphere, namely the Meliata Ocean, were consumed.

(2) After this obduction event, major deformations accompanied by the stacking of the Austroalpine nappe units started during the Late Valanginian (ca. 135 Ma). This is indicated by the development of the syn-orogenic Rossfeld sedimentary basin in the Northern Calcareous Alps (Faupl & Wagreich 2000) in the Northern Calcareous Alps. It is this shortening, referred to as the Eo-Alpine tectono-metamorphic event, that we relate

to the final closure of the westernmost parts of the Neotethys oceanic realm. A SE- to E-dipping subduction zone developed within and/or near the western termination of the Neotethys oceanic embayment into Adria (Fig. 2), possibly along a Jurassic strike-slip fault (see discussions in Schuster & Frank 1999; Frank & Schlager 2006). In the Alps and along this intra-continental subduction zone located at the western end of the Meliata Ocean, crustal rocks were transported to great depths some 90 Ma ago (Thöni 2006).

(3) The intra-continental, partly eclogitic, former subduction zone, referred to as *Eoalpine high-pressure belt* in Plate 1, subdivides the Upper Austroalpine basement nappe sequence into two parts (Schmid et al. 2004a): the Silvretta-Seckau nappe system in its footwall (*northern margin of Meliata* in Plate 1, together with the Northern Calcareous Alps and the Grauwackenzone) and the Ötztal-Bundschuh and Drauzug-Gurktal nappe systems in its hanging-wall (part of the *southern margin of Meliata* in Plate 1, together with the Southern Alps).

Correlation of the Upper Austroalpine units of the Alps with the major tectonic units of the West Carpathians (Plate 1) has to contend with considerable difficulties, since major changes occur along strike in the architecture of the Cretaceous-age (Eoalpine) orogen. Hence, individual Upper Austroalpine units cannot be cylindrically traced eastwards. The absence of exposed Eoalpine high-pressure rocks east of the Alps, possibly due to their burial beneath the fill of the Pannonian Basin, presents an additional difficulty.

We correlate the Drauzug-Gurktal nappe system with the Transdanubian ranges since we interpret both of these units to structurally represent the hanging-wall with respect to the Eoalpine high-pressure belt. Therefore Drauzug-Gurktal nappe system and Transdanubian ranges paleogeographically represent realms along the southern margin of the Meliata-Maliac Ocean. The Transdanubian ranges are made up of weakly metamorphosed Variscan basement that is overlain by a non-metamorphic Permo-Mesozoic cover. This cover exhibits close similarities to the Drauzug and the Southern Alps (e.g. Kazmer & Kovács 1985; Haas et al. 1995). This correlation is also warranted on structural grounds; the Transdanubian ranges are located immediately N of the Balaton Line, the eastern extension of the Periadriatic Line, along which the Austroalpine units (Drauzug and Transdanubian ranges) escaped to the east (Kazmer & Kovács 1985). Hence, the Drauzug-Gurktal nappe system and the Transdanubian Ranges are interpreted as allochthonous tectonic units that structurally overlie the postulated eastern extension of the Eoalpine high-pressure units (Plate 2, Profile 1).

Conversely we correlated all units of the Central and Inner West Carpathians with the Silvretta-Seckau nappe system, the Northern Calcareous Alps and the Grauwackenzone. We propose that the easternmost parts of these units were derived from the northern margin of the Meliata-Maliac Ocean. These units form the lower plate with respect to the Eoalpine high-pressure belt of the Alps and include the thick-skinned

Veporicum and Gemicum thrust sheets, as well as a series of detached sedimentary nappes. From external to internal, the latter are referred to as Fatricum, Hronicum and Silicicum units (Plašienka 1997a; see Plate 2, Profile 2). According to our interpretation this group also includes rock associations that crop out in isolated inselbergs, the Uppony, Szendrő and Zemplin mountains (Fig. 1), whose assignment to specific units is much debated. These inselbergs are located to the northwest and north of the southern boundary of ALCAPA, marked by the Darno and Nekészeny Faults (Fig. 1).

The structural and paleogeographic relationships between the most internal and structurally highest system of cover nappes (Silicicum in Slovakia or Aggtelek-Rudabánya Unit in Hungary; Haas 2001) and the Meliaticum are still enigmatic. One school of thought considers the Meliaticum as a suture zone, referred to as Rožňava suture (i.e. Plašienka et al. 1997a,b). In this case, however, the Silicicum, together with a weakly metamorphic cover slice at its base referred to as Tornaicum (Martonyi in Hungary; see Fodor & Koroknai 2000; Less 2000) or as South Rudabányaicum (Kozur & Mock 1997), would represent the upper plate with respect to this suture as they overlie the Meliaticum. Hence, these units ("Inner West Carpathians" of Plašienka 1997a) would, contrary to our interpretation (Plate 1 and Plate 2, Profile 2), represent the southern margin of the Meliata-Maliac Ocean.

We chose another option. According to our interpretation the Silicicum-Aggtelek Unit was derived from the northern passive continental margin of the Triassic Meliata-Maliac Ocean, with the Bodva sub-unit in northern Hungary (e.g. Kovács 1992; Kovács et al. 1997) representing its southernmost and most distal parts (Fig. 4a). The paleogeographic position of the Silicicum-Aggtelek Unit is very reminiscent of that of the Juvavic nappes of the Northern Calcareous Alps (Fig. 4a). Due to the development of a triangle structure formed during Late Jurassic obduction of the West Vardar Ophiolitic Unit, a part of the northern distal passive margin of the Meliata-Maliac Ocean (Silicicum-Aggtelek unit) now tectonically overlies ophiolitic mélanges with remnants of the Meliata-Maliac Ocean (Fig. 4b, right). Hence, for the Western Carpathians we propose that S-directed back thrusting, associated with the formation of this triangle structure, is responsible for the present-day tectonic position of the Silica-Aggtelek cover nappes in the hanging-wall of obducted remnants of the Triassic Meliata-Maliac Ocean (Plate 2, Profile 2; Fig. 4b, right). Our field observations support S-directed Jurassic thrusting for the southernmost exposures of the West Carpathians in Northern Hungary. Subsequent Cretaceous deformation was N-directed (Balla 1987), with in-sequence thrusting gradually propagating northward (Fig. 4c, right; Plašienka 1997a,b).

Consequently, we place the suture of the Meliata-Maliac Ocean further to the south, namely between the southernmost exposures of the Central and Inner West Carpathians of the Uppony Mountains in the north and the Bükk Mountains to the south. The latter represent a displaced part of the Dinarides. This suture formed during the Early Cretaceous and was

severely overprinted by Cenozoic strike-slip faulting along the Darno Line during the lateral eastward extrusion of the Alps and Dinaridic fragments (Plate 1 and Plate 2, Profile 2).

A geometrically similar situation is found in the easternmost Alps (Mandl & Ondrejickova 1991; Kozur & Mostler 1991; Neubauer et al. 2000; Frank & Schlager 2006). In spite of the great similarities between the nappe units of the West Carpathians and the Eastern Alps (Fig. 4), we prefer a different scenario for the Northern Calcareous Alps, largely following Mandl (2000) and Frank & Schlager (2006). In this interpretation Late Jurassic/Early Cretaceous emplacement of the most distal elements, the so-called "Tiefjuvavikum" including Meliata-type ophiolitic mélanges (Fig. 4b, left), was followed by out-of-sequence Cretaceous imbrication of the "Hochjuvavikum" (Fig. 4c, left).

The *Meliata* Unit of the West Carpathians and easternmost Eastern Alps includes different elements that do not represent ophiolitic bodies in a strict sense. The Meliaticum of the West Carpathians consists of two units: (1) the metamorphosed Bôrka Unit, that was derived from near the ocean-continent transition of the northern margin of the Meliata-Maliac Ocean and which underwent low-temperature, high-pressure (12 kbar) metamorphism (Faryad 1995a & b, 1997; Mello et al. 1998), and (2) the Meliata Unit s.str. (Mock et al. 1998), a non-metamorphic ophiolite-bearing mélangé which forms part of a Jurassic accretionary flysch complex containing radiolarites, olistostromes, mélanges and ophiolitic bodies (Kozur & Mock 1997). Glaucofane-bearing basalts from the base of the Meliata accretionary complex (Bôrka Unit) overriding the southernmost Gemicum yield Middle to Late Jurassic ages (150–160 Ma) for their HP-LT metamorphism (Maluski et al. 1993; Dallmeyer et al. 1996; Faryad & Henjes-Kunst 1997). This demonstrates that Mid-Jurassic intra-oceanic subduction processes preceded latest Jurassic obduction onto the distal northern continental margin of the Meliata-Maliac Ocean that was associated with the development of an accretionary wedge. This subduction clearly pre-dated, and is hence not related to the Late Valanginian onset of nappe stacking in the Eastern Alps (Gawlick & Frisch 2003) and West Carpathians.

We can only speculate that the Eoalpine high-pressure belt of the Eastern Alps, which represents a Cretaceous-age partly intra-continental suture that post-dates obduction of the Meliaticum onto the Juvavic and Gemic units of the Alps and West Carpathians, respectively, might also be present in the subsurface of the Pannonian plain. We suggest its presence along a geophysically defined belt of linear deep-seated faults consisting of the Raba and Hurbanovo-Diósjenő faults (Fig. 1), based on data from Plašienka et al. (1997a; their Fig. 2). This Cretaceous-age suture (Eoalpine high-pressure belt of Plate 1) would coincide with the northern limit of the Transdanubian Range Unit along the Diósjenő Fault, as proposed by Haas (2001). Borehole data analysed by Koroknai et al. (2001), revealed immediately north of the Diósjenő Line the occurrence of basement that is characterized by Eo-Alpine amphibolite-grade metamorphism, typical for the Veporic Unit of the West

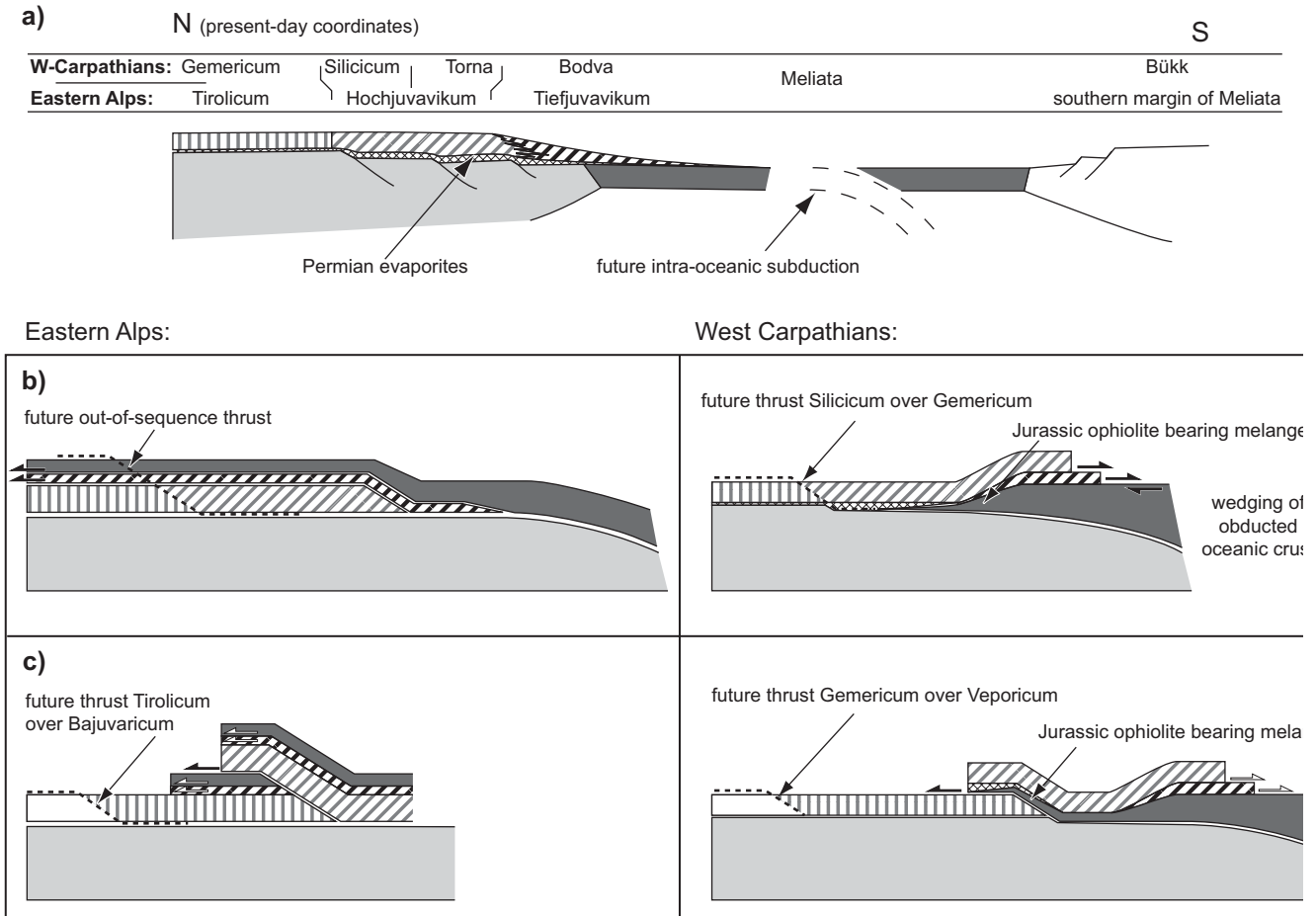


Fig. 4. Conceptual model for Late Jurassic and Cretaceous thrusting affecting the former passive continental margin adjacent to the Meliata Ocean Eastern Alps (Northern Calcareous Alps) and in the West Carpathians. a) Former passive margin of Neotethys and terminology of the various paleogeog domains and tectonic units as used in the West Carpathians (top line) and the Eastern Alps (bottom line). b) Late Jurassic thrusting in the Alps (left) and West Carpathians (right: triangle structure). c) Overprinting during Early Cretaceous orogeny in the Alps (left) and in the West Carpathians (right).

Carpathians. Moreover, these data indicate that this high-pressure belt probably wedges out eastward (Plate 1). In addition, these findings provide further evidence for the existence of an important tectonic boundary that separates the non-metamorphic Transdanubian Ranges, derived from south of the Meliata-Maliac Ocean, from the Veporic Unit of the Central West Carpathians that we place to the north of the Meliata oceanic embayment.

4.3. East Carpathians, South Carpathians, Transylvanian Basin and Carpatho- Balkanides (Danubian nappes and “Dacia”)

4.3.1. Overview

The internal tectonic units of the East and South Carpathians, which are fringed to the E and S by the external Miocene thrust belt, were emplaced in Cretaceous time (i.e. Săndulescu 1984, 1994; Kräutner et al. 1988; Kräutner 1996). Săndulescu (1984, 1994) referred to these units as the Marginal, Outer and Me-

dian Dacides. In the Hungarian literature, the Outer and Median Dacides are referred to as the Dacia Mega-Unit or ter (i.e. Csontos & Vörös 2004), whilst Burchfiel (1980) referred them as the “Rhodopian fragment”.

The Danubian nappes, also referred to as Marginal Dacia, however, were originally part of the Moesian foreland. The Outer and Median Dacides of the Dacia Mega-Unit, together with more internal units located below the Transylvanian I and cropping out in the North Apuseni Mountains (Tisza Nap Unit; e.g. Haas & Pero 2004, referred to as Internal Dacides; Săndulescu 1984), moved into the Carpathian embayment during Cenozoic times (i.e. Royden 1988; Fodor et al. 1999; Molnár 2000; Wortel & Spakman 2000; Csontos & Vörös 2004; Horváth et al. 2006). These internal units were finally docked against the European foreland during the Miocene, controlling the extension of the earlier described external fold-and-thrust belt. This extension involves Cretaceous to Tertiary-age flysch units.

Along the western margin of the Moesian Platform the South Carpathian units can be traced further southward

eastern Serbia and western Bulgaria. There they are referred to as the Carpatho-Balkanides. They also include, what Serbian authors refer to as the Serbo-Macedonian Massif (e.g. Dimitrijević 1997). Some of these units can then be traced eastward into the Balkan Orogen whilst others follow the eastern rim of the Eastern Vardar Ophiolitic Unit and extend southward into Northern Greece (Plate 1). Two curved strike-slip faults, the Cerna-Jiu Fault (Berza & Drăgănescu 1988) and the Timok Fault (Visarion et al. 1988; Moser 2001; Krätner & Krstić 2002, 2006), displace the Cretaceous nappe sequence along the contact between the Dacia Mega-Unit and the Moesian Platform. These faults accommodated Early Oligocene to Early Miocene dextral strike-slip motion with total displacements of up to 100 km (Moser 2001; Fügenschuh & Schmid 2005) as Dacia was mouldered around the western tip of the Moesian Platform (Ratschbacher et al. 1993). The Timok Fault can be traced southward and appears to be kinematically linked to extensional deformation in the Osogovo Mountains (Kounov et al. 2004) and along the Strymon fault system of Northern Greece (Dinter 1998; Kiliyas et al. 1999).

4.3.2. Danubian nappes

The **Danubian nappes** consist of a Neoproterozoic basement (e.g. Liégeois et al. 1996; Seghedi et al. 2005), Paleozoic rocks that were deformed during the Variscan cycle (e.g. Iancu et al. 2005) and Carboniferous to Late Cretaceous cover sequences (Berza et al. 1983, 1994). This imbricated nappe sequence developed by eastward thrusting during the latest Cretaceous (Late Campanian – Maastrichtian; often referred to as the “Laramide” phase in the Romanian literature; e.g. Krätner 1993; Berza et al. 1994) under low-grade (sub-greenschist to lowermost greenschist facies) metamorphic conditions (Berza & Iancu 1994). It is best exposed in a tectonic window in the South Carpathians referred to as the Danubian window (e.g. Murgoci 1905). After Late Cretaceous nappe emplacement this unit was exhumed during Late Eocene to Oligocene time (Schmid et al. 1998; Fügenschuh & Schmid 2005). The rocks in the Danubian nappes have a Neoproterozoic (“Panafrican”) tectono-metamorphic evolution similar to that of the basement in the Moesian Platform (e.g. Liégeois et al. 1996; Seghedi et al. 2005), a unit with Northern Gondwana paleogeographic affinities (Vaida et al. 2005). The Mesozoic cover of the Danubian nappes is characterized by Early Jurassic Gresten facies (e.g. Năstăseanu et al. 1981), followed by Late Jurassic to Early Cretaceous platform carbonates, Albian to Turonian deeper marine pelagic limestones and marls that give way to a Turonian and Senonian flysch sequence. Most authors regard the Danubian nappes as having been detached from the Moesian Platform, as shown in Profile 4 (Plate 2).

Following Visarion et al. (1978) and Ștefănescu et al. (1988) we suggest that the Danubian nappes continue northward in the subsurface below the East Carpathians (see Plate 3, Profile 3) as far north as the pre-Neogene Trotus Fault (Fig. 1). Southwards the Danubian nappe sequence extends into eastern

Serbia and western Bulgaria (see Plate 1 & Plate 3, Profile 5) as indicated by the 1 : 100'000 sheets of Geological Maps of former Yugoslavia (Osnovna Geološka Karta SFRJ) and data provided by Krätner & Krstić (2002, 2006) and Cheshitev et al. (1989). In Serbia (Dimitrijević 1997) the Danubian nappes are locally known as Miroč Unit (west of the Timok fault) and Vrška Čuka Unit (east of the Timok fault), or as Vrška Čuka-Miroč terrane (Karamata 2006). The Vrška Čuka Unit extends into western Bulgaria, where it is known as the West Balkan Unit (Kounov 2002). However, in the Balkan Mountains north-directed Eocene age thrusting overprinted many of the older Cretaceous structures (Boyanov et al. 1989).

4.3.3. The Ceahlau-Severin Ocean

The **Ceahlău nappe** (including the Black Flysch and Baraolt thrust sheets) of the East Carpathians and the equivalent ophiolite-bearing **Severin nappe** of the South Carpathians form a wedge that was accreted already in mid-Cretaceous (Aptian) time to the continental units of the overlying Bucovinian-Getic nappes (Șandulescu 1984). Ceahlău and Severin Ophiolitic Units represent the relics of what we refer to as the Ceahlău-Severin Ocean.

The Ceahlău nappe of the East Carpathians is the largest and main unit derived from this ocean. The Black Flysch and Baraolt thrust sheets occupy a higher tectonic position but were mapped as part of the Ceahlău-Severin Ophiolitic Unit in Plate 1. The Black Flysch nappe (Bleahu 1962; Șandulescu 1975) exposes a basement that consists of massive basaltic flows and dykes; younger basalts also intrude into the overlying Kimmeridgian-Aptian sediments. Since the mafic complex displays intra-plate geochemical characteristics it is not part of an ophiolitic sequence in the strict sense (Șandulescu et al. 1981a). These rocks were possibly located at the NW margin (in present day coordinates) of the Carpathian oceanic embayment and perhaps formed along large transtensional faults (Badescu 1997). Near the southern termination of the East Carpathians, the equivalent of the Black Flysch nappe is the Baraolt nappe (Ștefănescu 1970). This nappe is exclusively made up of Berriasian to Aptian sandy-calcareous turbidites. The large Ceahlău nappe consists of basal Late Jurassic radiolarites, with basic igneous rocks and other deep-water deposits (Azuga Facies), which are overlain by mostly shaly and calcareous Tithonian to Neocomian (Sinaia beds) and Barremian to Aptian proximal turbidites (Comarnic Beds). Late Aptian to Albian massive sandstones and conglomerates (Bucegi conglomerate) unconformably cover the tectonic contact between Ceahlău nappe and overlying Getic nappe (e.g. Patrușiu 1969; Ștefănescu 1976).

In the South Carpathians the Danubian nappes are overlain by Senonian “wildflysch”, which constitutes a tectonic mélange complex (Cosustea mélange; Seghedi & Oaie 1997). This complex, which is characterized by a block-in-sheared-matrix structure, formed during early stages of tectonic accretion of these sediments to the overlying ophiolitic Severin nappe during the

latest Cretaceous (presumably Maastrichtian). The basement of the overlying Ceahlau-Severin Ocean crops out in the Severin nappe and consists of strongly dismembered ophiolitic lithologies (Savu et al. 1985; Maruntiu 1987) such as harzburgitic ultramafics, gabbros and pillow basalts. The basalts show ocean-floor tholeiitic affinities (Cioflica et al. 1981). The overlying sediments are much thinner compared with units in the East Carpathians with which they are correlated and include Late Jurassic radiolarites (Azuga beds) followed by Early Cretaceous terrigenous turbidites (Sinaia and Comarnic Flysch) (see Codarcea 1940; Pop et al. 1997).

The tectonic units derived from the Ceahlau-Severin Ocean were thrust eastward in two stages (Ștefănescu 1976; Săndulescu et al. 1981a,b). During the earlier Aptian to Albian event (referred to as “Austrian” in the Romanian literature) they were accreted to the overlying Getic nappe related to west directed (in the East Carpathians and in present-day coordinates) subduction. The Baraolt and Black Flysch nappes of the Eastern Carpathians were emplaced over the more external Ceahlau nappe during the first stage, as dated by their Late Albian to Cenomanian post-tectonic cover (Săndulescu 1984). The second (“Laramide”) event occurred in the latest Cretaceous, when the Ceahlau-Severin Ophiolitic Units were thrust above more external units: the most internal flysch units of the Moldavides (Convolute Flysch nappe) in the East Carpathians and the Danubian nappes in the South Carpathians (Plate 3, Profile 3). The age of this second event is constrained by a Late Campanian to Maastrichtian post-tectonic cover (e.g. Săndulescu 1984; Melinte & Jipa 2005).

The Ceahlau-Severin Ophiolitic Unit can be followed southwards into the boundary region between eastern Serbia and western Bulgaria based on the compilation by Krätner & Krstić (2002, 2006). However, no traces of this ophiolitic unit (including the associated Sinaia-type turbidites) are present further south in the Carpatho-Balkan Orogen or further east in the Balkan Orogen. Hence, the oceanic Ceahlau-Severin rift, which represents a branch of the Alpine Tethys according to our interpretation, ended eastward within continental units of the European foreland and was not connected to any of the branches of Neotethys. This Ceahlau-Severin oceanic rift split off a narrow continental ribbon (Dacia), which later formed the Cretaceous-age Getic to Supragetic (or Bucovinian) nappe pile of the Carpathians described below (Fig. 2b). Because the Ceahlau-Severin Ocean ended to the east, the equivalents of this nappe pile in the Balkan Orogen (Central Balkan and Sredna Gora units; Ivanov 1988) are thrust above the Prebalkan Unit and the Moesian Platform without an apparent intermediate oceanic suture. Moreover main thrust contacts formed during the Cretaceous were reworked during Eocene times in the Balkan Orogen.

4.3.4. Getic-Supragetic (Bucovinian) nappe sequence

The east-facing Bucovinian nappe sequence of the East Carpathians developed during Early to mid-Cretaceous times

(e.g. Popescu-Voitesti 1929; Krätner 1938; Krätner 1980) (see Plate 3, Profile 3). It represents the lateral equivalent of the Getic-Supragetic nappe sequence of the South Carpathians (Săndulescu 1984, 1994) (see Plate 2, Profile 4). This nappe sequence has the general geometry of a large antiform and consists of low- to medium-grade metamorphic rocks of Late Precambrian to Cambrian age (e.g. Balintoni & Gheuca 1974) separated from each other either by pre-Alpine thrusts or by Triassic to Lower Cretaceous sedimentary series (Balintoni 1981). The uppermost Alpine tectonic unit is the **Bucovinian nappe** whose Mesozoic cover series grade upward into Early Cretaceous wildflysch that lies structurally below the over-riding ophiolite-bearing Transylvanian nappes (Patrulius et al. 1969; Ștefănescu 1976; Săndulescu 1984). A similar Paleozoic basement composition and Permian to Early Cretaceous sedimentary cover characterize the underlying **Sub-Bucovinian nappe**. The **Infra-Bucovinian nappe**, the lowermost unit of the thrust succession, contains medium-grade metamorphic basement overlain by a Permian to Jurassic sedimentary cover, which was locally metamorphosed in Cretaceous times (Krätner 1980; Gröger 2006; Dallmeyer et al. in press). This lowermost nappe crops out only in small isolated tectonic windows. Following Săndulescu (1984, 1994) we correlated the Infra-Bucovinian nappe of the East Carpathians with the **Getic nappe** of the South Carpathians, whereas the two higher units of the Bucovinian nappe sequence are correlated with the **Supragetic nappes** of the South Carpathians.

The Bucovinian nappe sequence of the East Carpathians and its lateral equivalent, the Getic and Supragetic nappes of the South Carpathians (Murgoci 1905; Streckeisen 1932), consist of Europe-derived continental crustal material (Dacia) that was separated from the European foreland along the Ceahlau-Severin oceanic rift. To the south, in Serbia and western Bulgaria, we also included the structurally highest unit, referred to as **Serbo-Macedonian “Massif”** (e.g. Dimitrijević 1957, 1997), into this nappe sequence. However we do not imply that this also applies to a unit that carries the same name in Greece and which experienced a severe Alpine metamorphic overprint (Kilias et al. 1999).

The Getic-Supragetic nappe sequence (see Plate 2, Profile 4) involves a medium- to high-grade metamorphic Neoproterozoic to Early Paleozoic gneissic basement and sub-green-schist to epidote-amphibolite grade Paleozoic successions. These are unconformably overlain by Late Carboniferous to Permian continental clastics and Mesozoic strata (Iancu et al. 2005). The Mesozoic rocks contain Middle Triassic carbonate platform deposits followed by detrital Early Jurassic strata (Gresten facies). Locally sedimentation ended with Middle Jurassic radiolarites, but was elsewhere followed by Late Jurassic to Early Cretaceous pelagic series. Post-tectonic strata begin with Albian to Cenomanian Molasse-type deposits, proving that this nappe sequence essentially formed during the mid-Cretaceous (“Austrian”) orogenic pulse. However, Late Cretaceous series were locally also affected by latest Cretaceous “Laramide” deformations (Săndulescu 1984, 1994).

We mapped the Getic nappe across the Danube into Serbia mainly based on the 1 : 100'000 Geological Map of former Yugoslavia (Osnovna Geološka Karta SFRJ) and the work of Krätner & Krstić (2002, 2006). In Serbia the Getic nappe, referred to as Kučaj-Ljubaš Zone by Krätner & Krstić (2002, 2006), is locally also known by many different names (Dimitrijević 1997; Karamata 2006). We also include a structurally higher and more internal nappe digitation (Saska-Gornjak Unit) as part of the Getic nappe in Serbia (see Plate 3, Profile 5).

Further south, in the border area between Serbia and Bulgaria, additional and tectonically higher nappes, referred to as *Kraishte units* by Krätner & Krstić (2002, 2006) have been mapped as part of what appears to be a Getic nappe “system” in Serbia and Bulgaria, rather than only one single Getic nappe. These Getic nappes and the overlying Struma unit now form part of the Osogovo-Lisets metamorphic core complex and were exhumed in Late Eocene to Oligocene times below a SW-dipping detachment below a Supragetic unit, locally known as Morava Unit (Kounov et al. 2004).

In Bulgaria the *Kraishte units* overlie the more external *Sredna Gora Unit*, also included as part of the Getic nappe system in Plate 1, together with the more external Luda Kamčija Zone of Ivanov (1988), identical with the East Balkan Unit of Georgiev et al. (2001). The *Sredna Gora Unit* extends eastward to the Black Sea and is well known for a superimposed thick Late Cretaceous volcano-sedimentary succession. This same succession and its associated magmatic rocks also extend westwards into eastern Serbia (Timok eruptive area of Dimitrijević 1997; Timok-Sofia Basin of Krätner & Krstić 2002, 2006). This Late Cretaceous basin and its associated Turonian to Campanian (92–78 Ma) magmatic activity (“banatites”) evolved in a back-arc setting with respect to the N- to NE-dipping Neotethys Ocean subduction zone (Fig. 2c) that lay farther to the south and southwest (i.e. Berza et al. 1998; Georgiev et al. 2001; Heinrich & Neubauer 2002; Neubauer & Heinrich 2003; von Quadt et al. 2005). Development of this continental back-arc basin is post-tectonic with respect to the Lower to mid-Cretaceous main deformation phase (“Austrian”) of the Getic-Supragetic nappe succession (Krätner & Krstić 2002, 2006; Osnovna Geološka Karta SFRJ). Post-tectonic sedimentation commenced in Bulgaria during the Cenomanian (Georgiev et al. 2001) and in eastern Serbia during the Albian (Dimitrijević 1997).

In the South Carpathians the Supragetic nappes consist of two alpine aged thrust sheets, that is, from bottom to top, the Locva and Boča units (Năstăseanu et al. 1991). These Supragetic nappes were traced across the Danube into Serbia based on Krätner & Krstić (2002 & 2006) and the 1 : 100'000 Geological Map of former Yugoslavia. There, these units are known as, from bottom to top, Ranovac and Vlasina units. They consist predominantly of low to intermediate-grade Proterozoic and Paleozoic rocks (Ranovac-Vlasina terrane of Karamata 2006). These units extend into Western Bulgaria, where they are known as the “Morava Unit” and form the upper plate of the Osogovo-Lisets core complex (Kounov et al. 2004), that we

assigned to the Getic nappe sequence. While some authors (e.g. Dimitrijević 1997) regard these Supragetic units as part of the Serbo-Macedonian Massif, others (i.e. Krätner & Krstić 2002, 2006) restrict the term Serbo-Macedonian Massif to a strip of high-grade units, which follows the Eastern Vardar Ophiolitic Unit along the western edge of Dacia. We interpret the contact between the high-grade Serbo-Macedonian Massif and the overlying low-grade units (“high-grade basement” and “low-grade Paleozoic” in Plate 3, Profile 5) to be of pre-Mesozoic age. Hence, we consider both high- and low-grade parts of the Serbo-Macedonian Massif in Serbia as a part of the Supragetic nappe sequence. In Serbia, Triassic sediments (Malešević et al. 1978) in sub-greenschist facies locally cover the high-grade part of the Serbo-Macedonian Massif. This shows that high-grade metamorphism of the westernmost part of the Serbo-Macedonian Massif of Serbia is pre-Mesozoic. Note that, by contrast, the Serbo-Macedonian Massif of Greece exhibits Cretaceous-age amphibolite-grade metamorphism (i.e. Kiliyas et al. 1999).

We interpret the entire Getic-Supragetic nappe sequence, formed in mid-Cretaceous times, to assume an upper plate position during the latest Cretaceous and Early Cenozoic suturing with the Dinarides. The latter, including the W-Vardar and Sava Ophiolitic Units, essentially occupy a lower plate position (see Plate 3, Profile 5). Our reconnaissance fieldwork, using the map by Malešević et al. (1978), showed that the Eastern Vardar ophiolites are located in a structurally higher position with respect to the Serbo-Macedonian Massif. Hence, in contrast to the generally accepted opinion, this easternmost branch of the “Vardar ophiolites” that in map view is spatially linked to the South Apuseni and Transylvanian ophiolites (Plate 1), tectonically overlies the Getic-Supragetic nappe sequence. This, together with findings presented below, led to the assignment of the Biharia nappe system of the Apuseni Mountains to the Getic-Supragetic nappe sequence, as shown in Plate 1.

The *Biharia* nappes of the Apuseni Mountains occupy the highest structural position in the N- to NW-facing North Apuseni Orogen (Bleahu et al. 1981; Balintoni 1994). Consequently, they are commonly regarded as an integral part of Tisza (i.e. Csontos & Vörös 2004). However, when combining surface mapping in the Apuseni Mountains (i.e. Balintoni 1994) with our own interpretation of subsurface data from the Transylvanian Basin (see also Krézsek & Bally 2006) it becomes clear that both the Biharia nappe system as well as the Bucovinian (= Getic-Supragetic) nappe sequence structurally underlie the ophiolitic units of the South Apuseni (“Metaliferous”) Mountains and the Transylvanian ophiolitic units. Both nappe sequences are parts of the same structural unit, the structurally highest unit of the East Carpathians (e.g. Săndulescu 1994). Hence we consider the Biharia nappe system as a part of the Dacia Mega-Unit.

Information available on the age of the tectonic contact between the South Apuseni ophiolites and the underlying Biharia nappe system is at first sight contradicting. In the Trascau Mountains the contact between island-arc-type volcanics that are part of the South Apuseni ophiolites and the underlying Biharia unit

appears to be of Jurassic age. According to Săsăran (2006) and our reconnaissance work, the contact between these volcanics and the continental Biharia basement is sealed by Late Jurassic (Late Oxfordian-Early Kimmeridgian) to Early Cretaceous platform limestones and, thus, must have formed prior to their deposition. As these platform carbonates are not metamorphosed, the low-grade metamorphism of the Biharia nappes system must be Jurassic rather than Cretaceous in age, at least locally in the Trascau Mountains. In this context it is interesting to note that Jurassic metamorphism, pre-dating the deposition of Late Jurassic platform carbonates that have not been metamorphosed, is also known from the ophiolite-bearing Circum-Rhodope Belt of Northern Greece (Michard et al. 1994) that we correlate with the Eastern Vardar Ophiolitic Unit as mapped in Plate 1. We interpret this Late Jurassic deformation and metamorphism as related to the obduction of the Eastern Vardar Ophiolitic Unit onto parts of the Dacia Mega-Unit in latest Jurassic times (see Fig. 2 and later discussion). The final east-directed emplacement of the Transylvanian ophiolites (the eastern continuation of the South Apuseni ophiolites) over the Bucovinian nappes (the eastern equivalents of the Biharia nappe system), however, is younger and did not occur before mid-Cretaceous times.

Radiometric dating by Dallmeyer et al. (1999) and fission track studies by Schuller (2004) indicate a poly-metamorphic history for the Biharia nappe system as a whole, with ages falling into two groups, namely Jurassic (186–156 Ma) and Early to middle Cretaceous (124–111 Ma). Thus, a Middle to Late Jurassic tectonic and metamorphic event, followed by Early Cretaceous top-E nappe stacking within the Dacia Mega-Unit, need to be distinguished. The final emplacement of the nappes in the North Apuseni Mountains involving top-W to NW superposition of the Biharia, Codru and Bihor nappe systems (see Plate 3, Profile 3), did not occur before Turonian time. This is documented by the Late Turonian “Gosau” unconformity (e.g. Balintoni 1994; Schuller 2004). This youngest tectonic event was preceded by two earlier thrusting events of latest Jurassic and Early Cretaceous ages.

The W-ward continuation of the Biharia nappe system beneath the subsurface of the Pannonian Basin as shown in Plate 1 is based on subsurface data compiled by Bleahu et al. (1994), Tari et al. (1999) and Lelkes-Felvari et al. (1996, 2003, 2005). We excluded, however, the Upper Codru nappes from the Biharia nappe system since they form an integral part of the Tisza Mega-Unit. On the other hand, we included parts of the Algyő basement high into the Biharia nappe system. This is based on the finding of Lelkes-Felvari et al. (2005) that in boreholes drilled on the Algyő basement high of southern Hungary, units characterized by a high-grade Cretaceous metamorphism (Dorozsma Complex) occur in the highest tectonic position.

4.3.5. Eastern Vardar Ophiolitic Unit (including South Apuseni Ophiolites and Transylvanian nappes)

The **Eastern Vardar Ophiolitic Unit** is part of the Carpatho-Balkan Orogen (or the Rhodopian fragment; Burchfiel 1980).

The Sava Zone separates this ophiolitic unit from the Western Vardar ophiolites of the Dinarides (Plate 1). Hence the unspecified term “Vardar” ought to be abandoned. In Plate 1 we trace the Eastern Vardar ophiolites of Macedonia and eastern Serbia in the subsurface of the southernmost Pannonian Basin across Vojvodina into the ophiolites of the South Apuseni Mountains (Kemenci & Čanović 1997; Čanović & Kemenci 1999). As mentioned above, the Eastern Vardar ophiolites, and their equivalents in the Guevgeli ophiolites and the Circum-Rhodope Belt of northern Greece (Kockel et al. 1971, 1977; Michard et al. 1994) were metamorphosed and tectonically emplaced eastward on the Serbo-Macedonian Massif during the Late Jurassic, probably by obduction. However, final emplacement of the Eastern Vardar Ophiolitic Unit (including the South Apuseni and Transylvanian ophiolites) occurred during Early Cretaceous east-facing nappe stacking that primarily shaped the Dacia Mega-Unit (Romanian Carpathians and their continuation into the Carpatho-Balkan Orogen).

The Eastern Vardar Ophiolitic Unit in Serbia (“Central Vardar Subzone” of Dimitrijević 1997, “Main Vardar Zone” of Karamata 2006) represents a piece of MORB-type oceanic lithosphere. Following their emplacement on the Serbo-Macedonian Massif these ophiolites were overstepped by Late Jurassic reef limestones (Karamata 2006) that are succeeded by a Cretaceous flysch (“Paraflysch”; Dimitrijević 1997). The Late Jurassic emplacement of the Eastern Vardar Ophiolitic Unit onto at least parts of the Biharia nappe system and its lateral equivalent, the Serbo-Macedonian Massif, is probably related to the obduction of the Eastern Vardar ophiolites onto parts of the Dacia Mega-Unit, i.e. the European margin. However, no metamorphic sole has yet been found at the base of the East Vardar ophiolites. The age of the Eastern Vardar ophiolites is constrained by modern radiometric dating in northern Greece only, where igneous rocks with ages between 164 Ma and 155 Ma are present (Guevgeli ophiolites; Anders et al. 2005). These ages are very similar to those reported from the Dinaridic and Western Vardar ophiolites (see later discussion concerning the Dinarides). However, the ages stem from granitoid igneous rocks that intrude the Guevgeli ophiolites and hence, are slightly younger. The presence of granitoids within the Guevgeli ophiolites indicates that the latter formed in an island arc or back-arc setting (Brown & Robertson 2004).

The ophiolite-bearing units of the **South Apuseni** Mountains are grouped together with ophiolitic nappes that occur beneath the Neogene sediments of the Transylvanian Basin and those that are exposed in the Transylvanian nappes of the East Carpathians. This group of ophiolitic nappes is also known as “Transylvanides” (Săndulescu 1984). Neither a metamorphic sole, nor associated Jurassic ophiolitic mélanges have so far been reported from this group of ophiolite-bearing nappes. Only parts of the South Apuseni ophiolites represent MORB-type oceanic lithosphere formed during the Middle Jurassic. Other parts represent Late Jurassic intra-oceanic island-arc volcanics (Savu et al. 1992; Bortolotti et al. 2002a; Nicolae & Saccani 2003; Bortolotti et al. 2004a). The latter include basalts,

andesites, rhyolites, as well as some granites. Similar to the Guevgeli ophiolites in Northern Greece these igneous rocks are only slightly younger than the surrounding MORB-type ophiolites, which they intrude. They are particularly widespread in the Trascău Mountains south of Cluj. Similar to the Eastern Vardar Ophiolitic Unit of Serbia, the South Apuseni ophiolites are also unconformably overlain by Late Jurassic to Early Cretaceous reef limestones (Bortolotti et al. 2002a; Săsăran 2006). As mentioned above, the Late Oxfordian to Early Kimmeridgian base of these reef limestones also oversteps the contact between the Apuseni ophiolites and the underlying basement of the Baia de Aries nappe, which forms part of the Biharia nappe system (Săsăran 2006 and our own observations). This suggests that the South Apuseni ophiolites were obducted over the Biharia nappe system before Late Oxfordian times.

The Late Jurassic to Early Cretaceous platform carbonates give way to Barremian to Aptian flysch deposits (Feneş Formation) and Aptian to Albian wildflysch (Meteş Formation; Bleahu et al. 1981; Săndulescu 1984; Suciú-Krausz et al. 2006). The wildflysch of the Meteş Formation formed during the second and main (pre-Cenomanian or “Austrian”) deformation event that affected the South Apuseni Mountains. It is during this event that the South Apuseni ophiolites, including their prolongation in the subsurface of the Transylvanian Basin (Plate 3, Profile 3), were finally thrust over the Bucovinian nappe sequence of the Dacia Mega-Unit. Late Campanian to Maastrichtian (“Laramide”) top-ESE thrusting (high-angle pop-up in the Trascău Mountains; see Profile 3, Plate 3) reflects a third compressional event that affected the South Apuseni and Transylvanian ophiolites including their Jurassic to Late Cretaceous sedimentary cover. “Laramide” thrusting is also reported from the Mures valley area where the most frontal tectonic slices of the South Apuseni units were imbricated towards the N to NW (Cris and Grosi nappes; Balintoni 1994) and thrust onto the Gosau-type sedimentary cover of the eastern parts of the Biharia nappe system (see Profile 4, Plate 2).

According to the interpretation given in Profile 3 of Plate 3 the *Transylvanian Ophiolites*, which are preserved beneath the Late Cretaceous to Cenozoic sedimentary fill of the Transylvanian Basin, represent the direct continuation of the South Apuseni ophiolites. This is based on the interpretation of numerous borehole, gravity, magnetic and seismic data (e.g. Săndulescu & Visarion 1977; de Broucker et al. 1998), that document their presence as well as that of the overlying latest Jurassic to Early Cretaceous platform carbonates beneath the western parts of the Transylvanian Basin. In the western and central-northern part of this basin, our own assessment of borehole data suggests a similar situation as in the South Apuseni Mountains, namely that Late Jurassic to Early Cretaceous reef limestones rest directly on the ophiolites. According to our interpretation (Profile 3, Plate 3) these ophiolites were eroded in the eastern parts of the Transylvanian Basin during an exhumation event that pre-dates the deposition of the Late Cretaceous post-tectonic cover, which in many parts of the westernmost Transylvanian Basin rests directly on the basement of

the Bucovinian nappe. This Late Cretaceous erosional event is genetically coupled with Late Cretaceous normal faulting (see normal fault east of the Tarnave Basin depocenter in Profile 3, Plate 3). Such normal faulting led to substantial exhumation of the previously metamorphosed Bucovinian nappe sequence (Dallmeyer et al. in press) along the northern margin of the Transylvanian Basin (Rodna horst; Gröger 2006; Gröger et al. in press). There, zircon fission track data yield evidence for rapid and substantial cooling from temperatures in excess of 300 °C during Coniacian to Campanian times.

These data support the interpretation that the Bucovinian nappe stack was originally covered by a substantial overburden and was exhumed in the footwall of the Tarnave normal fault. Seismic interpretation and wells in the hanging-wall of this large west-dipping normal fault demonstrate the presence of (half-) grabens. These grabens contain Late Cretaceous sediments, referred to as the “Uppermost Cretaceous rift mega-sequence” by Krézsek and Bally (2006). Our own reflection-seismic interpretations indicate that these series clearly pre-date syn-tectonic deposits that are associated with subsequent “Laramide” thrusting. Further to the west, development of these extensional structures is reflected in the South Apuseni Mountains by the gradual subsidence and deepening of a sedimentary basin in which the Bozes and Remeti flysch accumulated during the Late Cretaceous (Balintoni et al. 1984; Schuller 2004), that is, between the Austrian and Laramide tectonic events. Overall, the onset of extension-induced subsidence becomes gradually younger westward and highlights the importance of this Late Cretaceous (post-“Austrian”, pre-“Laramide”) extensional event. Note that juxtaposition of the South Apuseni ophiolites and the Getic-Supragetic nappe sequence across the South Transylvanian fault in the Mures Valley (Plate 2, Profile 4) largely results from the offsets across this large E–W oriented (in present-day coordinates) transfer fault produced during the Late Cretaceous extensional event, as evident in its eastern segment that is buried beneath the younger sedimentary fill of the Transylvanian Basin. During the Late Campanian to Maastrichtian “Laramide” event, the Tarnave and South Transylvanian faults were inverted, involving top-ESE thrusting and transpression, respectively.

The Transylvanian ophiolites crop out again as isolated tectonic klippen assigned to the so-called Transylvanian nappes that form the structurally highest unit of the East Carpathians. These nappes consist of Triassic to Albian sedimentary rocks, that were partly derived from continental margin units on the one hand, and from truly ophiolitic units on the other hand (Săndulescu 1974; Săndulescu & Russo-Săndulescu 1979; Săndulescu et al. 1981a; Săndulescu 1984). Modern geochemical work on these ophiolites by Hoeck & Ionescu (2006) evidence the occurrence of different types of magmatic rocks, namely true MORB and back-arc type ophiolites, but also a few andesites believed to have formed in a continental magmatic arc setting. The age of these ophiolites is still uncertain, although the above cited authors favour a Triassic age. The facies of the Triassic sediments occurring in some of the Transylvanian nappes (i.e. siliceous

limestones, Hallstatt-type limestones; Săndulescu 1975) suggests that the Transylvanian nappes as a whole were presumably derived from a continent-ocean transition of a Triassic-age Meliata-Maliac-type ocean. Note, however, that the structural position of the Transylvanian nappes, which according to our interpretation is similar to that of the Jurassic-age ophiolites occurring beneath the Transylvanian Basin, indicates that both Triassic and Jurassic ophiolites form part of one and the same oceanic Meliata-Maliac-Vardar Neotethys that is referred to by Săndulescu (1994) as the “Main Tethyan Suture Zone”.

Suturing of the Transylvanian nappes to Dacia (Bucovinian nappes) occurred during mid-Cretaceous times and is documented by the sealing of the nappe contacts by an Albian- to Cenomanian-age post tectonic cover. However, top-E compression had commenced already during the Late Barremian and was accompanied by the deposition of wildflysch, now occurring beneath the Transylvanian nappes (Săndulescu 1975). As shown in Profile 3 of Plate 3, we interpret the North Apuseni units (Tisza) to represent the upper plate with respect to this mid-Cretaceous suture. Note however, that the Transylvanian and South Apuseni ophiolites, that tectonically overlie the North Apuseni units, appear to be rootless in a present-day cross section view. This is the reason for depicting a large back-fold and -thrust, respectively, shown schematically and conceptually in Profile 3 of Plate 3, very similar to an interpretation that was advanced much earlier by Săndulescu & Visarion (1977). This structure developed presumably during a Turonian compressional event that post-dated the top-E mid-Cretaceous emplacement of the Transylvanian ophiolites but which is not documented at all within Dacia. During this Turonian event the NW-facing North-Apuseni nappe stack developed, that is so characteristic for the Tisza Mega-Unit, as will be described in the next chapter.

4.4. Tisza Mega-Unit of the southern Pannonian Basin and the N-Apuseni Mountains

4.4.1. Overview

The Tisza Mega-Unit (Haas & Pero 2004; Csontos & Vörös 2004) comprises a sequence of nappes consisting of basement and its Mesozoic cover with some common characteristics. According to our interpretation this Mega-Unit is surrounded by mobile zones, most if not all of them probably representing oceanic sutures. It was recognized early on that the faunal assemblages (“European” faunal province) contained in the Triassic and Early Jurassic sediments of units exposed in the Mecsek Mountains, located near the northern rim of this Mega-Unit, strongly contrast with those found in the northerly adjacent series that are exposed in the Transdanubian ranges (“Mediterranean” faunal province) which form part of ALCAPA (Vörös 1977, 1993). Moreover, paleomagnetic evidence indicates contrasting rotations and translations for Tisza and ALCAPA. Rotations during Cretaceous to Miocene times are generally counter clockwise in ALCAPA but clockwise in the

eastern parts of Tisza and adjacent Dacia (e.g. Patrascu et al. 1994; Panaiotu 1999; Márton 2000, 2001). The western parts of Tisza, however, were highly mobile, particularly during Tertiary times, and show small block rotations in opposing directions (Márton 2000).

The pre-Triassic basement of the Tisza Mega-Unit consists of various Variscan high-grade metamorphic series including anatectic granites and migmatites (Kovács et al. 2000). Recently Klötzli et al. (2004) provided evidence that the Late Paleozoic granitoids of the Mecsek Mountains likely formed at a location S or SSW of the Rastenberg granodiorite of the Bohemian Massif. This basement is therefore considered to represent a former part of the Moldanubian Zone.

The nappe succession that forms the Tisza Mega-Unit comprises, from external (NW) to internal (SE) the Mecsek, Bihar and Codru nappe systems (see Plate 2, Profile 2 & Plate 3, Profile 3). In general, thrusting occurred during the Turonian; it locally affects Early Turonian sediments and pre-dates the latest Turonian onset of deposition of the post-tectonic Late Cretaceous Gosau sediments (Balintoni et al. 1984; Schuller 2004). The Triassic cover sequences show substantial facies variations (Burchfiel & Bleahu 1976; Bleahu et al. 1981, 1994; Kovács et al. 2000; Haas & Pero 2004). A Germanic Muschelkalk-type facies of the most external units grades into more massive Mid-Triassic carbonate build-ups that are overlain by a Late Triassic Keuper facies (Haas & Pero 2004), and finally into the Schreyeralm-Hallstatt-type facies of the most internal and structurally highest units such as the Vascău nappe of the Codru nappe system (Bleahu et al. 1994). Hence, as pointed out by Burchfiel & Bleahu (1976), Triassic facies changes and nappe emplacement in the North Apuseni Mountains are reminiscent of what is known from the Central and Inner West Carpathians. A dramatic change occurred during the Bathonian, as documented in the Mecsek Unit by an increase in depositional water depths that can be related to the separation of the Tisza from the European continent, presumably in connection with the opening of the Alpine Tethys. Oxfordian radiolarites, followed by Rosso Ammonitico and Calpionella Limestone, combined with the faunal characteristics, indicate that Tisza had now become part of the Adriatic paleogeographic realm. Paleomagnetic data (Márton 2000) indicate, however, that rotations and translations of the Tisza micro-continent did not substantially depart from those of the European continent until about 130 Ma ago. This coincides with the Valanginian to Barremian volcanic activity of the Mecsek Mountains (Császár 1998). Interestingly, this event also approximately coincides with the opening of the Valais-Magura Ocean (e.g. Frisch 1979) and the onset of Early to mid-Cretaceous (“Austrian”) crustal shortening in the neighbouring Dacia and ALCAPA Mega-Units, as described earlier.

4.4.2. Tectonic contacts between Tisza and neighbouring units, timing of nappe stacking within the Tisza Mega-Unit

The *Mecsek* nappe system consists, according to Haas & Pero (2004), of the Mecsek and Szolnok Units. Since exposures are

restricted to the Mecsek Mountains, the internal structure of these units and their contacts with surrounding ones are poorly defined. The northern tectonic contact between the Mecsek nappe system and the Szolnok-Sava ophiolite-bearing belt of the Mid-Hungarian Fault Zone was mapped (Plate 1) according to Haas (2001) in the western sector, whilst in the area of Debrecen, we substantially departed from previous published compilations (e.g. Csontos & Vörös 2004). In this area the contact between the Mecsek nappe system and the Szolnok-Sava belt, as shown in Profile 2 (Plate 2), is based on a combination of borehole (Sáránd 1) and seismic data (Horvath & Rumpler 1984; Windhoffer et al. 2005). A Palaeogene thrust, overprinted by Miocene normal faulting, defines the contact between the previously stacked Mecsek and overlying Codru nappe systems with the Late Cretaceous Szolnok Flysch. The latter is considered as part of the Szolnok-Sava Zone (“ophiolite-bearing Intrapannonian Belt” of Channell et al. 1979) rather than simply the youngest cover of the Mecsek nappe system.

The **Bihor nappe** system (Villany-Bihor Zone or unit of Bleahu et al. 1994 and Haas & Pero 2004, respectively) crops out in the Villany Mountains of southern Hungary, as well as in the North Apuseni Mountains of Romania. We also included units that crop out in the Papuk inselberg of Croatia (Pamić et al. 1996) as part of the Bihor nappe system. We mapped its northern contact with the Mecsek nappe system after Csontos & Vörös (2004). However, we excluded the basement that crops out in the Moslavačka Gora inselberg in Croatia, previously considered as the westernmost tip of Tisza, from the Mecsek nappe system, and attributed it to the Sava Zone owing to the occurrence of mid-Cretaceous gabbros (109 ± 8 Ma; Balen et al. 2003) and Late Cretaceous-age high-temperature metamorphism and magmatism (Starijaš et al. 2006). The southern contact between the Bihor and the Codru nappe system is rather poorly constrained by subsurface data, except for the area south of Debrecen, where S-dipping reflectors indicate a shear zone (Posgay et al. 2006, their Fig. 2) that we interpret to mark the tectonic boundary between these two nappe systems. In the North Apuseni Mountains, however, the tectonic contact between Bihor “Autochthon” (Bleahu et al. 1981) and the Codru nappe system is well exposed and closely dated. The Codru nappe system (Bleahu et al. 1981) was thrust NW-ward over Early Turonian, the youngest sediments of the Bihor nappe system, whilst Late Turonian to Early Coniacian Gosau beds seal the tectonic contact between these two units (Schuller 2004).

The **Codru** nappe system, as mapped in Plate 1, corresponds to the Békés-Lower Codru nappe system of Bleahu et al. (1994) and Haas & Pero (2004), but it includes also the Upper Codru nappes that these authors considered as part of the Biharia nappe system. The Codru nappe system mostly consists of a succession of exclusively sedimentary nappes, mostly preserved in the western parts of the North Apuseni Mountains (Codru Mountains). Only the structurally lowest unit, the Finis-Girda Unit (Profile 3, Plate 3), also contains pre-Triassic basement. This basement can be traced eastwards around a structural dome of the Bihor nappe system exposed in the Bihor Moun-

tains. In contrast to the non-metamorphic Codru sediments, the pre-Triassic basement of the Girda Unit in the Bihor Mountains was mylonitized under greenschist facies conditions during Turonian nappe emplacement (Balintoni pers. comm. and our own observations). Stretching lineations and associated shear sense criteria in these mylonites indicate top-WNW nappe transport; kinematic indicators observed further W and within the sedimentary Codru nappe system indicate top-NW nappe transport.

Turonian-age top-NW thrusting also involved the structurally highest nappe system, the earlier described Biharia nappe system that we consider to form part of Dacia (see above). According to our interpretation (Profile 3, Plate 3) the Biharia nappe system, which was previously affected by mid-Cretaceous top-E nappe transport, was back-thrust towards the NW during the Turonian. Hence, it now forms the highest structural unit of the North Apuseni Mountains. This back-thrust is interpreted to be responsible for a substantial offset of the “Main Tethyan Suture Zone” (Săndulescu 1994), the suture zone between Tisza and Dacia that formed during the mid-Cretaceous orogeny. This interpretation is supported by the radiometrically constrained Jurassic (186–156 Ma) and Early Cretaceous (124–111 Ma) ages of metamorphism within the Biharia nappe system (Dallmeyer et al. 1999), which clearly pre-date Turonian thrusting.

In summary, and according to the interpretation presented above, the northern margin of Tisza, characterized by Germanic Muschelkalk-type facies, is preserved in the Mecsek Mountains and faced, during the Jurassic, a branch of the Alpine Tethys Ocean. The southern margin of the Tisza-block, however, faced the Triassic Meliata-Maliac Ocean that formed part of the Neotethys (Fig. 2b). Remnants of this Triassic passive continental margin are preserved in the highest sedimentary nappes (Vascou and Coltesti nappes) of the Codru nappe system and possibly in the Transylvanian nappes.

4.5. Dinarides

4.5.1. Overview

The tectonic units of the Dinarides were primarily compiled on the basis of the excellent geological 1 : 100'000 maps of former Yugoslavia (Osnovna Geološka Karta SFRJ). In some, but not all aspects we depart from schemes proposed by previous authors (i.e. Kossmat 1924; Petković 1961; Aubouin et al. 1970; Aubouin 1973; Dimitrijević 1982, 1997, 2001; Pamić et al. 2000; Hrvatović & Pamić 2005; Karamata 2006). The main difference with respect to previous compilations pertains to the distinction between a more external and a more internal ophiolitic belt, corresponding to the “Dinaridic and Mirdita-Pindos Oceanic Basin” and the “Vardar Zone Western Oceanic Basin” of Karamata (2006), respectively, as well as to their tectonic relationship with the continental Drina-Ivanjica and Jadar “blocks”. Almost all previous workers considered these two ophiolite belts as representing two distinct oceanic realms,

while the intervening continental blocks were regarded as terranes that separated them (e.g. Karamata 2006).

According to our interpretation, however, we have to deal with one single Jurassic ophiolite sheet in the Dinarides, namely the Western Vardar Ophiolitic Unit that was obducted onto the passive margin of Adria during latest Jurassic times (see Figs. 2 & 5). In this interpretation the Drina-Ivanjica and Jadar blocks simply represent tectonic windows below a single ophiolitic thrust sheet in which the most distal paleogeographic domains of Adria are exposed. Furthermore, we suggest that in map view the present-day separations between ophiolitic and continent-derived tectonic units resulted from Cretaceous to Cenozoic out-of-sequence thrusting, severely modifying the originally rather simple geometry that resulted from obduction (Plate 3, Profile 5). This view is not new and was already proposed by Bernoulli & Laubscher (1972) and Baumgartner (1985) for the southward adjacent Hellenides. Similarly, Smith & Spray (1984), Bortolotti et al. (2004b) and Bortolotti & Principi (2005) more recently emphasised the similarities between the ophiolitic belts in the Dinarides and Hellenides.

4.5.2. External Dinaridic Platform: Dalmatian Zone, Budva-Cukali Zone and High Karst Unit

The proximal parts of the Adriatic margin are characterized from the Triassic to Cenozoic times by carbonate platforms that are interspersed by intervening narrow deep-water basins (e.g. Bernoulli et al. 1990; Bernoulli 2001). One of these deep-water basins that are floored by crust of uncertain composition (thinned continental or oceanic) is the Pindos-Olonos Zone of Greece (e.g. Aubouin 1959) that is referred to as the Krasta-Cukali Zone in Albania (Aubouin & Ndojaj 1964; Robertson & Shallo 2000) and as the Budva Zone in Montenegro (Goričan 1994; Dimitrijević 1997).

The **Budva-Cukali Zone** of the Dinarides (Nopcsa 1921; Dimitrijević 1997), the sedimentary record of which starts with Triassic deep-water facies and ends with Cenozoic flysch, separates the relatively more external carbonate platform of the **Dalmatian Zone** from that of the more internal **High Karst Unit** (Aubouin et al. 1970). However, the Budva-Cukali Zone wedges out to the north between Kotor and Dubrovnik (Plate 1). Further north the Dalmatian Zone and High Karst Unit can still be separated by a thrust between the Dalmatian Zone and the High Karst Unit (Cadet 1970) that can be traced northwestward into the area of Split (Blanchet 1970) where it runs offshore, interfering with the N-S striking dextral Split-Karlovac transpressive zone (Chorowicz 1970, 1975, Fig. 1). According to the 1 : 100'000 Geological Map of former Yugoslavia (Osnovna Geološka Karta SFRJ) thrusting occurred exclusively during the Late Eocene to Early Oligocene (so-called Dinaridic phase of the Southern Alps), as documented by the accumulation of flysch-type sediments in an evolving flexural foreland basin from the Middle to the Late Eocene (e.g. Tari 2002). However, De Capoa et al. (1995), also found Miocene faunas along this flysch belt and hence provided evidence for

ongoing Late Miocene thrusting of the High Karst Unit onto the Dalmatian Zone. Also the Split-Karlovac transpressive zone was active later since it affected Miocene-age strata in intramontane basins. Merlini et al. (2002) report ongoing thrusting in the subsurface of the foreland of the Dinarides until Quaternary times for the Trieste area. All this indicates that shortening continued during Late Miocene to recent (?) times, as clearly documented in Albania (Carminati et al. 2004), and off-shore Montenegro within the Dalmatian Zone (e.g. Picha 2002).

Although many authors claim that the Pindos Trough of the Pindos-Olonos Zone was underlain by oceanic lithosphere (e.g. Stampfli & Borel 2004) no ophiolitic basement flooring this deep-water trough is exposed anywhere. Moreover, it is clear that the so-called Pindos Ophiolite Group of the Pindos Mountains in Greece, including its metamorphic sole and underlying, presumably Jurassic-age mélange formation (identical with the typical "Diabase-Radiolarite Formation" of the Dinarides), tectonically overlie the Cenozoic Pindos-Flysch, that is, the youngest sediments of the Pindos Zone (Aubouin 1959, Bornovas & Rondogianni-Tsiambaou 1983). This, and the fact that the Budva Zone has no northward continuation in Dalmatia, strongly argues in favour of the "one-ocean thesis" that was first formulated by Bernoulli & Laubscher (1972). We propose that the so-called, and in our opinion misnamed "Pindos ophiolites", form indeed the southern continuation of the Dinaridic-Mirdita ophiolite belt, but that these far-travelled ophiolite sheets have a more internal paleogeographic origin with respect to the Pindos Zone. Thus, the term "Mirdita-Pindos Ocean" is totally misleading and ought to be abandoned (see also Burchfiel 1980 who reached the same conclusion).

In Albania, the thin-skinned Miocene thrust belt of the Ionian Zone (Fraseri et al. 1996; Robertson & Shallo 2000; Carminati et al. 2004) is characterized by deeper marine slope and basin facies (Bernoulli 2001). It is external with respect to the Dalmatian Zone but does not reach the area of our map and strikes north-westward into the Adriatic Sea. The carbonate platform of the Dalmatian Zone is the northern equivalent of the more internal Kruja Zone of Albania (Aubouin & Ndojaj 1964; Robertson & Shallo 2000) and the Gavrovo-Tripolitza Zone of Greece (Jacobshagen 1986), which also crops out in the Olympos window of the Pelagonian Zone (Aubouin 1973). Moreover, in northeastern Albania, the Kruja (= Dalmatian) and Cukali (= Budva) zones, including Eocene-Oligocene sediments, are exposed in a window below the Korab (= Pelagonian) Massif and overlying Western Vardar ophiolites south of the area mapped in Plate 1 (Bortolotti et al. 2005). The carbonate platform of the High Karst Unit of Dalmatia, on the other hand, probably wedges out in Albania. In Greece, we interpret platform carbonates that are exposed in the Parnassos window of the Pelagonian Zone (Aubouin 1973; Jacobshagen 1986) as probable southern equivalents of the High Karst Unit. The existence of all these windows was the rationale for extrapolating at depth the external Dinaridic platform units over considerable distance (about 120 km) eastward beneath a Cenozoic thrust at the base of the more internal Dinaridic units (Pre-Karst

and Bosnian Flysch Unit and East Bosnian – Durmitor thrust sheet) and the Drina-Ivanjica (= Pelagonian) thrust sheet, as shown in Profile 5 of Plate 3.

4.5.3. Internal Dinaridic Platform: Pre-Karst and Bosnian Flysch Unit

The term ***Pre-Karst Unit***, introduced by Aubouin et al. (1970) and co-workers (Blanchet 1970; Cadet 1970; Charvet 1970), refers to a paleogeographic realm that was thought to be transitional between the carbonate platforms of the High-Karst Unit and a second and more internal tectono-stratigraphic unit, the so-called “Zone Bosniaque” of Aubouin et al. (1970), that is characterized by Late Jurassic to Cretaceous flysch. This flysch zone we refer to as ***Bosnian Flysch*** (“Flysch Bosniaque”) largely corresponds to the so-called “Sarajevo sigmoid” of Dimitrijević (1997). According to our own observations, however, the Bosnian Flysch does not represent a different first-order tectonic entity, and hence we interpret the Pre-Karst and Bosnian Flysch units as part of a single unit, the ***Pre-Karst and Bosnian Flysch Unit***. In western Bosnia, large parts of the Bosnian Flysch simply represent the latest Jurassic and younger sedimentary sequences of the Pre-Karst Unit, typically found in the more internal parts of one and the same tectonic unit. The Bosnian Flysch is, however, in tectonic contact with the overlying units, mostly the East Bosnian-Durmitor thrust sheet except in the NE where the latter wedges out (see Plate 1).

The Paleozoic of the Pre-Karst Unit, which exhibits no or only low-grade Variscan metamorphism, crops out in the Bosnian Schist Mountains and in the Sana-Una Paleozoic series of Bosnia and adjacent Croatia (Hrvatović 2000a; Hrvatović 2005; Hrvatović & Pamić 2005). Radiometric ages indicate Cretaceous (121–92 Ma) and Cenozoic (59–35 Ma) low-grade metamorphic overprints, respectively (Pamić et al. 2004). The external parts of the Pre-Karst Unit are characterized by Jurassic-Cretaceous transitional platform-slope facies. From Mid-Jurassic times onward, breccias were shed from the High Karst paleogeographic domain NE-ward towards the more distal parts of the Adria passive continental margin that was drowned during the Early Jurassic. Departures from the facies of the external Dinaridic platform occurred, however, locally already during Mid-Triassic times, as evidenced by the deposition of red nodular Rosso Ammonitico type limestones (the so-called “Han-Bulog” facies, first described by Hauer 1853). This facies is very widespread in the more distal parts of the Adriatic margin (Aubouin et al. 1970). In the more internal parts of the Pre-Karst and Bosnian Flysch Unit, pelagic sedimentation began during Early Jurassic times and well before the deposition of the Bosnian Flysch. The boundary between the Pre-Karst and Bosnian Flysch Unit and the High Karst Unit, as shown in Plate 1, in the SE follows essentially the one drawn by Aubouin et al. (1970) and Dimitrijević (1997). Further to the NE we based the mapping of the thrust contact between the Pre-Karst and Bosnian Flysch and the High Karst units in Plate 1 on the 1 : 100'000 Geological Map of former Yugoslavia (Os-

novna Geološka Karta SFRJ), this thrust being mostly accompanied by a narrow stripe of Cenozoic strata. Hence, we also included, for example, units such as the Mid-Bosnian Schist Mountains and the Raduša Unit (Hrvatović 2000a; Hrvatović 2005; Hrvatović & Pamić 2005), or the Sana-Una Paleozoic and its Mesozoic cover (Blanchet 1970; Pamić & Jurković 2002), in our combined Pre-Karst and Bosnian Flysch Unit.

The Bosnian Flysch s. str. (“Flysch Bosniaque” of Blanchet 1966 and Aubouin et al. 1970) comprises latest Jurassic (Tithonian) to Cenozoic flysch-type deposits that vary in depositional age, paleotectonic environment and source area both along and across strike. In the most internal zones of the Pre-Karst and Bosnian Flysch Unit, deposition of flysch started during the Late Jurassic but becomes progressively younger in the more external parts where it commenced variably during the Senonian, Maastrichtian or even the Palaeogene. Aubouin et al. (1970) recognised that the basal parts of the Bosnian Flysch represented syn-orogenic deposits with respect to what these authors referred to as the development of the Paleo-Dinarides. Other authors invoked, however, a passive margin scenario (distal Adriatic continental margin) to explain these flysch deposits (Pamić et al. 2000). According to our observations the latter model cannot be supported, at least for those parts of the Bosnian Flysch, which contain abundant ophiolitic detritus, such as the Late Jurassic to Berriasian age Vranduk Flysch that is exposed along the river Bosna north of Sarajevo (Blanchet 1966; Olujić 1978; Hrvatović 2000b). This flysch, which contains also radiolaritic pelagic intervals, formed at the leading edge of the Western Vardar Ophiolitic Unit during its obduction onto the Adria passive margin, the most distal parts of which were obviously converted into an active margin during the Late Jurassic.

The younger parts of the Bosnian Flysch in the Bosna Valley section, referred to as Ugar Flysch (Hrvatović 2000b) represent, however, a younger and entirely different type of flysch basin. According to our observations this Turonian to Senonian flysch rests unconformably either on previously deformed Vranduk Flysch or on Jurassic to Early Cretaceous strata of the Pre-Karst Unit. Hence it formed in response to a pre-Turonian orogenic event and, in this sense, represents a kind of Gosau Basin. Clasts contained in this flysch include large olistostoliths consisting of carbonates derived from the External Dinaridic platform. In Western Bosnia and Montenegro the base of similar flysch deposits is also Senonian in age (Mirković et al. 1972). Deposition of the so-called Durmitor Flysch in Montenegro (Dimitrijević 1997), however, commenced even later during Maastrichtian time and lasted into the Palaeogene. Accumulation of this flysch can be related to Late Cretaceous to Early Cenozoic top-SW thrusting and emplacement of the structurally next higher tectonic unit, the East Bosnian-Durmitor thrust sheet.

4.5.4. East Bosnian – Durmitor thrust sheet

The ***East Bosnian-Durmitor*** thrust sheet, as shown in Plate 1, comprises the unit of the same name defined by Dimitrijević

(1997), but includes also more internal tectonic units such as the Lim Paleozoic and overlying Triassic-Jurassic strata. The Triassic-Early Jurassic carbonate platform, which constitutes a large part of this unit, was drowned in Early Jurassic time and sunk below the CCD in the Middle Jurassic (Bajocian; Đerić pers. comm.) when the deposition of radiolarites started (e.g. Rampnoux 1970). The radiolarites give upward way to a Late Jurassic ophiolitic tectonic mélange (“Diabase-Radiolarite Formation”) that was deposited during the obduction of the directly overlying West Vardar Ophiolite Units. Hence the East-Bosnian-Durmitor thrust sheet is a composite tectonic unit; it consists in its basal part of Paleozoic and Mesozoic formations detached from the Adriatic passive margin in Cenozoic times, and in its upper part of the Western Vardar Ocean ophiolites that were obducted during the Late Jurassic to earliest Cretaceous. An out-of-sequence thrust, that post-dates the Late Jurassic obduction of the Western Vardar Ophiolitic Unit over the East-Bosnian-Durmitor Unit, is also found in the hanging wall of the East Bosnian-Durmitor composite thrust sheet. It juxtaposes the more external East Bosnian-Durmitor composite thrust sheet against a more internal structural unit, the Drina-Ivanjica Unit, which is also a composite tectonic unit (Plate 3, Profile 5). According to Dimitrijević (1997) the East Bosnian-Durmitor thrust sheet represents a far-travelled (>45 km) thrust sheet that corresponds to the “Zone Serbe” of Rampnoux (1970) and Aubouin et al. (1970). Note that on Plate 1 only the Paleozoic-Jurassic series, which underlie the ophiolitic mélange, were mapped as the East Bosnian-Durmitor thrust sheet, while the previously obducted ophiolites and associated mélanges were mapped as part of the Western Vardar Ophiolitic Unit; the same holds for the more internal Drina-Ivanjica and Jadar-Kopaonik composite thrust sheets, respectively.

The NW-SE striking external thrust contact between the East Bosnian-Durmitor thrust sheet and the Bosnian Flysch is strongly deflected towards N-S in the Sarajevo area (hence the term “Sarajevo sigmoid” for the underlying and more external Pre-Karst and Bosnian Flysch Unit). N of Sarajevo, the Paleozoic to Triassic formations of the East Bosnian-Durmitor thrust sheet laterally wedge out towards the NW. We regard, however, the so-called “Radiolarite Formation” (Pamić 2000), that is exposed in the Bosna River section and extends north-westward into the Banja Luka area (Plate 1), as forming part of the East Bosnian-Durmitor thrust sheet as well. In the Banja Luka area this Radiolarite Formation consists exclusively of late Middle Jurassic to earliest Cretaceous radiolarites (Vishnevskaya & Đerić 2005; Đerić pers. comm.) that are tectonically sandwiched between Vranduk Flysch in the footwall and an ophiolitic mélange at the base of the Western Vardar Ophiolitic Unit in the hanging wall.

The East Bosnian Durmitor thrust sheet can locally be subdivided into second-order tectonic units, such as the more external Durmitor sub-unit of Montenegro and the more internal Lim sub-unit of adjacent southern Serbia. These are involved in a number of domal anticlines that are upheld by

low-grade Paleozoic sediments (i.e. Foča and Lim Paleozoic). The Triassic (i.e. Rampnoux 1970) is either characterized by thick platform carbonates, such as those found in the Durmitor sub-unit, or by more distal slope or basinal facies typical for the more internal Lim sub-unit, which are occasionally characterized by siliceous thin-bedded limestones (Ladinian-Carnian age Grivska Formation defined by Dimitrijević & Dimitrijević 1991). This slope facies is very reminiscent of the so-called Pötschenkalk-facies of the Eastern Alps (e.g. Gawlick 2000) or a coeval deep-water limestone in Central Greece Adhami Limestone; Baumgartner 1985) and is also found in the more internal Drina-Ivanjica and Jadar-Kopaonik thrust sheets. Mid-Triassic rift-related volcanism is wide-spread throughout this unit (Pamić 1984). Very thick (>100 m) Jurassic radiolarite successions (Rampnoux 1970) are typical for the more internal Lim sub-unit in southern Serbia (Zlatar area) and resemble those of the late Middle Jurassic to earliest Cretaceous (Vishnevskaya & Đerić 2005) “Radiolarite Formation” of the Bosna Valley section (Pamić 2000) much further to the NW, which are also part of the East Bosnian-Durmitor thrust sheet and were deposited prior to the Late Jurassic to Early Cretaceous obduction of the Western Vardar ophiolites onto the distal Adriatic margin. Note that most previous authors (e.g. Dimitrijević 1997; Pamić 2000) erroneously interpreted these radiolarites, which according to our observations tectonically underlie the obducted Western Vardar Ophiolitic Unit, as part of the ophiolitic succession.

4.5.5. Drina-Ivanjica thrust sheet

The *Drina-Ivanjica* thrust sheet contains even more distal parts of the Adriatic passive margin. It was probably emplaced in Early to mid-Cretaceous times on top of the East Bosnian – Durmitor thrust sheet and, similar to the East Bosnian-Durmitor composite thrust sheet, also carried passively the previously obducted Western Vardar ophiolites (i.e. the Zlatibor ophiolites; see Plate 3, Profile 5). The front of this thrust sheet was mapped by compiling the 1 : 100'000 sheets of the Geological Map of former Yugoslavia (Osnovna Geološka Karta SFRJ). NE of Sarajevo (Devetak area), Triassic to Middle Jurassic strata form mainly the frontal parts of this thrust sheet. SW-wards, in the Zlatibor area, the sole of the thrust front locally ramps up into the previously obducted ophiolites. This caused a duplication of the ophiolitic units since the footwall of the “youngest” rocks of the East Bosnian – Durmitor nappe also consists of ophiolites (see Plate 3, Profile 5).

The more internal parts of the Drina-Ivanjica thrust sheet consist largely of low-grade metamorphic Paleozoic formations (Milovanović 1984) that form the basement of the Drina-Ivanjica Mesozoic. The facies of the Mesozoic strata shares many similarities with that of the East-Bosnian-Durmitor thrust sheet (Dimitrijević & Dimitrijević 1991). Local occurrences of red nodular Late Anisian limestones (Hambuloz facies; Sudar 1986), siliceous thin-bedded Ladinian to Carnian limestones (Grivska Formation) indicate that these

Mesozoic rocks also were deposited on a relatively distal part of the Adriatic passive margin, which started to form in Triassic times (Rampoux 1970; Dimitrijević & Dimitrijević 1991). Thick sequences of Jurassic radiolarites are also typical for this thrust sheet. In places, the drowning below the CCD started rather abruptly in Aalenian times, radiolarite deposition persisting until Callovian times (Đerić et al. 2007) and being followed by ophiolite emplacement. Above a major unconformity, Cenomanian to Maastrichtian sediments commence with shallow water clastics and rudist limestones, which grade upward into flysch (Kosovska Mitrovica Flysch; Dimitrijević & Dimitrijević 1976, 1987). These series progressively unconformably cover, from west to east, ultramafics and mélange of the Western Vardar Ophiolitic Unit, Mesozoic and finally Paleozoic strata of the Drina-Ivanjica thrust sheet (Plate 3, Profile 5). This sedimentary cover is post-tectonic and post-metamorphic with respect to the Late Jurassic to earliest Cretaceous obduction of the Western Vardar Ophiolitic Unit and to Early to mid-Cretaceous deformations.

We correlate the base of the Late Cretaceous sedimentary cover of the Drina-Ivanjica thrust sheet with the base of the Ugar Flysch that occurs in the Bosna Valley section and that is also post-tectonic with respect to Cretaceous compressional deformation affecting the Vranduk Flysch. Since neither Late Cretaceous nor Cenozoic flysch is present below the frontal thrust of the Drina-Ivanjica thrust sheet, we propose that thrusting of this unit also occurred during the Early to mid-Cretaceous deformation of the internal Dinarides. It is this thrust event, combined with subsequent erosional denudation, which we hold responsible for the development of the unconformity at the base of this more than 200 km long strip of Late Cretaceous Kosovska Mitrovica Flysch (Plate 3, Profile 5). This flysch extends from western Serbia southward into the Kosovo (Dimitrijević 1997) in the immediate footwall of the next higher and yet more internal unit: the Jadar-Kopaonik thrust sheet.

In summary, this interpretation strongly deviates from the view expressed by practically all previous authors who regarded the Drina-Ivanjica Unit as a continental terrane that was originally located between two separate oceanic basins (e.g. Dimitrijević & Dimitrijević 1973; Robertson & Karamata 1994; Dimitrijević 2001; Karamata 2006) or who postulated that this element was derived by out-of-sequence thrusting from the European margin (Pamić et al. 1998; Hrvatović & Pamić 2005). However, as the tectonic position of the Drina-Ivanjica thrust sheet is identical to that of the *Korab* element in Albania, referred to as *Pelagonides* in Macedonia and Greece, our re-interpretation has consequences for the entire Dinaridic-Hellenic Orogen. Based on our interpretation of the cross section through the Dinarides we challenge the postulate of most authors (i.e. Robertson & Karamata 1994; Stampfli et al. 2004) according to which in the area of the future Hellenides the Pelagonian micro-continent was originally located between a more external “Pindos” or “Sub-Pelagonian” Ocean and a more internal “Maliac” or “Vardar” Ocean.

4.5.6. Jadar-Kopaonik thrust sheet

The present-day tectonic contact between the Drina-Ivanjica thrust sheet and the Jadar-Kopaonik thrust sheet, derived from the most distal Adriatic passive margin, is very steep (Plate 3, Profile 5) and has a strong dextral strike-slip component (Gerzina & Csontos 2003). In the literature this contact is referred to as “Zvornik suture” (Dimitrijević 1997) that is supposed to mark the ophiolitic suture between the continental Drina-Ivanjica and Jadar block terranes (Karamata 2006). In our view also this innermost thrust sheet passively carries previously obducted ophiolites of the Western Vardar Ocean. Hence, according to our interpretation this Zvornik “suture” simply represents the northwestern continuation of the long belt of Senonian flysch, that marks the tectonic boundary between the Drina-Ivanjica and Jadar-Kopaonik thrust sheets. The Jadar-Kopaonik thrust sheet represents the third and innermost thrust sheet that was activated after the Late Jurassic obduction of the Western Vardar Ophiolitic Unit. Also elsewhere Late Cretaceous (“Senonian”) flysch unconformably overlies the Jadar-Kopaonik thrust sheet, the largest occurrence being present SSW of Belgrade in the Ljig area.

The so-called *Jadar* “block” consists of a non-metamorphic Paleozoic basement that is covered by Permian Bellerophon limestones, which are followed by a Triassic succession that is similar to the one of the Drina-Ivanjica thrust sheet (Dimitrijević 1997). Moreover, Filipović et al. (2003) recognized very strong similarities between these rocks and those in the *Bükk* Unit of Northern Hungary. This correlation provides one of the major arguments to consider the Bükk Mountains as a displaced fragment of the internal Dinarides (Kovács et al. 2000, 2004; Dimitrijević et al. 2003). Geographically, the Medvednica Mountain and neighbouring inselbergs near Zagreb occupy an intermediate position. Tomljenović (2000, 2002) showed that a low-grade metamorphic complex, partly consisting of Mesozoic rocks and partly of Paleozoic series, was covered by an ophiolitic mélange during a first deformation event that possibly equates with the Late Jurassic ophiolite obduction of the Western Vardar Ophiolitic Unit (see also Pamić & Tomljenović 1998; Pamić et al. 2002a). The low-grade metamorphism of the Paleozoic and Mesozoic rocks is of Aptian (115–123 Ma) age (Belak et al. 1995); moreover, a blueschist event of unknown age (Belak & Tibljaš 1998) has also been reported from this area.

In southern Serbia two other complexes crop out, which according to our interpretation belong to the most distal Adriatic margin, and are surrounded by the Western Vardar Ophiolitic Unit: a window in the *Kopaonik* area (Fig. 1) and a smaller westerly adjacent window below the Western Vardar ophiolites referred to as Studenica slice (Dimitrijević 1997). According to our investigations both these windows expose low-grade metamorphosed Paleozoic to Mesozoic rocks. Karamata (2006) considered the Kopaonik block as yet another continental terrane, which he traced northward into the Belgrade area. We regard, however, also the rocks in the Kopaonik and Studenica window,

together with the Jadar block and more southerly occurrences found in the Kosovo, as having been derived from the distal Adriatic passive margin. Southwest of Belgrade, the tectonic contact between the Drina-Ivanjica and Jadar-Kopaonik thrust sheets turns in map view NW-ward, owing to some differential rotation between the southeastern and northwestern Dinarides; this is one of the reasons for not extending the Kopaonik ridge into the Belgrade area in Plate 1.

According to a cross-section published by Grubić et al. (1995) and our observations, the Kopaonik window is a late-stage antiform structure that folded the previously obducted Western Vardar Ophiolitic Unit preserved on both sides of this structure (see also Sudar & Kovács 2006). On the eastern flank of this antiform, which was later intruded by an Oligocene granodiorite, occurs a strip of Senonian flysch. This flysch rests unconformably either on the Western Vardar ophiolites or on the underlying continental units of the Kopaonik window and is over-thrust by the Eastern Vardar Ophiolitic Unit that was earlier obducted onto the Serbo-Macedonian Massif (Profile 5, Plate 3). We regard the corresponding E-dipping thrust fault as a first order tectonic contact that marks the suture between the Dinarides in a lower-plate position and the Carpatho-Balkan orogen in an upper-plate position. Towards the hangingwall this Senonian flysch contains huge olistoliths, as well as abundant detrital material that was eroded from the overriding Eastern Vardar Ophiolitic Unit, thus dating the closure of this flysch basin as Late Senonian. We interpret this strip of Senonian flysch, which here marks a suture, as the southerly extension of the Sava Zone (Plate 3, Profile 5).

The continental units underlying the Western Vardar ophiolites in the Kopaonik area, as well as in the W-ward adjacent Studenica area, largely consist of Triassic carbonates, often transformed into marbles, and associated meta-basites (Zelić et al. 2005). Sudar (1986) determined Carnian and Norian ages for some of the carbonates occurring in the Kopaonik area and in other areas of the adjacent Kosovo (metamorphic Trepča series), proving their Mesozoic age. They stratigraphically rest on Early Triassic Werfen beds and Paleozoic schists. Sudar & Kovács (2006) estimated the temperature of this metamorphism to be slightly higher than 400 °C based on the colour alteration index established for conodonts and on microstructural observations. The exact age of this metamorphism, which pre-dates the unconformity at the base of the Senonian flysch, is still unknown (Jurassic or Early to mid Cretaceous?).

4.5.7. Ophiolites obducted onto the Adria margin: the Western Vardar Ophiolitic Unit

In former Yugoslavia the mapping of the Western Vardar ophiolites shown on Plate 1 is based on the 1 : 100'000 geological maps of former Yugoslavia (Osnovna Geološka Karta SFRJ) whilst for Albania we used the 1 : 200'000 map of Albania (Geological Map of Albania 2002) and an overview presented by Robertson & Shallo (2000). We mapped all ophiolitic occurrences west of the Sava belt as the same unit that is here col-

lectively referred to as Western Vardar Ophiolitic Unit. Also in Albania (Mirdita ophiolites) a traditional distinction between different ophiolitic belts cannot be made on structural grounds, although geochemical and petrological differences have been documented (see below). A high-grade metamorphic sole typically underlies the obducted ultramafic massifs. We also included the ophiolitic mélange underneath the metamorphic sole, as well as the post-obduction overlapping younger strata into this same tectonic unit on Plate 1.

In the territory of former Yugoslavia two belts of largely isolated ultramafic massifs forming klippen overlying the ophiolitic mélange (Diabase-Radiolarite Formation) are evident in map view (Plate 1). These belts are separated by a structural culmination of the continental Drina-Ivanjica thrust sheet. The more external belt, referred to by most authors as the Dinaridic ophiolites (or Dinaridic ophiolite belt; Pamić et al. 2002a; Karamata 2006), is also known as the Central Dinaridic ophiolite belt (Lugović et al. 1991). Most of the ophiolitic klippen of this external belt overly the external parts of Drina-Ivanjica thrust sheet and a few the internal parts of the East-Bosnian-Durmitor thrust sheet in Serbia and Montenegro. The more internal belt is referred to as Western Vardar ophiolites by Karamata (2006), but also referred to under a variety of names such as Inner Dinaridic ophiolite belt (Lugović et al. 1991), External Vardar Subzone (Dimitrijević 1997, 2001) or simply Vardar Zone (Pamić et al. 2002a). We propose that the collective term "Vardar" should not be used any longer, as the Eastern Vardar Ophiolitic Unit is part of the Carpatho-Balkan Orogen (or the Rhodopian fragment; Burchfiel 1980) and structurally separated from the Western Vardar Ophiolitic Unit by the Sava Zone (see below). Note that we excluded ophiolitic occurrences in the Fruška Gora Mountain NW of Beograd (Dimitrijević 1997) and in the northern parts of the Kozara Mountains in Bosnia (Karamata et al. 2000a) from the Western Vardar Ophiolitic Unit as we consider them as forming part of the more internal Sava Zone (Plate 1).

The SW ophiolite belt ("Dinaridic" in the sense of Karamata 2006) of the Western Vardar Ophiolitic Unit is dominated by fertile mantle rocks (lherzolites), though harzburgites occur locally as well. Extrusive rocks are relatively rare (Lugović et al. 1991; Trubelja et al. 1995). Depleted mantle rocks (harzburgites) predominate in the NE ophiolite belt ("Western Vardar" in the sense of Karamata 2006) of the Western Vardar Ophiolitic Unit that contains abundant extrusive rocks with a supra-subduction geochemical signature (i.e. Karamata et al. 1980; Spray et al. 1984; Lugović et al. 1991). Most authors concluded that the ophiolites of the western belt are predominantly of the MORB-type, whilst those of the eastern belt represent supra-subduction oceanic island-arc type ophiolites.

In northern Albania both belts merge into one larger thrust sheet, the *Mirdita* ophiolitic thrust sheet (e.g. Bortolotti et al. 1996, 2005; Gawlick et al. 2007) that was thrust over the Budva-Cukali Zone into a relatively more external structural position southwest of an important transverse zone known as Skutari-Pec line (Plate 1). This ophiolite unit, and other smaller

klippen in Central Albania, show a general trend from dominantly lherzolitic types in the west towards harzburgitic types in the east (e.g. Bortolotti et al. 2002b). Most authors working in Albania, however, express doubts that these two types of ophiolites represent different oceanic basins that were separated by a micro-continent. Some claim along-strike variations (e.g. Hoeck et al. 2002), whereas others infer that these ophiolites represent a single piece of oceanic lithosphere formed at a slow spreading ridge with variable amounts of amagmatic (west) vs. magmatic (east) spreading (Nicolas et al. 1999). Bortolotti et al. (2004b, 2005) also postulated a single oceanic basin, but invoked mature intra-oceanic NE-directed subduction to explain the supra-subduction-type ophiolites found in the eastern parts of the Albanian and Greek ophiolites. From a purely structural point of view (one sheet of obducted ophiolites), and owing to the widespread occurrence of metamorphic soles both in the western and eastern belt (see below), we subscribe to the latter interpretation.

The age of the ophiolitic ultramafic and mafic plutonic rocks of both belts is Middle to early Late Jurassic (163–148 Ma; Callovian to Early Tithonian), based on radiometric age determinations (Spray et al. 1984; Bazylev et al. 2006; Ustaszewski et al. submitted) and palaeontological data from the oldest overlying sediments (Late Bajocian to Early Oxfordian radiolarites, preserved in Albania only; Prela 1994; Chiari et al. 1994; Marcucci et al. 1994; Marcucci & Prela 1996). Interestingly, the range of ages obtained for of the metamorphic sole at the base of the obducted ophiolites appears to be slightly older (174–157 Ma, Aalenian-Oxfordian; Lanphere et al. 1975; Okrusch et al. 1978; Dimo-Lahitte et al. 2001). In Bosnia, Serbia and Albania a metamorphic sole is present almost everywhere at the base of the obducted ophiolites. Metamorphic conditions span a large range of temperatures from >300 to 850 °C while the range of the reported pressures (4–10 kbar) is relatively small (Carosi et al. 1996; Karamata et al. 2000b; Operta et al. 2003). Mafics (amphibolites) predominate, though interlayered meta-sediments, probably derived from the sedimentary cover of the lower plate during intra-oceanic subduction, occur as well (Karamata et al. 2000b; Bortolotti et al. 2005). Most authors agree that, given the inverted metamorphic field gradient and the large range of temperatures over only a few hundreds of meters, residual heat from the overlying young and still hot oceanic lithosphere represents the heat source for metamorphism affecting the protoliths of the lower plate rocks during the intra-oceanic obduction stage (Michard et al. 1991) of the future Western Vardar Ophiolitic Belt (Bortolotti et al. 2005). Shear sense indicators (Simpson & Schmid 1983) are preserved in the mylonitic metamorphic sole at Zlatibor Mountain (Dinaridic ophiolites of Southern Serbia, our observations), around the Bresovica locality in Kosovo (Karamata et al. 2000b and our observations), as well as in the Mirdita ophiolites of Albania (Carosi et al. 1996). The senses of shear consistently vary between top-W to top-NW. This indicates that intra-oceanic obduction was WNW-directed, that is oblique to nearly parallel to the present-day strike of the Dinaridic chain.

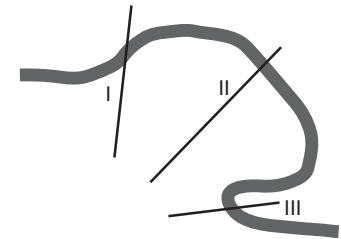
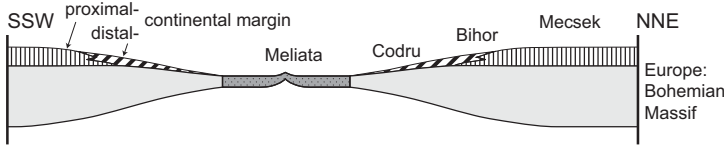
Given the Aalenian to Oxfordian ages for the formation of the metamorphic sole at a depth of 35 km (corresponding to 10 kbar), intra-oceanic subduction in the Meliata-Maliac-Vardar Neotethys Ocean must have started no later than at least some 5 Ma earlier (assuming a subduction rate of 1 cm per year and a 45° dipping subduction zone), namely at around 179 Ma ago (Toarcian). This suggests that older oceanic lithosphere (Early Jurassic and Triassic, see below) must have been present in this subducting lower plate (see Fig. 5).

The ophiolitic *mélange*, which occurs below the metamorphic sole flooring the obducted ophiolites (Diabase-Radiolarite Formation of former Yugoslavia, referred to as Rubik complex in Albania; e.g. Bortolotti et al. 2005), typically contains a mixture of (1) rock types derived from the lower plate, mechanically scraped off and accreted to the upper plate, and (2) gravitationally emplaced olistoliths derived from the upper plate. The blocks derived from the lower plate consist, amongst other lithologies, of Triassic ultramafics and mafics (MORB-type ophiolitic blocks up to several km in diameter) that were derived from the Meliata-Maliac-Vardar Ocean, the age of which was inferred from preserved stratigraphic contacts with Triassic radiolarites. Such Triassic ophiolites are found, for example, in the Darno-Complex adjacent to the Bükk Mountains (Dimitrijević et al. 2003), in the area around Zagreb (i.e. Halamić & Goričan 1995), in Serbia (Ovcar-Kablar gorge; N. Đerić pers. comm.) and in Albania (e.g. Kodra et al. 1993; Bortolotti et al. 1996; Gawlick et al. 2007). Amongst the blocks derived from the lower plate, Triassic strata derived from the adjacent Adria passive margin mafics predominate, however, over ophiolites. These Triassic strata consist of platform carbonates, slope to basal facies such as Hallstatt limestone, cherty limestone, thin-bedded radiolarite – pelagic limestone successions or radiolarites that are of Late Anisian to Norian age (e.g. Chiari et al. 1996; Dimitrijević et al. 2003; Goričan et al. 1999, 2005; Bortolotti et al. 2005; Gawlick et al. 2007). The composition of the rocks derived from the lower plate documents that the oceanic Triassic and Early Jurassic crust of the Meliata-Maliac-Vardar Neotethys Ocean, which was attached to the Adriatic passive margin was completely subducted, except for the blocks preserved in the Diabase-Radiolarite Formation. Hence we interpret the ophiolitic *mélange* as an accretionary prism that formed during the late emplacement stages of the obducted upper plate ophiolites (Western Vardar Ophiolite Unit) that are Jurassic in age. The gravitationally emplaced olistoliths mostly comprise blocks derived from the metamorphic sole and the Western Vardar ophiolites of the upper plate, including their overlying Jurassic radiolarites (e.g. Bortolotti et al. 2005).

The matrix of the ophiolitic *mélange* contains palynomorphs that yields ages ranging from the Hettangian to the Late Bajocian (Babić et al. 2002) in the area near Zagreb; hence *mélange* formation must post-date the Late Bajocian. The final obduction stages of ophiolites and associated ophiolitic *mélange* are dated by strata, which overstep the previously emplaced Western Vardar Ophiolitic Unit. After a period of erosion, during which parts of the obducted ophiolites were removed, sedimen-

Triassic - Jurassic boundary

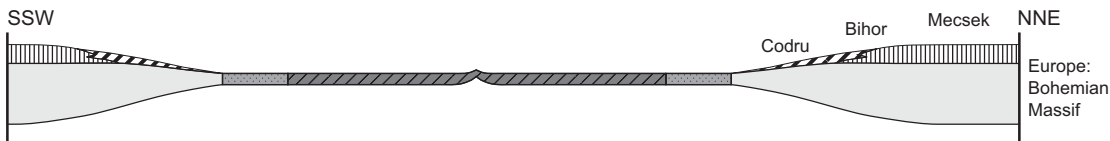
a) NW Dinarides - Tisza - Bohemian massif (I)



approximate orientations of the schematic section sketches in respect to the present-day Carpathian embayment

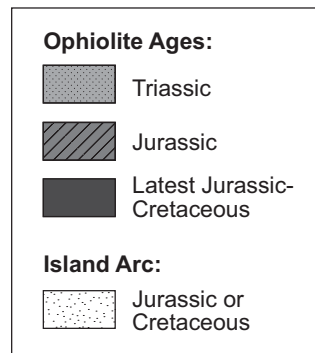
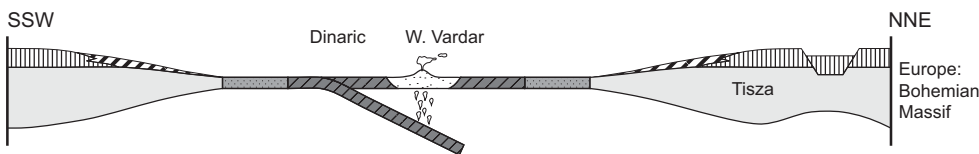
Early Jurassic

b) NW Dinarides - Tisza - Bohemian massif (I)



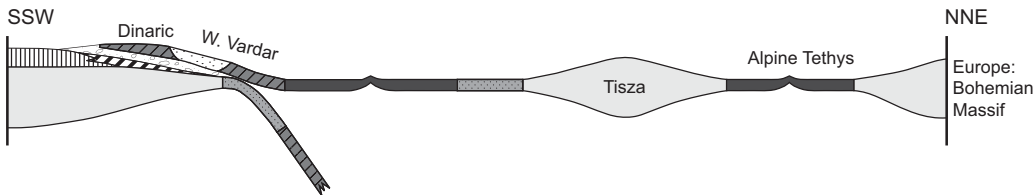
early Middle Jurassic

c) NW Dinarides - Tisza - Bohemian massif (I)



latest Jurassic

d) NW Dinarides - Tisza - Bohemian massif (I)



e) central Dinarides - Tisza - Dacia - Europe (II)

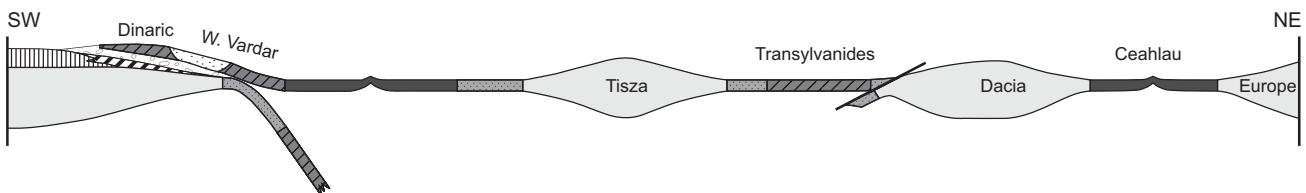
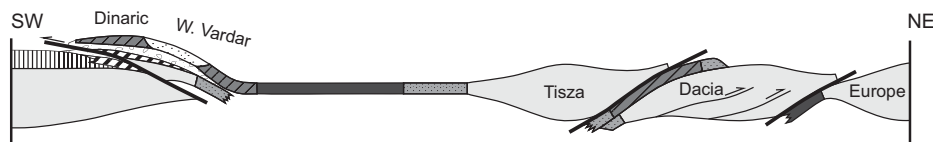


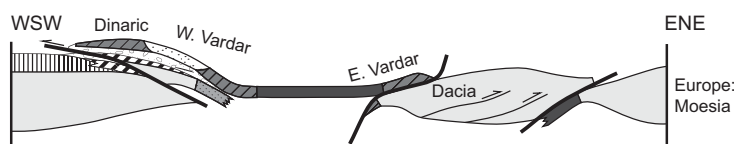
Fig. 5. Schematic serial sections depicting the plate tectonic evolution of the Alps-Carpathians-Dinarides system in pre-Cenozoic times. Given the complexity of the structures depicted in Plate 1, the sections were drawn in 3 different directions (see inset for location of the sections in present-day map view): a, b, c, d along section I; e, f, h along section II; g, i along section III. Note that important out-of-section translations of some of the units must have occurred (see Fig. 2). Furthermore, associated vertical axis rotations cannot be appropriately depicted in the sections alone. See text for detailed discussion.

late Early Cretaceous

f) central Dinarides - Tisza - Dacia - Europe (II)

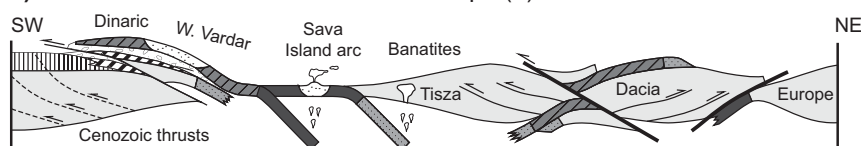


g) SE Dinarides - Dacia - Moesia (III)



Late Cretaceous

h) central Dinarides - Tisza - Dacia - Europe (II)



i) SE Dinarides - Dacia - Moesia (III)

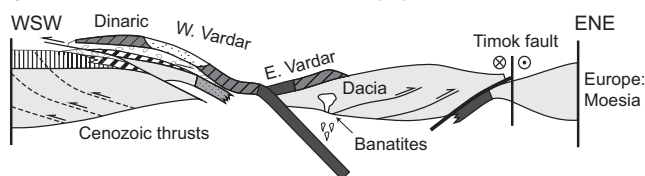


Fig. 5. (Continued).

tation locally resumed (e.g. Bosna River section) with fluvial conglomerates and sandstones (Pogari Formation; Blanchet et al. 1970; Pamić & Hrvatović 2000; Neubauer et al. 2003). These Tithonian to Berriasian conglomerates contain reworked ophiolitic as well as continental crustal material, including Late Permian granites (Neubauer et al. 2003). A similar over-step sequence that consists of mixed continental and ophiolitic detritus and ranges in age from Tithonian to Valanginian is known from Albania (Simoni mélange; Bortolotti et al. 2005). In former Yugoslavia platform carbonates and reefal build-ups of Late Jurassic (Kimmeridgian-Tithonian) and Early Cretaceous age are more widespread. These overlie erosionally truncated ophiolites and interfinger laterally with the Pogari conglomerates (Pamić & Hrvatović 2000). These overstepping formations indicate that the final stages of obduction occurred during Late

Jurassic times. Hence, final obduction onto the Adriatic margin closely followed, within some 10 Ma, intra-oceanic subduction. However, since the age range of radiolaria in the underlying radiolarites of the continental East Bosnian Durmitor thrust sheet extends into the Berriasian and Valanginian (Đerić & Vishnevskaya 2006; Đerić pers. comm.) this obduction possibly did not come to a halt before Early Cretaceous times. Our kinematic analysis in the Zlatibor area (Rudine locality), performed on the weakly metamorphosed matrix of ophiolitic mélange immediately underlying the metamorphic sole, indicated top-WNW thrusting. Thus, also the final stages of ophiolite obduction involved transport oblique to sub-parallel to the present-day strike of the Dinarides.

After the Late Jurassic to Early Cretaceous period of alluvial to neritic sedimentation, the overstep basin was involved

in Early to mid-Cretaceous folding and thrusting, subjected to erosion and subsequently unconformably covered by the Senonian series which locally rest on the non-ophiolitic parts of the Drina-Ivanjica and Jadar-Kopaonik thrust sheets. These series grade upward into latest Cretaceous flysch that immediately predates the Palaeogene development of the major tectonic contacts between the different units of the Inner Dinarides.

4.5.8. Sava Zone: the Cenozoic suture between Dinarides and Tisza-Dacia

According to our interpretation, the **Sava Zone** marks the position of a suture between the upper plate Tisza and the Dacia Mega-Units to the NE and SE, respectively, and the lower plate internal Dinarides (Fig. 5 and Plate 3, Profile 5). Originally this belt of ophiolitic, magmatic and metamorphic rocks that extends from Zagreb to Belgrade was referred to as “North-western Vardar Zone” (Pamić 1993) or “Sava-Vardar Zone” (Pamić 2002a). It was interpreted as a Late Cretaceous to Early Palaeogene volcanic (back-) arc basin that had remained open until the Mid-Eocene collision between the Dinarides and the Tisza Block by Pamić et al. (2002a). Since the Western and Eastern Vardar Ophiolitic Units were closed by obduction in Late Jurassic times (see above) we prefer not to use the term “Vardar” for the Sava Zone, which contains relics of a Cretaceous age back-arc ocean (Fig. 2c) and presently represents a Palaeogene-age suture zone. Southward from Belgrade we extend the Sava Zone as a narrow belt of Late Cretaceous ophiolite-bearing flysch (Senonian Flysch of Dimitrijević 1997). There the Sava Zone separates the Dinarides (including the Western Vardar Ophiolitic Unit) from the Carpatho-Balkan orogen (including the Eastern Vardar Ophiolitic Unit) (Plate 1; Plate 3, Profile 5).

Unfortunately, near Zagreb there are no exposures of the Sava Zone in the area of the junction of the Mid-Hungarian Fault Zone that includes the ophiolitic “Intra-Pannonian Belt” (Channell et al. 1979) and the westernmost parts of the ophiolite-bearing Sava belt of the Dinarides. Furthermore, the tectonic position of the Moslavačka Gora inselberg, characterized by Cretaceous-age gabbros (109 ± 8 Ma, Balen et al. 2003) and Late Cretaceous metamorphism and magmatism (Starijaš et al. 2006), is not very clear. Although traditionally attributed to the Tisza Mega-Unit, we interpreted the Moslavačka Gora inselberg as part of the Sava Zone, guided by the fact that areas with a strong Mesozoic metamorphic overprint are unknown from the adjacent internal Dinarides and the Tisza Unit.

The best exposures of the Sava Zone are present in northern Bosnia and Eastern Croatia (Kozara, Prosara, Motajica and Požeška inselbergs; Pamić 2002). In the northern part of the Kozara Mountains the southernmost and structurally lowest part of the Sava Zone is thrust SW-ward over the Western Vardar Ophiolitic Unit and its Cretaceous to Palaeogene post-obduction sedimentary cover. The structurally lowermost unit of the Sava Zone consists of Late Cretaceous ophiolites with bimodal volcanic suites (Karamata et al. 2000a; Ustaszewski et al. sub-

mitted). These younger ophiolites indicate that oceanic island arc-type crust (Sava Back-Arc Ocean in Fig. 2c) was generated during Late Cretaceous time within a remnant of the once much larger Neotethys Ocean. This confirms the view of Karamata et al. (2000a) that a remnant of the Vardar Ocean stayed open until Campanian times. Northward these Late Cretaceous ophiolites are covered by Maastrichtian to Eocene siliciclastic flysch (Cretaceous to Early Palaeogene flysch of Pamić et al. 2002a). Still further north, this flysch becomes progressively metamorphic (Pamić et al. 1992). This latest Cretaceous to Early Palaeogene metamorphism reaches lower amphibolite facies (Ustaszewski et al. 2007) and is followed during the Late Oligocene by the intrusion of S-type granites (Ustaszewski et al. 2006). This is in line with Pamić (1993, 2002) who provided evidence that the Sava Zone formed during the Palaeogene final collision of the Internal Dinarides with the Tisza Mega-Unit. The next and more easterly located inselberg occurs west of Belgrade in the Fruška Gora and exposes a very heterogeneous suite of blueschist metamorphic and non-metamorphic ophiolitic and non-ophiolitic rocks (Milovanović et al. 1995; Dimitrijević 1997). According to Milovanović et al. (1995) this metamorphism is Barremian in age (123 ± 5 Ma) and thus, documents an earlier stage of ongoing subduction of the Vardar Ocean.

South of Belgrade, a narrow strip of Senonian flysch represents the suture between the Dinarides and the Eastern Vardar Ophiolitic Unit that we consider as an integral part of the Carpatho-Balkan Orogen, and which, together with the Serbo-Macedonian “Massif”, forms here the upper plate during end-Cretaceous-Palaeogene suturing (Plate 3, Profile 5). Further to the east, a window through the Serbo-Macedonian Massif, the Jastrebac window (Fig. 1; Grubić 1999; Kräutner & Krstić 2002), exposes low-grade metamorphosed Late Cretaceous to Palaeogene flysch that is overlain by greenschists, marbles and meta-pelites. These rocks, which we attribute to the Sava Zone (Plate 3, Profile 5), clearly demonstrate that the previously E-facing thrust succession of the Carpatho-Balkan Orogen formed the upper plate with respect to the Dinarides during their Palaeogene final suturing. Furthermore, mantle xenoliths occurring within Palaeogene magmatic suites in the Carpatho-Balkan Orogen of eastern Serbia are evidence for deep reaching subduction of the Dinarides lower plate, causing magmatism in the upper plate according to Cvetković et al. (2004)

5. Summary and outlook

The bewildering geometric complexity of the Alpine-Carpathian-Dinaridic orogenic system largely results from its long lasting deformation history and local changes in polarity of subduction and thrusting. This led to multiple overprinting of older deformations by younger ones. In Figure 6 we attempted to group the age of tectonic contacts within this orogenic system into six time slices. We are aware that such a subdivision is rather artificial, particularly for those parts of the system that underwent a progressive and rather continuous history of deformation. In contrast, in other parts of this orogenic system,

the kinematics of deformation did change rather abruptly between the different deformation episodes. A second difficulty encountered during the construction of Figure 6 was that when along a given contact zone repeated tectonic activity had occurred we had to decide which deformation episode was the most important.

Late Jurassic deformations (170–150 Ma), associated with the obduction of parts of the Vardar Ocean, affected mainly the area of the future Dinarides (Figs. 5d,e), whereas the Eastern Alps were only marginally affected by this episode of deformation. The occurrences of ophiolitic *mélange* formations (Meliata unit) in the Western Carpathians show that the Jurassic Vardar Ocean was not only obducted onto the Adriatic southern margin of the Meliata-Maliac-Vardar Neotethys embayment in the domain of the Dinarides, but also less dramatically over its northern margin in the domain of the Western Carpathians. Note that in the Dinaridic domain this obduction occurred top-WNW with low-angle obliquity to the strike of the future orogen. On the other hand, the exact nature of the Late Jurassic, still rather enigmatic contact between the Eastern Vardar-South Apuseni and Transylvanian ophiolites with the Europe-derived Dacia units (Fig. 5e) is difficult to assess owing to a strong overprint by Early Cretaceous deformations.

Early Cretaceous orogenic processes strongly affected the Eastern Alps and the Dacia Mega-unit, but not the Tisza Mega-Unit. In the Eastern Alps, the Early Cretaceous orogeny was accompanied by the subduction of large volumes of continental crust along the western end of the Meliata embayment. This led to the development of an eclogitic subduction channel, which was subsequently exhumed. The onset of this orogeny around 135 Ma (Valanginian) is documented by the deposition of the Rossfeld Formation in the Northern Calcareous Alps (Faulpl & Wagreich 2000). In the Europe-derived Dacia Mega-unit, this deformation episode controlled the formation of the presently E-facing succession of nappes, closure of the Ceahlau-Severin Ocean and their suturing to the European foreland (Fig. 5f). At the same time, the Eastern Vardar Ophiolitic Unit overrode the internal, western margin of the Dacia Mega-Unit. In this area, the Early Cretaceous orogeny (“Austrian” phase) commenced during Late Barremian time (130 Ma), as evidenced by the onset of wildflysch accumulation, and ended prior to the deposition of the post-tectonic cover, between Aptian and earliest Cenomanian (125–100 Ma) times, depending on the location. Shortening was immediately followed by extensional collapse of the orogenic edifice. The Tisza Mega-Unit was, however, not affected by Early Cretaceous orogenic activity. This, and the fact that the kinematics of deformation of Turonian-age thrusting and nappe formation in the Tisza Mega-Unit are drastically different, i.e. top NW rather than top-E (see Plate 3, Profile 3), led us separate this Early Cretaceous episode from a younger one that started in early Late Cretaceous times.

The second, early Late Cretaceous, orogenic episode peaked during the Turonian. Typically, a Late Turonian to Coniacian-age unconformity truncates structures that resulted from this orogenic episode and forms the base of the overstepping

Gosau-type basins. In the area of the Tisza-Dacia Mega-Units, this second Cretaceous deformation episode can be rather clearly separated from the first one. Such a distinction is more problematic in the ALCAPA Mega-Unit of the Eastern Alps and the Western Carpathians. In these areas pre-Gosau deformation appears to have been rather continuous during the Cretaceous with the thrust front progressively migrating towards the European foreland. However, in both the Tisza-Dacia and ALCAPA Mega-Units Cretaceous-age metamorphism was followed by rapid exhumation (e.g. Thöni 2006), and the related Late Cretaceous extensional collapse that appears to have affected also the Dacia Mega-Unit. This indicates that in all areas considered the Early and early Late Cretaceous orogenic pulses were clearly separated from the Maastrichtian to Cenozoic orogenic phases.

In the Dinarides, Cretaceous orogenic events are currently not well dated. The most prominent angular unconformity occurs below the basal strata of the Turonian to “Senonian” overstep basins. For this reason we tentatively assigned the basal thrust of the Drina-Ivanjica thrust sheet to the early Late Cretaceous (100–85 Ma, Late Albian-Coniacian) compressional event (Figs. 5h,i). Rare radiometric ages so far available for the low-grade or blueschist metamorphism in the Dinarides available so far (Milovanović 1984; Belak et al. 1995; Milovanović et al. 1995; Pamić et al. 2004; Ilić et al. 2005) span, however, the entire 130–92 Ma time interval (Barremian–Cenomanian), suggesting that also in the Dinarides Cretaceous orogenic activity may have been rather continuous.

Compression resumed during the latest Cretaceous to Cenozoic orogenic cycle. A very short-lived orogeny affected during the latest Santonian and the Maastrichtian (“Laramide” phase) the East and South Carpathians, including the Transylvanian Basin. However, no Palaeogene compressional deformations have been recorded in the Tisza and Dacia Mega-Units. Indeed, some areas, such as the South Carpathians, underwent even extension during this period of time.

By contrast, the ALCAPA Mega-Unit and the Dinarides are characterized by a completely different Maastrichtian to Palaeogene deformation history. Palaeogene orogenic activity essentially shaped the present-day Alps, Western Carpathians and Dinarides and is thus recognized as the dominant deformation episode in this part of the Alpine-Carpathian-Dinaridic orogenic system. It was associated with a large magnitude of N–S convergence between Adria and Europe, estimated to be about 600 km in case of the Alps by Schmid et al. (1996). Contemporaneous shortening of this magnitude did not occur in the Tisza and Dacia Mega-Units during this time period. Hence, it is obvious that crustal shortening in the Alps, which was associated with a differential N-ward displacement of the Adria plate, must have been accommodated in the Dinarides by very substantial dextral strike-slip movements. The steepness of the more internal thrusts of the Dinarides indeed is suggestive of a transpressive tectonic setting during their Palaeogene evolution that essentially terminated at the Eocene-Oligocene transition when the subducted Adriatic slab was detached from

AGES OF MAJOR ACTIVITY OF MAJOR TECTONIC CONTACTS IN THE ALPS, CARPATHIANS AND DINARIDES

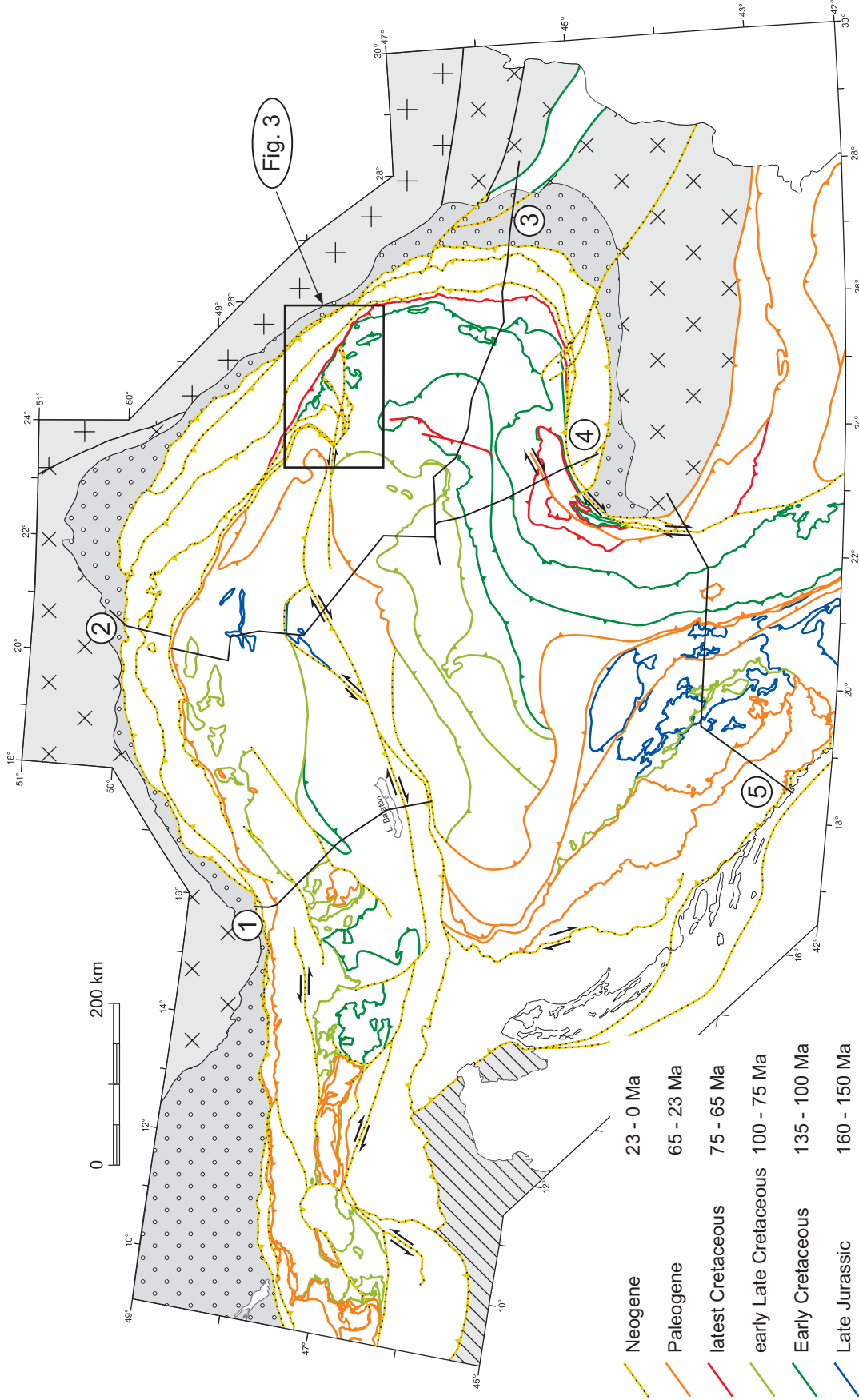


Fig. 6. Ages of main activity along major tectonic contacts in the Alps, Carpathians and Dinarides are colour-coded. Six time slices are depicted. Although some contacts were repeatedly active, only the age of the main deformation is shown. This figure also shows the locations of the traces of cross-sections given in Plates 2 and 3 and the area covered by Figure 3.

the lithosphere, giving rise to an Oligocene to Early Miocene high-K calc-alkaline and shoshonitic magmatism (Pamić et al. 2002b; Harangi et al., 2006). As already pointed out by Laubscher (1971) in his pioneering paper that addressed the Alps-Dinarides connection, a change in subduction polarity takes place between Alps and Dinarides. This change presumably occurs somewhere in the area now occupied by the Mid-Hungarian Fault Zone, i.e. the eastern continuation of the Periadriatic Line. However, this change in subduction polarity cannot be understood before the rather dramatic effects of Neogene deformation have been unravelled and palinspastically restored.

The Neogene tectonic setting of the Alpine-Carpathian-Dinaridic orogenic system is rather closely constrained. Continued crustal shortening in the Alps was accompanied by N-ward movement of the Adriatic plate, dextral wrench movements along the Periadriatic-Sava Zone of the Dinarides and E-ward lateral extrusion of the ALCAPA Mega-Unit along the Alpine Periadriatic-Mid-Hungarian Fault Zone. Retreat of the subducted European lithospheric slab beneath the inner Carpathians facilitated the advance of the ALCAPA and Tisza-Dacia Mega-Units into the Pannonian embayment and controlled the development of the back-arc-type Pannonian Basin (i.e. Horvath et al. 2006; Cloetingh et al. 2006). Simultaneously, the ALCAPA and Tisza Dacia Mega-Units invaded the still partly oceanic Carpathian embayment, involving substantial amounts of strike-slip faulting that interact with extension. Furthermore, the formation of this basin was kinematically linked to shortening in the external Miocene thrust belt of the Carpathians (Royden 1988).

Conclusions drawn from our correlations have serious paleogeographic implications. Alpine Tethys and Neotethys denote two separate groups of oceanic basins that opened during the break-up of Pangea (Fig. 2). The Neotethys opened during Triassic and Early to Mid-Jurassic times whilst the Alpine Tethys started to open during the Mid-Jurassic (Fig. 2; Figs. 5a-d). Remnants of the Triassic parts of the Neotethys, referred to as the Meliata Ocean, are preserved only in ophiolitic mélanges. Jurassic opening of the Alpine Tethys was largely contemporaneous with partial closure of the Neotethys oceanic lithosphere and the obduction of its Jurassic parts represented by the Eastern and Western Vardar Ophiolitic Units (Fig. 5d). Both, Triassic and Jurassic ophiolites formed part of one and the same branch of Neotethys, referred to as the Meliata-Maliac-Vardar Ocean (Fig. 2; Fig. 5b). By rooting the Transylvanian and South Apuseni ophiolites beneath the Tisza Mega-Unit, we postulate that a branch of the Jurassic Neotethys had separated the Tisza and Dacia Mega-Units. Erroneous interpretation of the complex geometries that resulted from out-of-sequence thrusting during the Cretaceous and Palaeogene deformations underlies a variety of multi-ocean concepts that were advanced in the literature. We propose that such models are incompatible with field evidence we have gathered and/or synthesized from the literature.

Moreover, different branches of the Alpine Tethys must have opened throughout the complex Alpine-Carpathian-Di-

naride orogenic system. For instance, the oceanic Valais and Piemont-Liguria units, including their eastern counterparts, were apparently only partly separated from each other by such ribbon continents as the Iberia Briançonnais micro-continent (Fig. 2c) and narrow elongated continental fragments found within parts of the Pieniny Klippen Belt (too small to be depicted in Fig. 2c). In present-day map view, the strike of the Piemont-Liguria main branch of the Alpine Tethys changed sharply in the Maramures area (area of the Pienides, see Fig. 1). From there, after turning south and southwest, it followed the Mid-Hungarian fault zone to finally link up with the Sava Zone, the ophiolitic constituents of which represent a back-arc basin of the Meliata-Vardar Ocean. The Ceahlau-Severin Ocean of the Eastern Carpathians represents an eastern branch of the Alpine Tethys, which in contrast, terminated eastwards and did not reach the present-day Balkan Mountains of Bulgaria (Fig. 2b).

Therefore we conclude that (1) none of the branches of the Alpine Tethys and Neotethys can be followed E-ward into the North Dobrogean Orogen, although such connections have been proposed in the past (e.g. Stampfli & Borel 2004). Instead, in the area of the Sava Belt the main branch of the Alpine Tethys was connected with the Neotethyan Meliata-Maliac-Vardar Ocean, representing the only oceanic realm that can be traced via the Dinarides and Hellenides eastward into Turkey (Fig. 2c). (2) We propose that all ophiolitic remnants of Neotethys found in the area under consideration formed part of one and the same oceanic basin that started to open in Triassic times and continued to open during the Jurassic, though its closure commenced during the Middle Jurassic at the same time as the Alpine Tethys began to open.

It is hoped that the correlation of tectonic units presented here will provide a solid basis for future research into the kinematics and dynamics of the Alpine-Carpathian-Dinaridic system and to better-constrained sequential palinspastic reconstructions of the various deformation episodes. Such research and testing of our interpretations will finally lead to a better understanding specifically of the kinematics and dynamics of pre-Neogene orogenies, orogenies that, in contrast to the Neogene deformations, still remain rather enigmatic.

Acknowledgements

We benefited from a close cooperation with: D. Balen (Zagreb), I. Balintoni (Cluj), T. Berza (Bucharest), L. Csontos (Budapest), C. Dinu (Bucharest), N. Đerić (Belgrade), D. Egli (Basel), L. Fodor (Budapest), W. Frank (Vienna), N. Froitzheim (Bonn), H.-J. Gawlick (Leoben), N. Gerzina (Belgrade), F. Horvath (Budapest), H. Hrvatović (Sarajevo), S. Karamata (Belgrade), A. Kounov (Basel), S. Kovács (Budapest), K. Krenn (Graz), C. Legler (Pristina), R. Lein (Vienna), M. Marović (Belgrade), E. Márton (Budapest), K. Onuzi (Tirana), J. Pamić (Zagreb), D. Plašienka (Bratislava), M. Săndulescu (Bucharest), E. Sasaran (Cluj), M. Sudar (Belgrade), V. Schuller (Tübingen), B. Tomljenović (Zagreb) and many others. Clark Burchfiel (Cambridge Mass.) and Peter Ziegler (Binningen) are thanked for their detailed and constructive comments; their reviews substantially improved a first version of the manuscript. Peter Nievergelt finalized the figures. This study was financed through the Swiss National Science Foundation grant Nr. 200021-101882/1 ("Tisza and

its role in the framework of the tectonic evolution of Alps, Dinarides and Carpathians”).

REFERENCES

- Anders, B., Reischmann, T., Poller U. & Kostopoulos, D. 2005: Age and origin of granitic rocks of the eastern Vardar Zone, Greece: new constraints on the evolution of the Internal Hellenides. *Journal of the Geological Society*, London 162, 857–870.
- Aubouin, J. 1959: Contribution à l'étude géologique de la Grèce septentrionale: les confins de l'Épire et de la Tessalie. Thèse, Paris, 1958. *Annales géologiques des Pays helléniques* 10, 483 pp.
- Aubouin, J. 1973: Des tectoniques superposées et de leur signification par rapport aux modèles géophysiques: l'exemple des Dinarides; paléotectonique, tectonique, tarditectonique, neotectonique. *Bulletin de la Société Géologique de France* 15/5–6, 426–460.
- Aubouin, J. & Ndojaj, I. 1964: Regards sur la géologie de l'Albanie et sa place dans la géologie des Dinarides. *Bulletin de la Société Géologique de France* 7/6, 593–625.
- Aubouin, J., Blanchet, R., Cadet, J.-P., Celet, P., Charvet, J., Chorowicz, J., Cousin, M. & Rampnoux, J.-P. 1970: Essai sur la géologie des Dinarides. *Bulletin de la Société Géologique de France* 12/6, 1060–1095.
- Babić, L., Hochuli, P. & Zupanić, J. 2002: The Jurassic ophiolitic mélange in the NE Dinarides: Dating, internal structure and geotectonic implications. *Eclogae geologicae Helveticae* 95, 263–275.
- Badescu, D. 1997: Tectono-thermal regimes and lithosphere behaviour in the external Dacides in the Upper Triassic and Jurassic Tethyan opening (Romanian Carpathians). *Tectonophysics* 282, 167–188.
- Baldi, T. & Baldi-Becke M. 1985: The evolution of the Hungarian Palaeogene basins. *Acta Geologica Hungarica* 28, 5–28.
- Balen, D., Schuster, R., Garašić, & Majer, V. 2003: The Kamenjača olivine gabbro from Moslavčka Gora (South Tisia, Croatia). *Rad Hrvatske akademije znanosti i umjetnosti knj.* 486, 57–76.
- Balintoni, I. 1981: The importance of the Ditrau Alcaline Massif emplacement moment for dating of the basement overthrusts in the Eastern Carpathians. *Revue Roumaine Géologie, Géophysique, Géographie, série Géologie* 25, 89–94.
- Balintoni, I. 1994: Structure of the Apuseni Mountains. In: ALCAPA II Field Guidebook «South Carpathians and Apuseni Mountains». *Romanian Journal of Tectonics and Regional Geology* 75, Suppl. 2, 37–58.
- Balintoni, I. & Gheuca, I. 1974: Metamorphism progresiv, metamorphism regresiv si tectonica in regiunea Zugreni-Barnar (Carpatii Orientali). *Anuarul Institutului de Geologie si Geofizica LXIII/5*, 11–38.
- Balla Z. 1987: Tertiary paleomagnetic data for the Carpatho-Pannonian region in the light of Miocene rotation kinematics. *Tectonophysics* 139, 67–98.
- Bauer, C., Rubatto, D., Krenn, K., Proyer, A., Hoinkes, G. 2007: A zircon study from the Rhodope metamorphic complex, N-Greece: Time record of a multistage evolution. *Lithos* 99, 207–228.
- Baumgartner, P.O. 1985: Jurassic sedimentary evolution and nappe emplacement in the Argolis Peninsula (Peloponnesus; Greece). *Mémoires de la Société Helvétique des Sciences Naturelles* 99, 111 pp.
- Bazylev, B., Zakariadze, G., Popević, A., Kononkova, N., Karpenko, S. & Simakin, S. 2006: Spinel peridotites from Bistrica Massif (Dinaridic ophiolite belt): The possible fragment of a sub-continental mantle. In: *Mesozoic ophiolite belts of the northern part of the Balkan Peninsula*; Proceedings of a Conference organized by the Serbian Academy of Sciences & Arts, Belgrade-Banja Luka, 12–14.
- Belak, M. & Tibljaš, D. 1998: Discovery of blueschists in the Medvednica Mountain (Northern Croatia) and their significance for the interpretation of the geotectonic evolution of the area. *Geologica Croatica* 51/1, 27–32.
- Belak, M., Pamić, J., Kolar-Jurkoviček, T., Pecsckay, Y. & Karan D. 1995: Alpinski regionalno metamorni kompleks Medvednice (Sjeverozapadna Hrvatska). In: Vlahović, I. et al. (Eds): 1st Croatian Geological Congress Proceedings 1: 67–70.
- Bernoulli, D. 2001: Mesozoic-Tertiary carbonate platforms, slopes and basins of the external Apennines and Sicily. In: Vai, G.B. & Martini, I.P. (Eds.): Anatomy of an orogen: the Apennines and adjacent Mediterranean basins. *Kluwer Academic Publishers*, 307–327.
- Bernoulli, D. & Laubscher, H. 1972: The palinspastic problem of the Hellenides. *Eclogae geologicae Helveticae* 65, 107–118.
- Bernoulli, D., Weissert, H. & Blome, C.D. 1990: Evolution of the Triassic Hawasina basin, Central Oman Mountains. In: Robertson, A.H.F., Searle, M.P. & Ries, A.C. (Eds.): *The Geology and Tectonics of the Oman Region*. Geological Society London Special Publications 49, 189–202.
- Berza, T. & Drăgănescu, A. 1988: The Cerna-Jiu fault system (South Carpathians, Romania), a major Tertiary transcurrent lineament. *Dări de Seamă Institutul de Geologie si Geofizică* 72–73, 43–57.
- Berza, T. & Iancu, V. 1994: Variscan events in the basement of the Danubian nappes (South Carpathians). In: ALCAPA II Field Guidebook. *Romanian Journal of Tectonics and Regional Geology* 75/2, 93–104.
- Berza, T., Krättner, H.G. & Dimitrescu, R. 1983: Nappe Structure of the Danubian window of the Central South Carpathians. *Anuarul Institutului de Geologie si Geofizica Bucharest* 60, 31–34.
- Berza, T., Balintoni, I., Iancu, V., Seghedi, A. & Hann, H.P. 1994: South Carpathians. In: ALCAPA II Field Guidebook. *Romanian Journal of Tectonics and Regional Geology* 75/2, 37–50.
- Berza, T., Constantinescu, E. & Vlad, S.N. 1998: Upper Cretaceous magmatic series and associated mineralization in the Carpathian-Balkan orogen. *Resource Geology* 48, 291–306.
- Bielik, M., Šefara, J., Kováč, M., Bezák, V. & Plašienka, D. 2004: The Western Carpathians – interaction of Hercynian and Alpine processes. *Tectonophysics* 393, 63–86.
- Birkenmajer, K. 1986: Stages of structural evolution of the Pieniny Klippen Belt, Carpathians. *Studia Geologica Polonica* 88, 7–31.
- Blanchet, R. 1966: Sur l'âge tithonique éocétacé d'un flysch des Dinarides internes en Bosnie. Le flysch de Vranduk (Yougoslavie). *Compte-Rendu Sommaire des Séances Société Géologique de France*, 401–402.
- Blanchet, R. 1970: Sur un profil des Dinarides, de l'Adriatique (Split-Omiš, Dalmatie) au Bassin panonique (Banja Luka – Doboj, Bosnie). *Bulletin de la Société Géologique de France* 12/6, 1010–1027.
- Blanchet, R., Durand Delga, M., Moullade, M. & Sigal J. 1970: Contribution à l'étude du Crétacé des Dinarides internes: la région de Maglaj, Bosnie (Yougoslavie). *Bulletin de la Société Géologique de France* 12/6, 1003–1009.
- Bleahu, M. 1962: Recherches géologiques dans le bassin supérieur de Valea Ruscova (Monts de Maramures). *Dări de Seamă Comision Géologique XLV*, 298–308.
- Bleahu, M., Lupu, M., Patrulius, D., Bordea, S., Stefan, A. & Panin, S. 1981: The Structure of the Apuseni Mountains. *Guide to Excursion B3*. 12th Carpatho-Balkan Geological Association Congress, Bucharest, Romania.
- Bleahu, M., Haas, J., Kovács, S., Péró, C., Mantea, G., Bordea, S., Panin, S., Bérczi-Makk, A., Ștefănescu, M., Konrád, G., Nagy, E., Ráliš-Felgenhauer, E., Sikić, K. & Török, A. 1994: Triassic facies types, evolution and paleogeographic relations of the Tisza Megaunit. *Acta Geologica Hungarica* 37, 187–234.
- Bocin, A., Stephenson, R., Tryggvason, A., Panea, I., Mocanu, V., Hauser, F. & Matenco, L. 2005: 2.5 D seismic velocity modelling in the southeastern Romanian Carpathians Orogen and its foreland. *Tectonophysics* 410, 273–291.
- Bombitá, G. & Savu, H. 1986: Sur les roches volcaniques associées aux klippes Piénines de Poiana Botizii (Maramouesh Roumain). *Annales Societatis Geologorum Poloniae* 56, 337–348.
- Bornovas, J. & Rondogianni-Tsiambaou, Th. 1983: Geological Map of Greece 1 : 500'000. Institute of Geology and Mineral Exploration, Athens.
- Bortolotti, V. & Principi, G. 2005: Tethyan ophiolites and Pangea break-up. *Island Arc* 14, 442–470.
- Bortolotti, V., Kodra, A., Marroni, M., Mustafa, F., Pandolfi, L., Principi, G.F. & Saccani, E. 1996: Geology and petrology of ophiolitic sequences in the Mirdita region (northern Albania). *Ofioliti* 21: 3–20.
- Bortolotti, V., Marroni, M., Ionel, N., Pandolfi, L., Principi, G.F. & Saccani, E. 2002a: Geodynamic Implications of Jurassic Ophiolites associated with Island-Arc Volcanics, South Apuseni Mountains, Western Romania. *International Geology Review* 44, 938–955.

- Bortolotti, V., Marroni, M., Pandolfi, L., Principi, G. & Saccani, E. 2002b: Interaction between mid-ocean ridge and subduction magmatism in Albanian ophiolites. *Journal of Geology* 110, 561–576.
- Bortolotti, V., Marroni, M., Ionel, N., Pandolfi, L., Principi, G.F. & Saccani, E. 2004a: An update of the Jurassic ophiolites and associated calc-alkaline rocks in the South Apuseni Mountains (Western Romania). *Ophioliti* 29/1, 5–18.
- Bortolotti, V., Chiari, M., Marcucci, M., Marroni, M., Pandolfi, L., Principi, G.F. & Saccani, E. 2004b: Comparison among the Albanian and Greek ophiolites: in search of constraints for the evolution of the Mesozoic Tethys Ocean. *Ophioliti* 29/1, 19–35.
- Bortolotti, V., Marroni, M., Pandolfi, L., Principi, G. 2005: Mesozoic to Tertiary tectonic history of the Mirdita ophiolites, northern Albania. *Island Arc* 14, 471–493.
- Boyakov, I., Dobovski, C.H., Gochev, P., Harkovska, A., Kostadinov, V., Tzankov, T.Z., and Zagorchev, I., 1989: A new view of the Alpine tectonic evolution of Bulgaria. *Geologica Rhodopica* 12, 107–121.
- Brown, S.A.M. & Robertson, A.H.F. 2004: Evidence for Neotethys rooted within the Vardar suture zone from the Voras Massif, northernmost Greece. *Tectonophysics* 381, 143–173.
- Brun, J.P. & Sokoutis, D. 2007: Kinematics of the Southern Rhodope Core Complex (North Greece). *International Journal of Earth Sciences* 96, doi: 10.1007/s00531-007-0174-2
- Burchfiel, B.C. 1980: Eastern European Alpine system and the Carpathian orocline as an example of collision tectonics. *Tectonophysics* 63, 31–61.
- Burchfiel, B.C. & Bleahu, M. 1976: Geology of Romania. Geological Society of America Special Paper 158, 82 pp.
- Burg, J.-P., Ricou, L.-E., Ivanov, Z., Godfriaux I., Dimov, D., Klain, L. 1996: Syn-metamorphic nappe complex in the Rhodope Massif: Structure and kinematics. *Terra Nova* 8, 6–15.
- Cadet, J.-P. 1970: Esquisse géologique de la Bosnie-Herzégovine méridionale et du Monténégro occidental. *Bulletin de la Société Géologique de France* 12/6, 973–985.
- Čanović, M. & Kemenci, R. 1999: Geologic setting of the Pre-Tertiary basement in Vojvodina (Yugoslavia). Part II: The north part of the Vardar zone in the south of Vojvodina. *Acta Geologica Hungarica* 42, 427–449.
- Carminat, E., Doglioni, C., Argnani, A. and 13 others 2004. Transect III, Massif Central – Provence – Gulf of Lion – Provençal Basin – Sardinia – Tyrrhenian Basin – Southern Apennine – Apulia – Adriatic Sea – Albanides – Balkans – Moesian Platform. In: Cavazza, W. Roure, F.M., Spakman, W., Stampfli, G.M. & Ziegler, P.A. (Eds.): *The TRANSMED Atlas – The Mediterranean Region from Crust to Mantle*. Springer, Berlin, Heidelberg, Part Two CD-ROM.
- Carosi, R., Cortesogno, L., Gaggero, L. & Marroni, M. 1996: Geological and petrological features of the metamorphic sole from the Mirdita ophiolites, northern Albania. *Ophioliti* 21, 21–40.
- Channell, J.E.T. & Horvath, F. 1976: The African/Adriatic promontory as a paleogeographical premise for Alpine orogeny and plate movements in the Carpatho-Balkan region. *Tectonophysics* 35, 71–101.
- Channell, J.E.T. & Kozur, H.W. 1997: How many oceans? Meliata, Vardar, and Pindos oceans in Mesozoic Alpine paleogeography. *Geology* 25, 183–186.
- Channell, J.E.T., D'Argenio, B. & Horvath, F. 1979: Adria, the African promontory in Mesozoic Mediterranean paleogeography. *Earth Science Reviews* 15, 213–292.
- Charvet, J. 1970: Aperçu géologique des Dinarides aux environs du méridien de Sarajevo. *Bulletin de la Société Géologique de France* 12/6, 986–1002.
- Cheshitev, I., Kánčev, I., Váľkov, V. & Marinova, R. 1989: Geological map of P.R. Bulgaria 1 : 500'000.
- Chiari, M., Marcucci, M. & Pella, M. 1994: Mirdita Ophiolite Project 2: Radiolarian assemblages in the cherts at Fushe Arrez and Shebaj (Mirdita area, Albania). *Ophioliti* 19, 313–318.
- Chiari, M., Marcucci, M., Cortese, G., Ondrejickova, A. & Kodra, A. 1996: Triassic Radiolarian assemblages in the Rubik area and Cukali zone, Albania. *Ophioliti* 21, 77–84.
- Chorowicz, J. 1970: La transversale de Zrmanja (Yougoslavie). *Bulletin de la Société Géologique de France* 12/6, 1028–1033.
- Chorowicz, J. 1975: Mechanics of Split-Karlovac transversal structure in Yugoslavian Dinarides. *Compte-Rendu Académie des Sciences Série D* 280/20: 2313–2316.
- Cioflica, G., Savu, H., Nicolae, I., Lupu, M., Vlad, S. 1981: Alpine Ophiolitic Complexes in South Carpathians and South Apuseni Mountains. *Carpatho-Balkan Geological Association, XII: Congress Guidebook Series* 18, Excursion A3, Bucharest.
- Čirić, B. & Karamata, S. 1960: L'évolution du magmatisme dans le géosynclinal dinarique au Mésozoïque et au Cénozoïque. *Bulletin de la Société Géologique de France* 7/2, 376–380.
- Cloetingh, S., Burov, E., Matenco, L., Toussaint, G., Bertotti, G., Andriessen, P.A.M., Wortel, M.J.R. & Spakman, W. 2004: Thermo-mechanical controls on the mode of continental collision in the SE Carpathians (Romania). *Earth & Planetary Science Letters* 218, 57–76.
- Cloetingh, S., Bada, G., Maţenco, L., Lankreijer, A., Horváth F. & Dinu, C. 2006: Modes of basin (de)formation, lithospheric strength and vertical motions in the Pannonian-Carpathian system: inferences from thermo-mechanical modelling. In: Gee, D.G. & Stephenson, R.A. (Eds.): *European Lithosphere Dynamics*. Geological Society London Memoirs 32, 207–221.
- Codarcea, A. 1940: Vues nouvelles sur la tectonique du Banat et du Plateau du Mehedinti. *Anuarul Institutului de Geologie si Geofizica* XX, 1–74.
- Császár G. 1998: The stratigraphy of the Early and Mid-Cretaceous formations of Mecsek and Villány Unit. In: Bérczi, I. & Jámor, Á. (Eds.): *The stratigraphy of the geological formations of Hungary (in Hungarian)*. MOL Rt & MÁFI, Budapest, 353–369.
- Csontos, L. 1995: Tertiary tectonic evolution of the Intra-Carpathian area: a review. *Acta Vulcanologica* 7/2, 1–13.
- Csontos, L. 1999: Structural outline of the Bükk Mts. (N Hungary). Text in Hungarian, abstract and figure captions translated. *Földtani Közlöny* 129/4, 611–651.
- Csontos, L. 2000: Stratigraphic re-evaluation of the Bükk Mts (N Hungary). Text in Hungarian, abstract and figure captions translated. *Földtani Közlöny* 130/1, 95–131.
- Csontos, L. & Nagymarosy, A. 1998: The Mid-Hungarian line: a zone of repeated tectonic inversions. *Tectonophysics* 297, 51–71.
- Csontos, L. and Vörös, A. 2004: Mesozoic plate tectonic reconstruction of the Carpathian region. *Paleogeography Paleoclimatology Paleocology* 210, 1–56.
- Csontos, L., Nagymarosy, A., Horváth, F. & Kováč, M. 1992: Cenozoic evolution of the Intra-Carpathian area: a model. *Tectonophysics* 208: 221–241.
- Cvetković, V., Downes, H., Prelević, D., Jovanović, M. & Lazarov, M. 2004: Characteristics of the lithospheric mantle beneath East Serbia inferred from ultramafic xenoliths in Palaeogene basanites. *Contributions Mineralogy & Petrology* 148, 335–357.
- Dallmeyer, R.D., Neubauer, F., Handler, R., Fritz, H., Müller, W., Pana, D. & Putiš, M. 1996: Tectonothermal evolution of the internal Alps and Carpathians: Evidence from ⁴⁰Ar/³⁹Ar mineral and whole-rock data. *Eclogae geologicae Helveticae* 89, 203–227.
- Dallmeyer, R.D., Pana, D.I., Neubauer, F. & Erdmer, P. 1999: Tectonothermal evolution of the Apuseni Mountains, Romania: Resolution of Variscan versus Alpine events with ⁴⁰Ar/³⁹Ar ages. *Journal of Geology* 107, 329–352.
- Dallmeyer, R.D., Neubauer, F., Krätner, H.G., Fritz, H. & Bojar, A.-V. in press: Variscan vs. Alpine tectonic processes in the Eastern Carpathian orogen: Evidence from ⁴⁰Ar/³⁹Ar mineral ages. *International Journal of Earth Sciences*.
- Dal Piaz, G.V., Martin, S., Villa, I., Gosso, G. & Marschalko, R. 1995: Late Jurassic blueschist facies pebbles from the Western Carpathian orogenic wedge and paleostructural implications for Western Tethys evolution. *Tectonics* 14, 874–885.
- de Brouker, G., Mellin, A. & Duindam P. 1998: Tectono-stratigraphic evolution of the Transylvanian Basin, pre-salt sequence, Romania. In: Dinu, C. & Mocanu, V.H. (Eds.): *Geological Structure and hydrocarbon potential of the Romanian areas*. Bucharest Geoscience Forum Volume 1, 36–69.
- De Capoa, P., Radoičić, R. and D'Argenio, B. 1995: Late Miocene deformation of the External Dinarides (Montenegro and Dalmatia): New biostratigraphic evidence. *Memorie Scienze Geologiche (Padova)* 47, 157–172.

- Dercourt J., & 18 others. 1986: Geological evolution of the Tethys belt from the Atlantic to the Pamirs since the Lias. In: Aubouin J., Le Pichon X. & Monin A.S. (Eds.): Evolution of the Tethys. *Tectonophysics* 123, 241–315.
- Dercourt, J., Ricou, L.E. & Vrielynck, B. (Eds.) 1993: Atlas Tethys Palaeoenvironmental Maps. Gauthier-Villars, Paris, 307 pp., 14 maps, 1 plate.
- Dicea, O. 1995: The structure and hydrocarbon geology of the Romanian East Carpathians border from seismic data. *Petroleum Geoscience* 1, 135–143.
- Dimitrijević, M.D. 1957: The structure of the crystalline region between Slišane and Preševo (English summary). Proceedings of the 2. Kongres geologa FNRJ, Sarajevo, 629–634.
- Dimitrijević, M.D. 1982: Dinarides: An outline of the tectonics. *Earth Evolution Sciences* 2/1, 4–23.
- Dimitrijević, M.D. 1997: Geology of Yugoslavia. Geological Institute GEMINI Special Publication, Belgrade, 187 pp.
- Dimitrijević, M.D. 2001: Dinarides and the Vardar Zone: a short review of the geology. *Acta Vulcanologica* 13, 1–8.
- Dimitrijević, M.D. (Ed.) 2002: Geological Atlas of Serbia. Serbian Ministry of Natural Resources and Environmental Protection, Beograd.
- Dimitrijević, M.N. & Dimitrijević, M.D. 1973: Olistostrome mélange in the Yugoslavian Dinarides and late Mesozoic plate tectonics. *Journal of Geology* 81/3, 328–340.
- Dimitrijević, M.N. & Dimitrijević, M.D. 1976: The Senonian Flysch of Kosovska Mitrovica. 2. Skup sedloga Jugoslavije, Beograd, 33–42.
- Dimitrijević, M.N. & Dimitrijević, M.D. 1987: The Titova Mitrovica Flysch. In: Dimitrijević, M.N. & Dimitrijević, M.D. (Eds.): The trubiditic basins of Serbia. Serbian Academy of Sciences and Arts Department of Natural & Mathematical Sciences 61, 25–64.
- Dimitrijević, M.N., Dimitrijević M.D. 1991: Triassic carbonate platform of the Drina-Ivanjica element (Dinarides). *Acta Geologica Hungarica* 34, 15–44.
- Dimitrijević, M.N., Dimitrijević M.D., Karamata S., Sudar M., Gerzina, N., Kovács, S., Dostály, L., Gulácsi, Z., Less, G. & Pelikán, P. 2003: Olistostrome/mélanges – an overview of the problems and preliminary comparison of such formations in Yugoslavia and NE Hungary. *Slovak Geological Magazine* 9, 3–21.
- Dimo-Lahitte, A., Monié, P. & Vergély, P. 2001: Metamorphic soles from the Albanian ophiolites: Petrology, $^{40}\text{Ar}/^{39}\text{Ar}$ geochronology, and geodynamic evolution. *Tectonics* 20, 78–96.
- Dinter, D.A. 1998: Late Cenozoic extension of the Alpine collisional orogen, northeastern Greece: Origin of the north Aegean basin. *Geological Society of America Bulletin* 110, 1208–1230.
- Đerić, N. & Vishnevskaya, V.S. 2006: Some Jurassic to Cretaceous radiolarians of Serbia. In: Mesozoic ophiolite belts of the northern part of the Balkan Peninsula, Proceedings of a Conference organized by the Serbian Academy of Sciences & Arts, Belgrade-Banja Luka, 29–36.
- Đerić, N., Gerzina N. & Schmid, S.M. 2007: The age of the Jurassic radiolarian chert formation from the Zlatar Mountains (SW Serbia). *Ophioliti*. 32, 101–108.
- Dumont, T., Wiczorek, J. & Bouillin, J.-P. 1996: Inverted Mesozoic rift structures in the Polish Western Carpathians (High-Tatric units). Comparison with similar features in the Western Alps. *Eclogae geologicae Helveticae* 89, 181–202.
- Ellouz, N., Roure, F., Săndulescu, M. & Badescu, D. 1994: Balanced cross sections in the eastern Carpathians (Romania): a tool to quantify Neogene dynamics. In: F. Roure, N. Ellouz, V.S. Shein & I. Skvortsov (Eds.): Geodynamic evolution of sedimentary basins. International Symposium Moscow 1992 Proceedings. Technip, Paris 305–325.
- Faryad, S.W. 1995a: Phase petrology and P-T conditions of mafic blueschists from the Meliata unit, West Carpathians, Slovakia. *Journal of Metamorphic Geology* 13, 701–714.
- Faryad, S.W. 1995b: Petrology and phase relations of low-grade high-pressure metasediments of the Meliata Unit, Western Carpathians, Slovakia. *European Journal of Mineralogy* 7, 71–87.
- Faryad, S.W. 1997: Lithology and metamorphism of the Meliata unit high-pressure rocks. In: Grečula P., Hovorka D. & Putiš M. (Eds): Geological evolution of the Western Carpathians. *Mineralia Slovaca Monograph* 131–144.
- Faryad, S.W. & Henjes-Kunst, F. 1997: Petrological and K-Ar and ^{40}Ar - ^{39}Ar age constraints for the tectonothermal evolution of the high-pressure Meliata unit, Western Carpathians (Slovakia). *Tectonophysics* 280, 141–156.
- Faupl, P. & Wagreeich, M. 2000: Late Jurassic to Eocene paleogeography and geodynamic evolution of the Eastern Alps. *Mitteilungen Österreichische Geologische Gesellschaft* 92, 70–94.
- Favre P. & Stampfli, G.M. 1992: From rifting to passive margin: the example of the Red Sea, Central Atlantic and Alpine Tethys. *Tectonophysics* 215, 69–97.
- Filipović, I., Jovanović D., Sudar M., Pelikán, P., Kovács, S., Less, G. & Hips, K. 2003: Comparison of the Variscan – Early Alpine evolution of the Jadar Block (NW Serbia) and “Bükkium” (NE Hungary) terranes; some paleogeographic implications. *Slovak Geological Magazine* 9, 23–40.
- Fodor, L. & Koroknai, B. 2000: Ductile deformation and revised lithostratigraphy of the Martonyi subunit (Torna Unit, Rudabánya Mts.), northeastern Hungary. *Geologica Carpathica* 51, 355–369.
- Fodor, L., Jelen B., Márton, M., Skaberne, D., Car, J. & Vrabec M. 1998: Miocene-Pliocene tectonic evolution of the Slovenian Periadriatic fault: Implications for Alpine-Carpathian extrusion models. *Tectonics* 17, 690–709.
- Fodor, L., Csontos, L., Bada, G., Györfi, I. & Benkovic, L. 1999: Tertiary tectonic evolution of the Pannonian basin system and neighbouring orogens: a new synthesis of paleostress data. In: Durand B., Jolivet, L., Horváth, F. & Séranne, M. (Eds.): The Mediterranean basins: Tertiary Extension within the Alpine Orogen. Geological Society London Special Publications 156, 295–334.
- Frank, W. 1987: Evolution of the Austroalpine elements in the Cretaceous. In: Flügel, H.W. & Faupl, P. (Eds.): Geodynamics of the Eastern Alps. Deuticke, Vienna, 379–406.
- Frank, W. & Schlager, W. 2006: Jurassic strike slip versus subduction in the Eastern Alps. *International Journal of Earth Sciences* 95, 431–450.
- Fraseri, A., Nishani, P., Bushati, S. & Hyseni, A. 1996: Relationship between tectonic zones of the Albanides, based on results of geophysical studies. In: Ziegler P.A. & Horváth, F. (Eds.) Peri-Tethys Memoir 2: Structure and Prospects of Alpine Basins and Forelands. Mémoires du Muséum National d'Histoire Naturelle 170, 485–511.
- Frisch, W. 1979: Tectonic progradation and plate tectonic evolution of the Alps. *Tectonophysics* 60, 121–139.
- Froitzheim, N., Schmid, S.M. & Frey, M. 1996: Mesozoic paleogeography and the timing of eclogite-facies metamorphism in the Alps: A working hypothesis. *Eclogae geologicae Helveticae* 89, 81–110.
- Fügenshuh, B. & Schmid, S.M. 2005: Age and significance of core complex formation in a very curved orogen: Evidence from fission track studies in the South Carpathians (Romania). *Tectonophysics* 404, 33–53.
- Fülöp, J. & Dank, V. (Eds.) 1987: Geological Map of Hungary without Cenozoic formations 1 : 500'000. Geological Institute, Budapest.
- Fülöp, J., Brezsnýánszki, K. & Haas, J. 1987: The new map of basin basement of Hungary. *Acta Geologica Hungarica* 30, 3–20.
- Gawlick, H.-J. 2000: Paläogeographie der Ober-Trias Karbonatplattform in den nördlichen Kalkalpen. *Mitteilungen der Gesellschaft der Geologie- & Bergbaustudenten Österreich* 44, 45–95.
- Gawlick, H.-J. & Frisch, W. 2003: The Middle to late Jurassic carbonate clastic radiolaritic flysch sediments in the Northern Calcareous Alps: sedimentology, basin evolution, and tectonics – an overview. *Neues Jahrbuch Geologisch- Paläontologische Abhandlungen* 230, 163–213.
- Gawlick, H.J. & Schlagintweit, F. 2006: Berriasian drowning of the Plassen carbonate platform at the type-locality and its bearing on the early Eoalpine orogenic dynamics in the Northern Calcareous Alps (Austria). *International Journal of Earth Sciences* 95, 451–462.
- Gawlick, H.J., Frisch, W., Hoxha, L., Dumitrica, P., Krystyn, L., Lein, R., Missoni, S. & Schlagintweit, F. 2007: Mirdita Zone ophiolites and associated sediments in Albania reveal Neotethys Ocean origin. *International Journal of Earth Sciences*. DOI 10.1007/s00531-007-01193-z.
- Geological Map of Albania 2002: Geological 1 : 200'000 map published by the Ministry of Industry & Energy and the Ministry of Education & Science, Tirana.
- Georgiev, G., Dabovski C. & Stanisheva-Vassileva, G. 2001: East Srednogie-Balkan Rift Zone. In: Ziegler P.A. et al. (Eds): Peri-Tethys Memoir 6:

- Peri-Tethyan Rift/Wrench Basins and Passive Margins. *Mémoires Muséum Histoire Naturelle Paris* 186, 259–293.
- Gerzina, N., & Csontos, L. 2003: Deformation sequence in the Vardar Zone: surroundings of Jadar block, Serbia. *Annales Universitatis Scientiarum Budapestinensis, Sectio Geologica* 35, 139–140.
- Girbacea, R. & Frisch, W. 1998: Slab in the wrong place: Lower lithospheric mantle delamination in the last stage of the eastern Carpathians subduction retreat. *Geology* 26, 611–614.
- Golonka, J. 2004: Plate tectonic evolution of the southern margin of Eurasia in the Mesozoic and Cenozoic. *Tectonophysics* 381, 235–273.
- Goričan, S. 1994: Jurassic and Cretaceous radiolarian biostratigraphy and sedimentary evolution of the Budva zone (Dinarides, Montenegro). *Mémoires de Géologie Lausanne* 18, 176 pp.
- Goričan, S., Karamata, S., Batočanin-Srećković, D. 1999: Upper Triassic (Carnian-Norian) radiolarians in cherts of Sjenica (SW Serbia) and the time span of the oceanic realm ancestor of the Dinaridic Ophiolite Belt. *Bulletin de l'Académie Serbe des Sciences et des Arts Classe Sciences Mathématiques et Naturelles* 39, 141–149.
- Goričan, S., Halamić, J., Grgasović, T. & Kolar-Jurkovsek 2005: Stratigraphic evolution of Triassic arc-backarc system northwestern Croatia. *Bulletin de la Société Géologique de France* 176, 3–22.
- Gröger H.R. 2006: Thermal and structural evolution of the East Carpathians in northern Romania: from Cretaceous orogeny to final exhumation during Miocene collision. Unpublished PhD Thesis, Basel University.
- Gröger, H.R., Fügenschuh B., Tischler R., Schmid, S.M. & Foeken, J. submitted: Tertiary cooling and exhumation history in the Maramures area (Internal Eastern Carpathians, Northern Romania): thermochronology and structural data. *Geological Society of London Special Publications*.
- Grubić, A. 1999: Tektonika Jastreba i njen opštiji značaj. *Rud. Geol. i Metal.* 50, 13–17.
- Grubić, A., Đoković, I. & Marović, M. 1995: Tectonic outline of the Kopaonik area (in Serbian, English abstract). In: Symposium "Geology and Metallogeny of Kopaonik Mt.". June 19–22 1995, 46–53.
- Gvirtzman, Z. 2002: Partial detachment of a lithospheric root under the southeast Carpathians: Toward a better definition of the detachment concept. *Geology* 30, 51–54.
- Haas, J. 2001: *Geology of Hungary*. Eötvös University Press, Budapest, 317 pp.
- Haas J. & Pero S. 2004: Mesozoic evolution of the Tisza Mega-unit. *International Journal of Earth Sciences* 93, 297–313.
- Haas, J., Kovács S., Krystyn L. & Lein, R. 1995: Significance of Late Permian-Triassic facies zones in terrane reconstructions in the Alpine-North Pannonian domain. *Tectonophysics* 242, 19–40.
- Haas, J., Mioč, P., Pamić, J., Tomljenović, B., Arkai, P., Berczi-Makk, A., Koroknai, B., Kovács, S., and Felgenhauer, E.R. 2000: Complex structural pattern of the Alpine-Dinaridic-Pannonian triple junction. *International Journal of Earth Sciences* 89, 377–389.
- Halamić, J. & Goričan, Š. 1995: Triassic radiolarites from Mts. Kalnik and Medvednica. *Geologica Croatica* 48, 129–146.
- Harangi, S., Downes, H. & Seghedi I. 2006: Tertiary-Quaternary subduction processes and related magmatism in the Alpine-Mediterranean region. In: Gee, D.G. & Stephenson, R.A. (Eds.): *European Lithosphere Dynamics*. Geological Society London Memoirs 32, 167–190.
- Hauer, F.V. 1853: Über die Gliederung der Trias, Lias und Juragebilde in den nordöstlichen Alpen. *Jahrbuch Geologische Reichsanstalt* 4, 715–748.
- Hauser, F., Raileanu, V., Fielitz, W., Dinu, C., Landes, M., Bala, A. & Prodehl, C. 2007: Seismic crustal structure between the Transylvanian Basin and the Black Sea, Romania. *Tectonophysics* 430/1–4, 1–25.
- Heinrich, C.A. & Neubauer, F. 2002: Cu-Au-Pb-Zn-Ag metallogeny of the Alpine-Balkan-Carpathian-Dinaride geodynamic province. *Mineralium Deposits* 37, 533–540.
- Hippolyte, J.-C. 2002: Geodynamics of Dobrogea (Romania): new constraints on the evolution of the Tornquist-Teisseyre Line, the Black Sea and the Carpathians. *Tectonophysics* 357, 33–53.
- Hoeck, V. & Ionescu, C. 2006: Basic and intermediate volcanics in the Eastern Carpathians (Rarau; Romania): are all of them ophiolites? Proceedings of the 18th Congress of the Carpathian-Balkan Geological Association, Belgrade, 219–221.
- Hoeck, V., Koller, F., Meissel, T., Onuzi, K. & Kneringer, E. 2002: The Jurassic South Albanian ophiolites: MOR- vs. SSZ-type ophiolites. *Lithos* 65, 143–164.
- Horvath, F. & Rumpler, J. 1984: The Pannonian basement: extension and subsidence of an Alpine orogen. *Acta Geologica Hungarica* 27, 229–235.
- Horvath, F., Bada, G., Szafian, P., Tari, G., Adam, A. & Cloetingh, S. 2006: Modes of basin (de)formation, lithospheric strength and vertical motions in the Pannonian-Carpathian system: inferences from thermo-mechanical modeling. In: Gee, D.G. & Stephenson, R.A. (Eds.): *European Lithosphere Dynamics*. Geological Society London Memoirs 32, 191–206.
- Hrvatović, H. 2000a: Paleozoic of the Mid-Bosnian Schist Mountains. In: Pamić, J. & Tomljenović, B. (Eds.): *PANCARDI 2000 Fieldtrip Guidebook*, *Vijesti* 37/2, 75–77.
- Hrvatović 2000b: Passive continental margin formations (Bosnia Flysch). In: Pamić, J. & Tomljenović, B. (Eds.): *PANCARDI 2000 Fieldtrip Guidebook*, *Vijesti* 37/2, 71–72.
- Hrvatović, H. 2005: *Geological Guidebook through Bosnia and Hercegovina*. Geological Survey of Bosnia and Hercegovina, Sarajevo, 155 pp.
- Hrvatović, H. & Pamić, J. 2005: Principal thrust-nappe structures of the Dinarides. *Acta Geologica Hungarica* 48/2, 133–151.
- Huismans, R.S., Bertotti, D., Ciulavu, D., Sanders, C.A.E., Cloetingh, S., & Dinu, C., 1997: Structural evolution of the Transylvanian Basin (Romania): A sedimentary basin in the bend of the Carpathians. *Tectonophysics* 272, 249–268.
- Iancu, V., Berza, T., Seghedi, A. & Mărunțiu, M. 2005: Paleozoic rock assemblages in the South Carpathian Alpine thrust belt (Romania and Serbia): a review. *Geologica Belgica* 8/4, 48–68.
- Ilić, A., Neubauer, F. & Handler, R. 2005: Late Paleozoic-Mesozoic tectonics of the Dinarides revisited: Implications from 40Ar/39Ar dating of detrital white micas. *Geology* 33, 233–236.
- Jacobshagen, V. 1986: *Geologie von Griechenland*. Beiträge zur regionalen Geologie der Erde Band 19. Gebrüder Bornträger Berlin, 363 pp.
- Jipa, D. 2006: Bazinul Dacic: arhitectură sedimentară, evoluție, factori de control (The Dacic basin: sedimentary architecture, evolution, controlling factors), Ed. GeoEcoMar, Bucharest, 306 pp.
- Ivan, P., Sykora, M. & Demko, R. 2006: Blueschists in the Cretaceous exotic conglomerates of the Klape unit (Pieniny Klippen Belt, Western Carpathians): their genetic types and implications for source area. *Geologia* 32, 47–63.
- Ivanov, Z. 1988: Aperçu général sur l'évolution géologique et structurelle du massif des Rhodopes dans le cadre des Balkanides. *Bulletin de la Société Géologique de France* 84/2, 227–240.
- Karamata, S. 2006: The geological development of the Balkan Peninsula related to the approach, collision and compression of Gondwana and Eurasian units. In: Robertson, A.H.F. & Mountrakis, D. (Eds.): *Tectonic Development of the Eastern Mediterranean Region*. Geological Society London Special Publications 260, 155–178.
- Karamata, S., Majer, V. & Pamić, J. 1980: Ophiolites of Yugoslavia. *Ophioliti, Special Issue Tethyan Ophiolites* 1, 105–125.
- Karamata, S., Olujić, J., Protić, L., Milovanović, D., Vujnović, L., Popević, A., Memović, E., Radovanović, Z., & Resimić-Sarić, K., 2000a: The western belt of the Vardar Zone – the remnant of a marginal sea. In: Karamata, S. & Janković, S. (Eds.): *International Symposium Geology and Metallogeny of the Dinarides and the Vardar zone*, Academy of Sciences & Arts Republic of Srpska Vol. 1, Banja Luka, Sarajevo, 131–135.
- Karamata, S., Korikovskiy, S. & Kurdyukov, E. 2000b: Prograde contact metamorphism of mafic and sedimentary rocks in the contact aureole beneath the Bresovica harzburgite Massif. In: Karamata, S., & Janković, S. (Eds.): *International Symposium Geology and Metallogeny of the Dinarides and the Vardar zone*, Academy of Sciences & Arts Republic of Srpska Vol. 1, Banja Luka, Sarajevo, 171–177.
- Kazmer, M. & Kovács, S. 1985: Permian-Palaeogene paleogeography along the eastern part of the Insubric-Periadriatic Lineament system: evidence for continental escape of the Bakony-Drauzug Unit. *Acta Geologica Hungarica* 28, 71–84.

- Kemenci, R. & Čanović, M. 1997: Geologic setting of the Pre-Tertiary basement in Vojvodina (Yugoslavia). Part 1: The Tisza Mega-unit of North Vojvodina. *Acta Geologica Hungarica* 40, 1–36.
- Kılıas, A., Falalakis, G. & Mountrakis, D. 1999: Cretaceous-Tertiary structures and kinematics of the Serbomacedonian metamorphic rocks and their relation to the exhumation of the Hellenic hinterland (Macedonia, Greece). *International Journal of Earth Sciences* 88, 513–531.
- Kissling, E., Schmid, S.M., Lippitsch, R., Ansoerge, J. & Fügenschuh, B. 2006: Lithosphere structure and tectonic evolution of the Alpine arc: new evidence from high-resolution teleseismic tomography. In: Gee, D.G. & Stephenson R.A. (Eds.): *European Lithosphere Dynamics*. Geological Society of London Memoirs 32, 129–145.
- Klötzli, U.S., Buda, G. & Skiöld, T. 2004: Zircon typology, geochronology and whole rock Sr-Nd isotope systematics of the Mecsek Mountain granitoids in the Tisia Terrane (Hungary). *Mineralogy and Petrology* 81, 113–134.
- Knapp, J.H., Knapp, C.C., Raileanu, V., Matenco, L., Mocanu, V. & Dinu, C. 2005: Crustal constraints on the origin of mantle seismicity in the Vrancea Zone, Romania: The case for active continental lithospheric delamination. *Tectonophysics* 410, 311–323.
- Kockel, F., Mollat, H. & Walther, H.W. 1971: *Geologie des Serbo-Mazedonischen Massivs und seines mesozoischen Rahmens (Nordgriechenland)*: Geologisches Jahrbuch 89, 529–551.
- Kockel, F., Mollat, H. & Walther, H.W. 1977: *Erläuterungen zur Geologischen Karte der Chalkidiki und angrenzender Gebiete 1:100'000, Nordgriechenland*. Bundesanstalt für Geowissenschaften und Rohstoffe, Hannover, 119 pp.
- Kodra, A., Vergély, P., Gjata, K., Bakalli, F. & Godroli, M. 1993: La formation volcano-sédimentaire du Jurassique supérieur: Témoin de l'ouverture du domaine ophiolitique dans les Albanides internes. *Bulletin de la Société Géologique France* 164, 61–70.
- Koroknai, B., Horvath, P., Balogh K. & Dunkl, I. 2001: Alpine metamorphic evolution and cooling history of the Veporic basement in northern Hungary: new petrological and geochronological constraints. *International Journal of Earth Sciences* 90, 740–751.
- Kossmat, F. 1924: *Geologie der zentralen Balkanhalbinsel, mit einer Übersicht des dinarischen Gebirgsbaus*. In: Wilder J. (Ed.): *Die Kriegsschauplätze 1914–1918 geologisch dargestellt*. Verlag Gebrüder Bornträger, Berlin, 198 pp.
- Kounov, A. 2002: *Thermotectonic evolution of Kraishite, Western Bulgaria*. Unpublished PhD ETH Nr. 14946, ETH Zürich, 219 pp.
- Kounov, A., Seward, D., Bernoulli, D., Burg, J.-P. & Ivanov, Z. 2004: Thermotectonic evolution of an extensional dome: the Cenozoic Osogovo-Listes core complex (Kraishite zone, western Bulgaria). *International Journal of Earth Sciences* 93, 1008–1024.
- Kováč, M., Kováč, P., Marko, F., Karoli, S., Janočko, J. 1995: The East Slovakian Basin – a complex back arc basin. *Tectonophysics* 252, 453–466.
- Kováč, M., Nagymarosy, A., Oszczytko, N., Slaczká, A., Csontos, L., Marunteanu, M., Matenco, L. & Márton, E. 1999: Palinspastic reconstruction of the Carpathian – Pannonian region during the Miocene. In: M. Rakus (Ed.): *Geodynamic development of the Western Carpathians*. Dionyz Stur, Bratislava, 189–218.
- Kovács, S. 1992: Tethys “western ends” during the Late Paleozoic and Triassic and their possible genetic relationships. *Acta Geologica Hungarica* 35, 329–369.
- Kovács, S., Szederkényi, T., Arkai, P., Buda, G.Y., Lelkes-Felvári, G. & Nagymarosy, A. 1997: Explanation of the terrane map of Hungary. *Annales Géologiques des Pays Helléniques* 37, 271–330.
- Kovács, S., Haas S., Császár, G., Szederkényi, T., Buda, G. & Nagymarosy, A. 2000: Tectonostratigraphic terranes in the pre-Neogene basement of the Hungarian part of the Pannonian area. *Acta Geologica Hungarica* 43/3, 225–328.
- Kovács, S., Brezsnaynszky, K., Haas, J., Szederkényi, T., Ebner, F., Pamić, J., Tomljenović, B., Gaetani, M., Vai, G.-B., Krätner, H.G., Karamata, S., Krstić, B., Vozar, J., Vozarova, A. & Mioč, P. (Eds.) 2004: *Tectonostratigraphic terrane and paleoenvironment maps of the Circum-Pannonian region. 1 : 2'500'000*. Geological Institute of Hungary, Budapest.
- Kozur, H. 1991: The evolution of the Meliata-Hallstatt ocean and its significance for the early evolution of the Eastern Alps and Western Carpathians. *Palaeogeography Palaeoclimatology Palaeoecology* 87, 109–135.
- Kozur, H. & Mock, R. 1997: New paleogeographic and tectonic interpretations in the Slovakian Carpathians and their implications for correlations with the Eastern Alps. Part II: Inner Western Carpathians. *Mineralia Slovaca* 29, 164–209.
- Kozur, H. & Mostler, H. 1991: Erster paläontologischer Nachweis von Meliaticum und Süd-Rudabanyaicum in den nördlichen Kalkalpen (Österreich) und ihre Beziehungen zu den Abfolgen in den Westkarpathen. *Geologisch Paläontologische Mitteilungen Innsbruck* 18, 87–129.
- Krätner, H.G. 1980: Lithostratigraphic correlation of the Romanian Carpathians. *Anuarul Institutului de Geologie si Geofizica LVII*, 229–296.
- Krätner, H.G. 1993: Pre-Alpine evolution in the southern Carpathians and adjacent areas. *Geologica Carpathica* 44, 203–212.
- Krätner, H.G. 1996: Alpine and pre-Alpine terranes in the Romanian South Carpathians and equivalents south of the Danube. In: Knezevic, V. & Krstić, B. (Eds.): *Terranes of Serbia*, Belgrade, 53–58.
- Krätner, H.G. & Krstić, B. 2002: Alpine and Pre-Alpine structural units within the Southern Carpathians and the Eastern Balkanides, Proceedings of XVII. Congress of Carpathian-Balkan Geological Association Bratislava, September 1–4 2002. *Geologica Carpathica* 53 Special Issue, available online under <http://www.geologicacarpatica.sk/src/main.php>.
- Krätner, H.G. & Krstić, B. 2006: Geological map of the Carpatho-Balkanides between Mehadia, Oravita, Nis and Sofia. CD-version provided at the 18th Congress of the Carpathian-Balkan Geological Association, Belgrade 2006.
- Krätner, H.G., Berza, T. & Dimitrescu, R., 1988. South Carpathians. In: Zoubek V. (Ed.): *Precambrian in younger fold belts*. J. Wiley, London, 639–664.
- Krätner, T.H. 1938: Das kristalline Massiv von Rodna. *Anuarul Institutului Geologie Romania* XIX, 164–287.
- Krézsek, C. & Bally, A. 2006: The Transylvanian Basin (Romania) and its relation to the Carpathian fold and thrust belt: Insights in gravitational salt tectonics. *Marine & Petroleum Geology* 23, 405–442.
- Krzywiec, P. 2001: Contrasting tectonic and sedimentary history of the central and eastern parts of the Polish Carpathian foredeep basin – results of seismic data interpretation. *Marine & Petroleum Geology* 18, 13–38.
- Kurz, W. 2005: Tectonic map and overall architecture of the Alpine orogen. Comment on an article by Stefan M. Schmid, Bernhard Fügenschuh, Eduard Kissling & Ralf Schuster 2004, *Eclogae geologicae Helveticae* 97, 93–117. *Eclogae geologicae Helveticae* 98, 97–98.
- Lanphere, M., Coleman, R.G., Karamata, S. & Pamić, J. 1975: Age of amphibolites associated with Alpine peridotites in the Dinaride ophiolite zone, Yugoslavia: Earth and Planetary Science Letters 26, 271–276.
- Laubscher, H. 1971: Das Alpen-Dinariden-Problem und die Palinspastik der südlichen Tethys. *Geologische Rundschau* 60, 813–833.
- Laubscher, H. & Bernoulli, D. 1977: Mediterranean and Tethys. In: Nairn, A.E.M., Kanes, W.H. & Stehli, F.G. (Eds.): *The Ocean Basins and Margins V. 4A*, Plenum Publ. Comp., New York, 1–28.
- Leever, K., Matenco, L., Bertotti, G., Cloetingh, S. and Drijkoningen, K.G. 2006: Late orogenic vertical movements in the Carpathian Bend Zone – seismic constraints on the transition zone from orogen to foredeep. *Basin Research* 18, 521–545.
- Lelkes-Felvári, G., Arkai P. & Sassi, F.P. 1996: Main features of the regional metamorphic events in Hungary: a review. *Geologica Carpathica* 47/4, 257–270.
- Lelkes-Felvári, G., Frank, W. & Schuster, R. 2003: Geochronological constraints of the Variscan, Permian-Triassic and Eo-Alpine (Cretaceous) evolution of the Great Hungarian Plain basement. *Geologica Carpathica* 54, 299–315.
- Lelkes-Felvári G., Schuster, R., Frank, W. & Sassi R. 2005: Metamorphic history of the Algyő basement-high (Tisza Mega-Unit, basement of the Great Hungarian Plain) – A counterpart of crystalline units of the Korlpe-Wölz nappe system (Austroalpine, Eastern Alps). *Acta Geologica Hungarica* 48/4, 371–394.

- Less, G. 2000: Polyphase evolution of the structure of the Aggtelek-Rudabánya mountains (NE Hungary), the southernmost element of the Inner Western Carpathians – a review. *Slovak Geological Magazine* 6, 260–268.
- Less, G. & Mello J. (Eds.) 2004: Geological map of the Gemer-Bükk area 1 : 100'000. Geological Institute of Hungary, Budapest.
- Liégeois, J.P., Berza, T., Tatu, M., Duchesne, J.C. 1996: The Neoproterozoic Pan-African basement from the Alpine Lower Danubian nappe system (South Carpathians, Romania). *Precambrian Research* 80, 281–301.
- Lugović, B., Altherr, R., Raczek, I., Hofmann, A.W., & Majer, V., 1991: Geochemistry of peridotites and mafic igneous rocks from the Central Dinaric Ophiolite Belt, Yugoslavia: Contributions to Mineralogy and Petrology 106, 201–216.
- Lupu, M. 1984: Problems of the European continental margin in the Transylvanian-Pannonian area. *Annuaire de l'Institut de Géologie et de Géophysique Bucharest XLV*, 323–332.
- Mahel, M. 1973 (Ed.): Tectonic map of the Carpathian-Balkan mountain system and adjacent areas. Carpathian-Balkan Association Tectonic Commission. Published by D. Stur's Geological Institute in Bratislava and UNESCO.
- Malešević, M., Vukanović, M., Brković, T., Obradović, Y., Karajičić, L., Dimitrijević, M.D. & Stanislavijević, R. 1978: Osnovna Geološka Karta SFRJ, 1 : 100'000, Sheet Kuršumlja and explanations.
- Maluski, H., Rajlich, P. & Matte, P. 1993: ⁴⁰Ar-³⁹Ar dating of the Inner Carpathians Variscan basement and Alpine mylonitic overprinting. *Tectonophysics* 223, 313–337.
- Mandl, G. 2000: The Alpine sector of the Tethyan shelf – Examples of Triassic to Jurassic sedimentation and deformation from the Northern Calcareous Alps. *Mitteilungen der Österreichischen Geologischen Gesellschaft* 92, 61–77.
- Mandl, G. & Ondrejickova, A. 1991: Über eine triadische Tiefwasserfazies (Radiolarite, Tonschiefer) in den Nördlichen Kalkalpen – ein Vorbericht. *Jahrbuch der Geologischen Bundesanstalt* 136, 841–871.
- Marcucci, M. & Prela, M. 1996: The Luni zi (Puke) section of the Kalur cherts: radiolarian assemblages and comparison with other sections in northern Albania. *Ophioliti* 21, 71–76.
- Marcucci, M., Kodra, A., Pirđeni, A. & Gjata, T. 1994: Radiolarian assemblages in the Triassic and Jurassic cherts of Albania. *Ophioliti, Special Issue on Albanian ophiolites: state of the art and perspectives* 19: 105–115.
- Marović, M., Đoković, I., Pešić, Radovanović, S., Toljić, M. & Gerzina N. 2002: Neotectonics and seismicity of the southern margin of the Pannonian Basin in Serbia. *EGU Stephan Mueller Special Publication Series* 3, 277–295.
- Marroni, M., Molli, G., Montanini, A., Ottria, G., Pandolfi, L. & Tribuzio, R. 2002: The External Ligurian Units (Northern Apennine, Italy): From rifting to convergence of a fossil ocean-continent transition zone. *Ophioliti* 27, 119–132.
- Martin, M., Ritter, J.R.R. & CALIXTO working 2005: High-resolution teleseismic body-wave tomography beneath SE Romania – I. Implications for three-dimensional versus one-dimensional crustal correction strategies with a new crustal velocity model. *Geophysical Journal International* 162, 448–460.
- Martin, M., Wenzel, F. & Group, C.W. 2006: High-resolution teleseismic body wave tomography beneath SE – Romania – II. Imaging of a slab detachment scenario. *Geophysical Journal International* 164, 579–595.
- Márton, E. 2000: The Tisza Megatectonic Unit in the light of paleomagnetic data. *Acta Geologica Hungarica* 43/3, 329–343.
- Márton, E. 2001: Tectonic implications of Tertiary paleomagnetic results from the PANCARDI area (Hungarian contribution). *Acta Geologica Hungarica* 44, 135–144.
- Márton, E., Tischler, M., Csontos, L., Fügenschuh, B. & Schmid, S.M. 2007: The contact zone between the ALCAPA and Tisza-Dacia mega-tectonic units of Northern Romania in the light of new paleomagnetic data. *Swiss Journal of Geosciences* 100, 109–124.
- Maruntiu, M. 1987: Studiul geologic complex al rocilor ultrabazice din Carpatii Meridionali. Unpublished Ph.D. Thesis, University Bucharest.
- Matenco, L. & Bertotti, G. 2000: Tertiary tectonic evolution of the external East Carpathians (Romania). *Tectonophysics* 316, 255–286.
- Matenco L., Bertotti G., Cloetingh S. & Dinu C. 2003: Subsidence analysis and tectonic evolution of the external Carpathian-Moesian Platform region during Neogene times. *Sedimentary Geology* 156, 71–94.
- Matenco, L., Bertotti, G., Leever, K., Cloetingh, S., Schmid, S.M., Tărăpoancă, M. & Dinu, C. 2007: Large scale deformations at a locked collisional boundary: coeval Pliocene-Quaternary differential tectonic movements in the foreland of the SE Carpathians. *Tectonics* 26, TC4011, doi:10.1029/2006TC001951.
- Melinte, M.C. & Jipa, D. 2005: Campanian-Maastrichtian marine red beds in Romania: biostratigraphic and genetic significance. *Cretaceous Research* 26, 49–56.
- Mello, J., Reichwalder, P. & Vozárová, A. 1998: Bôrka nappe: high-pressure relic from the subduction-accretion prism of the Meliata ocean (Inner Western Carpathians, Slovakia). *Slovak Geological Magazine* 4, 261–273.
- Merlini, S., Doglioni, C., Fantoni, R. & Ponton, M. 2002: Analisi strutturale lungo un profilo geologico tra la linea Fella-Sava e l'avampaese adriatico (Friuli Venezia Giulia-Italia). *Memorie Società Geologica Italiana* 57, 293–300.
- Michard, A., Chopin, C. & Goffé, B. 1991: Obduction versus subduction and collision in the Oman case and in the other Tethyan settings. In: Peters, T.J., Nicolas, A. & Coleman R.G. (Eds.): *Ophiolite Genesis and Evolution of the Oceanic Lithosphere. Petrology & Structural Geology* 5, Kluwer Acad. Publ. Dordrecht, 447–467.
- Michard, A., Goffé, B., Liathi, A. & Mountakis, D. 1994: Découverte de faciès schiste bleu dans les nappes du Circum-Rhodope; un élément d'une ceinture HP-BT éohellénique en Grèce septentrionale. *Compte Rendu Académie des Sciences* 318 Série II, 1535–1542.
- Milovanović, D. 1984: Petrology of low metamorphosed rocks of the central part of the Drina-Ivanjica Palaeozoic. *Bulletin du Musée de l'Histoire Naturelle Beograd* A39: 1–139.
- Milovanović, D., Marchig, V. & Karamata, S. 1995: Petrology of crossite schists from Fruška Gora Mts. (Yugoslavia): Relic of a subducted slab of the Tethyan oceanic crust. *Journal of Geodynamics* 20/3, 289–304.
- Mirković, M., Kalezić, M., Pajović, M., Rašković, S., Čepić, M. & Vujisić, P. 1972: Sheet Gačko of the 1 : 100'000 geological map of former Yugoslavia.
- Mock, R., Sýkora, M., Aubrecht, R., Ožvoldová, L., Kronome, B., Reichwalder, P. & Jablonský, J. 1998: Petrology and stratigraphy of the Meliaticum near the Meliata and Jaklovce Villages, Slovakia. *Slovak Geological Magazine* 4, 223–260.
- Morley, C.K. 1996: Models for relative motion of crustal blocks within the Carpathian region, based on restorations of the outer Carpathian thrust sheets. *Tectonics* 15, 885–904.
- Moser, F. 2001: Tertiäre Deformation in den rumänischen Südkarpathen: Strukturelle Analyse eines Blattverschiebungskorridors am Westrand der mösischen Plattform. *Tübinger Geowissenschaftliche Arbeiten Reihe A*, Band 63, 169 pp.
- Motaş, C. & Tomescu, L. 1983: L'avant-fosse carpathique roumaine; évolution et contenu. *Anarul Institutului Geologie si Geofizica* 60, 147–158.
- Mposkos, E. & Krohe, A. 2006: Pressure-temperature-deformation paths of closely associated ultra-high-pressure (diamond-bearing) crustal and mantle rocks of the Kimi complex: implications for the tectonic history of the Rhodope Mountains, northern Greece. *Canadian Journal of Earth Sciences* 43, 1755–1776.
- Murgoci, G.M. 1905: Sur l'existence d'une grande nappe de recouvrement dans les Carpathes Méridionales. *Comptes Rendus Académie Paris*, 31 juillet.
- Murgoci, G.M. 1915: Études géologiques dans la Dobrogea du Nord. La tectonique de l'aire cimmérienne. *Annuaire de l'Institut de Géologie Roumain VI/2*, 443–568.
- Murgoci, G.M. 1929: Sur l'Aire Cimmérienne. *Compte Rendus des Scéances de l'Institut de Géologie Roumain VIII*, 207–226.
- Năstăseanu, S., Bercia, I., Iancu, V., Vlad, S. & Hartopanu, I. 1981: The Structure of the South Carpathians. Guide to Excursion B2 of the 12th Carpatho-Balkan Geological Association Congress, Bucharest, Romania.
- Neubauer, F. & Heinrich, Ch. 2003: Late Cretaceous and Tertiary geodynamics and ore deposit evolution of the Alpine-Balkan-Carpathian-Dinaride orogen. In: Eliopoulos et al. (Eds.): *Mineral Exploration and Sustainable Development*. Millpress Rotterdam, 1133–1136.

- Neubauer, F., Genser, J. & Handler, R. 2000: The Eastern Alps: Result of a two-stage collision process. *Mitteilungen Österreichische Geologische Gesellschaft* 92, 117–134.
- Neubauer, F., Pamić, J., Dunkl, I., Handler, R. & Majer, V. 2003: Exotic granites in the Cretaceous Pogari Formation overstepping the Dinaric Ophiolite Zone mélange in Bosnia. *Annales Universitatis Scientiarum Budapestensis, Sectio Geologica* 35, 133–134.
- Nemčok, M. 1993: Transition from convergence to escape: field evidence from the West Carpathians. *Tectonophysics* 217, 117–142.
- Nemčok, M., Pospisil, L., Lexa, J. & Donelick, R.A., 1998: Tertiary subduction and slab break-off model of the Carpathian-Pannonian region. *Tectonophysics* 295: 307–240.
- Nicolae, I. & Saccani, E. 2003: Late Jurassic calc-alkaline series in the South Apuseni mountains. *Schweizerische Mineralogisch-Petrographische Mitteilungen* 83, 81–96.
- Nicolae, A., Boudier, F. & Meshi, A. 1999: Slow spreading accretion and mantle denudation in the Mirdita ophiolite (Albania). *Journal of Geophysical Research* 104 B7, 15155–15167.
- Nopcsa, F. Baron 1921: Geologische Grundzüge der Dinariden. *Geologische Rundschau* 12, 1–19.
- Okay, A.I., Satir, M., Tüysüz, O., Akyüz, S. & Chen F. 2001: The tectonics of the Strandja Massif: late Variscan and mid-Mesozoic deformation and metamorphism in the northern Aegean. *International Journal of Earth Sciences* 90, 217–233.
- Olujić, J. 1980: Occurrences and genesis of Mesozoic flyschs of Bosnia and Hercegovina (in Serbian, summary in English). Unpublished Report Institute of Geology, Sarajevo, 210 pp.
- Okrusch, M., Seidel, E., Kreuzer, H. & Harre, W. 1978: Jurassic age of metamorphism at the base of the Brezovica peridotite (Yugoslavia): *Earth and Planetary Science Letters* 39, 291–297.
- Operta, M., Pamić, J., Balen, D. & Tropper P. 2003: Corundum-bearing amphibolites from the metamorphic basement of the Krivaja-Konjuh ultramafic massif (Dinaride Ophiolite Zone, Bosnia). *Mineralogy and Petrology* 77, 287–295.
- Osnovna Geološka Karta SFRJ: Geological maps of former Yugoslavia, 1 : 100.000, Beograd, Savezni Geoloski Zavod.
- Oszyzypko, N. 2006: Late Jurassic-Miocene evolution of the Outer Carpathian fold-and-thrust belt and its foredeep basin (Western Carpathians, Poland). *Geological Quarterly* 50, 169–194.
- Pamić, J. 1984: Triassic magmatism of the Dinarides in Yugoslavia. *Tectonophysics* 109, 273–307.
- Pamić, J. 1993: Eoalpine to Neoalpine magmatic and metamorphic processes in the northwestern Vardar Zone, the easternmost Periadriatic Zone and the southwestern Pannonian Basin. *Tectonophysics* 226, 503–518.
- Pamić, J. 2000: Radiolarite Formation. In: Pamić, J. & Tomljenović, B. (Eds.): *Pancardi 2000 Fieldtrip Guidebook*. *Vijesti* 37/2, 70.
- Pamić, J. 2002: The Sava-Vardar Zone of the Dinarides and Hellenides versus the Vardar Ocean. *Eclogae geologicae Helveticae* 95, 99–113.
- Pamić, J. & Hrvatović, H. 2000: Dinaride Ophiolite Zone (DOZ). In: Pamić, J. & Tomljenović, B. (Eds.): *Pancardi 2000 Fieldtrip Guidebook*. *Vijesti* 37/2, 60–68.
- Pamić, J. & Jurković I. 2002: Paleozoic tectonostratigraphic units of the northwestern and central Dinarides and the adjoining South Tisia. *International Journal of Earth Sciences* 91, 538–554.
- Pamić, J. & Tomljenović, B. 1998: Basic geological data on the Croatian part of the Mid-Transdanubian Zone. *Acta Geologica Hungarica* 41, 389–340.
- Pamić, J., Árkay, P., O'Neil, J.O. & Lantal, C. 1992: Very low- and low-grade progressive metamorphism of Upper Cretaceous sediments in Mt. Motajica, northern Dinarides. In: Vozar, J. (Ed.): *Western Carpathians, Eastern Alps, Dinarides, IGCP project No. 276*, Bratislava, 131–146.
- Pamić, J., Lanphere, M. & Belak, M. 1996: Hercynian A-type and S-type granites from the Slavonian Mountains (Southern Pannonian Basin, northern Croatia). *Neues Jahrbuch Mineralogische Abhandlungen* 171, 155–186.
- Pamić, J., Gušić, I. & Jelaska, V. 1998: Geodynamic evolution of the Central Dinarides. *Tectonophysics* 297, 251–268.
- Pamić, J., Gušić, I. & Jelaska, V. 2000: Basic geological features of the Dinarides and South Tisia. In: Pamić, J. & Tomljenović, B. (Eds.): *Pancardi 2000 Fieldtrip Guidebook*. *Vijesti* 37/2, 9–18.
- Pamić, J., Tomljenović, B. & Balen, D. 2002a: Geodynamic and petrogenetic evolution of Alpine ophiolites from the central and NW Dinarides: an overview. *Lithos* 65, 113–142.
- Pamić, J., Balen, R.T. & Herak, M., 2002b: Origin and geodynamic evolution of late Palaeogene magmatic associations along the Periadriatic-Sava-Vardar magmatic belt. *Geodinamica Acta* 15, 209–231.
- Pamić, J., Balogh, K., Hrvatović, H., Balen, D., Jurković I. & Palinkaš, L. 2004: K-Ar and Ar-Ar dating of the Paleozoic metamorphic complex from the Mid-Bosnian Schist Mts., Central Dinarides, Bosnia and Hercegovina. *Mineralogy and Petrology* 82, 65–79.
- Panaiotu, C. 1999: Paleomagnetic studies in Romania: Tectonophysics implications. Unpublished PhD thesis University Bucharest.
- Patrascu, S., Panaiotu C., Seclaman, M. & Panaiotu C.E. 1994: Timing of rotational motion of Apuseni Mountains (Romania) – Paleomagnetic data from Tertiary magmatic rocks. *Tectonophysics* 233, 163–176.
- Patrulus, D. 1969: *Geologia masivului Bucegi si a culoarului Dimbovicioara*. Editia Academie RSR, Bucuresti.
- Patrulus, D., Popa, E. & Popescu, I. 1969: Structura pinzei bucovinice in partea meridionala a masivului cristalin moldav (Carpatii Orientali). *Annaire de la Commission Géologique de la Roumanie XXXVII*, 71–118.
- Perraki, M., Proyer, A., Mposkos, E., Kaindl, R. & Hoinkes, G., 2006: Raman micro-spectroscopy on diamond, graphite and other carbon polymorphs from the ultrahigh-pressure metamorphic Kimi Complex of the Rhodope Metamorphic Province, NE Greece. *Earth and Planetary Science Letters* 241, 672–685.
- Petković, K. 1961: La carte tectonique de la RFP de Yougoslavie. *Glas. Srp. akad. nauka* 149, Odelj. prir. mat. nauka 22, 129–144.
- Pharaoh, T.C., Winchester, J.A., Verniers, J., Lassen, A., Seghedi, A., 2006: The western accretionary margin of the East European Craton: an overview. In: Gee, D.G., Stephenson, R.-A. (Eds.): *European Lithosphere Dynamics*. Geological Society London Memoirs 32, 291–311.
- Picha, F.J. 2002: Late orogenic strike-slip faulting and escape tectonics in frontal Dinarides-Hellenides, Croatia, Yugoslavia, Albania, and Greece. *American Association of Petroleum Geologists Bulletin* 86, 1659–1671.
- Picha, F.J. & Stranič, Z. 1999: Late Cretaceous to early Miocene deposits of the Carpathian foreland basin in southern Moravia. *International Journal of Earth Sciences* 88, 475–495.
- Pinter, N., Greneczy, G., Weber, J., Stein, S. & Medak, D. 2005: The Adria Microplate: GPS Geodesy, Tectonics and Hazards (NATO Science Series IV: Earth and Environmental Sciences). Springer, 413 pp.
- Plašienka, D. 1995a: Passive and active margin history of the northern Tatricum (Western Carpathians, Slovakia). *Geologische Rundschau* 84, 748–760.
- Plašienka, D. 1995b: Mesozoic evolution of Tatric units in the Malé Karpaty and Považský Inovec Mts.: Implications for the position of the Klape and related units in western Slovakia. *Geologica Carpathica* 46, 101–112.
- Plašienka, D. 2003: Dynamics of Mesozoic pre-orogenic rifting in the Western Carpathians. *Mitteilungen der Österreichischen Geologischen Gesellschaft* 94, 79–98.
- Plašienka D., Michalik J., Gross P. & Putiš M. 1991: Paleotectonic evolution of the Malé Karpaty Mts. – an overview. *Geologica Carpathica* 42, 195–208.
- Plašienka, D., Grecula, P., Putiš, M., Hovorka, D. & Kovač, M. 1997a: Evolution and structure of the Western Carpathians: an overview. In: Grecula, P. Hovorka, D. & Putiš M. (Eds.): *Geological Evolution of the Western Carpathians, Mineralia Slovaca Monograph*, Bratislava, 1–24.
- Plašienka, D., Putiš, M., Kovač, M., Šefara, J. & Hruščeký, I. 1997b: Zones of Alpidic subduction and crustal underthrusting in the Western Carpathians. In: Grecula, P., Hovorka, D. & Putiš M. (Eds.): *Geological Evolution of the Western Carpathians, Mineralia Slovaca Monograph*, Bratislava, 35–42.
- Pop, G., Marantiu, M., Iancu, V., Seghedi, A. & Berza, T. 1997: Geology of the South Carpathians in the Danube Gorges (Field guide book). *Int. Symposium Geology of the Danube Gorges*. Institut & Geozavod Belgrade and Geological Institute of Romania Bucharest, 28 pp.
- Popescu-Voitești, I. 1929: Aperçu synthétique sur la structure des régions carpathiques. *Revue du Musée de Géologie et Mineralogie Cluj III/1*.
- Posgay, K., Bodoky, T., Hajnal, Z., Toth, T.M., Fancsik, T., Hegedus, E., Kovács, A.C. & Takacs, E. 2006: Interpretation of subhorizontal crustal reflections

- by metamorphic and rheologic effects in the eastern part of the Pannonian Basin. *Geophysical Journal International* 167, 187–203.
- Prela, M. 1994: Mirdita Ophiolite Project: 1. Radiolarian biostratigraphy of the sedimentary cover of the ophiolites in the Mirdita area (Albania): Initial data. *Ophioliti* 19, 279–286.
- Răbăgia, T. and Matenco, L. 1999: Tertiary tectonic and sedimentological evolution of the South Carpathians foredeep: tectonic versus eustatic control. *Marine & Petroleum Geology* 16/7, 719–740.
- Răbăgia, T., Matenco, L. & Cloetingh, S. 2007: The balance between tectonics and sedimentation in highly oblique collisional settings: A case study from the South Carpathians and their foreland. *Sedimentary Geology*, submitted.
- Rampnoux, J.-P. 1970: Regards sur les Dinarides internes yougoslaves (Serbie-Monténégro oriental): stratigraphie, évolution paléogéographique, magmatisme. *Bulletin Société géologique de France* 12/6, 948–966.
- Ratschbacher, L., Merle, O., Davy, P. & Cobbold, P. 1991a: Lateral extrusion in the Eastern Alps; Part 1: Boundary conditions and experiments scaled for gravity. *Tectonics* 10(2), 245–256.
- Ratschbacher, L., Frisch, W., Linzer, H.G. & Merle, O. 1991b: Lateral extrusion in the Eastern Alps; Part 2: Structural analysis. *Tectonics* 10(2), 257–271.
- Ratschbacher, L., Linzer, H.G., Moser, F., Strusievicz, R.O., Bedeleian, H., Har, N. & Mogos, P.A. 1993: Cretaceous to Miocene thrusting and wrenching along the central South Carpathians due to a corner effect during collision and orocline formation. *Tectonics* 12, 855–873.
- Robertson, A.H.F. 2002: Overview of the genesis and emplacement of Mesozoic ophiolites in the Eastern Mediterranean Tethyan region. *Lithos* 65, 1–67.
- Robertson, A.H.F. & Karamata, S. 1994: The role of subduction-accretion processes in the tectonic evolution of the Mesozoic Tethys in Serbia. *Tectonophysics* 234, 73–94.
- Robertson, A.H.F. & Shallo, M. 2000: Mesozoic-Tertiary tectonic evolution of Albania in its regional Eastern Mediterranean context. *Tectonophysics* 316, 197–254.
- Roca, E., Bessereau, G., Jawor, E., Kotarba, M. & Roure, F. 1995: Pre-Neogene evolution of the Western Carpathians: Constraints from the Bochnia-Tatra Mountains section (Polish Western Carpathians). *Tectonics* 14, 855–873.
- Rögl, F. 1999: Mediterranean and Paratethys. Facts and hypotheses of an Oligocene to Miocene paleogeography. *Geologica Carpathica* 50, 339–349.
- Roure, F., Roca, E. & Sassi, W. 1993: The Neogene evolution of the outer Carpathian flysch units (Poland, Ukraine and Romania): kinematics of a foreland/ fold-and-thrust belt system. *Sedimentary Geology* 86, 177–201.
- Royden, L.H. 1988: Late Cenozoic Tectonics of the Pannonian Basin System. In: L.H. Royden and F. Horvath (Eds.): *The Pannonian Basin, a study in basin evolution*. American Association of Petroleum Geologists Memoir 45, 27–48.
- Royden, L.H. 1993: Evolution of retreating subduction boundaries formed during continental collision. *Tectonics* 12/3, 629–638.
- Royden, L.H. & Báldi, T. 1988: Early Cenozoic Tectonics and Paleogeography of the Pannonian and Surrounding Regions. In: Royden, L.H. & Horváth, F. (Eds.): *The Pannonian Basin: A Study In Basin Evolution*. American Association of Petroleum Geologists Memoir 45, 1–16.
- Royden, L.H. & Horváth, F. 1988: The Pannonian Basin: A Study In Basin Evolution. American Association of Petroleum Geologists Memoir 45.
- Saintot, A., Stephenson, R.A., Stovba, S., Brunet, M.F., Yegorova, T. & Starostenko, V. 2006: The evolution of the southern margin of Eastern Europe (Eastern European and Scythian platforms) from the latest Precambrian-Early Paleozoic to the Early Cretaceous. In: D.G. Gee and R.A. Stephenson (Eds.): *European Lithosphere Dynamics*. Geological Society London Memoir 32, 481–505.
- Săndulescu, M. 1974: Corelarea seriilor mezozoice din sinclinalele Rarău și Hăghimas (Carpații Orientali). *Dări de Seama Institutului Geologie și Geofizică* 60/5, 119–142.
- Săndulescu, M. 1975: Essai de synthèse structurale des Carpathes. *Bulletin de la Société Géologique de France* 17/3, 299–358.
- Săndulescu, M. 1980: Analyse géotectonique des chaînes alpines situées autour de la Mer Noire occidentale. *Annuaire Institutului Geologie și Geofizică* LVI, 5–54.
- Săndulescu, M. 1984: *Geotectonica României* (translated title: *Geotectonics of Romania*). Ed. Tehnică, Bucharest, 450 pp.
- Săndulescu, M. 1988: Cenozoic Tectonic History of the Carpathians. In: Royden, L.H. & Horvath F. (Eds.): *The Pannonian Basin, a study in basin evolution*. American Association of Petroleum Geologists Memoir 35, 17–25.
- Săndulescu, M. 1989: The structure and tectonic development of the East and South Carpathians. In: Rakus M. et al. (Eds.): *Evolution of the Northern Margin of Tethys Volume 2. Mémoires de la Société Géologique de France, Nouvelle Série* 154, 59–61.
- Săndulescu, M. 1994: Overview on Romanian Geology. 2. Alcapa Congress Field Guidebook. *Romanian Journal of Tectonics and Regional Geology* 75 Suppl. 2, 3–15.
- Săndulescu, M. & Russo-Săndulescu, D. 1979: The ophiolites from the Rarău and Hăghimas synclines – their structural position, age and geotectonic evolution. *Dări de Seama Institutului Geologie și Geofizică* 66, 103–114.
- Săndulescu, M. & Visarion, M. 1978: Considérations sur la structure tectonique du soubassement de la dépression de Transylvanie. *Dări de Seama Institutului Geologie și Geofizică, Tectonică și Geologie Regională* 64, 153–173.
- Săndulescu, M. & Visarion, M. 1988: La structure des plate-formes situées dans l'avant-pays et au-dessous des nappes du flysch des Carpathes orientales. *St. Tehn. Econ. Geofiz.* 15, 62–67.
- Săndulescu, M., Krätner, H., Borcos, M., Năstăseanu, S., Patrulius, D., Ștefănescu, M., Ghenea, C., Lupu, M., Savu, H., Bercia, I. & Marinescu, F. 1978: Geological map of Romania 1 : 1.000.000. Institut de Géologie Roumain, Bucharest.
- Săndulescu, M., Neagu, T. & Antonescu, E. 1979/1980: Contributions à la connaissance des Klippes de type Pienin de Poiana Botizei (Maramures). *Dări Seama Institutului Geologie și Geofizică* 67/4, 79–96.
- Săndulescu, M., Krätner, H.G., Balintoni, I., Russo-Săndulescu, D. & Micu, M. 1981a: The Structure of the East Carpathians. Guide Book to Excursion B1 of the Carpatho-Balkan Geological Association 12th Congress, Bucharest, pp 1–92.
- Săndulescu, M., Ștefănescu, M., Butac, A., Patrut, I. & Zaharescu, P. 1981b: Genetic and structural relations between flysch and molasse (The East Carpathians Model). Guidebook to Excursion A5 of the Carpatho-Balkan Geological Association 12th Congress, Bucharest, Romania, 95 pp.
- Săndulescu, M., Visarion, M., Stanica, D., Stanica, M. & Atanasiu, L. 1993: Deep Structure of the inner Carpathians in the Maramures-Tisa zone (East Carpathians). *Romanian Journal of Geophysics* 16, 67–76.
- Săsăran, E. 2006: *Calcarele Jurasicului superior – Cretacului inferior din Munții Trascău*. Unpublished Ph D thesis University Cluj-Napoca. Presa Universitară Clujeană, 249 pp.
- Savu, H., Udrescu, C. & Neacsu, V. 1977: Structural, petrological and genetic study of the ophiolites from the Niculitel Zone (North Dobrogea). *Dări de Seama Institutului de Geologie și Geofizică, Mineralogie-Petrologie-Geochimie* 65, 41–64.
- Savu, H., Udrescu, C., Neacsu, V., Bratosin, I. & Stoian, M. 1985: Origin, geochemistry and tectonic position of the Alpine ophiolites in the Severin nappe (Mehedinti Plateau, Romania). *Ophioliti* 10, 423–440.
- Savu, H., Udrescu, C. & Neacsu, V. 1992: On the presence of ocean floor rocks (Liassic ophiolites) in the Trascău Mountains (Mures Zone). Their petrology and geochemistry. *Romanian Journal of Petrology* 75, 53–62.
- Schmid, S.M. & Kissling, E., 2000: The arc of the Western Alps in the light of geophysical data on deep crustal structure. *Tectonics* 19, 62–85.
- Schmid, S.M., Pfiffner, O.A., Froitzheim, N., Schönborn, G. & Kissling, E. 1996: Geophysical-geological transect and tectonic evolution of the Swiss-Italian Alps. *Tectonics* 15, 1036–1064.
- Schmid, S.M., Berza, T., Diaconescu, V., Froitzheim, N. & Fügenschuh, B., 1998: Orogen-parallel extension in the Southern Carpathians. *Tectonophysics* 297, 209–228.
- Schmid, S.M., Fügenschuh, B., Kissling, E. & Schuster, R. 2004a: Tectonic map and overall architecture of the Alpine orogen. *Eclogae geologicae Helveticae* 97, 93–117.
- Schmid, S.M., Fügenschuh, B., Kissling, E. & Schuster, R. 2004b: TRANSMED Transects IV, V and VI: Three lithospheric transects across the Alps and their forelands. In: Cavazza W., Roure, F.M., Spakman, W., Stampfli G.M. & Ziegler, P.A. (Eds.): *The TRANSMED Atlas: The Mediterranean Re-*

- gion from Crust to Mantle. Springer, Berlin and Heidelberg, attached CD (version of the explanatory text available from the first author as pdf-file upon request).
- Schmid, S.M., Fügenschuh, B., Kissling, E. & Schuster, R. 2005: Reply to Comment by W. Kurz on "Tectonic map and overall architecture of the Alpine orogen". *Eclogae geologicae Helvetiae* 98, 99–101.
- Schnabel, W. 1992: New data on the Flysch zone of the Eastern Alps in the Austrian sector and new aspects concerning the transition to the Flysch Zone of the Carpathians. *Cretaceous Research* 13, 405–419.
- Schuller V. 2004: Evolution and geodynamic significance of the Upper Cretaceous Gosau basin in the Apuseni Mountains (Romania). *Tübinger Geowissenschaftliche Arbeiten Reihe A* 70, 112 pp.
- Schuster, R. & Frank W. 1999: Metamorphic evolution of the Austroalpine units east of the Tauern window: indications for Jurassic strike slip tectonics. *Mitteilungen der Gesellschaft der Geologie & Bergbaustudenten Österreichs* 42, 37–58.
- Schuster, R., Scharbert, S., Abart, R. & Frank W. 2001: Permo-Triassic extension and related HT/LP metamorphism in the Austroalpine – Southalpine realm. *Mitteilungen der Gesellschaft der Geologie & Bergbaustudenten Österreichs* 45, 111–141.
- Schuster, R., Koller, F., Hoek, V., Hoinkes, G. & Bousquet, R. 2004: Explanatory notes to the map: Metamorphic structure of the Alps – Metamorphic evolution of the Eastern Alps. *Mitteilungen der Österreichischen Mineralogischen Gesellschaft* 149, 175–199.
- Seghedi, A. 2001: The North Dobrogea orogenic belt (Romania). A review. In: Ziegler, P.A. et al. (Eds.): *Peri-Tethys Memoir 6, Peri-Tethyan Rift/Wrench Basins and Passive Margins*. Mémoires Musée Histoire Naturelle Paris 186, 237–257.
- Seghedi, A. & Oaie, G. 1997: Sedimentology and petrography of sandstones in cover nappes in the central South Carpathians: constraints for geotectonic setting. In: Grubić, A. & Berza, T. (Eds.): *Geology of the Djerdap area*. Internat. Symposium Geology of the Danube Gorges, 277–279.
- Seghedi, A., Berza, T., Jancu, V., Măruntiu, M. & Oaie, G. 2005: Neoproterozoic terranes in the Moesian basement and in the Alpine Danubian nappes of the South Carpathians. *Geologica Belgica* 8/4, 4–19.
- Seghedi, I., Downes, H., Szakacs, A., Mason, P.R.D., Thirlwall, M.F., Rosu, E., Pecskey, Z., Márton, E. & Panaiotu, C. 2004: Neogene-Quaternary magmatism and geodynamics in the Carpathian-Pannonian region: a synthesis. *Lithos* 72, 117–146.
- Simpson, C. & Schmid, S.M., 1983: An evaluation of criteria to deduce the sense of movement in sheared rocks. *Bulletin Geological Society America* 94, 1281–1288.
- Smith, A.G. & Spray, J.G. 1984: A half-ridge transform model for the Hellenic-Dinaric ophiolites. In: Dixon, J.E. et al. (Eds.): *The Geological Evolution of the Eastern Mediterranean*. Geological Society London Special Publications 17, 589–603.
- Sokoutis, D., Brun, J.P., van der Driessche, J & Pavlides, S. 1993: A major Oligo-Miocene detachment in southern Rhodope controlling north Aegean extension. *Journal of the Geological Society*, 150, 243–246.
- Soták, J., Rudinec, R. & Spišiak, J. 1993: The Penninic "pull-apart" dome in the pre-Neogene basement of the Transcarpathian Depression (Eastern Slovakia). *Geologica Carpathica* 44, 11–16.
- Soták, J., Spišiak, J. & Biroň, A. 1994: Metamorphic sequences with "Bündnerschiefer" lithology in the pre-Neogene basement of the East Slovakian Basin. *Mitteilungen der Gesellschaft der Geologie & Bergbaustudenten Österreichs* 86 (1993), 111–120.
- Soták, J., Biron, A., Dunkl, I., Prokesova, R., Magyar, J., Rudinec, R. & Spišiak, J. 1999: Alpine Penninics in the Eastern Slovakia: from crustal updoming to basin downfaulting. *Geologica Carpathica* 50 (Special Issue), 172–174.
- Soták, J., Biroň, A., Prokešová, R. & Spišiak, J. 2000: Detachment control of core complex exhumation and back-arc extension in the East Slovakian Basin. *Slovak Geological Magazine* 6, 130–132.
- Sperner, B., Ratschbacher, L. & Nemčok, M. 2002: Interplay between subduction retreat and lateral extrusion: Tectonics of the Western Carpathians. *Tectonics* 21/6.
- Sperner, B. & CRC 461 team 2005: Monitoring of Slab Detachment in the Carpathians. In: *Perspectives in modern Seismology* (Wenzel, F. Ed.): *Lecture Notes in Earth Sciences* 105, 187–202.
- Spray, J.G., Bébien, J., Rex, D.C. & Roddick, J.C. 1984: Age constraints on the igneous and metamorphic evolution of the Hellenic-Dinaric ophiolites. In: Dixon, J.E. et al. (Eds.): *The Geological Evolution of the Eastern Mediterranean*. Geological Society London Special Publications 17, 619–627.
- Stampfli, G. 1993: Le Briançonnais: Terrain exotique dans les Alpes? *Eclogae Geologicae Helvetiae* 86, 1–45.
- Stampfli, G., Mosar, J., Favre, Ph., Pilleveit A. & Vannay, J.-C. 2001: Permo-Mesozoic evolution of the western Tethys realm: the Neo-Tethys East Mediterranean Basin connection. In: *Peri-Tethys Memoir 6: Peri-Tethyan Rift/Wrench Basins and Passive Margins* (Ed. by P.A. Ziegler et al.). Mémoires Musée Histoire Naturelle Paris 186, 51–108.
- Stampfli, G.M. & Borel, G. 2004: The TRANSMED transects in space and time: constraints on the paleotectonic evolution of the Mediterranean domain. In: Cavazza, W., Roure, F.M., Spakman, W., Stampfli G.M. & Ziegler, P.A. (Eds.): *The TRANSMED Atlas: The Mediterranean Region from Crust to Mantle*. Springer, Berlin and Heidelberg, 53–80.
- Starijaš, B., Gerdes, A., Balen, D., Tibljaš, D., Schuster, R., Mazer, A., Humer, B. & Finger F. 2006: Geochronology, metamorphic evolution and geochemistry of granulites of the Moslavačka Gora Massif (Croatia). *Proceedings 18. Congress of the Carpathian-Balkan Geological Association*, Belgrade, 594–597.
- Ștefănescu, M., 1970: Pinza de Baraolt. *Dari de Seama Institutului Geologie si Geofizica LXII*, 107–124.
- Ștefănescu, M., 1976: O noua imagine a structurii fisului intern din regiunea di curbura a Carpatilor. *Dari de Seama Institutului Geologie si Geofizica LXII*, Bucuresti.
- Ștefănescu, M., 1995: Stratigraphy and structure of Cretaceous and Palaeogene flysch deposits between Prahova and Ialomita valleys. *Romanian Journal of Tectonics and Regional Geology* 76, 1–49.
- Ștefănescu, M. and working group, 1988: Geological cross sections 1 : 200'000, Nr. 5-B, Section Biharia – Malu Mare Institutului Geologie si Geofizica, Bucharest.
- Ștefănescu, M., Dicea, O. & Tari, G. 2000: Influence of extension and compression on salt diapirism in its type area, East Carpathians Bend area, Romania. In: B.C. Vendeville, Y. Mart and J.L. Vigneresse (Eds.): *Salt, shale and igneous diapirs in and around Europe*. Geological Society London Special Publications 174, 131–147.
- Stephenson, R.A., Mart, Y., Okay, A., Robertson, A., Saintot, A., Stovba, S. & Khriachtchevskaia, O. 2004: TRANSMED Section VIII; East-European Craton-Crimea-Black Sea-Anatolia-Cyprus-Levant Sea-Sinai-Red Sea. In: W. Cavazza, F. Roure, W. Spakman, G.M. Stampfli and P.A. Ziegler (Eds.): *The TRANSMED Atlas: The Mediterranean Region from Crust to Mantle*. Springer, Berlin.
- Streckeisen, A. 1932: Sur la tectonique des Carpathes Méridionales. *Extrait de l' "Anarul Institutului Geologic al României"*, Vol. XVI 1931, Omprinerie Nationale Bucarest, 96 pp.
- Suciu-Krausz, E., Bălc, R. & Borbei, F. 2006: New data on the Western Transilvanides along Ampoi valley (Southern Apuseni Mts., Romania). *Studia Univ. Babeș-Bolyai Geologia* 51, 55–60.
- Sudar, M. 1986: Triassic microfossils and biostratigraphy of the Inner Dinarides between Gučevo and Ljubišnja Mts., Yugoslavia (in Serbian, English summary). *Annales Géologiques de la Péninsule Balkanique* 50, Beograd, 151–394.
- Sudar, M. & Kovács S. 2006: Metamorphosed and ductilely deformed conodonts from Triassic limestones situated between ophiolite complexes: Kopaonik Mountain (Serbia) and Bükk Mountains (NE Hungary) – a preliminary comparison. *Geologica Carpathica* 57, 157–176.
- Tărăpoancă, M., Bertotti, G., Matenco, L., Dinu, C. & Cloetingh, S. 2003: Architecture of the Focșani depression: A 13 km deep basin in the Carpathians bend zone (Romania). *Tectonics* 22/6, 1074.
- Tari, G. 1994: Alpine tectonics of the Pannonian basin. Unpublished PhD thesis, Rice University, Houston Texas, 501 pp.
- Tari, G. 1996: Extreme crustal extension in the Raba River extensional corridor (Austria/Hungary). *Mitteilungen der Gesellschaft der Geologie & Bergbaustudenten Österreichs* 41, 1–17.
- Tari, G., Dicea, O., Faulkerson, J., Georgiev, G., Popov, S., Ștefănescu, M. & Weir, G. 1997: Cimmerian and Alpine stratigraphy and structural evolution of the Moesian Platform (Romania/Bulgaria). In: A.G. Robinson

- (Ed.): Regional and petroleum geology of the Black Sea and surrounding regions. American Association of Petroleum Geologists Memoir 68, 63–90.
- Tari, G., Dövényi, P., Dunkl, I., Horvath, F., Lenkey, L., Ștefănescu, M., Szafian, P. & Toth T. 1999: Lithosphere structure of the Pannonian basin derived from seismic, gravity and geothermal data. In: Durand, B. et al. (Eds.): *The Mediterranean basins: Tertiary extension within the Alpine orogen*. Geological Society London Special Publications 156, 215–250.
- Tari, V. 2002: Evolution of the northern and western Dinarides: a tectonostratigraphic approach. EGU Stephan Mueller Special Publications 1, European Geosciences Union, 223–236.
- Thöni, M. 2006: Dating eclogite-facies metamorphism in the Eastern Alps – approaches, results, interpretations: a review. *Mineralogy and Petrology* 88, 123–148.
- Tischler, M. 2005. A combined structural and sedimentological study of the Inner Carpathians at the northern rim of the Transylvanian basin (N. Romania). Unpublished PhD Thesis Basel University.
- Tischler, M., Gröger, H.R., Fügenschuh, B. & Schmid, S.M. 2007: Miocene tectonics of the Maramures area (Northern Romania): implications for the Mid-Hungarian fault zone. *International Journal of Earth Sciences* 96, 473–496.
- Tomek, C. 1993: Deep crustal structure beneath the central and inner West Carpathians. *Tectonophysics* 226, 417–431.
- Tomljenović, B. 2000: Zagorje-Mid-Transdanubian zone. In: Pamić, J. & Tomljenović, B. (Eds.): *PANCARDI 2000 Fieldtrip Guidebook*. *Vijesti* 37/2, 27–33.
- Tomljenović, B. 2002: *Strukturne Znacajke Medvednice i Samoborskoj gorja*. Unpublished PhD Thesis, Zagreb, 208 pp.
- Trubelja, F., Marchig, V., Burgath, K.P. & Vujović, Ž. 1995: Origin of the Jurassic Tethyan ophiolites in Bosnia: A geochemical approach to tectonic setting. *Geologica Croatica* 48/1, 49–66.
- Trümpy, R. 1988: A possible Jurassic-Cretaceous transform system in the Alps and the Carpathians. *Geological Society of America Special Paper* 218, 93–110.
- Turpaud, Ph. 2006: Characterization of igneous terranes by zircon dating: implications for the UHP relicts occurrences and suture identification in the Central Rhodope, Northern Greece. Unpublished PhD thesis, University Mainz, 107 pp.
- Ustaszewski, K., Fügenschuh, B., Schmid, S.M., Kounov, A. & Schaltegger, U. 2006: Kinematics and timing of convergence between the Tisza block and the internal Dinarides along the Sava-Zone: from Mid-Eocene collision to Mid-Miocene exhumation. Abstract 4th Swiss Geoscience Meeting Bern, 203–204.
- Ustaszewski, K., Krenn, E., Fügenschuh, B., Schmid, S.M., and Finger, F. 2007: Tracing the Alpine collision zone towards east: the Sava Zone – a Late Cretaceous to Palaeogene suture between Tisza and the Dinarides, EGU General Assembly 2007, Volume 9: Geophysical Research Abstracts: Vienna, p. 04357.
- Ustaszewski, K., Schmid, S.M., Lugović, B., Schuster, R., Schaltegger, U., Kounov, A., Bernoulli, D., Hottinger, L. & Schefer S. submitted: Late Cretaceous island arc magmatism in the internal Dinarides (northern Bosnia and Herzegovina): Implications for the collision of the Adriatic and European plates. *Lithos*.
- Vaida, M., Seghedi, A. & Verniers, J. 2005: Northern Gondwana affinity of the east Moesian terrane based on chitinozoans. *Tectonophysics* 410, 397–387.
- Velledits, F. 2006: Evolution of the Bükk Mountains (NE Hungary) during the Middle – Late Triassic asymmetric rifting of the Vardar-Meliata branch of the Neotethys. *International Journal of Earth Sciences* 95, 395–412.
- Visarion, M., Veliciu, S. & Ștefănescu, M. 1978: Thermal field in the Romanian Carpathians and some aspects of its interpretation. *Studia geoph. & geod.* 22, 196–199.
- Visarion, M., Săndulescu, M., Stanica, D., Veliciu, S. 1988: Contributions à la connaissance de la structure profonde de la plate-forme Moesienne en Roumanie. *Stud. The. Econ. Geofiz.* 15, 68–92.
- Vishnevskaya, V. & Đerić, N. 2005: The first finding of Jurassic radiolarians in Bosnia and Hercegovina. *Micropaleontology on eve of centuries*. Abstracts of the Proceedings of the 13. Russian Micropaleontological Conference, Moscow, 77–79.
- von Quadt, A., Moritz R., Peytcheva, I. & Heinrich, C.A. 2005: 3: Geochronology and geodynamics of Late Cretaceous magmatism and Cu–Au mineralization in the Panagyurishte region of the Apuseni–Banat–Timok–Srednogie belt, Bulgaria. *Ore Geology Reviews* 27, 95–126.
- Vörös, A. 1977: Provinciality of the Mediterranean Lower Jurassic brachiopod fauna: causes and plate-tectonic implications. *Paleogeography Paleoclimatology Paleogeology* 21, 1–16.
- Vörös, A., 1993: Jurassic microplate movements and brachiopod migrations in the western part of the Tethys. *Paleogeography Paleoclimatology Paleogeology* 100, 125–145.
- Weber J., Vrabec M., Stopar B., Pavlovčič-Prešeren P. & Dixon T. 2005: The PIVO-2003 experiment: A GPS study of Istria peninsula and Adria microplate motion, and active tectonics in Slovenia. In: Pinter N., Grenczy G., Weber J., Medak D. & Stein S. (Eds.): *The Adria microplate: GPS Geodesy, Tectonics, and Hazards*. NATO Science Series 61, Kluwer Academic Publishers, 305–320.
- Weidle, C., Widiyantoro, S. & CALIXTO Working Group 2005: Improving depth resolution of teleseismic tomography by simultaneous inversion of teleseismic and global P-wave traveltimes data – application to the Vrancea region in Southeastern Europe. *Geophysical Journal International* 162, 811–823.
- Wessely, G. 1987: Mesozoic and Tertiary evolution of the Alpine-Carpathian foreland in eastern Austria. *Tectonophysics* 137, 45–59.
- Windhoffer, G., Bada, G., Nieuwland, D., Worum, G., Horvath, F. & Cloetingh, S. 2005: On the mechanics of basin formation in the Pannonian basin: Inferences from analogue and numerical modelling. *Tectonophysics* 410, 389–415.
- Wortel, M.J.R. & Spakman, W. 2000: Subduction and slab detachment in the Mediterranean-Carpathian region. *Science* 290, 1910–1917.
- Zacher, W. & Lupu, M. 1999: Pitfalls on the race for an ultimate Tethys model. *International Journal of Earth Sciences* 88: 111–115.
- Zelić, M., D’Orazio, M., Malasoma, A., Marroni, M. & Pandolfi, L. 2005: The metabasites from the Kopaonik Metamorphic Complex, Vardar Zone, Southern Serbia: Remnants of the rifting-related magmatism of the Mesothethyan domain or evidence for Paleotethys closure of the Dinaric-Hellenic belt? *Ophioliti* 30, 91–101.
- Ziegler, P.A. 1981: Evolution of Sedimentary Basins in North-West Europe. In Illing, L.V. et al. (Eds.): *Petroleum Geology of the Continental Shelf of North-West Europe*. London Institute of Petroleum, Heyden & Son, London, 3–39.
- Ziegler, P.A. 1990. *Geological Atlas of Western and Central Europe*. 2nd Ed. Shell Internationale Petroleum Maatschappij, distributed by Geological Society London, Publishing House Bath, 239 pp.
- Ziegler, P.A., Cloetingh, S. & van Wees, J.D. 1995: Dynamics of intra-plate compressional deformation: the Alpine Foreland and other examples. *Tectonophysics* 252, 7–59.
- Zonenshain, L.P., Kuzmin, M.I. and Natapov, L.M. 1990: *Geology of the USSR: a Plate-Tectonics Synthesis*. American Geophysical Union Geodynamics Series 21.
- Zweigel, P., Ratschbacher, L. & Frisch, W. 1998: Kinematics of an arcuate fold-thrust belt: the southern Eastern Carpathians (Romania). *Tectonophysics* 297, 177–207.

Manuscript received March 21, 2007

Revision accepted December 20, 2007

Published Online first March 24, 2008

Editorial Handling: Clark Burchfiel & Stefan Bucher

Electronic supplementary material: The online version of this article (DOI: 10.1007/s00015-008-1247-3 contains 3 fold-out plates as supplementary material, which is available to authorized users.

MAJOR TECTONIC UNITS OF THE ALPS

S.M. Schmid, D. Bernoulli, B. Fügenschuh, L. Matenco, S. S. Schmid

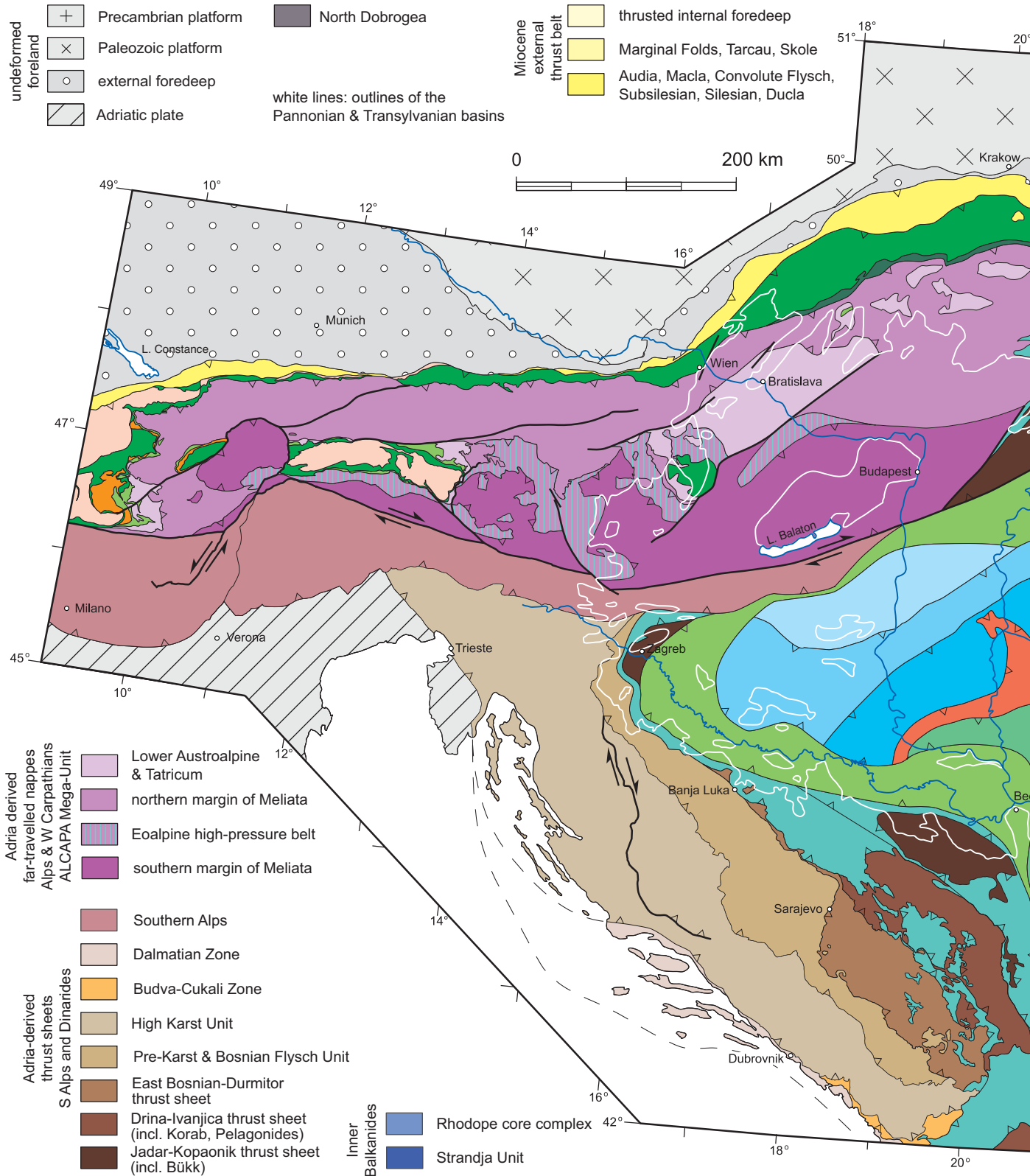
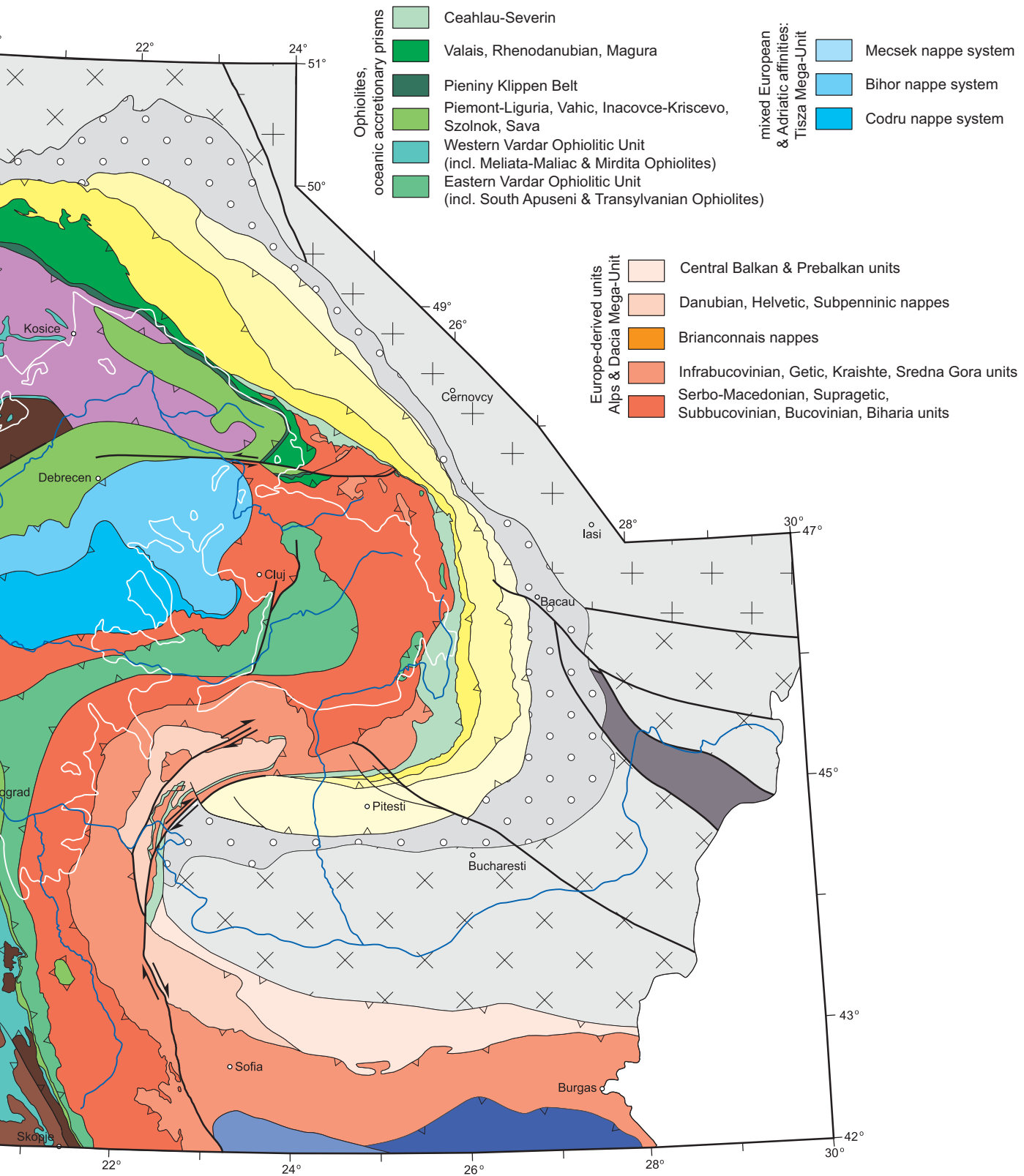


Plate 1: Major tectonic units of the Alps, Carpathians and Dinarides 1:5'000'000. Note that the locations of the cross-sections given

S, CARPATHIANS AND DINARIDES

hefer, R. Schuster, M. Tischler and K. Ustaszewski



in Fig. 3 and Plates 2 & 3 are found in Fig. 6.

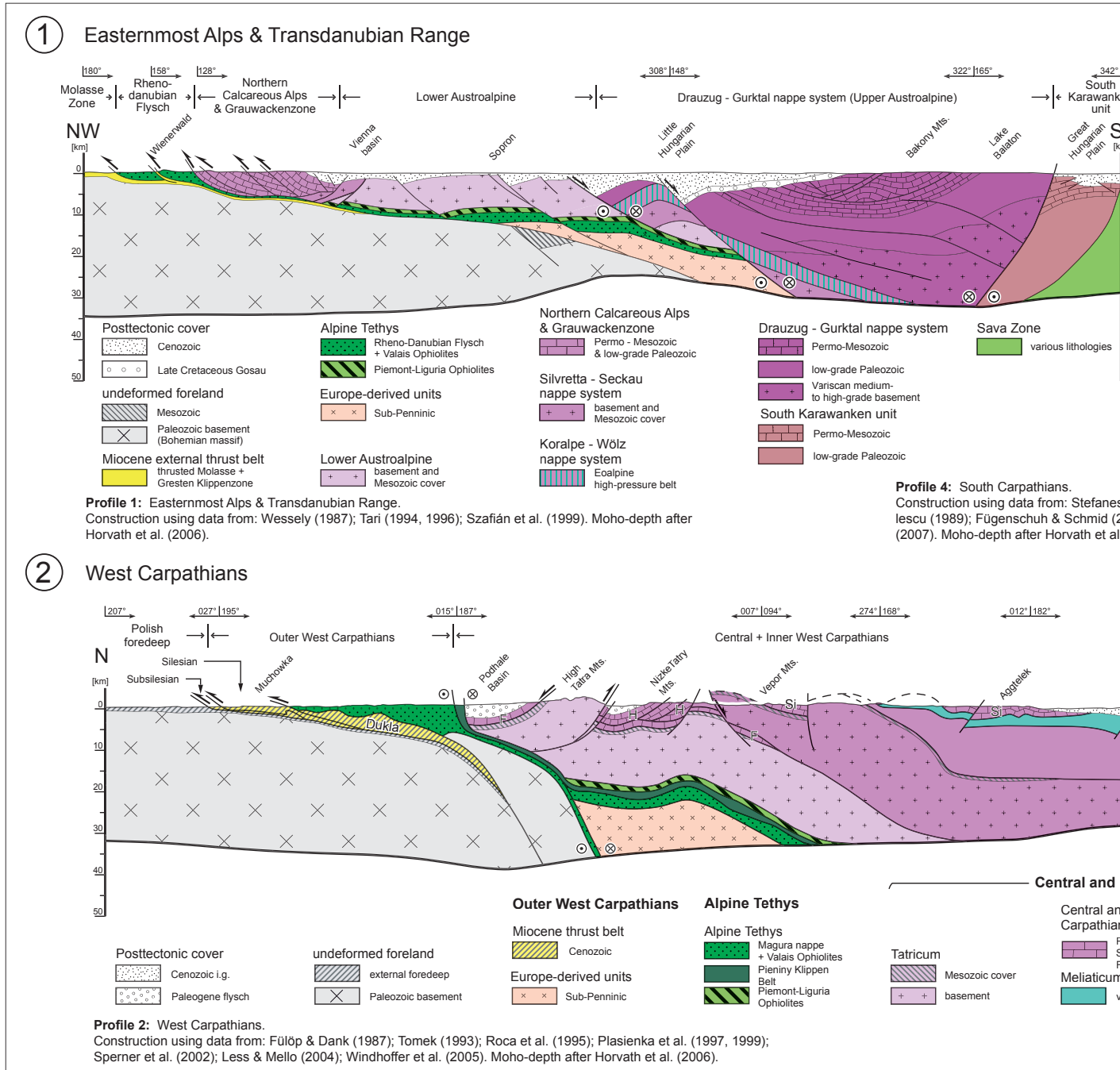
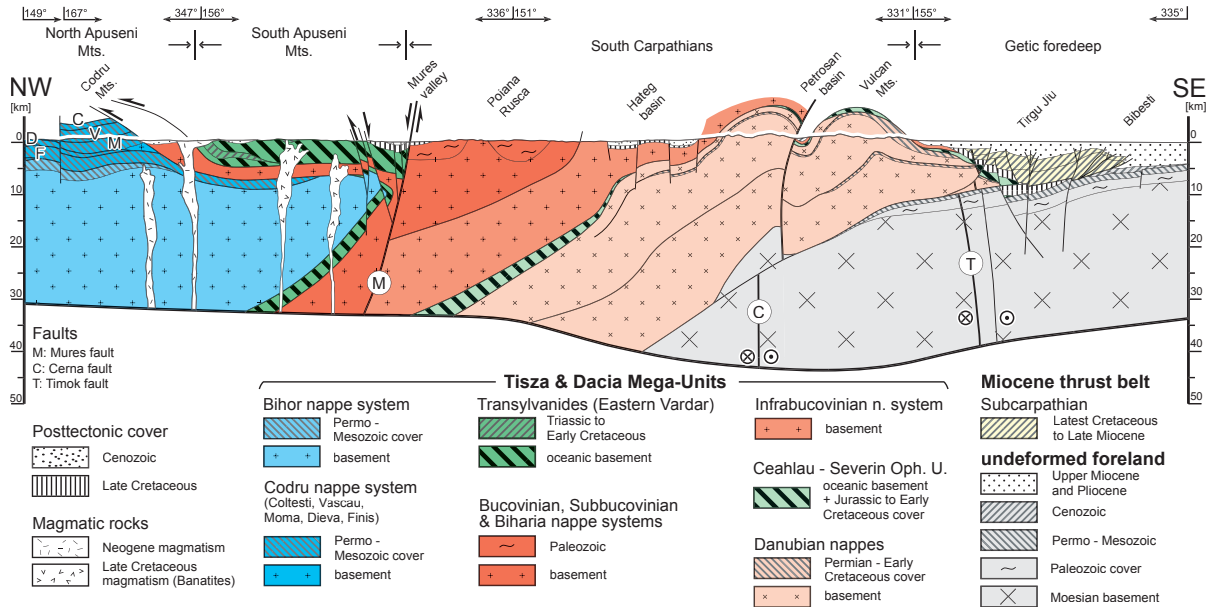


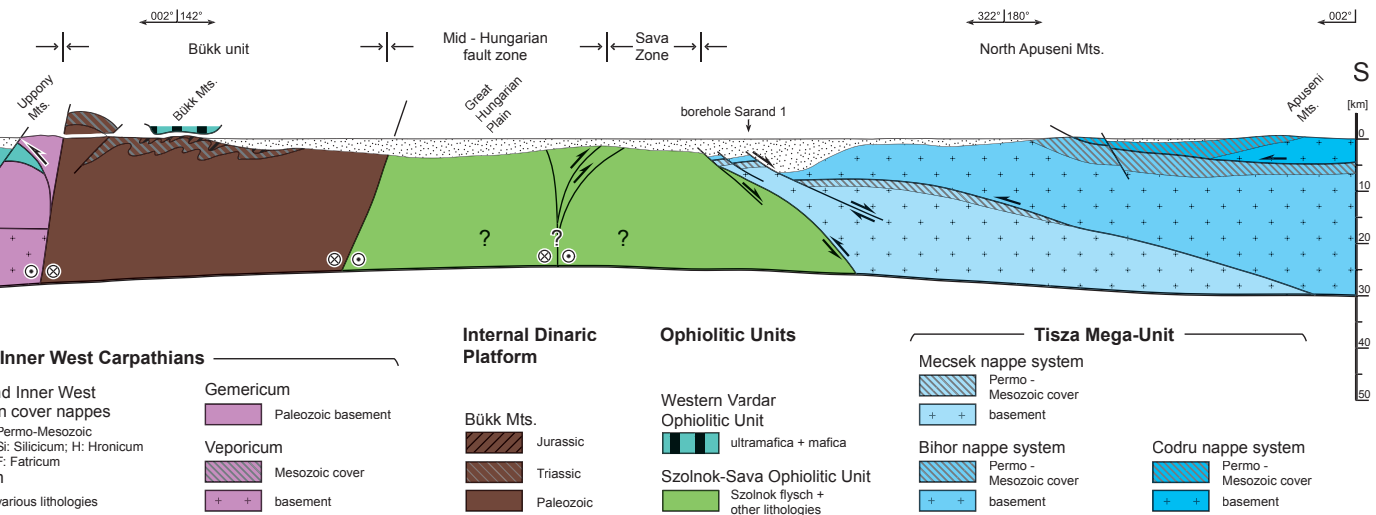
Plate 2: Crustal-scale cross-sections through the Alps, Carpathians and Dinarides (for location see Fig. 6).

S. M. Schmid et al.

④ South Carpathians



scu (1988); Sandu-
2005); Rabagia et al.
(2006).



d Inner West
n cover nappes
Permo-Mesozoic
Si: Silicium; H: Hronicum
F: Faticum
various lithologies

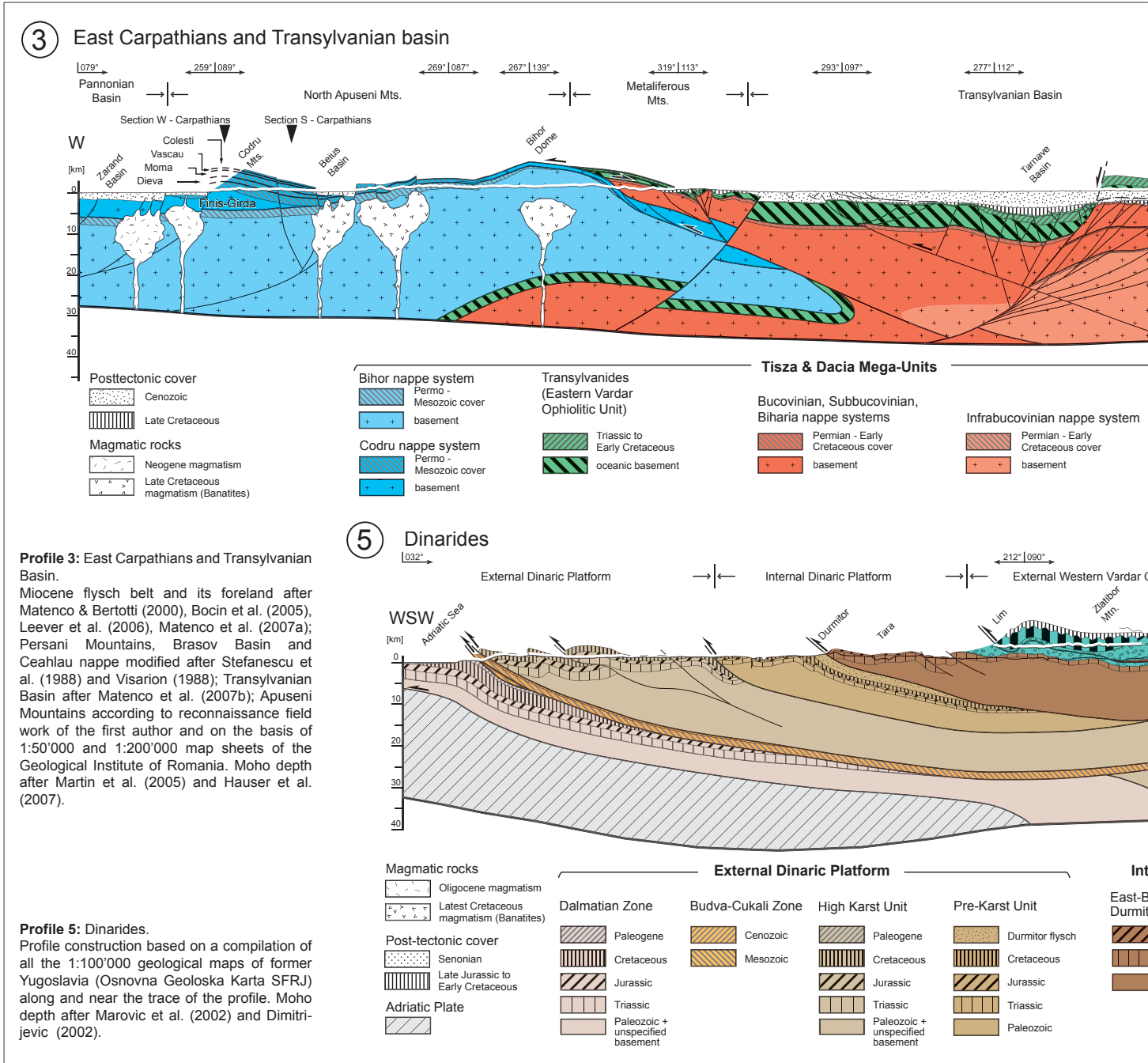
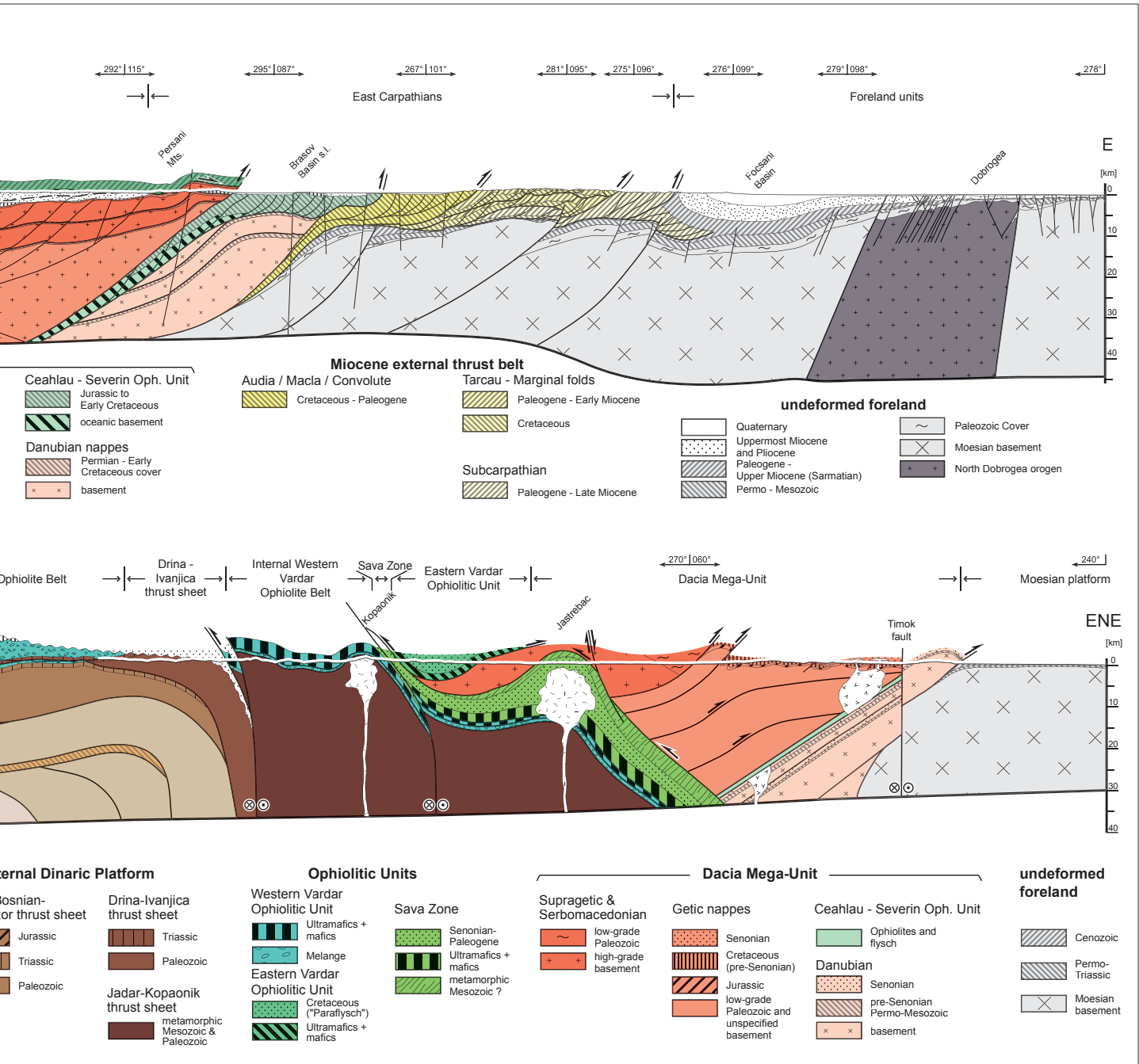


Plate 3: Crustal-scale cross sections through the Alps, Carpathians and Dinarides (for location see Fig. 6).

S. M. Schmid et al.



Alps-Carpathians-Dinarides

Appendix II: Ustaszewski et al. 2009

Lithos 108 (2009) 106–125



Contents lists available at ScienceDirect

Lithos

journal homepage: www.elsevier.com/locate/lithos

Late Cretaceous intra-oceanic magmatism in the internal Dinarides (northern Bosnia and Herzegovina): Implications for the collision of the Adriatic and European plates

Kamil Ustaszewski^{a,*}, Stefan M. Schmid^a, Boško Lugović^b, Ralf Schuster^c, Urs Schaltegger^d, Daniel Bernoulli^a, Lukas Hottinger^a, Alexandre Kounov^a, Bernhard Fügenschuh^e, Senecio Schefer^a^a Institute of Geology and Paleontology, Bernoullistrasse 32, University of Basel, CH-4056 Basel, Switzerland^b Rudarsko-geološko-naftni fakultet, HR-10000 Zagreb, Croatia^c Geologische Bundesanstalt, A-1030 Wien, Austria^d Département de Minéralogie, CH-1205 Genève, Switzerland^e Geologisch-Paläontologisches Institut, A-6020 Innsbruck, Austria

ARTICLE INFO

Article history:

Received 17 September 2007

Accepted 17 September 2008

Available online 7 October 2008

Keywords:

Ophiolites
Sm–Nd-dating
U–Pb dating
Geochemistry
Dinarides
Vardar Ocean

ABSTRACT

The Kozara Mountains of northern Bosnia and Herzegovina form part of the internal Dinarides and host two tectonically juxtaposed ophiolitic successions of different age. The southern part of the Kozara Mountains exposes the Western Vardar Ophiolitic Unit, which was obducted onto the Adriatic margin in the Late Jurassic. The northern part exposes a bimodal igneous succession that was thrust onto the Western Vardar Ophiolitic Unit during the latest Cretaceous to Early Paleogene. This bimodal igneous succession comprises isotropic gabbros, doleritic dikes, basaltic pillow lavas and rhyolites. Pelagic limestones, intercalated with pillow lavas, yielded a Campanian globotruncanid association, consistent with concordant U–Pb ages on zircons from dolerites and rhyolites of 81.39 ± 0.11 and 81.6 ± 0.12 Ma, respectively.

Chondrite-normalised rare earth element patterns of the bimodal igneous rocks show enrichment of LREE over HREE. Primitive mantle-normalised multi-element diagrams do not reveal significant depletion of HFSE. The $\epsilon_{\text{Nd}}(\text{T})$ and initial $^{87}\text{Sr}/^{86}\text{Sr}$ isotopic values range from +4.4 to +6.3 and from 0.70346 to 0.70507 respectively, suggesting an intraoceanic origin.

The bimodal igneous succession is unconformably overlain by Maastrichtian to Paleocene siliciclastics that contain abundant ophiolitic detritus, suggesting reworking of the Campanian magmatics. An Eocene turbiditic sandstone succession unconformably covers both the Western Vardar Ophiolitic Unit and the Late Cretaceous bimodal igneous successions. These observations suggest that the Adriatic Plate and the Europe-derived Tisza and Dacia Mega-Units were still separated by a deep basin floored by oceanic lithosphere until the Campanian and that its closure did not occur before the Maastrichtian to earliest Paleogene. This Late Cretaceous oceanic domain probably represented a remnant of the Vardar Ocean, or alternatively, the Alpine Tethys; possibly the traces of both oceanic domains were connected in the area.

© 2008 Elsevier B.V. All rights reserved.

1. Introduction

1.1. Large-scale tectonic setting

The widespread occurrence of ophiolites is one of the most distinctive features of the Dinarides and Hellenides of the Balkan Peninsula. They can be traced for about 1000 km along strike, from the area of Zagreb (Croatia) in the northwest to the Peloponnesus (Greece) in the southeast and beyond (Fig. 1). In map view, the ophiolites exposed west of a line Zagreb–Beograd–Skopje form two parallel, spatially separate belts (Smith and Spray, 1984). Petrographic

and geochemical differences between the ophiolites of the two belts were used as evidence for the existence of two distinct oceanic basins, originally separated by one or several Adria-derived micro-continents that included the Drina-Ivanjica, Jadar and Pelagonian blocks (Robertson and Karamata, 1994; Dimitrijević, 1997, 2001; Karamata, 2006; Dilek et al., 2008). This ‘two ocean’ model contrasts with that of Bernoulli and Laubscher (1972), Smith and Spray (1984) and Pamić et al. (2002), who suggested an origin of both ophiolitic belts in one ocean. Schmid et al. (2008) support the ‘single ocean’ model and consider the two belts of ophiolites as relics of the same, formerly coherent ophiolitic sheet (their Western Vardar Ophiolitic Unit) that was obducted onto the Adriatic passive margin in the Late Jurassic and was disrupted by Cretaceous to Tertiary thrusting. Thrusting has exposed units derived from the Adriatic margin below the ophiolitic units in the form of windows, which were interpreted as micro-continents by earlier authors (Fig. 1).

* Corresponding author. Now at: Department of Geosciences, National Taiwan University, 10617 Taipei, Taiwan.

E-mail address: kamilu@ntu.edu.tw (K. Ustaszewski).

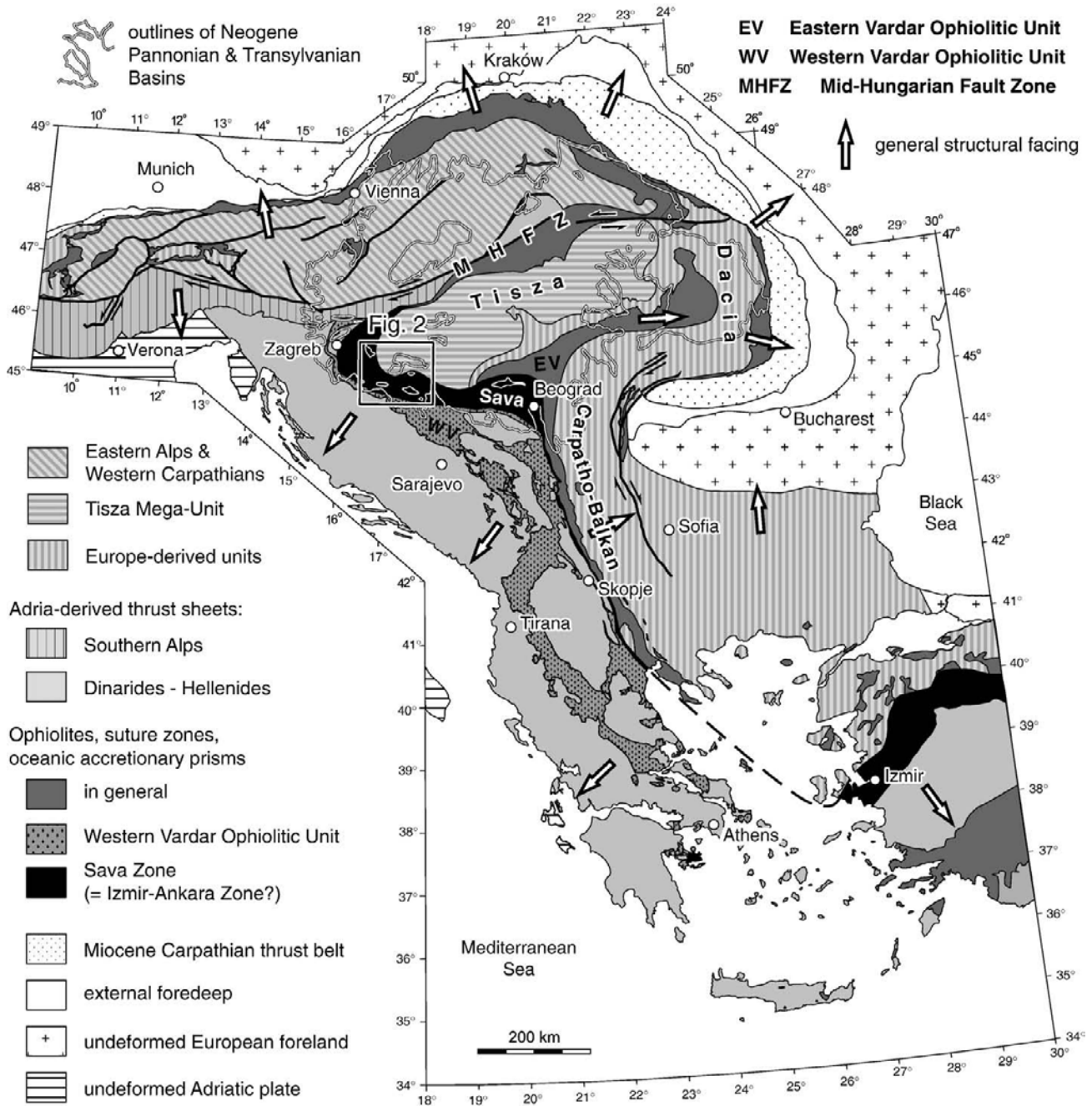


Fig. 1. Major tectonic units of the Alps, Carpathians, Dinarides and Hellenides (north of 42°N, simplified after Schmid et al., 2008).

The spatial separation of these ophiolitic belts gave rise to a number of different names. The western (external) belt is referred to as Dinaride (or Dinaridic) ophiolite belt (Robertson and Karamata, 1994; Pamić et al., 2002), or as the Central Dinaridic ophiolite belt (Lugović et al., 1991). The eastern (internal) belt has a variety of names: Western Vardar ophiolites (Karamata, 2006), Inner Dinaridic ophiolite belt (Lugović et al., 1991), External Vardar Subzone (Dimitrijević, 1997, 2001) or simply Vardar Zone (Robertson and Karamata, 1994; Pamić et al., 2002). The terminology adopted here follows that of Schmid et al. (2008), who refer to the two belts located west and east of the Drina-Ivanjica unit as Dinaridic and Western Vardar ophiolites, respectively, in a struc-

tural sense. Since Schmid et al. (2008) regard the two ophiolitic belts as having formed in the same ocean, they use “Western Vardar Ophiolitic Unit” (WV; Fig. 1) when collectively referring to both the ophiolite belts and the ocean from which the ophiolites were derived. There is yet another ophiolitic branch of the Vardar Ocean, located further to the east, referred to as the Eastern Vardar Ophiolitic Unit (Fig. 1).

1.2. When did the Vardar Ocean close?

A controversial topic is the time of the closure of the Vardar Ocean that led to collision of Adria with smaller Europe-derived plates like the

Tisza and Dacia Mega-Units (see Schmid et al., 2008 and references therein). The different branches of the Vardar Ocean (and the Alpine Tethys) were involved in two orogens of different age and structural facing direction: 1) the Early to middle Cretaceous, Europe-vergent South Carpathians (Dacia Mega-Unit) including the Carpatho-Balkan orogen in the NE, and 2) the SW-vergent Dinarides, which, with the obducted Western Vardar Ophiolitic Unit, form the NE edge of the Adriatic Plate (Fig. 1). The Tisza Mega-Unit, located NE of the Vardar suture, referred to as Sava Zone by Schmid et al. (2008), was originally separated from the Dacia Mega-Unit by another oceanic branch represented by the Eastern Vardar Ophiolitic Unit. The Tisza and Dacia Mega-Units were juxtaposed along the East-Vardar suture in the late Early Cretaceous (Săndulescu and Visarion, 1977). The West-Vardar suture, i.e. the consumed oceanic domain between Tisza–Dacia on the one hand and Adria on the other hand, belonged to a branch of the Triassic to Jurassic Meliata–Maliac–Vardar Ocean (Schmid et al., 2008), part of the Neotethys *sensu* Ricou (1994). The Neotethys was probably linked to the Alpine Tethys somewhere in the area around Zagreb. For simplicity, we use the name Vardar Ocean for this ocean that closed to form the Sava Zone suture. The closure of this ocean was hitherto inferred to have occurred in the Late Cretaceous–Early Paleogene, based on the following observations:

- a.) Blueschist-facies metamorphosed metabasalts in Fruška Gora (N of Beograd) yielded glaucophane K–Ar ages of 123 ± 5 Ma (Milovanović et al., 1995). They are believed to mark subduction of oceanic lithosphere of the Vardar Ocean ongoing at that time.
- b.) The stratigraphic minimum age of strongly deformed, very low- to low-grade metamorphosed sediments in the most internal

Dinarides, containing olistoliths of mafics and ultramafics as well as tectonically incorporated Mesozoic platform carbonates, is Late Cretaceous (“Senonian”) flysch of Dimitrijević, 1997; Pamić, 2002; Schefer et al., 2007).

- c.) A belt of Late Cretaceous, mainly calc-alkaline igneous rocks, stretching from central Bulgaria across eastern Serbia into western Romania, is informally referred to as “banatites”. They are mostly associated with Late Cretaceous (Turonian to Campanian age, 92–78 Ma) volcano-sedimentary basins and are interpreted to have formed in a back-arc setting related to the N- to NE-directed subduction of the Vardar Ocean beneath Europe-derived units (e.g. Georgiev et al., 2001; Heinrich and Neubauer, 2002; Neubauer et al., 2003; von Quadt et al., 2005).
- d.) Greenschist- to amphibolite-facies metapelites in North Bosnia (Pamić and Prohić, 1989; Pamić, 1993a) with a biostratigraphically determined Maastrichtian protolith age (Pantić and Jovanović 1970; Šparica et al., 1980, 1984; Jovanović and Magaš 1986) are thought to mark a post-collisional metamorphic event (Pamić, 2002).

In Central Serbia, the surface expression of the Sava Zone suture is a N–S-trending, few kilometre wide belt of Late Cretaceous (“Senonian”) flysch. At the latitude of Beograd this suture bends into an E–W trend and opens into a 50 km wide corridor parallel to the Sava River (therefore termed Sava Zone, Fig. 1, corresponding to the “Northwestern Vardar Zone” of Pamić, 1993a, or the “Sava–Vardar Zone” of Pamić, 2002). Between Beograd and Zagreb the suture is exposed in a few isolated inselbergs located at the southwestern margin of the Pannonian Basin (Fig. 2).

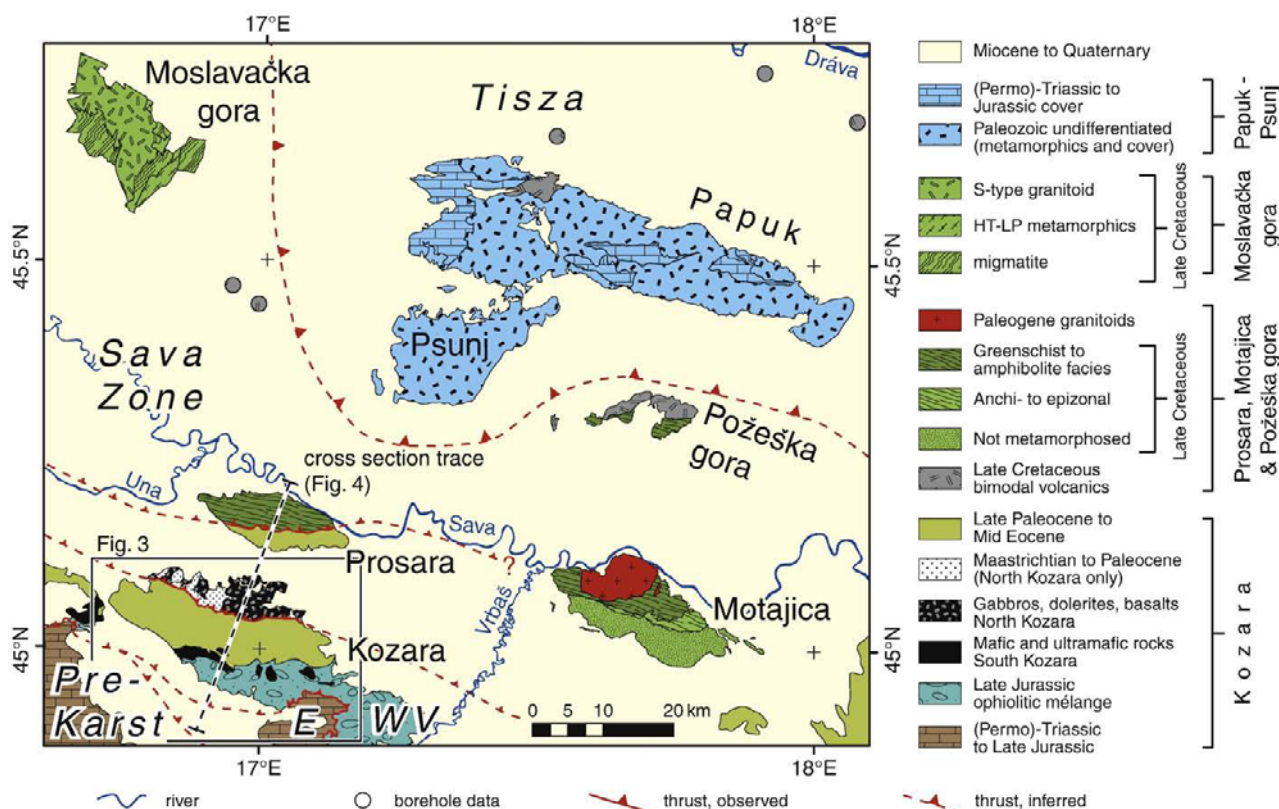


Fig. 2. Simplified geologic–tectonic map of the study area, compiled from 1:100,000 map sheets of former Yugoslavia (referenced in the text) and Pamić et al. (2000). Well locations are from Pamić (1997). Tectonic contacts between major tectonic units (in italics) are from Schmid et al. (2008). Only inferred Paleogene and older contacts are shown, while faults related to the Neogene extension of the Pannonian Basin are neglected. WV=Western Vardar Ophiolitic Unit, E=East-Bosnian–Durmitor unit.

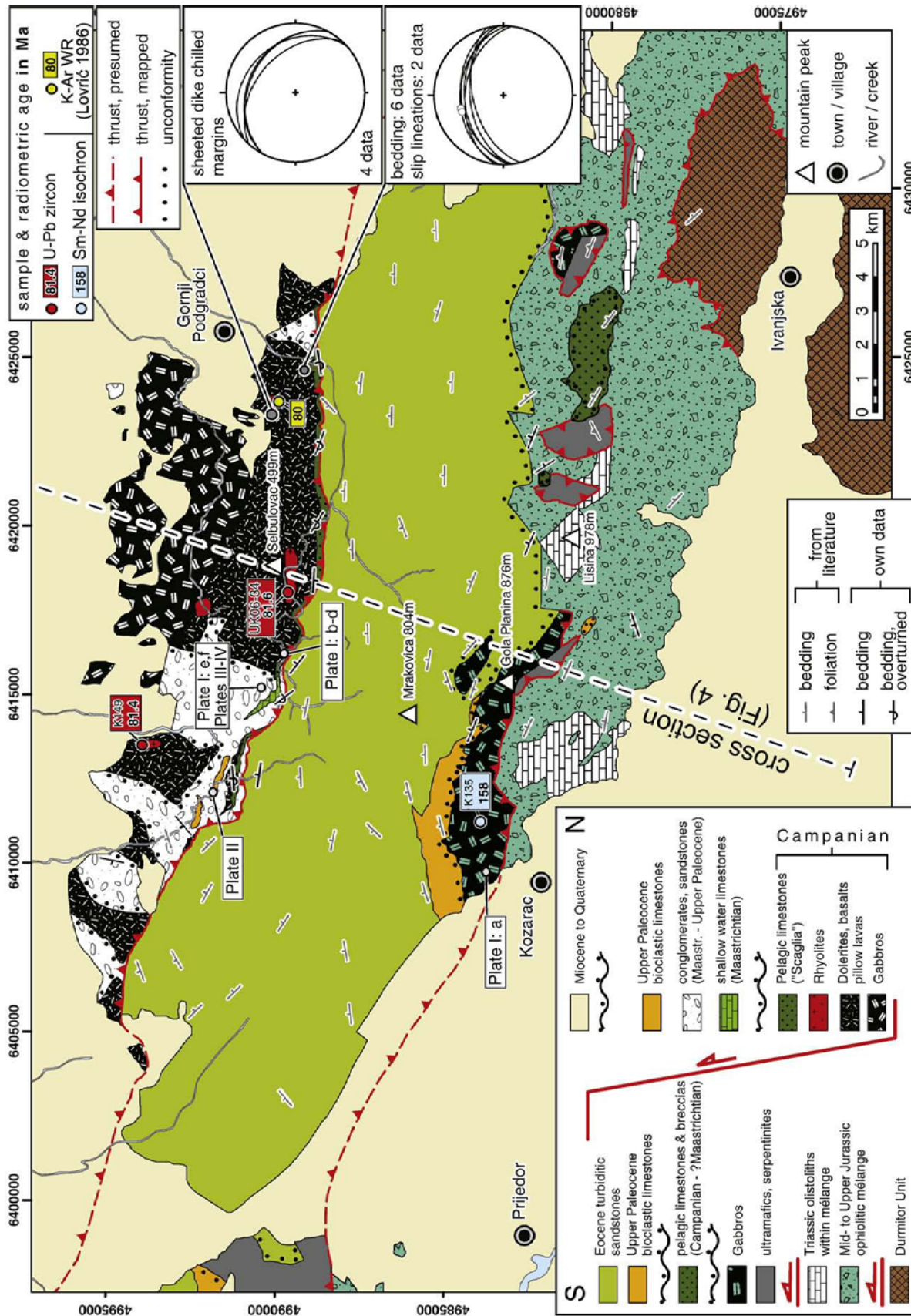


Fig. 3. Geological map of the Kozarac Mountains, compiled from 1:100,000 geological map sheets of former Yugoslavia (see text for references) and modified according to own observations. Numbers at the edges of the map are MGI Balkan 6 Cartesian coordinates. Structural data plotted at the right edge are lower hemisphere, equal area projections.

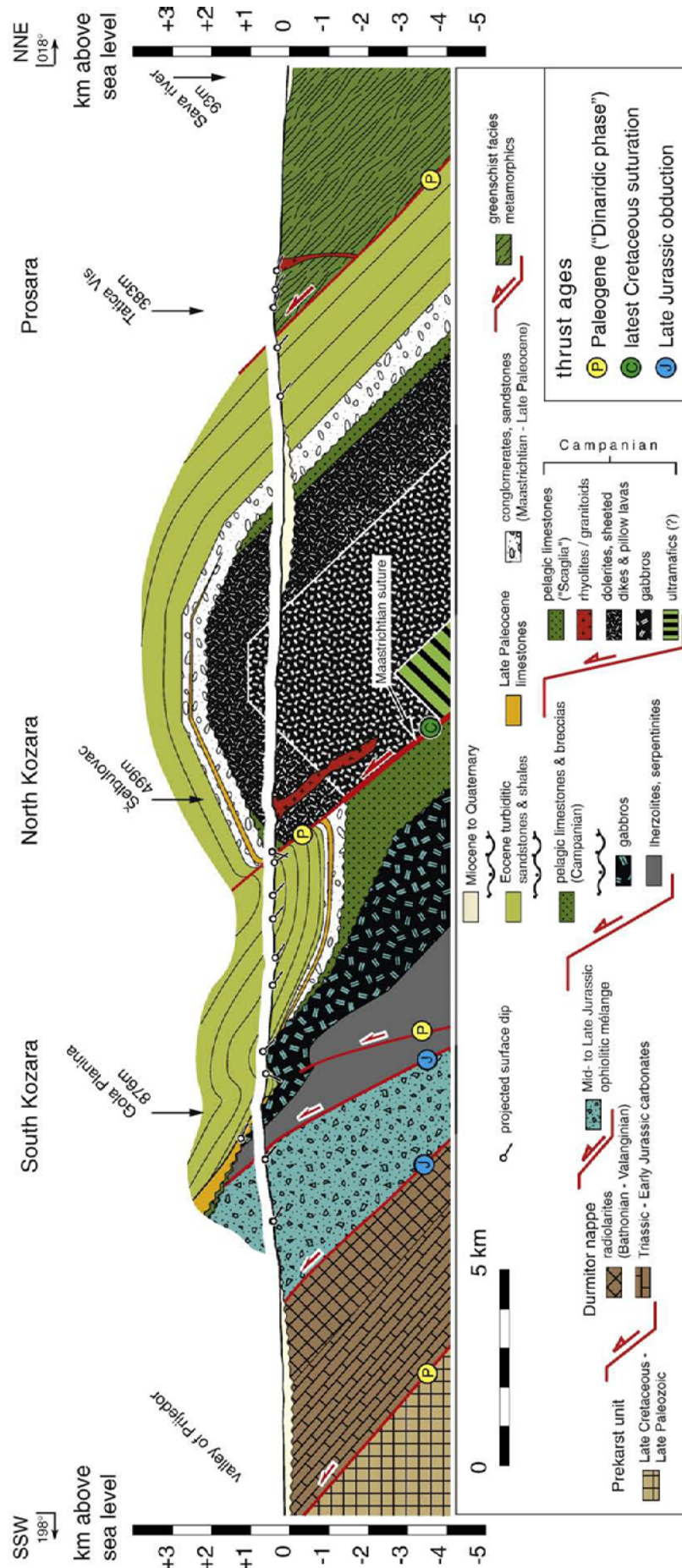


Fig. 4. Geological cross-section across the Kozara and Prosara Mountains. See Figs. 2 and 3 for location.

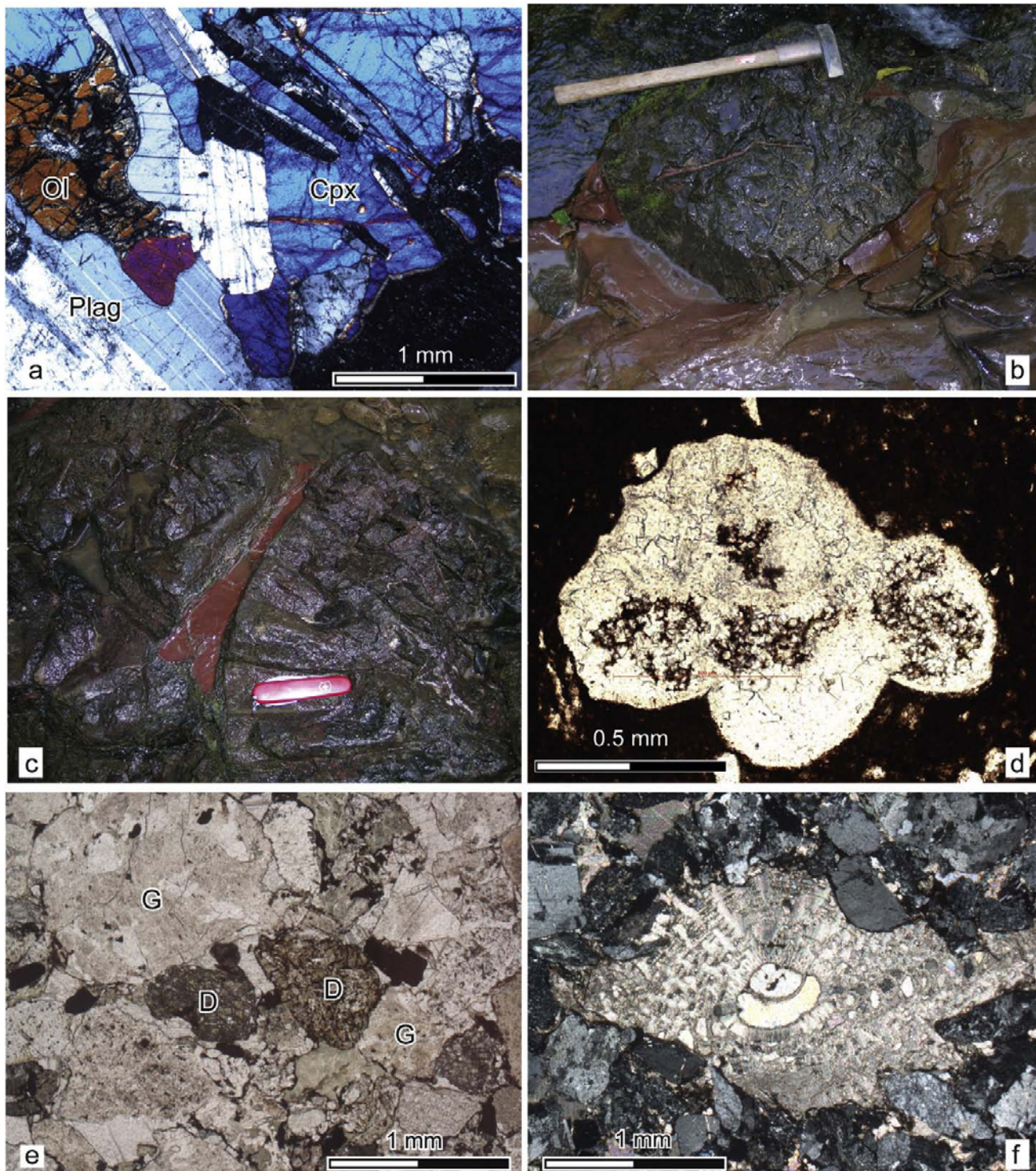


Plate I.

- a. Thin-section photomicrograph of an olivine-bearing cumulate gabbro (sample K135) from South Kozara, selected for Sm–Nd isochron dating. Crossed nicols.
- b and c. Outcrop (no. 142, see Table 5 in electronic supplement) of basaltic pillow-lavas and intercalated red pelagic limestones containing globotruncanids. Note the radial crack filled with limestones in b.
- d. Thin section photomicrograph of *Contusotruncana* (anc. *Rosita*) *patelliformis* (Gandolfi, 1955) in pelagic limestone (sample K142s) from the locality in (b), dating the limestones to the Early Campanian. Fossil determination courtesy of M. Caron (Fribourg).
- e. Late Cretaceous–Early Paleogene (?) lithic sandstone (sample K144) containing reworked volcanic material from the North Kozara magmatics of both mafic and felsic affinity. D=dolerite clasts with ophitic textures, G=coarse-grained clasts with granophyric texture.
- f. Late Cretaceous–Early Paleogene lithic sandstone (sample K144) containing reworked shallow-water benthic foraminifera of the species *Orbitoides gruenbachensis* Papp and Küpper, indicative of Maastrichtian age.

Our paper presents new biostratigraphic, geochronological and geochemical evidence for Late Cretaceous intra-oceanic magmatism within the Sava Zone. These results constrain the earliest possible age for the closure of the Vardar Ocean to the latest Cretaceous. This supports the assumption of Karamata et al. (2000, 2005) that a remnant or a “marginal basin” of the Vardar Ocean stayed open until the Campanian. Our results are also in line with Pamić (1993a, 2002), who interpreted the Sava Zone as a suture that formed during the collision of the Internal Dinarides with Tisza during the Paleogene.

2. Regional geological setting

Outcrops of pre-Neogene rocks in the study area are restricted to isolated inselbergs separated by Neogene fill (Fig. 2). Pre-Neogene rocks cropping out in the Papuk–Psunj inselberg belong to the Tisza Mega-Unit. This is characterised by a pre-Mesozoic basement that experienced a pre-Variscan and Variscan metamorphic overprint (Balén et al., 2006, and references therein), and an autochthonous Permo-Mesozoic, non-metamorphic cover. By contrast, the westerly and southerly adjacent inselbergs of Moslavačka Gora, Požeška Gora, Prosara and Motajica all underwent middle or Late Cretaceous metamorphism. In Moslavačka Gora olivine gabbros were intruded in the late Early Cretaceous (c. 110 Ma, Balén et al., 2003), followed by Late Cretaceous LP-HT (Abukuma-type) metamorphism. This event was accompanied by the formation of migmatites and granites that yielded electron-microprobe-based monazite ages around 80 Ma (Starijaš et al., 2004, 2006). ^{40}Ar – ^{39}Ar ages obtained on hornblende (81–83 Ma) and white mica (74 Ma) document cooling from peak metamorphic conditions between 83 and 74 Ma (Balén et al., 2001).

The northern part of Požeška Gora exposes a bimodal igneous rock suite including (gabbro-) dolerites, pillow basalts, basic and acidic tuffs and volcanoclastics, as well as alkali-feldspar rhyolites and subordinate granites (Pamić and Šparica 1983; Belak et al., 1998). The basalts and tuffs are intercalated with red, pelagic limestones that yielded Late Campanian to Early Maastrichtian globotruncanids (Pamić and Šparica 1983). Dolerite dikes intruded both acidic rocks and Late Cretaceous sediments (Belak et al., 1998). Rhyolites and cogenetic granites have a Rb–Sr age of 71.5 ± 2.8 Ma (Pamić et al., 1988), whereas K–Ar ages of the dolerites range between 66 and 68 Ma (Pamić, 1993b). In the south of Požeška Gora, greenschist-facies phyllites predominate. K–Ar whole rock ages obtained on muscovite-rich phyllites yielded an age of ca. 49 Ma (Pamić et al., 1988), which may reflect cooling from earlier peak metamorphic conditions. Due to poor outcrop conditions, the structural relationships between the Late Cretaceous bimodal volcanics and the greenschist-facies metamorphics are presently unknown (see Šparica et al., 1980).

The inselberg of Motajica (Fig. 2) is characterised by a Late Cretaceous, mostly siliciclastic succession that underwent Barrovian-type metamorphism (Pamić and Prohić, 1989; Pamić et al., 1992) and is comparable to the metamorphic series found in Požeška Gora. Electron-microprobe-based analysis of monazites in lower amphibolite-grade metapelites from Motajica yielded an age of 63 ± 9 Ma for this metamorphic event (Krenn et al., 2008).

The inselberg of Prosara exposes a lower tectonic unit in the S and an upper tectonic unit in the N. These units are separated by a N-dipping thrust associated with a top-S shear sense. The lower unit consists of a non-metamorphic succession of sandstones and shales of most likely Paleogene age (Šparica et al., 1984; Jovanović and Magaš, 1986). The higher unit comprises, from bottom to top, a greenschist-facies succession of mylonitic metarhyolites, prasinities, followed by metasandstones, phyllites and subordinate calcite marbles. Palynomorph studies performed on the phyllites suggested a Maastrichtian protolith age (Šparica et al., 1984; Jovanović and Magaš, 1986). Metarhyolites and phyllites are intruded by meter-scale pegmatite dykes and decametric bodies of coarse-grained, leucocratic alkali-feldspar granites. While the dikes are mostly boudinaged, the larger

intrusions acquired a schistosity together with their host rock. Thin-section analyses suggest that the schistosity formed in a solid state. These observations suggest that the fabric-forming event occurred after the intrusion of the leucocratic magmatics.

3. Geology and petrography of the Kozara Mountains

The Kozara Mountains (Fig. 3) form a WNW–ESE-trending massif at the southwestern margin of the Pannonian Basin. The outline of this massif follows the general strike of the geological units. Igneous rocks dominate in the northern and southern parts of the Kozara Mountains and are separated from each other by a belt of Eocene turbiditic sandstones (Fig. 3). From south to north, across strike, or in cross-section from bottom to top (Fig. 4), the following geological units can be distinguished.

3.1. South Kozara

The lowermost unit exposed consists of Bathonian to Valanginian-age radiolarites (Djerić and Vishnevskaya, 2006; Djerić et al., 2007), which belong to the East Bosnian–Durmitor unit (Schmid et al., 2008). The Durmitor unit tectonically overlies the Pre-Karst unit, which is characterised by a Late Paleozoic to Late Cretaceous sedimentary succession. The radiolarites of the Durmitor unit are tectonically overlain by an ophiolitic mélangé that consists predominantly of disrupted lithic sandstones and shales. Numerous extra-formational blocks of mafics, ultramafics and Late Triassic shallow-water limestones and dolomites occur within the mélangé. The Triassic olistoliths are up to several km across and often form the highest mountains (Lisina 978 m, Fig. 3). The lithic sandstones are moderately to poorly sorted and both texturally and compositionally immature. The most frequent detrital components are euhedral, often embayed quartz grains of volcanic origin, plagioclase, white mica and basalt fragments. The shales typically exhibit an intense, closely spaced cleavage. The exact age of formation of the ophiolitic mélangé in Kozara and elsewhere in the Dinarides is still poorly constrained. Near Zagreb, the shaly matrix of the ophiolitic mélangé was dated by palynomorphs, yielding ages from Hettangian to Late Bajocian (Babić et al., 2002). In our opinion, the Bajocian age indicates the maximum age of the mélangé formation (see below).

In South Kozara, an ultramafic to mafic succession tectonically overlies the ophiolitic mélangé. In contrast to other ophiolite exposures in the Dinarides, no metamorphic sole has yet been found here. The ultramafics are often serpentinised lherzolites (Djerković et al., 1975; Mojićević et al., 1976). The mafics include gabbros and dolerites. Volumetrically subordinate dolerites occur usually as dikes cutting the gabbros. No doleritic sheeted dike complex was recognised; basalts are totally absent. Gabbros show both isotropic, cumulate and, rarely, pegmatitic textures. The cumulates are olivine bearing and coarse grained with ophitic to subophitic textures. Olivine is partly transformed into iddingsite (made up of cryptocrystalline chlorite and goethite). Plagioclase and clinopyroxene are fresh in some samples (Plate 1a; sample K135). Clinopyroxene forms large, poikilitic grains. Subordinately, albite-rich felsic intrusives and dikes occur. The latter cut both gabbros and dolerites, show granophyric textures and contain zoned plagioclase.

The mélangé together with the ultramafics and mafics are unconformably overlain by reddish pelagic marly limestones and clast-supported micro-conglomerates with pebbles of pelagic limestone (Fig. 3). The age of the pebbles ranges from latest Albian to Coniacian–Santonian, as indicated by different species of planktonic foraminifera (M. Caron pers. comm. 2006). The matrix, and hence the conglomerate formation, is thus most likely of Campanian age or younger.

Higher up in the section, the lithologies so far described are unconformably overlain by an Upper Paleocene to Eocene succession starting with often bioclastic shallow-water limestones (column “S

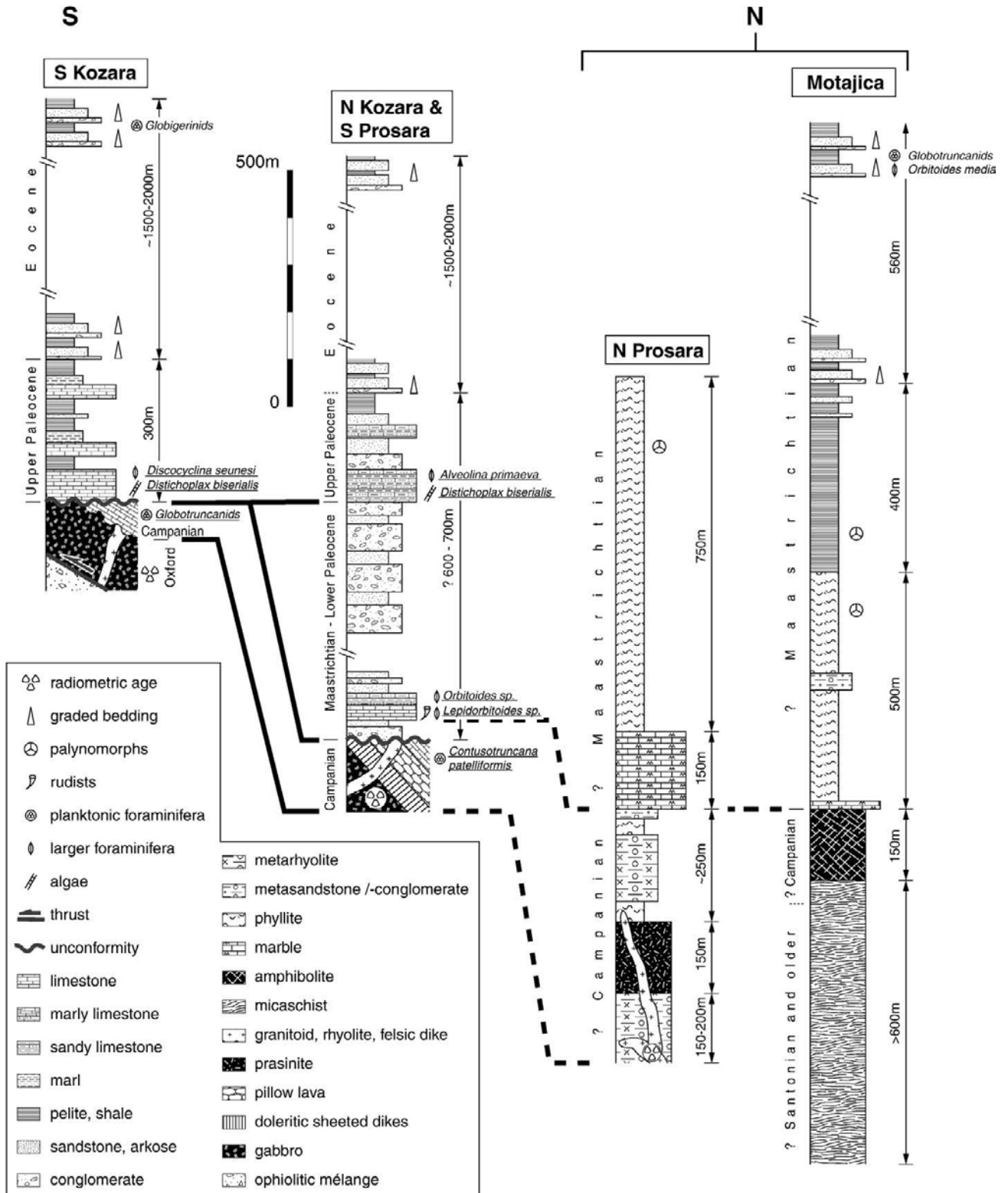


Fig. 5. Tectono-stratigraphic correlation of the North Bosnian inselbergs (south of the Sava River, see Fig. 2). Bold black lines mark correlated stratigraphic intervals and unconformities. Fossils identified in this study are underlined. Correlations between the exposures in South and North Kozara rely on both litho- and biostratigraphy, whereas further correlations with Prosara and Motajica are largely based on lithostratigraphy. For simplicity, the (Late Oligocene) Motajica granitoid (shown in Fig. 2) is omitted in the corresponding stratigraphic column.

Kozara” in Fig. 5). The limestones are packstones, grainstones and rudstones, containing *Discocyclus*, red algae (*Distichoplax biserialis*), coral fragments, alveolinids, and rare globigerinids (Jovanović and Magaš, 1986; M. Caron pers. comm., 2006). Up-section, they grade into marls and shales (Fig. 5). Still higher up follows a succession of thick-bedded siliciclastic turbiditic sandstones (arkoses, lithic arenites, lithic sandstones) and subordinate pelites. The basal part of this succession includes reworked bioclasts. The detrital components are mostly quartz (often embayed quartz of volcanic origin), plagioclase, microcline, white mica and biotite. Rock fragments are mostly basalts, granophyres and metamorphics of both low and high grade. Bed thickness ranges from about 10 cm to 1 m. Individual beds are commonly graded. Globigerinids within hemipelagic intercalations (Jelaska, 1981), as well as benthic foraminiferal assemblages (Šparica et al., 1984), constrain the minimum age of this succession to the middle Eocene.

3.2. North Kozara

The turbiditic sandstone succession of South Kozara dips N and is overlain by the igneous succession of North Kozara, separated by a major thrust (Fig. 4). The igneous succession comprises gabbros, dolerites, doleritic sheeted dikes, basalts and subordinate peraluminous (Shand, 1947) felsic dikes and extrusives (Figs. 3, 4), and substantially differs from that of South Kozara. Ultramafics do not crop out: the structurally lowest exposed levels are gabbros, and hence there is no direct proof that the latter are underlain by ultramafics. The gabbros are coarse to very coarse grained with isotropic textures. The main mineral phases are plagioclase and brown and green amphibole. Green amphibole is formed by replacement (uralitisation) of primary clinopyroxene. Common accessory minerals are biotite, apatite, zircon and Fe–Ti-oxides.

The dolerites are subophitic with idiomorphic plagioclase laths, clinopyroxene, brown and green hornblende. Biotite has formed at the expense of brown hornblende. Accessories are zircon, apatite and Fe–Ti-oxides. Plagioclase is often zoned.

The basalts are usually phaneritic and typically show intersertal textures formed by elongated laths of idiomorphic plagioclase. Porphyritic varieties with idiomorphic olivine phenocrysts are also found. The top of the mafic igneous succession consists of pillow lavas, containing amygdules with calcite. The pillow lavas are intercalated with red pelagic limestones of Scaglia facies that are also found as inter-pillow sediment and along radial cracks in the pillows (Plate Ib and Ic). This indicates that the extrusion of the pillow lavas and the sedimentation of the pelagic limestones were contemporaneous. The occurrence of *Contusotruncana* (anc. *Rosita*) *patelliformis* (Gandolfi) constrains the age of the pelagic limestones and, indirectly, the pillow basalts, to the Early Campanian (Plate Id, determination by M. Caron). Karamata et al. (2000, 2005) suggested a Late Campanian to Early Maastrichtian for these same limestones.

The mafics are often intruded by felsic dikes on the outcrop scale. On the map scale, rhyolites are found in numerous locations (Fig. 3). Composite dikes of mafic amphibole-bearing segments in diffuse contact with granophyric segments are occasionally found, suggesting simultaneous mafic and felsic intrusion. Rhyolites are mostly altered, fine-grained, banded and commonly of aphyric texture.

The map view alignment of the gabbros (in the north), dolerites and pillow basalts, including their cover of pelagic limestones (in the south) suggests that the igneous succession is tilted towards the S and even overturned in proximity to the north-dipping thrust fault (Fig. 4). This is corroborated by the following observations: (a) The beds of the pelagic limestones, intercalated with the pillow lavas, dip to the S or are even overturned and then topographically overlain by igneous rocks and (b) the chilled margins within the originally subvertical doleritic sheeted dike complex dip to the NNE- to NE (upper stereoplott in Fig. 3).

Arkoses, lithic sandstones, conglomerates and shallow-water limestones unconformably overlie the igneous rocks of North Kozara. The shallow-water limestones contain abundant rudist fragments and benthic foraminifera indicating a Maastrichtian age (Fig. 3, column “N Kozara & S Prosara” in Fig. 5). Lithic sandstones, overlying the shallow water limestones, contain reworked benthic foraminifera of Maastrichtian age and abundant fragments of basalt and granophyre (Plate Ie and If, Plates II and III in electronic supplement). Quartz, plagioclase and detrital white mica are also very common. Thick beds of poorly sorted conglomerates with well-rounded boulders/clasts, ranging from a few cm up to several dm in diameter, consist of basalts, dolerites and granite clasts. Metamorphic rocks are absent. Up-section, the average clast size of the conglomerates decreases. Bioclastic limestones with alveolinids, indicating a Late Paleocene (Thanetian) age (Fig. 5, Plate IV in electronic supplement) are intercalated.

4. Geochemistry and age of the Kozara Mountains igneous rocks

A geochemical comparison of the two tectonically separated igneous complexes exposed in the South and North Kozara Mountains, respectively, is precluded by the fact that both igneous complexes

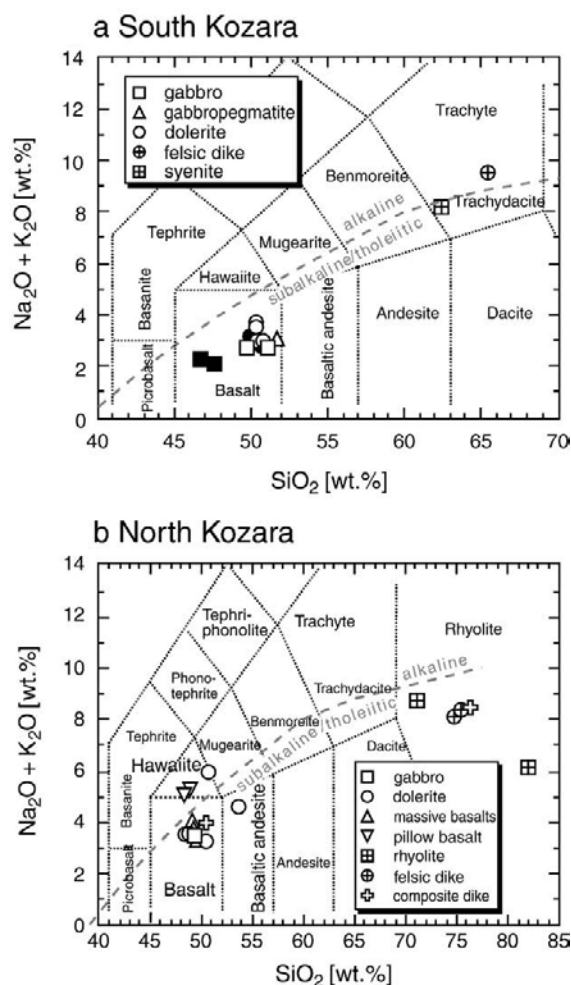


Fig. 6. TAS diagrams (after Le Bas et al., 1986) of (a) South and (b) North Kozara igneous rocks. Open symbols are samples from this study; black symbols in (a) are samples from Lugović et al. (1991).

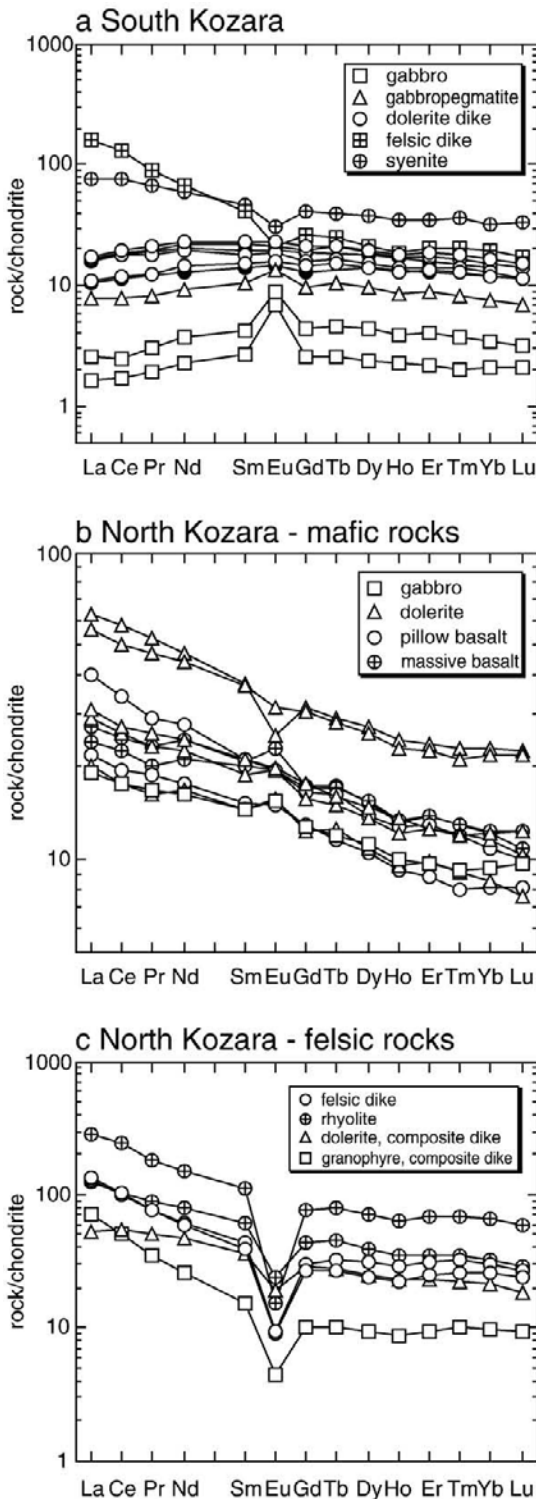


Fig. 7. Rare earth element concentrations normalised over chondrite composition. a: South Kozara, b: North Kozara mafic rocks, c: North Kozara felsic rocks. Chondrite normalisation is according to Boynton (1984). Open symbols are from this study; filled symbols are from Lugović et al. (1991).

represent incomplete ophiolitic successions, each comprising different crustal levels. The absence of extrusive rocks in South Kozara makes it impossible to directly compare the South Kozara rocks with

the unfractionated basaltic rocks from North Kozara. Hence, our interpretation of the tectonic setting of the South and North Kozara igneous successions does not solely rely on the analysis of geochemical discrimination diagrams, but, in addition, on isotopic evidence as well as on the field geological constraints given above. 26 whole-rock samples were analysed for major and trace elements (Table 1). The majority of the analysed samples (23) yielded loss-on-ignition (LOI) values of <4 wt.% indicating that their degree of alteration is low to moderate. LOI is generally higher for the North Kozara samples (up to 9 wt.%) and apparently in line with the occurrence of hydrous mineral phases.

4.1. South Kozara

4.1.1. Major and trace element characteristics

In the TAS-diagram (total alkali (Na₂O+K₂O) vs. SiO₂ ratio; Le Bas et al., 1986), samples from South Kozara almost exclusively plot in the field of subalkaline/tholeiitic basalts (Fig. 6a). Gabbros from South Kozara are low in TiO₂ (<0.3%) and K₂O (<0.4%) with Mg# between 69 and 74 (Mg# = 100 * molar MgO / (MgO + FeO_{total})). Dolerites show slightly higher contents of TiO₂ (up to 1.6%) and Mg# between 57 and 62. Mg# and Ti-content are negatively correlated. Concentrations

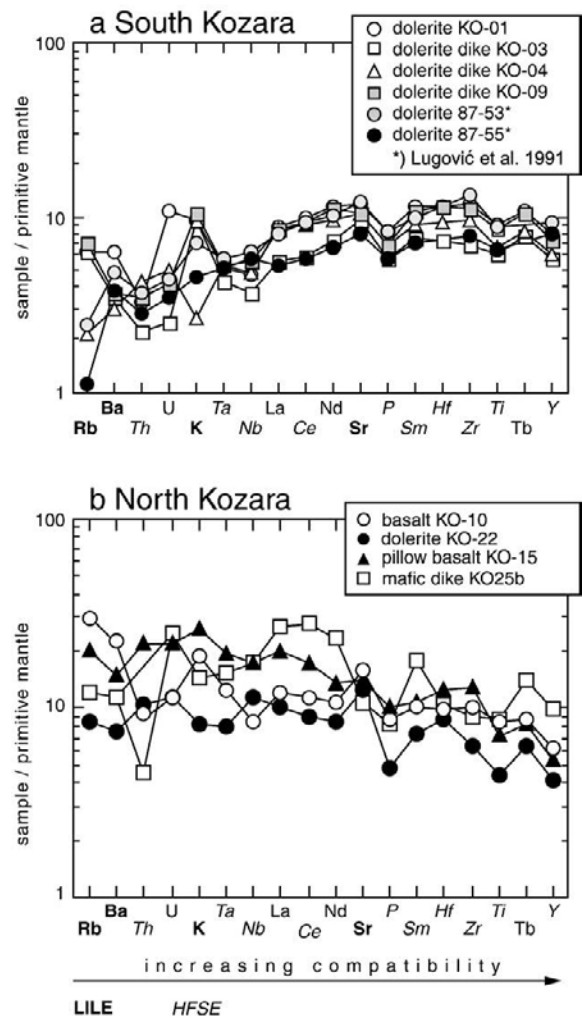


Fig. 8. Primitive mantle-normalised multi-element diagrams of non-cumulate South Kozara mafic rocks (a) and North Kozara mafic rocks (b). Normalisation values are after Hofmann (1988).

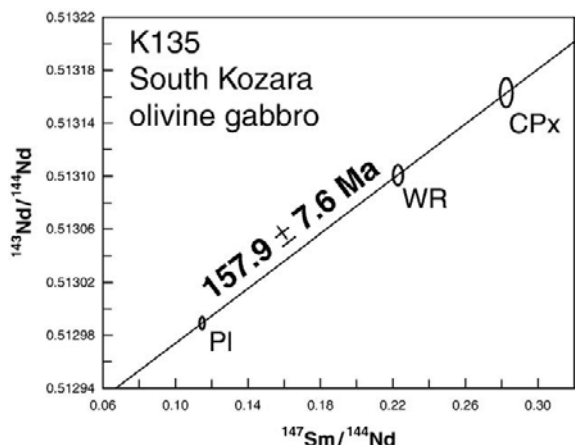


Fig. 9. Sm–Nd–isochron plot of an olivine-bearing cumulate gabbro from South Kozara. The three data points (PI=Plagioclase, WR=whole-rock, CPX=clinopyroxene) fit onto an isochron with an age of 158 ± 8 Ma (MSWD 0.0109). The initial $^{143}\text{Nd}/^{144}\text{Nd}$ value is 0.512871 ± 9 (see Table 2). See Figs. 4 and 12 for sample locality.

of compatible elements, like Ni and Cr, correlate positively with Mg#. Chondrite-normalised REE concentration diagrams of samples from South Kozara (particularly gabbros) reveal essentially flat REE patterns (Fig. 7a), with a slight depletion of LREE. The felsic dikes and intrusives show enrichment of LREE over HREE. Positive Eu-anomalies in the gabbros are attributed to fractionation of Eu^{2+} into plagioclase, a main constituent phase in the gabbros. Primitive mantle-normalised multi-element diagrams of non-cumulate mafic samples show gently positive slopes and unpronounced depletions in P and Ti (Fig. 8a).

4.1.2. Sm–Nd dating, Sr and Nd isotopes

A well-preserved, coarse-grained olivine gabbro from South Kozara, with fresh plagioclase and clinopyroxene, was chosen for dating (sample K135). A whole-rock powder, clinopyroxene and plagioclase were used for dating. The data points fit onto an isochron, yielding an age of 158 ± 8 Ma (MSWD 0.0109). The initial $^{143}\text{Nd}/^{144}\text{Nd}$ value is 0.512871 ± 9 (Fig. 9 and Table 2).

Sr- and Nd-isotopic values were also analysed on a whole-rock powder of the same sample, yielding an $^{87}\text{Sr}/^{86}\text{Sr}$ -ratio of 0.702703 and a $^{143}\text{Nd}/^{144}\text{Nd}$ -ratio of 0.513067. Its initial isotopic values, calculated for an age of 160 Ma, are +8.6 for $\epsilon\text{Nd}(T)$ and 0.70264 for $^{87}\text{Sr}/^{86}\text{Sr}$, respectively (Fig. 10 and Table 3). The sample plots in the MORB field.

4.2. North Kozara

4.2.1. Major and trace element characteristics

In the TAS-diagram (Le Bas et al., 1986), samples from North Kozara plot as subalkaline/tholeiitic basalts, basaltic andesites, hawaiites and rhyolites, and they show a bimodal distribution (Fig. 6b). Mg# of all samples (except felsic dikes or intrusives) are between 40 and 66 (Table 1), i.e. they are generally more evolved than comparable samples from South Kozara. The basalts and basaltic andesites reveal K_2O contents between 0.25 and 1.14 wt.%. Based on this, they can be classified as low- to medium-K tholeiites (Gill, 1981).

Chondrite-normalised REE patterns of samples from North Kozara show strong enrichment of LREE over HREE (Fig. 7b and c). None of the essentially flat REE patterns that characterise the South Kozara mafic igneous rocks are encountered here. The REE slopes of both mafic and felsic samples are essentially parallel. A primitive mantle-normalised multi-element diagram is shown for four mafic igneous rocks (Fig. 8b). This shows no significant depletion of HFSE (particularly Ta, Nb, P, Zr and Ti) over LILE (Rb, Ba and Sr).

4.2.2. Sr and Nd isotopes

The $^{143}\text{Nd}/^{144}\text{Nd}$ -ratios of the North Kozara samples are similar, varying between 0.512844 and 0.512945 (Table 3). By contrast, the $^{87}\text{Sr}/^{86}\text{Sr}$ -ratios of the same samples exhibit a relatively large spread between 0.703531 and 0.706224. The initial isotopic values for 80 Ma (see below) are +4.4 to +6.3 for $\epsilon\text{Nd}(T)$ and 0.70346 to 0.70507 for $^{87}\text{Sr}/^{86}\text{Sr}$, respectively (Fig. 10). The $\epsilon\text{Nd}(T)$ values and initial $^{87}\text{Sr}/^{86}\text{Sr}$ -ratios from North Kozara plot at the intersection of the MORB, island arc and ocean island basalt fields. Two “outliers” with the highest $^{87}\text{Sr}/^{86}\text{Sr}$ -ratios (samples K142 and K147b) are an altered pillow basalt with calcite-filled amygdules and a veined dolerite, respectively; they also yielded LOI values of up to 9% (Table 1).

4.2.3. U–Pb dating

Three igneous rock samples have been selected for high accuracy isotope-dilution thermal ionisation mass spectrometry (ID-TIMS) dating using zircon single crystals. Two samples (a dolerite and a rhyolite, samples K149 and UK06-34, respectively) are from North Kozara, a third sample is from Provara Mountain (an alkali-feldspar granite, sample UK04-4) located still further north (Figs. 2 & 4). The results are presented in Fig. 11 and Table 4. The three dated samples (K149, UK06-34 and UK04-02) yielded weighted mean $^{206}\text{Pb}/^{238}\text{U}$ ages of 81.4 ± 0.11 Ma, 81.6 ± 0.12 Ma and 82.68 ± 0.13 Ma, respectively.

5. Discussion

5.1. Tectonic interpretation of the geochemical and isotopic data

From a tectonic point of view, the ultramafic and igneous succession of South Kozara represents the northwesternmost occurrences of the Western Vardar Ophiolitic Unit. This is evident from the overall geological framework and is further corroborated by our new geochronological data.

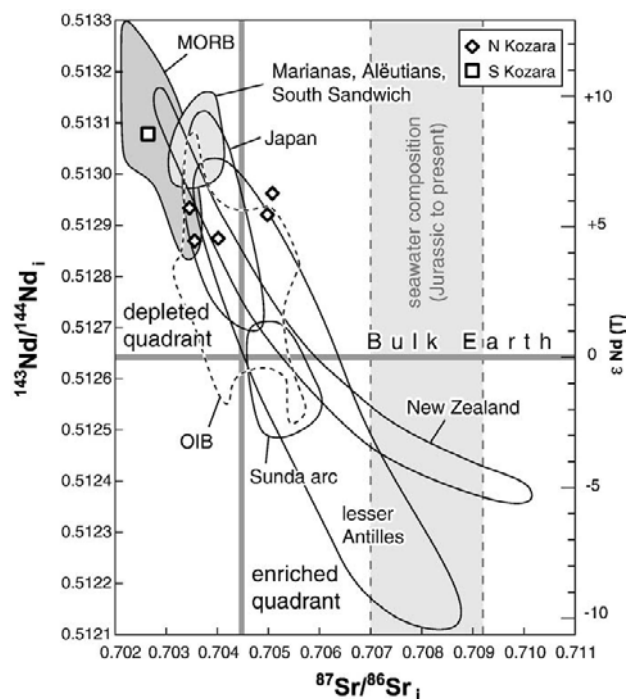


Fig. 10. Initial Nd- and Sr-isotopic ratios of selected North and South Kozara mafics in comparison to various basaltic rocks from different oceanic environments. The samples with elevated $^{87}\text{Sr}/^{86}\text{Sr}$ values are likely affected by syn- or postmagmatic alteration in contact with seawater, the average composition of which is shown by light-grey shading. The OIB field is after Hofmann (1997), all other fields are from Murphy (2007).

Table 1
Whole rock chemical analyses of igneous rocks from South and North Kozara

South Kozara										
Sample rock remark	K135 ol-gabbro cumulate	KO-05 gabbro cumulate	KO-07 gabbro pegm	KO-01 dolerite massive	KO-03 dolerite dike	KO-09 dolerite dike	KO-04 dolerite dike	KO-08 TD dike	KO-H alb.sy intr	
SiO ₂	49.09	49.70	50.13	49.08	49.69	49.48	49.25	64.21	60.46	
TiO ₂	0.25	0.31	0.70	1.64	1.09	1.52	1.22	0.89	1.28	
Al ₂ O ₃	19.62	17.62	14.70	15.33	15.48	15.59	16.15	18.99	15.19	
Fe ₂ O ₃ total	6.46	5.88	7.52	10.60	9.08	10.37	9.08	2.00	6.17	
MnO	0.11	0.09	0.12	0.17	0.15	0.17	0.15	0.02	0.09	
MgO	9.08	8.77	9.04	7.25	8.41	7.41	7.95	1.67	1.74	
CaO	11.42	12.29	11.88	9.85	10.92	10.17	10.91	0.82	3.54	
Na ₂ O	2.56	2.61	2.60	3.29	2.60	3.16	2.81	9.40	6.19	
K ₂ O	0.13	0.07	0.37	0.30	0.30	0.33	0.08	0.00	1.78	
P ₂ O ₅	0.03	0.01	0.04	0.17	0.12	0.14	0.14	0.18	0.49	
LOI	1.51	2.02	2.24	1.29	1.32	1.30	1.51	1.20	3.10	
Total	100.25	99.37	99.34	98.97	99.16	99.64	99.25	99.38	100.03	
Mg#	73.5	74.7	70.4	57.5	64.7	58.6	63.4	62.3	35.8	
Rb	1.8	1.6	5.3	3.3	3.4	3.8	1.1	1.0	22	
Ba	27	13	33	38	21	22	18	20	158	
Th	0.02	0.05	0.20	0.26	0.18	0.27	0.34	15.0	8.3	
U	<0.01	0.01	0.06	0.22	0.05	0.08	0.10	2.14	2.80	
Ta	0.25	0.01	0.06	0.18	0.15	0.19	0.19	1.39	1.00	
Nb	0.22	0.29	1.0	2.8	2.3	3.5	3.0	18	13	
Pb	<1	<5	<5	<5	<5	<5	<5	6.74	0.70	
Sr	189	222	192	215	173	190	193	49	137	
Zr	7	12	34	116	66	109	94	284	428	
Hf	0.23	0.45	1.04	3.11	1.95	3.08	2.51	8.15	11.8	
Y	5	7	15	31	23	28	24	34	72	
V	70	104	182	241	212	226	194	98	128	
Cr	371	407	153	220	353	260	260	82	7	
Ni	178	113	107	57	101	57	93	35	4	
Co	57	34	37	38	39	38	38	8	11	
Zn	40	32	37	73	72	80	62	<30	52	
La	0.50	0.79	2.4	5.4	3.4	5.1	5.2	50.3	23.7	
Ce	1.4	2.0	6.3	15.8	9.4	14.9	14.4	103.9	61.3	
Pr	0.24	0.37	1.0	2.5	1.5	2.4	2.2	10.8	8.1	
Nd	1.34	2.26	5.54	13.7	8.66	13.2	11.4	39.7	35.4	
Sm	0.51	0.82	2.03	4.39	2.95	4.23	3.43	7.88	9.00	
Eu	0.508	0.657	0.987	1.66	1.16	1.57	1.38	1.57	2.21	
Gd	0.68	1.1	2.5	5.4	3.7	5.0	4.1	6.7	10.7	
Tb	0.12	0.22	0.49	1.02	0.72	0.99	0.77	1.19	1.87	
Dy	0.77	1.4	3.1	6.2	4.4	5.9	4.8	6.7	11.8	
Ho	0.16	0.28	0.62	1.28	0.92	1.22	0.99	1.34	2.46	
Er	0.46	0.85	1.83	3.93	2.77	3.65	2.98	4.29	7.42	
Tm	0.065	0.123	0.264	0.574	0.412	0.533	0.447	0.667	1.16	
Yb	0.44	0.73	1.56	3.49	2.52	3.23	2.70	4.04	6.76	
Lu	0.069	0.101	0.228	0.482	0.360	0.451	0.370	0.562	1.08	
North Kozara										
Sample rock remark	K150 a-gabbro isotropic	K146* dolerite massive	K147b K-TB a-opx-	K149b a-BA massive	KO-22 dolerite massive	KO-24 dolerite pegm	KO-10 Basalt aphyric	KO-23 basalt aphyric	KO-12 basalt porphyric	
SiO ₂	48.25	46.51	47.27	53.01	49.67	47.19	48.05	48.97	48.09	
TiO ₂	1.36	1.45	2.43	2.05	0.81	2.45	1.55	2.21	1.70	
Al ₂ O ₃	16.93	18.43	13.61	14.67	16.18	16.26	15.20	14.94	17.30	
Fe ₂ O ₃ total	9.32	9.43	12.78	11.30	8.09	10.27	10.32	13.31	10.08	
MnO	0.14	0.22	0.22	0.20	0.21	0.14	0.16	0.13	0.15	
MgO	6.83	5.95	4.39	4.90	8.02	6.75	6.90	5.66	5.11	
CaO	11.25	10.10	6.71	8.04	12.01	10.50	11.49	10.10	11.17	
Na ₂ O	3.04	2.95	3.49	3.68	2.91	3.23	2.96	3.79	2.82	
K ₂ O	0.40	0.42	2.07	0.85	0.26	0.24	0.58	0.25	0.43	
P ₂ O ₅	0.11	0.18	0.32	0.26	0.10	0.17	0.18	0.26	0.21	
LOI	1.67	3.37	7.18	1.26	1.31	1.82	2.54	0.25	1.62	
Total	99.30	99.00	100.47	100.22	99.57	99.02	99.93	99.87	98.68	
Mg#	59.2	55.5	40.5	46.2	66.3	56.6	57.0	45.7	50.1	
Rb	4.7	11	56	18	4.6	3.5	16	2.7	11	
Ba	70	113	326	189	46	47	133	46	96	
Th	0.57	1.00	2.08	4.17	0.86	1.95	0.71	0.61	0.51	
U	0.21	0.35	0.75	1.36	0.23	0.48	0.23	0.30	0.16	
Ta	0.60	0.64	1.10	2.36	0.28	0.67	0.44	0.69	0.51	
Nb	5.5	6.6	14	17	6.9	12	5.3	12	7.8	
Pb	<1	2.2	8.1	3.2	<5	<5	<5	<5	<5	
Sr	238	266	149	209	226	288	288	226	266	
Zr	73	100	220	223	62	111	99	139	92	
Hf	1.95	2.49	5.16	5.40	2.36	3.24	2.60	4.10	2.62	
Y	20	29	47	50	17	21	24	34	24	

(continued on next page)

Table 1 (continued)

North Kozara									
Sample rock remark	K150 a-gabbro isotropic	K146* dolerite massive	K147b K-TB a-opx-	K149b a-BA massive	KO-22 dolerite massive	KO-24 dolerite pegm	KO-10 Basalt aphyric	KO-23 basalt aphyric	KO-12 basalt porphyric
V	203	212	227	252	158	261	228	281	207
Cr	269	282	34	82	241	62	270	73	140
Ni	71	63	17	28	74	76	64	63	21
Co	43	46	34	84	33	35		37	32
Zn	38	82	165	101	39	34	79	33	74
La	6.0	9.6	17.3	19.5	6.2	8.9	7.5	13.5	8.3
Ce	14.3	21.9	40.8	46.8	14.4	20.9	18.3	31.0	20.2
Pr	2.07	3.14	5.72	6.41	1.99	2.83	2.48	4.43	2.86
Nd	9.77	14.76	26.28	28.28	10.11	13.57	12.80	22.15	14.74
Sm	2.84	4.10	7.19	7.33	2.82	3.69	3.90	6.16	4.05
Eu	2.84	4.10	7.19	7.33	2.82	3.69	3.90	6.16	1.68
Gd	3.32	4.62	7.90	8.10	3.23	4.08	4.47	6.71	4.52
Tb	0.57	0.76	1.32	1.38	0.59	0.72	0.81	1.23	0.83
Dy	3.58	4.74	8.25	8.58	3.48	4.36	4.94	7.28	4.91
Ho	0.72	0.97	1.65	1.75	0.69	0.88	0.97	1.48	0.95
Er	2.03	2.66	4.74	4.95	2.07	2.66	2.91	4.45	2.93
Tm	0.299	0.390	0.689	0.740	0.295	0.396	0.420	0.634	0.423
Yb	1.98	2.53	4.57	4.81	1.78	2.42	2.58	3.84	2.55
Lu	0.313	0.396	0.707	0.732	0.246	0.333	0.400	0.526	0.351
Sample rock remark	KO-15 basalt pillow	K142 basalt pillow	KO-14 rhyolite dike	KO-16 rhyolite dike	KO-17 rhyolite massive	KO-20 rhyolite massive	KO-25c Granoph cmp.dk	KO-25b a-dol cmp.dk	
SiO ₂	45.15	44.97	73.98	73.85	68.53	80.91	75.30	49.98	
TiO ₂	1.29	1.32	0.28	0.22	0.59	0.16	0.11	1.58	
Al ₂ O ₃	15.91	14.26	13.57	13.06	13.81	9.46	13.07	14.92	
Fe ₂ O ₃ total	9.31	9.00	1.85	1.80	4.09	1.48	0.86	11.68	
MnO	0.19	0.19	0.01	0.04	0.07	0.01	0.01	0.13	
MgO	6.22	5.65	0.32	0.38	0.53	0.42	0.16	6.87	
CaO	10.05	11.57	0.76	0.33	0.21	0.10	0.84	9.91	
Na ₂ O	3.87	3.80	5.23	3.15	1.26	0.26	3.99	3.47	
K ₂ O	0.80	1.14	2.82	5.08	7.21	5.77	4.35	0.45	
P ₂ O ₅	0.21	0.14	0.05	0.05	0.15	0.03	0.01	0.17	
LOI	6.18	8.72	0.58	2.02	2.56	1.46	0.34	0.76	
Total	99.18	100.77	99.45	99.97	99.01	100.06	99.05	99.92	
Mg#	57.0	55.4	25.5	29.5	20.4	36.0	26.9	53.8	
Rb	11	19	60	119	125	170	151	6.5	
Ba	89	165	258	551	867	294	222	68	
Th	1.76	0.61	18.9	16.4	11.3	20.6	28.6	0.37	
U	0.44	0.45	6.09	7.37	3.94	2.52	2.64	0.51	
Ta	0.69	0.58	1.68	1.67	1.70	4.52	1.51	0.54	
Nb	11	7.6	19	18	25	57	8.6	11	
Pb	<5	8.2	<5	8.0	16.1	8.2	<5	<5	
Sr	255	245	82	59	36	18	49	198	
Zr	124	86	321	256	454	972	108	86	
Hf	3.38	2.11	9.75	8.25	11.7	26.2	5.42	2.78	
Y	21	19	41	52	58	104	16	39	
V	167	186	4	3	8	2	7	252	
Cr	313	278	<20	<20	<20	20	20	156	
Ni	139	77	<20	<20	<20	<20	42	47	
Co	44	33	1	2	4	<1	3	39	
Zn	72	73	<30	42	1980	75	<30	33	
La	12.4	6.8	41.2	40.2	38.0	89.0	22.4	16.6	
Ce	27.6	15.9	84.6	81.3	85.1	194.6	41.8	44.9	
Pr	3.55	2.29	9.49	9.32	10.80	22.58	4.27	6.24	
Nd	16.40	10.70	36.05	36.89	47.63	91.37	15.36	27.93	
Sm	4.15	3.00	7.48	8.38	11.90	21.49	2.93	6.96	
Eu	1.43	1.10	0.654	0.691	1.79	1.12	0.324	6.96	
Gd	4.28	3.35	6.83	7.91	11.22	20.10	2.66	7.40	
Tb	0.77	0.55	1.27	1.55	2.12	3.84	0.49	1.32	
Dy	4.44	3.36	7.74	9.85	12.50	22.91	2.97	7.99	
Ho	0.91	0.66	1.60	2.10	2.46	4.58	0.62	1.63	
Er	2.72	1.84	5.28	6.63	7.29	14.38	2.01	4.92	
Tm	0.387	0.260	0.849	1.047	1.124	2.252	0.324	0.729	
Yb	2.28	1.70	5.45	6.33	6.73	13.69	2.07	4.40	
Lu	0.321	0.262	0.777	0.851	0.925	1.884	0.302	0.603	

Major element oxides in wt.%, trace elements in ppm. LOI=loss on ignition. Mg#=100·molar MgO/(MgO+FeO_{total}). Rock abbreviations: TD=trachydacite; alb.sy=albite syenite; K-TB=potassic trachybasalt; BA=basaltic andesite; pegm=pegmatitic rocks; granoph=granophyre; dol.=dolerite. a-, opx-=igneous amphibole and orthopyroxene bearing assemblage. dol=dolerite; cmp.dk=composite dike (of granophyre and amphibole dolerite).

*Sample was a c. 50 cm diameter pebble retrieved from conglomerates overlying the igneous succession.

Table 2
Sm–Nd–isotopic data of sample K135 from South Kozara

Sample	Nd [ppm]	Sm [ppm]	$^{147}\text{Sm}/^{144}\text{Nd}$	$^{143}\text{Nd}/^{144}\text{Nd}$	2Sd (m)
K135WR	2.610	0.962	0.2228	0.513101	0.000006
K135 Cpx	5.580	2.607	0.2825	0.513163	0.000009
K135 Pl	0.767	0.146	0.1147	0.512989	0.000004

Given Sm and Nd concentrations were detected by isotope dilution. For calculating the isochron age an error of 1% at the $^{147}\text{Sm}/^{144}\text{Nd}$ ratio was assumed. WR=whole rock, Cpx=Clinopyroxene, Pl=Plagioclase.

The bimodal igneous succession of North Kozara tectonically overlies the Western Vardar Ophiolitic Unit and – according to the available geological and geochronological data – is of different age. However, the available geochemical and isotopic data do not allow the North Kozara igneous succession to be assigned to any particular geodynamic setting. The bimodal nature of volcanism is not distinctive of a mid-ocean ridge (MOR), ocean island (OI) or island-arc (IA) setting. The enrichment of LREE over HREE at least opposes a normal mid-ocean ridge (N-MOR) origin (Schilling et al., 1983). The negative and mutually parallel REE slopes of both mafic and felsic rocks suggest that they were derived from the same magma source. Primitive mantle-normalised multi-element diagrams do not show depletion of HFSE (particularly Nb, Ta and Ti) over LILE. There is no spiked pattern, which is typical of subduction-related magmatics (Sun and Stern, 2001; Murphy, 2007). Instead, they are more consistent with an OI origin (Hofmann, 1997; Winter, 2001). The absence of boninitic lavas (Cameron et al., 1979), considered typical of intraoceanic island arcs (Hickey and Frey, 1982; Crawford et al., 1981; Kim and Jacobi, 2002), is another argument against an IA setting.

The $^{143}\text{Nd}/^{144}\text{Nd}$ -ratios of the analysed mafic rocks from North Kozara are uniform and further suggest that the North Kozara magmatics are co-genetic. The larger scatter in $^{87}\text{Sr}/^{86}\text{Sr}$ -ratios with two outliers, on the other hand, is likely to be caused by syn- or post-magmatic alteration. The isotopic ratios are equivocal in terms of attributing the North Kozara magmatics to an IA, OI or MOR setting, as these fields strongly overlap (Fig. 10; Hofmann, 1997). In any case, the isotopic ratios do not suggest that the North Kozara magmatics formed in a continental (“Andean”) volcanic arc setting, which typically yields much higher $^{87}\text{Sr}/^{86}\text{Sr}$ - and lower $^{143}\text{Nd}/^{144}\text{Nd}$ -ratios (e.g. Mahlburg Kay et al., 2005). Hence, the pertinent conclusion from a tectonic viewpoint is that it is far more likely that the bimodal igneous succession of North Kozara represents intraoceanic rather than continental magmatism. We take this as evidence that the Adriatic and Europe-derived smaller plates (the Tisza and Dacia Mega-Units) were still separated by a deep basin that was floored by oceanic lithosphere in the Late Cretaceous.

5.2. Growth and demise of Late Cretaceous intraoceanic volcanic islands in the Sava Zone

In spite of the ambivalent geochemical and isotopic data, there is additional geological evidence that favours an interpretation of the Campanian igneous succession documented in the North Kozara and

Prosara Mountains (as well as other inselbergs in the Sava Zone) as intraoceanic. Volcanism in North Kozara was present in the Early Campanian in a deep-water environment. At about the same time, the South Kozara ophiolites were unconformably covered by pelagic limestones and microconglomerates that also contain clasts of older pelagic limestones, but no igneous rock debris. This implies that the South Kozara succession did not receive much, if any, detrital input from the time-equivalent volcanic edifice developing in North Kozara. Apart from the structural evidence, this suggests that the two igneous rock massifs must have originally been located at a considerable distance from each other and that they were tectonically juxtaposed later.

Throughout the Campanian, the volcanic build-ups had apparently grown high enough to become exposed above the sea level, as evidenced by the unconformably overlying alluvial conglomerates and sandstones that exclusively rework the underlying igneous succession. As yet, there is no evidence for reworked metamorphic rocks that would indicate a continental source. It is hence conceivable that the formations exposed in the North Kozara and Prosara Mountains became oceanic islands. Intercalations of Maastrichtian and, higher up-section, Paleocene neritic limestones, which may have fringed the volcanic island, constrain the timing of erosion of the volcanic complex. The absence of any intercalated lavas or volcanoclastics within the unconformable cover suggests that volcanic activity was probably confined to the Campanian, in agreement with our radiometric ages.

The South Kozara igneous rocks also possess a similar cover of Paleocene neritic limestones of about the same age. A gradual transition from the Paleocene neritic limestones into an Eocene turbiditic sandstone succession is observed in both South and North Kozara. This suggests that these two units were tectonically juxtaposed earlier, most likely by Maastrichtian-age top-to-the-south thrusting (Fig. 4). This older (Maastrichtian) thrust appears to have been reactivated after the deposition of the turbiditic sandstone succession, i.e. after the middle Eocene. An upper time bracket for the age of this Cenozoic thrust reactivation and displacement along a northerly adjacent thrust in Prosara Mountain is provided by the Neogene sediments of the Pannonian Basin that seal these thrusts. The Paleogene age of this thrusting therefore corresponds to the main phase of nappe stacking that is well known throughout the entire Dinarides (Tari-Kovačić and Mrinjek, 1994).

In summary, the area of the Kozara Mountains documents three phases of compressional tectonics, each separated by one or more unconformities: (1) Late Jurassic obduction, (2) Cretaceous subduction, followed by latest Cretaceous collision, as is evidenced by the juxtaposition of the North Kozara intraoceanic volcanic island with the Western Vardar Ophiolitic Unit and (3) Paleogene (post-Middle Eocene and pre-Miocene) top-to-the-south thrusting (Fig. 4).

5.3. Geodynamic significance of the new radiometric ages

Fig. 12 provides an overview of radiometric ages for ophiolitic lithologies of the northern Balkan Peninsula. The age of the South Kozara gabbro (157.9 ± 7.6 Ma) is among the youngest ages from the

Table 3
Nd- and Sr-isotopic data of selected mafic samples from South and North Kozara

Sample	locality	$^{143}\text{Nd}/^{144}\text{Nd}$	+/-Sm	$^{87}\text{Sr}/^{86}\text{Sr}$	+/-Sm	Rb [ppm]	Sr [ppm]	Sm [ppm]	Nd [ppm]	$^{87}\text{Rb}/^{86}\text{Sr}$	Age [Ma]	Io	$^{147}\text{Sm}/^{144}\text{Nd}$	e0 Nd (Chur)	Age [Ma]	et Nd _(Chur)	T Nd _(DM) [Ma]
K 135	S Kozara	0.513101	0.000004	0.702703	0.000005	1.7	188	0.96	2.61	0.0261	160	0.70264	0.2228	9.0	160	8.6	
K 142	N Kozara	0.512945	0.000004	0.705330	0.000005	19	245	3	10.7	0.2243	80	0.70507	0.1695	6.0	80	6.3	492
K 146	N Kozara	0.512855	0.000004	0.704150	0.000004	11	266	4.1	14.8	0.1196	80	0.70401	0.1675	4.2	80	4.5	725
K 147b	N Kozara	0.512900	0.000004	0.706224	0.000004	56	149	7.2	26.3	1.0872	80	0.70499	0.1655	5.1	80	5.4	577
K 149b	N Kozara	0.512844	0.000005	0.703838	0.000004	18	209	7.3	28.3	0.2491	80	0.70356	0.1560	4.0	80	4.4	624
K 150	N Kozara	0.512917	0.000004	0.703531	0.000004	5	238	2.8	9.8	0.0608	80	0.70346	0.1727	5.4	80	5.7	610

All given element concentrations were detected by ICP MS, except for Sm- and Nd-concentrations and isotope ratios of sample K135, which were detected by isotope dilution.

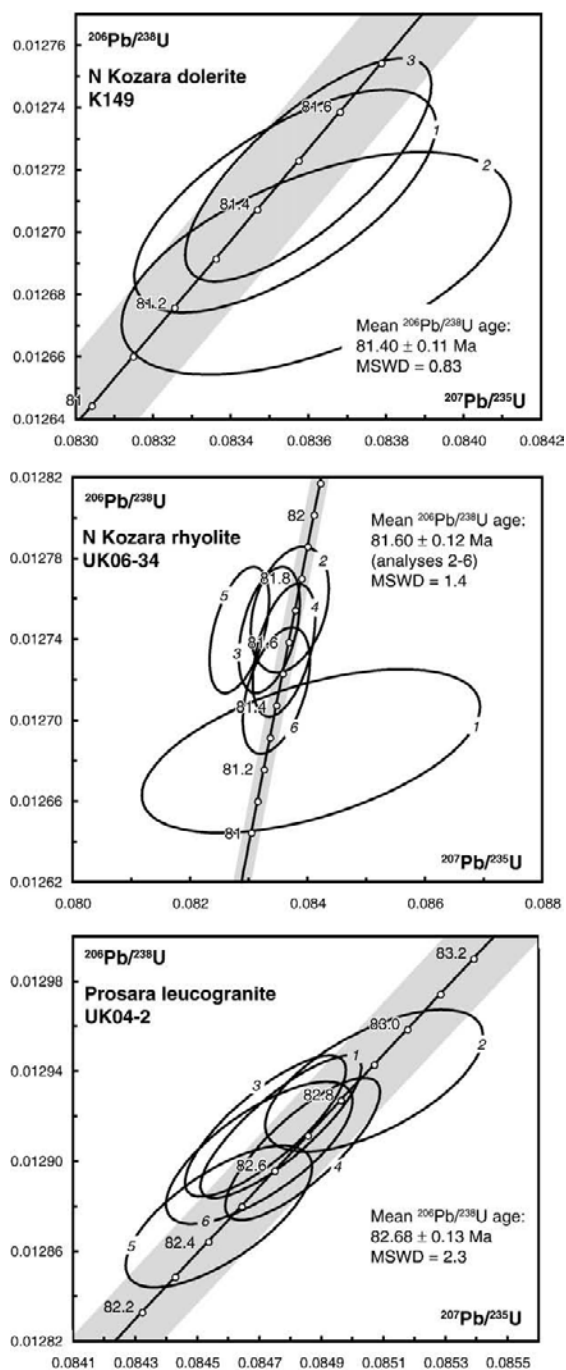


Fig. 11. Concordia diagrams showing the results of single zircon analyses from North Kozara and Prosara samples. Individual analyses are shown as 2σ error ellipses. Given ages are weighted mean $^{206}\text{Pb}/^{238}\text{U}$ ages. Grey shading indicates the uncertainties of the decay constants. See Figs. 4 and 12 for sample localities.

igneous part of the Western Vardar Ophiolitic Unit. Comparable ages were obtained from ophiolites in Albania (outside Fig. 12; see Fig. 2 in Dilek et al., 2008, for a recent compilation), from the frontal part of the obducted ophiolites (derived from the Western Vardar Zone according to Gawlick et al., 2008): a mafic dike from the Bulqiza Massif yielded a Rb–Sr biotite age of 158 ± 4 Ma, equivalent to a K–Ar age of 160.5 ± 7.5 Ma (Tashko and Teršana, 1988; cited in Dimo-Lahitte et al., 2001).

The mafic igneous rocks within the Greek ophiolites seem to be older. Gabbros and plagiogranites from the Vourinos complex (outside Fig. 12) yielded ages of 168.5 ± 2.4 and 172.9 ± 3.1 Ma, respectively, obtained by U–Pb ion-microprobe (SHRIMP) dating of zircons (Liati et al., 2004). The same study also reports ages of 171 ± 3 Ma for gabbros from the Greek so-called “Pindos ophiolite” (in our view the frontal part of the obducted Western Vardar Ophiolitic Unit, see also Gawlick et al., 2008).

Most radiometric ages obtained from the Western Vardar Ophiolitic Unit are from amphibolites of the metamorphic sole (Lanphere et al., 1975; Okrusch et al., 1978; Lugović et al., 2006). The two K–Ar ages obtained by Lanphere et al. (1975) for amphibolites from Konjuh (157 ± 4 Ma) and Zlatibor (171 ± 14 Ma) underwent a slight correction by Spray et al. (1984) on the basis of the new decay constant of Steiger and Jäger (1977) and thus became 161 ± 4 and 178 ± 14 Ma, respectively. Fig. 12 shows the corrected ages. Higher ages of 182–187 Ma were obtained from a metamorphic sole of the Eastern Vardar ophiolite at Razbojna (Karamata and Popević, unpubl.; in Karamata, 2006). The most recent age obtained for a metamorphic sole in the Dinarides is a pooled Sm–Nd isochron obtained with garnet, plagioclase, clinopyroxene, amphibole and whole rock on five granulites from Borja, which gave 171.4 ± 3.7 Ma (Lugović et al., 2006). All ages regarding metamorphic sole formation in the former Yugoslavian sector of the Western Vardar Ophiolitic Unit are thus in agreement with those reported from the Albanian (159 ± 2.6 to 171.7 ± 1.7 Ma; Dimo-Lahitte et al., 2001) and Greek ophiolites (see Spray et al., 1984).

Within the analytical errors, the crystallisation age for the South Kozara gabbro (157.9 ± 7.6 Ma) overlaps with the age of metamorphism or cooling of the geographically closest metamorphic soles (Borja 171.4 ± 3.7 Ma; Konjuh 161 ± 4 Ma). This suggests a rapid transition from seafloor spreading and associated MOR magmatism to intraoceanic subduction, which presumably occurred between the Bathonian and early Oxfordian (c. 166–157 Ma in the time-scale of Gradstein et al., 2004), as implied from the following line of reasoning. Growth of the dated minerals in the metamorphic soles occurred at a depth of c. 30–40 km according to thermobarometric estimates (Dimo-Lahitte et al., 2001). Given a subduction angle of 30° (young, hot, buoyant oceanic lithosphere entering subduction), this corresponds to a length of 60–80 km of subducted oceanic lithospheric slab. Hence, at a subduction velocity of, say, 5 cm a^{-1} , a metamorphic sole would have formed 1.2–1.6 Ma after subduction has started. This time span cannot be resolved with the available ages and their inherent analytical errors.

The age of the South Kozara gabbro is in conflict with the Hettangian to Late Bajocian age for the underlying ophiolitic mélangé inferred by Babić et al. (2002), as the gabbro would be younger than the tectonically underlying mélangé. Since the ages reported by Babić et al. (2002) give a maximum age of sedimentation of the matrix – the palynomorphs could even be reworked – we merely regard them as maximum ages for mélangé formation related to obduction.

Radiometric ages from the ultramafic parts of the ophiolites are scarce. Fig. 12 shows a Sm–Nd isochron age of 146.8 ± 3.7 Ma, obtained on a garnet-plagioclase-pyroxenite vein that cuts the dominantly lherzolitic peridotites of the Zlatibor massif (Bazylev et al., 2006 and pers. comm.). This age corresponds well with a pooled Sm–Nd isochron age of 136 ± 15 Ma (Fig. 6 in Lugović et al., 1991), constructed with clinopyroxenes and whole rock from lherzolites of three different localities (Borja, Konjuh and Zlatibor massifs; not shown in Fig. 12). Both ages are clearly younger than any of the adjacent metamorphic soles. It hence appears that the formation of oceanic lithosphere in parts of what presently constitutes the Western Vardar Ophiolitic Unit, that was in a suprasubduction position at that time, postdates the initiation of intraoceanic subduction but pre-dated final obduction (Fig. 13).

Another conclusion to be drawn from Fig. 12 is that Late Cretaceous magmatism is restricted to the Sava Zone. The U–Pb ages obtained on zircons from North Kozara (Fig. 11) correspond well with K–Ar whole-rock ages of 79 and 82 Ma obtained on dolerites from a sheeted dike complex near Gornji Podgradci (Lovrić, 1986; location given in Fig. 4).

Table 4
U–Pb isotopic data of analysed zircons from North Kozara and Prosara igneous rocks

Number ^a	Weight [mg]	Concentrations			Th/U ^b	Atomic ratios						Apparent ages			Error corr.	
		U [ppm]	Pb rad. [ppm]	Pb nonrad [pg]		²⁰⁶ Pb/ ²⁰⁴ Pb ^c	²⁰⁷ Pb/ ²³⁵ U ^d	Error 2 s [%]	²⁰⁶ Pb/ ²³⁸ U ^d	Error 2 s [%]	²⁰⁷ Pb/ ²⁰⁶ Pb ^d	Error 2 s [%]	²⁰⁶ Pb/ ²³⁸ U	²⁰⁷ Pb/ ²³⁵ U		²⁰⁷ Pb/ ²⁰⁶ Pb
<i>Dolerite, North Kozara (K149)</i>																
K149/1	0.0033	342	4.81	1.39	0.74	686	0.08354	0.38	0.01271	0.23	0.04768	0.28	81.40	81.47	83.50	0.68
K149/2	0.0015	502	7.25	1.30	0.85	494	0.08362	0.49	0.01269	0.23	0.04777	0.42	81.32	81.54	88.10	0.55
K149/3	0.0025	599	8.52	1.97	0.79	641	0.08360	0.31	0.01272	0.23	0.04767	0.20	81.49	81.53	82.60	0.76
K149/4	0.0046	34	0.44	2.55	0.48	68	0.08462	3.65	0.01254	0.33	0.04894	3.44	80.34	82.48	144.80	0.66
K149/5	0.0017	154	2.05	1.92	0.54	130	0.08345	2.35	0.01265	0.74	0.04785	2.12	81.03	81.38	91.70	0.45
<i>Rhyolite, North Kozara (UK06-34)</i>																
UK06-34/1	0.0033	134	1.78	4.47	0.51	100	0.08406	2.80	0.01268	0.26	0.04806	2.68	81.26	81.96	102.23	0.54
UK06-34/2	0.0025	143	1.92	1.41	0.55	228	0.08370	0.65	0.01275	0.20	0.04759	0.61	81.70	81.62	78.88	0.34
UK06-34/3	0.0009	579	7.75	0.98	0.55	456	0.08360	0.52	0.01273	0.21	0.04761	0.46	81.57	81.53	80.03	0.47
UK06-34/4	0.0018	222	2.97	0.79	0.55	437	0.08335	0.51	0.01274	0.20	0.04743	0.47	81.64	81.29	70.93	0.43
UK06-34/5	0.0015	488	6.52	0.82	0.55	752	0.08284	0.50	0.01274	0.20	0.04714	0.45	81.64	80.81	56.34	0.48
UK06-34/6	0.0016	622	8.28	2.83	0.53	306	0.08347	0.56	0.01271	0.20	0.04761	0.51	81.45	81.40	79.91	0.47
<i>Alkalifeldspar granite, Prosara (UK04-2)</i>																
UK04-2/1	0.0025	884	11.46	0.50	0.38	3739	0.08477	0.25	0.01292	0.20	0.04760	0.14	82.72	82.62	79.46	0.83
UK04-2/2	0.0023	1112	13.94	4.78	0.25	463	0.08507	0.34	0.01294	0.20	0.04770	0.26	82.85	82.90	84.38	0.63
UK04-2/3	0.0025	862	19.32	0.62	0.30	2959	0.08472	0.25	0.01292	0.20	0.04757	0.15	82.73	82.57	77.97	0.80
UK04-2/4	0.0025	1473	18.91	0.69	0.34	4534	0.08484	0.24	0.01291	0.20	0.04762	0.13	82.66	82.69	80.43	0.80
UK04-2/5	0.0020	875	11.20	0.89	0.34	1665	0.08457	0.29	0.01288	0.20	0.04764	0.21	82.47	82.43	81.40	0.69
UK04-2/6	0.0027	695	9.91	0.63	0.74	2529	0.08470	0.29	0.01290	0.20	0.04761	0.20	82.65	82.55	79.91	0.73

^a All zircons annealed–leached (Mattinson, 2005).

^b Calculated on the basis of radiogenic Pb²⁰⁸/Pb²⁰⁶ ratios, assuming concordancy.

^c Corrected for fractionation and spike.

^d Corrected for fractionation, spike, blank and common lead (Stacey & Kramers, 1975).

Furthermore, they are in agreement with the biostratigraphic evidence (Karamata et al., 2000, 2005; our data). The tectonically higher unit in the northerly adjacent Prosara Mountain exposes a succession of greenschist-facies, mylonitic rhyolites and prasinites, followed up-section by metasandstones (see above). Based on the lithostratigraphic resemblance of the Prosara succession with that of North Kozara and the compatible U–Pb ages, we assigned it a Campanian age (Figs. 3 and 5). The greenschist- to lower amphibolite-grade succession exposed in Mount Motajica contains amphibolites overlain by calcite marbles. The protolith of the amphibolites could be mafic volcanics or volcanoclastics related to Campanian intraoceanic magmatism (Fig. 5).

Požeška Gora also shares great similarities with the North Kozara succession in terms of lithostratigraphy, igneous rock suite and ages. Late Cretaceous (to Early Paleogene) bimodal magmatism has furthermore been documented in numerous outcrops and oil wells in the Tisza Mega-Unit (Pamić, 1997; Pamić et al., 2000; see Fig. 2). The ages, obtained by K–Ar dating of whole-rock samples or amphibole concentrates, span a considerably wide range between c. 110 and 51 Ma (Pamić, 1997; Pamić et al., 2000). Excluding all samples reported as altered by Pamić et al. (2000), the age range reduces to c. 110 to 62 Ma. Basalts from the Voćin area (northern part of Papuk mountain, Fig. 2) are intercalated with sediments containing a Late Cretaceous microfauna (Pamić and Pécskay, 1994).

5.4. Paleotectonic significance of the Campanian igneous succession

Our data document the existence of Late Cretaceous intraoceanic magmatism and hence an area floored by oceanic lithosphere between the Adriatic and the Europe-derived Tisza and Dacia Mega-Units. Still unresolved is the question concerning the original tectonic position of the oceanic lithosphere that was subsequently subducted underneath the Europe-derived Tisza and Dacia Mega-Units in the latest Cretaceous. Was it a fragment of (a) the Neotethys, parts of which would have escaped Late Jurassic obduction onto the Adriatic passive margin or (b) part of the Alpine Tethys or (c) of both, the two being connected along the Sava Zone corridor? Option (a) is possibly in line with the reasoning of Karamata et al. (2000, 2005), who

regarded the North Kozara igneous succession as representing a remnant oceanic area that remained open after parts of the Vardar Ocean had been obducted onto the Adriatic passive margin. This setting bears a close resemblance to the present-day situation in the Gulf of Oman. There, a remnant marine area, floored by oceanic crust, has remained open after the obduction of the Semail ophiolite onto the Arabian margin between c. 80 and 70 Ma (Coleman, 1981; see also Fig. 3.28 in Nicolas, 1989). At present, this remnant oceanic branch in the Gulf of Oman is being subducted underneath the Makran accretionary wedge to the north.

The closure of the remnant oceanic area in what is now the Sava Zone must have occurred stepwise (Fig. 13). An earlier step involved Campanian intraoceanic magmatism, possibly forming on Jurassic-age oceanic lithosphere of the Vardar Ocean that had escaped obduction onto the Adriatic passive margin (Fig. 13a). We leave it open, whether this Campanian intraoceanic magmatism occurred in an ocean-island (Fig. 13, “b1”) or back-arc basin setting (Fig. 13, “b2”). A later step involved the installation of a more internally positioned subduction (Fig. 13c), which ultimately led to the closure of this oceanic branch by Maastrichtian to early Paleogene times. Greenschist-facies metamorphism in the formations exposed in the Prosara, Motajica and Požeška Gora areas suggests that the Late Cretaceous igneous succession positioned more internally in respect to North Kozara became involved in thrusting and deep burial after collision. By contrast, the lack of a metamorphic overprint in the Mesozoic cover of Psnj–Papuk Mountains shows that the Tisza Mega-Unit occupied an upper-plate position during this closure. The widespread occurrence of Late Cretaceous (to Early Paleogene) subduction-related bimodal volcanics in the Tisza Mega-Unit itself (Pamić, 1993b, 1997; Pamić et al., 2000) suggests the installation of a continental volcanic arc on top of the upper plate above a north-dipping subduction zone. This magmatism might be considered as a prolongation of the “banatite” belt of Bulgaria, Serbia and Romania.

Possibility (b) is unlikely given the fact that subduction of the Alpine Tethys slab in the Alps during Late Cretaceous to Early Palaeogene times was south-directed, and hence opposed to the northeast-directed subduction inferred for the Sava Zone. Possibility (c) cannot be excluded

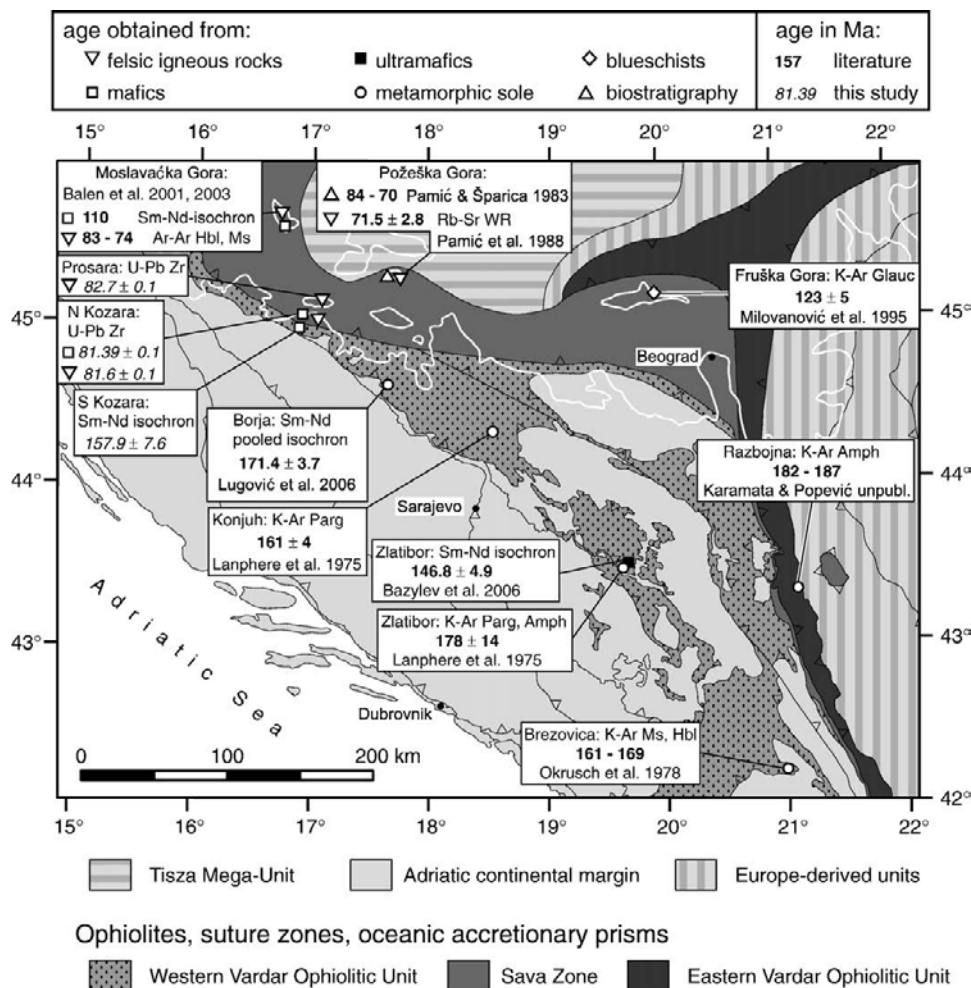


Fig. 12. Compilation of radiometric ages from the Western Vardar Ophiolitic Unit and the Sava Suture Zone. Ages from igneous rocks are interpreted as crystallisation ages. Ages from peridotites are considered as formation ages of the oceanic lithosphere. Ages from metamorphic sole rocks and blueschists are formation or cooling ages. The original ages of Lanphere et al. (1975) were corrected by Spray et al. (1984) to match the new decay constants of Steiger and Jäger (1977). Mineral abbreviations: Amph=amphibole, Glauc=glauconite, Hbl=hornblende, Ms= muscovite, Parg=pargasite, WR=whole rock, Zr=zircon.

however, for the following reason, discussed in more detail in Schmid et al. (2008): In order to account for the late Mesozoic to Cenozoic northward drift of the Adriatic Plate, the Alpine Tethys must have been spatially connected eastwards to a northwesternmost, still open branch of Neotethys. Such a link may indeed have existed in the area of the Sava Zone of Northern Bosnia. However, it should be noted that in a structural sense, the Sava Zone is definitely part of Tertiary collision in the Dinarides. The polarity of subduction probably changed somewhere along the present-day Mid-Hungarian Fault Zone ENE of Zagreb (Márton et al., 2007; Tischler et al., 2007).

The bimodal volcanics of the northernmost internal Dinarides (Pamić, 1997; Pamić et al., 2000) have already been suggested as a potential source area of volcanic ash layers found in the Late Cretaceous of the Central Apennines (Bernoulli et al., 2004). The radiometric ages reported here strongly support this hypothesis.

6. Conclusions

1.) Campanian to Early Maastrichtian intra-oceanic magmatism is reported in several inselbergs in the Sava Zone and implies that the Adriatic and Europe-derived smaller plates (such as the Tisza and the Dacia Mega-Unit) were still separated by a deep basin flooded

by oceanic lithosphere at this time. The earliest possible timing for the collision of these plates is hence the latest Cretaceous.

2.) Final closure of the oceanic fragment was the consequence of subduction of the Dinarides underneath the Tisza Mega-Unit representing the upper plate.

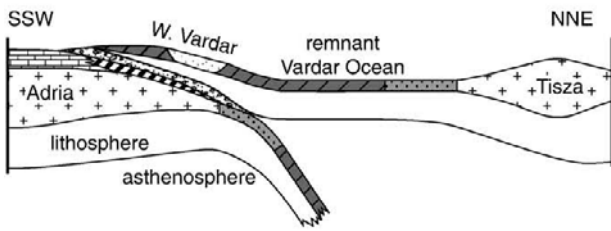
3.) Late Cretaceous to Early Paleogene bimodal volcanism in the Tisza Mega-Unit is attributed to the formation of a continental volcanic arc located in the upper plate during subduction. The end of subduction is marked by both the cessation of volcanic activity and the end of turbidite sedimentation in the Sava Zone in the Paleocene to Eocene.

4.) The Campanian to Early Maastrichtian oceanic crust can be considered as a northwesternmost extension of the Vardar Ocean, which at the same time was linked with the Alpine Tethys in the investigated area.

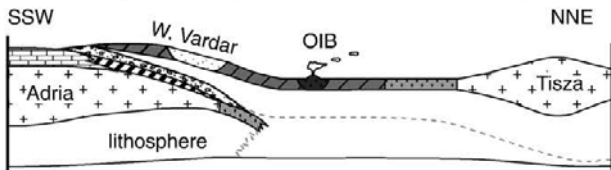
Acknowledgments

Stevan Karamata (Beograd) made us aware of the location and importance of the splendid outcrop of Campanian pillows and Scaglia Rossa in North Kozara. We are also deeply indebted to Michèle Caron (Fribourg) for her generous help with biostratigraphic determinations. Fred Gaidies and Cédric Rettenmund (Basel) performed whole rock XRF analyses. Monika Jelenc (Vienna) is thanked for help in measuring

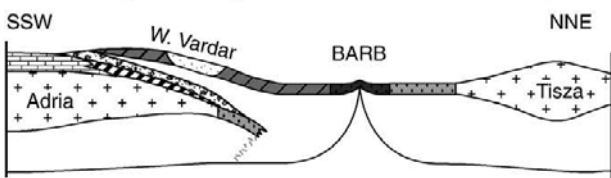
a. Late Jurassic



b1. Campanian (ocean island model)



b2. Campanian (back-arc basin model)



c. Late Campanian - Maastrichtian

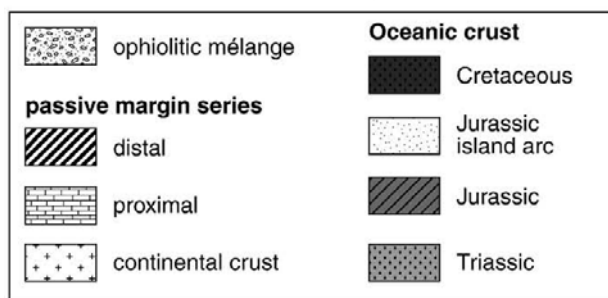
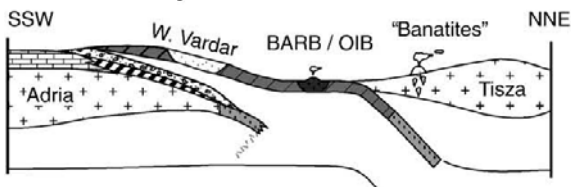


Fig. 13. Schematic sketches illustrating the invoked geodynamic evolution of the northern, E–W trending part of the Sava Suture Zone (not to scale). a: after Late Jurassic obduction of the Western Vardar Ophiolitic Unit onto the Adriatic passive margin, b: Campanian intraoceanic magmatism, c: before final ocean closure and subsequent collision of the Adriatic plate and the Tisza Mega-Unit.

Sr- and Nd-isotopes. The help of Maria Ovtcharova (Geneva) for U–Pb age determinations is also kindly acknowledged. Hazim Hrvatović (Sarajevo) is greatly thanked for logistic and scientific support. Thorough and very constructive reviews by Vladica Cvetković (Beograd), Alastair Robertson (Edinburgh) and Bruno Tomljenović (Zagreb), as well as additional helpful comments by Milica Božović (Mainz) and Sun-Lin Chung (Taipei) helped in further improving the

manuscript. Greg Shellnutt (Taipei) refined the English. Financial support for the Basel group through the Swiss National Science Foundation (projects “Tisza” Nrs. 200021-101883/1 and 200020-109278/1) is kindly acknowledged.

Appendix A1. Analytical techniques

A1.1. Whole rock major and trace element analyses

The analysed samples presented in this study consist of two different subsets that were collected during separate field campaigns. Whole rock (WR) analyses of the two subsets were performed separately in different laboratories before combining the results into one dataset for the present study. One subset consists of samples collected by B. Lugović (sample labels starting with “KO-”, Table 3). The other sample subset was collected by K. Ustaszewski between 2004 and 2006 (sample labels starting with “K”, followed by a three-digit number, Table 3). Analytical techniques are described below.

Sample subset “KO-” (sampled by B. Lugović)

Bulk-rock powders for chemical analyses were obtained from rock chips free of visible veins and weathering surfaces. Major elements and trace elements Rb, Ba, Sr, Zr, Cr and Ni were measured by wavelength dispersive X-ray fluorescence analysis (WD-XRFA) on fused and pressed pellets using conventional techniques. Trace elements Th, U, Nb, Ta, Hf, Y and REE were analysed by ICP-MS at Actlab Laboratories in Toronto, Canada. Trace elements were determined from diluted solution after leaching 500 mg sample in 3 ml HCl–HNO₃–H₂O at 95 °C for 1 h and REE were analysed after LiBO₂/Li₂B₄O₇ fusion of 200 mg sample.

Sample subset “K” (sampled by K. Ustaszewski)

Bulk-rock powders for chemical analyses were obtained from fresh specimens devoid of weathering surfaces. Major element concentrations were obtained from glass pellets by WD-XRFA using a Bruker AXS SRS-3400 at the Mineralogical and Petrographical Institute, University of Basel. Trace element concentrations were determined by ICP-MS on a Perkin Elmer 5000 at the Service d’Analyse des Roches et des Minéraux of the CNRS-CRPG Nancy, France (<http://www.crpq.cnrs-nancy.fr/SARM>).

A1.2. Isotopic analyses

Sm–Nd and Sr isotope analyses were performed at the Department of Geological Sciences at the University of Vienna. Sample weights of handpicked mineral separates used for dissolution were about 100 mg. The chemical sample preparation followed the procedure described by Sölvä et al. (2005). Spiked Sm and Nd ratios were measured at a Finnigan[®] MAT 262, whereas unspiked Nd and Sr ratios were analysed at a ThermoFinnigan[®] Triton TI TIMS. All elements were run from Re double filaments. On the Triton TI the La Jolla standard yielded ¹⁴³Nd/¹⁴⁴Nd = 0.511846 ± 2 (n = 7) whereas ⁸⁶Sr/⁸⁷Sr = 0.710246 ± 2 (n = 7) were determined for the NBS987.

A1.3. U–Pb dating

Zircons were prepared by standard mineral separation techniques (crushing, milling, concentration via Wilfey table, magnetic separation and heavy liquid separation in methylene iodide (density > 3.1 g cm⁻³)). Suitable grains were then handpicked in ethanol under a binocular microscope. In order to minimise the effects of secondary lead-loss, the chemical abrasion “CA-TIMS” technique, involving high-temperature annealing followed by a subsequent HF leaching step (Mattinson, 2005) was applied. Isotopic analyses were performed at the Department of Earth Sciences at the University of Geneva. The analytical techniques are described in Ovtcharova et al. (2006) in more detail. Calculation of ²⁰⁶Pb/²³⁸U ages was done with the Isoplot/Ex v.3 program (Ludwig, 2005).

Appendix A2. Supplementary data

Supplementary data associated with this article can be found, in the online version, at doi:10.1016/j.lithos.2008.09.010.

References

- Babić, L., Hochuli, P., Zupanić, J., 2002. The Jurassic ophiolitic mélange in the NE Dinarides: dating, internal structure and geotectonic implications. *Eclogae Geologicae Helveticae* 95, 263–275.
- Balen, D., Schuster, R., Garašić, V., 2001. A new contribution to the geochronology of Mt. Moslavačka Gora (Croatia). In: Ádam, A., Szarka, L., Szendrői, J. (Eds.), *PANCARDI 2001. Geodetic and Geophysical Research Institute of the Hungarian Academy of Science, Sopron, Hungary*, pp. DP–2.
- Balen, D., Schuster, R., Garašić, V., Majer, V., 2003. The Kamenjača Olivine gabbro from Moslavačka Gora (South Tisia, Croatia). *Rad Hrvatske akademije znanosti i umjetnosti* 486 (27), 57–76.
- Balen, D., Horváth, P., Tomljenović, B., Finger, F., Humer, B., Pamić, J., Ārkai, P., 2006. A record of pre-Variscan Barrovian regional metamorphism in the eastern part of the Slavonian Mountains (NE Croatia). *Mineralogy and Petrology* 87, 143–162.
- Bazylev, B., Zakariadze, G., Popević, A., Kononkova, N., Karpenko, S., Simakin, S., 2006. Spinel peridotites and garnet pyroxenes from Bistrica massif (Dinaridic ophiolite belt): the possible fragment of a sub-continental mantle. *International Symposium on the Mesozoic ophiolite belts of the northern part of the Balkan Peninsula*. Serbian Academy of Sciences and Arts, Committee of Geodynamics, Belgrade, pp. 12–14. May 31st–June 6th, 2006.
- Belak, M., Halamić, J., Marchić, V., Tibljas, D., 1998. Upper Cretaceous–Palaeogene tholeiitic basalts of the southern margin of the Pannonian Basin: Požeška Gora Mt. (Croatia). *Geologia Croatica* 51, 163–174.
- Bernoulli, D., Laubscher, H., 1972. The palinspastic problem of the Hellenides. *Eclogae Geologicae Helveticae* 65, 107–118.
- Bernoulli, D., Schaltegger, U., Stern, W.B., Frey, M., Caron, M., Monechi, S., 2004. Volcanic ash layers in the Upper Cretaceous of the Central Apennines and a numerical age for the early Campanian. *International Journal of Earth Sciences* 93, 384–399.
- Boynton, W.V., 1984. Cosmochemistry of the rare earth elements: meteorite studies. In: Henderson, P. (Ed.), *Rare Earth Element Geochemistry, Development in Geochemistry*. Elsevier, Amsterdam, pp. 63–114.
- Cameron, W.E., Nisbet, E.G., Dietrich, V.J., 1979. Boninites, komatiites and ophiolitic basalts. *Nature* 280, 550–553.
- Coleman, R.G., 1981. Tectonic setting for ophiolite obduction in Oman. *Journal of Geophysical Research* 86, 2497–2508.
- Crawford, A.J., Beccaluva, L., Serri, G., 1981. Tectono-magmatic evolution of the West Philippine-Mariana region and the origin of boninites. *Earth and Planetary Science Letters* 54, 346–356.
- Dilek, Y., Furnes, H., Shallo, M., 2008. Geochemistry of the Jurassic Mirdita Ophiolite (Albania) and the MORB to SSZ evolution of a marginal basin oceanic crust. *Lithos* 100, 174–209.
- Dimitrijević, M.D., 1997. Geology of Yugoslavia. Geological Institute GEMINI, Beograd. 190 pp.
- Dimitrijević, M.D., 2001. Dinarides and the Vardar Zone: a short review of the geology. *Acta Vulcanologica* 13, 1–8.
- Dimo-Lahitte, A., Monié, P., Vergély, P., 2001. Metamorphic soles from the Albanian ophiolites: Petrology, ⁴⁰Ar/³⁹Ar geochronology, and geodynamic evolution. *Tectonics* 20, 78–96.
- Djerić, N., Vishnevskaya, V.S., 2006. Some Jurassic to Cretaceous radiolarians of Serbia, Mesozoic Ophiolite Belt of the Northern Part of the Balkan Peninsula, pp. 29–36. Belgrade-Banja Luka, 31. 05–06. 06. 2006.
- Djerić, N., Vishnevskaya, V.S., Schmid, S.M., 2007. New data on radiolarians from the Dinarides (Bosnia and Serbia). Abstract Volume 8th Workshop on Alpine Geological Studies Davos, pp. 17–19.
- Djerković, B., Djordjević, D., Hohrajin, J., Jojić, D., Jurić, M., Kačar, B., Kapeler, I., Kovačević, R., Kujundžić, S., Ložajčić-Maglov, M., Maksimčev, S., Marić, L., Pamić, J., Sunarić-Pamić, O., Vejlović, R., Vilovski, S., 1975. Basic geological map sheet of Yugoslavia 1:100,000, sheet Prijedor L 33-118. Federal Geological Institute Beograd.
- Gawlick, H.-J., Frisch, W., Hoxha, L., Dumitrica, P., Krystyn, L., Lein, R., Missoni, S., Schlagintweit, F., 2008. Mirdita Zone ophiolites and associated sediments in Albania reveal Neotethys Ocean origin. *International Journal of Earth Sciences* 97, 865–881.
- Georgiev, G., Dabovski, C., Stanisheva-Vassileva, G., 2001. East-Srednogorie–Balkan Rift Zone. In: Ziegler, P.A., Cavazza, W., Robertson, A.H.F., Crasquin-Soleau, S. (Eds.), *Peri-Tethys Memoir 6: Peri-Tethyan Rift/Wrench Basins and Passive Margins*. Mémoires du Muséum National d'Histoire Naturelle Paris, pp. 259–293.
- Gill, J., 1981. Orogenic Andesites and Plate Tectonics. Minerals and Rocks, vol. 16. Springer Verlag, Berlin. 390 pp.
- Gradstein, F., Ogg, J., Smith, A.G., 2004. A Geologic Time Scale. Cambridge University Press, Cambridge. 589 pp.
- Heinrich, C.A., Neubauer, F., 2002. Cu–Au–Pb–Zn–Ag metallogeny of the Alpine–Balkan–Carpathian–Dinaride geodynamic province. *Mineralium Deposita* 37, 533–540.
- Hickey, R.L., Frey, F.A., 1982. Geochemical characteristics of boninite series volcanics. implications for their source. *Geochimica et Cosmochimica Acta* 46, 2099–2115.
- Hofmann, A.W., 1988. Chemical differentiation of the Earth: the relationship between mantle, continental crust, and oceanic crust. *Earth and Planetary Science Letters* 90, 297–314.
- Hofmann, A.W., 1997. Mantle geochemistry: the message from oceanic volcanism. *Nature* 385, 219–229.
- Jelaska, V., 1981. Facial characteristics of the Mt. Kozara flysch (North Bosnia) (in Croatian with English summary). *Vesnik, Serija A: Geologija* 38/39, 137–145.
- Jovanović, C., Magaš, N., 1986. Basic geological map sheet of Yugoslavia 1:100,000, sheet Kostajnica L 33-106. Federal Geological Institute Beograd.
- Karamata, S., 2006. The geological development of the Balkan Peninsula related to the approach, collision and compression of Gondwanan and Eurasian units. In: Robertson, A.H.F., Mountrakis, D. (Eds.), *Tectonic Development of the Eastern Mediterranean Region*. Geological Society Special Publications. Geological Society of London, London, pp. 155–178.
- Karamata, S., Olujić, J., Protić, L., Milovanović, D., Vujnović, L., Popević, A., Memović, E., Radovanović, Z., Resimić-Sarić, K., 2000. The western belt of the Vardar Zone – the remnant of a marginal sea. In: Karamata, S., Janković, S. (Eds.), *International Symposium Geology and metallogeny of the Dinarides and the Vardar zone*, Banja Luka, Sarajevo, pp. 131–135.
- Karamata, S., Sladić-Trifunović, M., Cvetković, V., Milovanović, D., Šarić, K., Olujić, J., Vujnović, L., 2005. The western belt of the Vardar Zone with special emphasis to the ophiolites of Podkozarje – the youngest ophiolitic rocks of the Balkan Peninsula. *Bulletin T. CXXX de l'Académie serbe des sciences et des arts. Classe des Sciences mathématiques et naturelles* 43, 85–96.
- Kim, J., Jacobi, R.D., 2002. Boninites: characteristics and tectonic constraints, north-eastern Appalachians. *Physics and Chemistry of the Earth* 27, 109–147.
- Krenn, E., Ustaszewski, K., Finger, F., 2008. Detrital and newly formed metamorphic monazite in amphibolite-facies metapelites from the Motajica Massif, Bosnia. *Chemical Geology* 254, 164–174. doi:10.1016/j.chemgeo.2008.03.012.
- Lanphere, M., Coleman, R.G., Karamata, S., Pamić, J., 1975. Age of amphibolites associated with Alpine peridotites in the Dinaride ophiolite zone, Yugoslavia. *Earth and Planetary Science Letters* 26, 271–276.
- Le Bas, M.J., Le Maitre, R.W., Streckeisen, A.L., Zanettin, B., IUGS Subcommittee on the Systematics of Igneous Rocks, 1986. A chemical classification of volcanic rocks based on the total alkali-silica diagram. *Journal of Petrology* 27, 745–750.
- Liati, A., Gebauer, D., Fanning, C.M., 2004. The age of ophiolitic rocks of the Hellenides (Vourinos, Pindos, Crete): first U–Pb ion microprobe (SHRIMP) zircon ages. *Chemical Geology* 207, 171–188.
- Lovrić, A., 1986. Ages of Magmatic and Metamorphic Rocks by Isotopic Methods (in Serbian), *Bulletin of the Fund for Scientific Investigations*. Serbian Academy of Sciences and Arts, Beograd, p. 18.
- Ludwig, K., 2005. Isoplot/Ex v.3, USGS Open File report.
- Lugović, B., Altherr, R., Raczek, I., Hofmann, A.W., Majer, V., 1991. Geochemistry of peridotites and mafic igneous rocks from the Central Dinaric Ophiolite Belt, Yugoslavia. *Contributions to Mineralogy and Petrology* 106, 201–216.
- Lugović, B., Šegvić, B., Babajić, E., Trubelja, F., 2006. Evidence for short-living intraoceanic subduction in the Central Dinarides, Konjuh Ophiolite Complex (Bosnia–Herzegovina). *International Symposium on the Mesozoic Ophiolite Belts of the Northern Part of the Balkan Peninsula*. Serbian Academy of Sciences and Arts, Committee of Geodynamics, Belgrade, pp. 72–75. May 31st–June 6th, 2006.
- Mahlburg Kay, S., Godoy, E., Kurtz, A., 2005. Episodic arc migration, crustal thickening, subduction erosion, and magmatism in the south-central Andes. *Geological Society of America Bulletin* 117, 67–88.
- Márton, E., Tischler, M., Csontos, L., Fügenschuh, B., Schmid, S., 2007. The contact zone between the ALCAPA and Tisza-Dacia mega-tectonic units of Northern Romania in the light of new paleomagnetic data. *Swiss Journal of Geosciences* 100, 109–124.
- Mattinson, J.M., 2005. Zircon U–Pb chemical abrasion (“CA-TIMS”) method: combined annealing and multi-step partial dissolution analysis for improved precision and accuracy of zircon ages. *Chemical Geology* 220, 47–66.
- Milovanović, D., Marchig, V., Karamata, S., 1995. Petrology of the crossite schist from Fruška Gora Mts (Yugoslavia), relic of a subducted slab of the Tethyan oceanic crust. *Journal of Geodynamics* 20, 289–304.
- Mojićević, M., Vilovski, S., Tomić, B., 1976. Basic geological map sheet of Yugoslavia 1:100,000, sheet Banja Luka L 33-119. Federal Geological Institute, Sarajevo.
- Murphy, J.B., 2007. Igneous Rock Associations 8: Arc Magmatism II: geochemical and isotopic characteristics. *Geoscience Canada* 34, 7–36.
- Neubauer, F., Heinrich, C.A., GEODE ABCD Working Group, 2003. Late Cretaceous and Tertiary geodynamics and ore deposit evolution of the Alpine–Balkan–Carpathian–Dinaride orogen. In: Eliopoulos, D.G. et al. (Eds.), *Mineral Exploration and Sustainable Development. Proceedings of the Seventh Biennial Society for Geology Applied to Mineral Deposits Meeting on Mineral Exploration and Sustainable Development*, Athens, Greece. Millpress Science Publishers, Rotterdam, pp. 1133–1136. August 24–28, 2003.
- Nicolas, A., 1989. Structures of Ophiolites and Dynamics of Oceanic Lithosphere. *Petrology and Structural Geology*, 4. Kluwer Academic Publishers, Dordrecht. 367 pp.
- Okrusch, M., Seidel, E., Kreuzer, H., Harre, W., 1978. Jurassic age of metamorphism at the base of the Brezovica peridotite (Yugoslavia). *Earth and Planetary Science Letters* 39, 291–297.
- Ovtcharova, M., Bucher, H., Schaltegger, U., Galfetti, T., Brayard, A., Guex, J., 2006. New Early to Middle Triassic U–Pb ages from South China: calibration with ammonoid biochronozones and implications for the timing of the Triassic biotic recovery. *Earth and Planetary Science Letters* 243, 463–475.
- Pamić, J., 1993a. Eoalpine to Neoalpine magmatic and metamorphic processes in the northwestern Vardar Zone, the easternmost Periadriatic Zone and the southwestern Pannonian Basin. *Tectonophysics* 226, 503–518.
- Pamić, J., 1993b. Late Cretaceous volcanic rocks from some oil wells in the Drava depression and adjacent mountains of the southern parts of the Pannonian Basin (North Croatia). *Nafta* 44, 203–210.
- Pamić, J., 1997. Volcanic rocks of the Sava–Drava interfluvium and Baranja (in Croatian with English summary). *Nafta*, 8, Zagreb. 192 pp.
- Pamić, J., 2002. The Sava–Vardar Zone of the Dinarides and Hellenides versus the Vardar Ocean. *Eclogae Geologicae Helveticae* 95, 99–113.

- Pamić, J., Šparica, M., 1983. The age of the volcanic rocks of Požeška Gora (Croatia, Yugoslavia). In Croatian with English abstract. *Rad Jugosl. Akad. znan. umjet.* 404, 183–198.
- Pamić, J., Prohić, E., 1989. Novi prilog petrološkom poznavanju alpskih granitnih i metamorfnih stijena Motajice u sjevernim Dinaridima u Bosni. (A new contribution to the petrology of Alpine granite and metamorphic rocks from Motajica Mt. in the northernmost Dinarides, Yugoslavia). *Geološki Glasnik* 13, 145–176.
- Pamić, J., Pécsekay, Z., 1994. Geochronology of Upper Cretaceous and Tertiary igneous rocks from the Slavonija–Srijem Depression. *Nafta* 45, 331–339.
- Pamić, J., Lanphere, M., McKee, E., 1988. Radiometric ages of metamorphic and associated igneous rocks of the Slavonian Mountains in the southern part of the Pannonian Basin, Yugoslavia. *Acta Geologica* 18, 13–39.
- Pamić, J., Árkai, P., O'Neil, J., Antai, C., 1992. Very low- and low-grade progressive metamorphism of Upper Cretaceous sediments of Mt. Motajica, northern Dinarides, Yugoslavia. In: Vozar, J. (Ed.), *Special Volume to the Problems of the Paleozoic Geodynamic Domains; Western Carpathians, Eastern Alps*. Dionýz Stur Institute of Geology, Bratislava, pp. 131–146.
- Pamić, J., Belak, M., Bullen, T.D., Lanphere, M.A., McKee, E.H., 2000. Geochemistry and geodynamics of a Late Cretaceous bimodal volcanic association from the southern part of the Pannonian Basin in Slavonija (Northern Croatia). *Mineralogy and Petrology* 68, 271–296.
- Pamić, J., Tomljenović, B., Balen, D., 2002. Geodynamic and petrogenetic evolution of Alpine ophiolites from the central and NW Dinarides: an overview. *Lithos* 65, 113–142.
- Pantić, N., Jovanović, O., 1970. On the age of "Azoic" or "Palaeozoic slates" in Motajica Mountain based on microfloristic remnants (in Serbocroatian with English abstract). *Geološki Glasnik* 14, 190–214.
- Ricou, L.E., 1994. Tethys reconstructed: plates, continental fragments and their boundaries since 260 Ma from Central America to South-eastern Asia. *Geodinamica Acta* 7, 169–218.
- Robertson, A.H.F., Karamata, S., 1994. The role of subduction–accretion processes in the tectonic evolution of the Mesozoic Tethys in Serbia. *Tectonophysics* 234, 73–94.
- Săndulescu, M., Visarion, M., 1977. Considérations sur la structure tectonique du soubassement de la dépression de Transylvanie. *Dări de seamă ale şedinţelor* 66, 153–173.
- Schefer, S., Fügenschuh, B., Schmid, S.M., Egli, D., Ustaszewski, K., 2007. Tectonic evolution of the suture zone between Dinarides and Carpatho-Balkan: field evidence from the Kopaonik region, southern Serbia, EGU General Assembly 2007. *Geophysical Research Abstracts* 03891 Vienna.
- Schilling, J.G., Zajac, M., Evans, R., Johnston, T., White, W., Devine, J.D., Kingsley, R., 1983. Petrologic and geochemical variations along the Mid-Atlantic Ridge from 29 degrees N to 73 degrees N. *American Journal of Science* 283, 510–586.
- Schmid, S.M., Bernoulli, D., Fügenschuh, B., Matenco, L., Schefer, S., Schuster, R., Tischler, M., Ustaszewski, K., 2008. The Alpine–Carpathian–Dinaridic orogenic system: compilation and evolution of tectonic units. *Swiss Journal of Geosciences* 101, 139–183.
- Shand, S.J., 1947. *Eruptive Rocks. Their Genesis, Composition, Classification, and Their Relation to Ore-Deposits, with a Chapter on Meteorite*. John Wiley & Sons, New York. 488 pp.
- Smith, A.G., Spray, J.G., 1984. A half-ridge transform model for the Hellenic–Dinaric ophiolites. In: Dixon, J.E., Robertson, A.H.F. (Eds.), *The geological evolution of the Eastern Mediterranean*. Geological Society Special Publications, vol. 17. Blackwell Scientific Publications, pp. 629–644.
- Sölvä, H., Grasmann, B., Thöni, M., Thiede, R., Habler, G., 2005. The Schneeberg Normal Fault Zone: normal faulting associated with Cretaceous SE-directed extrusion in the Eastern Alps (Italy/Austria). *Tectonophysics* 401, 143–166.
- Šparica, M., Bužaljko, R., Jovanović, C., 1980. Basic geological map sheet of Yugoslavia 1:100,000, sheet Nova Kapela L 33–108. Federal Geological Institute Beograd.
- Šparica, M., Bužaljko, R., Jovanović, C., 1984. Basic geological map sheet of Yugoslavia 1:100,000, sheet Nova Gradiška L 33–107. Federal Geological Institute Beograd.
- Spray, J.G., Bèbien, J., Rex, D.C., Roddick, J.C., 1984. Age constraints on the igneous and metamorphic evolution of the Hellenic–Dinaric ophiolites. In: Dixon, J.E., Robertson, A.H.F. (Eds.), *The Geological Evolution of the Eastern Mediterranean*. Geological Society Special Publication, vol. 17. Blackwell Scientific Publications, pp. 619–627.
- Stacey, J.S., Kramers, J.D., 1975. Approximation of terrestrial lead isotope evolution by a two-stage model. *Earth and Planetary Science Letters* 26, 207–221.
- Starjaš, B., Balen, D., Tibljaš, D., Schuster, R., Humer, B., Finger, F., 2004. The Moslavačka Gora Massif in Croatia: part of a Late Cretaceous high-heat-flow zone in the Alpine–Balkan–Carpathian–Dinaride collision belt, Pangea Austria 2004: "Erwissenschaften und Öffentlichkeit". *Berichte des Institutes für Erdwissenschaften der Karl-Franzens Universität Graz*, Graz, pp. 453–454.
- Starjaš, B., Gerdes, A., Balen, D., Tibljaš, D., Schuster, R., Mazer, A., Humer, B., Finger, F., 2006. Geochronology, metamorphic evolution and geochemistry of granitoids of the Moslavačka Gora Massif (Croatia). *Congress of the Carpathian–Balkan Geological Association, Beograd (Serbia)*, pp. 594–597.
- Steiger, R.H., Jäger, E., 1977. Subcommittee on geochronology: convention on the use of decay constants in geo- and cosmochronology. *Earth and Planetary Science Letters* 36, 359–362.
- Sun, C.H., Stern, R.J., 2001. Genesis of Mariana shoshonites: contribution of the subduction component. *Journal of Geophysical Research* 106, 589–608.
- Tari-Kovačić, V., Mrinjek, E., 1994. The Role of Palaeogene Clastics in the Tectonic Interpretation of Northern Dalmatia (Southern Croatia). *Geologia Croatica* 47, 127–138.
- Tashko, A., Tërshana, A., 1988. Mafic segregations with phlogopite in the Bulqiza Massif (English Translation). *Bull. Shkencave. Gjeol.* 2, 87–95.
- Tischler, M., Gröger, H., Fügenschuh, B., Schmid, S., 2007. Miocene tectonics of the Maramures area (Northern Romania): implications for the Mid-Hungarian fault zone. *International Journal of Earth Sciences* 96, 473–496.
- von Quadt, A., Moritz, R., Peytcheva, I., Heinrich, C.A., 2005. 3: Geochronology and geodynamics of Late Cretaceous magmatism and Cu–Au mineralization in the Panagyurishte region of the Apuseni–Banat–Timok–Srednogie belt, Bulgaria. *Ore Geology Reviews* 27, 95–126.
- Winter, J.D., 2001. *An introduction to igneous and metamorphic petrology*. Prentice–Hall, Upper Saddle River, New Jersey. 697 pp.

Acknowledgments

The present thesis would not have been possible without the help and support of numerous colleagues and friends. I am very grateful for whatever support I got from all the different people, may it be geological, musical, intellectual, computational or just ‚distractinal‘...

First of all I would like to thank my two supervisors, Stefan Schmid and Bernhard Fügenschuh. During the time of my thesis we spent a lot of time during fieldwork in the Balkan, on terrain-courses with students, and on excursions everywhere and we developed not only a professional relationship but also a friendship – there was a time when I spent more time with you than with my family... Stefan Schmid taught me a lot about the way how to work as a geologist in the field, how to read all kind of maps (and yes, concerning roadmaps we sometimes had hard discussions), to integrate the different branches of geology and helped me to get in touch with a lot of very interesting people. You always supported me in my ideas and gave me plenty of new input when I was lacking creativity. Precise argumentation and the importance of beautiful, informative yet simply kept figures was something I learnt during this time, and all my manuscripts are very grateful for your efficient, meticulous and thorough revising! Bernhard Fügenschuh gave the initial idea for this project. We had wonderful long discussions about geology and the meaning of life, and you always built me up when my spirits were low. I will never forget the enthusiasm you showed for me becoming a father, exactly what one needs in the middle of the Serbian outback when such news come out of the blue! I am also grateful for the accomodation during my stays in Innsbruck, for perfect espresso and the support during the latest stage of my PhD, when revising manuscripts and figures became a daily routine.

During my PhD I repeatedly spent a considerable amount of time doing fieldwork in Serbia. The reception and hospitality I got from the local people was outstanding and I am very grateful for this experience! Most of all I like to thank Peđa and Zorica Đorđević and their sons Oli and Miloš who provided me not only an excellent accommodation in Vila Đorđević but became very good friends and I felt like a member of their family. Hvala najlepše!

The most important thing when working in a foreign country is the ability to lead a basic conversation in the national language. I found a wonderful and patient teacher in Tatjana Simeunović. Natalie Špoljarić helped me for my homework and we exercised the serbian-croatian friendship with plenty of pivo... Moreover, all Serbian people I met were very patient and creative when it came to understand my broken Serbian with all the newly invented words (ja znam, da sam govorać!).

Although I was unable to establish a close collaboration with the University in Belgrade, there were some Serbian geologists who helped me getting access to literature and important local knowledge: Milan Sudar, Vladica Cvetković, Dejan Prelević, Kristina Sarić, Nataša Gerzina. Milica Božović introduced me to the serbian parties in Belgrade and most of all to Café Breza, a wonderful place in Kosjerić, and she translated my abstract to Serbian language, so that anyone can read it – thank you very much!

Urs Schaltegger, Maria Ovtcharova and Blair Schoene introduced me into the magic of isotope geochemistry at their lab in Geneva. I was very impressed by the cleanliness of the lab and fascinated by the precision of the analyses and I was sure I would never be able to work as precise to comply with your standards... Nevertheless, you all encouraged me and I somehow managed to work clean enough to produce quite precise results.

Daniel Egli spent two summers of fieldwork with me in Serbia and we shared our office. It was a great time, and I very much appreciate that he rarely called me an old man. We had plenty of good discussions on geology (and a lot more...), and his stratigraphic work was an important contribution to this thesis.

Kamil Ustaszewski introduced me to the study area and the serbian restaurants on a very brief field trip at the beginning of my thesis. He also participated a lot in the complicated topic of the geodynamic evolution in the Balkan Peninsula and the awful work of separating fine-fraction of pelitic rocks as preparation for argon isotopic analyses.

Daniel Bernoulli taught me the law of Occam's razor and how to methodically prepare and revise a manuscript. He also revised some of my texts and helped me with sedimentary, stratigraphic and regional geologic questions. I am glad for the open door of his office he shares with Alexandre Kounov, who introduced me to the art of counting and interpreting apatite track-length data.

Willy Tschudin prepared numerous thin-sections for my thesis, sometimes from samples far away from being a proper rock, but always in no time! Apart from that, I am very glad we managed to keep our small smokers-lounge in front of your workshop despite the non-smoking policy of the University... Michael Wiederkehr was usually the first to meet in the morning, always in a good mood, and always ready for a little chit-chat. Rüdiger Kilian helped me with computer problems I could not solve myself, he opened my eyes for security and privacy issues on the internet, and introduced me to the world of podcasting.

Furthermore I thank all my colleagues and the entire staff (former and present) at the Geological-Mineralogical Department for the mostly beautiful ten years I spent at the Bernoullianum. Special thanks go to Christian de Capitani for all scientific and not so scientific discussions, Leander Franz for help with metamorphic petrology, Stefan Gräser for his enthusiasm in mineralogy, Horst Dresmann for his help with GoCAD, Joëlle Glanzmann for the excellent culinary treatment, Verena Scheuring for support in accessing well hidden literature from the Balkan, and Koni Leu for introducing me to the possibilities of local area networking. Special thanks go to the Freie Akademische Gesellschaft Basel who supported my family and myself during five of the last months of the thesis in a non-bureaucratic way.

I thank my family, especially my parents, for being just that. I always knew I've had a wonderful childhood, but now I am beginning to understand what it means to provide it.

Christina Serr helped me a lot by taking so good care of Lou during the final stage of my PhD, when nights got longer and weekends shorter – I am sure Lou liked these days as much as Christina did!

Most of all I thank Hélène Chassin for her love and our daughter Lou Stoja! You always supported me in whatever I did, even if it meant me being abroad for a long time. You tolerated my moods when I was too deep in seemingly unsolvable geological problems, and while you did not solve them, you always cheered me up and you believed that I could do it. Thank you so much!

And even if might be easier to finish a thesis without a small child at home (it is hard to work when you could also go on the playground slide...), I am definitively better off having such a wonderful little person like our daughter being part of my life. And since my thesis is printed only in 2012, I also want to mention our wonderful son Jules Vanja - suppressing all possible jealousy in the beginning... :-)

Curriculum Vitae

Senecio Claudio Schefer

Personal Details

Date of birth: September 23rd 1971
Place of birth: Basel (Switzerland)
Marital status: married to H el ene Chassin
Children: Lou Stoja Schefer, born on April 8th 2008
Jules Vanja Schefer, born on January 17th 2012
Citizenship: Swiss citizen (Teufen, AR)

Professional Address:

Geothermal Explorers International Ltd.
Wasserturmplatz 1
4410 Liestal

Home Address:

Fatiostrasse 29
4056 Basel
061 321 55 66

Email: senecio.schefer@geothermal.ch

Education

2005–2010: PhD in Earth Sciences at University of Basel:
„Tectono-metamorphic and magmatic evolution of the Internal Dinarides (Kopaonik area, southern Serbia) and its significance for the geodynamic evolution of the Balkan Peninsula“
Supervisors: Prof. S.M. Schmid & Prof. B. F ugenschuh

Oct. 2005: Diploma in Earth Sciences at University of Basel
Diploma thesis (including mapping in the Alps of northern Italy):
„Tectonic und Metamorphic Evolution in the Gruf-Unit“
Supervisors: Prof. S.M. Schmid & Prof. R. Bousquet

2000–2005: Studies in Earth Sciences at the University of Basel

1988–1993: Studying Primary Teacher at Lehrerseminar Kreuzlingen (TG)

Professional experience

- since 2010: Exploration Geologist Geothermal Explorers International Ltd.
- 2005–2010: Teaching assistant at the Institute of Geology, University of Basel:
Excursions, field courses and lectures in structural and regional geology
- 08–10. 2005: Substitute teacher for mathematics at the „Schule für Brückenangebote“, Basel (BS)
- 2002–2004: Salesman (incl. consultation) in the Condomeria in Basel (BS)
- 1996–2000: Primary teacher at the elementary school in Münchwilen (TG), third to sixth grade,
last year as principal
- 1994–1995: Substitute teacher at different primary and secondary schools alternating with travelling in
Eastern Europe and North America
- 1993–1994: Cook and waiter in the cooperative Restaurant Löwen, Sommeri (TG)

Publications in journals with review procedure

- Schefer S**, Cvetković V, Fügenschuh B, Kounov A, Ovtcharova M, Schaltegger U & Schmid SM (2011): Cenozoic granitoids in the Dinarides of southern Serbia: age of intrusion, isotope geochemistry, exhumation history and significance for the geodynamic evolution of the Balkan Peninsula. *International Journal of Earth Sciences*, 100, DOI 10.1007/s00531-010-0599-x.
- Schefer S**, Egli D, Missoni S, Bernoulli D, Fügenschuh B, Gawlick HJ, Jovanović D, Krystyn L, Lein R, Schmid SM & Sudar MN (2010a): Triassic metasediments in the Internal Dinarides (Kopaonik area, southern Serbia): stratigraphy, paleogeographic and tectonic significance. *Geologica Carpathica*, 61: 89–109.
- Ustaszewski K, Schmid SM, Lugović B, Schuster R, Schaltegger U, Bernoulli D, Hottinger L, Kounov A, Fügenschuh B & **Schefer S** (2009): Late Cretaceous intra-oceanic magmatism in the internal Dinarides (northern Bosnia and Herzegovina): Implications for the collision of the Adriatic and European plates. *Lithos*, 108: 106–125.
- Schmitz S, Möller A, Wilke M, Malzer W, Kanngiesser B, Bousquet R, Berger A & **Schefer S** (2009): Chemical U-Th-Pb dating of monazite by 3D-Micro X-ray fluorescence analysis with synchrotron radiation. *European Journal of Mineralogy*, 21: 927–945.
- Schmid SM, Bernoulli D, Fügenschuh B, Matenco L, **Schefer S**, Schuster R, Tischler M & Ustaszewski K (2008): The Alpine-Carpathian-Dinaridic orogenic system: correlation and evolution of tectonic units. *Swiss Journal of Geosciences*, 101: 139–183.